UNIVERSITY OF CAPE TOWN

DEPARTMENT OF MECHANICAL ENGINEERING

RONDEBOSCH, CAPE TOWN, SOUTH AFRICA

SITE LOCATION AND TECHNO-ECONOMIC ANALYSIS OF UTILITY-SCALE CONCENTRATING SOLAR POWER PLANTS IN SOUTH AFRICA

A dissertation submitted in partial fulfilment of the requirements for the degree of Master of Philosophy in Sustainable Energy Engineering

Author:

Joshua J.L. Brodrick

17th November 2011

Abstract

This dissertation comprises a two-part study concerned with the identification and quantification of potential Concentrating Solar Power (CSP) sites in South Africa; and the performance and cost modelling, optimisation and analysis of two CSP technologies in three locations. A further theme of the study is the consideration of the availability of water for plant cooling purposes, and hence the comparison between, and analysis of optimal CSP technologies and cooling methods for each location.

A Geographic Information System (GIS) based analysis was created and presented in order to identify potential CSP sites, with an emphasis placed on levels of incoming direct normal solar irradiation, as well as proximity to the national electricity grid, and large water sources for cooling purposes. Additional analysis criteria include a suitably flat land slope, and the exclusion of areas deemed unsuitable for construction, or not classed as possessing 'least threatened' vegetation. Five separate analysis cases were considered resulting in a total identified potential land area of between 2,180.5 km^2 and 18,785.6 km^2, total available solar energy levels of between 16.5 TWh/day and 144.3 TWh/day, a power generation potential of between 77.9 GW and 670.9 GW at a land use value of 28 km^2 per GW, and a net energy generation potential of between 264.7 and 3,526.3 TWh/annum, depending on the analysis cases and CSP technologies considered.

A number of computer-based performance and cost models were then created within the Solar Advisor Model (SAM) software for both parabolic trough and central receiver technologies, incorporating both wet and dry cooling at three locations. Of the two CSP technologies considered, central receiver technology was found to be preferable, while wet-cooling was found to be more economical than dry cooling. Dry cooling, however was shown to reduce water consumption by more than 90%. The resulting LCOE from the SAM models was found to be most sensitive to the financing assumptions of the project, rather than the project capital costs, while the cost of cooling water was found to have the least effect on the resulting plant LCOE. Based on these results, in conjunction with the classification of South Africa as a water stressed country, it was thus deduced that the availability of raw cooling water, rather than its current cost, would likely be the limiting factor in the use of wet cooling technology. According to the comparisons between the final model results, it was found that it may be more beneficial to construct a central receiver CSP plant in a region with high DNI levels but limited access to cooling water, as opposed to an area with lower DNI levels but access to large volumes of water.

Declaration

I know the meaning of plagiarism, and declare that all the work in the document, save for that which is properly acknowledged, is my own.

Joshua J.L. Brodrick
17th November 2011
University of Cape Town

Acknowledgements

First and foremost I would like to acknowledge and thank my supervisor, Professor Kevin Bennett, whose leadership was invaluable. His guidance made this research possible and it was a privilege to have worked with him.

My sincerest thanks also go to Nicholas Lindenberg and Thomas Slingsby, both of whom have been an unfathomable source of knowledge, and assistance. Their never ending attitude to help – complimented by their skill with GIS software – allowed for the realization of this project, that otherwise may not have been attempted.

I would also like to acknowledge and thank Paul Gilman, previously from NREL, whose advise and experience regarding the SAM software was invaluable. In particular, his advice relating to the adaptation of SAM to local conditions proved extremely beneficial, and his help was highly valued.

My acknowledgements and thanks also go to South Africa's National Energy Research Institute (SANERI) and the University of Cape Town, for funds allocated towards the fulfilment of my degree. Their financial support allowed for the realisation of this research, and is greatly appreciated.

To Oisin 'Ush' Tummon, whose most cherished friendship, competitive spirit, and constant support have made my engineering years some of the best of my life, thank you for all the encouragement and inspiration.

To my parents, who have given me never ending support, and sacrificed to give me the best education possible. I would not have accomplished what I have today without you. Thank you.

And finally to Or, whose undying support and constant encouragement kept inspiring me through it all.

Table of Contents

List of Tables

List of Figures

Nomenclature

Acronyms and Abbreviations

CLFR	Compact Linear Fresnel Reflector
CPV	Concentrating Photovoltaic
CSIR	Council for Scientific and Industrial Research
CSP	Concentrating Solar Power
DEAT	Department of Environmental Affairs and Tourism
DEM	Digital Elevation Model
DME	Department of Minerals and Energy
DNI	Direct Normal Irradiation
DOE	Department of Energy
DSCR	Debt Service Coverage Ratio
DWA	Department of Water Affairs (formerly the DWAF)
DWAF	Department of Water Affairs and Forestry (now the DWA)
EIA	Environmental Impact Assessment
EPRI	Electric Power Research Institute
EPW	EnergyPlus Weather Data
GHG	Greenhouse Gas
GHI	Global Horizontal Irradiation
HCE	Heat Collection Element
HTF	Heat Transfer Fluid

HVAC	Heating, Ventilation, and Air Conditioning
IEA	International Energy Agency
IPCC	Intergovernmental Panel on Climate Change
IPP	Independent Power Producer
IRR	Internal Rate of Return
LCOE	Levelised Cost of Energy
LTMS	Long Term Mitigation Scenarios
NASA	National Aeronautics and Space Administration
NERSA	National Energy Regulator of South Africa
NREL	National Renewable Energy Laboratory
O&M	Operation and Maintenance
PCM	Phase Change Material
PPA	Power Purchase Agreement
PV	Photovoltaic
REFIT	Renewable Energy Feed-In Tariff
SAM	Solar Advisor Model
SARS	South African Revenue Service
SCAs	Solar Collector Assemblies
SEGS	Solar Energy Generating Systems
SETP	Solar Energy Technologies Program
SRTM	Shuttle Radar Topography Mission
SWERA	Solar and Wind Energy Resource Assessment
TES	Thermal Energy Storage
TMY	Typical Meteorological Year
USGS	United States Geographic Service

UTM	Universal Transverse Mercator
WMAs	Water Management Areas

Units of Measure

$/kl	U.S. Dollars per Kilolitre
$/MWh	U.S. Dollars per Megawatt Hour
¢/kWh	U.S. cents per Kilowatt Hour
GW	Gigawatt
GWh/d	Gigawatt Hours per Day
kl	Kilolitre
kW	Kilowatt
kW_e	Kilowatt Electric
kW.yr	Kilowatt Year
kWh_{th}	Kilowatt Hour Thermal
kWh/m^2	Kilowatt Hours per Square Meter
$kWh/m^2/d$	Kilowatt Hours per Square Meter per Day
MW	Megawatt
MW_e	Megawatt Electric
MW_{th}	Megawatt Thermal
MWh	Megawatt Hour
R	South African Rand
R/kl	South African Rand per Kilolitre
R/MWh	South African Rand per Megawatt Hour
TWh/a	Terrawatt Hours per Annum
TWh/d	Terrawatt Hours per Day
Wh/m^2	Watt Hour per Square Meter

1 Introduction

1.1 Subject and Reason for Investigation

Climate change, unsustainable development, and the depletion of finite fossil resources are some of the prominent issues facing the world in the 21st century. With the increase in extreme weather phenomena, alterations in global climate patterns, and the rise in average global temperatures, the effect that human kind is having on the biosphere is becoming more evident. The Intergovernmental Panel on Climate Change (IPCC), cited by Pegels (2009), confirms this fact, and points to human activity as one of the major causes of global warming, as a direct result of greenhouse gas (GHG) emissions.

In addition, the diminishing supply of crude oil, as well as other fossil fuels, poses a threat to the energy security of all countries worldwide. According to the DME (2003), the South African economy in particular is strained by the import of dollar based fuels, whose burden could be greatly diminished by reducing the need to import them. Furthermore, should global measures such as carbon taxing be introduced that limit the use of fossil fuels, the South African economy would be negatively impacted, as it currently generates revenue from the processing and export of coal.

The increasing global realisation of the need to reduce GHG emissions and progress towards sustainable power production has resulted in renewable energy sources receiving a great deal of attention, and becoming an increasingly important factor in the world energy balance (European Commission, 2004). According to the International Energy Agency (IEA, 2008), solar energy is the most abundant of all renewable energy sources, leading to solar power being considered as a primary contender for renewable power generation. In regions with high levels of direct solar radiation, Concentrating Solar Power (CSP) systems in particular are considered to have the potential to replace conventional fossil fuel technologies (European Commission, 2004; IEA, 2008).

In South Africa, however, even though there are vast renewable resources present – in particular some of the best solar resources in the world – investment in renewable energy technology has been relatively low and these resources have remained largely untapped (DME, 2003). Although financial incentives, such as the Renewable Energy Feed-In Tariff (REFIT), have been proposed by the National Energy Regulator of South Africa (NERSA, 2009), they have yet to realise the development of a large renewable energy sector, and as a result renewable energy targets defined in policy papers still have to be met (Pegels, 2009).

South Africa is also classified as a water-stressed country, with an average annual rainfall less than 60% of the world average (Mukheibir, 2007). The effects of climate change, coupled with a growing population and future development, are expected to add additional pressure to the limited availability of future water resources. As thermal power stations can use in the region of 1.89 - 2.84 litres of water per kilowatt hour (500 - 750 gallons/MWh) of energy produced when employing conventional wet cooling technology (DOE, U.S., 2010), it is thus imperative to consider all future energy generation technologies in the context of their water consumption. Alternative cooling technologies such as dry cooling – which is already adopted in some of the country's newer coal-fired plants – should also be considered as an alternative to more conventional wet cooling methods.

In light of these facts, the subject of this dissertation comprises a multi-part study concerned with the determination of locations for potential CSP plants in South Africa, and subsequently, the conduction of a computer-based performance and cost simulation of parabolic trough and central receiver CSP technologies at a number of locations representing the identified potential sites. Particular attention is paid to the availability of water for plant cooling purposes, and hence the use of both wet cooling and dry cooling technologies is considered. For each location, an attempt is made to identify the optimal CSP technology type, as well as to ascertain whether it would be preferable to adopt wet or dry cooling.

It is hoped that through the conduction of this research, a better understanding of the local technical and economic aspects and key variables associated with the implementation of CSP systems in South Africa will be gained. It is also hoped that by studying multiple CSP technologies at different locations, the relative metrics arising from their comparisons will prove more valuable than if only an absolute value prediction of a single technology or location was made. As stated by the European Commission (2004), a better understanding of the key issues will be beneficial for financiers, researchers and developers, if a successful CSP sector is to be realised globally, as well as here in South Africa.

1.2 Background to Investigation

In the past, the energy sector in both the developed and developing world has been the primary source of GHG emissions, as a direct result of a heavy reliance on fossil fuels as a source for energy production. South Africa in particular relies heavily on fossil fuels for its energy supply, with fossil fuels accounting for 90% of primary energy, and coal representing 75% of the fossil-based supply (DME, 2003). According to the DME, the abundant naturally occurring coal resources have resulted in extensive capital investments in a large-scale, coal-based energy supply system. This in turn saw low electricity prices and relatively little new capacity development taking place in the last decade (Pegels, 2009). However, according to Edkins, cited by Morse (2009), the lack of new capacity investment resulted in South Africa facing an electricity supply crisis and diminishing reserve margin towards the end of 2007. Morse (2009) continues to state that the national electricity supplier, Eskom, proposed two mitigation scenarios to increase capacity while reducing the effects of climate change, both of which include increasing the share of renewables. The first scenario envisages 8.5 GW of solar energy by 2050, while the second sees 30 GW of solar installed.

One of the key reason for the inclusion of solar power is that the majority of South Africa receives more than 2500 hours of sunshine per annum, with an average solar-radiation level ranging between 4.5 and 6.5 kWh/m^2 in one day. This is one of the highest local solar resources in the world, and according to the DME (2003), makes South Africa a prime candidate for solar power generation. In particular, the extremely high levels of annual direct solar irradiation makes the country a prime candidate for CSP systems. Certain CSP technologies are also considered to be relatively mature, with the first commercial parabolic trough plants being commissioned in 1984 as a result of the 1970s oil price shock (Wagner, 2008). Furthermore, as CSP systems typically make use of thermal energy as an intermediate energy phase, they possess the added benefit of being able to store thermal energy for later use, thereby reducing their variability and rendering them more applicable for base-load power generation. In areas with high levels of direct solar radiation, CSP plants prove to be far cheaper then photovoltaic (PV) solar systems, however, they are currently still not yet competitive with fossil fuels or wind power (IEA, 2008). The long-term viability of renewable energy technologies such as CSP therefore depends on the availability of financial subsidies, carbon emission disincentives, and their reliability when competing with more conventional fossil-based power generation systems (Morse, 2009).

Although no major utility-scale CSP plants are currently under construction in South Africa, initial research has been conducted to determine and quantify the potential for CSP plants in South Africa. A geographic information systems (GIS) study conducted by Fluri (2009) identified potential CSP locations throughout the country, however, no consideration was made for plant proximity to sources of cooling water. According to the Renewable Energy Policy Network (REN21, 2008), it is certain that renewable energy technologies will need to be implemented, and that they offer a viable solution to satisfying the growing energy demand, while simultaneously reducing GHG emissions and mitigating climate change. Before the successful and commercially-competitive implementation of these technologies is realised in South Africa, however, favourable policy and financial backing will also be required, and hence additional research will be beneficial in providing a deeper insight into the available technologies and their relationship with the economic environment.

1.3 Objectives

Thus, in light of the identification of South Africa's vast solar resource potential yet water stressed nature, coupled with the fact that Eskom has proposed renewable energy targets which have yet to be fully realised, and the fact that no utility-scale commercial CSP plants have yet been commissioned in South Africa, the objectives of this dissertation, considered in the context of current conditions and boundaries, and with the aim to aid the commencement of CSP in South Africa, are as follows:

1. To develop a methodology for the identification and quantification of potential CSP sites in South Africa, and subsequently, present an approach for creating South African specific, high-level techno-economic models of current commercial CSP technologies at select identified locations.

2. A further aim is to use this approach to attempt to ascertain which of the current commercial CSP technologies modelled would be considered optimal for a considered location, and to determine whether the use of wet cooling or dry cooling technology would be more beneficial.

3. Finally, as at the time of writing, no utility-scale commercial CSP plants have yet been realised in South Africa, a further objective of this study is to derive useful insight into and understanding of the techno-economic criteria and their effect on CSP developments, through the comparison of different model results and hence the arising relative metrics; as opposed to absolute value predictions which are not

the focus of this high level study. This objective is based on advise given by Gilman (2011) – previously of the United States National Renewable Energy Laboratory (NREL) Solar Advisor Model (SAM) division – which was that through consistency in the modelling, and only varying metrics of key interest, the relative metrics will provide more useful information as opposed to the less important and potentially less accurate absolute value predictions.

1.4 Research Questions

Based on the three key objectives of this dissertation, four research questions were posed, which encompassed specific aspects of the objectives, and whose analysis was deemed beneficial in aiding the understanding and accomplishment of the objectives. The research questions posed were:

1. Is it more beneficial in terms of the Levelised Cost of Energy (LCOE) to locate a South African CSP plant in a region with high DNI levels but limited access to cooling water, hence adopting dry cooling; or in a region with lower DNI levels but greater access to larger volumes of water, hence adopting wet cooling?

2. Of the CSP technologies considered in this analysis, which would be deemed most optimal at each location?

3. Which financial and cost-related model input variables have the greatest effect on the resulting LCOE of the plant, and hence which are the key items to consider when implementing a utility-scale parabolic trough or central receiver CSP plant in South Africa?

4. Can a high level analysis and methodology be developed to achieve the objectives of this study, by making use of existing software and modelling tools, available data, or data adapted to reflect South African conditions; and if so, how accurately can this be achieved?

1.5 Methodology

In order to achieve the objectives of this study, as well as to assess the research questions posed, the following methodology was developed and employed:

1. Conduct an in-depth literature review regarding the current environment for Concentrating Solar Power (CSP) stations in South Africa, in particular, considering previous studies on solar resource potential, and the availability of water for power-plant consumption.

2. In addition, assess the current status of CSP plants worldwide, paying particular attention to the latest technological developments, including cooling technology and thermal energy storage.

3. Identify and source the relevant data required to construct a Geographic Information Systems (GIS) model of potential CSP stations in South Africa.

4. Conduct a high-level GIS analysis, in order to identify potential CSP sites in South Africa, based on defined criteria.

5. Acquire detailed hourly weather data for the locations of a select few of the potential CSP sites identified in the GIS analysis.

6. Conduct an in-depth literature review of existing CSP plant designs and costs, in order to determine the necessary technical and financial data required to model various CSP technologies in South Africa.

7. Create performance and cost models for various CSP plants and locations in South Africa with the Solar Advisor Model (SAM) software, and subsequently simulate and optimise the various CSP plant configurations within the SAM models.

8. Analyse the various model results, and attempt to identify the optimal CSP technology for each of the considered locations. Thereafter, compare the results to, and validate them against, results contained in the literature.

9. Perform a sensitivity analysis of various model inputs in order to ascertain their effect on the model results.

10. Draw conclusions from the findings of the study, and make recommendations for further research and potential improvements.

1.6 Scope and Limitations

In light of the aforementioned objectives, this dissertation will include the identification and analysis of potential CSP sites in South Africa by means of a high-level GIS analysis. A performance and cost model will then be constructed within the Solar Advisor Model (SAM) computer software for two utility-scale CSP technology types, namely parabolic trough and central receiver, employing both wet and dry cooling at three identified potential locations. Attempts will be made to identify optimal choices for both CSP technology type and cooling technology within the context of current conditions and boundaries, and the sensitivity of the models to input variables will be assessed.

Due to limitations in the SAM software, and that fact that at the time of writing no utility-scale commercial CSP plants have yet been realised in South Africa, the more established parabolic trough and central receiver systems will thus receive key focus as CSP commencement technologies, and be will be considered and modelled at each location. Emerging technologies will therefore not be considered in this study. Furthermore, due to time constraints, no photovoltaic (PV) or concentrating photovoltaic (CPV) systems will be considered in this study. Due to the lack of freely available, detailed weather data, potential CSP site locations will be approximated with hourly weather data from the closest major town or city. Although the use and modelling of thermal energy storage will be included for CSP plants, time constraints lead to the exclusion of considering and modelling a fossil backup fuel system. Additionally, due to time constraints, and based on the guidelines in the REFIT documentation (NERSA, 2009, 2010), only 6 hours of thermal energy storage will be considered and this capacity will not be varied. Finally, as at the time of writing no utility-scale CSP plants were in existence in South Africa, detailed plant technical, design and cost data had to be sourced from the literature for plants outside of South Africa, before attempts were made to adjust these data to local conditions.

1.7 Plan of Development

The dissertation begins with a review of the literature, pertaining to the current state of CSP research in South Africa, as well as an overview of the SAM software, its method of operation, and its application.

Chapter 3 presents an overview of solar thermal technology, incorporating a review of current CSP technologies as well as their history and current applications worldwide. Chapter 4 then describes thermal power cycles, and the application of various wet and dry cooling technologies, before discussion their respective costs, and effect on plant water consumption. Chapter 5 concludes the initial theory and review chapters, with an overview of thermal energy storage, motivation for its use with CSP plants, and finally a description of various thermal storage technologies and their application.

The GIS analysis is conducted in Chapter 6, which concludes with the identification and quantification of potential CSP sites in South Africa. Chapter 7 then presents a detailed description of the SAM software user interface and its various input pages as a means to better identify required model input data, as well as to determine the applications and limitations of the software. In Chapter 8, a full and detailed description of all the methods and sources used in the determination of the SAM model inputs is given. The optimisation of various plant design criteria is also presented.

The final results from the various models, and the analysis thereof, are presented in Chapter 9, where they are subsequently compared to and validated against similar results contained in the literature. A sensitivity analysis of various key input variables is then conducted in Chapter 10, whereby the effect of varying input conditions on final model outputs is gauged.

In the final two chapters, conclusions are drawn from the findings, before recommendations are made based on the conclusions. The full documentation of the developed GIS methodology, as well as all CSP plant comparison databases and final model inputs are presented in the appendices.

2 Literature Review

Before commencing this research, it was first necessary to review the literature pertaining to the analysis of CSP systems in South Africa. This was done not only in order to gain the theoretical knowledge and data required to completed this analysis, but also to achieve a better understanding and refined scope through the review of the findings and limitations of similar studies that have previously been conducted.

In light of this, the following chapter will present a review of South Africa's solar and CSP potential, and the issues regarding water scarcity and security. A review of the relevant computer software used for the analysis of CSP technologies in this study will also be presented. The review of literature will not be confined to this chapter alone, however, but instead the relevant theory and literature specific to each section will be discussed and developed throughout the course of this dissertation. Furthermore, the data required for the various models and analyses in this study will be sourced from the literature and presented both in the subsequent sections of the report and in the appendices.

2.1 Analysis of South Africa's CSP Potential

The use of geographic information systems (GIS) software to conduct initial high-level evaluations and identify potential CSP sites is becoming more common. In their paper on the *GIS approach to the definition of capacity and generation ceilings of renewable energy technologies*, Bravo et al. (2007) made use of GIS software and modelling to identify and quantify the energy generation potential of CSP sites in Spain. More recently, Fluri (2009) conducted a study on the potential of CSP in South Africa, making use of similar GIS analysis criteria and methodologies to those of Bravo et al. (2007), as well as GIS studies conducted by Pletka et al. and Dahle et al. (as cited by Fluri, 2009).

Fluri (2009) concluded that when considering the potential CSP sites identified in his study with a land use profile of 28 km^2 per gigawatt (GW), South Africa possesses 510.3 GW of nominal generation capacity in the Northern Cape, 25.3 GW in the Free State, 10.5 GW in the Western Cape and 1.6 GW in the Eastern Cape. This results in a total nominal power generation capacity of 547.6 GW for the whole of South Africa. Furthermore, if parabolic trough CSP technology is considered at all locations, with an assumed annual capacity factor of 38.8%, a net energy generation potential of 1861.4 terrawatt hours per annum (TWh/a) could be realised.

Although Fluri (2009) states that a CSP sector of this magnitude would require 6086.7 million m^3 of water per annum, the requirement for potential sites to be within a certain proximity of cooling water was not included in the study. What is noted, however, is that according to the water management areas (WMAs) defined by the South African Department of Water Affairs (DWA) – then the Department of Water Affairs and Tourism (DWAF), and cited by Fluri, 2009) – most potential CSP sites are situated in areas where there is little or no potential for any future development requiring water for consumption purposes. Fluri (2009) therefore concludes that a large roll-out of CSP in South Africa will only be possible if dry-cooling is considered.

2.2 Water Scarcity

As stated in the introduction of this report, South Africa is classified as a water-stressed country, receiving an annual average rainfall of 500mm – less than 60% of the world average (Mukheibir, 2007). Of the 19 water management areas (WMAs) defined by the DWA – then the DWAF – 11 of these faced water deficits in 2004. The Northern Cape province is particularly affected by supply concerns, and had a water supply deficit of 8 million m^3 in 2000 (Mukheibir, 2007). This is of especial concern, as the Northern Cape is one of primary areas considered for potential CSP development.

As CSP plants consume large quantities of water per year – in the region of 500 - 750 gallons per megawatt hour (1.89 - 2.84 litres/kWh) (DOE, U.S., 2010) – it is thus imperative to consider water availability when analysing any potential CSP development site. Should there be insufficient water to supply the plant, or should the price of water become a limiting factor, it may be necessary to consider other areas or provinces with lower solar resources but access to water, or conversely, make use of alternative plant cooling technologies such as dry-cooling – at the expense of plant efficiency and cost.

2.3 The Solar Advisor Model Software

2.3.1 Overview

The Solar Advisor Model (SAM) is a performance and economic software model which was developed by the National Renewable Energy Laboratory (NREL), in collaboration with Sandia National Laboratories and in partnership with the U.S. Department of Energy (DOE) Solar Energy Technologies Program (SETP). Development on SAM was begun in 2004 by SETP to aid and support their analyses. It has since evolved the capacity to model a range of renewable technologies, and is currently used worldwide for planning and evaluating research and development programs, developing project cost and performance estimates, and for academic research (NREL, 2011b). SAM is now designed to aid in the decision making process for many involved in the solar industry, ranging from project managers, engineers, technology developers, incentive designers and researchers (SAM, 2010).

In general, SAM calculates both the performance characteristics for the renewable technology in question, and economic estimates for grid-connected solar power projects in the distributed and central generation markets (SAM, 2010). These attributes, as well as the fact that it has been used and validated in the fields of industry and research for a number of years, make it an ideal choice for use in this study to model, analyse and compare grid-connected, utility-scale parabolic trough and central receiver CSP technologies, incorporating the effects of both wet and dry cooling technologies, at various locations around South Africa.

In order to aid understanding of how SAM accomplishes its task of calculating the performance and economic characteristics of a plant, a brief overview of the workings of the SAM performance and economic components will now be briefly discussed. For the sake of brevity, detailed technical descriptions and actual thermodynamic and economic formulae will not be presented, however, these are available in the SAM (2010) documentation should the need or interest arise to consult them.

2.3.2 Performance Model Component

The SAM plant performance component is based on an hourly simulation engine that runs on the TRNSYS software, developed at the University of Wisconsin Madison, but combined with additional customised components. TRNSYS is a time-series based transient systems simulation program which can simulate the performance of solar thermal and photovoltaic systems, low energy buildings and HVAC systems, renewable energy systems, co-generation, and fuel cells. The TRNSYS software has been commercially available since 1975, and through years of validation has become reference software for engineers and researchers, across multiple fields worldwide (SAM, 2010; TRNSYS, 2011).

TRNSYS makes use of hourly resource data combined with user specified components that represent the power system and the manner in which they are connected. TRNSYS includes a detailed library of multiple components found in thermal and electrical energy systems, but also allows for the creation of additional, user-defined components through a system description language. Once a system is defined by means of components, connections and their interactions, the model then solves the representing mathematical equations in order to describe and predict the system performance (TRNSYS, 2011).

There is no need to purchase or make use of TRNSYS in conjunction with SAM, however, as it is integrated directly into the SAM software. Hence, there is also no requirement of familiarity with the use of TRNSYS in order to run SAM (SAM, 2010). The user need only define the inputs and specifications for the components of a plant in SAM, and when a simulation or model is run, SAM passes these defined inputs, as well as the relevant connection and interaction data, directly into its TRNSYS simulation engine for processing. The results can then used with the economic model components in SAM.

2.3.3 Economic Model Component

The economic model in SAM calculates the cost of generating electricity and the project's cash flow over a specified analysis period, based on provided location, direct and operating cost, financial, and design specification data. In order to accomplish this, the system's hourly output for a single year, as generated by the aforementioned performance model component, is used to calculate a series of annual cash flows for revenues generated from electricity sales and incentive payments, tax liabilities (including any tax credits for which the project is eligible), and loan principal and interest payments.

SAM then produces economic output metrics such as the levelised cost of energy (LCOE), internal rate of return (IRR), minimum debt service coverage ratio (DSCR), and yearly cash flows. The economic model also possesses the ability to represent projects in the residential, commercial, and utility markets, while incorporating a variety of incentive payments and tax credits – which can be based on investment amounts, capacity ratings, and annual electricity production (SAM, 2010).

2.3.4 Model Output and Simulations

Thus in summary, SAM functions by the means of interaction with performance, cost, and finance models to calculate energy output, energy costs, and cash flows. A final means of functionality provided in SAM is the option to run various simulations of the same case study, comprising parametric analyses, sensitivity analyses, optimisation, and statistical analyses. These additional simulations allow for the investigation of the effect that any variation or uncertainty in any of the input data will have on final model results (SAM, 2010).

An overview of the various input pages and layout of the SAM user interface will be covered in greater detail in Chapter 7, while detailed descriptions, methods and motivations for the definition and derivation of inputs used in the SAM model for this study will be given in Chapter 8.

3 Concentrating Solar Technologies

3.1 Solar Thermal Overview

In a concentrating solar power (CSP) system, the sun's rays are focussed by means of optical devises in order to generate large quantities of heat. The heat generated can then be used to power a Stirling engine, generate steam to drive a turbine for electricity production, or alternatively, to drive chemical reactions (European Commission, 2004; IEA, 2010a).

CSP systems make use of mirrors or reflective surfaces which continuously track the sun in order to concentrate and focus the incoming incident radiation onto one or multiple receivers. However, as predicted by classical optical theory, only direct, parallel light rays are capable of being reflected and concentrated. CSP systems are therefore only capable of using the Direct Normal Irradiation (DNI) component of irradiation from the sun, and hence are only suitable in areas that receive high annual averages of DNI (European Commission, 2004; IEA, 2010a). According to the International Energy Agency (IEA), the minimum yearly DNI considered acceptable for the consideration of CSP plants is 2000 kWh/m^2/year (5.48 kWh/m^2/day) (IEA, 2008). This limits the placement of CSP plants to regions such as North Africa, Southern Africa, Western India, the South Western United States, Mexico, some parts of South America, part of Central Asia, and Australia. These promising areas for CSP are presented in Figure 3.1.

The main components of a CSP plant comprise the aforementioned *solar collector field* – constituting the tracking mirrors and reflectors – the *solar receiver*, and an *energy conversion system*. The high temperature heat that is produced when the mirrors or reflectors focus and concentrate the irradiation onto the receiver is then captured and transported to the energy conversion system by a working fluid circulating through the receiver. This process can be accomplished in two ways; either *directly* by using water as the working fluid and generating steam directly in the receiver, or alternatively in an *indirect* process, where a heat transfer fluid (HTF) is circulated through the receiver

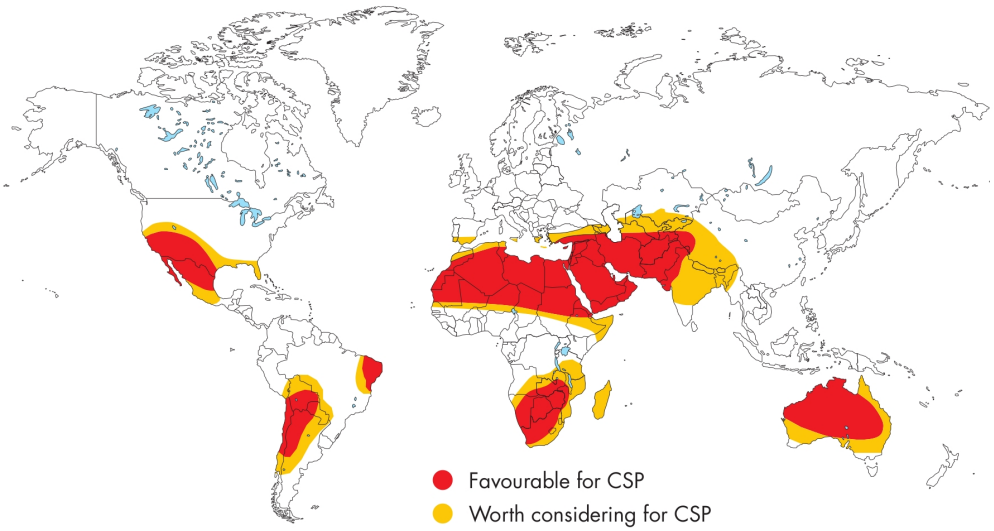

Figure 3.1: Most Promising Areas for CSP Sites (IEA, 2008).

before being used to produce steam in the energy conversion system via a heat exchanger mechanism (EPRI, 2010). The final step of the energy conversion process occurs at the power block or energy conversion system. In an electricity producing CSP plant, the heat can either be used to power a Stirling engine, or alternatively, to generate steam for driving a Rankine cycle turbine. CSP plants also possess the potential to be used in solar desalination projects, or to produce chemical fuels like hydrogen (IEA, 2008).

There are currently four major types of CSP technology, namely *Parabolic Trough*, *Central Receiver* (also know as a Power Tower), *Linear Fresnel*, and *Parabolic Dish* (or Dish Stirling). A schematic representation of each technology is presented in Figure 3.2 below.

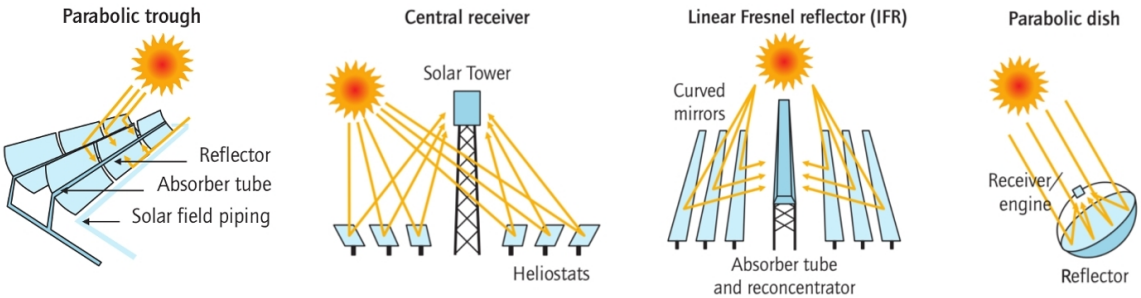

Figure 3.2: Various CSP Technologies. *Source of Images*: (IEA, 2010b).

From the figure, it can be seen that parabolic trough and linear Fresnel systems are line focus technologies, which track the sun along a single axis. Central receiver and parabolic trough technologies, however, are point focus technologies which track the sun across two axes (IEA, 2010a). A brief description of each of the technologies will now be presented under their respective headings.

3.2 Parabolic Trough

Figure 3.3: Parabolic Trough CSP Technology. *Source of Images:* Meyer (2010), Meyer (2010) and Müller-Steinhagen (2011).

Parabolic trough technology, as depicted in Figure 3.3, is the most mature of the CSP technologies, and consists primarily of a large field of single-axis tracking, parabolically-shaped troughs. The troughs are lined with parabolically shaped mirrors, or reflectors, which focus and concentrate the sun's beam radiation onto an integral linear receiver tube running along the length of each trough's focus. The troughs, which can span up to 150m in length, are usually installed in multiple parallel rows, known as solar collector assemblies (SCAs), which can cover areas of multiple square kilometers. The SCAs are typically aligned along a North-South horizontal axis, with each trough – driven by motors and control systems – tracking the sun from East to West throughout the day to ensure that the maximum incoming radiation is captured (EPRI, 2010).

The solar receiver tube, termed a heat collection element (HCE), is usually black-coated and housed in a glass vacuum tube to reduce thermal losses. Currently, all commercial plants make use of an indirect system with a high temperature thermal oil HTF which is circulated through the receiver tube, absorbing heat and reaching temperatures up to 400℃. The HTF is then piped to the power block and fed through heat exchangers in order to produce high temperature steam for the power cycle. Finally, the HTF is piped back to the HCEs for reheating. As a means to reduce costs, and limit the requirement for additional heat exchangers and maintenance, research is also being conducted in the field of direct steam generation (DSG) parabolic trough systems. In these DSG systems, water

is circulated through the receiver tubes to produce superheated steam. The superheated steam is then transported to the power block, where it drives a steam turbine to produce electricity. The water is then condensed and cycled back through the HCEs (EPRI, 2010; European Commission, 2004; Sargent & Lundy, 2003).

3.3 Central Receivers

Figure 3.4: Central Receiver CSP Technology. *Source of Images:* EPRI (2010), Müller-Steinhagen (2011) and Meyer (2010).

A central receiver system, also known as a 'power tower' and depicted in Figure 3.4, makes use of hundreds or thousands of individual two-axis sun-tracking mirrors, known as heliostats, to focus the sun's direct radiation onto a relatively small receiver situated on top of a tower. The receiver usually comprises an area of only a few square meters, while the tower ranges in height from 50m to over 100m depending on the capacity of the plant. Due to the large number of heliostats in the solar field, and the relatively small receiver size, central receiver plants produce extremely high concentration ratios in the order of 1000 suns, which in turn results in higher working temperatures and higher overall efficiencies when compared to parabolic trough plants (EPRI, 2010; European Commission, 2004; Sargent & Lundy, 2003).

The *receiver* is generally classed according to two categories, namely an *indirect irradiation* receiver, or a *direct irradiation* receiver. In an indirect configuration, the receiver consists of a number of metal or ceramic tubes through which the HTF flows. The outer surface of the receiver is heated by the concentrated solar irradiation, and this heat is then transferred to the working fluid. The heat can then be used to generate steam to drive a Rankine cycle turbine for electricity production, or alternatively to provide process heat for chemical processes. In such systems, the HTF typically comprises either water which generates steam within the receiver (as used in the Solar One, PS10 and PS20 plants), or a molten salt (as used in the Solar Two and Gemasolar plants) which is circulated throughout the system and heated to temperatures around 565 ℃ (Wagner, 2008).

In a direct irradiation receiver, also referred to as a volumetric receiver, the atmospheric air absorbs the solar radiation directly, or by intimate contact with a solid surface. The heated air can then be used to drive an open Brayton cycle or to heat nitrogen or helium for closed Brayton cycle operation (Wagner, 2008). At the time of writing, however, this technology is still undergoing research and development.

The use of a molten nitrate salt in a central receiver system has many distinct advantages over the thermal oil typically used in parabolic trough plants. Molten salt has a superior heat transfer capability compared to thermal oil, and is also significantly cheaper. The elimination of the thermal oil also greatly reduces the environmental risks associated with leaks. Molten salt can also be used directly as an energy storage mechanism, thereby reducing system component costs by eliminating the need for additional oil-to-salt heat exchangers – should storage be incorporated in a CSP system. The main disadvantage of a molten salt HTF, however, is that is solidifies at a relatively low temperature of 221 ℃, and therefore requires the use of additional electrical freeze protection mechanisms (EPRI, 2010; Wagner, 2008). The topic of thermal storage, however, will be discussed in more detail in Chapter 5.

Central receiver systems do, however, have larger associated parasitic loads when compared to parabolic trough plants. These arise due to the the fact that each heliostat requires an individual electric drive motor for tracking, and in the case of molten salt systems, the aforementioned electrical freeze protection system. Therefore, due to their size and economies of scale, central receiver systems are best suited for utility-scale application in the 30 MW to 400 MW range (European Commission, 2004). As a final note, due to the modelling limitation in SAM, only indirect irradiation central receiver systems will be considered, with the analysis of volumetric receivers considered beyond the scope of this report and recommended for future studies.

3.4 Linear Fresnel

Linear Fresnel technology, as depicted in Figure 3.5, is similar to the parabolic trough in the sense that it is a line focus technology. A linear Fresnel system differs from the parabolic trough, however, in that it approximates the parabolic shape by using long ground-level rows of flat or slightly curved mirrors. These mirrors are all individually controlled, single axis-tracking reflectors, which focus and concentrate the sun's incoming radiation onto a *fixed* downward-facing linear receiver which is suspended above the collectors (IEA, 2010a; Mills, 2004).

Figure 3.5: Linear Fresnel CSP Technology. *Source of Images:* Müller-Steinhagen (2011), Fahy (2009) and Meyer (2010).

A linear Fresnel system makes use of water as the working fluid and is thus a direct steam generation technology. According to Mills (2004), linear Fresnel systems can be classified into two different design categories, namely; the *Solarmundo* linear Fresnel system and the *Compact Linear Fresnel Reflector* (CLFR) system. The Solarmundo system is a classical linear Fresnel system, with one receiver per field and a relatively high receiver-to-field width ratio. The Solarmundo system makes use of a cavity receiver with a single receiver tube and secondary internal reflector. Mills (2004) continues to state that a Solarmundo system can be expected to deliver an annual average solar to electricity efficiency of between 10% and 12%. An example of a linear Fresnel cavity receiver with an internal secondary reflector, as produced by Novatec Solar (2011), is shown in Figure 3.6.

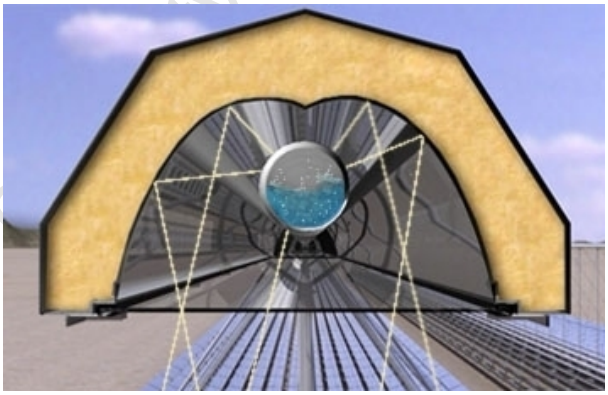

Figure 3.6: Linear Fresnel Cavity Receiver with Internal Secondary Reflector (Novatec Solar, 2011).

The CLFR system differers from a classical linear Fresnel system in that is employs the partial inter-meshing of adjacent fields with multiple receiver towers. This allows for a more efficient use of land space, as well as a significant increase in the optical efficiency of the system. The CLFR system makes use of a flat cavity receiver attached to boiling tubes, but unlike the Solarmundo system, does not make use of a secondary reflector. The CLFR system is reported to possess a peak solar to electricity conversion efficiency

of 19% (Mills, 2004). Both types of linear Fresnel system generate steam directly, which can then be used for electricity production through a Rankine cycle power block, or alternatively generate process heat. A linear Fresnel system is currently in use in Liddell, Australia, where it preheats boiler water for use in a conventional fossil fuel power station (Meyer, 2010).

Linear Fresnel technology is one of the newer developing CSP technologies, but possesses great potential as a low cost and effective system. Due to limitations in the SAM software, and the non-commercial nature of linear Fresnel technology, its use will not be considered or modelled in this analysis, but is recommended for further study.

3.5 Parabolic Dish

Figure 3.7: Parabolic Dish CSP Technology. *Source of Images:* Müller-Steinhagen (2011), Morse (2009) and Meyer (2010).

A parabolic dish system, as show in in Figure 3.7, makes use of a parabolically shaped dish, supported by a single structure and covered in mirrors or reflectors used to focus the sun's incoming radiation onto a receiver. The receiver unit is fixed at the dish's focus, with the whole dish and receiver unit tracking the sun along two axes. Parabolic dishes usually have an independent engine or generator coupled to the receiver, which is typically an external combustion Stirling engine. It is for this reason that a parabolic dish system may also referred to as a Dish Stirling system. Stirling engines are not the only engine used, however, with the possibility existing to make use of Brayton micro-turbines, or alternatively generating steam directly at the receiver. In the case of a Stirling or Brayton cycle, electricity would be generated directly at each receiver unit, while the use of direct steam generation would conversely require a separate power block and Rankine cycle turbine. (European Commission, 2004; IEA, 2010a).

Due to their extremely high concentration ratios, parabolic dish systems offer the greatest conversion efficiencies out of all the current CSP technologies, however, their commercial use is generally limited by their prohibitively high cost (Meyer, 2010). The dishes are generally small in size with diameters ranging between 8 and 10 meters (larger examples do exist, however, such as the *Big Dish* in Canberra, Australia). Due to their size, parabolic dish systems are considered modular by nature, but large installations are generally required to benefit from economies of scale. Their low compatibility with thermal storage, as well as the fact that they do not required cooling water, also puts them in direct competition with photovoltaic systems (European Commission, 2004; IEA, 2010a).

Due to the non-commercial nature of parabolic dish technology, parabolic dish systems will will not be considered in this analysis, however, their analysis is recommended for future studies.

3.6 Efficiency and Availability

The efficiency with which the incoming solar radiation can be converted into thermal energy, and electricity is dependent on a combination of the optical efficiency of the mirrors or reflectors, the heat absorption efficiency of the receiver, and the thermal to electric efficiency of the power block. According to the European Commission (2004), optical efficiencies in the region of 98% are achievable, while heat conversion efficiencies are in the range of 70% to 95%. Experimental parabolic dish systems have shown a peak solar to electric efficiency of 29%, but this is dependent on the technology type. Technologies with the highest concentration ratios, such as parabolic dishes and central receivers, generally achieve higher over all efficiencies when compared to more mature technologies such as parabolic troughs, which only achieve efficiencies around 20% (European Commission, 2004). The choice of cooling system for the power block – either wet or dry cooled – also affects the overall plant efficiency, as well as the system cost. A detailed discussion of thermal power plant cooling technologies will therefore be presented in Chapter 4.

CSP systems are also variable power producers by nature, due to their reliance on the sun and sensitivity to weather conditions. As a means to improve their availability and capacity factors, and hence render them better suited to base-load power generation, some CSP plants incorporate thermal energy storage devices, or are supplemented with a fossil fuel backup boiler (EPRI, 2010; IEA, 2010a). A detailed discussion of thermal storage for CSP systems will therefore be presented in Chapter 5.

3.7 History and Current State of Development of CSP Plants

Initial interest in CSP technology began in the late 1970s, with development beginning in early 1980s, and was primarily a result of the late 1970s world oil crisis. Experimental plants were set up in many countries, including Spain, the United States (U.S.), Japan and Australia, all of which were parabolic trough systems (Meyer, 2010).

CSP technology is still under active development today, however, having received a renewed revival as a result of the growing awareness of climate change and the need to reduce greenhouse gas (GHG) emissions (European Commission, 2004). Research is currently being conducted to improve the efficiency and reduce the cost of all aspects of CSP systems including, mirrors, receivers, HTFs, power blocks and cooling systems. Special attention is also being given to thermal energy storage systems, which would allow CSP plants to meet evening peaks loads, as well as become a firm option for base-load power generation, and hence economically viable competition to fossil fuel plants (IEA, 2010a).

A brief time-line of the development and operational lifetimes of some of the key CSP plants worldwide will now be presented under their respective headings. For the sake of brevity, not every single plant will be mentioned, but an effort made to include some of the major plants representing each technology. A summary of all the technologies covered is also presented in Table 3.1.

Parabolic Trough Plants

The first commercially operating CSP plant was the Solar Energy Generating Systems (SEGS) I parabolic trough plant, commissioned in the Mojave Desert of California in 1984. The plant was expanded in capacity every year from 1984 till 1991 and incorporates SEGS I through to SEGS IX. The total combined capacity of the plant is 354 MW, and the it has been operational ever since it was commissioned. Over the years, its output has increased by 35% while operation and maintenance (O&M) costs decreased by 40%. The plant is supplemented by a natural gas backup, with an upper limit of 25% imposed on supplementation. In the best years, however, only 5% gas backup was required (European Commission, 2004; Meyer, 2010).

Another key CSP plant is that of Nevada Solar One, which is a 64MW parabolic trough plant first commissioned in 2007 in the Nevada Desert. As of writing, this is the largest parabolic trough plant in the U.S. since the the original SEGS plants in 1980s (Meyer, 2010).

A final notable parabolic trough development is that of the Andasol I, II and III plants in Southern Spain. Andasol I and II are currently in operation, with the first plant commissioned in 2009. At the time of writing, Andasol III is still under development. Each plant outputs 50 MW to the electricity grid, which is the upper limit as currently regulated in Spain (Solar Millennium AG, 2008).

Central Receiver Plants

Some of the earliest central receiver CSP plants were the 10 MW Solar One and then later upgraded Solar Two plants in the Mojave Desert, California. Solar One was commissioned in 1982, and subsequently upgraded in 1988 to Solar Two, which incorporated 3 hours of full load thermal energy storage. Both plants operated reliably as development and test plants, and formed the design basis for the Gemasolar (Solar Tres) plant (Sargent & Lundy, 2003; Meyer, 2010).

Gemasolar, which was commissioned in 2011, is a 19.9 MW central receiver in southern Spain, and represents the worlds first central receiver system with 15 hours of molten salt storage. It also makes use of 15% limited natural gas backup (Torresol Energy, 2011).

Two other notable central receiver plants are PS10 and PS20 situated near Seville in southern Spain. Commissioned in 2007, PS10 was Europe's first commercial central receiver system and comprises an 11 MW direct steam system, as well as a steam energy storage system. PS20 was based on PS10 and was commissioned in 2009. At 20 MW rated capacity, it is currently the world's largest central receiver system, and makes use of direct steam generation (Meyer, 2010; Wagner, 2008).

A slightly different and new concept for central receiver systems is that of the 5 MW eSolar plant which was commissioned in 2009 in the U.S. The plant's focus is on modularity and ease of construction, and comprises approximately 12,000 small heliostats in a rectangular field, as opposed to the fewer, larger heliostats is elliptical arrangements, as adopted by many other systems (Meyer, 2010).

Linear Fresnel Plants

Linear Fresnel technology is still relatively undeveloped when compared to parabolic troughs and central receiver systems, however, a few commercial installations have been realised. The first implementation was a 1 MW thermal plant used to preheat boiler water for a coal-fired power station in Liddell, Australia. The plant was commissioned in 2004, and later upgraded to 10 $MW_{thermal}$. Other installations include the 5 MW Kimberlina CLFR plant installed in California in 2008, and the more recent 1.4 MW PE 1 plant installed by Novatec Solar in 2009 in Murcia, Spain (Meyer, 2010; Novatec Solar, 2011).

Parabolic Dish Plants

Parabolic dish technology, like linear Fresnel, is still relatively underdeveloped. Although a number of experimental systems do exist, as of the time of writing there are currently no commercially operating parabolic dish CSP plants (Meyer, 2010).

Table 3.1: Summary of Select Commercial CSP Plant Developments. *Source of Data:* European Commission (2004), Sargent & Lundy (2003), Meyer (2010), Novatec Solar (2011), Torresol Energy (2011) Solar Millennium AG (2008) and Wagner (2008).

Project	CSP Technology	Capacity	Country	Year Commissioned
SEGS I - IX	Parabolic Trough	354 MW	U.S.	1984
Nevada Solar One	Parabolic Trough	64 MW	U.S.	2007
Andasol I	Parabolic Trough	50 MW	Spain	2009
Andasol II	Parabolic Trough	50 MW	Spain	2009
Solar One	Central Receiver	10 MW	U.S.	1982
Solar Two	Central Receiver	10 MW	U.S.	1988
Gemasolar	Central Receiver	19.9 MW	Spain	2011
PS10	Central Receiver	11 MW	Spain	2007
PS20	Central Receiver	20 MW	Spain	2009
eSolar	Central Receiver	5 MW	U.S.	2009
Liddell	Linear Fresnel	10 MW_{th}	Australia	2004
Kimberlina	Linear Fresnel	5 MW	U.S.	2008
Novatec PE 1	CLFR	1.4 MW	Spain	2009

4 Power Plant Cooling Technologies

The Rankine steam power cycle forms the basis for the majority of all thermal power stations, as a means to generate electricity from heat (Cengel and Boles, 2006). The majority of all CSP technologies used for electricity generation are also based on the steam power cycle, the exception being the Stirling dish system which operates on the Stirling cycle (DOE, U.S., 2010). Furthermore, according to the DOE, U.S. (2010), all of the existing commercial parabolic trough CSP plants in the United States use a Rankine steam cycle to convert their thermal energy to electricity, in a similar manner to that used by coal-fired, natural gas and nuclear power stations.

The Rankine steam cycle functions according to the principle that heat enters the system from an external high temperature source, and is rejected to the sink at a low temperature. In an ideal cycle and ignoring any losses, the work done by the steam turbine – and thus the work extracted from the system – is equivalent to the difference in temperatures of the heat source and the heat rejected at the sink (DOE, U.S., 2010). This can be seen in Figure 4.1.

The efficiency of the Rankine cycle is largely affected by the temperatures and pressures at the source and sink of the system, and hence in the case of electricity generation from a steam turbine, the difference in the temperatures and pressures of the steam at the turbine inlet and outlet. The efficiency of the system – and thus power generation potential – can therefore be improved by either increasing the temperature and pressure of the inlet steam, or decreasing the temperature and pressure of the outlet steam (Kelly, 2006). The exit steam in the condenser is a saturated mixture, existing at the saturation temperature relating to the pressure in the boiler. Thus the lower the temperature of the condenser, the lower the exit steam pressure of the turbine, and the greater the efficiency and hence the amount of work that can be extracted from the system (Cengel and Boles, 2006). The process of decreasing the temperature and pressure of the exit steam is illustrated in Figure 4.2.

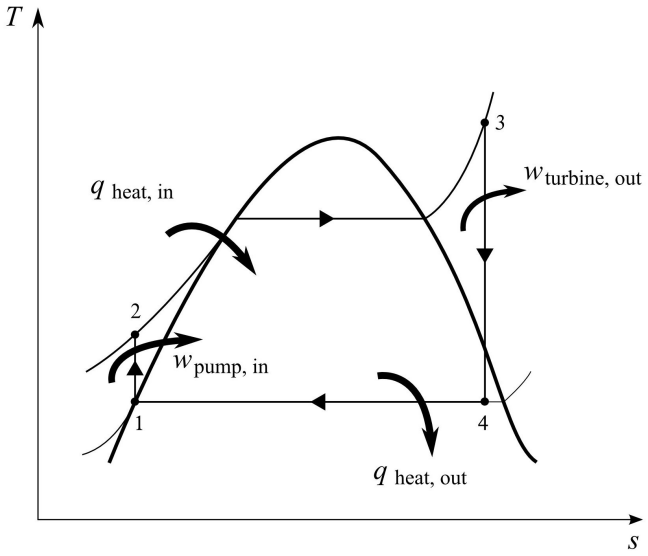

1 - 2 Isentropic compression in pump
2 - 3 Constant pressure addition of heat inside a boiler
3 - 4 Isentropic expansion through a turbine
4 - 1 Constant pressure rejection of heat in a condenser

Figure 4.1: Temperature - Enthalpy Diagram of the Simple Ideal Rankine Cycle.

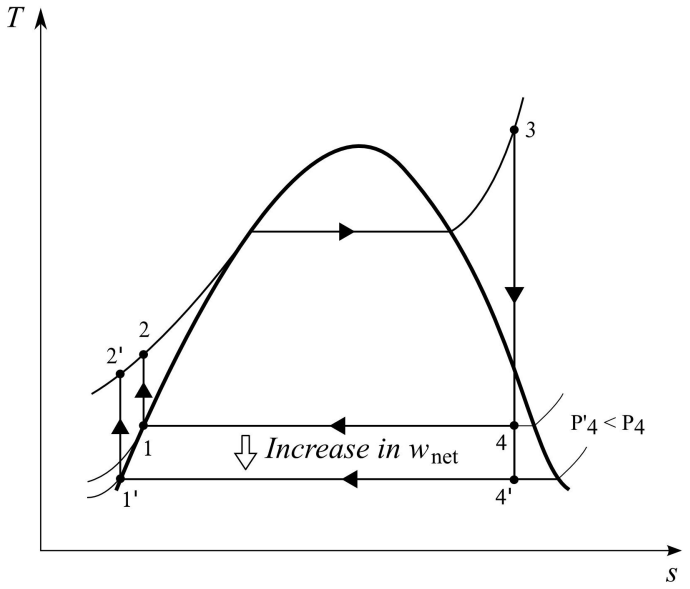

Figure 4.2: Effect of Decreasing Condenser Temperature and Pressure on the Efficiency of the Simple Ideal Rankine Cycle.

The condenser in most systems is therefore maintained at a low pressure, but in order to maintain it, a form of cooling is required in order to decrease its temperature. According to Kelly (2006), the lowest ambient temperature available is the wet bulb temperature, and thus most conventional power plants make use of an evaporation process and cooling towers to provide cooling water to the condenser, thereby achieving a high efficiency. Kelly (2006) continues to state that as the principal of heat transfer for wet cooling requires evaporation, large quantities of water are consumed – as much as 725 000 tons of water for an 80 MW_e parabolic trough CSP plant. In a report to congress concerning the reduction of water consumption in CSP electricity generation plants, the U.S. Department of Energy (DOE, U.S., 2010) state that all the operational CSP plants in the U.S. make use of water cooling, but due to the fact that water use for power plants is becoming more constrained, incentives exist to investigate alternative cooling technologies such as dry cooling, or hybrid wet-dry cooling. The following sections will thus briefly outline the methods and functionality of wet cooling, dry cooling and hybrid wet-dry cooling.

4.1 Wet Cooling

A 2003 study concerning the *Consumptive Water Use for U.S. Power Production* conducted by Torcellini et al. (2003) for NREL, showed that in the year 2000, 89% of electricity in the United States was produced by thermal driven, water-cooled energy conversion cycles. These water-cooled cycles used in thermoelectric plants were shown to evaporate an average of 1.8 litres of water for every kWh of electricity consumed at the point of end use (Torcellini et al., 2003).

In general, water-cooled cycles can be divided into two main categories or methods of accomplishment, namely, *once-through cooling*, and *recirculating evaporative cooling* (DOE, U.S., 2010). These two categories of wet cooling will now be briefly described.

4.1.1 Once-Through Cooling

In a once-through wet cooling cycle, large quantities of water are withdrawn from a waterbody, passed through a heat exchanger in the power cycle's steam condenser, and then returned back to the water source at elevated temperatures. The elevated temperature of the water returned to the source results in increased evaporation of the source itself. This process is represented graphically in Figure 4.3.

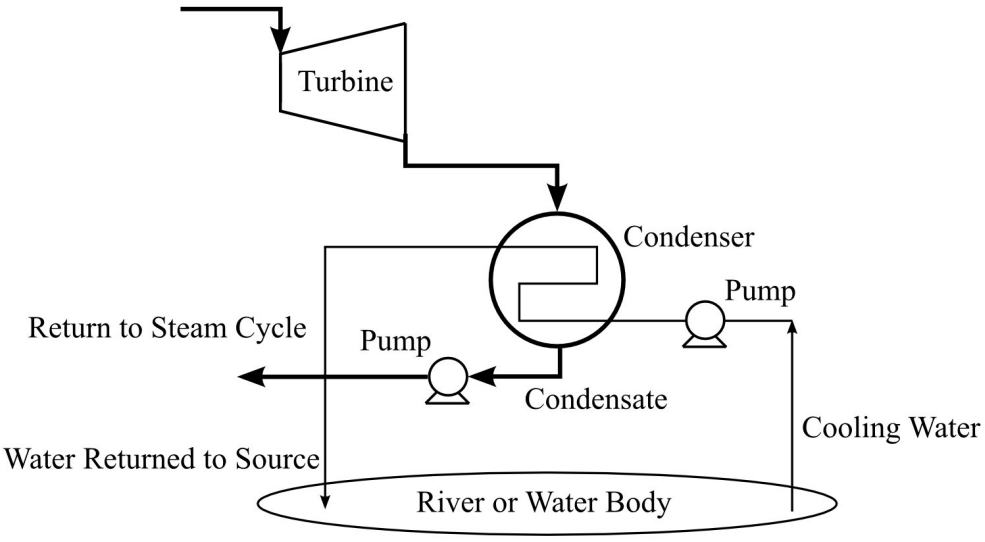

Figure 4.3: Schematic Representation of a Once-Through Wet Cooling System.

The method of once-through wet cooling typically requires volumes of between 87 and 102 litres of water per kWh being extracted from the source, the majority of which is returned and rapidly increases the evaporation rates of the source (DOE, U.S., 2010; Torcellini et al., 2003). The DOE, U.S. (2010) continues to note that the future use of once-through wet cooling in thermoelectric power plants may be restricted, due to environmental concerns regarding the impact of the elevated source temperatures on aquatic life and ecosystems. As a means to reduce these negative environmental impacts associated with this practice, evaporative cooling towers are thus preferred and hence more actively pursued.

4.1.2 Evaporative Cooling

In an evaporative cooling cycle, heat is removed from the system and transferred to the surrounding air by means of the evaporation of water. Unlike the once-through wet cooling cycle, the cooling water in the evaporative cycle is recirculated through the system, with a portion of it being continually evaporated in a draft cooling tower (Torcellini et al., 2003). Make-up water is thus required, and is drawn from the source to replenish the water evaporated in the draft cooling tower. This process is represented graphically in Figure 4.4.

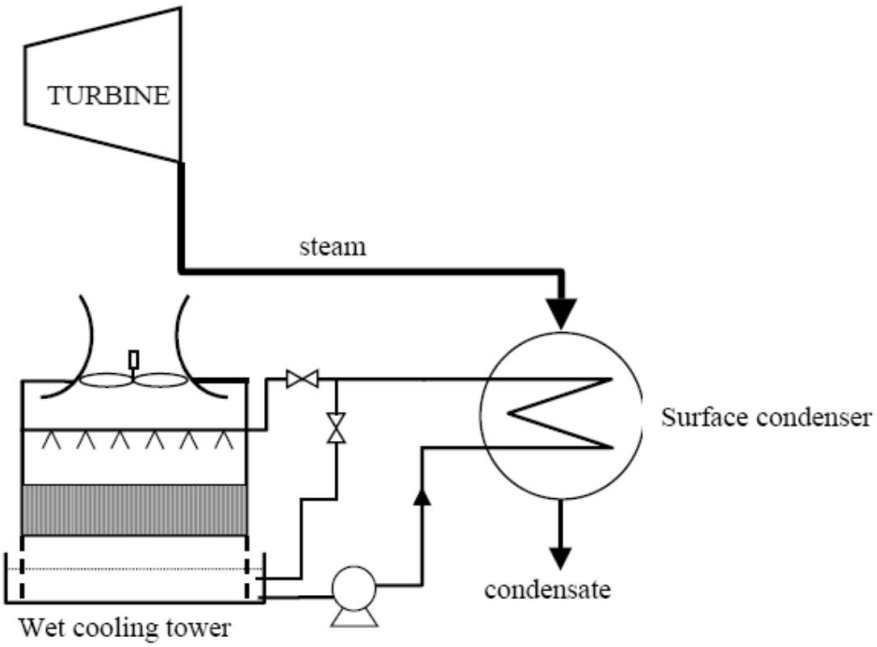

Figure 4.4: Schematic Representation of an Evaporative Wet Cooling System (DOE, U.S., 2010).

The recirculating evaporative cooling process results in far lower quantities of water being withdrawn from the source – between 1.89 and 2.46 litres per kWh – but the majority of the water which is withdrawn is consumed through evaporation (DOE, U.S., 2010). These figures are thus in agreement with the consumption figure of 1.8 litres per kWh stated by Torcellini et al. (2003) in section 4.1.

A further item for consideration with evaporative cooling is that any minerals, salts or water treatment chemicals present in the cooling water will become more concentrated over time as they are left behind in the evaporation process. This creates the need to drain a portion of the cooling water in order to remove these particulates. The waste drainage water is known as *blowdown*, and is a potential environmental hazard. Furthermore, any chemicals which are evaporated along with the cooling water can be a source a particulate pollution (DOE, U.S., 2010).

Therefore in summary of wet cooling, if a recirculating evaporative system is used, the volume of water withdrawn from the source is low, but the consumption of that water is relatively high. Conversely, if a once-through cooling system is used, larger quantities of water are drawn from the source, with evaporation rates at the power plant being low, but the elevated water source temperatures resulting in greater evaporation at the source, and increased total evaporation overall (Torcellini et al., 2003).

4.2 Dry Cooling

A dry cooling cycle operates without the need for cooling water, instead rejecting the heat from the steam cycle to the surrounding air. This process can be achieved through a number of methods, which will be described in the following sections.

A typical thermoelectric plant operating with dry cooling is thus a highly attractive alternative when considering water withdrawals and consumption. The only water withdrawal required for a conventional plant operating with dry cooling is for the steam cycle blowdown and make-up water, as well as domestic uses on site. A CSP plant using this technology, however, would require additional water withdrawals for mirror cleaning. The DOE, U.S. (2010) suggest that a conventional thermoelectric plant making use of dry cooling consumes less than 10% of the water of an equivalent plant employing evaporative wet cooling.

Although dry cooling was seen primarily as a means to address water limitations in areas where there was abundant fuel but little water, there are a number of additional or alternate reasons for its consideration. The majority of these considerations either stem from environmental or aesthetic concerns and comprise items such as reduction of waste-water discharge, and the abatement of the evaporation vapour plume visibility. According to EPRI and California Energy Commission (2002), in many cases the use of dry cooling also reduces licensing approval times by removing the need for a review of water related issues and rights, thus shortening the "time to market".

The use of dry cooling is becoming increasingly common with thermoelectric plants, but there are, however, disadvantages associated with the technology. Dry cooling represents a higher initial capital investment cost, and requires more auxiliary power to run when compared to wet cooling cycles. As the lowest temperature available to dry cooling is the dry bulb temperature – which is higher than the wet bulb temperature, especially on hotter days – the Rankine cycle efficiency is also reduced. This is a result of the increased temperature causing an increase in the condenser pressure and decreasing the turbine efficiency. The IEA (2010b) state that the use of dry cooling with a parabolic trough CSP plant can reduce its efficiency and annual electricity production by 7%, increasing the cost of the electricity it produces by 10%, when compared to the same plant using wet cooling technology. These figures are comparable to the 5% electricity production reduction and 7-9% increase in electricity price, as found by the DOE, U.S. (2010) in their analysis.

As with wet cooling, dry cooling cycles can also be differentiated according to two main categories or methods of accomplishment, namely, *direct* dry cooling, and *indirect* dry cooling. These two categories will now be briefly described.

4.2.1 Direct Systems

Direct dry cooling systems are the most common, and function by means of routing the turbine exhaust steam directly to an air-cooled condenser. The air cooled condenser is essentially a liquid-to-air surface heat exchanger with multiple finned tubes, usually arranged in an A-frame configuration. The multiple fins serve to increase the surface area for heat exchange and thus the heat transfer efficiency. The heat exchanger is typically fitted with fans in order to aid the heat transfer process via forced convection (DOE, U.S., 2010; Torcellini et al., 2003). The process is represented in Figure 4.5.

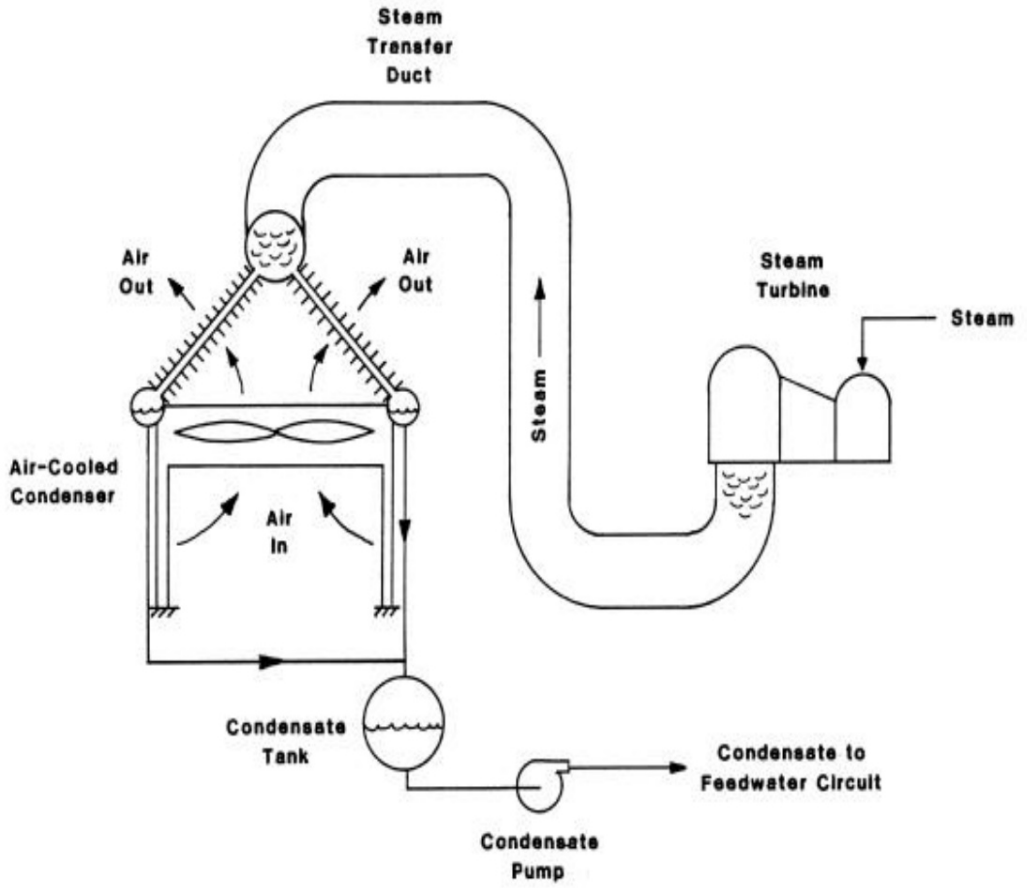

Figure 4.5: Schematic Representation of a Direct Dry Cooling System (EPRI and California Energy Commission, 2002).

4.2.2 Indirect Systems

In an indirect dry cooling system, a separate condenser is used in which the steam is condensed. This can be either a conventional shell-and-tube surface condenser, or a barometric condenser which condenses the steam directly on a spray of cooling water. In both types, the cooling water used to condense the steam is then circulated in a separate cycle through an air-cooled heat exchanger which ultimately rejects the heat to the atmosphere (EPRI and California Energy Commission, 2002). The former system is illustrated in Figure 4.6 and the latter in Figure 4.7.

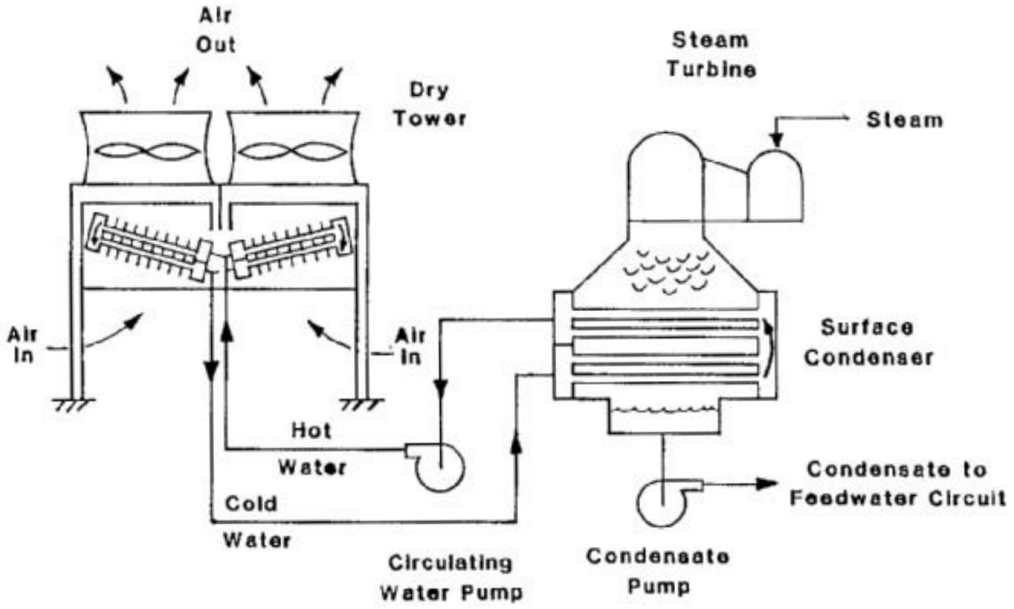

Figure 4.6: Schematic Representation of an Indirect Dry Cooling System with Surface Condenser and Mechanical Draft Tower (EPRI and California Energy Commission, 2002).

The latter system depicted in Figure 4.7 – which makes use of the barometric condenser – is usually coupled to a natural draft cooling tower, and known as a *Heller* system. As with all dry cooling technologies, they are characterised by a high initial capital cost, and generally a high operational and maintenance cost as well. They are used in several installations around the world, and represent the most likely retrofit solution for the rare occasion that an existing wet cooled plant would want to convert to dry cooling (EPRI and California Energy Commission, 2002).

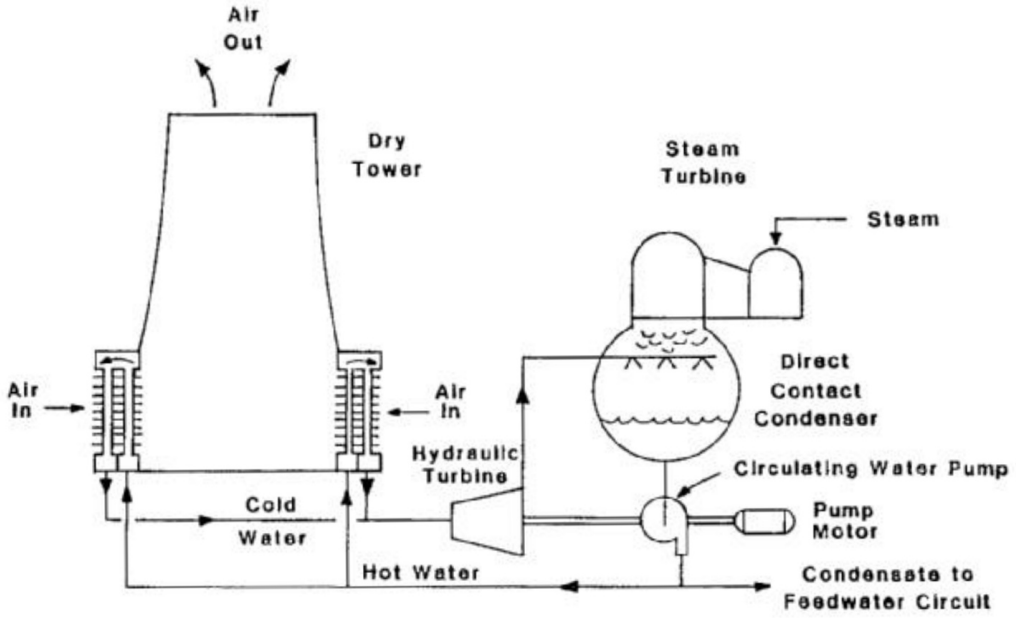

Figure 4.7: Schematic Representation of a Indirect Dry Cooling System with Direct Contact Condenser and Natural Draft Tower (EPRI and California Energy Commission, 2002).

4.3 Hybrid Wet-Dry Cooling

A hybrid wet-dry cooling system functions by means of employing a combination of both wet and dry cooling technologies. The use of hybrid cooling can generally be classified according to its purpose, namely a water conservation system or a plume abatement system. Initial interest in the technology occurred primarily in the 1970s – at the same time interest and research in dry cooling was taking place – and the primary focus was on plume abatement design. According to EPRI and California Energy Commission (2002), this trend in prioritising hybrid systems for plume abatement design as opposed to water conservation is still largely the case today.

4.3.1 Plume Abatement Systems

A plume abatement system is essentially a wet cooling system with a small dry-cooled component. The dry component's sole purpose is to dry out the exhaust plume during particularly cold and highly humid periods, when it would be most visible. Although this is primarily as aesthetic purpose, other benefits include reducing winter icing (caused by the exhaust plume) on nearby roads. The cold and highly humid conditions mentioned

are generally not present in areas deemed most suitable for CSP generation, however, and thus plume abatement is not considered a pressing issue for CSP sites (DOE, U.S., 2010; EPRI and California Energy Commission, 2002).

4.3.2 Water Conservation Systems

The purpose of a water conservation system is to reduce, but not completely eliminate the use of cooling water for power cycle heat rejection. The idea is that the plant will operate on a dry cooling cycle for the majority of the year – as a means to drastically reduce water consumption – but during the hottest periods of the year, a small amount of cooling water is used as a means to mitigate the largest losses in system efficiency that would be experienced in an all-dry system. According to EPRI and California Energy Commission (2002), water conservation hybrid schemes can limit annual water usage to between 2% and 5% (but generally between 20% to 80%) of that consumed by an all-wet cooling system, while simultaneously achieving greater efficiency and capacity advantages over an all-dry system during the hottest periods of the year. The DOE, U.S. (2010) echo this view, and estimate that water conservation hybrid systems save about 80% of water when compared to all-wet systems, while reducing the energy cost penalty below that of dry-cooled systems. Water conservation systems also possess the added advantage of plume abatement due to the wet part of the system not operating during the colder periods of the year when a plume is most likely to be visible.

4.3.3 Design Arrangements

A multitude of different designs exist for hybrid cooling systems, and can be summarised according to the following tower and condenser designs (EPRI and California Energy Commission, 2002):

Tower Designs

- Single structure with combined tower
- Separate wet and dry towers
- Parallel or series airflow paths through the wet and dry systems
- Parallel or series connected cooling water circuits

Condenser Designs

- Common condenser
- Separate condenser
- Divided water box separating the cooling water flows from the wet and dry towers

A generic hybrid parallel cooling system is shown in Figure 4.8. The system functions by making use of a dry cooling system as the primary heat rejection system for the majority of the year. During hot periods, the system efficiency is enhanced by routing some of the turbine exit steam to a separate wet cooling system which only rejects a portion of the total waste heat.

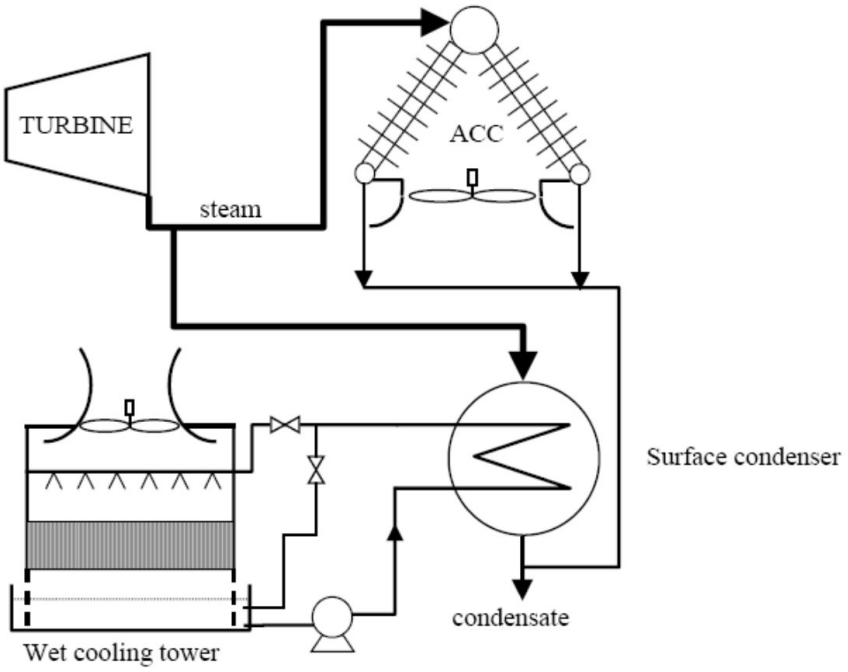

Figure 4.8: Schematic Representation of a Generic Parallel Hybrid Wet-Dry Cooling System (DOE, U.S., 2010).

4.4 Technology Comparisons and Costs

The majority of all new fossil fuel based plants make us of an evaporative wet cooling cycle to reject the steam power cycle heat to the atmosphere. A typical coal or nuclear power station will consume in the region of 500 gallons of water per MWh (1.89 litres per kWh) of electricity produced. In comparison, a typical parabolic trough or central receiver CSP plant making use of an evaporative wet cooling will consume similar amounts of water, with the parabolic trough plant consuming slightly more on average – in the region of 800 gallons per MWh (3.03 litres per kWh). Of this water consumed, approximately 2% is used for mirror washing and cleaning (DOE, U.S., 2010).

As discussed in Section 4.2, dry cooling is typically far less economical than wet cooling due to its poorer thermal efficiency characteristics (especially during hotter periods of the year) as well as its higher initial capital investment costs. This is also true for CSP plants. However, as the most suitable CSP sites are generally located in regions with high levels of solar irradiation resulting from many hours of direct sunlight, these sites also tend to have minimal access to water sources (DOE, U.S., 2010). With the ever increasing pressure for power plants to reduce their water consumption, coupled with the great difficulty and expense of having to secure water in these arid regions, new CSP sites need to consider dry cooling technologies more than ever before.

According to the DOE, U.S. (2010) studies have shown that plant location as well as power plant type affect the efficiency and cost associated with dry cooling. As an example a parabolic trough plant located in the Mojave Desert operating on dry cooling would produce 5% less electricity and the cost of electricity would increase by 7% - 9%. A similar dry cooled plant located in New Mexico would only see an electricity price increase of 2%, however, as the maximum daytime temperatures are lower.

Furthermore, additional studies predicted that central receiver plants would only see a reduction in efficiency of 1.3% compared to a 4.6% reduction for parabolic trough plants. This is though to be due to the higher concentration ratios and associated high operating temperatures of the central receiver plants compared to parabolic trough plants, which diminishes the effect of the increased dry cooled condenser temperature. It has also been suggested that the net present value of a dry cooled CSP plant could be improved by using a larger collector field in order to offset the lower Rankine cycle efficiencies associated with dry cooling (DOE, U.S., 2010).

It is thus concluded that although dry cooling may increase plant initial capital investment costs, as well as running costs and ultimately the final electricity price in the short term, it will most likely become a necessity for all new CSP plants in the future. Finally, the costs associated with dry cooling are both location and technology dependent, with the local micro-climate, local water availability and extraction costs, as well as demand for electricity, all playing a significant role.

For ease of comparison purposes, the above section data is summarised and presented in Table 4.1 with water consumption, relative efficiency, and electricity cost data.

Table 4.1: Comparison of Water Consumption and Relative Electricity Costs for Different Power Plants using Different Cooling Technologies. *Source of Data:* DOE, U.S. (2010)

Power Plant Type	Cooling Technology	Gallons/MWh	Litres/kWh	Efficiency Reduction*	Elec. Cost Increase
Coal / Nuclear	Once Through Wet	23 000 - 27 000**	87.06 - 102.21		
	Recirculating Wet	400 - 750	1.51 - 2.84		
	Dry Cooled	50 - 60	0.19 - 0.23		
Natural Gas	Recirculating Wet	200	0.76		
Central Receiver	Recirculating Wet	500 - 750***	1.89 - 2.84		
	Hybrid Parallel	90 - 250	0.34 - 0.95	1 - 3%	5%
	Dry Cooled	90	0.34	1.3%	
Parabolic Trough	Recirculating Wet	800	3.03		
	Hybrid Parallel	100 - 450	0.38 - 1.70	1 - 4%	8%
	Dry Cooled	78	0.30	4.5 - 5%	2 - 9%
Linear Fresnel	Recirculating Wet	1000***	3.79		
Dish Stirling	Mirror Washing	20	0.08		

* Annual energy output loss compared to most efficient cooling technology

** Majority returned to source, but at elevated temperature

*** Estimate

5 Thermal Energy Storage

5.1 Need and Motivation for Energy Storage

The solar energy received on earth's surface is not a constant, but is instead a time-dependant energy resource, affected by both the time of day and variable weather conditions. The energy demands that are met by thermal power station are also time-dependant, and vary throughout the day, but usually in a different manner to the solar energy supply. Consequently, if a solar energy generation system or CSP plant is required to meet the majority of this demand, or operate as a base-load plant, energy storage in some form will be required (Duffie and Beckman, 1974). By extending the operational hours of a CSP plant, the incorporation of energy storage can increase plant capacity factors from below 25% to above 50% and hence greatly increase a plant's dispatchability (Morse, 2009).

5.1.1 Advantages of Energy Storage in CSP Plants

The incorporation of a low capacity energy storage system in a CSP plant allows for the storage of energy as a 'buffer', which can be used to smooth electricity production considerably, as well as be dispatched during periods of intermittent cloud cover. This eliminates the short-term variations in CSP plant output, thereby increasing turbine efficiency (IEA, 2010b; Pilkington Solar International GmbH, 2000; Wagner, 2008).

A moderate size energy storage system is also beneficial in areas where peak energy demand occurs after sunset, or at a different time to the daily solar irradiation peak. In these situations, a plant can store energy during periods of high solar radiation and dispatch it later, allowing for a separation between the collection of energy and the operation of the power block. This in turn extends the operational hours of the plant without the need to burn an axillary fossil back-up fuel, and hence reduces the unpredictability in-

herent in the use of solar energy, rendering CSP technology closer to the dispatchability of a base-load plant (Pilkington Solar International GmbH, 2000; SAM, 2010; Wagner, 2008).

In some CSP plants the size of the solar field is increased relative to the rated turbine output capacity – thereby increasing the plant solar multiple – to allow the power block to operate at its rated capacity for more hours of the day. In these plants, with an absence of an energy storage system, some of the solar collectors would need to be 'defocussed' during the periods of maximum solar irradiation, as the solar field would produce more heat then the system could utilise. The incorporation of an energy storage system, however, would allow for this excess energy to be diverted to storage, thereby reducing unnecessary energy loss whilst simultaneously extending the operating hours of the plant after sunset (SAM, 2010). The discussion of the trade-off's associated with the increase in solar multiple, as well the the optimisation of CSP plant solar multiples will be presented in Section 8.8.5.

5.1.2 Method of Operation

The method of operation for energy storage in a CSP plant is fairly simple to define. Throughout the day, during periods of high solar irradiation, excess energy generated by the solar field is diverted to a storage system. During any periods of intermittent solar irradiation, and primarily after the sun sets or solar irradiation levels drop below those required to run the power block at rated capacity, the stored energy is released into the steam power generation cycle to either supplement the solar energy, or solely run the power block (IEA, 2010b).

In some instances, a backup or supplementary fossil fuel boiler is incorporated into the power cycle, to provide further energy to run the power block. This system, defined as hybridisation, is beyond the scope of this study, however, and will not be considered in any of the forthcoming analyses. The modelling of its inclusion is recommended for further studies. A graphic representation of the effect of energy storage (as well as hybridisation) on a CSP plant is shown in Figure 5.1.

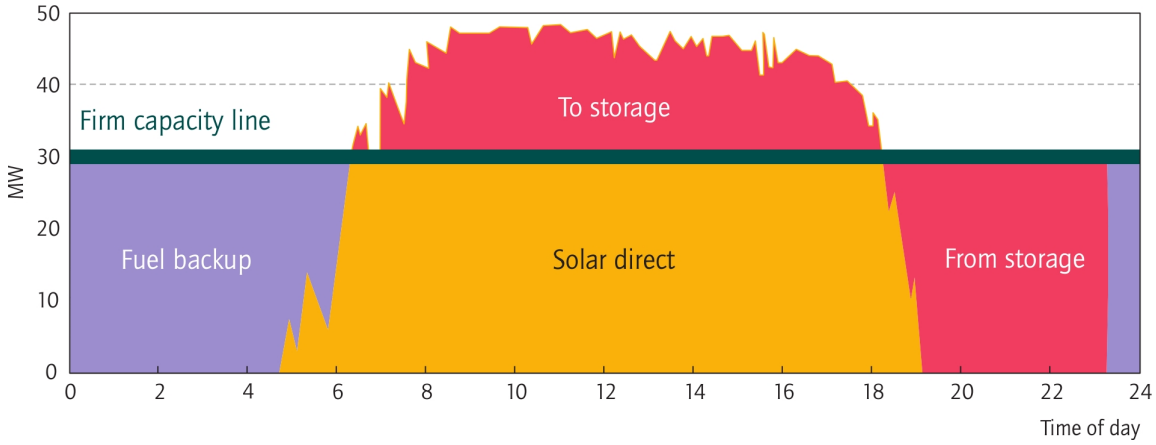

Figure 5.1: Effect of Energy Storage and Hybridisation on a CSP Plant (IEA, 2010b).

5.2 Classification of Energy Storage Technologies

5.2.1 Primary Forms of Energy Storage

Energy storage can exist in many forms, but can generally be classified according to four primary forms; namely *electrical* energy storage, *mechanical* energy storage, *thermal* energy storage (TES) and *chemical* energy storage. Of these primary forms, thermal energy storage is considered by many to be the most viable energy storage mechanism for use with CSP plants (EPRI, 2010; Morse, 2009; Wagner, 2008; Pilkington Solar International GmbH, 2000), with many of the existing commercial and pilot CSP plants already incorporating a form of TES. The characteristics, as well as advantages and disadvantages, of the remaining primary energy storage forms will thus not be discussed in this report, and instead, readers are referred to the dissertation by Morse (2009) for an in-depth review.

CSP plants therefore possess a distinct advantage when compared to other renewable energy technologies such as wind or photovoltaics, in that they produce thermal energy directly, which can easily be stored without the need to first convert energy from another form. The direct storage of electricity generated by these other technologies is considered to be far more complex and costly when compared to thermal energy storage (Pilkington Solar International GmbH, 2000; Wagner, 2008).

5.2.2 Thermal Energy Storage Mechanisms

Thermal energy storage can be classified according to three main storage mechanisms, namely; *sensible-heat*, *latent heat* – or phase change materials (PCMs), and *thermo-chemical*. Each one of these mechanisms can be further classified as *active* or *passive* depending on the storage design (Pilkington Solar International GmbH, 2000; Stine and Geyer, 2001).

Sensible-Heat Storage

Sensible-heat storage refers to the process of storing energy by increasing the the temperature, and thus internal energy, of the storage medium. The magnitude of energy stored by the medium can be calculated by the product of the mass, average specific heat and temperature change of the medium. Sensible-heat storage systems usually employ solids or liquids as the heat storage medium, however combinations resulting in mixed-media storage are also used (Pilkington Solar International GmbH, 2000; Stine and Geyer, 2001).

Typical examples of sensible-heat storage technologies include solid media such as concrete, packed-bed media such as rock and sand, as well as mixed-media systems comprising a packed bed with a liquid such as thermal oil. Mixed-media systems generally make use of thermal stratification; however, parasitic losses and high pressure drops are some of the disadvantages associated with this system (Pilkington Solar International GmbH, 2000).

Other examples include the use of liquids for sensible-heat storage. Water can be used to generate high pressures steam for storage purposes, however, thermal oils and molten salts are often used due to their higher temperature limits. Liquids used for TES can either be stored in single tanks, making use of thermal stratification, or alternatively in a two-tank system. Due to concerns over the negative environmental impacts of synthetic thermal oils, molten salts are often preferred; however, due to their higher melting points, auxiliary heaters are required to prevent freezing (Pilkington Solar International GmbH, 2000). More detailed descriptions of some of the sensible-heat storage technologies, however, will be give in Section 5.3.

Latent Heat Storage

Latent heat storage is based on the principle that energy can be released or absorbed nearly isothermally during the phase change of a material. This phase change can be from solid-to-liquid, liquid-to-vapour, or solid-to-solid crystalline, however, in terms of CSP thermal storage, solid-to-liquid phase change materials (PCMs) are most common. One of the major advantages of using PCMs for energy storage is that the latent heat of fusion is typically much higher than the sensible-heat, which allows for a greater energy density of the storage media. This in turn allows for a reduction in volume and size of latent heat storage systems when compared to single-phase sensible-heat systems, thereby reducing material costs (Duffie and Beckman, 1974; Pilkington Solar International GmbH, 2000; Stine and Geyer, 2001).

The selection of a suitable PCM is a difficult task, however, as the material must be able to sustain a large number of phase change cycles without degrading. Furthermore, as a PCM can exist in solid phase, it is not possible to circulate the storage media directly as the HTF. Instead, a separate cycle is required, with additional heat exchangers carefully designed to accommodate the typically low thermal diffusivity of the solid material. This ultimately results in an increased system cost (Stine and Geyer, 2001).

As latent heat energy storage is nearly an isothermal process, the storage media remains at a fairly constant temperature whether charging or discharging. Conversely, sensible-heat storage systems typically undergo a large temperature change during charging or discharging, rendering them more suited to conditions in a high temperature CSP plant. The lower temperature latent heat storage systems are thus deemed more suited to applications which required constant temperatures and compact designs. According to Stine and Geyer (2001), due to the high cost of latent heat storage systems, as well as the availability of sensible-heat storage systems, latent heat storage systems have yet to be widely adopted in high-temperature CSP systems.

Thermochemical Storage

A thermochemical energy storage system is based on the principle of using heat to drive completely reversible, endothermic chemical reactions, thereby storing energy. As the rupture of chemical bonds is highly energy intensive, this mechanisms results in a storage media with a high energy density. The products of the thermochemical reaction are also typically non-reactive at ambient temperatures, and can be stored separately, rendering them suitable for long term energy storage. When energy is required from storage, the reaction can be reversed at elevated temperatures, releasing the stored energy in the

process. Catalysts are also sometimes required to release the stored energy, adding to the level of system control (Duffie and Beckman, 1974; Pilkington Solar International GmbH, 2000; Stine and Geyer, 2001).

Some of the key advantages of thermochemical energy storage comprise its associated high energy density, nearly infinite storage potential as a result of the chemical product stability at ambient temperatures, and the potential to create 'solar-fuels' such as hydrogen, which can be easily transported. However, although thermochemical energy storage systems are theoretically promising, uncertainties regarding the thermodynamic properties of the reaction components and long term reversibility of the reactions, have resulted in it being far from the point of adoption in CSP plants. As of writing, there are currently no utility-scale commercial CSP plants employing thermochemical energy storage (Pilkington Solar International GmbH, 2000; Stine and Geyer, 2001).

5.2.3 Thermal Energy Storage Design Concepts

Direct and Indirect Active Systems

In an active TES system, the storage medium itself circulates, and is generally characterised by forced convection heat transfer. Active systems also usually make use of tank storage to contain the storage medium.

An active system can be further subdivided into *direct* and *indirect* systems. In a direct system, the heat transfer fluid (HTF) itself – which receives energy from the solar field – serves as the storage medium, eliminating the need for an additional storage medium and heat exchangers. Conversely, an indirect active system makes use of a separate secondary loop containing a storage medium, which is charged and discharged by the HTF via means of heat exchangers (Pilkington Solar International GmbH, 2000; SAM, 2010).

Passive Systems

A passive TES system – also referred to as a regenerator – differs from an active systems in that the storage medium itself does not circulate. Instead, the HTF passes through the storage medium only when charging or discharging. Passive systems usually make use of dual-medium storage, which can comprise liquids, solids or PCMs. A disadvantage with passive systems, however, is that the heat transfer rates are low, especially when using solid media, and there is usually no direct contact between the HTF and storage media as a result of heat exchangers (Pilkington Solar International GmbH, 2000).

5.3 Thermal Energy Storage Technologies

As a means of concluding the review of thermal energy storage, this final section will present and briefly outline the method of operation for some of the more prominent TES technologies.

5.3.1 Molten Salt Energy Storage

Indirect Two-Tank Molten Salt System

In an indirect two-tank molten salt system, thermal energy from the solar field is circulated by means of an HTF – typically a synthetic thermal oil – in a separate cycle to the storage system. During periods of peak solar irradiation, excess heat collected by the synthetic oil HTF is directed via heat exchangers to molten salt in the storage system cycle. During the charging process, the molten salt flows from the cold tank into the hot tank, where it is stored for later use. When additional energy is required to drive the power block, the hot salt flows back from the hot tank, through the storage system heat exchangers, to the cold tank, adding additional energy to the HTF. The energy from the synthetic oil HTF passes through an additional heat exchanger used to heat water and generate steam for the Rankine power cycle (Sargent & Lundy, 2003). This process, usually adopted in parabolic trough plants, is illustrated graphically in Figure 5.2.

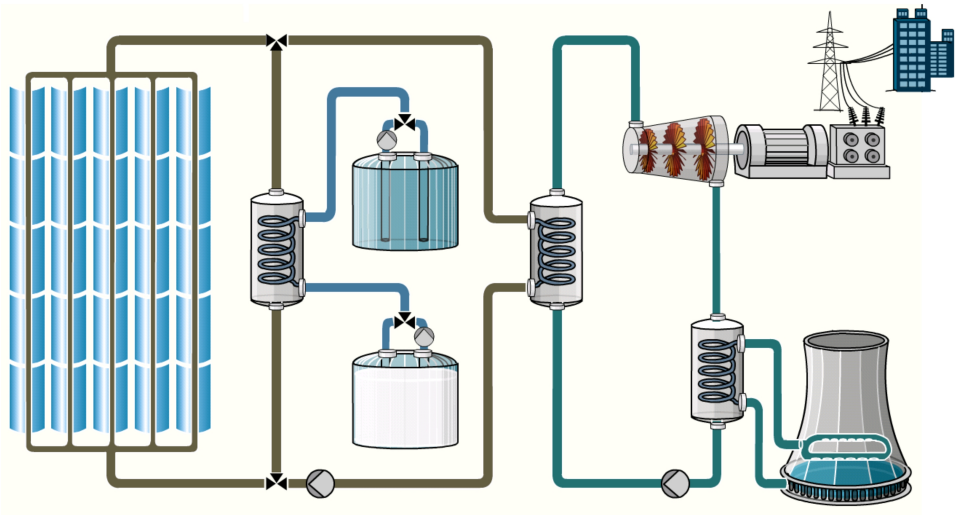

Figure 5.2: Schematic of Parabolic Trough Plant with Two-Tank Indirect Molten Salt Storage (Solar Millennium AG, 2011).

Direct Two-Tank Molten Salt System

Unlike the indirect molten salt storage system with synthetic oil HTF adopted by parabolic trough systems, some central receiver CSP plants adopt a direct molten salt system, where the HTF is the same fluid as the storage media. This allows for the direct thermal energy storage of the HTF itself, resulting in a substantial cost reduction through the elimination of the oil-to-salt heat exchangers (with their associated parasitic losses) as well as the need for thermal oil (EPRI, 2010).

In such a system, liquid salt at 290 ℃ is pumped from the cold storage tank through the receiver, where it is heated to 565 ℃. The heated molten salt then flows to the hot tank where it is stored for later use. When additional energy is required to drive the power block, the hot salt is pumped from the hot tank through the steam generating heat exchangers, used to heat water and generate steam for the Rankine power cycle. Once through the heat exchanger, the salt is then pumped back to the cold tank where it is stored until pumped back through the receiver for reheating (Sargent & Lundy, 2003). This process is illustrated graphically in Figure 5.3.

Images of a two-tank molten salt storage system under construction at the Andasol I parabolic trough plant in Spain, and a direct two-tank system at the Solar Two central receiver plant in the U.S. are shown in Figure 5.4

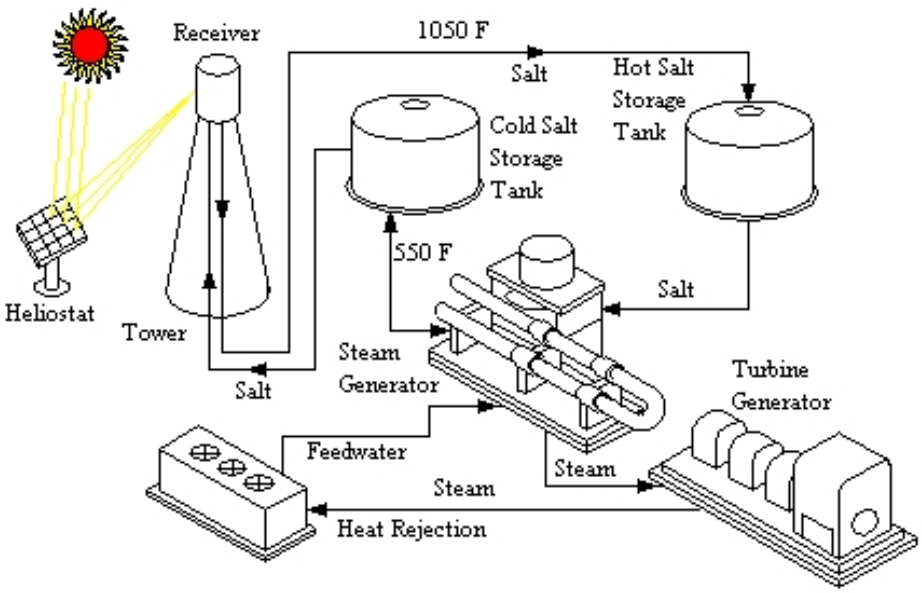

Figure 5.3: Schematic of Central Receiver Plant with Two-Tank Direct Molten Salt Storage (Sargent & Lundy, 2003).

Figure 5.4: Two-Tank Molten Salt Storage at Andasol I in Spain and Solar Two in the United States. *Source of Images:* Müller-Steinhagen (2011) and Meyer (2010).

5.3.2 Thermal Oil, Rock and Sand Thermocline Systems

As a means to reduce thermal energy storage costs associated with two-tank systems, thermocline system make use of a single tank to store both the hot and cold storage medium. This system relies on thermal buoyancy to maintain thermal stratification, with the hot fluid remaining at the top of the tank and the cold fluid sinking to the bottom. The boundary area within the tank where the hot and cold fluids meet is defined as a thermocline (Brosseau et al., 2004; NREL, 2011a; SAM, 2010).

As a means to reduce the thermal storage fluid volume – and thus further reduce costs – the single tank can be filled with a low-cost packed-bed filler material, comprising rock and sand, or potentially, other materials. This low-cost filler material then becomes the primary energy storage media in the mixed-media system, with a liquid such as thermal oil circulating through it (Brosseau et al., 2004; NREL, 2011a).

A thermocline system can either act as a direct system, with the HTF fluid itself flowing through the storage media when charging, or alternatively it can be adopted as an indirect system, utilising a separate thermal storage fluid such as thermal oil. The Solar One central receiver CSP plant in the U.S. utilises thermal oil combined with rock and sand in a single tank thermocline TES system (Brosseau et al., 2004; Meyer, 2010). A schematic of an indirect thermocline system is presented in Figure 5.5 while an image of the Solar One single tank storage system is shown in Figure 5.6.

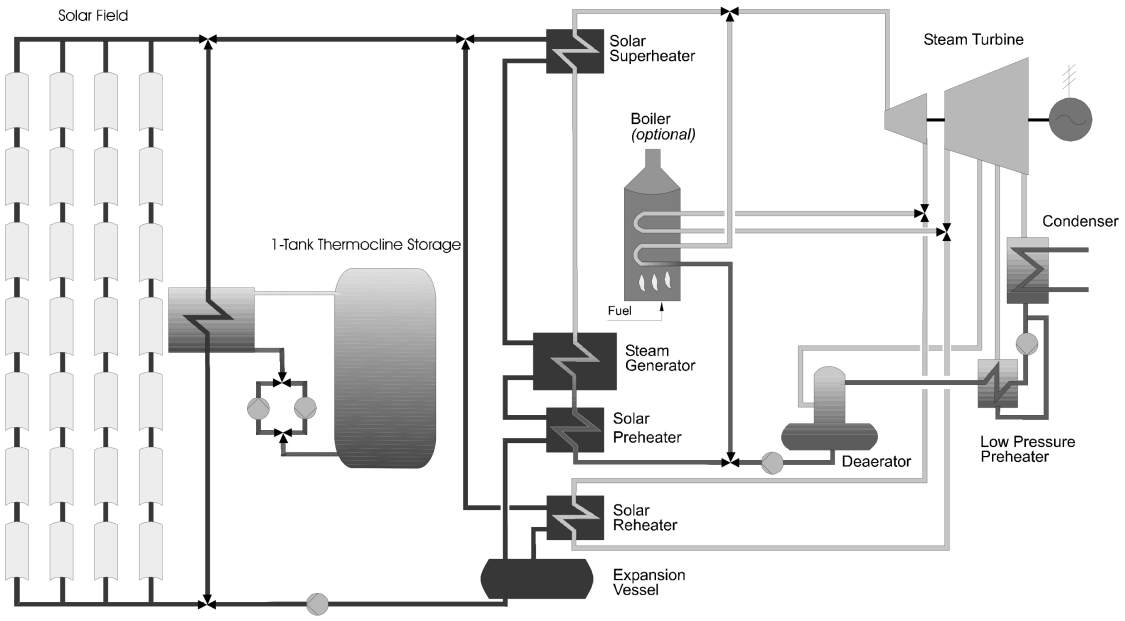

Figure 5.5: Schematic Diagram of Indirect Thermocline Energy Storage (Herrmann et al., 2002).

Figure 5.6: Solar One's Single-Tank Thermocline Energy Storage Comprising Thermal Oil, Rock and Sand (Meyer, 2010).

5.3.3 High Pressure Steam Storage

In plants which make use of water as the HTF – hence operating as direct steam generation systems – it is possible store the high pressure steam itself in a direct steam thermal energy storage system. The high pressure saturated steam is stored in a number of tanks, depending on their level of charge. During periods of intermittent solar irradiation, the stored energy in the steam storage tanks is release to power the Rankine cycle turbine (SolarPACES, 2011).

This method of direct steam storage was adopted in the PS10 central receiver plan in Spain, and allowed for a storage capacity of 20 $MWh_{thermal}$ – which equates to 50 minutes of turbine operation at 50% load (Meyer, 2010; SolarPACES, 2011). Direct steam storage systems – also referred to as a steam accumulators – are only economically suitable as buffer storage devices, however, and are not economically applicable for long term energy storage (Morse, 2009). A schematic of a central receiver with direct steam storage is presented in Figure 5.7, while an image of the four steam storage tanks at PS10 plant in Spain is shown in Figure 5.8.

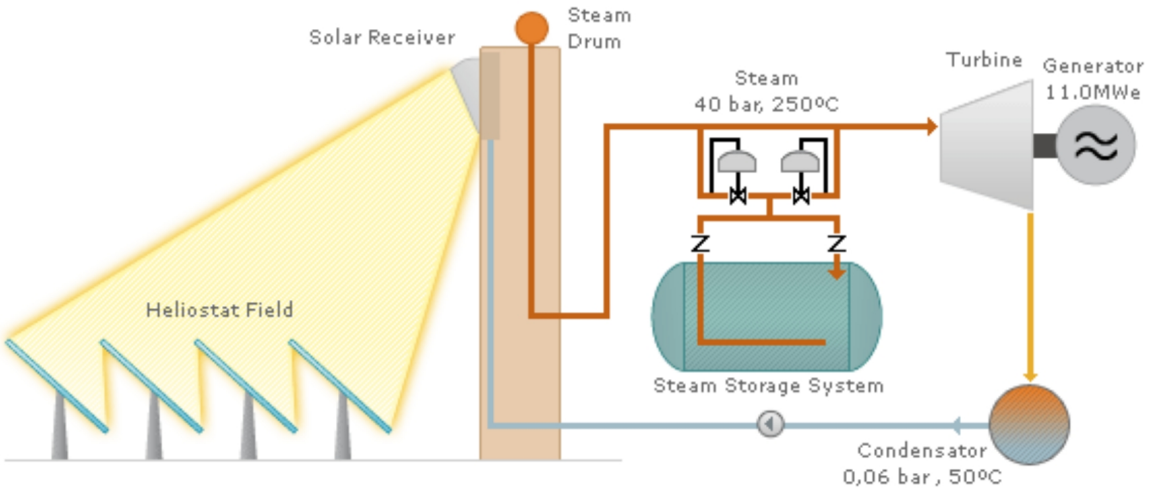

Figure 5.7: Schematic Diagram of Central Receiver Plant with Steam TES (IEA, 2007).

Figure 5.8: The Four Steam Storage Tanks at the Base of the PS10 Central Receiver Plant (SolarPACES, 2011).

5.3.4 Concrete and Solid Media Storage

As a means to reduce the cost of thermal energy storage system, as well as increase their modularity, the German Aerospace Center (DLR) has been conducting research into the use of solid media storage devices comprising concrete, or cast ceramics. In such a system, the standard HTF fluid from the solar field is circulated through an array of pipes embedded in the solid storage medium, thereby transferring the thermal energy to and from storage during the charging and discharging processes (DLR, 2003; NREL, 2011a).

As previously stated, the main advantage of such a system over other TES systems is the low cost of the storage media, however, primary issues such as large pressures drops, low thermal transfer rates, and maintaining good contact between the concrete and piping do exist (NREL, 2011a; Pilkington Solar International GmbH, 2000). A schematic of a concrete energy storage system is depicted in Figure 5.9, while images of concrete storage test blocks from the DLR are shown in Figure 5.10.

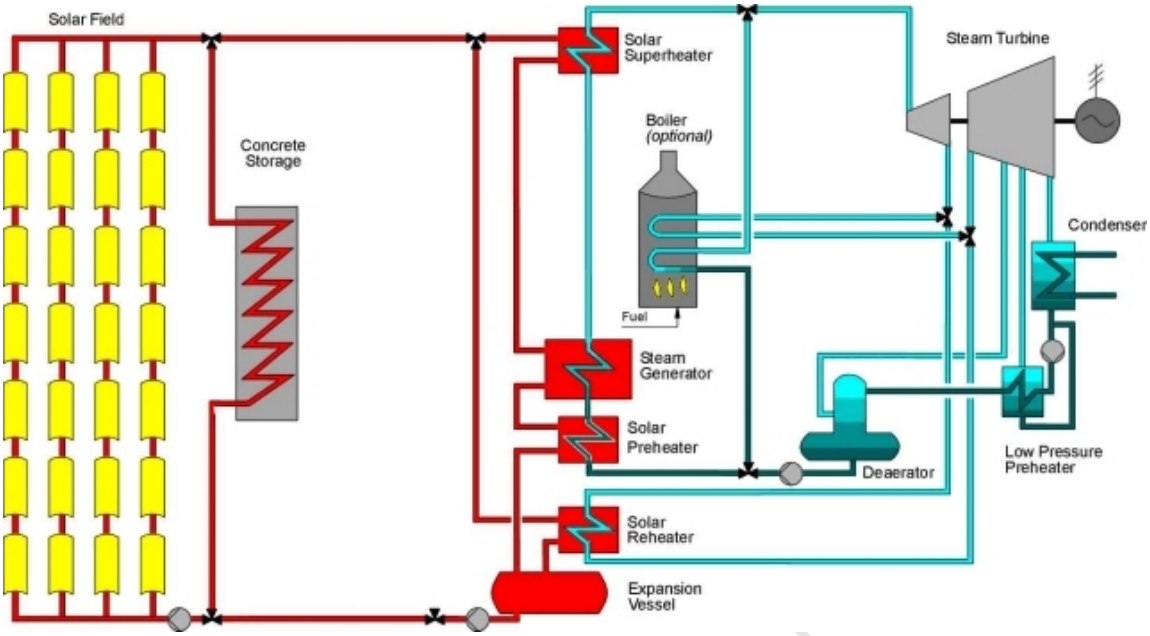

Figure 5.9: Schematic of a CSP Plant with Concrete TES (Herrmann et al., 2002).

Figure 5.10: Concrete Storage Test Blocks (DLR, 2003).

5.3.5 Phase Change Materials

The use of phase change materials (PCMs) in a storage system allows for large amounts of energy to be stored in relatively small volumes, resulting in low energy storage costs. Although PCMs were initially considered for use with thermal oil parabolic trough plants, research conducted by the DLR has shown them to be more suitable for use with direct steam generation parabolic trough plants (NREL, 2011a).

In such a system, a single PCM material – chosen such that its phase change occurs in the temperature region of the HTF thermal source – is either encapsulated within a highly conducive thermal solid, or within a matrix of expanded graphite (Morse, 2009). The HTF fluid from the receiver then flows through a heat exchanger embedded in the PCM storage, allowing for charging and discharging of the storage media. Due to the complexity of these systems, however, further research on the use of PCMs is still being conducted (NREL, 2011a). A graphic representation and an image of a salt PCM latent heat storage module is presented in Figure 5.11.

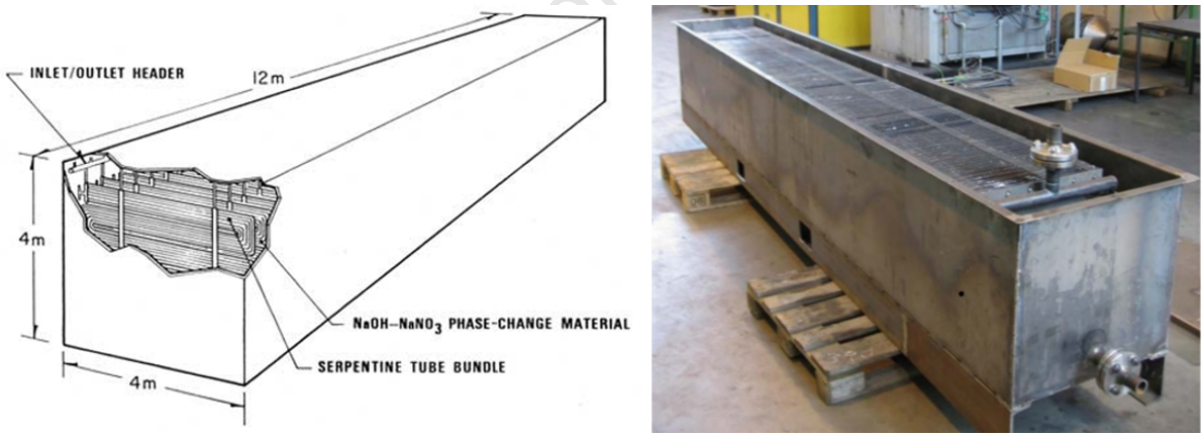

Figure 5.11: Latent-Heat Thermal Energy Storage Module with Salt PCM. *Source of Images*: Stine and Geyer (2001) and Müller-Steinhagen (2011).

6 Site Location and Geographic Information Systems Analysis

6.1 Overview of GIS Software and Analysis

A Geographic Information System (GIS) is defined by ESRI (2010b) as the integration of hardware, software and data, which is used for the capture, management, analysis and display of all forms of geographically referenced information.

As previously stated, the use of GIS software to identify and quantify potential CSP sites is becoming more common, as it allows for one to visualise, analyse and interpret data in a unique and efficient manner. This in turn not only renders trends and relationships in data more evident, but also allows for identification of locations based on specified criteria, the mapping of these locations, and the extraction and calculation of new data that would otherwise not be readily visible (ESRI, 2010b).

In this study, GIS software was used extensively to identify and quantify potential sites for CSP plants in South Africa. The GIS analysis and methodology was based on the use of a number of predefined analysis criteria, which were created and represented in the software in the form of data layers. These data layers were then used as screens, whereby the software was set to search for instances, or locations, where all of the analysis criteria were satisfied simultaneously. The search was performed at a predefined spacial resolution of 90m by 90m cells – as governed by the spacial resolution of the majority of the analysis layers. Once potential CSP sites were identified, it was then possibly to analyse and calculate various attributes, as well as depict the findings visually in topographical format. Key characteristics and attributes of the identified potential sites are also presented numerically in tabular format. The full GIS analysis and methodology will now be presented in the following sections of this chapter, while a more detailed description of the exact GIS procedure developed for this study is given in Appendix A.

6.2 Previously Conducted Studies

When considering a potential CSP site, a number of physical and topographical criteria – such as minimum solar irradiation levels and close proximity to suitable infrastructure – need to be satisfied to ensure that construction is not only possible, but also economically viable. In addition, it is imperative to consider the environmental connotations of such a project, and take precautions to avoid causing any negative impacts.

As discussed briefly in the literature review of Chapter 2, previous studies making use of GIS software to analyse CSP potential in various counties and regions have been conducted, with a more recent study by Fluri (2009) focussing specifically on South Africa. When reviewing previous GIS studies conducted by Bravo et al. (2007), Pletka et al., Dahle et al. (cited by Fluri, 2009) and Fluri (2009), it can be seen that they all make use of similar analysis criteria to a varying degree.

In their assessment of capacity and generation ceilings of renewable energy technologies for Spain, Bravo et al. (2007) required that all potential sites have a land slope of between 2% and 7% for slopes facing SE to SW and a slope below 2% for all other orientations. In addition, potential sites were considered and grouped according to average daily solar direct normal irradiation (DNI) values of 1500, 1750 and 2000 kWh/m^2/annum, which equates to approximately 4.1, 4.8 and 5.5 kWh/m^2/day respectively.

In their studies on potential CSP sites in the United States, Pletka et al. and Dahle et al. (as cited by Fluri, 2009) both required a land slope of less than 1%, and DNI values greater than 6.5 and 6.75 kWh/m^2/day respectively.

In his study on *the potential of concentrating solar power in South Africa*, Fluri (2009) stipulated a land slope of less than 1% and a daily DNI value of 7.0 kWh/m^2/day. Furthermore, Fluri also included the additional analysis criteria comprising the exclusion of: sensitive or 'threatened' vegetation areas, built-up areas, water surfaces and other unsuitable areas. Potential sites were also required to be of an area larger than 2 km^2 in order to be considered.

A final consideration for potential CSP site locations is the proximity to high voltage transmission lines and/or substations. Distances considered acceptable in the aforementioned studies range from 1 km to 25 miles (40.2 km) (Fluri, 2009). The analysis criteria of the previous studies are summarised in Table 6.1.

Table 6.1: GIS Analysis Considerations from Select Previous Studies. *Source of Data:* Bravo et al. (2007), Fluri (2009).

Reviewed Study:	Bravo et al. (2007)	Pletka et al. (2007)	Dahle et al. (2008)	Fluri (2009)
Slope (%)	$< 7\%$ (SE to SW) $< 2\%$ (other)	$< 1\%$	$< 1\%$	$< 1\%$
DNI (kWh/m^2/day)	> 4.1, > 4.8, > 5.5	> 6.5	> 6.75	> 7.0
Proximity to Transmission Lines	Not Considered	< 1.0km	< 40.2km	< 20.0km

In order to quantify the energy generation potential from the identified potential sites in South Africa, Fluri assumed a land use profile of 28 km^2/GW, with a 38.8% capacity factor for parabolic trough plants. Furthermore he assumed a specific water requirement of 3.27 m^3/MWh for the CSP plants. His study identified a vast number of suitable locations for potential CSP plants in South Africa, and a summary of the key results is given in Table 6.2.

Table 6.2: Results and Findings of Fluri's Study on the Potential for CSP in South Africa. *Source of Data:* Fluri (2009).

	Total for South Africa
Suitable Land Area (km^2)	15334.0
Power Generation Potential (GW)	547.6
Net Energy Generation (TWh/a)	1861.4
Water Requirement Wet-Cooled (million m^3/a)	6086.7

What is noted, however, is that although Fluri (2009) states that a CSP sector of this magnitude would require 6086.7 million m^3 of water per annum, the close proximity to large water bodies was not considered as a requirement for a potential CSP site in Fluri's study. Considering the previously discussed water-stressed classification of South Africa, as well as the large water requirements of wet-cooled CSP plants for cooling and mirror cleaning purposes (Cohen et al., 1999; Edkins et al., 2009), it was decided to include the proximity to large water bodies as a key requirement in this study. An initial GIS assessment was conducted by the author in a preliminary unpublished GIS study (Brodrick, 2010), however, the GIS analysis conducted and presented in this dissertation serves to improve upon and greatly extend the scope and validation of the initial investigation.

6.3 Analysis Criteria

Based on the various data layers and analysis criteria stated in the aforementioned literature, it was decided to adopt a similar GIS methodology, and make use of a similar number of data layer analysis criteria in the GIS section of this study. The multiple analysis criteria used to analyse potential CSP sites in this study will now be identified and discussed under their respective headings.

6.3.1 Solar Irradiation

When incoming solar radiation enters the Earth's atmosphere, a portion of it is scattered, resulting in ambient white light classified as *diffuse irradiation*. The remaining light, which is seen to come directly from the sun – or solar disk – consist of parallel rays capable of casting a shadow, and is classified as *direct irradiation* or *beam irradiation*. The light that is 'seen' on the Earth's surface is thus a combination of diffuse and direct irradiation, the ratio of which depends on the amount of cloud cover and other light refracting particles in the atmosphere (Boyle, 2004).

Although the diffuse irradiation portion may contain high amounts of energy, in general, CSP technologies are only capable of focussing the direct irradiation portion onto the receiver (Duffie and Beckman, 1974). Thus for the remainder of this analysis, only the level of solar *direct normal irradiation* (DNI) will be considered for the identification of potential CSP site locations.

DNI can be described as a measure of the sun's energy falling on the Earth's surface, and is quantified in the units of watt hours per square meter (Wh/m^2). As defined in Table 6.1, previous studies required a potential CSP site to have total daily DNI values in a range above 4 kWh/m^2/day (Fluri, 2009). In this analysis, three initial cases will be considered with required daily DNI values ranging from > 6.0 kWh/m^2/day, > 6.5 kWh/m^2/day and > 7.0 kWh/m^2/day, depending on the availability of water. The exact requirements, however, will be described in detail in Section 6.4.

The solar irradiation data used in this analysis was derived from satellite imagery and was processed by the United States National Renewable Energy Laboratory (NREL). The data has a spacial resolution of 40 km $\times$ 40 km with an accuracy of 10% (Fluri, 2009; SWERA, 2010). The data was made publicly available by means of the Solar and Wind Energy Resource Assessment website (SWERA, 2010).

The solar data was included in the GIS software as the first data analysis layer. Based on this data, a map depicting the average daily DNI values over South Africa for different months of the year was created, and is presented in Figure 6.1. A second map depicting the data analysis layer for the annual average daily DNI values for South Africa can be seen in Figure 6.2. From the figures it is evident that the DNI values for the summer months are considerably higher than those of the winter months, with areas in the Northern Cape receiving the highest DNI values throughout the year. It can also be seen that the Northern Cape receives average annual daily DNI values in excess of 7.0 kWh/m^2/day, which are though to be some of the highest worldwide, and in excess of areas such as California, Nevada, Morocco and Spain (Edkins et al., 2009).

6.3.2 Land Slope

Large utility-scale CSP sites generally require relatively large, flat areas of land, usually comprising areas greater than 2 km^2 in size (Broesamle et al., 2001; Morse, 2009). Of all the commercially implemented CSP plant technologies, parabolic trough plants are the most sensitive to land slope, and require flatter areas of land when compared to technologies such as central receiver systems. This is a result of parabolic troughs making use of single-axis tracking, where as the two-axis tracking heliostats used in central receiver systems provide more flexibility with regard to land slope (EPRI, 2010). In previous studies, the land slope requirement for parabolic trough plants was usually a slope of less than 1% (Fluri, 2009) – as can be seen in Table 6.1 – however, some studies such as that done by Broesamle et al. (2001) only required a land slope of 2% or less. In their study on South Africa EPRI (2010), suggest a land slope criteria of between 1% and 3%.

In this study, a land slope requirement of less than 1% was enforced, in order to allow for the consideration of both parabolic trough and central receiver CSP systems. The land slope data used in this study to create the land slope GIS analysis layer was derived from a 90 m Digital Elevation Model (DEM), courtesy of NASA's Shuttle Radar Topography Mission (SRTM), and published by the United States Geographic Service (USGS). The DEM has a spacial resolution of 90 m $\times$ 90 m.

Using this DEM data, a map depicting the percentage land slope analysis layer was created, and is shown in Figure 6.3. It is noted that a large majority of areas with between 0% and 1% slope also coincide with the regions with high DNI values in the Northern Cape, North West Province and Free State, as evident when compared to Figure 6.2.

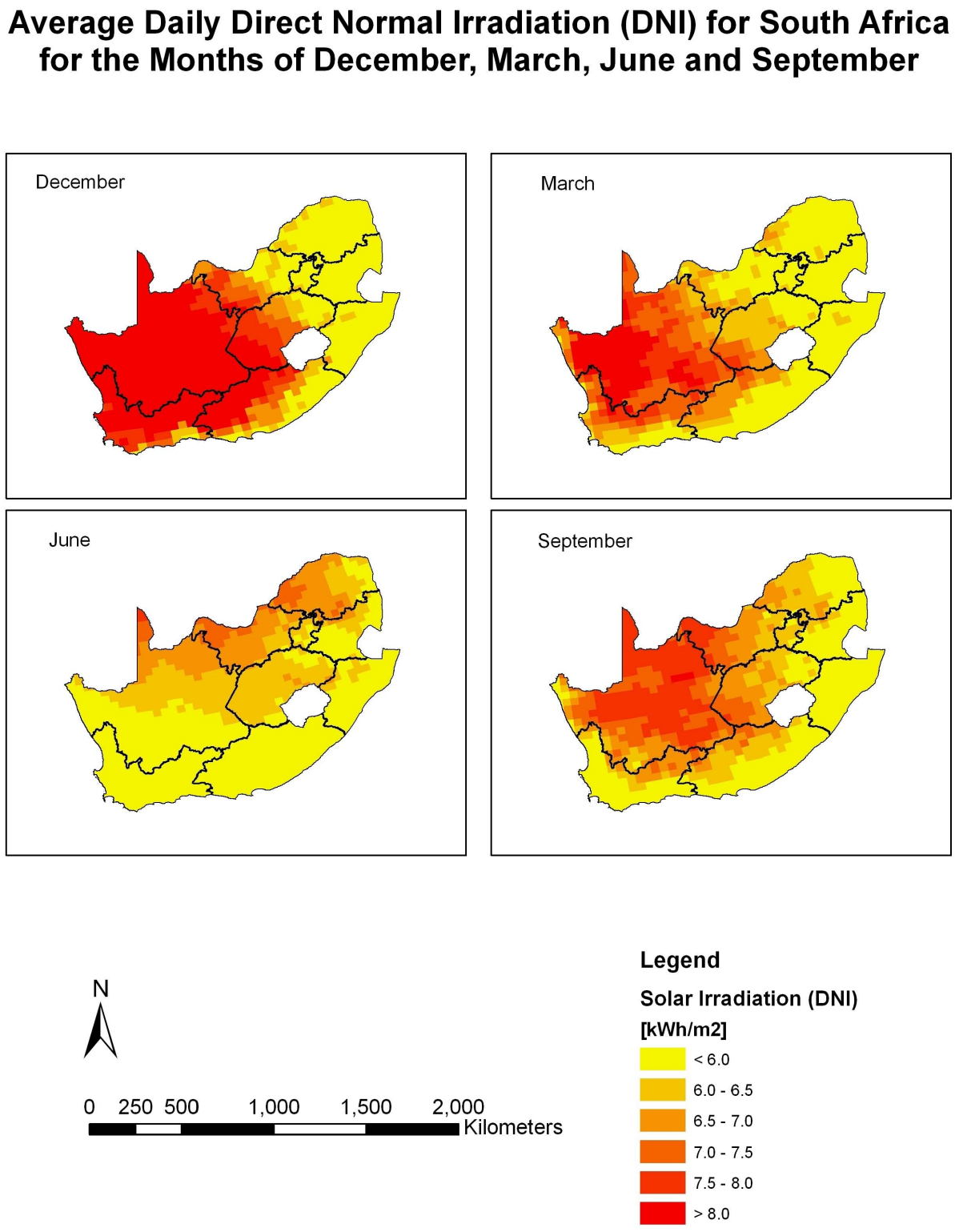

Figure 6.1: Map of Monthly Average Daily Direct Normal Irradiation (DNI) for South Africa for the Months of December, March, June and September (Brodrick, 2010). *Source of Data:* SWERA (2010) and CSIR (2001c).

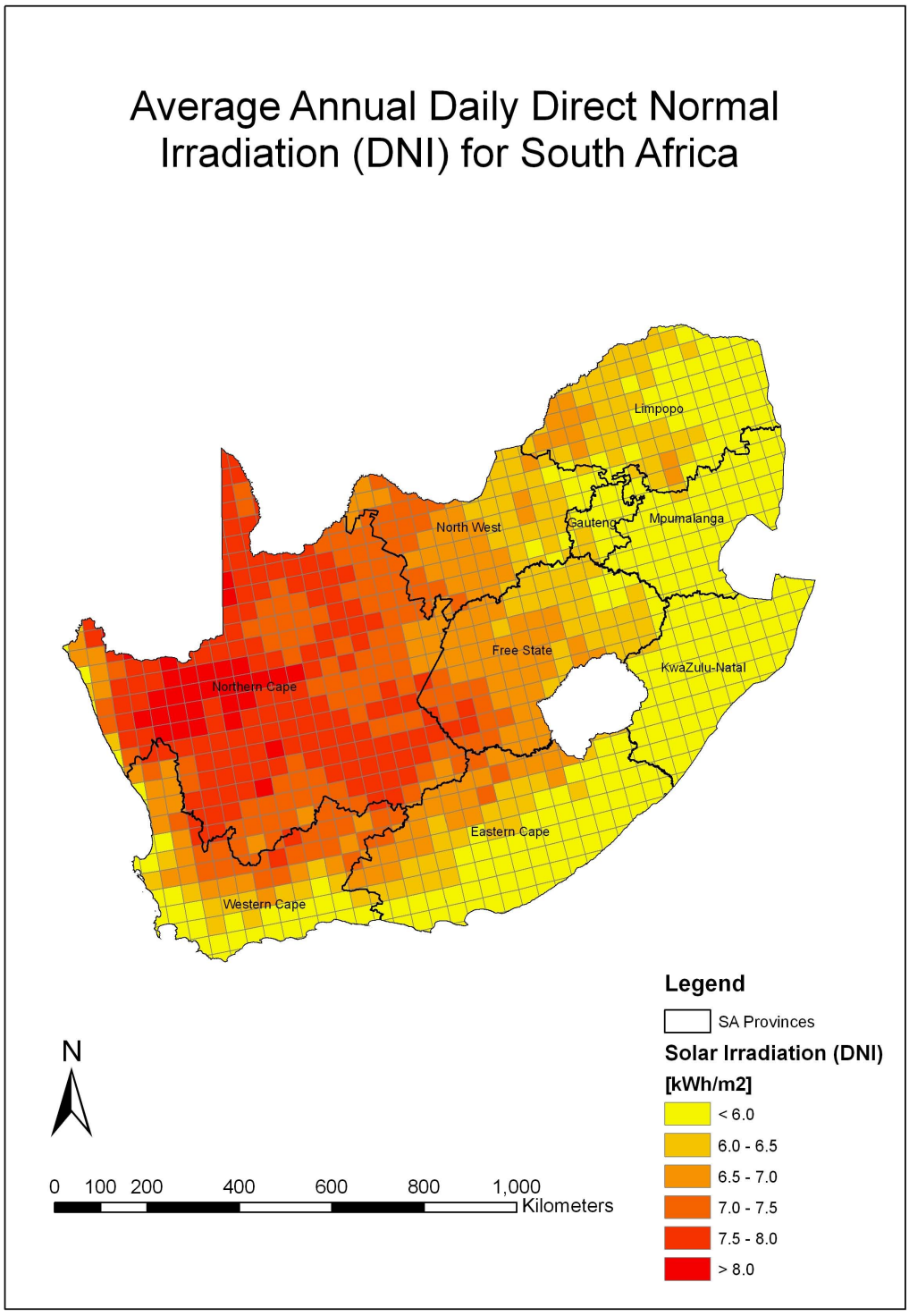

Figure 6.2: Map of Annual Average Daily Direct Normal Irradiation (DNI) for South Africa (Brodrick, 2010). *Source of Data:* SWERA (2010) and CSIR (2001c).

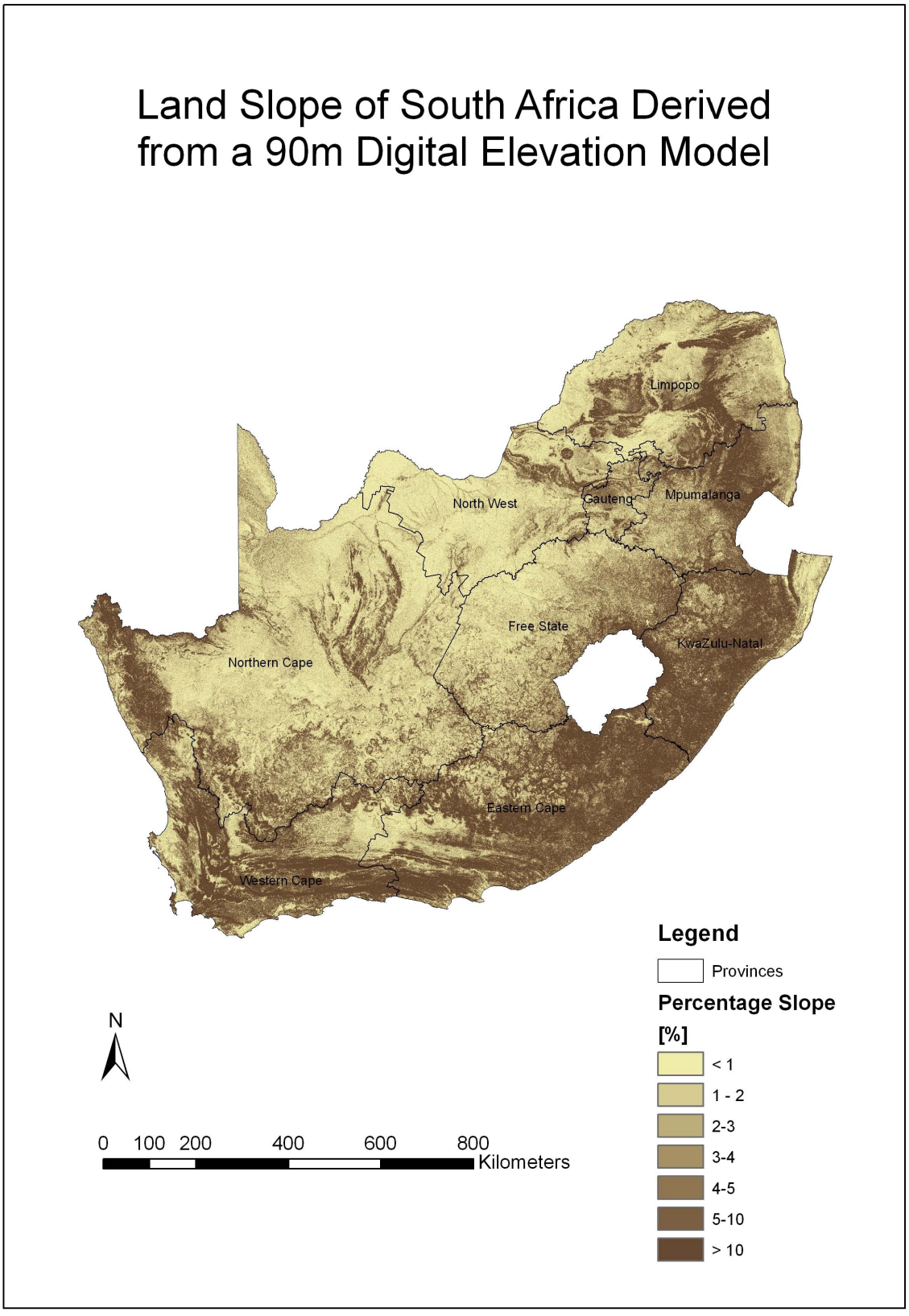

Figure 6.3: Map of the Land Slope of South Africa Derived from a 90m Digital Elevation Model (DEM) (Brodrick, 2010). *Source of Data:* SRTM (2006) and CSIR (2001c).

6.3.3 Excluded Areas

When choosing a potential suitable location for any power station, certain areas must be excluded from the analysis due to the unsuitable nature of their land class. In his study of the potential of CSP in South Africa, Fluri (2009) excluded areas such as water surfaces, built–up areas, military bases and airports.

In this analysis, land use was classified according to the *South African 30m Land Cover Data* published by the CSIR (2001a), and the following land class areas were excluded from consideration:

- Water-bodies
- Wetlands
- Forests
- Plantations
- Urban Areas

By making use of the land class data, and merging the various excluded land classes into one body of excluded areas, the excluded areas data analysis layer was created in the GIS software. A map created depicting the data analysis layer of the excluded land class areas is presented in Figure 6.4. From the figure, it can be seen that the majority of the Northern Cape – except for cultivated areas near the Orange river – is not excluded from the analysis, as it is one of the least urbanised provinces in South Africa. It is also noted, when compared to the map of Solar Irradiation in Figure 6.2, that the majority of areas with the highest DNI values coincide with the non-excluded areas.

6.3.4 Vegetation

In terms of the Environmental Impact Assessment (EIA) Regulations of South Africa, before any construction project can begin in a particular area, it must be authorised by the National Department of Environmental Affairs and Tourism (DEAT). In order to obtain this authorisation, multiple independent EIAs must be conducted, in order to minimize potentially negative environmental impacts (Eskom, 2006).

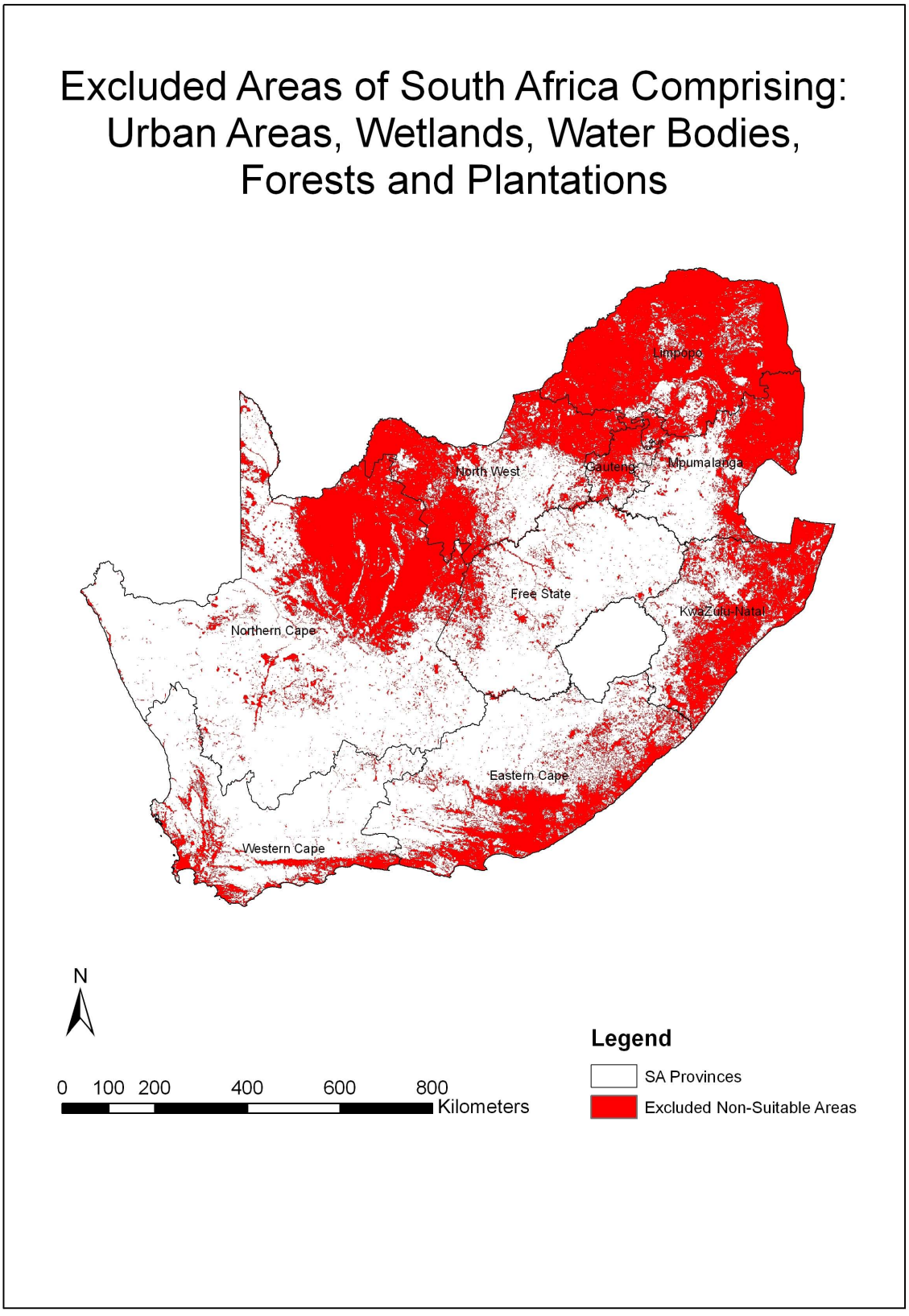

Figure 6.4: Map of Areas in South Africa Excluded from the GIS Analysis (Brodrick, 2010). *Source of Data:* CSIR (2001a) and CSIR (2001c).

Obtaining EIAs for potential sites was beyond the scope of this analysis; however, in order to reduce the likelihood of possible negative environmental impacts, potential CSP sites were only considered if they fell inside areas classed by Mucina and Rutherford (2006) as *'least threatened'* vegetation.

Using the data presented by Mucina and Rutherford (2006) in their publication, *The Vegetation of South Africa, Lesotho and Swaziland*, a data analysis layer comprising areas classified as 'least threatened' was created in the GIS software. A map was then created depicting this data analysis layer, which can be seen in Figure 6.5. It is noted, when compared to the map of solar DNI in Figure 6.2, that the majority of areas with high DNI values also coincide with the areas classed as 'least threatened' vegetation.

6.3.5 Water Availability

As previously discussed, the availability of water for plant cooling purposes is deemed an important factor for consideration in the implementation of any large CSP plant, and the analysis thereof is one of the key themes of this study. According to Edkins et al. (2009), the 100 Megawatt (MW) Central Receiver plant planned by Eskom for Upington is expected to consume in the region of 300,000 m^3 of water per annum. Furthermore, Cohen et al. (1999) state that for the Solar Energy Generating Systems (SEGS) CSP parabolic trough plants in the United States, more than 90% of water usage is a result of the Rankine power cycle cooling, while only 1.4% is used for mirror cleaning. Hence, the proximity to large water sources, water bodies and rivers was included as a data analysis layer and was considered as a requirement for some of potential CSP site locations.

In some of the GIS analysis cases, potential CSP sites were required to be situated within 20 km of a large perennial river, dam, or the Atlantic Ocean on the West Coast of South Africa. In order to represent this requirement, data comprising the *1:10,000 River and Dam Data* from the South African Department of Water Affairs and Forestry (DWAF) – supplied by the CSIR (2001b) – and the *South African River Data* from the South African Department of Environmental Affairs and Tourism – supplied by ENPAT (2000) – was used in the creation of the water proximity analysis layer. A map created depicting the data analysis layer of the 20 km buffer from large perennial rivers, dams, and the South African West Coast can be seen in Figure 6.6.

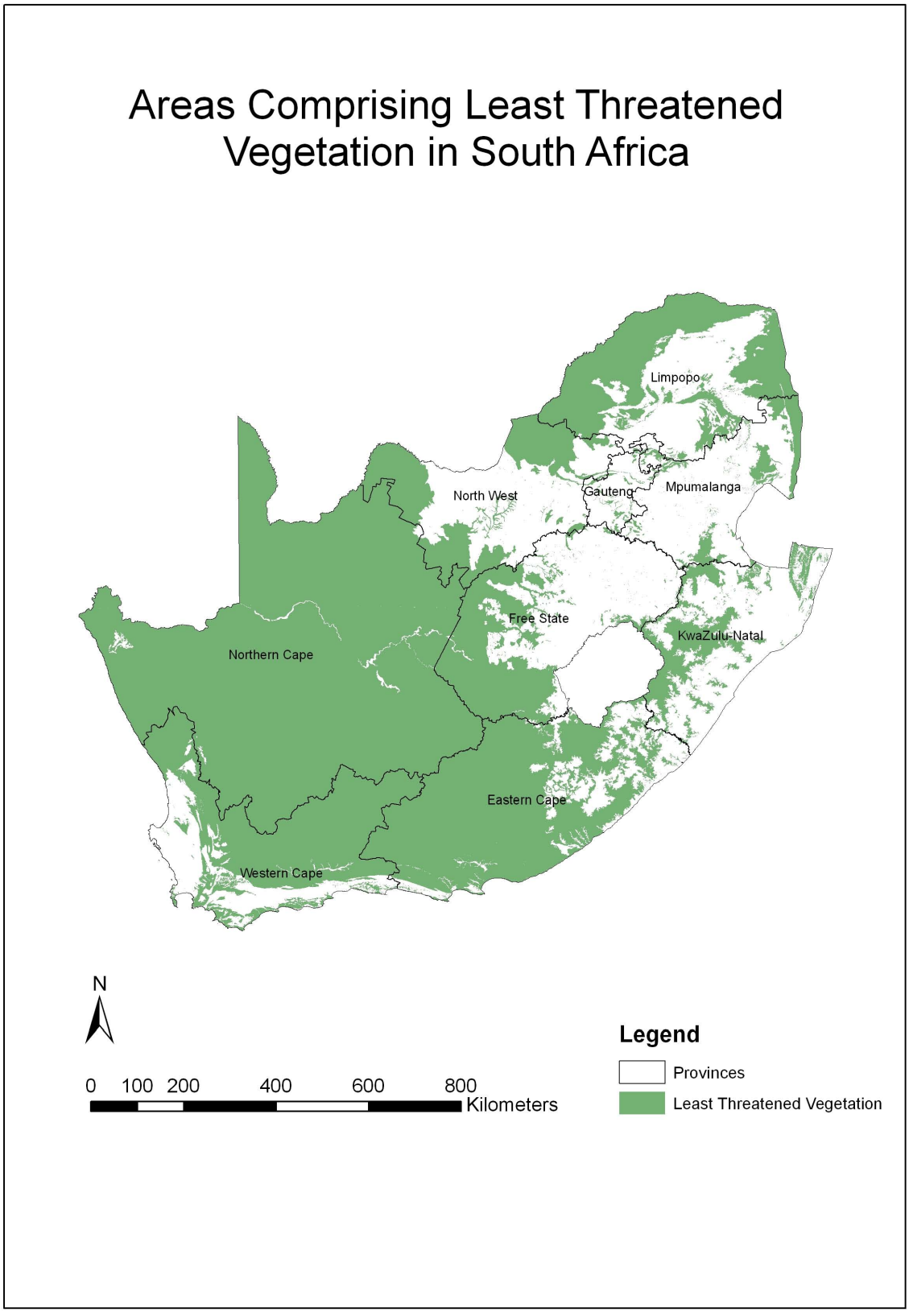

Figure 6.5: Map showing Areas of Least Threatened Vegetation in South Africa (Brodrick, 2010). *Source of Data:* Mucina and Rutherford (2006) and CSIR (2001c).

6.3.6 Proximity to Power Grid

A close proximity to high voltage transmission lines in a necessity for any large power station, in order to allow for the electricity produced to be distributed efficiently and economically to the rest of the country (Morse, 2009). Morse (2009) continues to state that for a 100 MW CSP plant, a minimum transmission line power rating of 132 kV with a line length not exceeding 100 km is required in order to reduce electrical losses. Thus for the final analysis layer criterion, and in keeping with the analysis figures used by Fluri (2009) and stated by Edkins et al. (2009), potential sites were only considered if they fell within a 20 km radial buffer from transmission lines. In addition, only transmission lines with a power rating greater than or equal to 132 kV were considered.

The data used in the creation of this analysis layer comprised the major Eskom national grid, whose spacial data in turn was implemented through the digital geo-referencing of a poster issued by Eskom (2010). A map created using this data, and depicting the analysis layer of the 20 km buffer from the Eskom national gird can be seen in Figure 6.6. It is noted that there is not a large portion or capacity of the national grid in the Northern Cape; however, according to Morse (2009) there are plans for further development of grid capacity in this region.

As a means to investigate potential areas and corridors for future grid expansion, further GIS analyses were conducted by removing the criteria for potential CSP sites to be in close proximity to the existing national grid. This method therefore allowed for the identification of potential sites that would otherwise have been excluded. Furthermore, the identification of large concentrations of sites could be used as a means to guide future grid expansion. This topic, however, will be discussed further in Section 6.5.2.

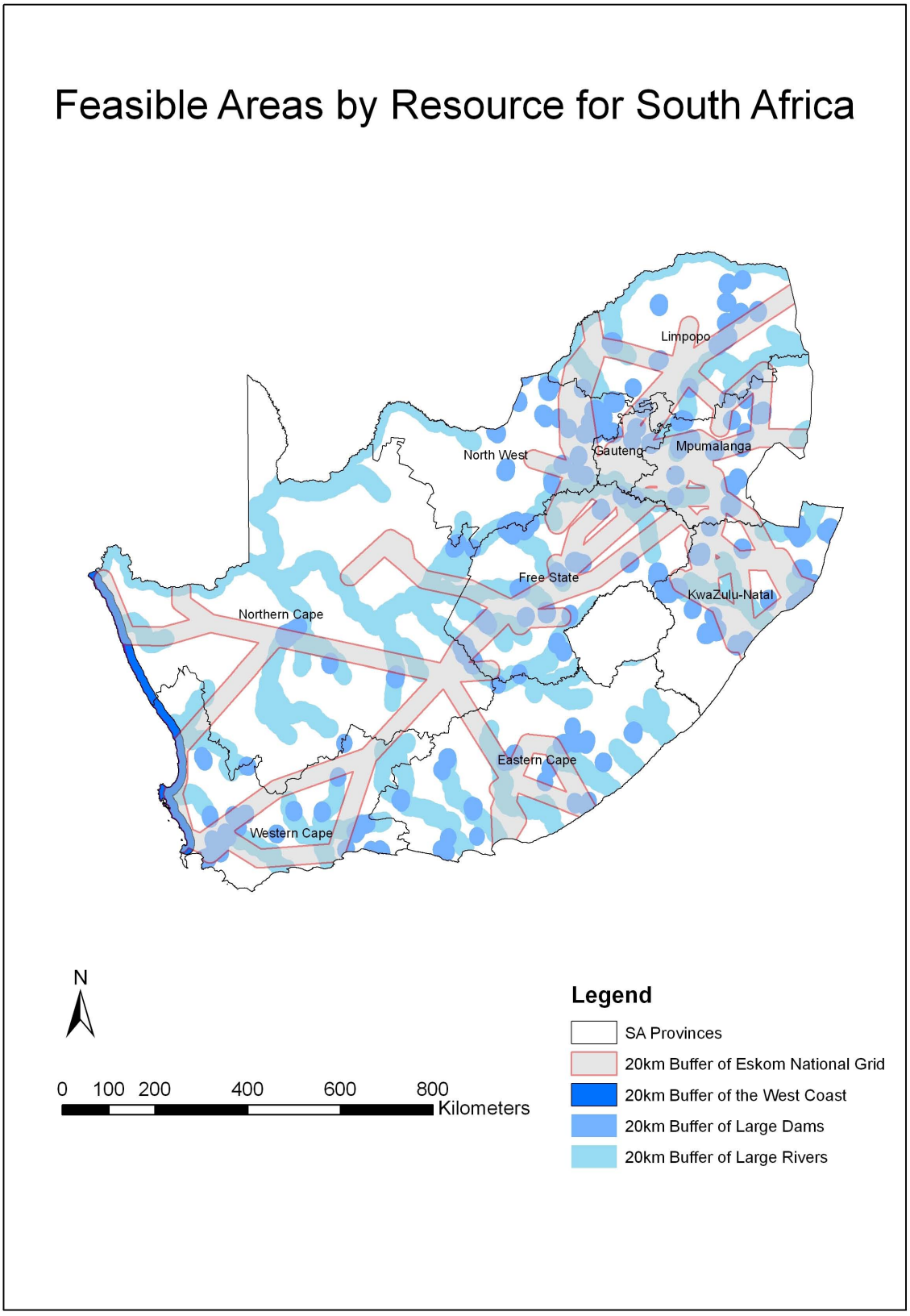

Figure 6.6: Map showing Areas in South Africa within a 20 km Radius of Large Water Bodies and of the National Grid (Brodrick, 2010). *Source of Data:* Eskom (2010), ENPAT (2000), CSIR (2001b) and CSIR (2001c).

6.4 Analysis Cases

The analysis criteria discussed in Section 6.3 were then grouped to create a number of unique analysis cases. The various analysis cases were created in order to allow for the identification of potential CSP sites with differing characteristics, depending on the criteria that needed to be satisfied. Five different analysis cases, or scenarios, were created in total, all of which will now be described and discussed in the following sections.

6.4.1 Cases Concerned with and without Proximity to Water

The initial three analysis cases were created in order to considered and identify various potential CSP sites based on the availability of water in the surrounding regions. Case 1 and Case 2 both require a potential CSP site to be within a certain distance from large water bodies, but have less stringent DNI requirements – of which Case 1 possesses the lowest DNI requirement. Conversely, Case 3 has no requirement for close proximity to cooling water – hence assuming the probable adoption of dry cooling – but requires the highest DNI levels of all the cases in order to offset the efficiency reductions if dry cooling were adopted at the site. The three cases are defined technically as follows:

Case 1: DNI > 6 kWh/m^2/d, Proximity to Large Water Bodies

- DNI greater than 6.0 kW/m^2 per day
- Less than 20 km from large water bodies
- Less than 20 km from transmission lines
- Less than 1% land slope
- Region classified as 'least threatened' vegetation
- Region not excluded due to land class restrictions of Section 6.3.3
- Site area greater than 2 km^2

Case 2: DNI > 6.5 kWh/m^2/d, Proximity to Large Water Bodies

- DNI greater than 6.5 kW/m^2 per day
- Less than 20 km from large water bodies
- Less than 20 from transmission lines
- Less than 1% land slope
- Region classified as 'least threatened' vegetation
- Region not excluded due to land class restrictions of Section 6.3.3
- Site area greater than 2 km^2

Case 3: DNI > 7 kWh/m^2/d, No Proximity to Large Water Bodies

- DNI greater than 7.0 kW/m^2 per day
- Less than 20 km from transmission lines
- Less than 1% land slope
- Region classified as 'least threatened' vegetation
- Region not excluded due to land class restrictions of Section 6.3.3
- Site area greater than 2 km^2

6.4.2 Cases Considering Future Grid Expansion

The final two cases that were considered were derived from Case 2 and Case 3 respectively, but were modified by removing the single condition for a 20 km proximity to transmission lines. This was done in order to assess the country's CSP potential if it were not limited by the location and density of the existing grid. Furthermore, the identification of large concentrations of potential CSP sites in areas without grid access could be used as a guide for possible future grid expansions, as mentioned at the end of Section 6.3.6 and described in Section 6.5.2.

Case 4: DNI > 6.5 kWh/m^2/d, Proximity to Large Water Bodies, No Grid Proximity

- DNI greater than 6.5 kW/m^2 per day
- Less than 20 km from large water bodies
- Less than 1% land slope
- Region classified as 'least threatened' vegetation
- Region not excluded due to land class restrictions of Section 6.3.3
- Site area greater than 2 km^2

Case 5: DNI > 7 kWh/m^2/d, No Proximity to Large Water Bodies, No Grid Proximity

- DNI greater than 7.0 kW/m^2 per day
- Less than 1% land slope
- Region classified as 'least threatened' vegetation
- Region not excluded due to land class restrictions of Section 6.3.3
- Site area greater than 2 km^2

6.4.3 GIS Methodology

A completed and detailed description of the GIS methodology and procedures that were developed and followed in order to successfully complete the GIS analysis – comprising the import and processing of data as well as the quantification of results – is given in Appendix A. Due to its length, and hence for the sake of brevity, the full methodology will not be presented in the body of the report.

6.5 Model Results and Identified Sites

A separate GIS analysis was conducted for each of the five analysis cases outlined in Section 6.4. The results obtained regarding the identified potential sites for each of the five cases will now be presented and discussed.

6.5.1 Identified Potential Sites with Close Gird Proximity

Case 1: DNI > 6 kWh/m^2/d, Proximity to Large Water Bodies

The identified potential CSP sites for Case 1, superimposed on the Digital Elevation Model (DEM), were recorded in topographical format and are presented in Figure 6.7. From the figure it can be initially observed that the large majority of the identified potential sites – depicted in black – fall within the boundaries of the Northern Cape, which is to be expected due to the Northern Cape receiving the highest average daily DNI levels throughout the year. Potential sites in the Free State and the Western Cape provinces are also identified; however, these to a much lesser extent.

Although not clearly visible from the country-sized scale of the map, the potential sites are constituted of a multitude of small square cells, which is a direct result of the 90m × 90m spacial resolution adopted in the analysis. Furthermore, the potential sites are not always completely uniform in shape, which is caused by the strict land slope requirement resulting in the elimination of some of the smaller 90m × 90m grid cells. These features are more evident in subsequent maps, however, which depict areas in greater detail.

When reviewing the results in conjunction with national grid data, it can be seen that the potential sites are limited by the lack of national grid capacity in the Northern Cape, made evident by the fact that all the sites are clustered around the few large transmission lines. Lack of water also plays a limiting role, however, as the only potential sites are situated close to the very few large water bodies. Although these results are expected due to the analysis criteria that were stipulated in Section 6.3, the resulting map greatly aids in coherent display of this information, that would otherwise be hard to visualise.

A final observation from this particular analysis is that only a very small portion of the West Coast appears suitable for CSP plants. This is mainly due to the combination of a lack of large grid capacity in the region, the decrease of DNI levels towards the coast, and the 'threatened vegetation' on the West Coast of the Western Cape.

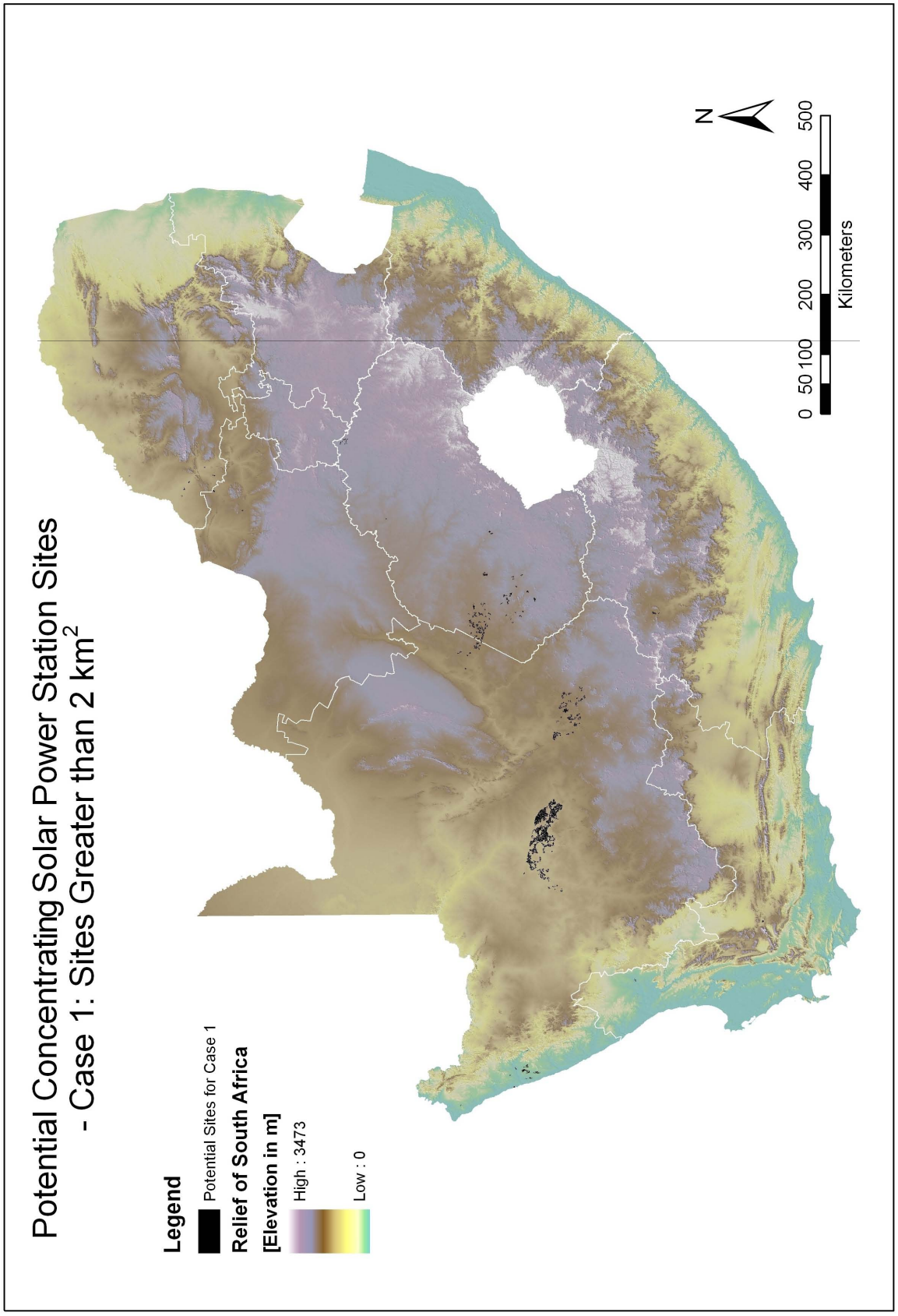

Figure 6.7: Map Identifying Potential Locations for CSP Plants in South Africa, as Governed by the Criteria in Case 1. *Source of Data:* Same as included layers.

Case 2: DNI > 6.5 kWh/m^2/d, Proximity to Large Water Bodies

The identified potential CSP sites for Case 2, superimposed on the DEM, were recorded in topographical format and are presented in Figure 6.8. From the map it is evident that the results are very similar to those of Case 1, only with a slight decrease in the total number – and area – of potential CSP sites. This is to be expected, however, as the only difference between the requirements for Case 1 and Case 2 is the higher DNI requirement of 6.5 kWh/m^2/day for Case 2, which in turn results in additional sites being excluded due to their slightly lower DNI values. For the remainder of the potential sites, the explanation is unchanged from that given in Case 1.

Case 3: DNI > 7 kWh/m^2/d, No Proximity to Large Water Bodies

The identified potential CSP sites for Case 3, superimposed on the DEM, were recorded in topographical format and are presented in Figure 6.9. It is immediately clear that, when compared to the previous two analysis cases, Case 3 produces the largest number and area of potential CSP sites. This is primarily due to the removal of the requirement for a close proximity to large water bodies, the reason being that even though the DNI requirement is increased to above 7.0 kWh/m^2/day, the Northern Cape does not possess many large water resources, but the majority of it does, however, possess solar resources in excess of 7.0 kWh/m^2/day.

The implications of this are that by reducing the need for cooling water and using alternative cooling technologies such as dry cooling, a far greater CSP potential could be realised in terms of mere number of sites and potential area. Finally, as in the previous cases, the potential CSP sites are clustered around the national grid transmission network, and the lack of extensive grid capacity in the region is again one of the limiting factors.

6.5.2 Identified Potential Sites with No Grid Proximity Requirement

As previously stated, the final two cases, Case 4 and Case 5, are derivatives of Case 2 and Case 3 respectively, but with the removal of the condition for a 20 km proximity to the national grid.

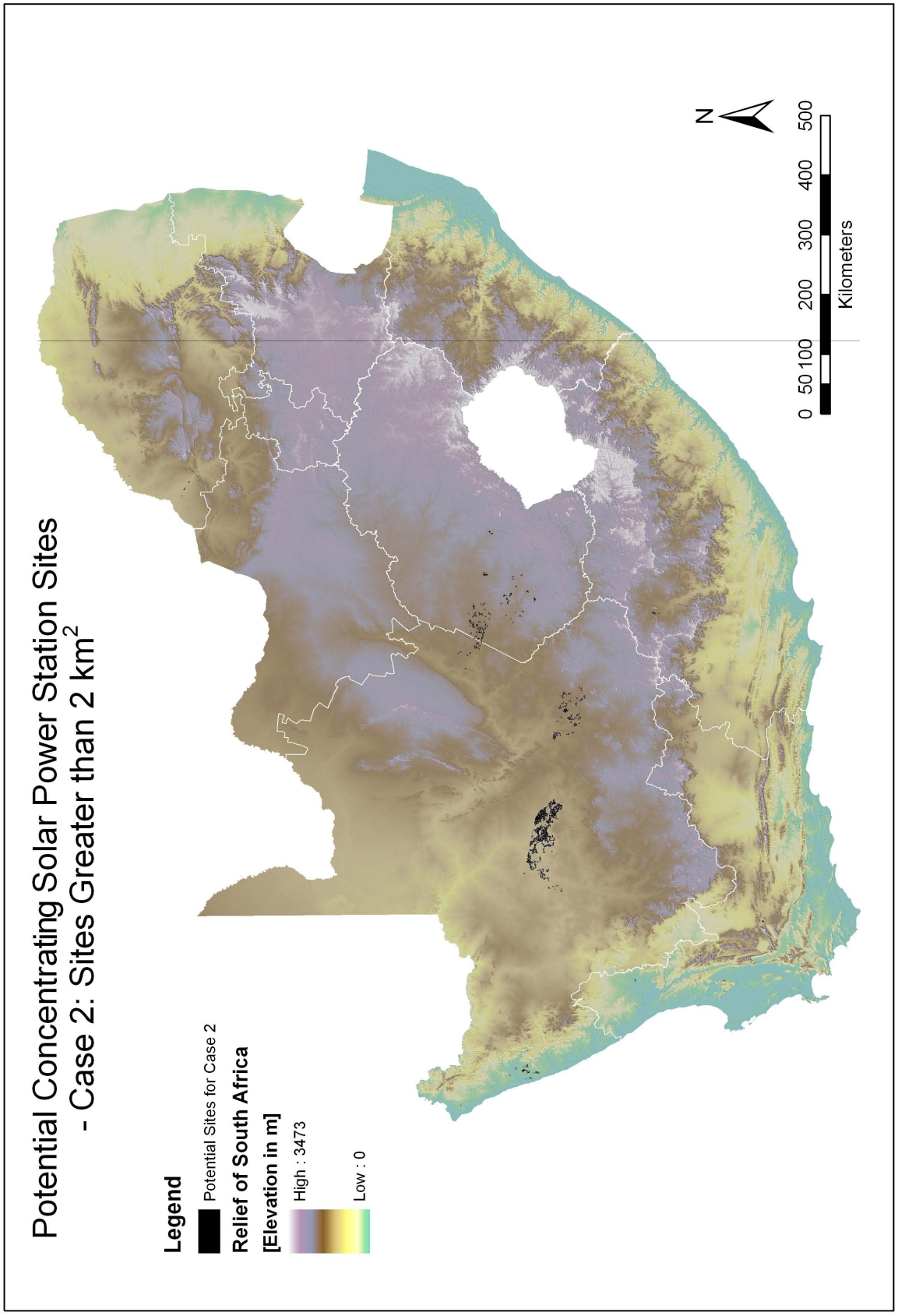

Figure 6.8: Map Identifying Potential Locations for CSP Plants in South Africa, as Governed by the Criteria in Case 2. *Source of Data:* Same as included layers.

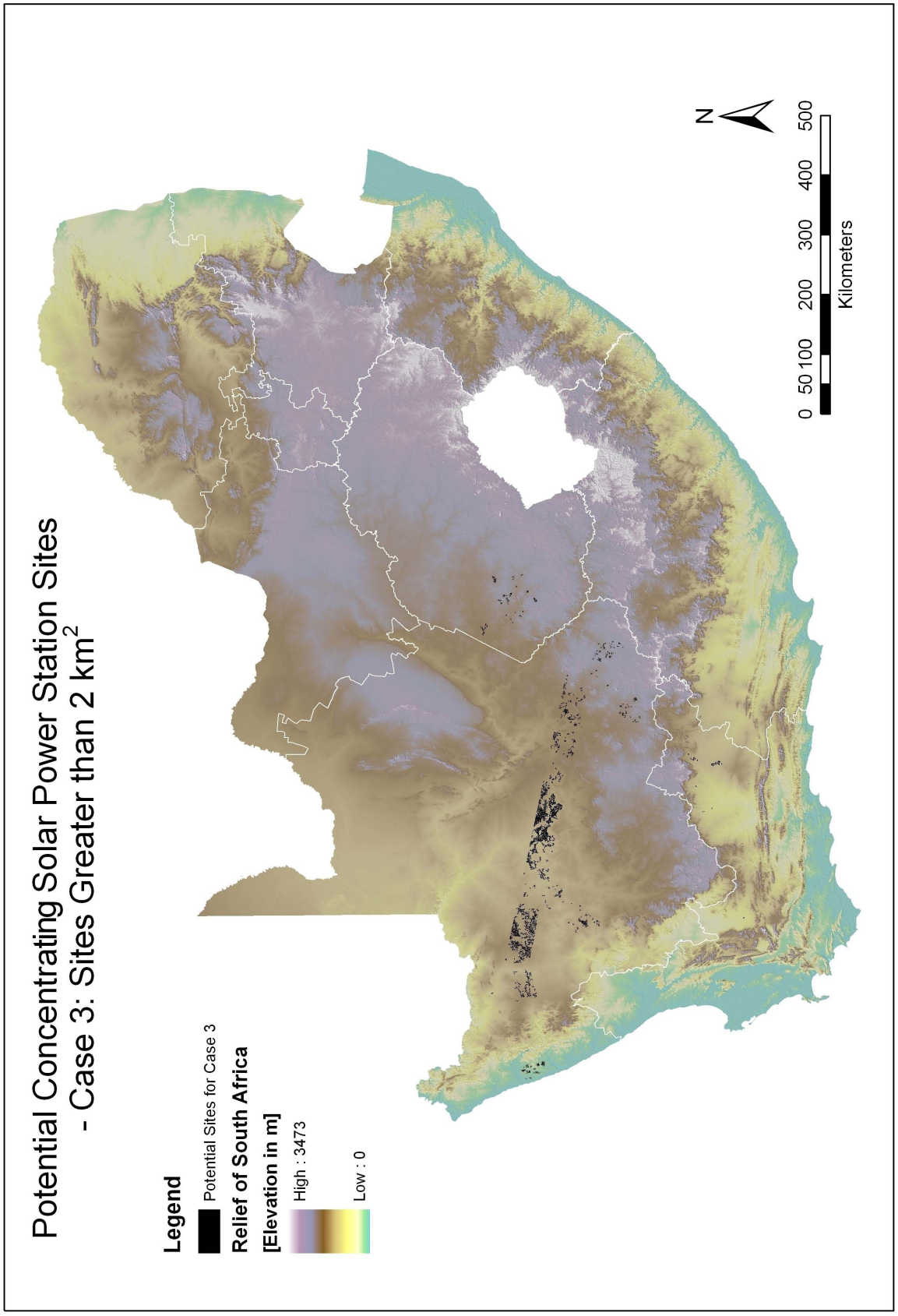

Figure 6.9: Map Identifying Potential Locations for CSP Plants in South Africa, as Governed by the Criteria in Case 3. *Source of Data:* Same as included layers.

Case 4: DNI > 6.5 kWh/m^2/d, Proximity to Large Water Bodies, No Grid Proximity

The identified potential CSP sites for Case 4, superimposed on the DEM, were recorded in topographical format and are presented in Figure 6.8. The existing Eskom national grid was also included in the map – represented by the grey dashed lines – in order to better illustrate how close the identified sites are to the existing infrastructure, as well as to highlight potential areas that may not be close to the existing grid at all.

When reviewing the map of the Case 4 potential sites, it can be seen that although there is no requirement for the potential sites to be near the existing grid, a large number of the sites are still situated fairly close, particularity in the Northern Cape. The limited distribution of sites is thought to be primarily a result of the requirement for close proximity to cooling water, as well as the strict land slope requirement. When compared to Case 2 – from which Case 4 is derived – it is clear that there is certainly a large increase in the number of identified potential sites, particularity in the Western Cape, Eastern Cape, Free State and North West Provinces, This is to be expected, however, due to the relaxation of the 20 km grid proximity requirement.

Case 5: DNI > 7 kWh/m^2/d, No Proximity to Large Water Bodies, No Grid Proximity

The identified potential CSP sites for Case 5, superimposed on the Digital Elevation Model (DEM), were recorded in topographical format and are presented in Figure 6.8. As in Case 4, the existing Eskom national grid was also included in the map – represented by the grey dashed lines.

From the map of Case 5 potential sites, it is immediately clear that the removal of both the requirements for close proximity to the national grid and large water bodies greatly increases the number of identified potential sites, with Case 5 identifying by far the largest number compared to any other analysis case. As was the situation in Case 4, a large number of the identified sites are still located fairly close to the national grid in the Northern Cape, primarily due to its high DNI values and level ground. An additional number of sites are also identified further North of the Orange River, as well as on the border between the Northern Cape and North West Province. Due to the increase in the DNI requirement to 7.0 kWh/m^2/day, however, a number of potential sites identified by Case 4 in the Free States Province have now been eliminated.

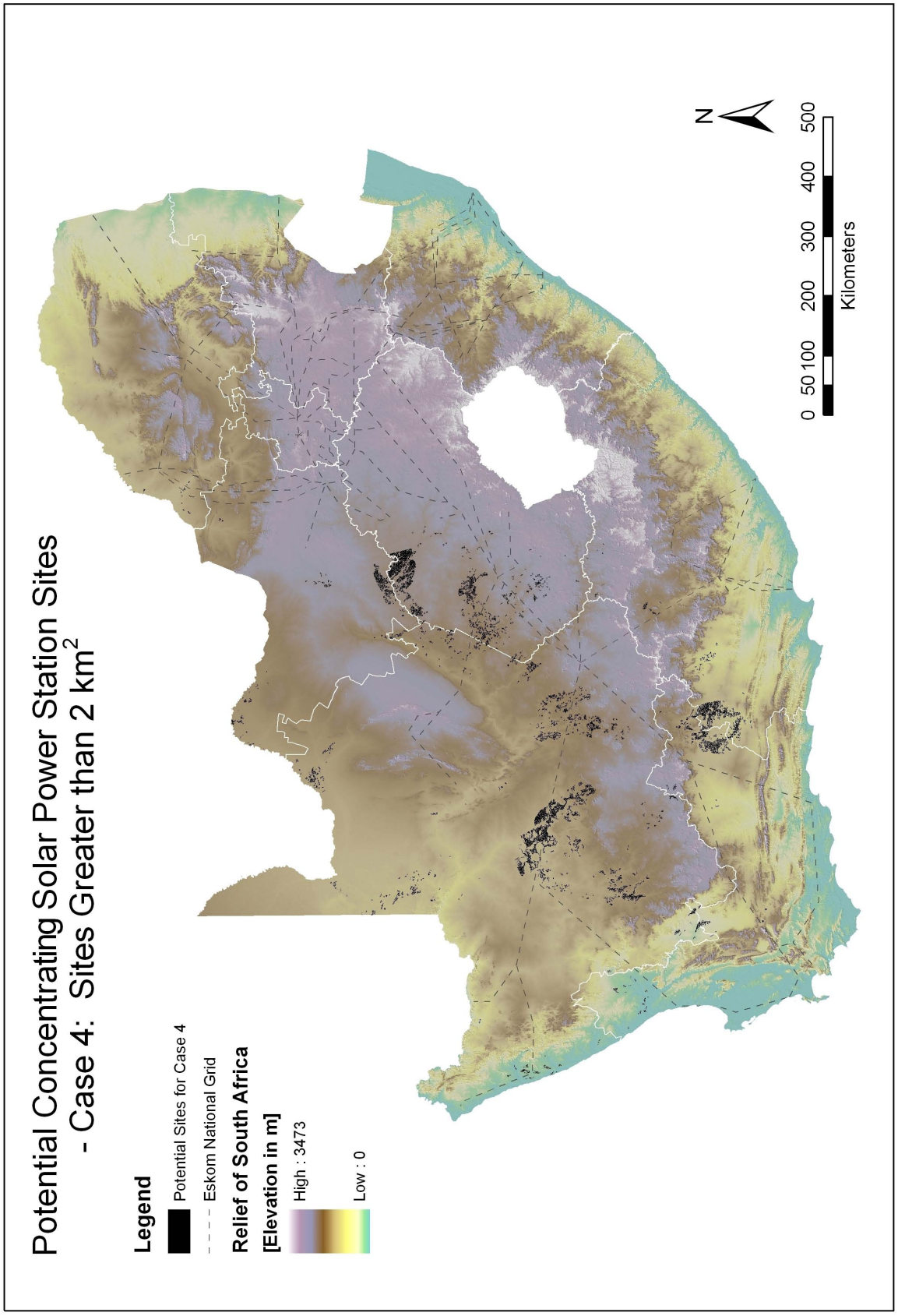

Figure 6.10: Map Identifying Potential Locations for CSP Plants in South Africa, as Governed by the Criteria in Case 4. *Source of Data:* Same as included layers.

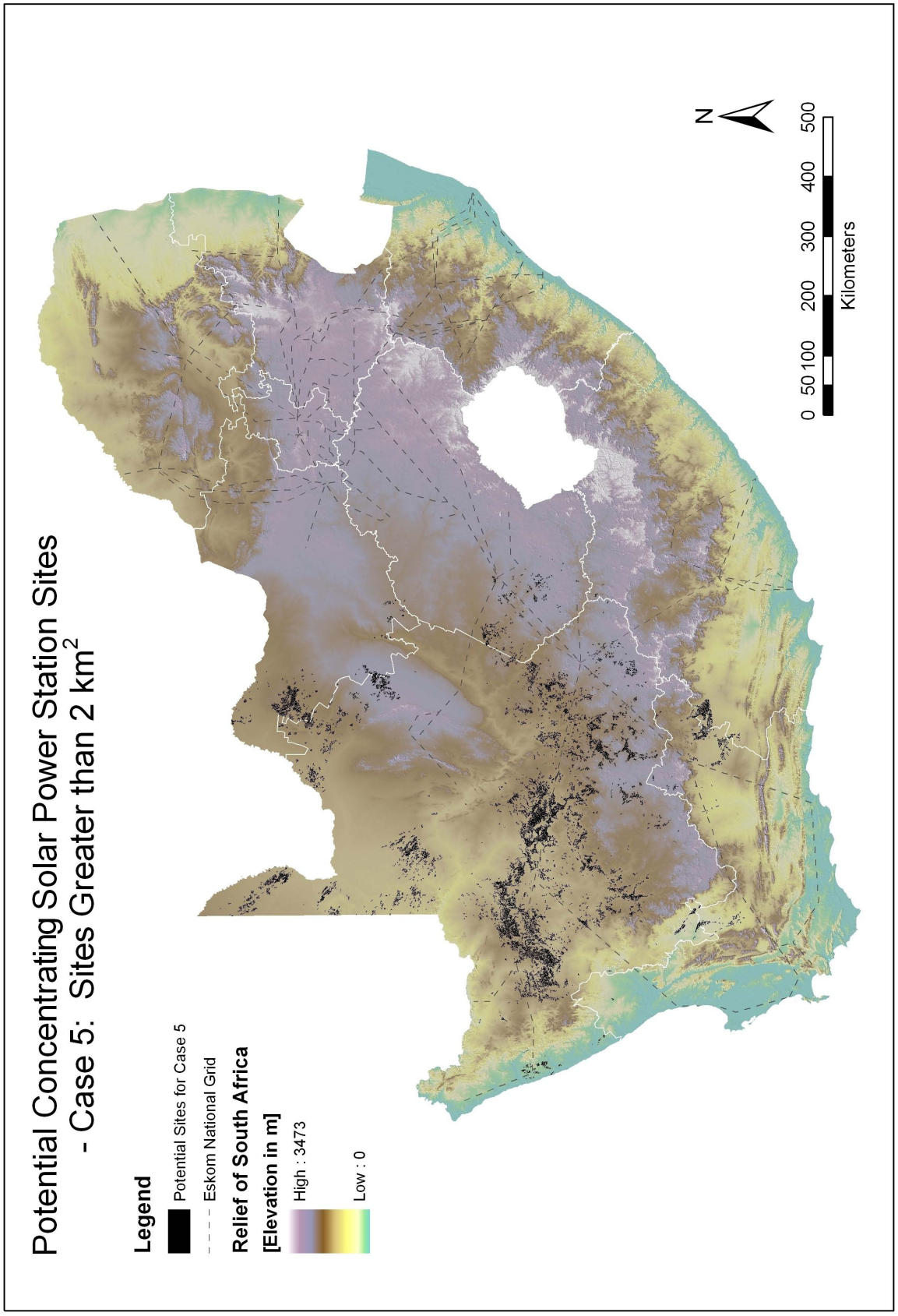

Figure 6.11: Map Identifying Potential Locations for CSP Plants in South Africa, as Governed by the Criteria in Case 5. *Source of Data:* Same as included layers.

6.5.3 Quantification and Characteristics of Potential Sites

In order to allow for the quantification of the results for the potential CSP sites, database files containing the total area, perimeter, location, and DNI values for each of the sites were created within the GIS software. The total available solar energy in terrawatt hours per day (TWh/d) was then calculated for each site by multiplying the site area by its particular DNI value. As the cell size for each analysis block is 90 m × 90 m – as dictated by the special resolution of the Digital Elevation Model (DEM) – each cell in a potential site was also assigned the identification number of the site containing it. This was done in order to overcome the possible scenario that a potential site fell across the boundary of differing DNI values on the larger 40 km × 40 km DNI grid, which would then cause the GIS software to consider it as two separate sites. The sites were then redefined according to their original site numbers, as described in Item 6 of Appendix A on page 214. This method allowed for the correct calculation of the total area and hence solar energy available for each potential site. The method is illustrated graphically in Figure 6.12.

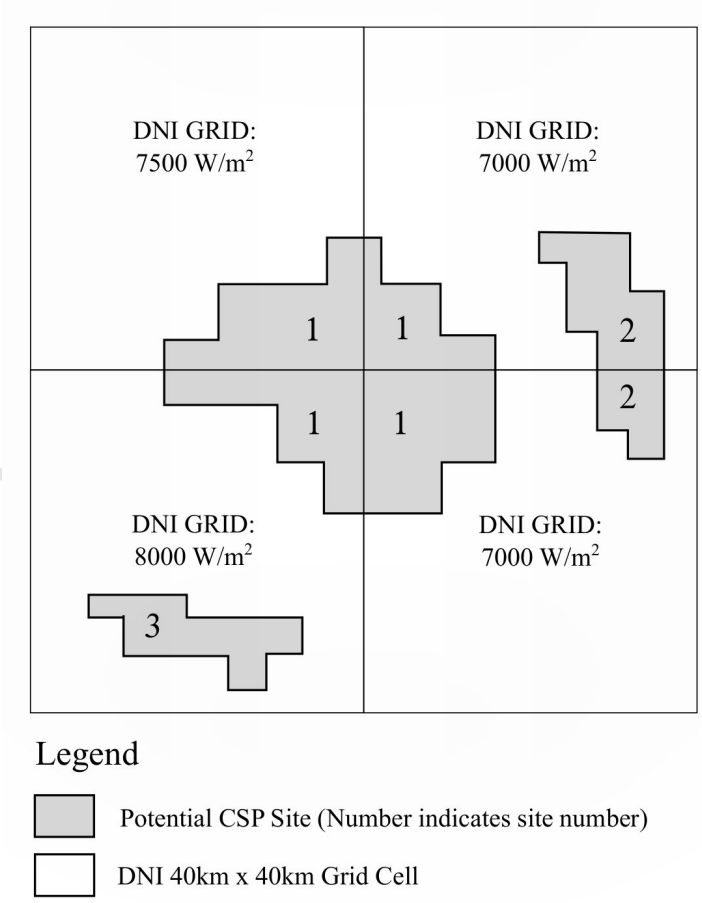

Figure 6.12: Method of Summarising Sites to Overcome Splitting by DNI Grid.

Once the total available solar energy had been calculated for each site, the total power generation potential in gigawatts (GW) was then calculated. This was accomplished by adopting a land use value of 28 km^2 per GW, in accordance with Pletka et al. (as cited by Fluri, 2009). Finally, an average plant capacity factor of 38.8% was assumed for parabolic trough plants (Fluri, 2009), while a capacity factor of 60.0% was assumed for central receivers (Winkler, H., editor, 2007), which allowed for the prediction of the net energy generation potential in Terrawatt hours per annum (TWh/a).

For the first set of calculations, all potential site areas were included in the quantification, even those with areas less than 2 km^2. Theses results are presented in Table 6.3. However, due to the extremely large amount of data produced from the Case 5 analysis when sites smaller than 2 km^2 weren't excluded, the resulting database file was too large to be completely imported and analysed in Microsoft Excel®. The Case 5 values could therefore not be included in the table. All these values were only calculated for interest sake, however, and were not deemed critical for the completion of this investigation.

For the second set of calculations, only sites with areas greater than 2 km^2 were considered and quantified, as stipulated in the actual analysis cases. These results are presented in Table 6.4. In this instance, the data for Case 5 was now small enough to be analysed completely, and its results are therefore included in the table along with those of the first four analysis cases.

Table 6.3: Total Potential Area, Average Daily DNI, Total Available Solar Energy, Power Generation Potential and Net Energy Generation (Including potential sites with areas less than 2 km^2).

	Case 1	Case 2	Case 3	Case 4	Case 5
Total Potential Area (km^2)	7,158.0	6,848.4	15,337.3	32,917.8	–
Average Daily DNI (kWh/m^2/day)	7.2	7.3	7.7	7.4	–
Total Available Solar Energy (TWh/d)	52.4	50.5	118.7	241.0	–
Power Generation Potential at 28 km^2/GW (GW)	255.6	244.6	547.8	1,175.6	–
Net Energy Generation - Parabolic Trough with 38.8% Capacity Factor (TWh/a)	868.9	831.3	1,861.8	3,995.8	–
Net Energy Generation - Central Receiver with 60.0% Capacity Factor (TWh/a)	1,343.7	1,285.5	2,879.0	6,179.1	–

Table 6.4: Total Potential Area, Average Daily DNI, Total Available Solar Energy, Power Generation Potential and Net Energy Generation (Excluding potential sites with areas less than 2 km^2).

	Case 1	Case 2	Case 3	Case 4	Case 5
Total Potential Area (km^2)	2,219.3	2,180.5	4,294.0	9,994.3	18,785.6
Average Daily DNI (kWh/m^2/day)	7.3	7.4	7.8	7.3	7.6
Total Available Solar Energy (TWh/d)	16.8	16.5	33.5	72.5	144.3
Power Generation Potential at 28 km^2/GW (GW)	79.3	77.9	153.4	356.9	670.9
Net Energy Generation - Parabolic Trough with 38.8% Capacity Factor (TWh/a)	269.4	264.7	521.2	1,213.2	2,280.4
Net Energy Generation - Central Receiver with 60.0% Capacity Factor (TWh/a)	416.6	409.3	806.0	1,876.1	3,526.3

When reviewing the results presented in the two tables, it is observed that they affirm the trends identified from the maps of the analysis cases. Case 2 results in the lowest identified site area and hence energy generation potential, caused by its stricter DNI requirement of 6.5 kWh/m^2/day (compared to 6.0 kWh/m^2/day of Case 1). Case 3 results in the greatest site area and energy generation potential of the first three cases that consider grid proximity. Furthermore, the increase in site area and energy generation potential in Case 4 and Case 5 is dramatic – more than four times that of the equivalent Case 2 and Case 3 scenarios – and is attributed to the removal of the grid proximity requirement. Finally, although the exclusion of sites with areas less than 2 km^2 greatly reduces the total overall area and energy generation potential, vast areas still remain for consideration.

As a means of validating these results, a comparison was made to the those achieved by Fluri (2009) in his GIS study of CSP potential in South Africa. Fluri (2009) calculated a total suitable land area of 15,334.0 km^2, a power generation potential of 547.6 GW and a net energy generation potential of 1861.4 TWh/annum. Comparing this to the suitable land area of 15,337.3 km^2, a power generation potential of 547.8 GW and a net energy generation potential of 1,861.8 Wh/annum calculated in Case 3 in this study – which made use of virtually identical analysis criteria to those used by Fluri – and *including* sites smaller than 2 km^2, a strong resemblance is visible. However, when compared to the results from Case 1 and Case 2, which required a close proximity to water bodies, the values calculated in this study are considerably lower – 2180.5 km^2, 77.9 GW and 264.7 TWh/annum for Case 2 *excluding* sites smaller than 2 km^2.

The reasons for these discrepancies are twofold: Firstly, the obvious factor that the requirement for a close proximity to water greatly reduces the number of potential sites in this study, compared to Fluri's, which didn't require a water proximity characteristic. And secondly, even though the analysis criteria in this study for Case 3 were virtually identical to Fluri's, different data was used for some analysis layers, and different land class exclusions were applied in this study, as can be see in Figure 6.4.

It is therefore concluded that although the requirement for a close proximity to large water bodies greatly reduces the area and energy generation potential of CSP sites in South Africa, a large number of sites do still exist. In order to truly realise the solar resource potential in South Africa, however, it may be more beneficial to make use of dry cooling technologies to reduce the need for plant cooling water, and hence greatly expand the total potential area and number of potential sites for future CSP installations. The investigation of this possibility will thus be conducted in Chapter 8 through to Chapter 10. Finally, if the the national grid were to be further extended into areas with high CSP potential, the total available area and energy generation potential could be greatly increased. The cost benefit analysis of the extension of the national grid is beyond the scope of this study however, and will not be considered.

6.6 Solar Shading and DNI Calculation Model

6.6.1 Background and Motivation

The DNI data used in this analysis, as stated in Section 6.3.1, was processed by NREL and has a spacial resolution of 40 km × 40 km with an accuracy of 10%. At the time of writing, this data was the best freely available data for South Africa with the highest spacial resolution, and was used by Fluri (2009), as well as recommended by Meyer (2010).

All the remaining raster-based analysis criteria, however, have a spacial resolution of 90 m × 90 m, as derived from the spacial resolution of the DEM. Potential CSP sites thus comprise a collection of 90 m × 90 m cells, and can total an area of a number of kilometers. This in turn results in the DNI data having a far coarser resolution than than other analysis layer or identified potential CSP sites. The sun's irradiation, however, is thought to be far more constant over a larger area, than that of land slope for instance, and thus for the sake of this study, the resolution is considered acceptable.

The 40 km × 40 km spacial resolution of the DNI grid, however, is not able to capture variations in DNI caused by local terrain and surroundings. These potential variations could arise from hills or mountains casting shadows on nearby flatter areas at certain times of the day. Although the analysis cases used should generally exclude areas that would be shaded by hills – as a result of the strict land slope criteria (less than 1%) – there may be the odd case where a potential CSP site could fall in a valley that is flat but surrounded by high hills or mountains. Thus, as a means to verify the eligibility of potential CSP sites, it was decided to make use of the shading and DNI calculation algorithm from the *Area Solar Radiation* toolbox within the ArcGIS software package.

The Area Solar Radiation calculation algorithm is fairly complex in nature, with a large number of user defined variables, and is able calculate and output the incoming direct radiation, diffuse radiation, and duration of direct radiation for any area defined by a DEM raster (ESRI, 2010a). This makes it an ideal tool not only for calculating the average hours of daylight that a particular sight may experience over a year – taking into account shading from surrounding elevations – but also as a means to verify the actual DNI values of the NREL data through comparison with its algorithmically calculated values.

6.6.2 Theory and User Defined Inputs

The Solar Radiation Algorithm calculates solar irradiation and duration of direct radiation based on a number of input parameters, and the surrounding topography contained within the DEM. It is thus purely a calculated indication, and is not based on any actual measurements at the potential sites. The accuracy of the calculations can be increased by controlling a number of the algorithm's input parameters, however, as stated by ESRI (2010a) in the documentation, it is imperative to obtain the correct balance between processing time and accuracy. This is due to the fact the radiation calculations can be time consuming, with calculations for large DEMs running for hours and sometimes days.

The algorithm functions by dividing the sky into a hemispherical dome comprising a number of defined cells. Then, by making use of the latitude of the area in question as well as times and dates, the position and track of the sun is calculated as it moves across the sky for each defined day interval. The direct radiation received on a surface is then calculated by the positions and tracks of the sun – as stored in the *sunmap* – for a specified period of time. In this case the simulation was run for an entire year to obtain an annual daily average. A specified number of *viewsheds* are created and horizon

angles are traced for all areas within the DEM, in order to take into account shading and blocking by topographical features, and thereby yield a quantified duration of received daily direct radiation (ESRI, 2010a).

As the latest NREL DNI data used in this study was for the year 2006, the Solar Radiation algorithm was run for the same time period – from 1st January 2006 to 31st December 2006. This was done in order to allow for an equal comparison between the measured and calculated results. The majority of the remaining solar area model inputs were left at the suggested default values, in order to obtain adequate accuracy without significantly increasing processing time. Location specific inputs such as the site latitude were automatically calculated by the software based on the input data of the areas in question.

6.6.3 Unsuccessful Methods

It was initially thought that the most efficient method for calculating the direct irradiation and duration of radiation from the solar area radiation algorithm would be to import the 90 m DEM for South Africa, and run the calculation algorithm for the entire country. This method would therefore cover all previously identified potential sites, and allow for the direct comparison and verification between them. It soon became apparent, however, that the algorithm was extremely computationally intensive, and crashed before any results could be obtained. After reading user's reviews and comments regarding the algorithm on ESRI's online forums (ESRI Online Forums, 2010) it was revealed that this was a common issue encountered when processing large DEMs for long time periods, especially when running the algorithm on 32 bit operating systems with their associated memory limit – as opposed to a 64 bit operating system.

In order to reduce the computational size of the data extent that needed to be processed by the solar radiation algorithm, it was subsequently decided to divide the South African 90m DEM into multiple geographic $1° \times 1°$ grid cells, and then only run the solar radiation algorithm on those $1° \times 1°$ grid cells that contained identified potential sites. In theory, once the algorithm had run for each of the $1° \times 1°$ grid cells, the separate results could then be merged back together to form one single data layer.

It was also decided to add a small euclidean distance buffer around each of the $1° \times 1°$ grid cells, as recommended by Lindenberg and Slingsby (2010). This was done in an attempt to reduce edge effects on the resulting calculated data, that would not have arisen had the algorithm been run once over the entire country as a whole. These edge effects could appear along the boundaries of each of the $1° \times 1°$ grid cells as a result of there not being any data on the external surrounding, which, in reality, would have affected the calculations for the included data. By increasing the extent of each of the $1° \times 1°$ grid cells by a certain distance, the edge effects would then also be moved outwards. Then, in theory, when merging all the calculation results from the $1° \times 1°$ grid cells together after the algorithm had been run, the excess overlapping euclidean buffers could be clipped away, thereby reducing the model's edge effects. Full details and description of this method are given in Appendix A.

The solar radiation calculation was subsequently run on the chosen $1° \times 1°$ grid cells and their buffers. The algorithm and calculation process was still highly computationally intensive, and took multiple days to run. It did, however, ultimately produce results without crashing. Attempts where made to merge, or *mosaic*, the processed individual $1° \times 1°$ grid cells back together, however, due to unknown and unexplained reasons, the results produced from the merge were erroneous and unreliable.

The graphic results of the DNI, and duration of average daily DNI for the $1° \times 1°$ grid cells calculated by the algorithm, as well as the failed attempt at their re-merging are presented in topographical format in Figure 6.13 and Figure 6.14 respectively. In the figures, boundary lines can clearly be seen that appear to suggest that the calculations for each $1° \times 1°$ grid cell were not consistent between cells, with the resulting merge not appearing continuous. Furthermore, two of the $1° \times 1°$ grid cells contained erroneous DNI values of 0 kWh/m^2/d for the entire cell, depicted by the two yellow cells in Figure 6.13.

6.6.4 Modified Successful Method

Due to the lack of success in calculating the DNI and duration of daily DNI for large areas of South Africa, it was decided to adopt a more focussed approach. As the calculation of DNI and duration of daily DNI is primarily for the purpose of validating the NREL DNI data – and hence the results achieved in the analysis cases – it was deemed acceptable to only run the calculation algorithm for a few small areas containing a few potential CSP sites, thereby reducing the size of calculation for the algorithm, and hence computational time.

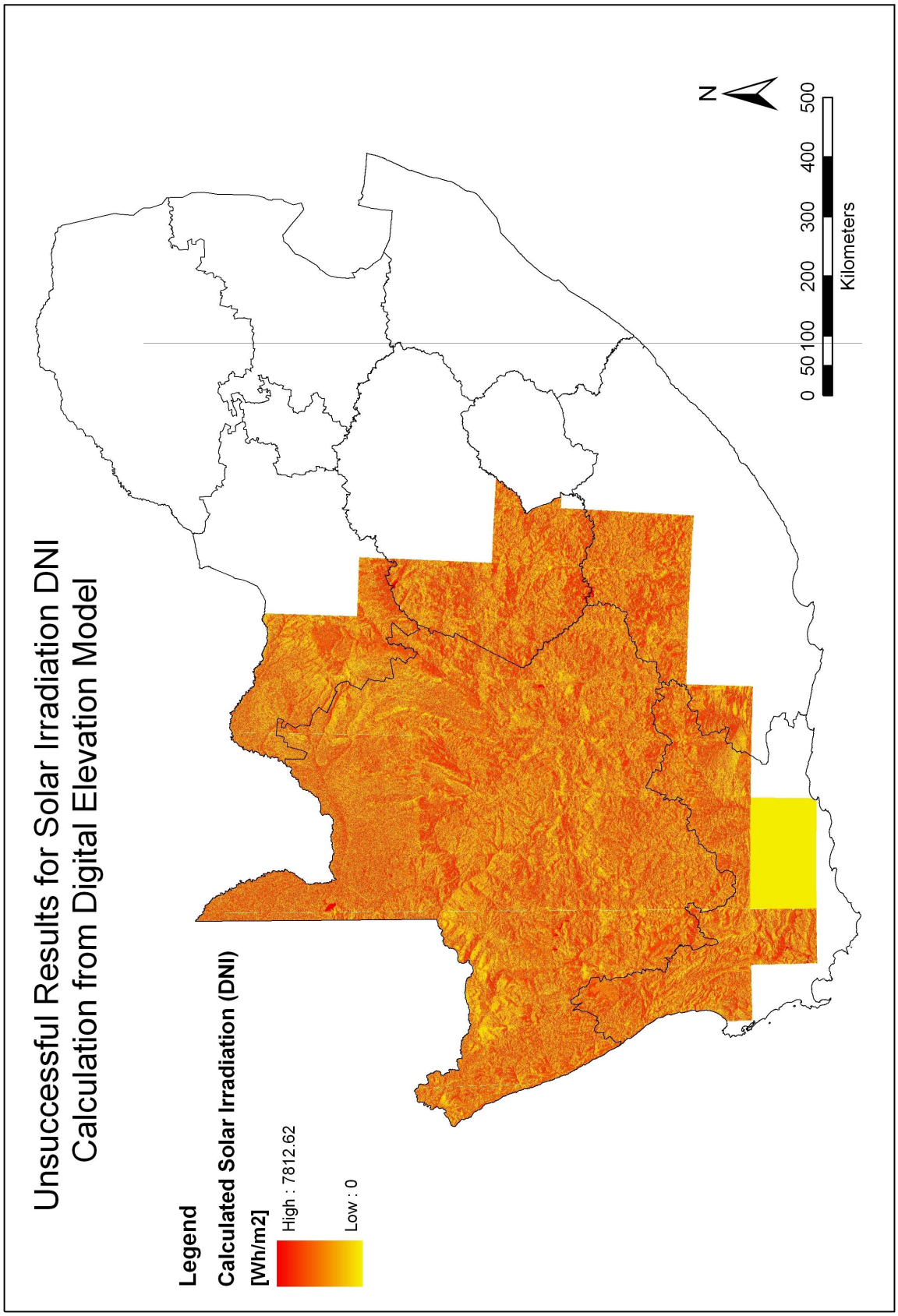

Figure 6.13: Map Illustrating the Failed Merge and Edge Effects for the Daily Solar DNI Calculation Algorithm. *Source of Data:* CSIR (2001c) and DNI Calculation Algorithm.

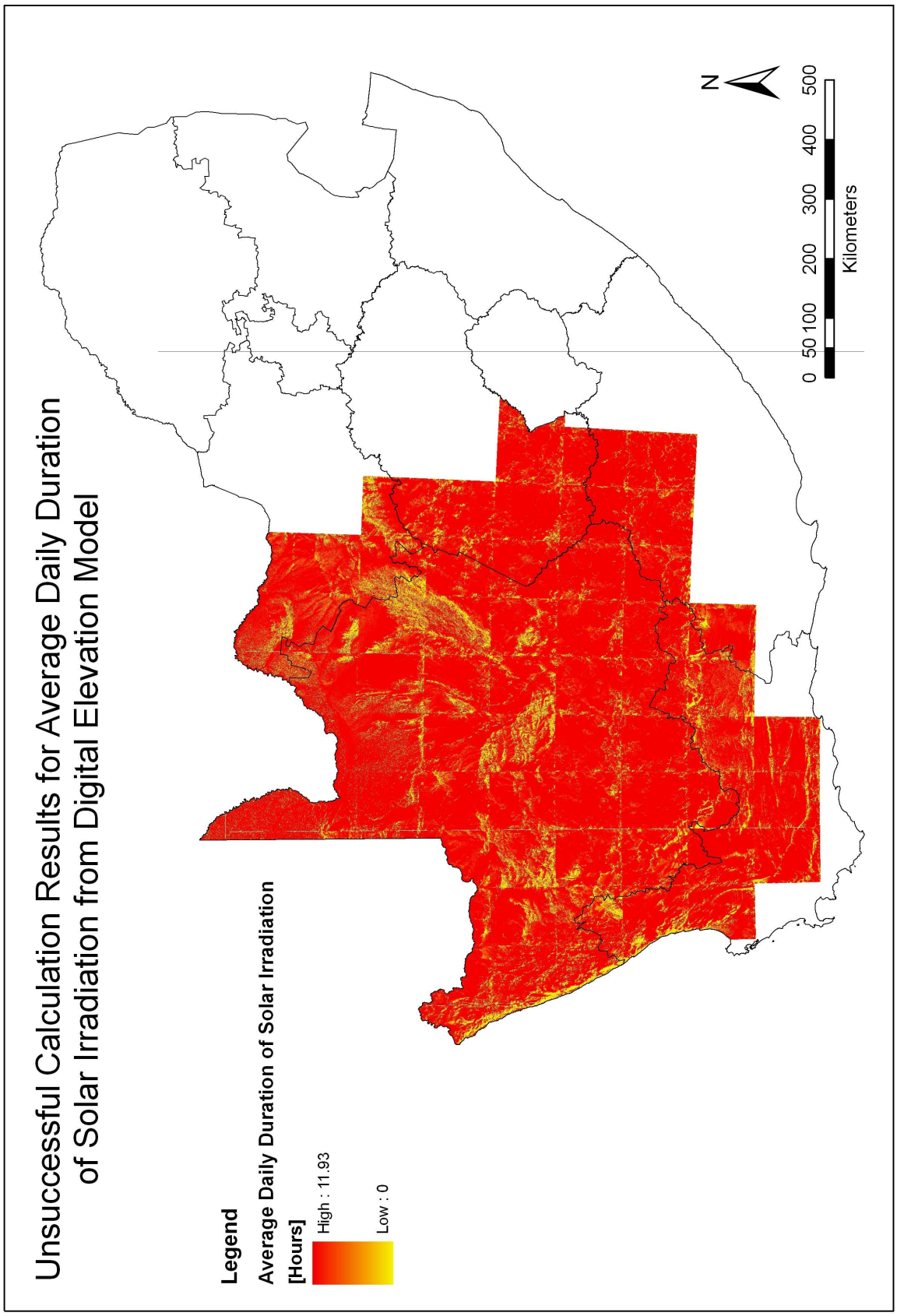

Figure 6.14: Map Illustrating the Failed Merge and Edge Effects for the Solar Shading and Duration Calculation Algorithm. *Source of Data:* CSIR (2001c) and DNI Calculation Algorithm.

In order to accomplish this task, two potential sites identified from Case 4 with fairly high DNI values and large total areas were chosen, while one site closer to the West Coast was chosen from Case 5. A 50 km radial buffer was then created around each of the sights to account for edge effects. The calculation algorithm was run on each one these three buffered site areas. As the areas for each calculation were smaller than a $1° \times 1°$ geographic grid cell, no re-merging or 'mosaicing' was required. The results of the solar irradiation DNI calculation for Case 4 and Case 5 are presented in Figure 6.15 and Figure 6.17 respectively, while the results from the duration of solar irradiation calculations are presented in Figure 6.16 and Figure 6.18.

When reviewing the DNI calculation results shown in Figure 6.15 and Figure 6.17, a few trends were observed. Firstly the algorithm calculates DNI levels lower than those measured by the NREL satellite derived data. Secondly the identified potential CSP sites do indeed fall in areas with calculated high DNI levels, although the algorithm does predict some higher DNI levels on the more steeply sloped terrain (evident when reviewed in conjunction with the DEM over which the results are superimposed).

When reviewing the duration of daily solar irradiation maps shown in Figure 6.16 and Figure 6.18, however, it can be seen the the potential CSP sites identified in this study fall in areas which receive high average daily durations of solar irradiation – in the region of 11.8 hours. The areas on the steeper slopes that appeared to have higher calculated DNI levels in the first calculation can be seen to receive lower durations of average daily solar irradiation.

Therefore, based on this rather limited method of validation, it is concluded that the results for the potential CSP sites identified in the analysis cases do indeed coincide with areas receiving high amounts of annual DNI. It is also concluded that the analysis cases were completed successfully in the GIS software, with all the specified analysis criteria being satisfied simultaneously. However, as will be discussed in Chapter 12, further validation and more extensive analyses considering local-scale DNI levels are recommend for future studies.

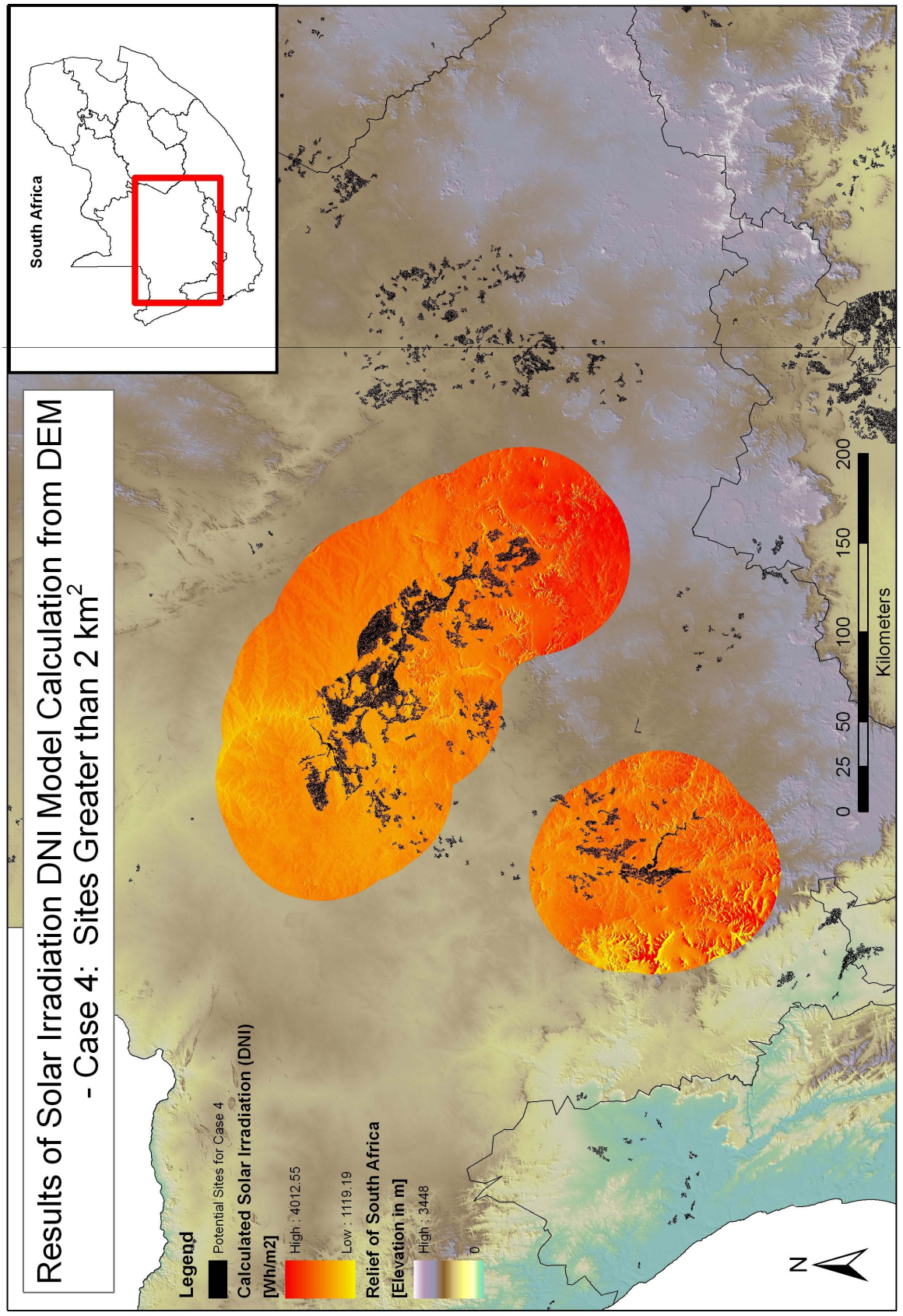

Figure 6.15: Map Illustrating the Successful Model Area Surrounding Potential Sites for the Daily Solar DNI Calculation Algorithm for Case 4. *Source of Data:* Same as included layers.

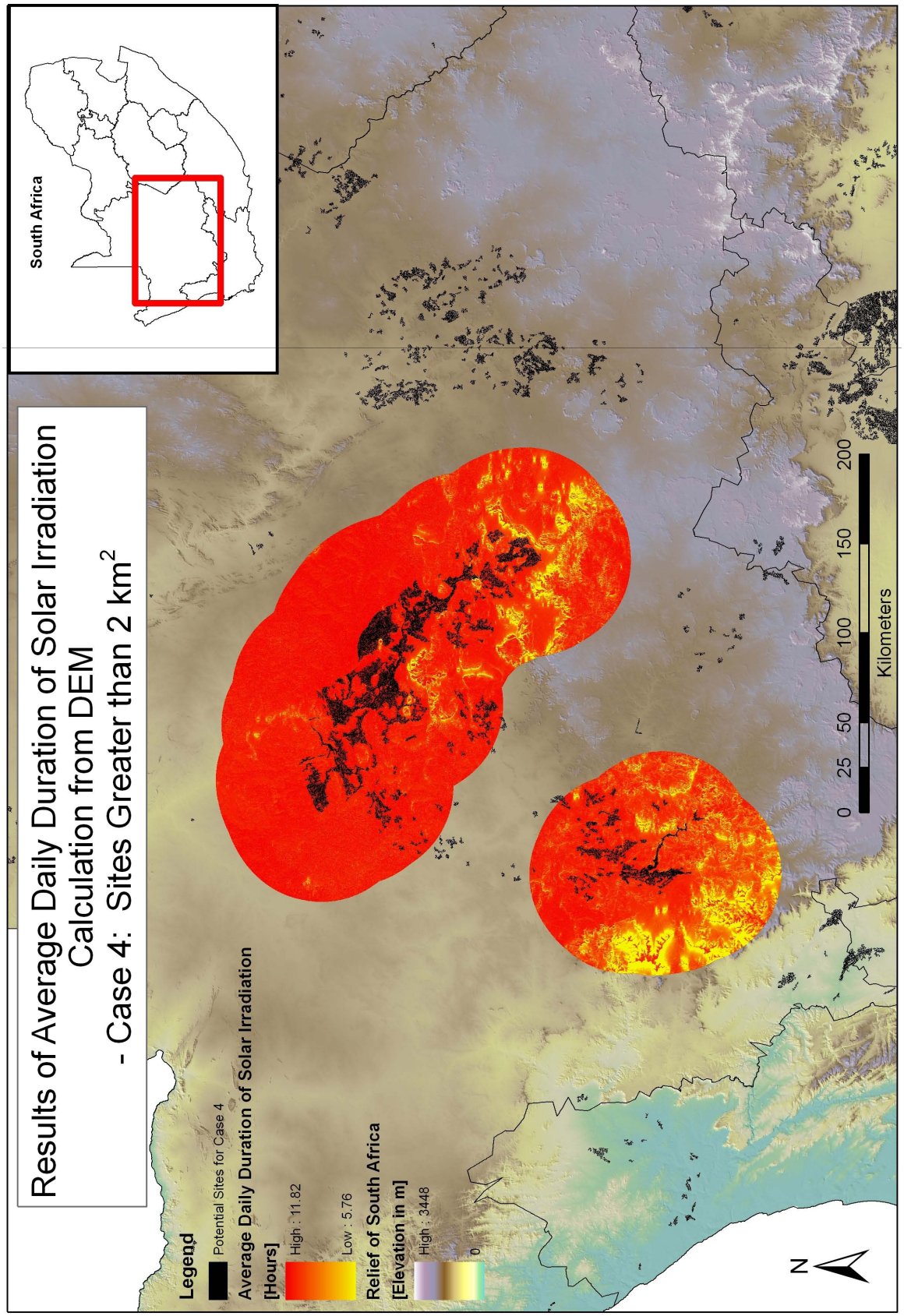

Figure 6.16: Map Illustrating the Successful Model Area Surrounding Potential Sites for the Solar Shading and Duration Calculation Algorithm for Case 4. *Source of Data:* Same as included layers.

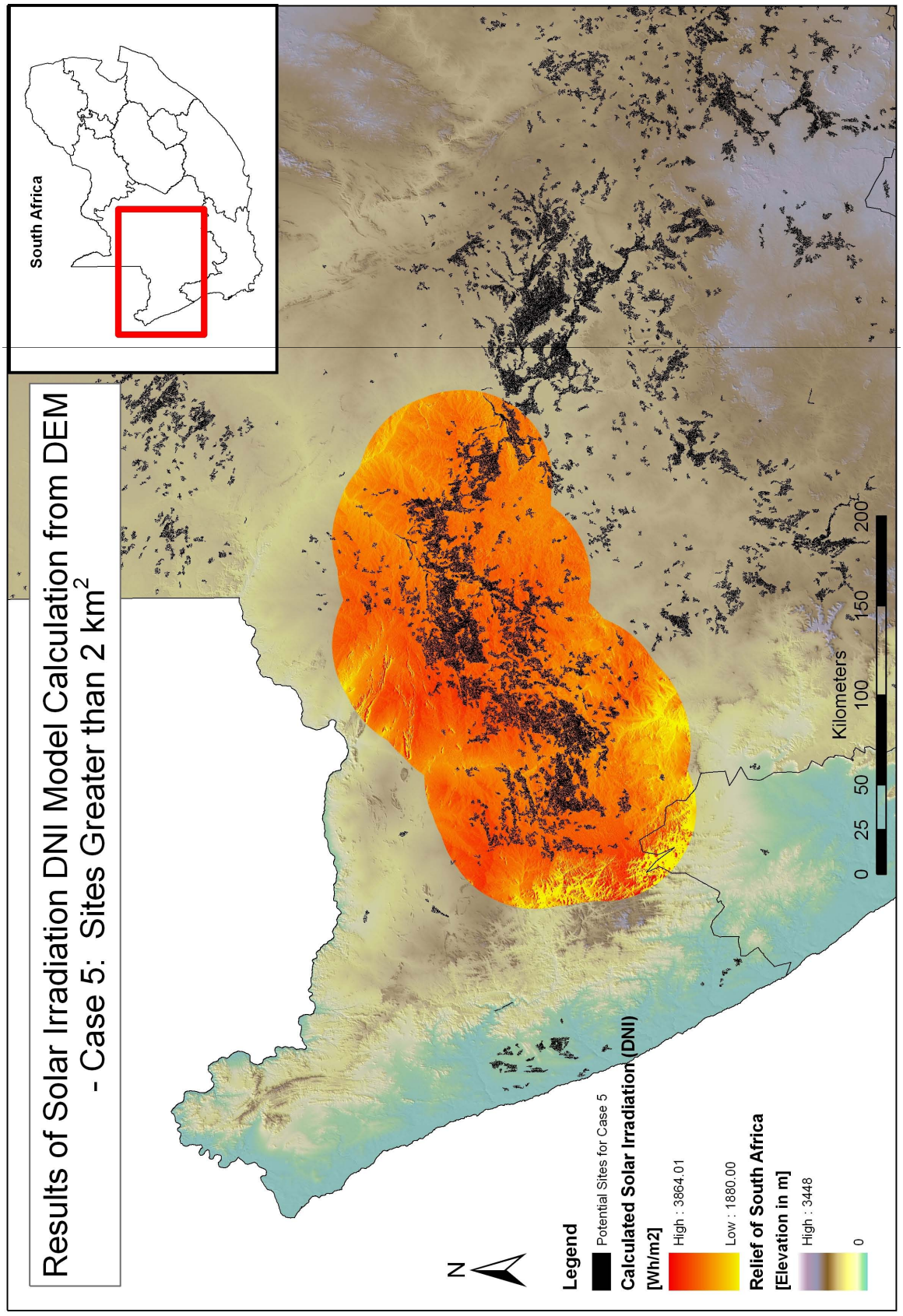

Figure 6.17: Map Illustrating the Successful Model Area Surrounding Potential Sites for the Daily Solar DNI Calculation Algorithm for Case 5. *Source of Data:* Same as included layers.

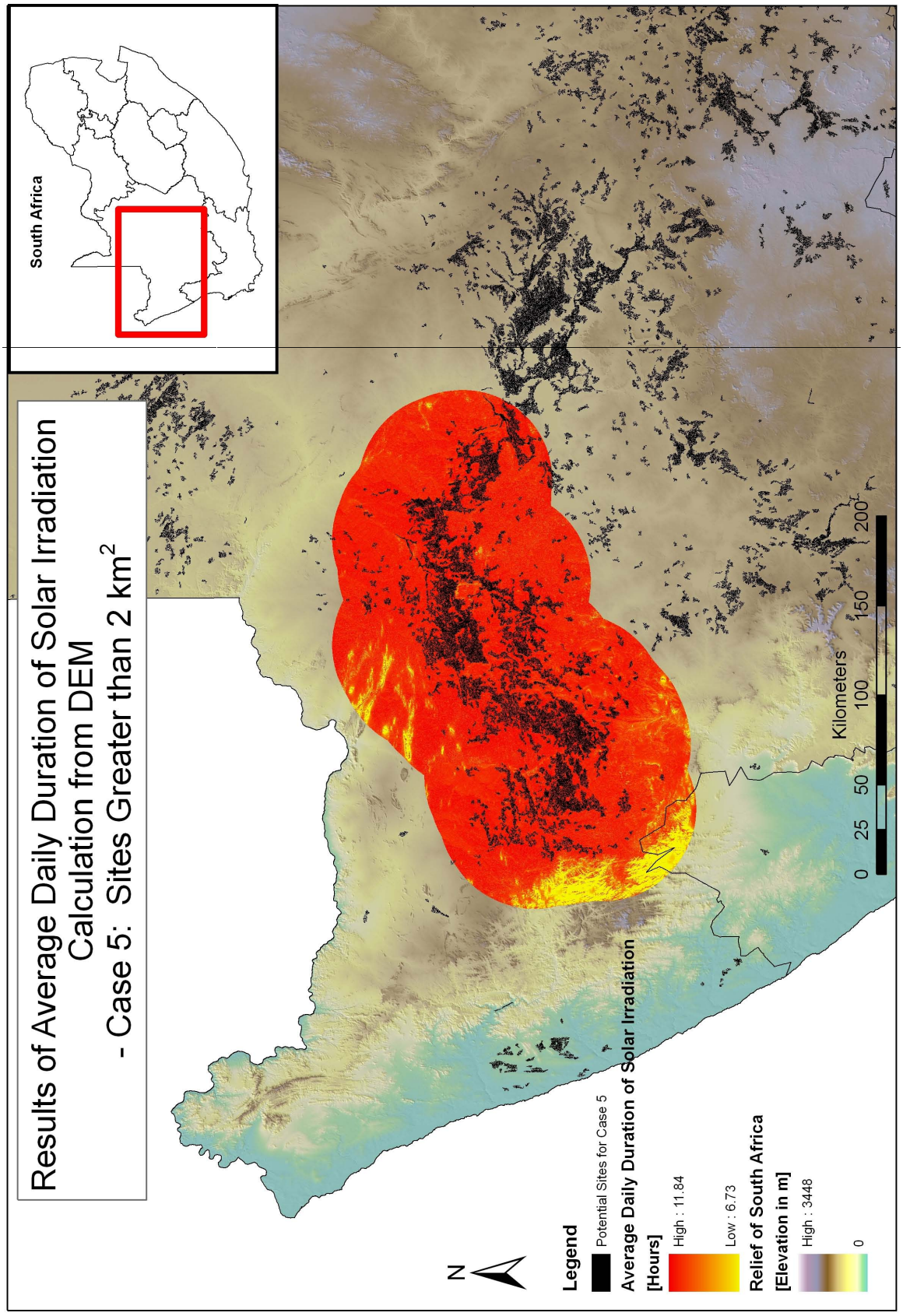

Figure 6.18: Map Illustrating the Successful Model Area Surrounding Potential Sites for the Solar Shading and Duration Calculation Algorithm for Case 5. *Source of Data:* Same as included layers.

7 System Modelling using SAM

The following chapter will present a brief overview of the SAM software user interface and input pages, reported in a similar order in which they would be found in the program. This not only allows for a better understanding of what input data is required in order to accurately model a CSP plant with SAM, but also further aids in the understanding of the applications and limitations of the software.

7.1 Program Version and User Interface

The latest version of the SAM software at the time of commencing this analysis was SAM version number 2010.04.12. This is the version that was used for the entirety of the study, and all further inputs and descriptions are made with reference to this version.

As mentioned in Section 2.3, the SAM software presents the user with a graphical user interface comprising a number of input pages, each of which requires a number of data inputs to be entered. Once all the data inputs on the relevant pages have been satisfied, the user is presented with options to configure and run various simulations, before viewing the results within the software or alternatively exporting them to a spreadsheet program. It is also possible to run a number of cases or scenarios for a project, changing only a few key variables in one in order to ascertain and compare their effects. Brief overviews of each of the input pages within SAM will now be outlined under their respective headings.

7.2 Technology and Market

The initial step in defining a project in SAM is to define which technology it comprises. Choices include *Concentrating Solar Power* (CSP), *Photovoltaic*, or a *Generic Fossil-fuel System*. Since this study is concerned with the modelling and analysis of CSP plants only, no further discussion will be presented on the other technology types. Further description of the different CSP technology types included in SAM is given in Section 7.5.

The second input of the technology and market pages requires the definition of the energy market which best describes the project in question. Depending on which technology choice was made initially, different financing option become available. Choices include *Residential*, *Commercial*, or *Utility IPP* projects. Once again, SAM will display different input variable pages depending on which market choice was made (SAM, 2010).

7.3 Weather Data

7.3.1 Overview of Accepted Data

The SAM software makes use of detailed weather data specific to each project location in order to run simulations and calculate the system performance outputs. SAM only accepts weather data in a text file format which contains hourly weather data describing solar resource, as well as a number of other environmental variables, for a specific location. The text data can be in either Typical Meteorological Year 3 (TMY3), Typical Meteorological Year 2 (TMY2) or EnergyPlus Weather Data (EPW) file format. The weather data encapsulated in these files may contain data for a single complete year, or for a typical year made up of assimilated data from a number of years. By definition, a TMY2 file normally represents data from a number of years ranging from 1961 - 1990, while a TMY3 represents more recent data from 1991 - 2005. These data types are generally suited for economic analysis and performance predictions of a project over a long analysis period. Single year data on the other hand is better suited for analysis of a project's economics and performance in a particular year, and for analyses involving rate structure or load data for a given year. All data sets, however, possess the standard assumption of 8760 hours per year, and do not account for leap years (SAM, 2010).

7.3.2 Weather Data Elements and Uses

The data encapsulated in the weather files contains information for a number of variables, including latitude and longitude, elevation, global horizontal irradiation (GHI), direct normal irradiation (DNI), diffuse irradiation, wind velocity, wet and dry bulb temperatures, pressure and albedo (SAM, 2010). Although not all these variables may be used in the simulation of each and every technology type, the SAM software only accepts a complete dataset with all variables as standard. For the CSP plants being analysed in this study, the key values of importance are the solar DNI levels, the location, and variables such as wind speed and temperature which would be needed for thermodynamic calculations and determining heat transfer losses to the environment.

7.4 Financing and Incentives

7.4.1 Economics and Financing

As discussed in Section 2.3.3, SAM possesses a detailed financial and economic model component. The financing inputs page displays the variables and inputs that are used by this model component to calculate the project cash flow, as well as other related financial metrics. As previously stated, the input variables available for each simulation depend on the technology choice and financing option as specified in the 'Technology and Market' section of the SAM software. As this study is concerned with utility scale CSP plants in South Africa, the *Utility IPP* market was deemed the obvious choice for the SAM model and simulations, and thus only Utility IPP model options will be discussed further.

According to the SAM (2010) definition, a utility project earns revenue by the selling of electricity at a rate determined through a power purchase agreement (PPA). The PPA rate is fixed for a year, and then either remains fixed, or escalates at a defined annual escalation rate. When a utility IPP market is chosen for a project, it is assumed that the utility owner pays cash for the equity portion of the total installed project cost in year zero, and makes interest and principal loan payments in the following years. SAM then calculates the electricity PPA price required to meet the internal rate of return (IRR), minimum debt service coverage ratio (DSCR) and positive cash flow requirements as defined by the user in the financial inputs page. Utility projects (and commercial projects for that matter) also have the added ability to be modelled with or without depreciation – using MACRS depreciation schedules or various other user-defined depreciation methods (SAM, 2010).

7.4.2 Tax Credit Incentives

SAM also allows for the optional inclusion of tax credit incentives in its economic model, with the option to include both investment based credits or production based credits. An investment tax credit will reduce the project's annual tax liability in the first year of the project cash flow, whereas a production tax credit will reduce the project's annual tax liability in the first year of the cash flow as well as subsequent years up to and including a specified final year. It is also possible to define whether tax credit amounts themselves are taxable, and whether or not they affect the depreciation of the project. Once calculated, SAM then displays the tax credits and income tax payments in the project cash flow results (SAM, 2010).

7.4.3 Payment Incentives

As with tax credit incentives, SAM can also optionally include payment incentives within the economic model. These can be defined either as investment based incentives, capacity based incentives or production based incentives. All types represent an amount paid towards the project that contributes to the project's annual income in the first or subsequent years of the project's life. Once again, as with tax credit incentives, it is possible to define whether the incentives themselves are taxable, and whether or not they affect the depreciation of the project. Once calculated, SAM then displays the payment incentives in the project cash flow results (SAM, 2010).

7.5 System Design and Costing

Depending on which technology choice was made initially, as described in Section 7.2, a number of technology specific design and cost input pages are shown, each of which require further data inputs to be defined. However, as previously mentioned, this study will only focus on those inputs relevant to CSP parabolic trough and central receiver technologies.

7.5.1 System Costs

The economic modelling component in SAM makes use of the system costs to calculate the project investment costs and annual operating costs as reported in the project cash flow output. SAM requires cost input data which describes the entire spectrum of the project, including detailed direct and indirect capital costs as well as operation and maintenance (O&M) costs.

A full description of all the costs data used in this project in given in Sections 8.5 to 8.7 of Chapter 8, with full tabulated data presented in Appendix B, Appendix C, Appendix F and Appendix G. Thus for the sake of brevity, and due to the sheer number of cost input categories available for both parabolic trough and central receiver plants, the various cost inputs will not be listed again in this section.

7.5.2 Parabolic Trough Model

When modelling a parabolic trough CSP plant, SAM offers the user a choice between two plant models. The first model developed is that of the *empirical parabolic trough model*, which makes use of a set of equations, based on empirical analysis of data collected from existing parabolic trough installations, in order to predict the performance of trough components. However, as the empirical model makes use of a set of curve-fit equations derived from the regression analysis of data measured from existing systems, one is limited to only being able to include system components for which measured data exists. The empirical model is based on the *Excelergy* model which was initially developed for internal use at the National Renewable Energy Laboratory (NREL) (SAM, 2010).

The second and most recent parabolic trough model available is that of the *physical trough system model*, which was first introduced in March 2010. This model differs from the empirical model in the fact that it characterises the performance of system components based on the first principals of thermodynamics and heat transfer. These mathematical models allow for far greater flexibility when defining system components and removes the limitation of only being able to model existing components with measured data. The disadvantage of the physical model, however, is that it does add more uncertainty to performance predictions when compared to the empirical model. The empirical model is technically reliable when modelling plants very similar in design to an existing plant from which it was derived, however, for new plant designs not based on existing plants, the physical trough model may be more applicable. A further key advantages of the physical model, apart from its added flexibility, is that its relatively short simulation run-time allows for additional simulations and parametric analyses to be run (SAM, 2010). The physical trough model is based on NREL's collector Excelergy model, and comprises a receiver heat loss model by Forristall (2003), a field piping pressure drop model developed by Kelly and Kearney (2006) and the power cycle performance model used in the SAM central receiver model, developed by Wagner (2008).

As with the system costs input page, the parabolic trough model contains multiple data input pages relating to the physical plant design. Once again, a full review of the design input data is given Section 8.8 of this report, with full tabulated data presented in Appendix D and Appendix F. These inputs will therefore not be presented again in this section.

7.5.3 Central Receiver Model

Unlike the parabolic trough technology model in the SAM software, there is only one choice of model for central receiver systems. The central receiver performance model makes use of TRNSYS components developed at the University of Wisconsin, and is described in the research conducted by Wagner (2008). The central receiver model was first included in the more recent versions of SAM.

Like the parabolic trough models, the central receiver model also presents the user with a number of data input pages relating to the physical design and layout of the plant. The number of inputs are greatly increased, however, by the fact that a central receiver system contains thousands of heliostats, all of which require positioning and layout data. Various mathematical algorithms do exist which aid in the generation of the heliostat field layout based on ray tracing or other methods, but in order to simply the process, SAM includes its own optimisation and layout wizard.

According to the SAM (2010) documentation, "the power tower optimization wizard simplifies the task of choosing values for the relatively large number of input parameters required to specify the power tower solar field and receiver." The optimisation of the heliostat field size is considered a crucial step in the design process, as the heliostat field alone accounts for more than 40% of the total installation cost (Sargent & Lundy, 2003). The SAM optimisation wizard functions by searching for a set of optimal design parameters that result in the lowest levelised cost of energy (LCOE). This optimisation process is separate and run prior to the full simulation process, and produces input variables which are then used to populate the data input fields used in the final performance simulation. Unlike other optimisation techniques such as genetic algorithms, the technique adopted in SAM is more of a 'brute-force' method, where a range and increment size is given for each input variable and then discrete combinations are run individually to see which produces the lowest LCOE while satisfying performance requirements (SAM, 2010). The wizard may not always produce an optimal field layout, however, and may require adjustment to value ranges through an iterative process. If the wizard is unable to locate a reasonable field layout, it will always display a message with suggestions for adjustments of limits or step sizes.

The optimisation wizard makes use of, and holds constant, the capital costs defined in the system costs input page, as well as the solar multiple, nameplate capacity, heliostat width and height, and the receiver maximum flux rating. The various heliostat optical and dimension inputs are also used.

The optimiser then finds and populates the following optimal design values:

- Receiver Diameter
- Receiver Height
- Tower Height
- Radial Step Size for Layout
- Total Reflective Area
- Number of Heliostats
- Number of Heliostats per Radial Zone

The optimisation wizard's underlying algorithm is based on the DELSOL3 code from Sandia National Laboratory (Kistler, 1986), and was implemented in SAM through the PTGen program described by Wagner (2008). A full review of the design input data is given in Section 8.9 of this report, with tabulated data presented in Appendix E and final input data (including inputs to the optimisation wizard) given in Appendix G.

7.6 Thermal Storage and Fossil Fuel Backup

The theory and motivation for thermal energy storage in CSP plants has already been covered in Chapter 5, and hence only its implementation and configuration within SAM will be covered in this section. The user inputs for thermal storage in SAM are divided into two categories, namely thermal energy storage (TES) design parameters, and thermal storage dispatch controls. Should it be required, SAM also possesses the ability to model and include a fossil fuel backup system, whose use is also defined and controlled within the dispatch schedule.

7.6.1 Thermal Storage Systems and Dispatch

The inputs in the TES category are used to define the TES storage capacity and its type – direct, indirect, single tank, two tank – as well as its efficiency parameters. The central receiver TES model differs slightly from the parabolic model, however, in the sense that it calculates the storage tank geometry, but requires that the heat transfer fluid volume, tank loss coefficients, and tank temperatures be specified in order to do so. SAM calculates the storage tank geometry by ensuring that the storage system can supply enough

energy to the power block at its rated design thermal input capacity, for the total number of hours specified (SAM, 2010). As with previous sections, the full list of all the inputs for each technology is presented in tabulated form along with the other plant design data in Appendix D, Appendix E, Appendix F and Appendix G.

The inputs in the thermal storage dispatch determine when energy from the TES system – and fossil backup system if included – is released to the power block. This process can be defined by up to six different dispatch schedule periods. The SAM software analyses the thermal dispatch process according to the following algorithm (SAM, 2010):

- For each hour in the simulation process, SAM makes a decision whether or not to operate the power cycle based on how much energy is available in the TES, how much energy is being delivered by the solar field, and the input values of the thermal storage dispatch control parameters. It is also possible to define when the power cycle operates according to the aforementioned six dispatch schedule periods for both weekdays and weekends.
- For each hour of the simulation, SAM analyses the amount of energy available in the TES at the beginning of the hour, and decides whether or not it should operate the power cycle, if it is not already running. This decision is based on two targets, namely one for periods of sunshine and one for periods without.
- During periods of sunshine when there is insufficient energy from the solar field to drive the power cycle at its specified load requirement, the system dispatches energy from storage, but only when energy in storage is greater than or equal to the dispatch target. A dispatch target exists for each dispatch period and is defined as the product of the storage dispatch fraction for that period, and the thermal storage capacity defined by the TES thermal capacity input variable.
- Similarly during periods of no sunshine, when no thermal power is being produced by the solar field, the power block will not run, except for when the energy available in TES is greater or equal to the dispatch target as defined above.

Thus in order to define and control the dispatch schedule, one simply defines a turbine output fraction and a storage dispatch fraction for each dispatch period. A turbine output fraction of 1.0 is equivalent to requiring an energy output defined by the systems nameplate gross output capacity. For hours when the system is not able to produce the required amount of energy from the solar field, the power cycle will then run on energy from both the solar field and TES. For hours when the energy from the solar field exceeds that of the output requirement defined, the power block will run at said capacity while excess energy is diverted to TES – provided it is not full.

7.6.2 Fossil Fuel Backup and Dispatch

If one decides to include a fossil fuel backup system with the CSP plant, its specification and schedule are defined within SAM by means of a dispatch schedule similar to that of the thermal storage system. The fossil fuel dispatch schedule is defined by means of a fossil fill fraction for each dispatch period. The fossil fill fraction defines the solar output level of the system for each hour at which the backup fossil fuel system runs. A fossil fill fraction of 1.0 requires the fossil backup to run and supplement the system to 100% design output power for every hour that the solar energy alone would not be enough to accomplish this. A fossil fill fraction of 0.5 would only allow the fossil backup to engage and supplement the system when the solar output of the plant drops below 50% (SAM, 2010).

SAM also incorporates and calculates the cost of fossil fuel for the backup system – as defined in the system costs page – and reports the results in the levelised cost of energy as well as other result metrics. The energy equivalent of the fuel consumption is also calculated and reported in the results.

A full description and graphic representation of the dispatch schedules used to define the thermal energy storage systems in this analysis is presented in Section 8.10 of this report, and hence no examples will be given here. The use of a fossil backup fuel is not considered in this study, however, and hence no modelling or data inputs relating to its use will be discussed or included.

7.7 Parasitics and Losses

The final input page in the SAM software is that of *Parasitics*, which allows for the inclusion of parameters that define the parasitic electrical loads and losses in the system. The parasitic losses are calculated according to two sections, namely the total parasitic losses used to calculate the power block design thermal input, and the hourly values calculated during the simulation of the system's performance. SAM includes a default set of parasitic parameters for a range of systems, which are then automatically scaled to match the size of the actual plant being modelled. The actual calculated parasitic losses are then reported in the results of the analysis (SAM, 2010). The parasitic loss inputs for the parabolic trough and central receiver systems are discussed in Section 8.8 and Section 8.9 respectively, and presented in tabular format along with the other design inputs for each technology in Appendix D, Appendix E, Appendix F and Appendix G.

8 System Inputs for SAM Model

The derivation and correct identification of inputs for the SAM model is extremely important, as with any model, the results achieved are only as good as the input data used to ascertain them. The following sections will thus describe in detail the methods and sources used in the determination of the inputs to the SAM software models in this study. The sections are described in an order relating to their structure in the SAM software.

8.1 Site Selection and Weather Data

8.1.1 Background and Method

After the successful conduction of the GIS potential site analysis, the next step was to select a number of potential sites for further analysis, and subsequently to obtain detailed weather data for these sites. The means of determining or selecting the *most* optimal sites is not a simple task, however, and would require a closer level of inspection and lower level analysis than the high level GIS analysis presented in this study. Furthermore, the selection of potential sites for a CSP project would depend on project-specific requirements, and would potentially require a method which ranked and weighted sites according to criteria considered most important for that particular project.

The difficulty of site selection for analysis in this study is compounded by the fact that the SAM software requires very detailed weather data for a potential site, as discussed in Section 7.3. Acquiring this weather data for a specific location given by geographic co-ordinates is either achieved by direct measurements from a weather station set up at the site in question, or otherwise from satellite derived or interpolated data (Meyer, 2010). The first method would require site measurements to be taken for a period of at least a year, which would be extremely costly and is thus judged beyond the scope of this study. The latter method, although technically easier and cheaper, still requires the use of proprietary software or data for any location not centred near a city, large town, or

weather station with publicly available data (Meyer, 2010). Software such as Meteonorm is capable of providing the required hourly data for any geographic location, accomplished by means of combining satellite derived data with interpolated weather data from known weather stations; however, at the time of writing this software was not freely available (Meteotest, 2011; Meyer, 2010).

Detailed hourly weather data for a meteorological year (in EPW format) was, however, available for a number of major cities and towns around South Africa, included with the SAM training course as presented by Gilman (2010) and Meyer (2010). The sites in South Africa for which data was supplied and possessed are listed in Table 8.1.

Table 8.1: South African Locations for which Detailed Hourly Data Weather Data was Already Obtained.

Location Name	Province
Bethlehem	Free State
Bloemfontein	Free State
Lephalale	Limpopo
Saldanha	Western Cape
Springbok	Northern Cape
Sutherland	Northern Cape
Upington	Northern Cape

After discussion with Bennett (2010), it was decided to make use of this weather data already in possession, and subsequently, select three potential CSP sites for consideration by means of comparison and superposition of the weather data locations and the potential sites identified in the GIS analysis. This would eliminate the need to invest in expensive weather data, as well as remove the need for a lower level analysis required for identifying the *absolute optimal* sites. This decision was made based on the scope and detail required for this high-level study; however, for future research, it is recommended to make use of more accurate site specific weather data as well as lower-level site evaluation and selection methods. The method adopted in this study for choosing the three locations will now be presented.

8.1.2 Chosen Sites

Of the locations for which weather data was available, only three were deemed close enough to the identified potential sites to be of value to the analysis. These sites comprise the town of *Upington* in the Northern Cape, the town of *Springbok* in the Northern Cape, and the city of *Bloemfontein* in the Free State. A map of these three chosen locations superimposed on the identified potential CSP sites from Case 5 (DNI > 7 kWh/m^2/day, No Proximity to Large Water Bodies, No Grid Proximity) is shown in Figure 8.1.

From the map it can be seen that the three chosen towns are not only located close to identified potential CSP sites, but are also evenly distributed across the region. Furthermore, each of the three locations possesses slightly different characteristics, either in a region with high DNI values and reasonably close to water sources (Bloemfontein), in an area of high DNI but further from water sources (Upington), or in a region of lower DNI but closer to the West Coast (Springbok).

8.1.3 Visualisation and Validation of Site Weather Data

As a means of validating that the assumption to make use of existing town weather data to approximate the weather data at optimal locations is acceptable, the weather data for each of the three town locations was processed and quantified, before being compared to that of the satellite derived NREL DNI data used in the GIS analysis in Section 6.3.1.

The first step in the validation process was to create daily solar profiles of the variation in DNI for an average day for a number of different months. This was done for each of the three locations, before an average annual daily profile was created for visualisation. The results of these daily profiles and average annual daily profiles for Upington, Springbok and Bloemfontein can be seen in Figure 8.2, Figure 8.3 and Figure 8.4 respectively.

From the graphs of the DNI profiles, it is immediately apparent that the daily profiles fit the correct and expected shape for DNI variation, with zero DNI during night hours and an increase to peak DNI around midday. A variation of the average daily profile is also visible from month to month, with the summer months of December and March experiencing a larger and longer plateau – and thus exposure to DNI – when compared to the winter months of June and September. Finally, variation is also observed between locations, with the Upington area receiving higher DNI values when compared to Springbok and Bloemfontein. This is agreement with the satellite derived DNI maps presented in Figure 6.1 and Figure 6.2 of this report.

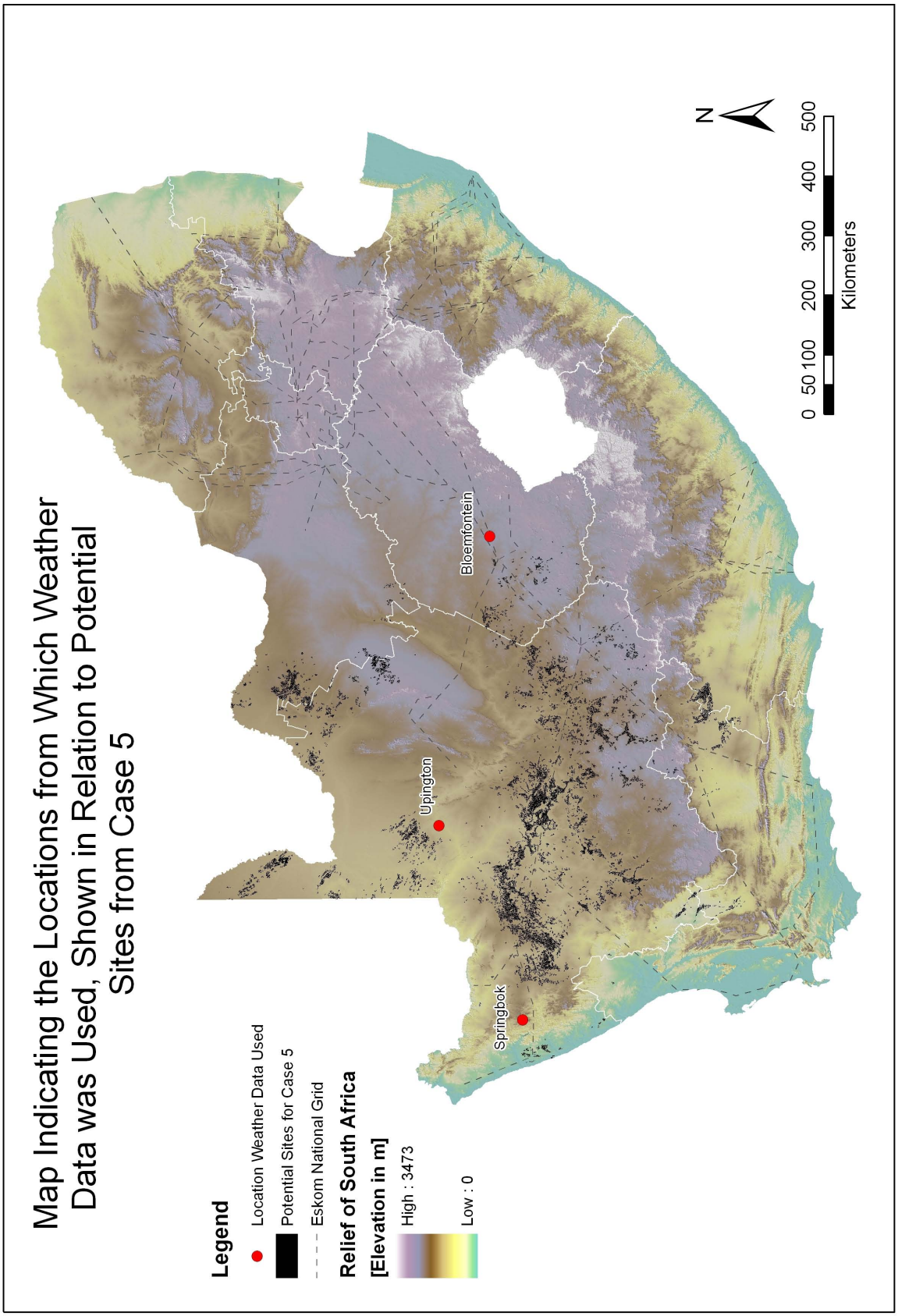

Figure 8.1: Map Indicating the Locations from which Weather Data was Used, Shown in Relation to Potential Sites from Case 5. *Source of Data:* Same as included layers and ENPAT (1998).

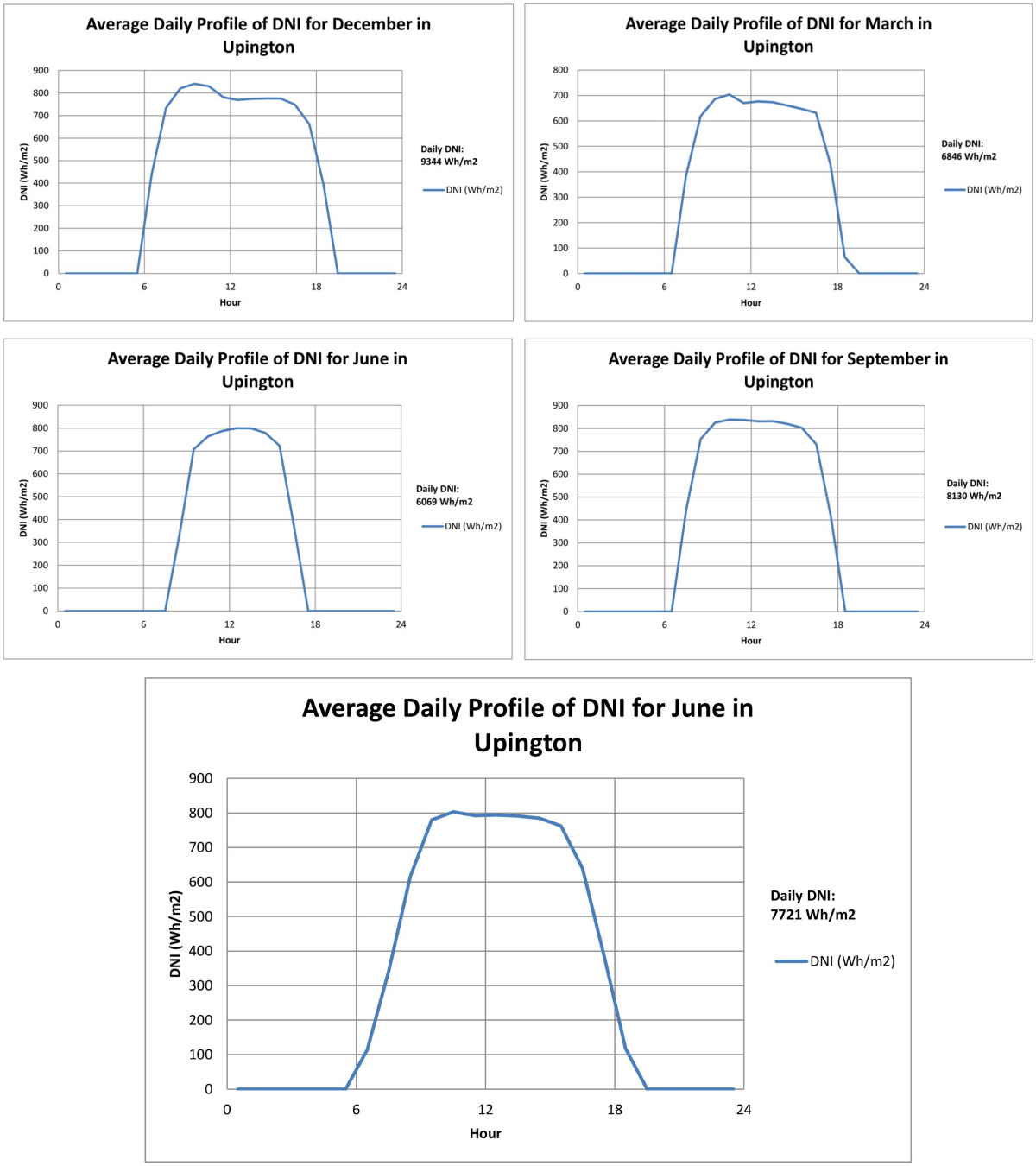

Figure 8.2: Average Daily DNI Profiles for Select Months and Annual Average Daily DNI Profile for Upington.

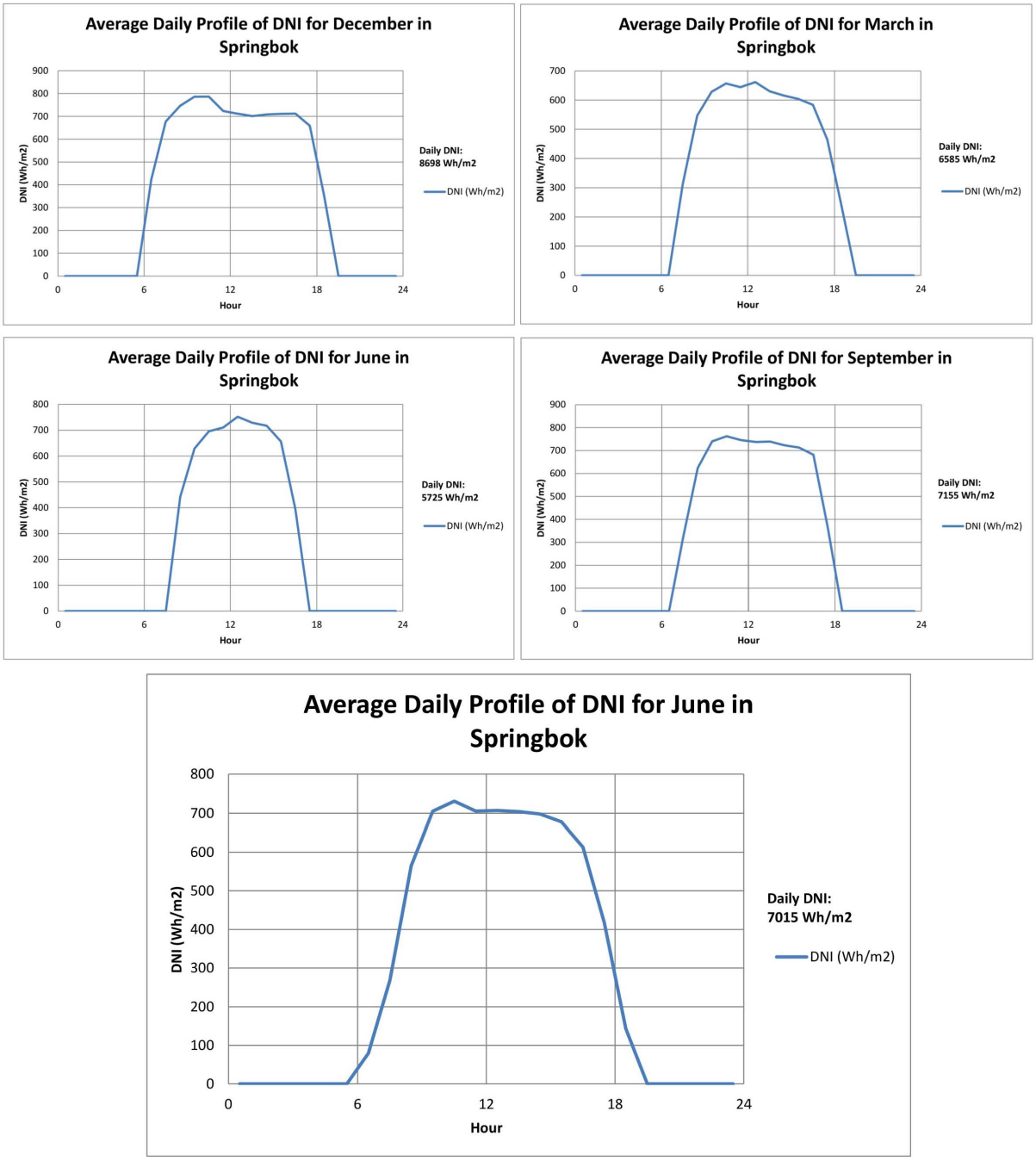

Figure 8.3: Average Daily DNI Profiles for Select Months and Annual Average Daily DNI Profile for Springbok.

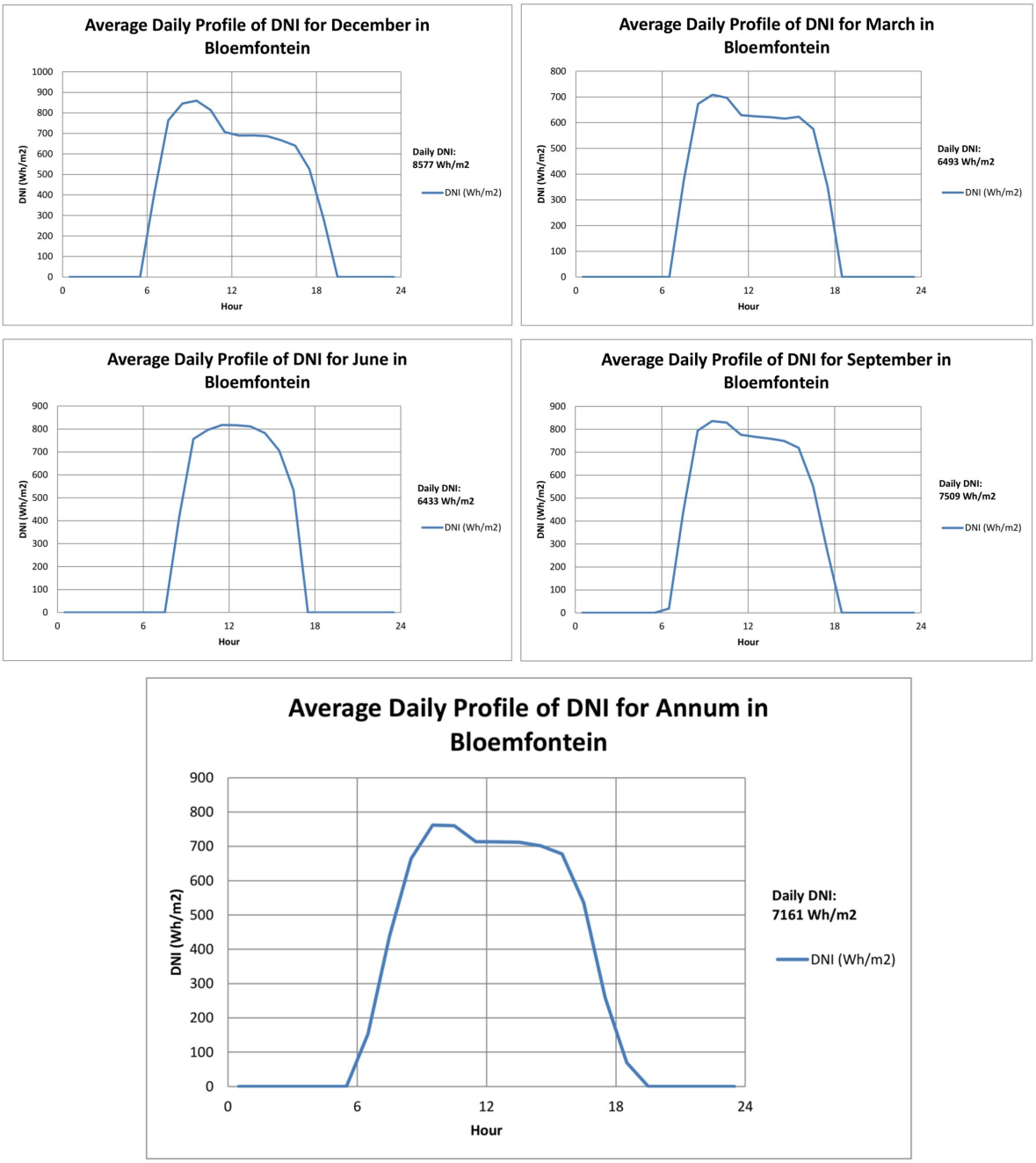

Figure 8.4: Average Daily DNI Profiles for Select Months and Annual Average Daily DNI Profile for Bloemfontein.

The second means of validating the weather data chosen for use in SAM, was to calculate the total daily DNI for an average day of each selected month, and an annual average daily total for the three locations, as a means to quantify and compare it to the satellite derived DNI values given by NREL (SWERA, 2010) and used in the GIS analysis of this report. The results of these calculations are presented in Table 8.2.

Table 8.2: Total Daily DNI for Select Months and Annual Average Total Daily DNI for Upington, Springbok and Bloemfontein.

	Upington	Springbok	Bloemfontein
Total Daily DNI for Average Day in December ($Wh/m^2/day$)	9344	8698	8577
Total Daily DNI for Average Day in March ($Wh/m^2/day$)	6846	6585	6493
Total Daily DNI for Average Day in June ($Wh/m^2/day$)	6069	5725	6433
Total Daily DNI for Average Day in September ($Wh/m^2/day$)	8130	7155	7509
Annual Average Total Daily DNI ($Wh/m^2/day$)	**7721**	**7015**	**7161**

From the above tabulated data, it is clear that the total daily DNI values for each of the locations shows strong agreement with the satellite derived DNI values given by NREL (SWERA, 2010) – and used to identify the potential sites in the GIS section of this report – with the annual daily average for each location being higher than the 7.0 $kWh/m^2/day$ required by the GIS analysis. Once again, the monthly variations are also in accordance with the values predicted by the satellite data in the GIS study, and can be compared to those given in Figure 6.2.

Thus although the towns used to approximate the CSP locations are not situated at any specific or optimal identified sites themselves, the weather data was deemed suitable from a DNI perspective to be used for the SAM model. It is noted that is was not possible to compare other weather data characteristics such as temperature, wind speed, wind direction, and albedo, as these variables were not considered in the GIS study and hence there was no means to quantify how they would differ when compared to the local town weather data. It was therefore assumed that the data used in this report was adequate for an initial high-level study, based on the assumption that the DNI data is considered the primary weather factor for CSP plants, however, it is once again recommended to obtain location specific weather data in future studies.

8.2 Financial Inputs and REFIT

8.2.1 Background and Overview

The SAM model contains a detailed financial analysis component, as discussed in Section 7.4, but the majority of the default values included, however, are specific to the United States (U.S.). It was therefore necessary to review the inputs and adjust them to reflect the local costs and environment in South Africa. In order to determine the financial assumptions required for a South African specific model, the draft reports for the South African Renewable Feed-In Tariff (REFIT) were reviewed. The REFIT is a revolutionary set of proposed tariffs, or rates, at which an appointed buyer is obliged to pay any independent power producer (IPP) for energy supplied to the South African national electricity grid. The feed-in tariffs were calculated for a number of various renewable energy technologies, and the assumptions made for their calculation in a South African environment are listed in the draft reports for REFIT Phase I (NERSA, 2009) and Phase II (NERSA, 2010). Of these assumptions, those of key interest comprised; a debt to equity ratio of 70% debt to 30% equity, a real discount rate of 8% for conventional plants and 12% for renewable plants, a tax rate of 28% and a real cost of debt 6.39%.

As a means to validate these values, as well as determine a number of remaining inputs, a study presented by the Electric Power Research Institute (EPRI) on *Power Generation Technology Data for the Integrated Resource Plan of South Africa* (EPRI, 2010) was reviewed. Their study was not only restricted to CSP plants, but covered most forms of modern electricity generation, and provided detailed descriptions of financial, cost and design inputs for each technology type considered. In their analyses, they adopted a debt to equity ratio of 60% debt to 40% equity, a real discount rate of 8.6%, a tax rate of 28% and a real cost of debt of 7.3%. Furthermore they made use of a combined property tax and insurance value of 2% of project value, and assumed a straight line depreciation model over the entire loan term of 30 years.

As can be seen when comparing the two data sets from NERSA and EPRI, the majority of the values are similar, with EPRI seeming to adopt slightly more conservative values in some cases. It was therefore decided to make use of the EPRI values in the cases where they were more conservative, or when NERSA values were not stated, and adopt the NERSA data for all other inputs. An insurance rate of 0.5% was adopted as suggested by Turchi (2010) and the SAM software, and thus a property tax of 1.5% was adopted in order to sum to the combined 2% value given by EPRI.

In order to assure that the inflation rate and tax rate data was as accurate and up to date as possible, the latest data from the South African Revenue Service (SARS) and Statistics South Africa was consulted. SARS (2011) confirmed the 28% federal tax level – with state tax being equal to zero with no differentiation between Federal and State in South Africa – and a sales tax of 14%. Statistics South Africa gave an average inflation rate for the year 2010 of 4.3% which was adopted in the study (StatsSA, 2011).

8.2.2 Definition of Inputs

The finally adopted values used in this analysis, as discussed above, are presented below in Table 8.3. The default SAM values are also included for reference and comparison purposes.

Table 8.3: Financial Inputs for SAM Model. *Source of Data:* EPRI (2010), NERSA (2010), SARS (2011), StatsSA (2011), Turchi (2010).

	Default SAM Value	Value Used in Analysis	Reference
Analysis Period	30 yr	30 yr	Turchi (2010), EPRI (2010)
Inflation Rate	2.5%	4.3%	StatsSA (2011)
Real Discount Rate	8%	8.6%	EPRI (2010)
Federal Tax	35%	28%	NERSA (2010), SARS (2011)
State Tax	8%	0%	
Property Tax	0%	1.5%	Derived from EPRI (2010)
Sales Tax	7.75%	14%	SARS (2011)
Insurance	0.5%	0.5%	Turchi (2010), EPRI (2010)
Loan Term	20 yr	30 yr	EPRI (2010)
Loan Rate	8%	7.3%	EPRI (2010)
Debt Fraction	40%	60%	EPRI (2010)
Depreciation	MARCS Mid-Quarter	Straight Line 30 Years	EPRI (2010)

8.3 Market Choice and Incentives

8.3.1 Electricity Market Choice

As discussed in Section 7.4, the choice of market type for this study is that of a *Utility IPP*. The choice of this market requires a definition of a PPA escalation rate, as well as a minimum required IRR and a minimum DSCR. In the REFIT Phase II document, NERSA (2010) makes use of an IRR value of 17%, which is 2% higher than the 15% default value given in SAM. No mention of any other values was found in the documents by NERSA (2010) or EPRI (2010), and thus it was decided to adopt the value of 17% for the IRR, and the SAM default value for minimum DSCR. Instead of specifying a PPA escalation rate, it was decided to let SAM automatically calculate the value that resulted in the lowest LCOE. The final adopted market inputs are given in Table 8.4 below.

Table 8.4: Market Constraint Inputs for SAM Model. *Source of Data:* SAM (2010).

	Default SAM Value	Value Used in Analysis
PPA Escalation Rate	1.2%	Automatically Minimize
Minimum IRR	15%	17%
Minimum DSCR	1.4	1.4

8.3.2 Tax Credits and Payment Incentives

At the time of writing, the author was not aware of any tax credit incentives nor any payment incentives for utility-scale CSP projects in South Africa. Therefore although SAM does possess the ability to incorporate the effects of tax credit and payment incentives into a project's financial model – as discussed in Section 7.4 – no allowance or inclusion of any incentives was made in this study.

8.4 Review and Compilation of Existing CSP Plant Designs and Costs

In order to accurately model and simulate a CSP plant within the SAM software, it is necessary to posses and input fairly detailed design and cost related data. However, the determination and acquisition of this plant design and costs data presented a fairly difficult task. This was found to be due to a combination of there being relatively few commercially operating CSP plants worldwide when compared to conventional power stations, and the fact that the level of detail of the data required for existing CSP plants is either not freely available, or otherwise not complete in terms of both cost and design specifications.

As a means to obtain the required data, an extensive literature review was conducted to locate detailed plant cost and design data for existing CSP plants worldwide. A spreadsheet database was then constructed in order to record and compare the reviewed data. Of the documents reviewed, all provided differing levels of detail for various aspects of different plants. The focus of some documents leaned more towards system costs, while others toward the design criteria. The sheer quantity and variety of the design and cost specifications represented in a typical CSP plant (and thus in the documents reviewed) also soon proved to be an issue, resulting in the scope and focus of the database becoming extensive and unclear. It was therefore decided to adopt a slightly different and more focused approach, first compiling all the required inputs from the existing SAM model into the database, and then only seeking those equivalent items out of the literature, as a means for comparison. This new approach allowed for a far more concise and focused database to be construed, without sacrificing any of the detail or accuracy required to construct a new SAM model.

The complete comparison database, adapted to fit on multiple A4 pages is presented in the appendices. The database contains comparison data for both parabolic trough and central receiver CSP plants, and comprises system costs and design data for various existing plants as well as the SAM default plants. Data was sourced from – but not limited to – reports and papers from EPRI (2010), Sargent & Lundy (2003), Turchi et al. (2010), Stoddard et al. (2006), Kelly (2006), Romero et al. (2002) and Dersch et al. (2002). Parabolic trough system costs are presented in Appendix B while Appendix C gives central receiver system costs. Parabolic trough design data is presented in Appendix D, while central receiver design data is presented in Appendix E.

After reviewing the constructed comparison database, it was apparent that no one report or paper presented a complete set of the required data, even after the scope had been narrowed as previously described. Furthermore, while some papers were more complete in terms of cost data, and others in design data, further discrepancies arose due to the fact that the existing CSP plants reviewed were of different sizes and ages. In order to accurately construct the complete set of data required, one would then need to obtain scaling factors as a means to compare all plants on an equal power-output size rating, as well as apply financial discounting to account for the different ages of the plants and associated years of their cost data.

The SAM software itself, however, includes a complete set of default data inputs for a number of different CSP plant types and configurations. The data was commissioned by NREL as part of a study conducted to update the ageing default inputs used in the 2009 version of SAM. The study's findings, as well as the plant designs and costs are given in the report by Turchi (2010). According to Turchi (2010), NREL contracted the WorleyParsons Group, Inc to conduct a design and cost analysis of a generic representative parabolic trough plant, with both wet and dry cooling. The 100 MW plant was given nominal design specifications by NREL, before the complete conceptual design and cost assessment was conducted by the WorleyParsons Group. Turchi (2010), continues to state that "the the primary purpose of the WorleyParsons contract was to develop a line-item cost model that SAM users could manipulate to represent cases of interest".

After reviewing the report and study conducted by NREL and the WorleyParsons Group, it was thought best to make use of the default design parameters and baseline costs for all the CSP plants in this study, but only in the instances that more appropriate and location specific South African values could not be identified or calculated. As a means to validate this reasoning, the method was discussed with Bennett (2011), and contact was made with Gilman (2011) who was previously involved with SAM at NREL. Both Bennett and Gilman affirmed the approach, with Gilman continuing to state that the absolute values are less important in the study then the relative metrics, and thus provided that the default assumptions remain constant across locations, and only the variables of interest are varied, the truly valuable information will arise in the comparison of results and effects measured. The various plant data presented in the comparison database already constructed is still included in the report, however, as a means for comparison and validation.

8.5 System Costs

As discussed in Section 8.4, it was decided to make use of the default cost inputs provided in the SAM software – as derived from the study conducted by NREL and the Worley-Parsons Group (Turchi, 2010) – but to then adapt them to equivalent costs that would have occurred had the same plant been constructed in South Africa. It was also decided to conduct the entire analysis with a base year of 2010 in currency terms, primarily due to the fact that this study was begun in 2010. Fortunately, the default SAM inputs were also defined in 2010 by the WorleyParsons Group, and hence listed in 2010 U.S. Dollars. This ensured that they were realistic and current, and also removed the need to make conversions to other years by means of discounting or appreciation.

The costs used in the SAM model could not simply be converted to local South African values by means of the current currency exchange rate, however, as the costs themselves are dependent on local factors such as local expertise and material availability, imports and shipping distances, labour wage rates and labour productivity. It was therefore decided to make use of a method presented and employed by EPRI (2010) in their aforementioned study and report on *Power Generation Technology Data for the Integrated Resource Plan of South Africa*. As previously stated, their study was not restricted to CSP plants only, but covered most forms of modern electricity generation. For all technologies their method remained the same, however, in the fact that the power plant costs were initially established for U.S. based plants with the same design basis and specifications as the South African plant in question. The costs were then adjusted based on adjustment factors developed by EPRI's subcontractor as well as in-house EPRI assumptions. Finally, once the adjustment was completed, the costs were converted to South African Rand by means of the current currency exchange rate.

This method was deemed ideally suited for use in this study owing to the fact that, like the EPRI study, the CSP plant cost data in this study are also given for U.S. based plants and require conversion in order to accurately represent an equivalent South African based plant. The method as well as the adjustment factors will now be discussed in detail for both the *direct* and *indirect* capital costs, as well as the *operation and maintenance* (O&M) costs.

8.5.1 Method for Direct and Indirect Capital Costs

It was first assumed that a portion of the equipment and materials required for the construction of a South African CSP plant would be imported from outside South Africa, while the remainder of the materials and construction labour would be supplied locally. It is also noted that for all CSP technologies included in this study, no provision was made for new infrastructure nor improvements to existing infrastructure, including transmission lines and roads, because as noted by EPRI (2010), these are "generally quite specific and design requirements can vary from one location to another". Based on cost data from the Medupi Coal Power Station Project, as well as in-house data, EPRI estimated the percentage breakdown of both imported and locally available plant components, labour and material costs for each technology. These percentages are given in Table 8.5.

Table 8.5: Assumptions for Percentage Breakdown of Imported and Locally Available CSP Plant Components, Labour and Material Costs. *Source of Data:* EPRI (2010).

Technology	Imported	Locally Available
CSP Parabolic Trough	50%	50%
CSP Central Receiver	50%	50%

It was then assumed that of the estimated breakdown of *local costs*, a certain percentage comprised material and equipment costs while the remainder comprised local labour costs. This was based on EPRI in-house labour to material ratio data, as well as the assumption that 95% of the imported costs were material or equipment costs (EPRI, 2010). These percentages are given Table 8.6.

Table 8.6: Assumptions for Percentage Breakdown of Materials and Labour for Locally Available CSP Costs. *Source of Data:* EPRI (2010).

Technology	Materials (Local)	Labour (Local)
CSP Parabolic Trough	45%	55%
CSP Central Receiver	45%	55%

A set of conversion factors for adjusting the construction costs in the U.S. gulf coast to the cost of construction in South Africa were developed by EPRI's subcontractor, and are given in Table 8.7 below. These conversion factors were then applied to the breakdown of local materials and local labour presented in Table 8.6 above.

Table 8.7: Conversion Factors for U.S. to South African Local Materials, Local Labour Productivity and Local Labour Wage Rate. *Source of Data:* EPRI (2010).

Category	Materials Factor (Local)	Labour Productivity Factor (Local)	Labour Wage Rate (Local)
Civil	1.00	1.75	0.72
Concrete	1.00	1.75	0.72
Structural Steel	1.00	2.10	0.57
Mechanical	1.00	2.10	0.67
Piping	1.10	2.25	0.68
Valves	1.10	2.25	0.68
Insulation	1.00	2.00	0.62
Electrical Bulks	1.00	1.95	0.52
Instrumentation	1.15	1.95	0.52
Painting	1.00	1.80	0.76
Electrical Equipment	1.00	1.90	0.62
Value Used	**1.00**	**2.10**	**0.65**

From the above data it can be seen that the majority of the materials used in the construction of power plants in South Africa are expected to cost approximately the same as in the U.S. This is due to the fact that the majority of the raw materials required are mined and refined locally (leading to less expensive pricing compared to the U.S.) but that less advanced production techniques and lower labour productivity in South Africa subsequently offset this.

The predicted lower labour productivity in South Africa also causes an increase in the hours required to complete the construction, with an increase ranging from 75% to 125% more labour hours. At the same time, however, the labour wage rates are lower in South Africa compared to the U.S., ranging from 24% to 48% lower. Thus in accordance with the recommendations made by EPRI's subcontractor, an average adjustment factor of 1.00 for materials, 2.10 for labour productivity, and 0.65 for labour wage rates was applied across all their respective cost divisions (EPRI, 2010).

Of the percentage of costs given in Table 8.5 that represent imports, no division was made between labour and materials, and only an shipping factor was applied. It was assumed, however, that the shipping factor would remain 1.00 based on the further assumption that the same transportation costs applied for shipping to the U.S. and South Africa (EPRI, 2010). This in turn resulted in the imported cost remaining the same as the U.S.

Therefore based on the aforementioned breakdowns and factors, the U.S. based direct and indirect capital costs were adjusted to South African costs in the following manner:

1. Each direct and indirect capital cost item was broken down into an imported portion and a locally available portion as per the percentages given in Table 8.5.
2. The imported portion of the cost was assumed to remain the same as the U.S. imported cost.
3. The locally available portion of the cost was then broken down into a materials portion and a labour portion as per the percentages given in Table 8.6.
4. These local material and labour portions were then converted to South African equivalent costs by means of the adjustment values given in Table 8.7.
5. The converted imported and local costs were then all combined to give the final equivalent South Africa cost (still in 2010 U.S. Dollars) for the particular direct or indirect capital cost in question.

It was decided not to complete the final conversion to South African Rand by means of the currency exchange rate at this point, however, due to the fact that the SAM software is based in U.S. dollars. It was instead decided to run the SAM software models using the above calculated South African equivalent U.S. Dollar values, and subsequently convert the final outputs of the model to South Africa Rand by means of the exchange rate. This method has the added benefit of allowing for easier comparisons and validation of the SAM output data to other existing CSP plant data (which is already given in U.S Dollars) at different steps of the analysis process.

A visual representation of the entire conversion process for direct and indirect capital costs is presented in Figure 8.5 in the form of a flow diagram.

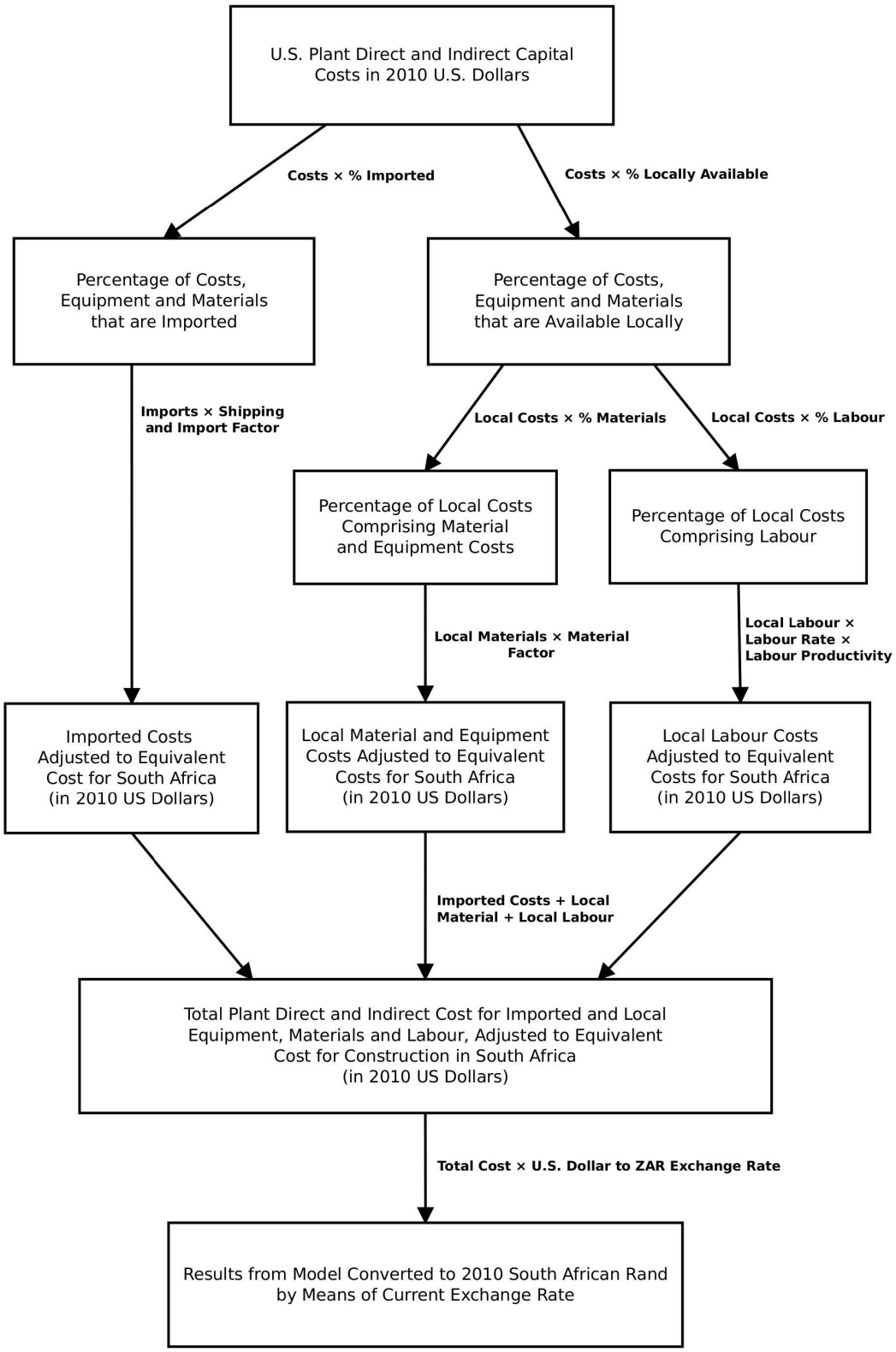

Figure 8.5: Visualisation of Method for Estimating and Converting Foreign CSP Plant Direct and Indirect Capital Costs to South African Based Equivalents.

8.5.2 Method for Operation and Maintenance Costs

The CSP plant operation and maintenance (O&M) costs also required adjusting to to South African conditions and currency. The method adopted for converting the O&M costs was similar to that of the direct and indirect capital costs described in Section 8.5.1. Based on the assumption that *fixed* O&M costs are often scaled with the capital costs of a plant, the same adjustment factors and conversion method used for the direct and indirect capital costs was adopted (EPRI, 2010), namely:

1. Each fixed O&M cost item was broken down into an imported portion and a locally available portion as per the percentages given in Table 8.5.
2. The imported portion of the cost was assumed to remain the same as the U.S. imported cost.
3. The locally available portion of the cost was then broken down into a materials portion and a labour portion as per the percentages given in Table 8.6.
4. These local material and labour portions were then converted to South African equivalent costs by means of the adjustment values given in Table 8.7.
5. The converted imported and local costs were then all combined to give the final equivalent South Africa cost (still in 2010 U.S. Dollars) for the particular O&M cost in question.

Variable O&M costs, however, prove more difficult to analyse with this method, and thus could not be broken down with material and labour factors (EPRI, 2010). Thus for *variable* O&M costs, only a currency exchange rate was applied after the completion of the SAM analysis. A visual representation of the entire conversion process for fixed and variable O&M costs is presented in Figure 8.6 in the form of a flow diagram.

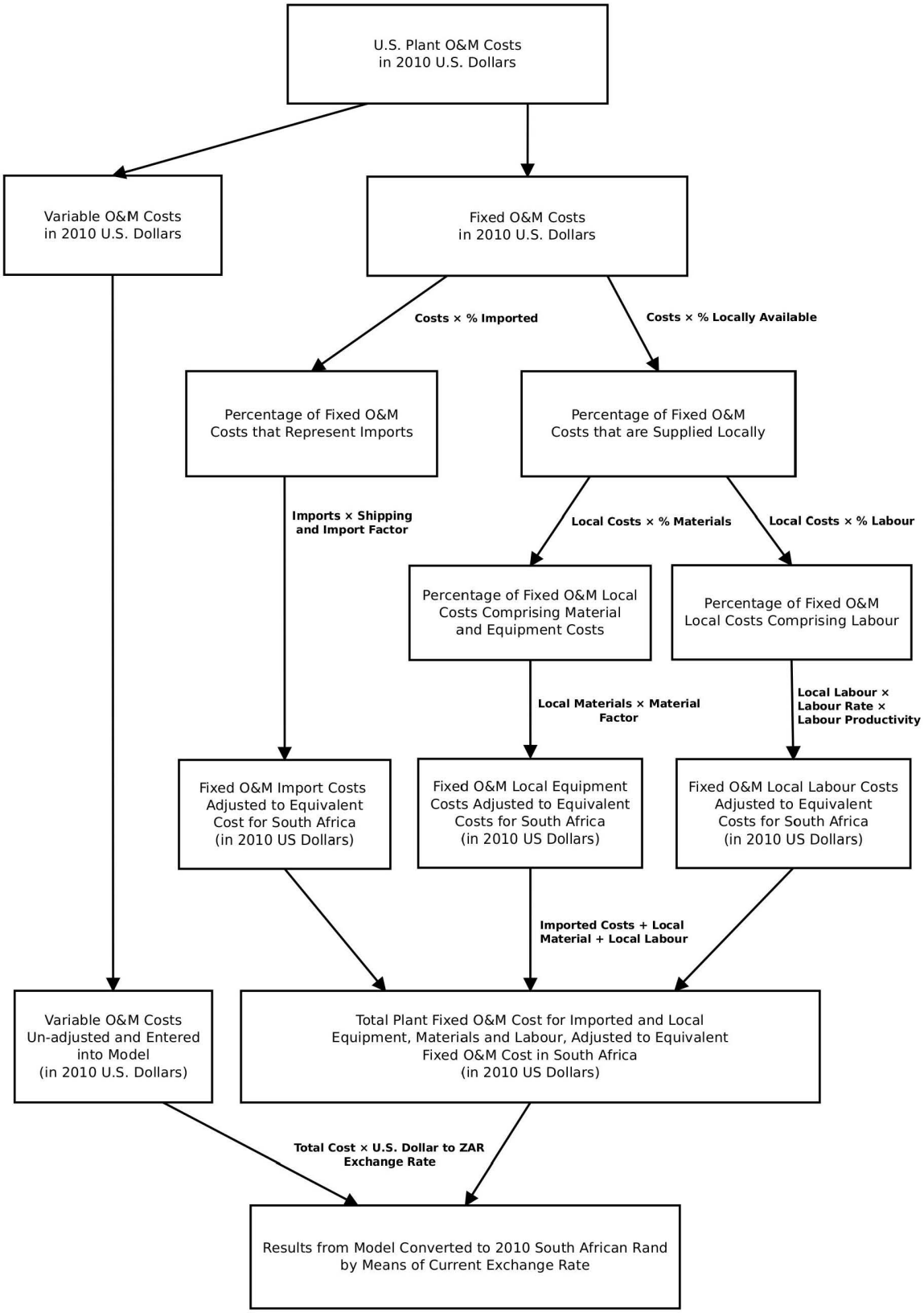

Figure 8.6: Visualisation of Method for Estimating and Converting Foreign CSP Plant O&M Costs to South African Based Equivalents.

8.6 Cost of Water

8.6.1 Background and Incorporation

The availability of cooling water, or lack thereof, is a key area of focus in this study, and its representation in the SAM model was therefore given specific consideration. The SAM software does not allow for, nor present a specific input dedicated to the cost or consumption of cooling water, and it was thus necessary to devise another means to represent it in the model. After discussion with Gilman (2010), it was recommended to incorporate the cost and use of cooling water by means of an additional user-defined O&M cost.

SAM offers the user the ability to add an O&M cost either as a fixed cost by capacity (in $/kW.yr), or as a variable cost by generation (in $/MWh). As the consumption of cooling water is directly dependent on the amount of power produced and not linked directly to the name plate capacity of the plant, it was decided to incorporate it as a variable O&M cost by generation (in $/MWh).

8.6.2 Method of Calculation

As no South African cooling water consumption data was found for parabolic trough or central receiver CSP plants in the required units of $/MWh (or R/MWh), a method was devised in order to calculate the required inputs. The review of cooling technologies in Chapter 4 provided data for water consumption of parabolic trough and central receiver plants. This data was extracted from Table 4.1 and the values used presented in Table 8.8. For the case of wet cooling for central receiver plants where a range of values was given, the average value of 625 Gallons per MWh (2.37 litres/kWh) was used. These values were then converted to metric units of kilolitres/MWh.

The next step in the calculation process required the determination of cost data for large quantities of cooling water from the local South African municipalities in the areas surrounding the potential sites. Initial searches only revealed the commercial and industrial treated water tariffs for City of Johannesburg Council, at a stated value of R14.82 per kl for consumption exceeding 200 kl (City of Johannesburg Council, 2011). It was therefore decided to contact the South African Department of Water Affairs (DWA) to obtain local tariffs for both treated and untreated water. Van der Merwe (2011) from the DWA stated that the unit charges for bulk raw water supplied from departmental water resource infrastructure to large Eskom coal-fired power stations in the Mpumalanga highveld region

– which supply base-load electricity to the national electricity grid – currently vary from around R2.30 to R8.25 per kl, depending on the physical attributes of the water supply infrastructure. These costs exclude any treatment cost of the raw water for cooling purposes, which would occur at the plant in addition to the aforementioned departmental unit charges. As these costs represent a fairly large range, further inquiry was made, and it was determined that one supplier, Namakwa Water in the Lower Orange River area, contended that it was able to supply its customers with bulk treated water at a cost of R5.50 per kl, although the sustainability of this supply at this price is not known (Van der Merwe, 2011).

As a final means to obtain a reasonable value for the cost of cooling water, the Sargent & Lundy (2003) report for NREL on the *Assessment of Parabolic Trough and Power Tower Solar Technology Cost and Performance Forecasts* was consulted. In their report, a review is given of the SunLab cost model, where SunLab estimates (based on the SEGSVI/VII CSP plants) give a raw water cost of $0.32 per kl, and treatment costs of $0.043 and $0.540 per kl for cooling water chemical treatment and demineralizer chemical treatment respectively. Thus at a rand-dollar exchange rate of R7.02 to the U.S Dollar as of the 16th May 2011 (Bloomberg, 2011) the SunLab raw water cost of $0.32 equates to a cost of approximately R2.25, which is very similar to the lower limit of R2.30 as stated by Van der Merwe (2011).

It was finally decided, however, to employ a conservative approach and adopt an average value from Van der Merwe (2011) of approximately R5.28 for raw water costs, but then to vary the range during the sensitivity analysis as described in Chapter 10. When converted using the aforementioned exchange rate, this resulted in a raw water cost of $0.75 per kl. The chemical treatment and demineralization costs from SunLab were then added to the raw water cost to yield the total cooling water cost in $/kl, as given in Table 8.8.

The final step in the calculation process was then to multiply the total cooling water cost in $/kl by the water usage in kl/MWh to obtain the final cooling water O&M cost in $/MWh. The results of the final calculation for each technology are give in Table 8.8. It is also noted that for the remainder of this report, the term 'wet cooling' will refer to the technology of recirculating wet cooling, as once through wet cooling is not a considered technology in this analysis.

Table 8.8: Values Used in Calculation of O&M Cost of Cooling Water for Various Power Plants using Different Cooling Technologies. *Source of Data:* DOE, U.S. (2010), Van der Merwe (2011), Sargent & Lundy (2003).

	Parabolic Trough		Central Receiver	
	Wet Cooling	Dry Cooled	Wet Cooling	Dry Cooled
Water Usage (Gallons/MWh)	800	78	625*	90
Water Usage (kl/MWh)	3.028	0.295	2.366	0.341
Raw Water Cost (R/kl)	5.275*	5.275*	5.275*	5.275*
Raw Water Cost ($/kl)	0.751	0.751	0.751	0.751
Cooling Water Chemical Cost ($/kl)	0.043	0.043	0.043	0.043
Demineraliser Chemical Cost ($/kl)	0.540	0.540	0.540	0.540
Total Water Cost ($/kl)	1.334	1.334	1.334	1.334
Calculated Cooling Water O&M Cost ($/MWh)	**4.04**	**0.39**	**3.16**	**0.45**

* Average Value

8.7 Final Locally Adjusted Cost Inputs for SAM

The conversion method as described in Section 8.5 was applied to the default cost data supplied with the SAM software, which is recorded in Appendix B and Appendix C. The additional cost for cooling water as calculated in Section 8.6 was then added to the existing O&M variable cost by generation section. The results from the conversion process and the final cost inputs as used in the SAM software model are recorded below in tabular format. Table 8.9 lists the final calculated inputs for the parabolic trough plant, while Table 8.10 lists the final calculated inputs for the central receiver plant. The final cost inputs for the various parabolic trough and central receiver models are also listed in their entirety in Appendix F and Appendix G respectively.

Table 8.9: Locally Adjusted Final Cost Inputs as Used in SAM Models for Parabolic Troughs.

Parabolic Trough	**Wet Cooled**	**Dry Cooled**
Direct Capital Costs		
Site Improvement	22.008 $/m^2	
Solar Field	385.131 $/m^2	
HTF System	55.019 $/m^2	
Storage	77.026 $/kWh$_{th}$	
Fossil Backup	0.000 $/kW$_e$	
Power Plant	1012.345 $/kW$_e$	1254.428 $/kW$_e$
Contingency	10%	
Indirect Capital Costs		
Engineer, Procure, Construct	15% of Direct Cost	
Project, Land, Management	3.5% of Direct Cost	
Sales tax Applies to:	80% of Direct Cost	
O&M Costs		
Fixed Annual Cost	0.000 $/yr	
Fixed Cost by Capacity	88.030 $/kW.yr	
Variable Cost by Generation	7.040 $/MWh	3.390 $/MWh
Fossil Fuel Cost	0.000 $/MMBTU	

* Unadjusted value left as SAM default

Table 8.10: Locally Adjusted Final Cost Inputs as Used in SAM Models for Central Receivers.

Central Receiver	Wet Cooled	Dry Cooled
Direct Capital Costs		
Site Improvement	22.008 $/m^2	
Heliostat Field	221.175 $/m^2	
Balance of Plant	379.629 $/kW$_e$	
Power Block	632.716 $/kW$_e$	874.798 $/kW$_e$
Storage	33.011 $/kWh$_{th}$	
Fixed Solar Field Cost	$ 0.000	
Fixed Tower Cost	$ 991,988.06	
Tower Cost Scaling Component	0.01298	
Fossil Backup	0.000 $/kW$_e$	
Receiver Reference Cost	$ 65,085,970.84	
Receiver Reference Area	1110 m^2	
Receiver Scaling Component	0.7	
Contingency	10%	
Indirect Capital Costs		
Engineer, Procure, Construct	15% of Direct Cost	
Project, Land, Management	3.5% of Direct Cost	
Sales tax Applies to:	80% of Direct Cost	
O&M Costs		
Fixed Annual Cost	0.000 $/yr	
Fixed Cost by Capacity	88.030 $/kW.yr	
Variable Cost by Generation	6.160 $/MWh	3.450 $/MWh
Fossil Fuel Cost	0.000 $/MMBTU	

* Unadjusted value left as SAM default

8.8 Parabolic Trough Design Specifications

The following sections will cover some of the key plant design and performance related inputs for the parabolic trough models in SAM. For the sake of brevity, only the inputs which have been specifically adapted for South African conditions, or otherwise modified from the SAM default inputs, will be covered in the following sections. A full list of the SAM default design inputs for the parabolic trough model is presented in Appendix D, while the final design and performance inputs used in this study for the parabolic trough models are presented in Appendix F.

8.8.1 Design Gross Output and Nameplate Capacity

As stated in Section 8.4 it was decided to adopt the WorleyParsons Group, and SAM default parabolic trough plant size of 100 MW nameplate capacity. This approach was adopted as all technical and design related data included in SAM is specific to a plant of this size. Furthermore, 100 MW is also the plant capacity adopted by Eskom (2006) for their prosed central receiver plant in the Northern Cape. In order to produce a nameplate capacity of 100 MW, a gross design output of 110 MW was required to account for the parasitic and other losses in the system (SAM, 2010). Although this value has not been changed from the SAM default, it is included in this section as a reference and reminder of the parabolic trough plant size in this study.

8.8.2 Availability and Performance

According to EPRI (2010), parabolic troughs are expected to have an annual availability of up to 95%. This is due to the existing commercial nature of parabolic trough plants, as well as the fact that the solar fields do not operate at night, thereby allowing for much of the maintenance to take place during this down time. Furthermore, the modular nature of the SCAs and HCEs means that repairs can be carried out on a single unit, while the remainder of the plant remains in operation.

As no mention of any degradation assumptions are made in the EPRI (2010) study, it was decided to adopt the SAM default value of 0% degradation, which assumes adequate maintenance is conducted on the plant throughout its lifetime.

8.8.3 Solar Irradiation Design Point Calculation

The solar irradiation design point value is generally defined as the maximum annual incident DNI value (in W/m^2) experienced at a location in a typical meteorological year. SAM makes use of this value to calculate the required solar field aperture from the user-specified solar multiple value. According to the SAM (2010) documentation, the choice of this value is of great importance, as the value has a significant impact on the calculated field aperture size. An example is given where a 110 MW plant with a solar multiple of 2 and an irradiation design point value of 950 W/m^2 requires a field aperture of 862,000 m^2, but the same system with an irradiation design point value of 800 W/m^2 requires a field aperture of 1,030,000 m^2. It is thus imperative to make use of an accurate value, as choosing too low a value will result in an oversized solar field which would then lead to excessive collector defocusing. Conversely, too high a value would result in an undersized solar field which can rarely drive the power block at its rated capacity.

The SAM documentation continues to state that an irradiation design point value of 950 W/m^2 would be suitable for a plant in the Mojave Desert in the U.S. while a value of 800 W/m^2 is typical for Southern Spain. It is suggested, however, to calculate the correct maximum irradiation design point value for each location being modelled, by making use of the location weather data and the field collector tilt and azimuth. This value can be calculated in SAM by the following method:

1. Initialise a parabolic trough simulation in SAM.
2. Choose and input the weather data for the site in question.
3. Adjust the solar field collector tilt and azimuth values from their default values of 0° tilt and 0° North-South orientations.
4. Run the simulation and view the hourly result database.
5. The maximum annual incident DNI value for each hour of the simulation is given by the the $Collector\_DNI\text{-}x\text{-}CosTh$ variable.
6. This data can then be exported and examined in a spreadsheet program in order to determine the absolute maximum value and hence the irradiation at design value.

The maximum annual incident DNI value, and hence the irradiation design point value, was calculated for the Upington, Springbok and Bloemfontein locations by following the above procedure. The resulting values are presented in Table 8.11.

Table 8.11: Calculated Solar Irradiation Design Point Values for Upington, Springbok and Bloemfontein.

	Calculated Solar Irradiation Design Point (W/m^2)	Value Used in Analysis (W/m^2)
Upington	1088.1	1088
Springbok	1084.1	1084
Bloemfontein	1085.4	1085

Although the calculated values above are slightly higher than the 950 W/m^2 values assumed for the Mojave Desert in the U.S., this is to be expected, as according to the Edkins et al. (2009) as stated in Section 6.3.1, the Northern Cape receives average annual daily DNI values which are though to be some of the highest worldwide, and in excess of areas such as California. This is further confirmed by the solar resource maps created for South Africa in the GIS section of this report.

8.8.4 Cooling Technology Choice

It has already been noted that the use of cooling water – and hence cooling technology choice – is one of the key points of interest in this study. It was therefore necessary to consider and model both a parabolic trough plant with wet cooling and one with dry cooling for each location, in order to ascertain the effects the cooling technology choice would have on water use, efficiency and ultimately cost.

The SAM software presents the user with a choice of two standard library models for cooling systems, namely an evaporative wet cooled system and an air-cooled condenser (dry cooled) system. For each location, one parabolic trough model was set up with wet cooling, and a second model with dry cooling. The resulting design-related input data for each technology is presented in Table 8.12. It is noted that for the case of wet cooling, the ambient temperature at design is the wet bulb temperature, while for the dry cooled system, the ambient temperature at design is the dry bulb temperature. The reference condenser water temperature change value and approach temperature are specific to evaporative cooling only, and are used by SAM in the calculation of the cooling water mass flow rate and turbine back pressure. Similarly, the initial temperature difference at design point value and condenser pressure ratio are specific to dry cooling only, and are used by SAM in the calculation of the pressure drop across the condenser and the corresponding parasitic power required to maintain the air flow rate (SAM, 2010).

Table 8.12: Parabolic Trough Cooling Technology Design Input Variables. *Source of Data:* SAM (2010).

Parabolic Trough	Wet Cooling	Dry Cooling
Condenser Type	Evaporative	Air-cooled
Ambient Temperature at Design	20 ℃	33 ℃
Reference Condenser Water dT	10 ℃	–
Approach Temperature	5 ℃	–
Initial Temperature Difference at Design Point	–	16 ℃
Condenser Pressure Ratio	–	1.0028
Power Block Rated Cycle Conversion Efficiency	0.3774	0.3390
Steam Cycle Blowdown Fraction	0.013	0.016

It is noted that the overall efficiency of the power block when running on a wet cooling cycle is higher than that of dry cooling, which is to be expected. In addition, the steam cycle blowdown fraction – which accounts for water used in steam cycle make-up and replenishment – is higher for dry cooling in order to account for wet-surface air cooling for critical Rankine cycle components (SAM, 2010).

8.8.5 Solar Multiple Optimisation

The solar multiple of a CSP system is defined as the ratio between the thermal power produced by the solar field at its design point, and the thermal power required by the power block under normal operational conditions (Montes et al., 2009). A solar multiple of 1.0 would imply that the solar field of a plant is just sufficient to drive the power block at full rated capacity when experiencing its maximum DNI design point value. A typical parabolic trough plant with a solar multiple of 1.0 would therefore only operate at its design point for only a few hours of every year. In an attempt to overcome this limitation, the majority of CSP plants possess oversized solar fields – and hence solar multiples greater than 1.0 – thereby allowing the plant to operate closer to its design point for more hours of the year. However, over-sizing the soar field does mean that excess thermal energy will be generated during times of high solar irradiation. In a system without storage, this excess energy is lost, while in a system with thermal energy storage, this excess energy will be diverted to the storage system for later use (Montes et al., 2009; SAM, 2010). This process is illustrated graphically in Figure 8.7.

A system with a solar multiple greater than 1.0 therefore produces more electricity, consequently reducing the system's LCOE. The increase in solar field size also increases the capital and O&M costs of the plant, however, and hence a balance needs to be found

between the increased electricity production and increased system cost. In most systems, a turning point will be reached, after which the higher system cost associated with increasing the solar multiple outweighs the benefit of the added electricity production. The complexity of the relationship is also increased when one considers a system with thermal storage, as TES can increase electricity output by storing energy from an even larger solar field, but has associated higher system costs and thermal losses. According to the SAM documentation, the optimal solar multiple for a parabolic trough system with no storage is between 1.4 and 1.5, while that for a system with storage is generally higher.

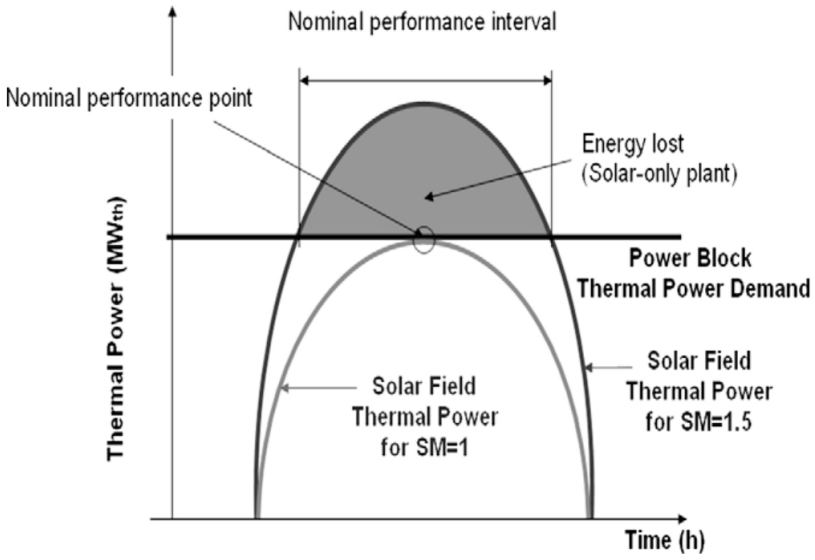

Figure 8.7: Daily Thermal Power Production from a Plant with No Thermal Storage for Different Solar Field Multiples (Montes et al., 2009).

In order to determine the optimal solar multiple value for each plant in this study, for all locations and cooling technologies, a parametric analysis within the SAM software was chosen. This method is recommended by the SAM documentation, due to the complex relationship between the solar multiple and LCOE for a plant with storage. For each of the parabolic trough models, both wet and dry cooled, and at each location, a simulation was run to calculate the LCOE of the plant with solar multiples ranging from 1.0 to 3.0 in increments of 0.1. Thus for each model with 6 hours of thermal storage, 21 simulations were run. The results were then exported to a spreadsheet program for analysis and graphing purposes. The simulations took a fair amount of time to run, and thus the incremental resolution was not increased to below 0.1. This value was considered acceptable, however, as the SAM software defaults to an increment of only 0.25. The graphic results of the optimisation process for each plant type situated at Upington, Springbok and Bloemfontein are presented in Figure 8.8, Figure 8.9 and Figure 8.10 respectively.

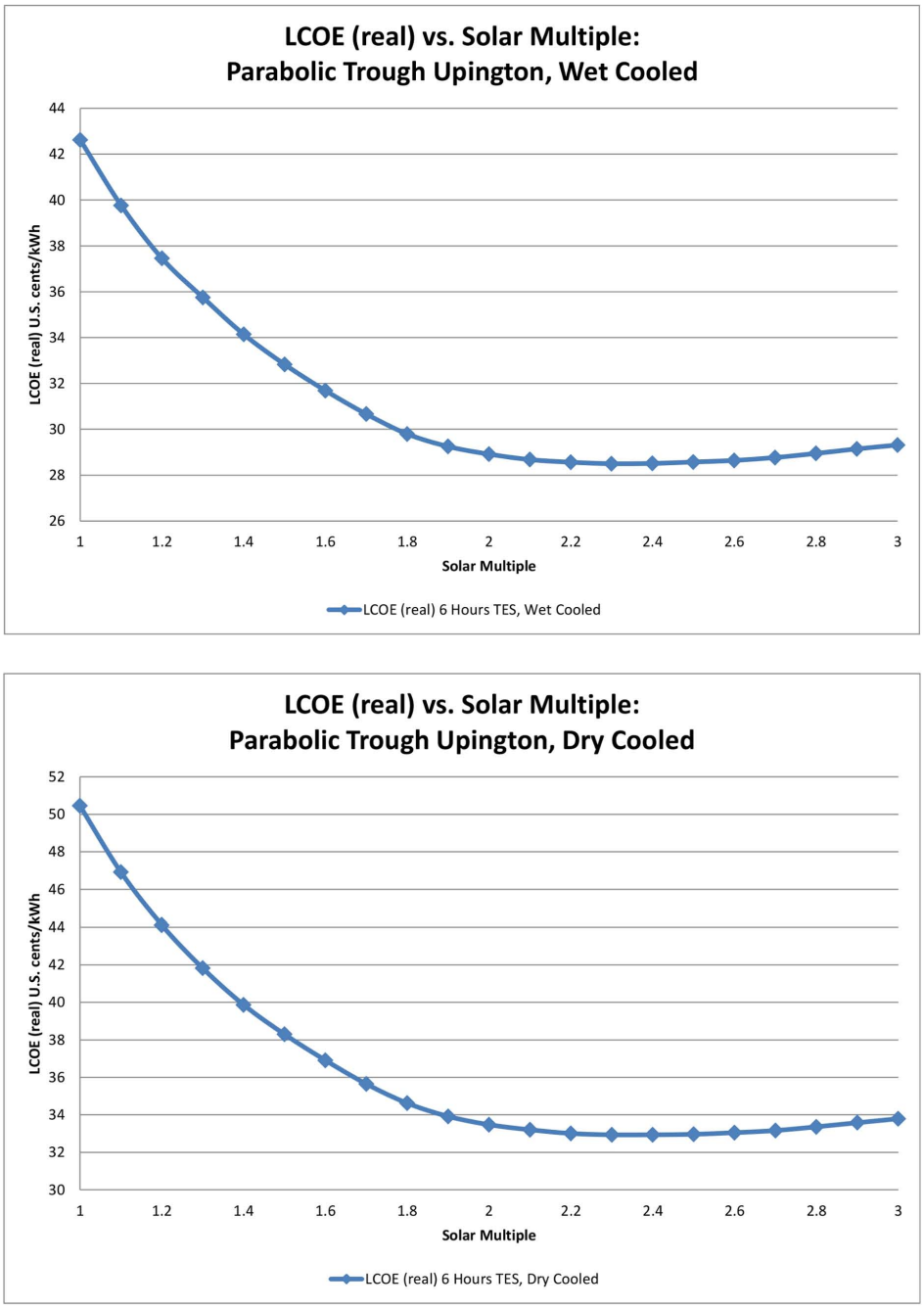

Figure 8.8: LCOE as a Function of Solar Multiple for Wet and Dry Cooling, Used to Determine Optimal Solar Multiple Value for Upington.

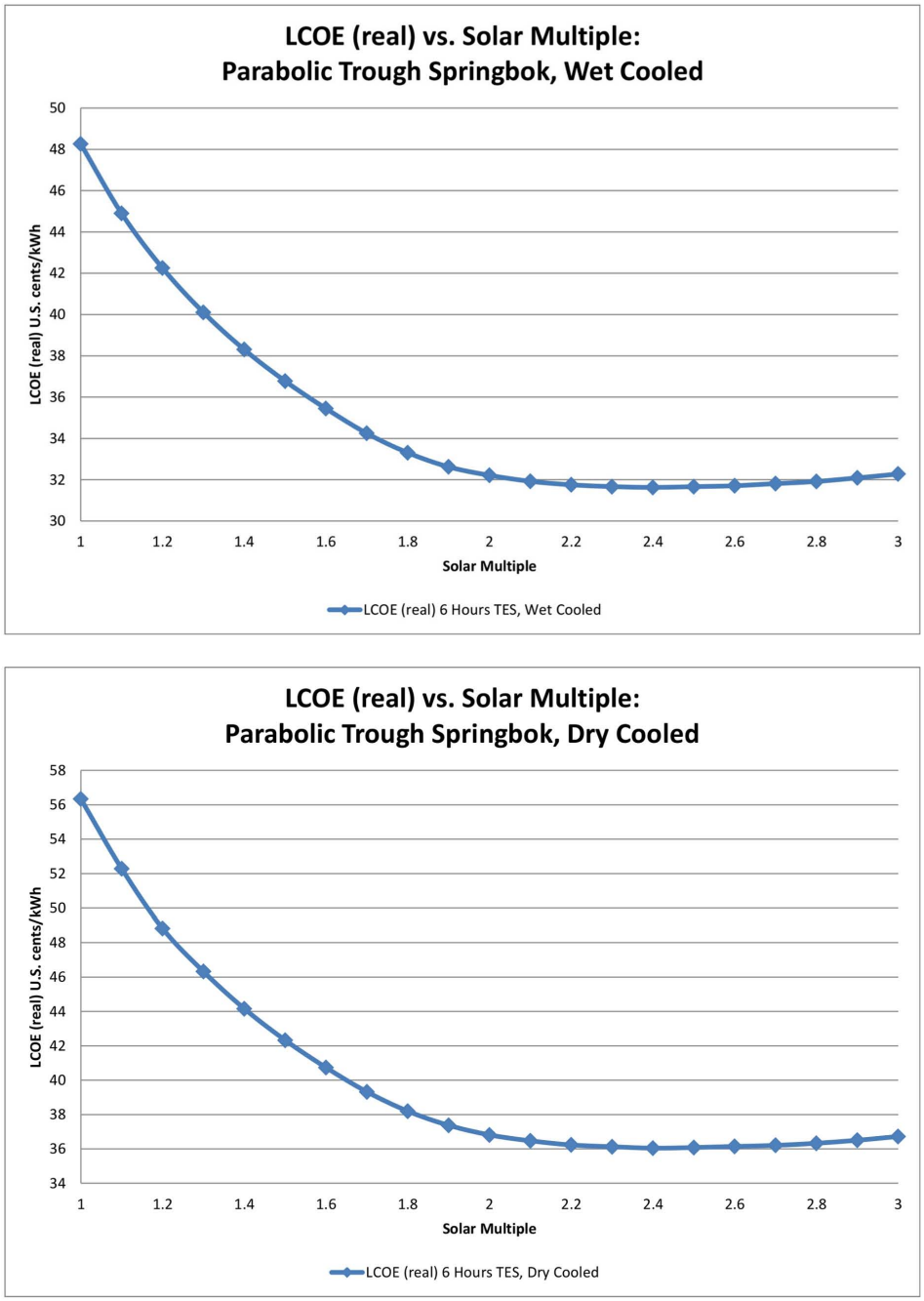

Figure 8.9: LCOE as a Function of Solar Multiple for Wet and Dry Cooling, Used to Determine Optimal Solar Multiple Value for Springbok.

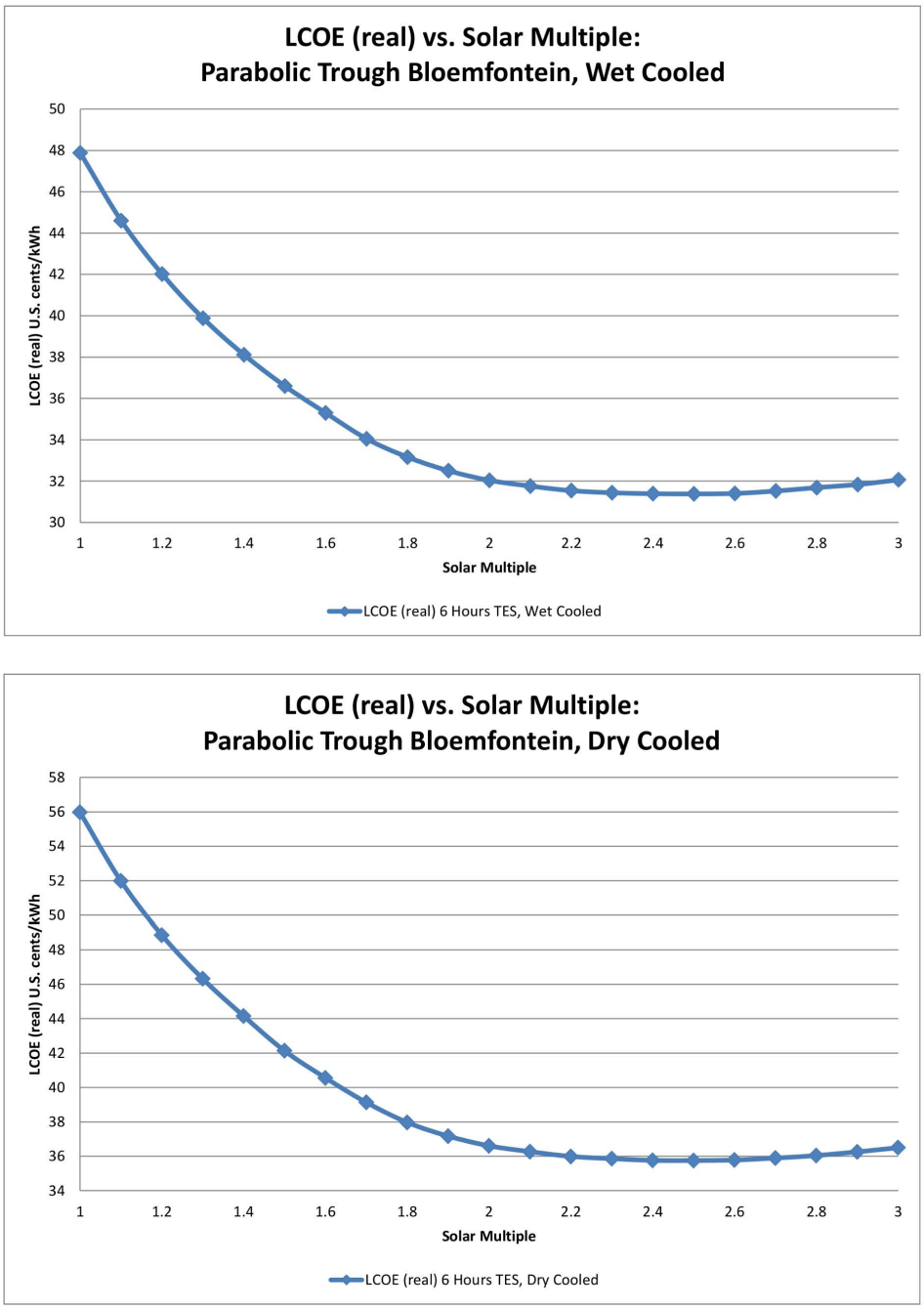

Figure 8.10: LCOE as a Function of Solar Multiple for Wet and Dry Cooling, Used to Determine Optimal Solar Multiple Value for Bloemfontein.

From the graphs, it is evident that the LCOE initially decreases rapidly with an increase in solar multiple, until it is eventually overwhelmed by the increasing system costs. For all three locations, the optimal solar multiple value occurs in the region of 2.3 to 2.5, with a slight variation in each location. Although there is an obvious difference in LCOE price between wet cooled and dry cooled systems, both system types possessed the same optimal solar multiple in each location. The optimal solar multiple values determined and used in the remainder of this study for each cooling technology and each location are presented in Table 8.13.

Table 8.13: Calculated Optimal Solar Multiples for Parabolic Trough Models with Wet and Dry Cooling in Upington, Springbok and Bloemfontein.

Location	Optimal Solar Multiple for Parabolic Trough Model	
	Wet Cooling	Dry Cooling
Upington	2.3	2.3
Springbok	2.4	2.4
Bloemfontein	2.5	2.5

As a means of validating the above results, the graphs from the solar multiple optimisation in this study were compared to those found by Montes et al. (2009) and depicted in Figure 8.11. The same shape and trend is found in both, while the difference in position of the optimal solar multiple observed is primarily due to the exclusion of thermal storage in the Montes et al. study. The optimal solar multiple values of 2.3 to 2.5 found in this study are also strongly comparable to the values of between 2.0 and 2.25 found in the SAM documentation optimisation example of a plant with 6 hours TES (SAM, 2010).

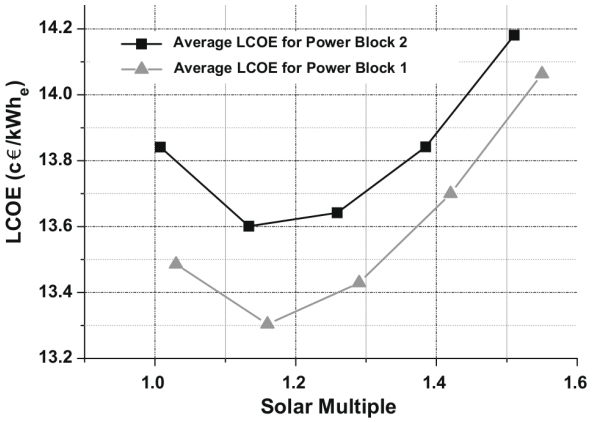

Figure 8.11: Average Electricity Cost for Every Solar Multiple Considered and Two Configurations of the Power Block with No Storage (Montes et al., 2009).

8.9 Central Receiver Design Specifications

As with the parabolic trough model, the following sections will cover some of the key plant design and performance related inputs for the central receiver models in SAM. Once again, for the sake of brevity, only the inputs which have been specifically adapted for South African conditions, or otherwise modified from the SAM default inputs, will be covered in the following sections. A full list of the SAM default design inputs for the central receiver model is presented in Appendix E, while the final design and performance inputs used in this study for the central receiver models are presented in Appendix G.

8.9.1 Design Gross Output and Nameplate Capacity

As for the case of the parabolic trough models, a plant size of 100 MW nameplate capacity was adopted for all central receiver models. Once again, a gross design output of 110 MW was needed in order to produce a nameplate capacity of 100 MW due to parasitics and losses. Although this value has not been changed from the SAM default, it is included in this section as a reference.

8.9.2 Availability and Performance

EPRI (2010) state that central receivers are expected to have an availability of 92%, which is less than the 95% for parabolic troughs. This is primarily due to the early commercial status of central receivers, however, this value is expected to increase in the future as more systems are deployed. For this analysis, the stated value of 92% was adopted.

As with the parabolic trough model, it was also decided to adopt the SAM default value of 0% degradation, which assumes that adequate maintenance is conducted on the plant throughout its lifetime.

8.9.3 Tower, Heliostat Field and Solar Multiple Optimisation

The central receiver optimisation wizard attempts to locate the best design parameters for the heliostat field, tower and receiver by searching through a discrete number of inputs defined by the search range. However, all calculations are based on a specified solar multiple value for the model in question, whose value is *not* varied or optimised by the wizard. As in the case of the parabolic trough model, the optimal solar multiple value for the central receiver plants at each location was also unknown prior to the analysis. It

was therefore decided to first run the optimisation wizard with a number of different solar multiples covering a similar range of values to those for the parabolic trough models, for each cooling technology type and at each location, but to retain the default search ranges and increments. The wizard would then define the optimal heliostat field layout, tower height and receiver dimensions for *that particular* solar multiple. Subsequently, using the resulting heliostat field layout, tower and receiver dimensions for that particular solar multiple, a full simulation was then run for each possible configuration in order to determine which solar multiple produced the heliostat field layout, tower height and receiver design which resulted in the lowest LCOE.

The results for each optimisation wizard run with each solar multiple, and full simulation calculated LCOE are presented in the following sections. For the sake of brevity, the full heliostat field layout, tower, and receiver dimensions will not be presented for each and every optimisation wizard run, but only for the run with the *optimal* solar multiple which resulted in the lowest LCOE in the full simulation.

Solar Multiple Optimisation

From the results of the previous solar multiple optimisation performed in the parabolic trough model, it was expected that the optimal solar multiple would occur in the region of 2.0; however, in order to determine the optimal solar multiple values for each plant, the solar multiple values were iterated from 1.0 to 2.6, by which stage it could be observed that the turning point had been passed. As was the case for the parabolic trough models, the calculated LCOE values from the simulation runs for each solar multiple were then exported to a spreadsheet program for analysis and graphing purposes. Due to the added step of having to run the tower and heliostat optimisation wizard first for each solar multiple value (and hence not being able to make use of a parametric analysis) the simulation and optimisation process took a fair amount of time to complete. The same parabolic trough incremental resolution of 0.1 was therefore adopted. The graphic results for the variation of LCOE with solar multiple for central receiver plants at all locations utilising wet cooling technology are presented in the first graph of Figure 8.12, while those for dry cooling at all locations are presented in the second graph of Figure 8.12.

The graphic results suggest that the optimal solar multiple for all the central receiver plants with *wet* cooling at all three locations in this study is 2.0. Similarly, the predicted optimal solar multiple for all the central receiver plants with *dry* cooling at all three locations in this study is 1.9. These values are strongly comparable to the solar multiple value of 1.9 as used by the SAM example central receiver model with 6 hours TES in California, and were therefore adopted for the remainder of this study.

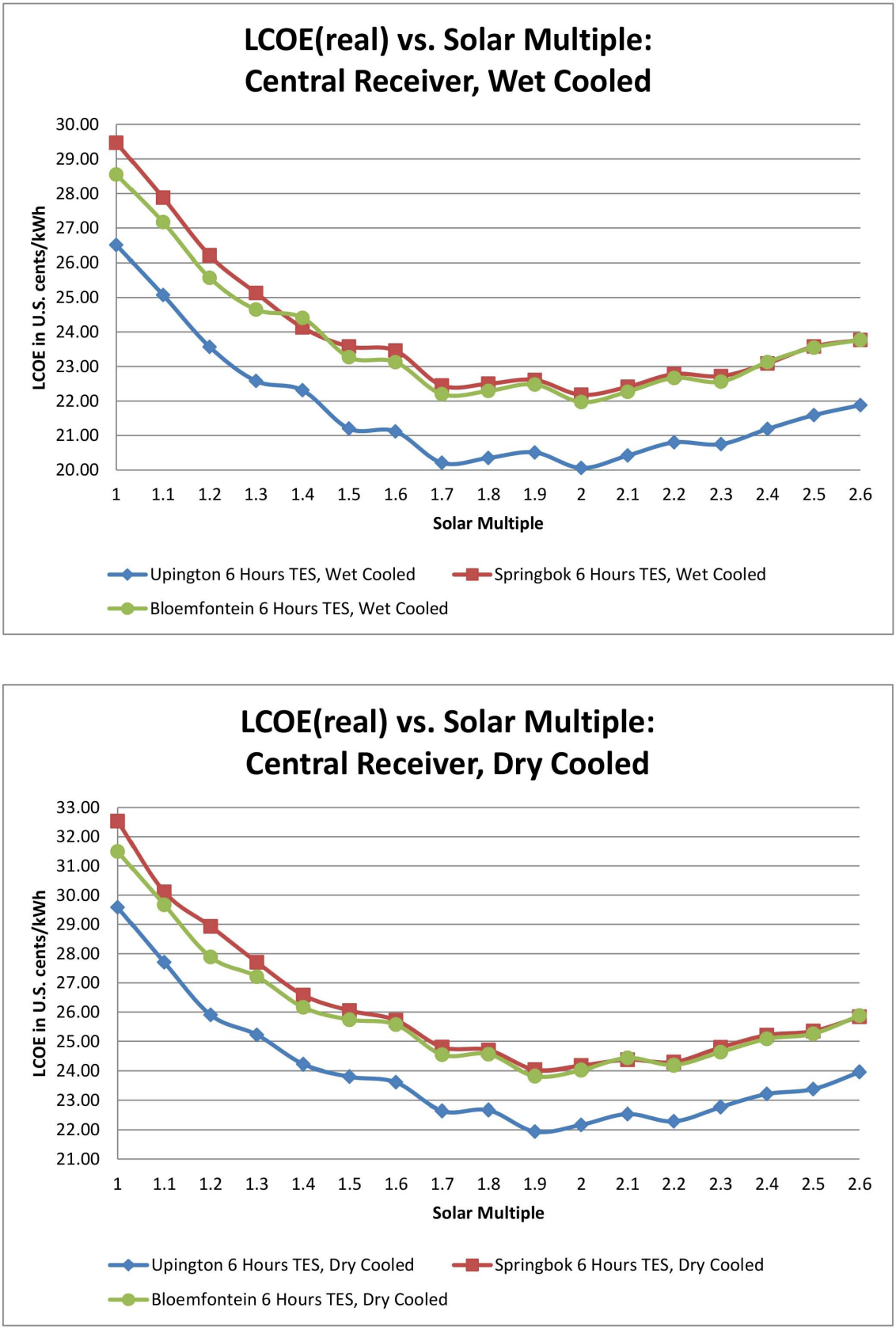

Figure 8.12: LCOE as a Function of Solar Multiple for Wet and Dry Cooling, Used to Determine Optimal Solar Multiple for Central Receiver Plants.

Heliostat Field Layout and Characteristics

The optimal heliostat field layouts generated by the optimisation wizard for each location and each cooling technology type – utilising a solar multiple of 2.0 for wet systems and 1.9 for dry systems – are depicted visually in Figure 8.13 and Figure 8.14. Each image represents an aerial view of the circular fields, which are divided into 12 radial segments with 12 rows each. The darker red areas indicate a higher density of heliostats.

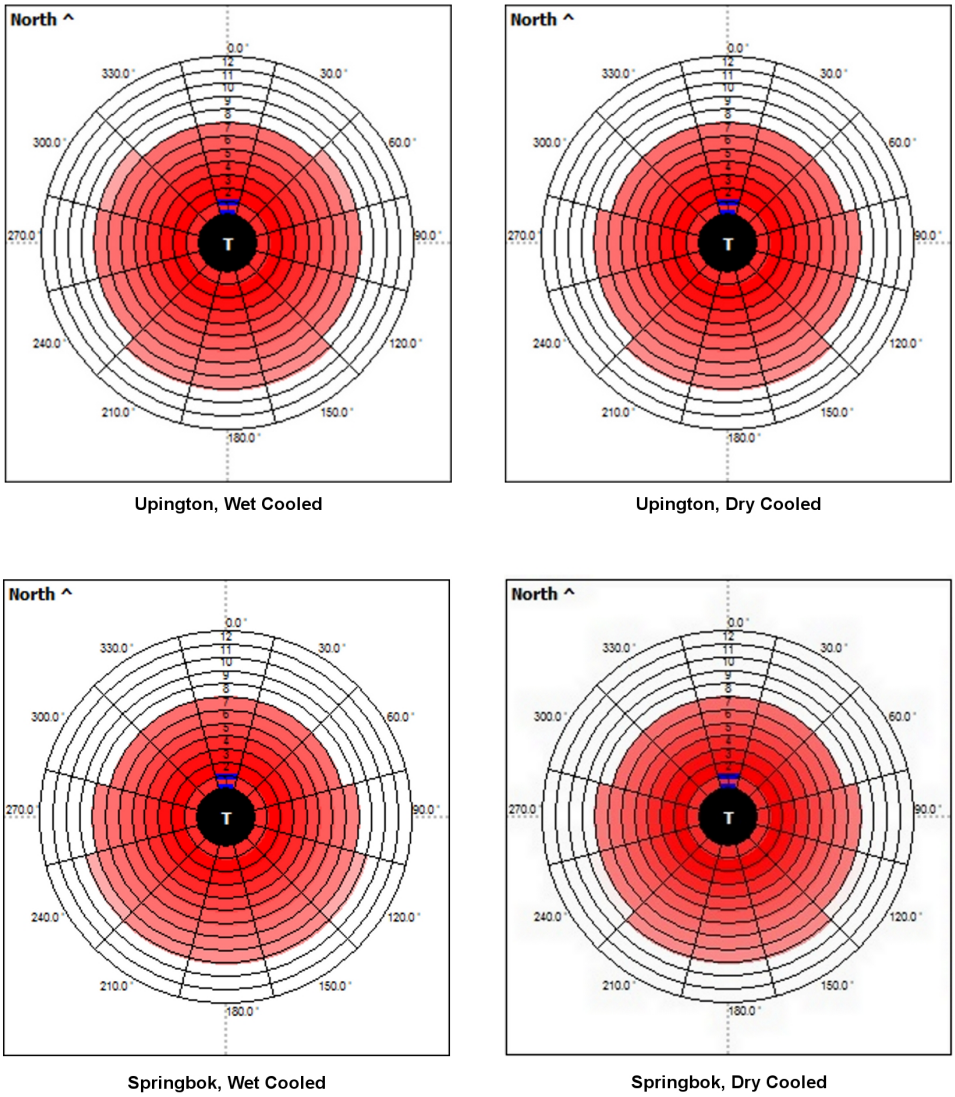

Figure 8.13: Optimal Heliostat Field Layout Diagram for a Central Receiver Plant with Wet and Dry Cooling at Upington and Springbok.

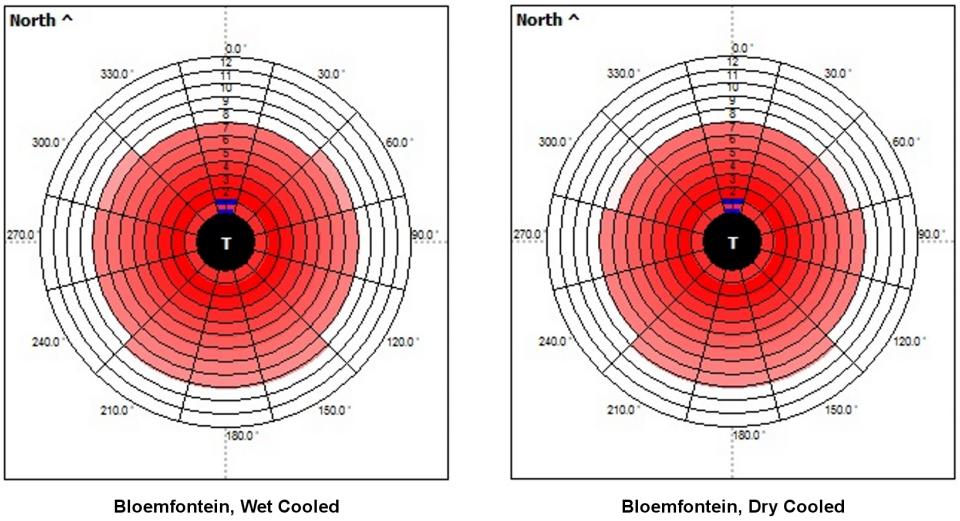

Figure 8.14: Optimal Heliostat Field Layout Diagram for a Central Receiver Plant with Wet and Dry Cooling at Bloemfontein.

As one would expect, the large majority of the heliostats in the field are located on the Southern side of the tower, thereby reducing cosine effect losses and increasing optical efficiency for locations in the Southern Hemisphere. This process is best visualised by means of the diagram shown in Figure 8.15. In order to focus the sun's rays onto the receiver, a heliostat must position itself so that its surface normal bisects the angle between the sun's rays and the line from the heliostat to the tower. The effective reflection area of the heliostat is then reduced by the cosine of one-half of the angle subtended. In the Southern Hemisphere, heliostats in the South field generally have their surface normal pointing Northwards towards the tower, thereby suffering less cosine reduction when compared to heliostats in the North field (Stine and Geyer, 2001).

The total number of heliostats in the field, as well as the total reflective area, and minimum and maximum distances from the tower calculated for each location and cooling technology are presented in Table 8.14. From the results it is evident that all of the plants have approximately 7000 heliostats, which is strongly comparable to the estimate of 6000 heliostats suggested by Eskom (2006) for their proposed 100 MW central receiver plant in the Northern Cape. The maximum distance from the tower of approximately 1260 m is also within the 2.0 km range for a large CSP plant, as suggested by the SAM (2010) documentation.

Table 8.14: Calculated Optimal Heliostat Field Layout Parameters for Central Receiver Models with Wet and Dry Cooling in Upington, Springbok and Bloemfontein.

		Number of Heliostats	Total Reflective Area (m^2)	Min. Distance from Tower (m)	Max. Distance from Tower (m)
Upington	Wet:	7119	1,027,804.2	162.5	1259.4
	Dry:	6997	1,010,190.5	162.5	1259.4
Springbok	Wet:	7125	1,028,670.4	162.5	1259.4
	Dry:	7011	1,012,211.7	162.5	1259.4
Bloemfontein	Wet:	7129	1,029,247.9	162.5	1259.4
	Dry:	7005	1,011,345.5	162.5	1259.4

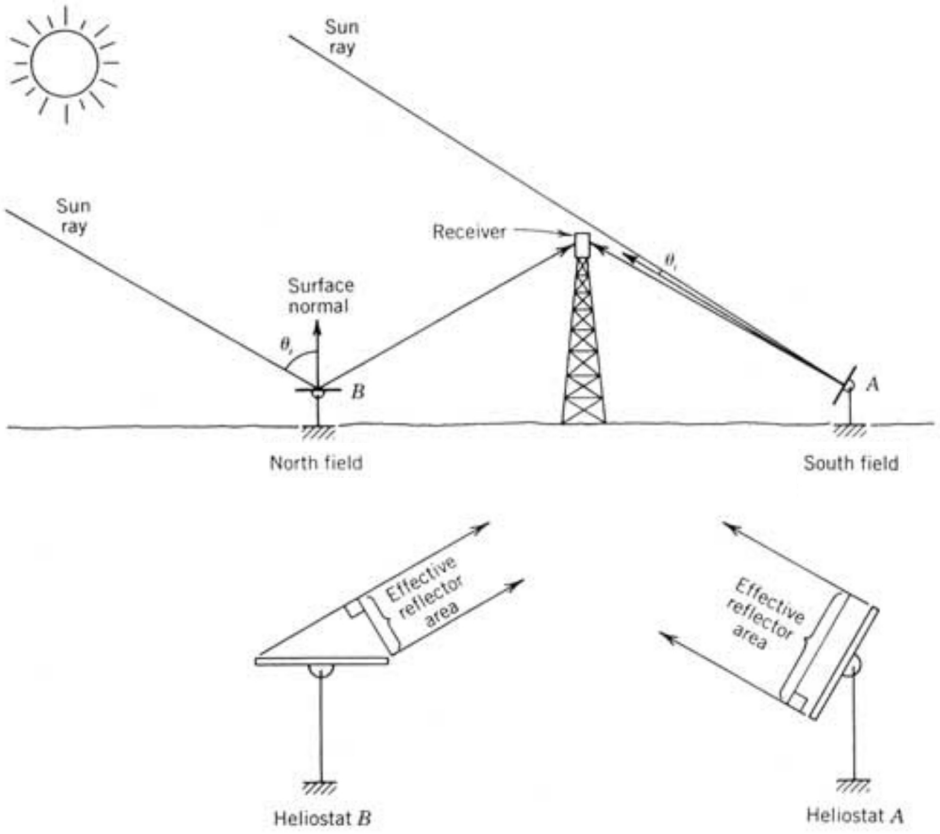

Figure 8.15: Cosine Effect of Two Heliostats in the Southern Hemisphere. *Adapted from Image:* Stine and Geyer (2001).

Tower and Receiver Dimensions

The optimal tower heigh as defined by the optimisation wizard occurred at a height of 216.67 m. This height was deemed the optimum value for all locations with both wet and dry cooling – with associated solar multiples of 2.0 and 1.9 respectively. This value is also strongly comparable to the estimated tower heigh of 210 m suggested by Eskom (2006) for their 100 MW proposed plant in the Northern Cape.

The optimal receiver heigh and diameter predicted by the optimisation wizard were 15.49 m and 12.44 m respectively. Once again this was standard when considering all locations, cooling types and solar multiples. Eskom (2006) estimated a receiver height in the region of 20 m for their 100 MW plant, thus once again affirming the credibility of the optimisation wizard results. The results for both tower height and receiver dimensions are presented in Table 8.15.

Table 8.15: Calculated Optimal Tower and Receiver Dimensions for Central Receiver Models with Wet and Dry Cooling in Upington, Springbok and Bloemfontein.

		Tower Height (m)	Receiver Height (m)	Receiver Diameter (m)
Upington	Wet Cooling:	216.67	15.49	12.44
	Dry Cooling:	216.67	15.49	12.44
Springbok	Wet Cooling:	216.67	15.49	12.44
	Dry Cooling:	216.67	15.49	12.44
Bloemfontein	Wet Cooling:	216.67	15.49	12.44
	Dry Cooling:	216.67	15.49	12.44

8.9.4 Receiver HTF Flow Configuration

In his study and creation of the central receiver model for SAM, Wagner (2008) identified 8 possible flow configurations for the HTF through the receiver. These flow configurations are presented in Figure 8.16. The cross-over flow pattern labelled as *Configuration 1* in the image is the one adopted at Solar II and is also the SAM default for its example plant in the Northern Hemisphere. In this configuration, the HTF enters through the Northern-most panels and then proceeds in series through half of the panels, before finally exiting from the two Southern-most panels of the receiver.

In this study, however, it was decided to adopt the same cross-over flow configuration, but to instead use the configuration identified by *Configuration 2* in the figure. This is due to the CSP plants in this study being located in the Southern Hemisphere, thereby requiring the HTF to enter from the Southern-most panels of the receiver.

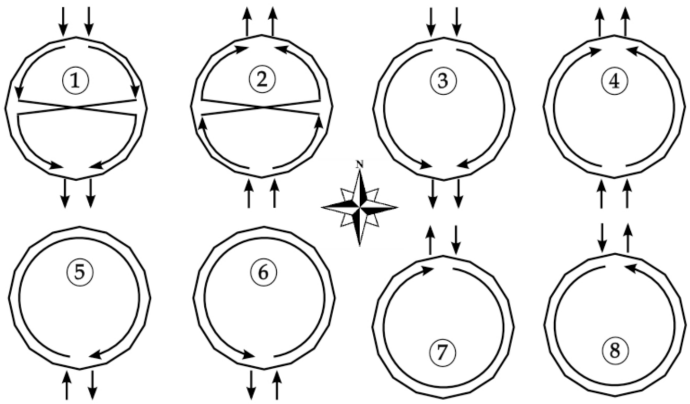

Figure 8.16: Possible Flow Configurations for External Receiver (Wagner, 2008).

8.9.5 Cooling Technology Choice

As for the case of the parabolic trough model, for each location, one central receiver model was set up with wet cooling, and a second model with dry cooling. The resulting design-related input data for each cooling technology is presented in Table 8.16. Once again it is noted that the overall efficiency of the power block when running on a wet cooling cycle is higher than that of dry cooling, while the steam cycle blowdown fraction is higher for dry cooling in order to account for wet-surface air cooling for critical Rankine cycle components (SAM, 2010).

Table 8.16: Central Receiver Cooling Technology Design Input Variables. *Source of Data:* SAM (2010).

Central Receiver	Wet Cooling	Dry Cooling
Condenser Type	Evaporative	Air-cooled
Ambient Temperature at Design	20 ℃	33 ℃
Reference Condenser Water dT	10 ℃	–
Approach Temperature	5 ℃	–
Initial Temperature Difference at Design Point	–	16 ℃
Condenser Pressure Ratio	–	1.0028
Power Block Rated Cycle Conversion Efficiency	0.425	0.408
Steam Cycle Blowdown Fraction	0.013	0.016

8.10 Thermal Storage

A thermal energy storage system comprising two-tank molten salt storage was chosen for both the parabolic trough and central receiver CSP models in this study, as per the SAM software defaults. The two-tank molten salt storage system was considered an appropriate choice, based on the review of thermal storage technologies in Chapter 5, which identified sensible-heat storage as the current most commercially viable TES technology. Furthermore, molten salt storage is also the adopted storage technology in the more recent CSP plants such as Andasol I - III, Solar Two and Gemasolar (Solar Tres) (Meyer, 2010; Torresol Energy, 2011).

In keeping with the plant design data assumptions from the previous sections, the default thermal storage design inputs were adopted for both the parabolic trough and central receiver models. An indirect two-tank molten salt system was specified for the parabolic trough plant, while a direct two-tank molten salt system was specified for the central receiver plants. Once again, the complete set of input variables for the parabolic trough and central receiver plants is presented in Appendix F and Appendix G respectively.

8.10.1 Full Load Hours of Thermal Storage

Although it is possible to simulate both parabolic trough and central receiver models with varying hours of thermal storage, it was decided to only study systems with 6 hours of full load TES in this analysis. This decision was made primarily due to time constraints, as the inclusion of a variation in hours of storage would more than double the number of models being run in this study. Furthermore, the value of 6 hours was chosen not only because is it the default SAM value for both parabolic trough and central receiver systems – hence full data for its inclusion is available – but it also represents the required number of storage hours specified by NERSA for both parabolic trough and central receiver plants in the South African REFIT (NERSA, 2010).

8.10.2 Storage Dispatch Schedule

As discussed in Section 7.6.1, the thermal storage dispatch schedule determines how and when the energy flows between the solar field, the thermal energy storage system and the power block, for up to six different dispatch periods. SAM presents a library of default dispatch schedules, with the SCE dispatch schedule representing the software default. The SCE default dispatch schedule is presented in Figure 8.17, with its legend shown in Table 8.17. A storage dispatch value of 0 indicates that the system will always

dispatch stored energy in any hour assigned to the given dispatch period, if required. A turbine output fraction of 1.0 requires the turbine gross output to be met in full, with supplementation from storage if it is available. A value of 0 for fossil fill fraction ensures that no fossil backup is utilised under any circumstance.

It was decided to employ the SAM default SCE dispatch schedule for thermal storage in this study, however, it was first necessary to modify it for conditions relevant to the Southern Hemisphere. This is evident, as it can be seen in Figure 8.17 that the default peak turbine output occurs over the months of June to September, instead of the Southern Hemisphere summer months of December to March. The entire dispatch schedule was thus shifted forward by six months, thereby retaining its form but adapting it to the local Souther Hemisphere climate. The resulting adapted dispatch schedule used in this study is presented in Figure 8.18.

Weekday Schedule

	12am	1am	2am	3am	4am	5am	6am	7am	8am	9am	10am	11am	12pm	1pm	2pm	3pm	4pm	5pm	6pm	7pm	8pm	9pm	10pm	11pm
Jan	6	6	6	6	6	6	5	5	4	4	4	4	4	4	4	4	4	4	4	4	4	5	5	5
Feb	6	6	6	6	6	6	5	5	4	4	4	4	4	4	4	4	4	4	4	4	4	5	5	5
Mar	6	6	6	6	6	6	5	5	4	4	4	4	4	4	4	4	4	4	4	4	4	5	5	5
Apr	6	6	6	6	6	5	5	4	4	4	4	4	4	4	4	4	4	4	4	4	5	5	5	6
May	6	6	6	6	6	5	5	4	4	4	4	4	4	4	4	4	4	4	4	4	5	5	5	6
Jun	3	3	3	3	3	3	3	2	2	2	2	1	1	1	1	1	1	2	2	2	2	2	3	3
Jul	3	3	3	3	3	3	3	2	2	2	2	1	1	1	1	1	1	2	2	2	2	2	3	3
Aug	3	3	3	3	3	3	3	2	2	2	2	1	1	1	1	1	1	2	2	2	2	2	3	3
Sep	3	3	3	3	3	3	3	2	2	2	2	1	1	1	1	1	1	2	2	2	2	2	3	3
Oct	6	6	6	6	6	5	5	4	4	4	4	4	4	4	4	4	4	4	4	4	5	5	5	6
Nov	6	6	6	6	6	6	5	5	4	4	4	4	4	4	4	4	4	4	4	4	4	5	5	5
Dec	6	6	6	6	6	6	5	5	4	4	4	4	4	4	4	4	4	4	4	4	4	5	5	5

Weekend Schedule

	12am	1am	2am	3am	4am	5am	6am	7am	8am	9am	10am	11am	12pm	1pm	2pm	3pm	4pm	5pm	6pm	7pm	8pm	9pm	10pm	11pm
Jan	6	6	6	6	6	6	5	5	5	5	5	5	5	5	5	5	5	5	5	5	5	5	5	5
Feb	6	6	6	6	6	6	5	5	5	5	5	5	5	5	5	5	5	5	5	5	5	5	5	5
Mar	6	6	6	6	6	6	5	5	5	5	5	5	5	5	5	5	5	5	5	5	5	5	5	5
Apr	6	6	6	6	6	5	5	5	5	5	5	5	5	5	5	5	5	5	5	5	5	5	5	6
May	6	6	6	6	6	5	5	5	5	5	5	5	5	5	5	5	5	5	5	5	5	5	5	6
Jun	3	3	3	3	3	3	3	3	3	3	3	3	3	3	3	3	3	3	3	3	3	3	3	3
Jul	3	3	3	3	3	3	3	3	3	3	3	3	3	3	3	3	3	3	3	3	3	3	3	3
Aug	3	3	3	3	3	3	3	3	3	3	3	3	3	3	3	3	3	3	3	3	3	3	3	3
Sep	3	3	3	3	3	3	3	3	3	3	3	3	3	3	3	3	3	3	3	3	3	3	3	3
Oct	6	6	6	6	6	5	5	5	5	5	5	5	5	5	5	5	5	5	5	5	5	5	5	6
Nov	6	6	6	6	6	6	5	5	5	5	5	5	5	5	5	5	5	5	5	5	5	5	5	5
Dec	6	6	6	6	6	6	5	5	5	5	5	5	5	5	5	5	5	5	5	5	5	5	5	5

Figure 8.17: Default SAM SCE Dispatch Schedule (SAM, 2011).

Table 8.17: Thermal Dispatch Schedule Legend. *Source of Data:* SAM (2010).

	Storage Dispatch: With Solar	Storage Dispatch: Without Solar	Turbine Output Fraction	Fossil Fill Fraction
Period 1	0	0	1.1	0
Period 2	0	0	1	0
Period 3	0	0	1	0
Period 4	0	0	1	0
Period 5	0	0	1	0
Period 6	0	0	1	0

Weekday Schedule

	12am	1am	2am	3am	4am	5am	6am	7am	8am	9am	10am	11am	12pm	1pm	2pm	3pm	4pm	5pm	6pm	7pm	8pm	9pm	10pm	11pm
Jan	3	3	3	3	3	3	3	2	2	2	2	1	1	1	1	1	1	2	2	2	2	2	3	3
Feb	3	3	3	3	3	3	3	2	2	2	2	1	1	1	1	1	1	2	2	2	2	2	3	3
Mar	3	3	3	3	3	3	3	2	2	2	2	1	1	1	1	1	1	2	2	2	2	2	3	3
Apr	6	6	6	6	6	5	5	4	4	4	4	4	4	4	4	4	4	4	4	4	5	5	5	6
May	6	6	6	6	6	6	5	5	4	4	4	4	4	4	4	4	4	4	4	4	4	5	5	5
Jun	6	6	6	6	6	6	5	5	4	4	4	4	4	4	4	4	4	4	4	4	4	5	5	5
Jul	6	6	6	6	6	6	5	5	4	4	4	4	4	4	4	4	4	4	4	4	4	5	5	5
Aug	6	6	6	6	6	6	5	5	4	4	4	4	4	4	4	4	4	4	4	4	4	5	5	5
Sep	6	6	6	6	6	6	5	5	4	4	4	4	4	4	4	4	4	4	4	4	4	5	5	5
Oct	6	6	6	6	6	5	5	4	4	4	4	4	4	4	4	4	4	4	4	4	5	5	5	6
Nov	6	6	6	6	6	5	5	4	4	4	4	4	4	4	4	4	4	4	4	4	5	5	5	6
Dec	3	3	3	3	3	3	3	2	2	2	2	1	1	1	1	1	1	2	2	2	2	2	3	3

Weekend Schedule

	12am	1am	2am	3am	4am	5am	6am	7am	8am	9am	10am	11am	12pm	1pm	2pm	3pm	4pm	5pm	6pm	7pm	8pm	9pm	10pm	11pm
Jan	3	3	3	3	3	3	3	3	3	3	3	3	3	3	3	3	3	3	3	3	3	3	3	3
Feb	3	3	3	3	3	3	3	3	3	3	3	3	3	3	3	3	3	3	3	3	3	3	3	3
Mar	3	3	3	3	3	3	3	3	3	3	3	3	3	3	3	3	3	3	3	3	3	3	3	3
Apr	6	6	6	6	6	5	5	5	5	5	5	5	5	5	5	5	5	5	5	5	5	5	5	6
May	6	6	6	6	6	6	5	5	5	5	5	5	5	5	5	5	5	5	5	5	5	5	5	5
Jun	6	6	6	6	6	6	5	5	5	5	5	5	5	5	5	5	5	5	5	5	5	5	5	5
Jul	6	6	6	6	6	6	5	5	5	5	5	5	5	5	5	5	5	5	5	5	5	5	5	5
Aug	6	6	6	6	6	6	5	5	5	5	5	5	5	5	5	5	5	5	5	5	5	5	5	5
Sep	6	6	6	6	6	6	5	5	5	5	5	5	5	5	5	5	5	5	5	5	5	5	5	5
Oct	6	6	6	6	6	5	5	5	5	5	5	5	5	5	5	5	5	5	5	5	5	5	5	6
Nov	6	6	6	6	6	5	5	5	5	5	5	5	5	5	5	5	5	5	5	5	5	5	5	6
Dec	3	3	3	3	3	3	3	3	3	3	3	3	3	3	3	3	3	3	3	3	3	3	3	3

Figure 8.18: Dispatch Schedule Used in Analysis and Adapted for Southern Hemisphere.

9 Model Results and Analysis

The final inputs for the various CSP technologies and models, as identified, determined and discussed in Chapter 8 were used to create twelve separate, final SAM simulations. These twelve simulations comprise parabolic trough models with wet cooling and with dry cooling, and central receiver models with wet and dry cooling for each of the three stipulated locations. The following chapter will now present and discuss the results obtained from the running of the twelve individual simulations, as well as identify any trends and discuss the optimal CSP configuration for each of the three locations in South Africa. Before the results are presented, however, a brief definition and description of the key considered output metrics will be given.

Annual Energy Production

The annual energy production metric is a measure of the total electric generation, in kWh, for the first year that a plant operates. This first year is equivalent to year one in the project's cash flow. The annual energy output may decrease over the plant's lifetime should a degradation rate value be included. The annual energy production value is a direct result of the plant performance calculations in the SAM model and is thus affected by the plant design and weather conditions (SAM, 2010).

Total Installed Cost per Net Capacity

The total installed cost per net capacity for a plant is simply a measure of the sum of all the capital costs, both direct and indirect, divided by the plant's nameplate rated net capacity (SAM, 2010). In this analysis, the total installed cost per net capacity is calculated by summing all the cost inputs stated in the final costs of Section 8.7 and in Table 8.9 and Table 8.10, and then dividing the total value by the nameplate capacity of 100,001.00 kW (100 MW).

Levelised Cost of Energy

The levelised cost of energy is a value in cents (or Rand) per kilowatt hour, whose value is the amount that a utility-scale project must receive for each unit of electricity it sells, in order to meet the financial requirements defined by a positive cash-flow, the minimum IRR and the minimum DSCR. The LCOE takes into account the project capital costs, financing, tax and operating costs over its lifetime, as well its electricity production (SAM, 2010). The LCOE is defined mathematically by the following formula:

$$\text{LCOE}_{\text{real}} = \frac{\sum_{n=0}^{N} \frac{R_n}{(1+d_{\text{nominal}})^n}}{\sum_{n=1}^{N} \frac{Q_n}{(1+d_{\text{real}})^n}} \tag{9.1}$$

Where,

N = Total project lifetime in years.
Q_n = Total annual energy production in year n.
R_n = The revenue generated from electricity sales in year n, calculated by the product of the annual energy production and electricity PPA price.
d_{real} = The real discount rate.
d_{nominal} = The nominal discount rate, calculated by the following formula:

$$d_{\text{nominal}} = (1+d_{\text{real}})(1+I) - 1$$

I = Inflation rate.

One of the key advantages of using an LCOE, is that it allows for the comparison of alternative technology choices, with different project lifetimes and performance characteristics. The LCOE provides a means to compare all technologies on an equal basis, while capturing the trade-off's between projects with different capital costs and O&M costs (SAM, 2010).

The SAM software calculates the LCOE in both real and nominal terms. According to the SAM (2010) documentation, it is generally advisable to make use of the nominal LCOE for projects with short lifetimes, while projects with longer lifetimes are generally analysed and compared with the real LCOE, thereby accounting for inflation over the project's life. Therefore, due to the 30 analysis periods used in this study, the *real* LCOE was adopted as the comparison metric of choice.

Capacity Factor

The capacity factor of a plant is defined as the ratio of the plant's actual energy output in the first year of operation, to the potential energy output that would have resulted had the plant operated at its nameplate capacity for the entire year. Capacity factors are an important consideration for the analysis of the merits of any plant, and also aid in the determination of whether a plant is better suited for base load generation, mid-merit, or for peaking loads (SAM, 2010).

The capacity factor is defined mathematically as:

$$\text{CF} = \frac{E_{\text{Actual Output Year 1}}}{P_{\text{Nameplate Capacity}} \cdot 8760} \tag{9.2}$$

Where,

CF = Capacity factor.
$E_{\text{Actual Output Year 1}}$ = Total annual energy generation in kWh in year 1 of the project cash-flow.
$P_{\text{Nameplate Capacity}}$ = The rated system nameplate capacity in kW.

9.1 Upington

Of the twelve final simulations, the first four were run for the Upington location. The key results and output metrics for these simulations are presented in Table 9.1. Each of the key areas for the different technologies in Upington will now be briefly discussed and compared under their relevant headings.

9.1.1 Annual Energy Production

The total annual energy produced by each plant type in Upington ranges from 370,088,244 kWh_e for the dry-cooled parabolic trough plant, to 417,100,874 kWh_e for the wet-cooled central receiver plant. As would be expected, the central receiver plants produce greater annual energy output, when compared to the parabolic trough plants, as a result of their higher concentration ratios and greater overall efficiency. The wet-cooled plants for both parabolic trough and central receiver plants also produce more energy than their dry-cooled equivalents as a result of the lower power cycle efficiencies associated with dry cooling.

Table 9.1: Cost and Performance Results for Parabolic Trough and Central Receiver Models with Wet and Dry Cooling in Upington.

Upington	Parabolic Trough		Central Receiver	
	Wet Cooling	Dry Cooling	Wet Cooling	Dry Cooling
Rated Net Capacity	100 MW	100 MW	100 MW	100 MW
Availability	95 %	95 %	92 %	92 %
Economic Life	30 yrs	30 yrs	30 yrs	30 yrs
Annual Energy Produced (kWh_e)	385,626,991.3	370,088,244.3	417,100,874.0	393,061,979.1
Total Direct Cost	$ 704,851,935.08	$ 800,658,637.32	$ 518,441,957.40	$ 545,371,791.37
Total Indirect Cost	$ 209,341,024.72	$ 237,795,615.28	$ 153,977,261.35	$ 161,975,422.04
Total Installed Cost	$ 914,192,959.80	$ 1,038,454,252.60	$ 672,419,218.75	$ 707,347,213.41
Total Installed Cost per Net Capacity	$ 9,141.84 /kW R 64,175.72 /kW	$ 10,384.44 /kW R 72,898.77 /kW	$ 6,724.12 /kW R 47,203.32 /kW	$ 7,073.40 /kW R 49,655.27 /kW
LCOE – real *	28.50 ¢/kWh R 2.00 /kWh	32.93 ¢/kWh R 2.31 /kWh	20.06 ¢/kWh R 1.41 /kWh	21.94 ¢/kWh R 1.54 /kWh
1st Year PPA Price	40.81 ¢/kWh R 2.86 /kWh	47.63 ¢/kWh R 3.34 /kWh	28.33 ¢/kWh R 1.99 /kWh	31.24 ¢/kWh R 2.19 /kWh
Capacity Factor	44.02 %	42.25 %	47.61 %	44.87 %
Annual Water Usage	1,507,891.7 m^3 3.91 l/kWh 1032.97 gal/MWh	89,460.5 m^3 0.24 l/kWh 63.86 gal/MWh	1,410,134.3 m^3 3.38 l/kWh 893.11 gal/MWh	82,446.8 m^3 0.21 l/kWh 55.41 gal/MWh

* ¢/kWh refers to U.S. cents per kilowatt hour.

9.1.2 Installed Cost per Net Capacity

The total installed cost per net capacity for the CSP models in Upington ranges from R47,203.32 /kW ($6,724.12 /kW) for the wet-cooled central receiver model, to R72,898.77 /kW ($10,384.44 /kW) for the dry-cooled parabolic trough plant. Both the central receiver plants are more economical when compared to the parabolic trough plants, which is a result of the difference in system component costs and plant designs between the two CSP technology types. Making use of dry cooling also increases plant costs, which is consistent with the higher capital and maintenance costs associated with the use of dry cooling technology. Furthermore, it is noted that the model predicts a central receiver plant with dry cooling in Upington is more economical in terms of cost per net capacity than the wet-cooled parabolic trough plant with equivalent 100 MW rating in the same location.

9.1.3 Levelised Cost of Energy

The LCOE for the different models in Upington ranges from R1.41 /kWh (20.06 U.S. ¢/kWh) to R2.31 /kWh (32.93 U.S. ¢/kWh) for the wet-cooled central receiver and dry-cooled parabolic trough respectively. The resulting LCOE for the central receiver plants is lower than that of the parabolic trough plants, while wet cooling is more economical than dry cooling for both technologies.

It is also noted that the calculated first year PPA prices of R1.99 /kWh and R2.19 /kWh for the central receiver models with wet and dry cooling respectively, are relatively close to the R2.31 /kWh 2009 value as stated in the REFIT Phase II document released by NERSA (2010) for central receiver plants with 6 hours TES. The PPA prices of R2.86 /kWh and R3.34 /kWh for the parabolic trough models with wet and dry cooling respectively, however, are higher than the 2009 value of R2.10 /kWh suggested by NERSA (2010) in the REFIT Phase II document for parabolic trough plants with 6 hours TES.

9.1.4 Capacity Factor

The capacity factors for the different plants in Upington range from 42.25% for the dry-cooled parabolic trough plant, to 47.61% for the wet cooled central receiver plant. The central receiver plants generally have higher capacity factors when compared to the parabolic trough plants, which is thought to be due the the previously mentioned higher concentration ratios and hence efficiency. Dry cooling also decreases capacity factors due to its negative effect on plant efficiency.

9.1.5 Annual Water Consumption

The difference in the annual water consumption between wet and dry cooling is vast, with the dry cooled central receiver consuming only 82,446.8 m^3 (0.21 litres/kWh) compared to the 1,507,891.7 m^3 (3.91 litres/kWh) of the wet-cooled parabolic trough. The central receiver plants also consume less water annually when compared to parabolic troughs, which is expected, and discussed in Section 4.4 of Chapter 4. Furthermore, the values of 3.91 litres/kWh and 3.38 litres/kWh for the wet-cooled parabolic trough and central receiver plants respectively, are similar to the values of 3.03 litres/kWh and 2.84 litres/kWh stated in Table 4.1, albeit approximately 0.54 - 0.88 litres/kWh higher.

9.1.6 Preferred Technology for Upington

Based on the above results, as well as the output data listed in Table 9.1, it is concluded that the central receiver plants in Upington are superior and more economical than their equivalent parabolic trough plants. It is also noted that of the two central receiver plants, the wet-cooled plant proves more economical in terms of LCOE and PPA price, which is to be expected. However, the scarcity of water in the Upington region of Northern Cape, as well as the negative impact on local farming and communities in the region should large quantities of water be drawn from the orange river for plant cooling (Morse, 2009), raise concerns over the security of supply of the cooling water and hence its cost. According to Morse (2009), the city of Upington consumes approximately 12.3 million m^3 of water per annum. A potential CSP plant with wet cooling would therefore consume more than a 10^{th} of the volume of water as the entire city of Upington.

In addition, according to the model results a central receiver plant with dry cooling is even more cost effective in terms of the LCOE and PPA price, than the same capacity parabolic trough making use of wet cooling. Therefore, due to these concerns over the security of supply of water in the region, it is thought that the optimal CSP plant for the Upington region would be a central receiver plant with dry cooling.

9.2 Springbok

The subsequent four simulations were run for the Springbok location. The key results and output metrics for these simulations are presented in Table 9.2. Each of the key areas for the different technologies in Springbok will now be briefly discussed and compared under their relevant headings.

Table 9.2: Cost and Performance Results for Parabolic Trough and Central Receiver Models with Wet and Dry Cooling in Springbok.

Springbok	Parabolic Trough		Central Receiver	
	Wet Cooling	Dry Cooling	Wet Cooling	Dry Cooling
Rated Net Capacity	100 MW	100 MW	100 MW	100 MW
Availability	95 %	95 %	92 %	92 %
Economic Life	30 yrs	30 yrs	30 yrs	30 yrs
Annual Energy Produced (kWh_e)	356,160,487.5	346,887,632.4	376,179,962.7	358,737,976.1
Total Direct Cost	$ 725,891,696.52	$ 823,611,104.34	$ 518,673,680.08	$ 545,912,477.63
Total Indirect Cost	$ 215,589,833.87	$ 244,612,497.99	$ 154,046,082.98	$ 162,136,005.86
Total Installed Cost	$ 941,481,530.38	$ 1,068,223,602.33	$ 672,719,763.06	$ 708,048,483.48
Total Installed Cost per Net Capacity	$ 9,414.72 /kW R 66,091.33 /kW	$ 10,682.13 /kW R 74,988.55 /kW	$ 6,727.13 /kW R 47,224.45 /kW	$ 7,080.41 /kW R 49,704.48 /kW
LCOE – real *	31.63 ¢/kWh R 2.22 /kWh	36.04 ¢/kWh R 2.53 /kWh	22.18 ¢/kWh R 1.56 /kWh	24.03 ¢/kWh R 1.69 /kWh
1st Year PPA Price	45.38 ¢/kWh R 3.19 /kWh	52.18 ¢/kWh R 3.66 /kWh	31.37 ¢/kWh R 2.20 /kWh	34.23 ¢/kWh R 2.40 /kWh
Capacity Factor	40.66 %	39.60 %	42.94 %	40.95 %
Annual Water Usage	1,388,420.6 m^3 3.90 l/kWh 1029.82 gal/MWh	88,879.7 m^3 0.26 l/kWh 67.69 gal/MWh	1,271,440.6 m^3 3.38 l/kWh 892.87 gal/MWh	79,800.6 m^3 0.22 l/kWh 58.76 gal/MWh

* ¢/kWh refers to U.S. cents per kilowatt hour.

9.2.1 Annual Energy Production

The total annual energy produced by each plant in Springbok ranges from 346,887,632.4 kWh_e for the dry-cooled parabolic trough plant, to 376,179,962.7 kWh_e for the wet-cooled central receiver. As was the case for Upington, the central receiver plants produce greater annual energy yields, when compared to the parabolic trough plants, as a result of their higher concentration ratios and greater cycle efficiency. Both the wet-cooled parabolic trough and central receiver plants once again produce more energy than their dry-cooled equivalents, as a result of the lower power cycle efficiencies associated with dry cooling.

9.2.2 Installed Cost per Net Capacity

The total installed cost per net capacity for the CSP models in Springbok ranges from R47,224.45 /kW ($6,727.13 /kW) for the wet-cooled central receiver model, to R74,988.55 /kW ($10,682.13 /kW) for the dry-cooled parabolic trough plant. As in Upington, both the central receiver plants are more economical when compared to the parabolic trough plants, while the use of dry cooling also increases plant costs. It is again noted that the model predicts a central receiver plant with dry cooling is more economical in terms of cost per net capacity than the equivalent 100 MW capacity wet-cooled parabolic trough plant in the same location.

9.2.3 Levelised Cost of Energy

The LCOE for the different models in Springbok ranges from R1.56 /kWh (22.18 U.S. ¢/kWh) to R2.53 /kWh (36.04 U.S. ¢/kWh) for the wet-cooled central receiver and dry-cooled parabolic trough respectively. Once again, the LCOE for the central receiver plants is lower than that of the parabolic trough plants, while wet cooling is more economical than dry cooling for both technologies.

The resulting required first year PPA prices of R2.20 /kWh and R2.40 /kWh for the central receiver models with wet and dry cooling respectively, are relatively close to R2.31 /kWh 2009 value as stated in the REFIT Phase II document (NERSA, 2010) for central receiver plants with 6 hours TES, albeit approximately R0.20 /kWh higher than the PPA prices for Upington. The PPA prices of R3.19 /kWh and R3.66 /kWh for the parabolic trough models with wet and dry cooling respectively, however, are considerably higher than the 2009 value of R2.10 /kWh suggested by NERSA (2010) in the REFIT Phase II document for parabolic trough plants with 6 hours TES, and are approximately R0.32 higher than the Upington trough prices. The higher energy prices experienced in

Springbok are related to the lower annual energy yields on account of the lower annual DNI levels at Springbok when compared to Upington.

9.2.4 Capacity Factor

The capacity factors for the different plants in Springbok range from 39.60% for the dry-cooled parabolic trough plant, to 42.94% for the wet cooled central receiver. Once again, the central receiver plants generally have higher capacity factors when compared to the parabolic trough plants, thought to be due the the aforementioned higher concentration ratios and efficiency. Dry cooling also decreases capacity factors due to its negative effect on plant efficiency. The capacity factors for Springbok are approximately 3% lower than those in Upington, which is likely due to the lower total annual DNI in Springbok resulting in the plants operating at their rated capacity for less time throughout the year.

9.2.5 Annual Water Consumption

The difference in the annual water consumption between wet and dry cooling in Springbok is also vast, with the dry-cooled central receiver consuming only 79,800.6 m^3 (0.22 litres/kWh) compared to the 1,388,420.6 m^3 (3.90 litres/kWh) of the wet-cooled parabolic trough. The central receiver plants in Springbok also also consume less water annually when compared to parabolic troughs. Furthermore, the values of 3.90 litres/kWh and 3.38 litres/kWh for the wet-cooled parabolic trough and central receiver plants respectively, are similar to the values of 3.03 litres/kWh and 2.84 litres/kWh stated in Table 4.1 and virtually identical (but slightly lower) to those in Upington.

9.2.6 Preferred Technology for Springbok

Based on the above results, as well as the output data listed in Table 9.2, it is concluded that the central receiver plants in Springbok are superior and more economical than their equivalent parabolic trough plants. It is also noted that of the two central receiver plants, the wet-cooled plant proves more economical in terms of LCOE and PPA price, which is to be expected. The decision for the optimal CSP technology near Springbok is complicated, however, as although plants in this region, like Upington, are situated in the dry Northern Cape, with its associated water scarcity – and hence security of water supply concerns – the possibility also exists for plants to be located along the west coast, as can be seen in Figure 8.1. A CSP plant situated at the coast could then potentially make use of wet cooling, drawing its cooling water from the Atlantic Ocean.

The use of sea water for wet cooling is not considered or incorporated into the SAM software in this study, however, and is considered beyond the scope of this report. A dry-cooled central receiver plant is also a potential candidate for the optimal CSP technology near Springbok, with it being more cost effective in terms of the LCOE and PPA price, than the same capacity parabolic trough making use of wet cooling. Additional modelling would therefore be required in order to determine whether a central receiver plant using sea water for wet cooling – with its associated complexities – would in fact be more economical than a dry-cooled central receiver plant. Hence, it can only be concluded, based on the results from this analysis, that the optimal CSP plant for the Springbok region would be a central receiver plant, but more research is required to determine whether wet cooling with sea water or dry cooling is preferable.

9.3 Bloemfontein

The final four simulations were run for the Bloemfontein location. The key results and output metrics for the these simulations are presented in Table 9.3. Each of the key areas for the different technologies in Bloemfontein will now be briefly discussed and compared under their relevant headings.

9.3.1 Annual Energy Production

The total annual energy produced by each plant in Bloemfontein ranges from 358,081,166.8 kWh_e for the dry-cooled parabolic trough plant, to 380,078,179.4 kWh_e for the wet-cooled central receiver plant. As was the case for both Upington and Springbok, the central receiver plants produce greater annual energy yields, when compared to the parabolic trough plants, as a result of their higher concentration ratios and greater overall efficiencies. The wet-cooled plants for both parabolic trough and central receiver plants once again also produced more energy than their dry-cooled equivalents, as a result of the lower power cycle efficiencies associated with dry cooling.

9.3.2 Installed Cost per Net Capacity

The total installed cost per net capacity for the CSP models in Bloemfontein ranges from R47,238.49 /kW ($6,729.13 /kW) for the wet-cooled central receiver model, to R76,904.17 /kW ($10,955.01 /kW) for the dry-cooled parabolic trough plant. As in the both the Upington and Springbok cases, both the central receiver plants are more economical when compared to the parabolic trough plants. Making use of dry cooling also

Table 9.3: Cost and Performance Results for Parabolic Trough and Central Receiver Models with Wet and Dry Cooling in Bloemfontein.

Bloemfontein	Parabolic Trough		Central Receiver	
	Wet Cooling	Dry Cooling	Wet Cooling	Dry Cooling
Rated Net Capacity	100 MW	100 MW	100 MW	100 MW
Availability	95 %	95 %	92 %	92 %
Economic Life	30 yrs	30 yrs	30 yrs	30 yrs
Annual Energy Produced (kWh_e)	367,781,069.3	358,081,166.8	380,078,179.4	361,868,799.9
Total Direct Cost	$ 745,018,752.37	$ 844,650,865.78	$518,828,161.87	$ 545,680,754.95
Total Indirect Cost	$ 221,270,569.45	$ 250,861,307.14	$ 154,091,964.07	$ 162,067,184.22
Total Installed Cost	$ 966,289,321.82	$ 1,095,512,172.91	$ 672,920,125.94	$ 707,747,939.17
Total Installed Cost per Net Capacity	$ 9,662.80 /kW R 67,832.86 /kW	$ 10,955.01 /kW R 76,904.17 /kW	$ 6,729.13 R 47,238.49 /kW	$ 7,077.41 R 49,683.42 /kW
LCOE – real *	31.38 ¢/kWh R 2.20 /kWh	35.75 ¢/kWh R 2.51 /kWh	21.97 ¢/kWh R 1.54 /kWh	23.82 ¢/kWh R 1.67 /kWh
1st Year PPA Price	45.05 ¢/kWh R 3.16 /kWh	51.76 ¢/kWh R 3.63 /kWh	31.06 ¢/kWh R 2.18 /kWh	33.93 ¢/kWh R 2.38 /kWh
Capacity Factor	41.98 %	40.88 %	43.39 %	41.31 %
Annual Water Usage	1,434,814.3 m^3 3.90 l/kWh 1030.61 gal/MWh	92,379.5 m^3 0.26 l/kWh 68.15 gal/MWh	1,283,893.8 m^3 3.38 l/kWh 892.37 gal/MWh	79,981.9 m^3 0.22 l/kWh 58.39 gal/MWh

* ¢/kWh refers to U.S. cents per kilowatt hour.

increased plant costs. It is again noted that the model predicts a central receiver plant with dry cooling in Bloemfontein is more economical in terms of cost per net capacity than the wet-cooled parabolic trough plant with an equivalent 100 MW rating in the same location.

9.3.3 Levelised Cost of Energy

The LCOE for the different models in Bloemfontein ranges from R1.54 /kWh (21.97 U.S. ¢/kWh) to R2.51 /kWh (35.75 U.S. ¢/kWh) for the wet-cooled central receiver and dry-cooled parabolic trough respectively. Once again, the LCOE for the central receiver plants is lower than that of the parabolic trough plants, while wet cooling is more economical than dry cooling for both technologies.

The resulting required first year PPA prices of R2.18 /kWh and R2.38 /kWh for the central receiver models with wet and dry cooling respectively, are relatively close to R2.31 /kWh 2009 value as stated in the REFIT Phase II document (NERSA, 2010) for central receiver plants with 6 hours TES, albeit R0.19 /kWh higher than the PPA prices for Upington. The PPA prices of R3.16 /kWh and R3.63 /kWh for the parabolic trough models with wet and dry cooling respectively, however, are considerably higher than the 2009 value of R2.10 /kWh suggested by NERSA (2010) in the REFIT Phase II document for parabolic trough plants with 6 hours TES, and are approximately R0.30 higher than the Upington trough prices. The higher energy prices experienced in Bloemfontein, as in Springbok, are thought to be primarily related to the lower annual energy yields on account of the lower annual DNI levels at Bloemfontein when compared to Upington.

9.3.4 Capacity Factor

The capacity factors for the different plants in Upington range from 40.88% for the dry-cooled parabolic trough plant, to 43.39% for the wet cooled central receiver plant. Once again, the central receiver plants generally have higher capacity factors when compared to the parabolic trough plants, which is thought to be due the the previously mentioned higher concentration ratios and efficiency. Dry cooling also decreases capacity factors due to its negative effect on plant efficiency. The capacity factors for Bloemfontein are also generally in the region of 2% lower than those in Upington, but approximately 1% higher than Springbok. This is again likely due to the differences in total annual DNI received at each location.

9.3.5 Annual Water Consumption

The difference in the annual water consumption between wet and dry cooling in Bloemfontein is again vast, with the dry cooled central receiver consuming only 79,981.9 m^3 (0.22 litres/kWh) compared to the 1,434,814.3 m^3 (3.90 litres/kWh) of the wet-cooled parabolic trough. The central receiver plants in Bloemfontein also also consume less water annually when compared to parabolic troughs. Furthermore, the values of 3.90 litres/kWh and 3.38 litres/kWh for the wet-cooled parabolic trough and central receiver plants respectively, are similar to the values of 3.03 litres/kWh and 2.84 litres/kWh stated in Table 4.1 and virtually identical (but slightly lower) to those in Upington.

9.3.6 Preferred Technology for Bloemfontein

Based on the above results, as well as all the output data listed in Table 9.3, it is concluded that the central receiver plants in Bloemfontein, as in the previous two location, are superior and more economical than their equivalent parabolic trough plants. It is also noted that of the two central receiver plants, the wet-cooled plant proves more economical in terms of LCOE and PPA price, which once again is to be expected. The decision for the optimal CSP technology near Bloemfontein is complex, however, as depending on the plant location, water for wet cooling may be accessible from large dams, rivers or other water sources in the region. This can be seen in Figure 6.6, which depicts rivers and large water bodies throughout the country in the GIS analysis section of this report. Nevertheless, it may still be more beneficial to make use of dry cooling, as a means to reduce the risk of water supply concerns. A dry-cooled central receiver plant near Bloemfontein, is still more cost effective in terms of the LCOE and PPA price, than the same capacity parabolic trough making use of wet cooling.

It is therefore concluded that more specific site analyses and local water availability studies would be required in order to determine whether a central receiver plant using wet cooling, or a dry-cooled central receiver plant would be more optimal. It can, however, be concluded that the optimal CSP technology – when only parabolic trough and central receiver technologies are considered – for the Bloemfontein region would be a central receiver.

9.4 Comparison of All Technologies and Locations

Although all the CSP technologies and cooling type configurations have been analysed at their various locations, it was deemed necessary to compare all the technologies at all locations based on four key metrics. This was done in order to address the third objective defined in this study through the comparison of the relative metrics; and to determine any trends in the results. The *LCOE*, *total installed cost per net capacity*, *annual water consumption*, and *annual energy production* data from Table 9.1, Table 9.2 and Table 9.3 was used to create the four graphs in Figure 9.1, to Figure 9.4 respectively. Any trends identified will be now discussed under their subsequent headings.

9.4.1 Comparison of Total Installed Cost per Net Capacity

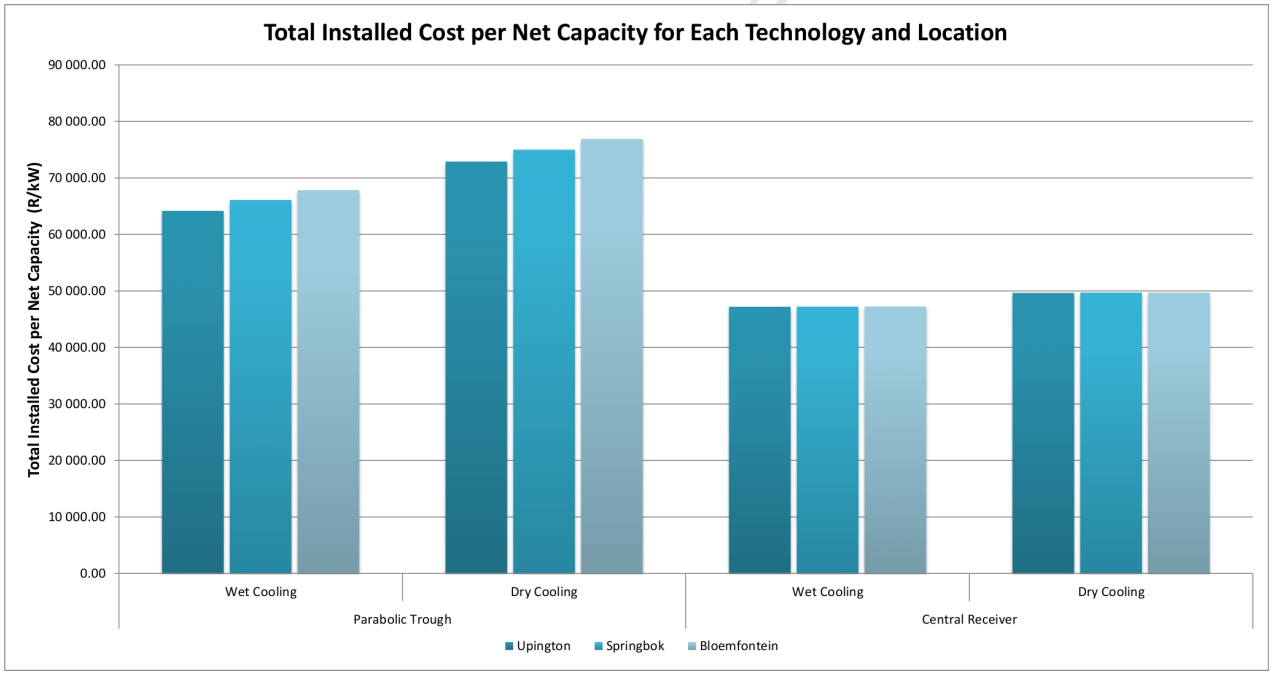

Figure 9.1: Comparison of Plant Total Installed Cost per Net Capacity for Each Technology and Location.

From Figure 9.1 three broad trends are initially evident. Firstly, for both wet and dry-cooled parabolic trough plants, the total installed cost per net capacity increases between Upington, Springbok and Bloemfontein, by approximately 3% between Upington and Springbok and a further 3% between Springbok and Bloemfontein; whereas for central receiver plants, the total installed cost per net capacity appears less influenced by location

with less than 0.1% variation. This is most likely related to the solar multiple of the plants, as the solar multiple influences the solar field size, and hence cost of the plant. As was discussed and shown in Table 8.13 and Figure 8.12, the parabolic trough plants have different solar multiples for each location (with Upington possessing the lowest and Bloemfontein the highest), while the central receiver plants have the same solar multiple for each location (but different solar multiples for wet and dry cooling).

Secondly, the dry-cooled plants for both parabolic trough and central receivers result in higher total installed costs, which is explained by their higher associated capital costs. The dry-cooled parabolic trough plants were shown to have approximately 13.5% greater total installed costs then their wet-cooled equivalents, while the dry-cooled central receivers were shown to have approximately 5% greater total installed costs then their wet-cooled equivalents. For the central receiver plants, the fact that the dry-cooled plants for all locations have a lower solar multiple than the wet-cooled plants (1.9 as opposed to 2.0) does help to reduce the difference in capital cost, however the dry-cooled systems are still more costly.

Finally, it is clear that central receiver plants have lower installed costs per net capacity than their equivalent capacity parabolic trough plants – approximately 26% – 30% less for wet cooling and approximately 31.5% – 35.5% less for dry cooling. As previously stated, this is due to different fundamental plant designs, components used, and component costs.

9.4.2 Comparison of Annual Energy Production

From Figure 9.2 the main trends identified are as follows; firstly, that location clearly has an effect on the annual energy production, with plants in Upington producing the most energy annually, followed by Bloemfontein and the least at Springbok. This trend closely follows the difference in annual DNI levels for each of the locations. Springbok was shown to produce approximately 6% – 10% less energy annually than Upington, while Bloemfontein was shown to produce approximately 3% – 9% less energy annually than Upington.

Secondly, all plant types making use of dry-cooling produce lower annual energy yields of approximately 2.5% – 6% less then their wet-cooled equivalents, which is attributed to the lower cycle efficiency of dry cooling.

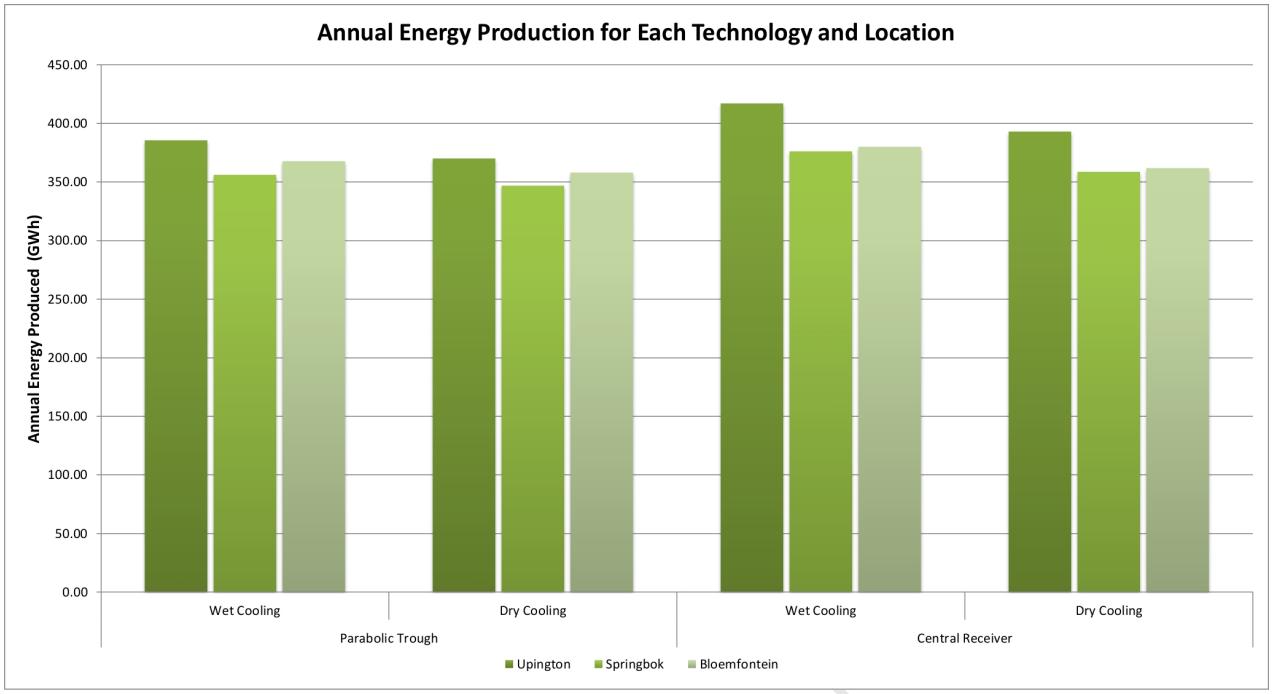

Figure 9.2: Comparison of Annual Energy Production for Each Technology and Location.

Finally, the results show that central receiver systems produce higher annual energy yields of between 1% – 8% more than their equivalent parabolic trough plants for all locations, which has previously been attributed to their higher concentration ratios and grater optical and overall efficiency. The magnitude of increase is also linked to location, however, with the Upington plants showing the greatest increase and the Bloemfontein plants the least.

9.4.3 Comparison of LCOE

The comparison of the LCOE for all technologies and locations, as presented in Figure 9.3 presents slightly different trends than those presented in the previous two graphs. Thus in order to attempt to understand these trends better, the results need to be considered in the context of the governing LCOE equation defined in Equation 9.1.

From the equation, it can be seen that the numerator contains a reference to the revenue generated from electricity sales, which in turn is related to the plant costs which need to be covered (PPA price). The denominator, however, contains a reference to the annual energy production of the plant. It is therefore evident that both the plant costs and energy production will have an effect on the LCOE of the plant in question.

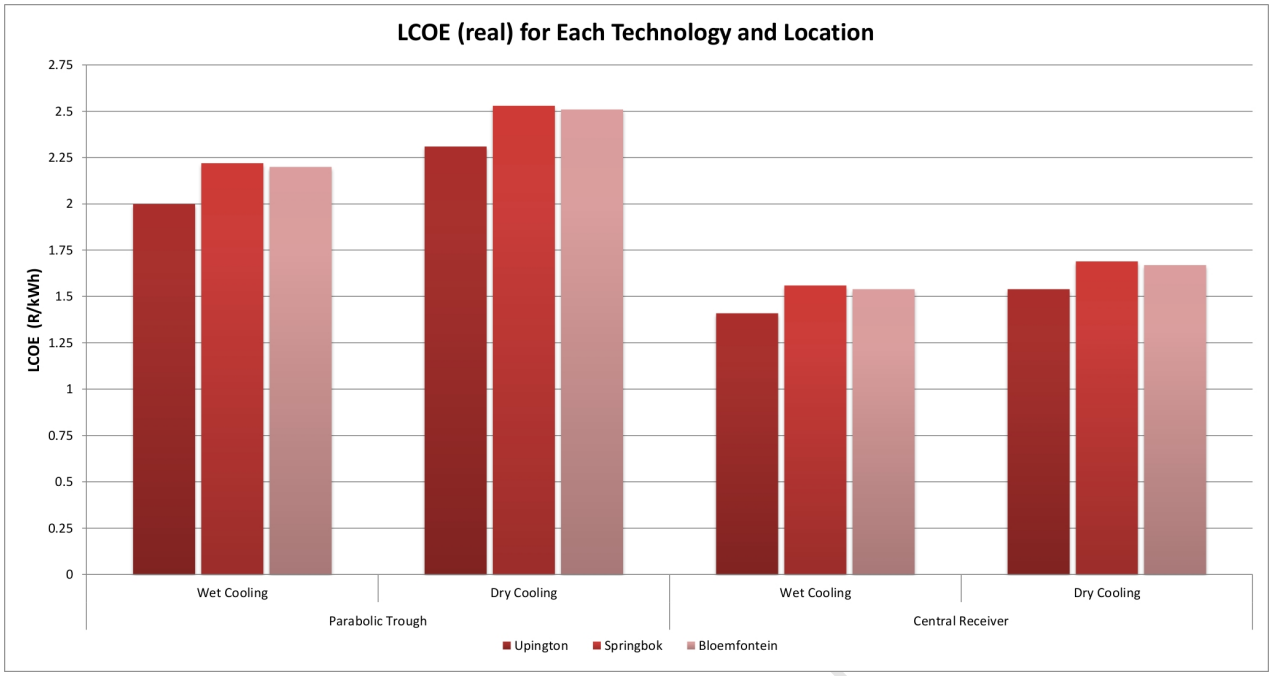

Figure 9.3: Comparison of LCOE (real) for Each Technology and Location.

The graph depicts that for both the parabolic trough and central receiver plants, the lowest LCOE occurs at Upington, whose location also represents the highest annual energy production with the lowest total system cost per net capacity. Bloemfontein, however, has the highest system cost on average, but also has a higher annual energy yield compared to Springbok, which in turn results in it having approximately an 8% – 10% higher LCOE than Upington (although lower than Springbok). Conversely, Springbok has a lower total installed cost per capacity than Bloemfontein, but also has a lower annual energy production value, which ultimately results in Springbok possessing the highest LCOE of all three locations – approximately 9% – 11% higher than Upington. This complex relationships between the LCOE, annual energy production and plant cost is a prime example of why it was necessary to perform the solar multiple optimisations in Chapter 8, in order to obtain the optimum balance between solar multiple (and hence plant size and cost) and energy production.

A second observation for the LCOE is that dry-cooled plants at all locations comprise higher LCOE values then their wet-cooled equivalents – between 14% and 15.5% higher for parabolic troughs and between 8% and 9.5% higher for central receivers. This is due to the higher system cost associated with dry cooling, as well as the reduction in efficiency and annual energy production.

Thirdly, the LCOE values for central receiver plants at all locations are lower than those of the parabolic trough plants – approximately 30% lower for wet-cooled plants and 33.5% lower for dry-cooled plants. This can be explained by both the lower system costs and higher energy output from the central receiver systems.

A final observation is that the LCOE for the dry-cooled central receiver plant in Upington (R1.54/kWh) is lower than that of the wet-cooled central receiver plant in Springbok (R1.56/kWh), and the same as the wet-cooled central receiver in Bloemfontein (R.154/kWh). The implications of this are that it may therefore be more beneficial to construct a central receiver CSP plant in a region with higher DNI levels but limited access to large volumes of cooling water, as opposed to an area with lower DNI levels but access to large volumes of water.

9.4.4 Comparison of Annual Water Consumption

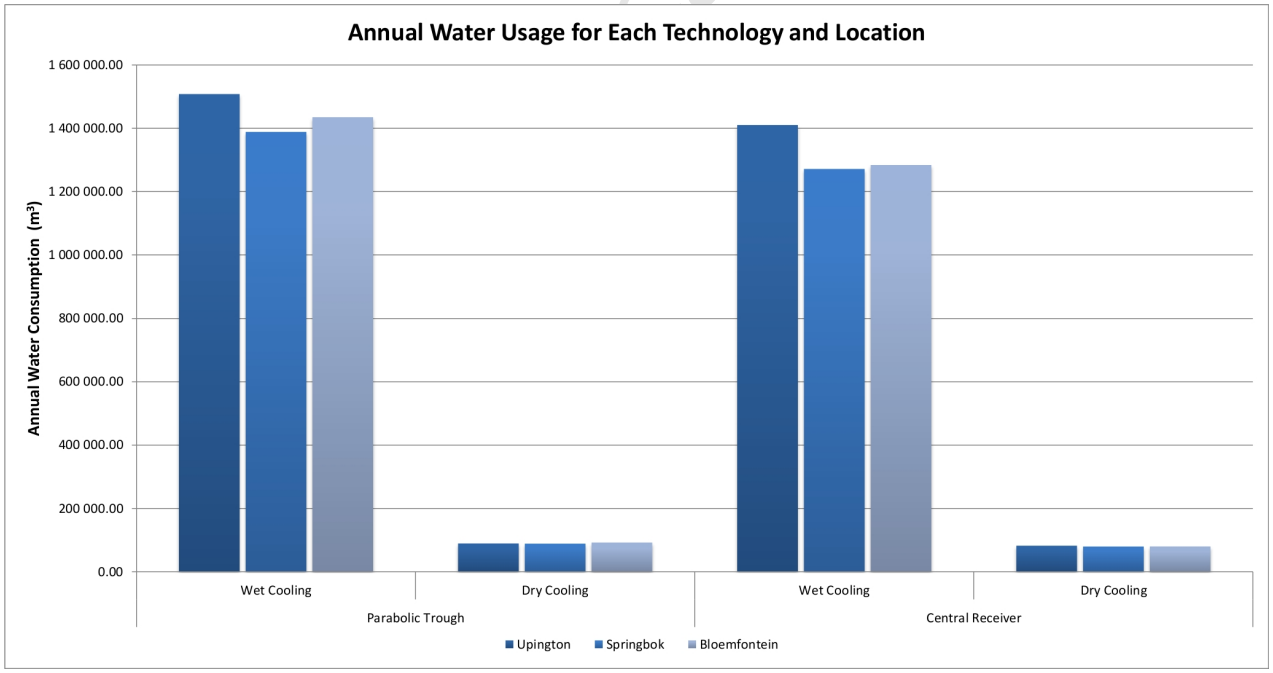

Figure 9.4: Comparison of Annual Water Usage for Each Technology and Location.

Figure 9.4 depicts three major trends for the water consumption of the CSP plants at all three locations. The first and most obvious is that wet-cooling consumes far more water annually than dry cooling. This is true for all locations for both parabolic trough and central receiver technologies, with the results showing dry cooling to eliminate more than 90% of annual plant water usage.

Secondly, as water consumption is directly linked to energy generation, the more energy a plant produces each year, the longer it runs closer to maximum capacity and the more water the power cycle consumes. This is can be seen for the plants located at Upington – as it receives the highest annual DNI values and produces the most energy annually, it also consumes the most water. Similar trends are visible when comparing the annual energy production depicted in Figure 9.2 to the water consumption shown in Figure 9.4.

Finally, it can be seen that all the central receiver plants consume less water by volume than their equivalent parabolic trough plants at all three locations – between 6% – 11% less for wet-cooled plants and between 7.5% – 13.5% less for dry-cooled plants. This has been previously discussed in Section 9.1.5 as well as in Section 4.4 of Chapter 4.

9.5 Validation and Comparison to Literature

In order to ensure that the results obtained in this analysis from the various model runs and simulations are reasonable and accurate, a comparison to similar results presented in the literature was conducted for validation purposes. Although the SAM software itself has been validated and used in industry and academia over the last few years, the comparison of the results in this study to those in the literature not only reaffirms SAM's credibility, but also helps to ensure that the assumptions and calculations made in this particular study in the adaptation of the simulations to South African conditions were reasonable and implemented accurately. In addition, the validation process also seeks to eliminate the possibility of user error when configuring and entering the data within the SAM software.

For the sake of brevity and due to time constraints, apart from in Table 9.8, only the results from the parabolic trough and central receiver models conducted for Upington were used in the validation and comparison process. It was assumed that as one of the primary differences between the Upington models and the others is in location, if the Upington models prove to be accurate, the models at the other locations would hopefully be as well.

The model results for the wet-cooled and dry-cooled parabolic troughs in Upington were compared to result data from the Sargent & Lundy (2003) report (containing both Sargent and Lundy, and SunLab data), as well as data from the International Energy Agency (IEA, 2010b) and the SAM (2010) default data. It is noted that for the wet-cooled parabolic trough models, no literature data was found pertaining to trough models in South Africa, and thus the comparison data presented is left in U.S. dollars for ease of comparison. For the dry-cooled trough, comparisons were made to data from the EPRI (2010) report, which was conducted for South Africa, and hence the results were reported in South African Rand. The results from the parabolic trough comparisons are tabulated and presented in Table 9.4 and Table 9.5.

The model results for both the wet-cooled and dry-cooled central receiver models were compared to the result data from the Sargent & Lundy (2003) report (which contained data for both the then Solar Tres and the proposed Solar100) and EPRI's own local South African modelling. The default SAM data was also used for validation purposes, with its results converted to South Africa Rand by means of the exchange rate stated in Chapter 8. The results from the central receiver comparisons are tabulated and presented in Table 9.6 and Table 9.7.

In addition, the model results for the percentage reduction in annual energy production and percentage increase in LCOE as a result of employing dry cooling instead of wet cooling, for both the parabolic trough and central receiver plants at all three locations, were compared to the percentage values stated in the literature by the IEA (2010b) and the DOE, U.S. (2010). The results of this comparison are present in Table 9.8. A brief discussion regarding the accuracy of each of the metrics will now follow under their respective headings.

Table 9.4: Validation of Upington Wet-Cooled Parabolic Trough Results. *Source of Data:* Sargent & Lundy (2003), IEA (2010b), SAM (2010).

Parabolic Trough	Wet-Cooled	SunLab	S&L	IEA	SAM	This Study
Total Plant Cost or Overnight Cost	($/kW)	4,859.00	4,816.00	–	7,987.66	9,141.84
LCOE	(¢/kWh)	±9.9	±10.2	20.0-29.5	15.34	28.50
Capacity Factor	(%)	53.5	–	–	41.25	44.02
Water Usage	(l/kWh)	–	–	–	3.97	3.91

Table 9.5: Validation of Upington Dry-Cooled Parabolic Trough Results. *Source of Data:* EPRI (2010), SAM (2010).

Parabolic Trough	Dry-Cooled	EPRI	SAM	This Study
Total Plant Cost or Overnight Cost	(R/kW)	43,385.00	63,745.81	72,898.77
LCOE	(R/kWh)	2.08	1.25	2.31
Capacity Factor	(%)	36.30	39.63	42.25
Water Usage	(l/kWh)	0.245	0.252	0.242

Table 9.6: Validation of Upington Wet-Cooled Central Receiver Results. *Source of Data:* Sargent & Lundy (2003), IEA (2010b), SAM (2010).

Central Receiver	Wet-Cooled	Solar Tres		Solar100		SAM	This Study
		SunLab	S&L	SunLab	S&L		
Total Plant Cost or Overnight Cost	($/kW)	7,135	9,090	3,103	4,608	5,730	6,724
LCOE	(¢/kWh)	11.5	14.3	4.8	6.8	10.46	20.06
Capacity Factor	(%)	–	–	–	–	46.21	47.61
Water Usage	(l/kWh)	–	–	–	–	3.30	3.38

Table 9.7: Validation of Upington Dry-Cooled Central Receiver Results. *Source of Data:* EPRI (2010), SAM (2010).

Parabolic Trough	Dry-Cooled	EPRI	SAM Default	This Study
Total Plant Cost or Overnight Cost	(R/kW)	32,190.00	43,935.65	49,655.27
LCOE	(R/kWh)	1.57	0.82	1.54
Capacity Factor	(%)	36.70	44.54	44.87
Water Usage	(l/kWh)	0.295	0.197	0.210

Table 9.8: Validation of Cooling Technology Effect on Plant Efficiency and Water Consumption. *Source of Data:* DOE, U.S. (2010), IEA (2010b).

Plant Type	Source	Reduction of Annual Energy Production*	Increase in LCOE*
Dry-Cooled Parabolic Trough	IEA (2010b)	7%	10%
Dry-Cooled Parabolic Trough	DOE, U.S. (2010)	4.5 - 5%	2 - 9%
Dry-Cooled Central Receiver	DOE, U.S. (2010)	1.3%	–
Upington, Dry-Cooled Trough	This Study	4.0%	15.5%
Upington, Dry-Cooled Tower	This Study	5.8%	9.2%
Springbok, Dry-Cooled Trough	This Study	2.6%	14.0%
Springbok, Dry-Cooled Tower	This Study	4.6%	8.3%
Bloemfontein, Dry-Cooled Trough	This Study	2.6%	14.1%
Bloemfontein, Dry-Cooled Tower	This Study	4.8%	8.4%

* When compared to equivalent plant with wet cooling technology

9.5.1 Validation of Total Installed Cost per Net Capacity

The total installed cost per net capacity for both the parabolic trough and central receiver models are in the same order of magnitude as those from the literature, albeit occasionally more than 50% higher. The only case where the costs in this study are less than those in the literature is for the then Solar Tres central receiver plant. The higher than average total installed costs for the plants in this study are attributed to both the SAM default costs (and hence the costs by the WorleyParsons Group) on which they are based, and to the conservative cost adjustment factors applied in Section 8.5.1 to represent the higher overall capital and O&M costs in South Africa. It is also noted, however, that the total installed cost per net capacity metric is variable for all plants in the literature, and therefore, the fact that the costs used in this study were based on SAM inputs, and that they were in the correct order of magnitude, renders them deemed acceptable.

9.5.2 Validation of LCOE

In contrast to the total installed cost per net capacity data, the LCOE values calculated in this study are not only in the same order of magnitude to those in the literature, but are approximately within 10% of those EPRI (2010) achieved for South Africa. The wet-cooled trough and central receiver models achieved slightly higher LCOE values than those in the literature, but the trough values were still within the range suggested by the IEA (2010b). The LCOE values were higher than the default SAM values, however, but this is primarily due to the SAM values representing plants in the U.S as opposed to South Africa.

9.5.3 Validation of Capacity Factor

The capacity factors achieved in this study were on average higher than those in the literature, but usually not by more than 20%. The higher capacity factors in this study can be attributed to the higher DNI levels in Upington compared to the plant locations in the literature, as well as the 6 hour storage capacity used in this analysis.

9.5.4 Validation of Annual Water Usage

The annual water consumption results from this study were extremely similar to those in the literature, usually with less than a 10% difference. As the water consumption is related to the annual energy output of the plant, some variability was experienced.

9.5.5 Cooling Technology Effect on Plant Efficiency and Water Consumption

The percentage reductions in annual energy production as a result of employing dry cooling for all the plants are in the same order of magnitude to those stated in the literature, and similar in *value* to within approximately 4.5%. The results for the parabolic trough models are slightly lower than those predicted in the literature, while the results for the central receivers are slightly higher than the literature values. The percentage increases in LCOE as a result of employing dry cooling are also in the same order of magnitude to those stated in the literature, with the parabolic trough values slightly higher by a *value* of approximately 4 - 5.5% and the central receiver values within the expected range stated for parabolic troughs. No value was found in the literature for the increase in LCOE as a result of dry cooling adoption in central receiver plants.

9.5.6 Major Cost Categories Breakdown

As a further means of verifying that the total installed costs are indeed primarily a result of the conservatively high SAM default values and South African conversion factors, and are not disproportionate to each other nor contain any other errors, a major cost category breakdown was created for comparison with the literature. Once again, for the sake of brevity, this major cost category breakdown was only created for the Upington plants, in particular only the wet-cooled parabolic trough and central receiver models. Both model cost breakdowns were compared to similar graphs presented in the Sargent & Lundy (2003) report. The graphic comparisons for the wet-cooled parabolic trough are presented in Figure 9.5 and Figure 9.6, while the wet-cooled central receiver comparisons are presented in Figure 9.7 and Figure 9.8.

From Figure 9.5 and Figure 9.6, it is evident that proportion and distribution of the major costs for the wet-cooled parabolic trough plants in this study are very similar to those of the 2004, 100 MW trough plant described in the Sargent & Lundy (2003) study, albeit that the Sargent and Lundy plant possesses 12 hours of TES compared to the 6 hours used in this study. The percentage cost distribution across all categories, except the solar field, are within 4% of each other, while the solar field values are within 7%.

From Figure Figure 9.7 and Figure 9.8, it is evident that proportion and distribution of the major costs for the wet-cooled central receiver plants in this study are very similar to those of the proposed Solar 220 plant outlined in the Sargent & Lundy (2003) study. The percentage cost distribution across all categories, except for the power block and balance of plant, are within 3% of each other. The power block and balance of plant values are within 7% of each other.

The strong agreement between the cost category results for both the wet-cooled parabolic trough and central receiver models in this study and those in the literature therefore suggests that although the final magnitude of the cost are slightly higher in this study, the distribution and proportion of the major cost categories are still strongly comparable to the literature.

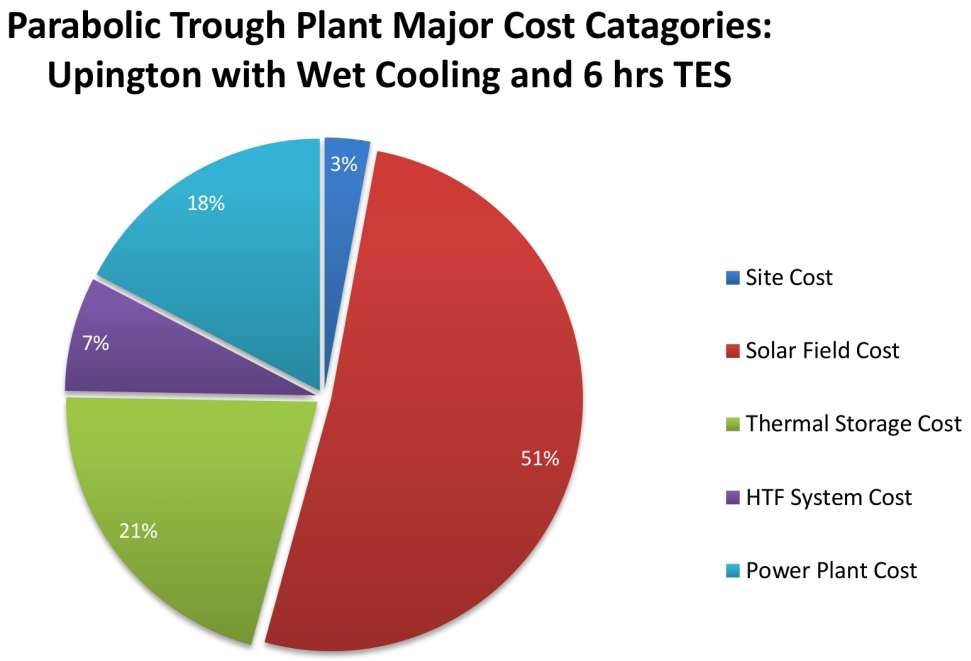

Figure 9.5: Parabolic Trough Major Cost Components for Upington with Wet Cooling.

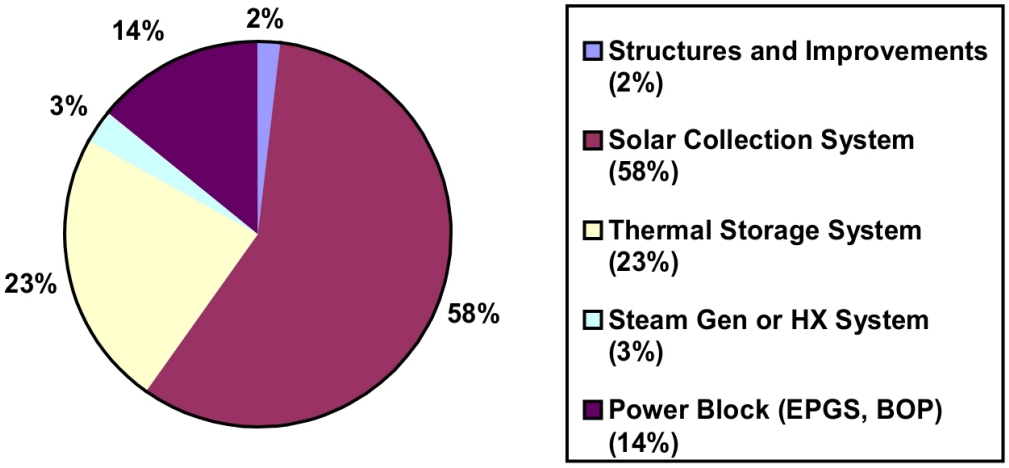

Figure 9.6: Major Cost Categories for Parabolic Trough Plant 2004 Near-Term Case: 100 MW_e, 12 hours TES, 2.5 Solar Multiple (Sargent & Lundy, 2003).

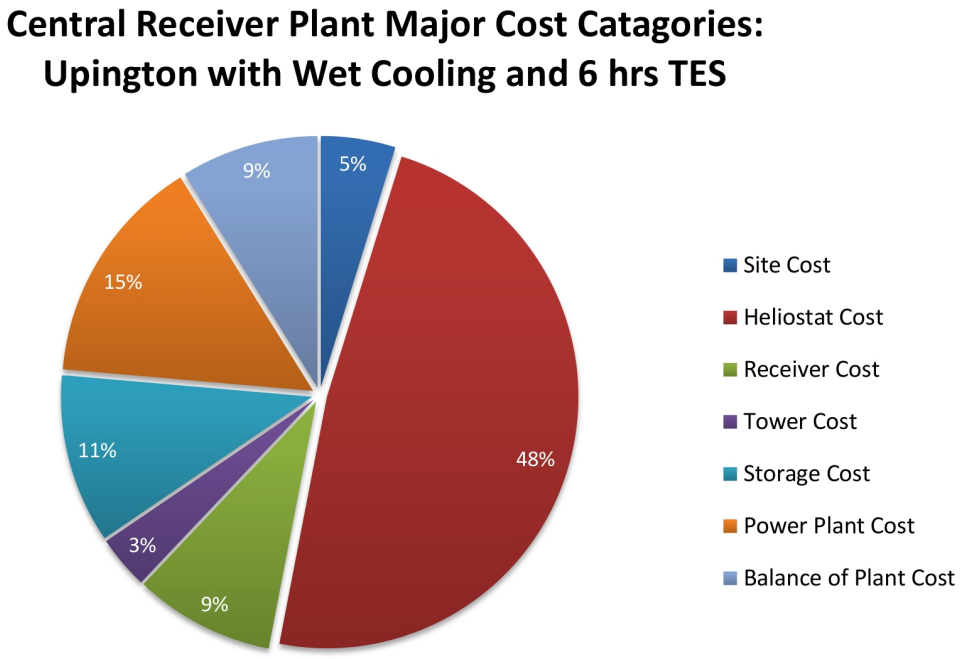

Figure 9.7: Central Receiver Major Cost Components for Upington with Wet Cooling.

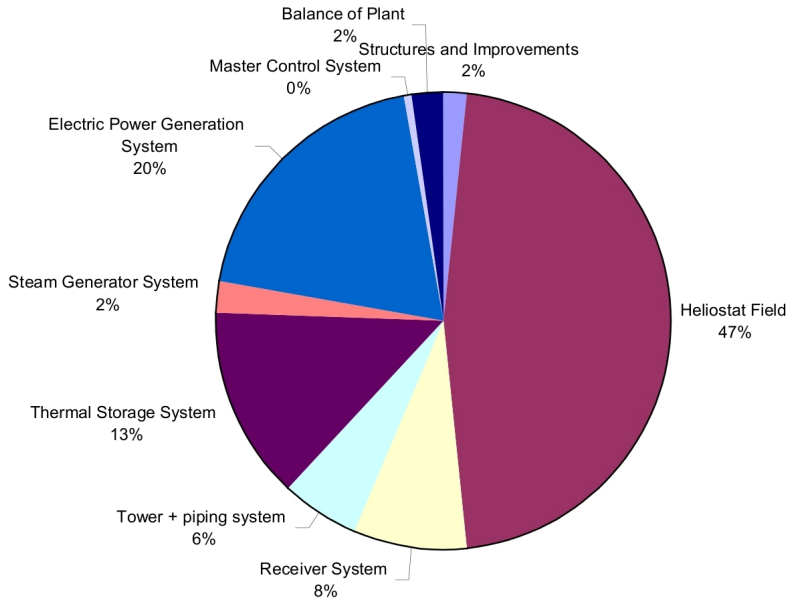

Figure 9.8: Capital Cost Categories for Solar 220 (Sargent & Lundy, 2003).

9.5.7 Daily Generation Profiles

As a final means of validation, solar generation profiles were created from the performance component of the SAM models, and compared to similar generation profiles presented in the EPRI (2010) report. The solar generation profiles display the total incident power from the solar field (Q_SF: in red), the thermal energy directed to the thermal energy storage (Q_to_TES: in blue), the thermal energy directed from the TES to the power block (Q_from_TES: in green), the total thermal energy entering the power block (Q_to_PB: in purple), the gross energy output from the power block (E_gross or Cycle_power: in orange), and finally the net output from the power plant (E_net: in yellow). The generation profiles depict these metrics at hourly intervals over a 24 hour period of a chosen day, and allow for the visual determination of magnitude, timing and distribution of energy flows within the plant. The review of this data can then be used as a means to visually determine whether the energy flows within the plant are reasonable, and hence that the performance model component is functioning accurately.

The solar generation profile for the dry-cooled central receiver plant in Upington for the 16th of January is shown in Figure 9.9 while the generation profile for the EPRI (2010) dry-cooled parabolic trough plant on the 15th of January is shown in Figure 9.10. It was not possible to include solar generation profiles for this study's parabolic trough models, however, as the variables used to depict the energy flow to and from storage (Q_to_TES and Q_from_TES) were not available as outputs in the SAM parabolic trough model.

By comparing the two figures, it is clear that both the model in this study and that used by EPRI follow the same overall trends. The incident solar power varies throughout the day, increasing to its maximum around midday, before decreasing towards the evening. Whenever there is excess energy from the solar field, usually during the hottest period of the day, some of the thermal energy is diverted to storage, as expected. During periods of intermittent solar irradiation, and towards the evening, the excess energy from the TES is then diverted back to the power block, supplementing the energy from the solar field (and replacing it after sunset), in order to allow for continued operation of the plant at its rated capacity. Finally, the energy output from the plant is observed to be less than the energy diverted to the power block, which is a result of losses in the cycle.

The plant generation profile clearly illustrates that the plant operates exactly as expected and designed, and in addition, follows the same pattern of the generation profile depicted in the literature. It is therefore confirmed that the SAM performance model used in this study was executed accurately, and that the results predicted by it are fair.

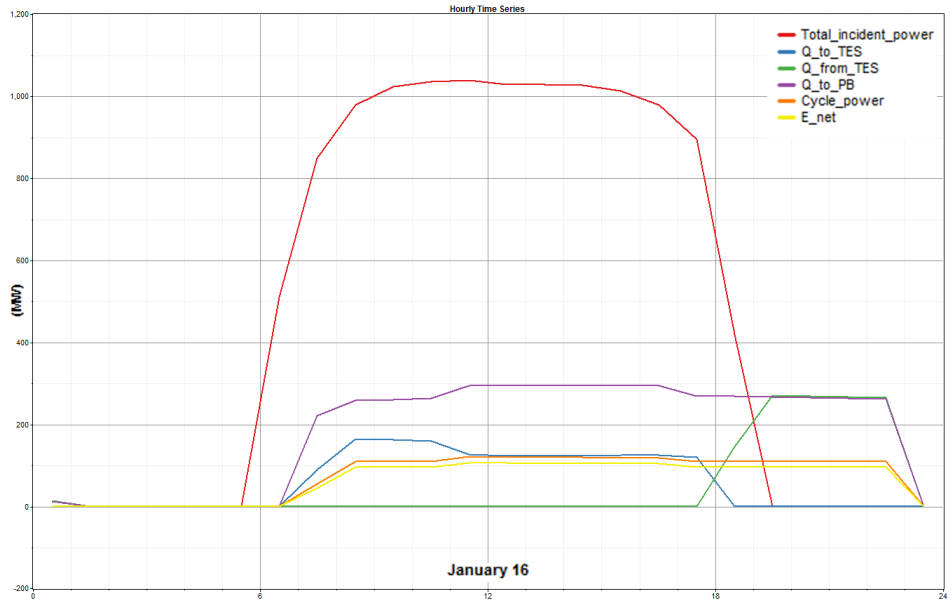

Figure 9.9: Solar Profile for Central Receiver with Dry Cooling and 6 Hours TES in Upington in Summer.

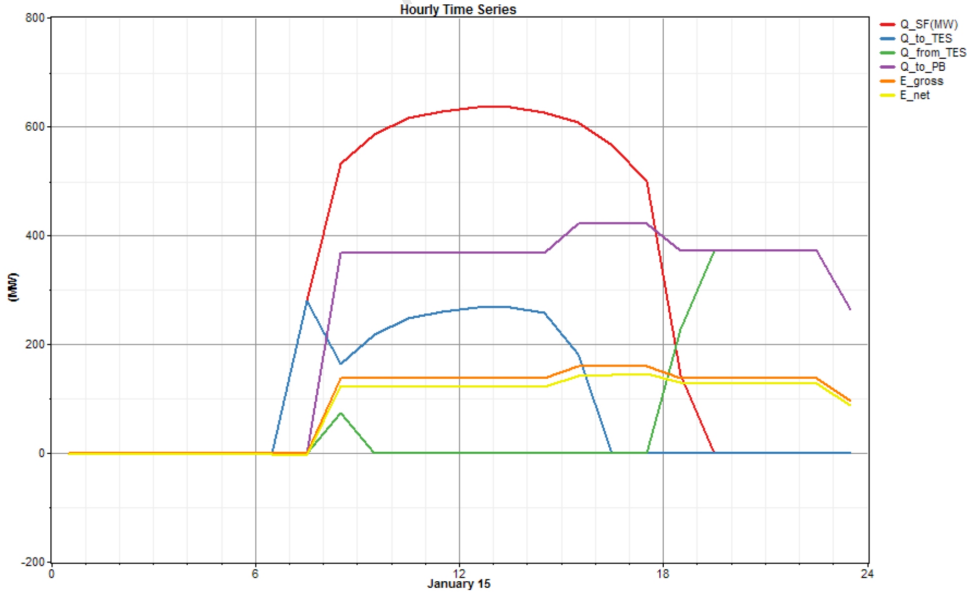

Figure 9.10: Solar Profile for Parabolic Trough with Dry Cooling and 6 Hours TES in Summer (EPRI, 2010).

10 Sensitivity Analysis of Model Inputs

Although the results from this study have been presented and validated, it is important to consider that for any technology, both new and mature, some degree of uncertainty is generally expected in the cost and performance input data used in its modelling. As eluded to in Chapter 8, fairly new or non-commercialised technologies such as the central receiver do not have extensive histories or track records from which to draw complete data, and thus estimates are often used. Even more mature or commercialised technologies such as the parabolic trough are prone to uncertainties stemming from the uniqueness of local conditions (EPRI, 2010). It is therefore necessary to no only be aware of the uncertainties in the input data, but also to attempt to predict and understand how these uncertainties will influence the model results, while determining which inputs have the greatest effect on the final model output.

In order to accomplish this, a sensitivity analysis was conducted for a various number of the input variables used in this study. The input variables considered comprise the following financial inputs: the debt fraction, inflation rate, loan rate (or cost of debt), minimum IRR and real discount rate. The following cost inputs were also analysed: the fixed cost by capacity, the cost of water (represented by the variable cost by generation), and for parabolic trough plants; the solar field cost. Due to the nature of the heliostat optimisation wizard for the central receiver model in SAM, it was not possible to directly integrate the solar field cost into the sensitivity analysis for central receiver plants. Once again, for the sake of brevity, the sensitivity analysis was only conducted for the models of plants in Upington, as it was assumed similar trends would occur for the plants in Springbok and Bloemfontein.

For each one of the input variables, a range of possible values were assigned, based on values suggested in the literature. These limits will now be discussed briefly, while a final summary is presented in Table 10.1.

10.1 Limits and Ranges for Input Variables

An upper limit of 70% was adopted for the debt fraction, based on the value stated in the REFIT Phase II document (NERSA, 2010). A lower limit of 50% was adopted in order to assess the effects of a lower debt fraction.

For the variation in inflation rate, it was decided to adopt a 1% variation in the lower limit and 2% in the upper limit, in order to account for the fluctuation in inflation rate. This resulted in a lower limit inflation rate value of 3.3% and an upper value of 6.3%.

The base case value of 7.3% for the cost of debt was adopted from EPRI (2010) as stated in Chapter 8, however, NERSA (2010) made use of a value of 6.39% while Sargent & Lundy (2003) adopted a value of 8.5%. Using these values as a reference, a lower cost of debt limit of 6.3% and an upper limit of 8.3% was adopted in this study.

Although NERSA (2010) make use of a minimum IRR value of 17% in the REFIT II document (which is the base case value adopted in this study) the SAM default value was 15%, while Sargent & Lundy (2003) made use of a value of 14%. As the adopted base case value of 17% is rather conservative, it was decided to use a lower limit of 15% while increasing the upper limit by only 1% to yield 18%.

NERSA (2010) make use of a real discount rate of 12% in the REFIT Phase II, which is considerably higher than the 8.6% adopted in this study. It was therefore decided to vary the discount rate between 8% and 12% to cover the majority of commonly accepted values.

For variations in both capital and O&M costs, Sargent & Lundy (2003) suggest making use of a ±10% variation around the base case value. This method was therefore chosen for the sensitivity analysis in this study.

As was discussed in Section 8.6 of Chapter 8, a wide range of water costs were listed, with ultimately the mean raw cost from Van der Merwe (2011) being adopted before being combined with treatment costs listed in the Sargent & Lundy (2003) report. For the sensitivity analysis, the full range of the costs given by Van der Merwe (2011) were considered, before being combined once again with the treatment costs from Sargent and Lundy. The final calculated values are listed in Table 10.1.

Table 10.1: Variation Limits of Input Variables for Sensitivity Analysis.

	Base Case	Lower Limit	Upper Limit	Reference
Financing Assumptions				
Debt Fraction	60%	50%	70%	NERSA (2010)
Inflation	4.3%	3.3%	6.3%	
Cost of Debt	7.3%	6.3%	8.3%	NERSA (2010); Sargent & Lundy(2003)
Minimum Required IRR	17%	15%	18%	SAM (2010)
Real Discount Rate	8.6%	8.0%	12.0%	NERSA (2010)
O&M Costs				
Fixed Cost by Capacity	$ 88.03	-10%	+10%	Sargent & Lundy (2003)
Variable Cost by Generation (Incorporating Cost of Water)				
Parabolic Trough Wet Cooling	$ 7.04	$ 5.76	$ 8.32	Calculated from: van der Merwe (2011); Sargent & Lundy (2003)
Parabolic Trough Dry Cooling	$ 3.39	$ 3.26	$ 3.52	
Central Receiver Wet Cooling	$ 6.16	$ 5.16	$ 7.16	
Central Receiver Dry Cooling	$ 3.45	$ 3.31	$ 3.59	
Capital Costs				
Solar Field Cost (Parabolic Trough Only)	$ 385.13	-10%	+10%	Sargent & Lundy (2003)

10.2 Sensitivity Analysis Results

The chosen output metric used to determine the sensitivity of the model to the aforementioned sensitivity input metrics, was that of the LCOE. The LCOE was chosen for the same reasons as stated in the beginning of Chapter 9, in that it provides a means to compare all technologies on an equal basis, while capturing the trade-offs between projects with different designs, capital and O&M costs, and financing parameters (SAM, 2010). The results from the sensitivity analysis are presented in graphical format for both the Upington wet-cooled and dry-cooled parabolic trough and central receiver plants in Figure 10.1 to Figure 10.4 respectively.

As can be seen from the figures, the LCOE is most sensitive to the values stipulated for the inflation rate, closely followed in second by the debt fraction. For both these inputs, an increase in their value results in a decrease in the LCOE, due to the reduction in comparable magnitude of the initial capital outlay. Variations in these inputs can see the LCOE ranging from approximately R1.81 to R2.16 per kWh for the wet-cooled parabolic trough, R2.10 to R2.51 per kWh for the dry-cooled parabolic trough, R1.28 to R1.52 per kWh for the wet-cooled central receiver, and R1.40 to R1.66 per kWh for the dry-cooled central receiver.

The third most influential input of those considered is that of the minimum required IRR, which sees an increase in LCOE with an increase in its value. This is in-line with it being one of the constraining inputs in the financial model. The solar field cost (only applied to the parabolic trough models) closely follows as the next most influential input, and represents a large portion of the project capital cost – as can be seen by its share in Figure 9.5. Intuitively, an increase in the capital cost sees an increase in the LCOE. Variations in these two inputs result in the LCOE ranging from approximately R1.90 to R2.09 per kWh for the wet-cooled parabolic trough, and R2.20 to R2.42 per kWh for the dry-cooled parabolic trough.

The subsequent three inputs, comprising the loan rate, real discount rate, and fixed cost by capacity all have a relatively small effect on the LCOE, with the *overall influence* ranging from approximately R0.10 per kWh down to R0.02 per kWh on either side of the base case value. For all three inputs, an increase in their value also results in an increase in the LCOE.

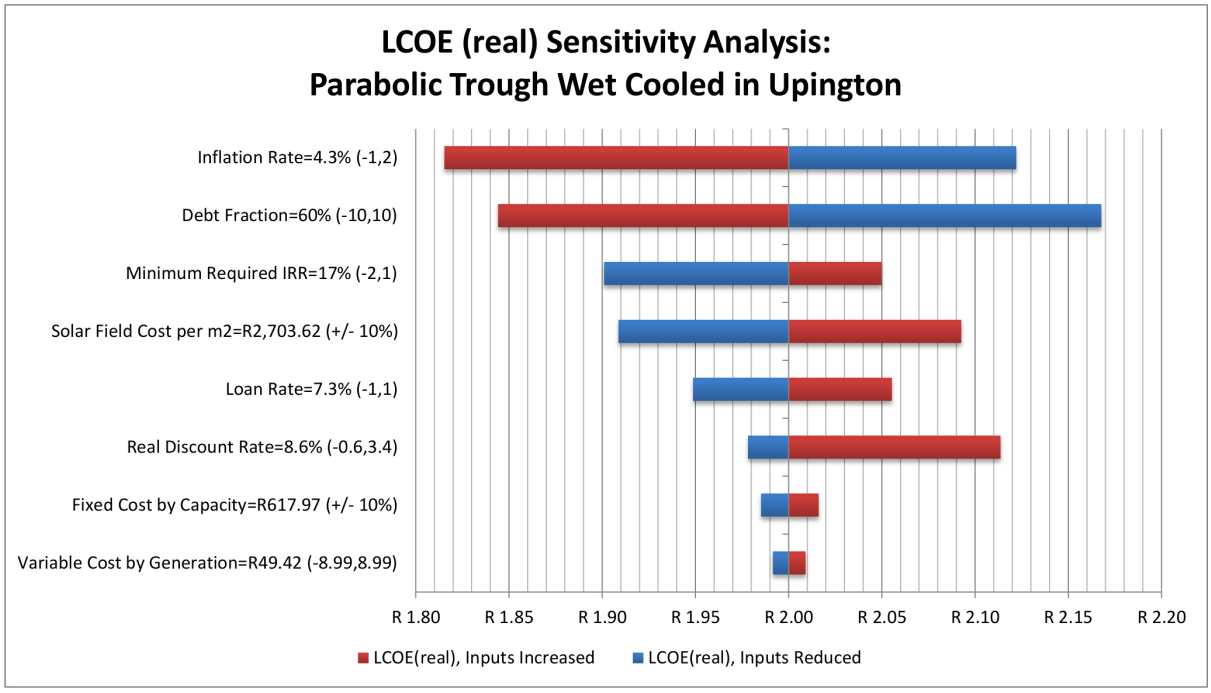

Figure 10.1: Sensitivity Analysis of LCOE (real) for Parabolic Trough with Wet Cooling in Upington.

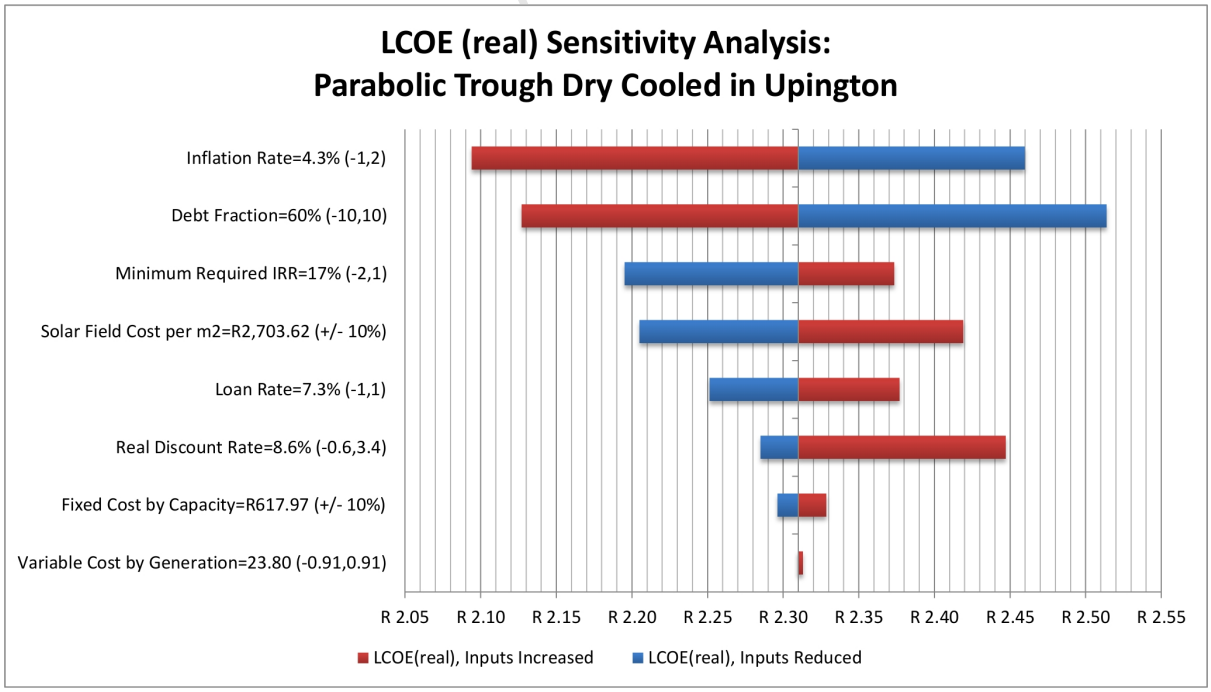

Figure 10.2: Sensitivity Analysis of LCOE (real) for Parabolic Trough with Dry Cooling in Upington.

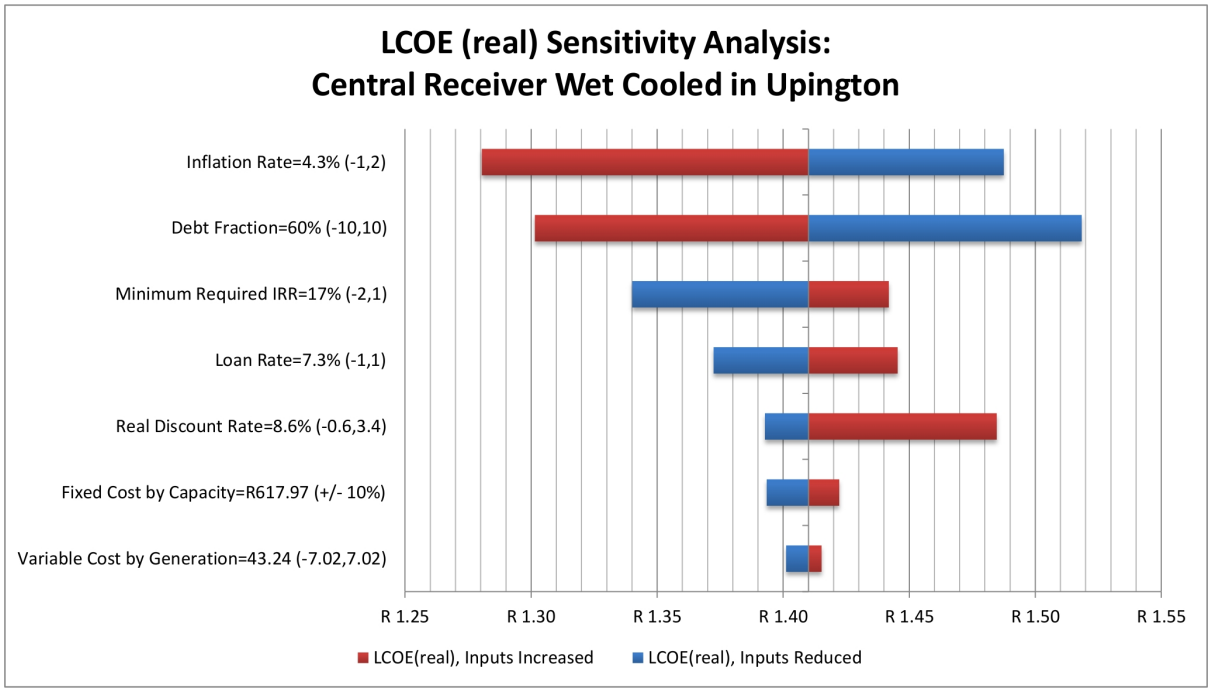

Figure 10.3: Sensitivity Analysis of LCOE (real) for Central Receiver with Wet Cooling in Upington.

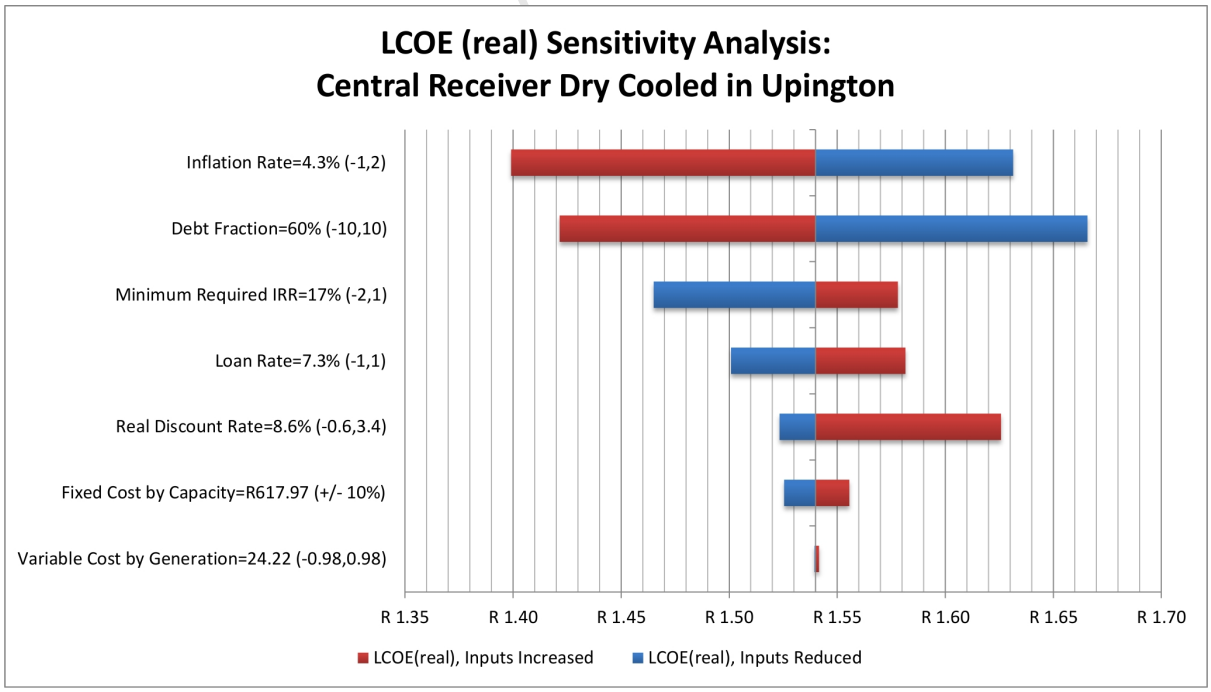

Figure 10.4: Sensitivity Analysis of LCOE (real) for Central Receiver with Dry Cooling in Upington.

Of all the input variables considered in the sensitivity analysis, that which has the least effect on the LCOE is the cost of water (represented by the variable cost by generation). Although an increase in the cost of cooling water does lead to an increase in the LCOE, the increase is approximately R0.01 per kWh for both the wet-cooled parabolic trough and central receiver plants, and less than R0.01 per kWh for the dry-cooled plants. Therefore, according to the model, it is implied that even if the cost of raw water increases to the upper limit of R8.25 per kilolitre, the wet-cooled plants will still be more cost affective – in terms of LCOE – than their dry-cooled equivalents. This in turn implies that the availability of raw cooling water, rather than its current cost, will limit the use of wet cooling technology.

10.3 Validation of Sensitivity Analysis Results

One of the major outcomes of the sensitivity analysis is the prediction that the financial constraints, rather than the plant capital costs, have the largest influence over the resulting LCOE. This result is consistent with statements made in the SAM (2010) documentation, which state that long term projects are very sensitive to values specified for the minimum IRR, minimum DSCR and the requirement of a positive cash flow. The documentation continues to state that in some instances it is possible that these financial constraints can render the project capital investment cost a relatively insignificant factor in the LCOE calculation (SAM, 2010).

11 Conclusions

The aims of this dissertation comprised thee key objectives, the first of which was to develop a methodology for the identification and quantification of potential CSP sites in South Africa, and subsequently, present an approach for creating South African specific, high-level techno-economic models of current commercial CSP technologies at select identified locations within the context of current conditions and boundaries. Secondly, to use this approach to attempt to ascertain which of the CSP technologies modelled would be considered optimal for each location, and to determine whether the use of wet cooling or dry cooling technology would be more beneficial. And thirdly, as at the time of writing, no utility-scale commercial CSP plants had yet been realised in South Africa, the final objective of this study was to derive useful insight into and understanding of the techno-economic criteria and their effect on CSP developments, through the comparison of different model results and hence the arising relative metrics, as opposed to absolute value predictions.

The work presented in this dissertation represents the fulfilment of these objectives, in that a methodology was developed whereby potential sites were successfully identified and quantified within the ArcGIS software package, and South African specific performance and cost-based models were created for both parabolic trough and central receiver technologies at each location by means of the SAM software package and the adaptation of model data to South African conditions. Attempts were made to identify the optimal CSP technology and cooling technology for each site considered, and key techno-economic criteria were identified through the comparison of model data and sensitivity analyses.

Thus, based upon the analyses, results and findings of this study, the following conclusions have been drawn and are presented in three categories relating to the GIS analysis, SAM analysis, and analysis of research questions:

11.1 Conclusions Drawn from GIS Analysis

11.1.1 Data, Analysis Criteria and GIS Methodology

Successful Sourcing of Data and Creation of GIS Methodology

Through the conduction of a literature review of previous studies concerned with GIS-based CSP-potential analysis, the characteristics required for potential CSP sites in this study were successfully identified, and relevant analysis criteria developed. The analysis criteria included the level of direct normal solar irradiation, a land slope of less than 1%, areas excluded due to land class, areas classed as 'least threatened' vegetation, and less than 20 km proximity to large water bodies and 132 kV transmission lines. The required data for the study was determined and sourced, thereby allowing for a comprehensive, high-level GIS analysis to be conducted.

An efficient GIS analysis methodology was also successfully researched and developed, and presented in its entirety in Appendix A. The implementation of the methodology in the GIS software allowed for the visualisation, analysis and interpretation of the imported data, which in turn made the creation of maps and the extraction and quantification of information possible.

Potential for Data Improvements

The solar data from NREL (SWERA, 2010) only had a spacial resolution of 40 km $\times$ 40 km, and hence could not depict small-scale variations in DNI caused by changes in local terrain or surroundings. Although this data was the best freely available data for South Africa with the highest spacial resolution, it was decided to make use of the shading and DNI calculation algorithm within the ArcGIS software package, as a means to verify the NREL data (and hence the results achieved), and attempt to predict location specific DNI levels. The DNI calculation algorithm was run with mixed success, and ultimately only used to calculate location specific variations in DNI for a few potential sites. It is concluded, however, that the results for the identified potential CSP sites arising from the analysis cases do indeed coincide with areas receiving high amounts of annual DNI, and hence that the NREL DNI data is acceptable for a high-level study. Further validation and more extensive analyses including the sourcing of higher resolution DNI data is recommended, however.

A further conclusion drawn regarding the data used in the GIS analysis, is that the large water bodies and rivers analysis layer, although suitable for this high-level study, did not contain information regarding the magnitude of water flow-rates, nor the volumes that are permissible for extraction. It was therefore not possible to determine whether a potential site situated near one of these water bodes would in fact be permitted to extract water from it, and if were, what quantities would be available. Furthermore, the transmission and national grid data employed was digitised and geo-referenced from an image, and it is hence concluded that the sourcing of a primary source of grid data would be beneficial for future studies.

A final conclusion regarding data for the GIS analysis surrounds the adopted land class data. The land class data employed in the study did not contain any information regarding the land value associated with a particular area. Data regarding various land area costs could be greatly beneficial to developers in further determining optimal CSP sites, based on the ranking of sites according to the cost associated with either the purchase or rental of the land in question.

11.1.2 Potential CSP Site Identification

Potential CSP Sites Successfully Identified and Quantified

The GIS analysis allowed for the successful identification of a large number of potential CSP sites for each of the five analysis cases. Of the identified potential CSP sites, the vast majority were situated in the Northern Cape, but were limited by the lack of national grid capacity and availability of large water sources in the cases where they formed part of the analysis criteria. Other provinces which contained identified potential sites included the Western and Eastern Cape, the Free State and North West Province.

A number of potential sites were also identified along the West Coast of South Africa, however, the identified potential areas only comprised a small portion of the total West Coast coastline. This is mainly attributed to the combination of a lack of extensive grid capacity in the region, the decrease of DNI levels towards the coast, and the 'threatened vegetation' on the West Coast of the Western Cape. The few potential sites identified could prove to be viable locations if sea water is to be adopted for plant cooling purposes, however as stated in Section 9.2.6, the modelling of sea water cooling was beyond the scope of this report, and thus further analysis is required – including the local measurement of coastal DNI levels and other weather data – in order to determine whether it would be more economical than adopting dry cooling.

The quantification of the five analysis cases – when only considering sites with individual areas grater than 2 km^2 – predicted a total potential land area for CSP in South Africa of anywhere between 2,180.5 km^2 and 18,785.6 km^2, with total available solar energy levels between 16.5 TWh/day and 144.3 TWh/day, depending on which analysis criteria were adopted. These values were more than tripled if the requirement for a site to have an area greater than 2 km^2 was removed and hence all potential areas were included. Of the five analysis cases, Case 2 resulted in the lowest identified site area and hence energy generation potential, caused by its stricter DNI requirement of 6.5 $kWh/m^2/day$ (compared to 6.0 $kWh/m^2/day$ of Case 1) as well a requirements for a 20 km proximity to both large water bodies and the national grid. Of the first three analysis cases (concerned with existing grid proximity) Case 3 resulted in the greatest site area and energy generation potential. When the requirement for close proximity to the national grid was excluded, as in Case 4 and Case 5, the increase in site area and energy generation potential was dramatic, with increases of more than fourfold being realised over their equivalent Case 2 and Case 3 scenarios. From these analysis case results the following additional conclusions are drawn:

Vast Potential for CSP in South Africa

Even when constrained by the requirement for CSP sites to be larger than 2 km^2 in order to be considered, vast potential still exists for a utility-scale CSP sector in South Africa. Furthermore, if one considers the higher capacity factors of central receiver plants compared to parabolic troughs, as well as the central receiver's better tolerance for land slope, central receiver technology is deemed a superior choice for adoption.

Requirement for Site Proximity to Large Water Bodies a Limiting Factor

The requirement for a close site proximity to large water bodies greatly reduces the area and hence energy generation potential of CSP sites in South Africa. The implications of this are that by reducing reliance on cooling water or adopting alternative cooling technologies such as dry cooling, a far greater CSP potential could be realised in terms of number of sites and total potential area. It is thus concluded that in order to fully realise the solar resource potential in South Africa, it may be necessary to make use of dry cooling technologies for the majority of all new CSP plants.

Limitations Arising from Existing National Gird

The number of potential CSP sites are also limited by the lack of national grid capacity in regions with high DNI levels, especially in the Northern Cape. This is evident by the

fact that all the identified sites are clustered around the few large transmission lines in the region. If the the national grid were to be further extended into areas with high CSP potential, the total available area and energy generation potential for CSP could be greatly increased. The site areas identified in Case 4 and Case 5, or similar areas identified by future analyses, could also be used to determine the optimal areas in which future national grid expansion would be beneficial. The cost benefit analysis of the extension of the national grid was considered beyond the scope of this study, but it is deemed a key requirement for future studies.

11.1.3 Validation of CSP Site Identification

Successful Validation of CSP Site Identification

The results achieved in the various GIS analyses were validated by means of comparison with those achieved in a study on South Africa's CSP potential by Fluri (2009). The results achieved in Case 3 of this study – which made use of virtually identical analysis criteria to those used by Fluri – and including sites smaller than 2 km^2, showed a strong resemblance to those achieved by Fluri. The other cases showed less of a resemblance due to the use of different analysis criteria to those used by Fluri. It is therefore concluded that the GIS methodology and analysis conducted in this study was implemented and conducted successfully.

11.2 Conclusions Drawn from SAM Analyses

11.2.1 SAM Model Input Data

Inputs for SAM Models Successfully Sourced and Calculated

The conduction of an extensive literature review of both CSP plant technical design and cost data allowed for the creation of a detailed comparison database, and ultimately lead to the decision to adopt the default SAM input values in the instances where relevant, South African specific data could not be sourced or calculated. A complete set of data inputs for each of the twelve SAM models, adapted to reflect local South African conditions, was successfully created within the SAM software, thereby allowing for a comprehensive performance and cost based analysis to be conducted for each technology at each considered location.

Weather Data from Towns Used to Approximate Potential Sites

The three locations of Upington, Springbok and Bloemfontein – whose weather data was used to represent conditions at potential CSP sites – were chosen due to the lack of freely available detailed weather data for specific geographic coordinates or regions containing potential CSP sites. It is therefore concluded that although this weather data was considered acceptable for this initial study, it will be necessary to obtain detailed, location-specific weather data for future analysis of potential sites. This location-specific data could be obtained commercially, however, the conduction of actual weather and DNI measurements at potential sites will likely be necessary.

11.2.2 Key Findings of SAM Analyses

Each of the twelve SAM models were successfully simulated within the SAM software. Through the analysis and review of the results obtained, the following key conclusions are drawn:

Wet Cooling Most Efficient when Available

The use of wet cooling technology with both parabolic trough and central receiver systems resulted in higher annual energy yields of between 2.5% and 6%, and greater capacity factors than equivalent plants at the same locations making use of dry cooling. This was attributed to the greater efficiencies achievable through the use of wet cooling, as a result of relying on lower wet-bulb temperatures as opposed to the higher dry-bulb temperatures of dry cooling.

The use of wet cooling was also found to result in lower total installed costs per net capacity and lower LCOEs than equivalent dry-cooled plants at the same location, with dry-cooled parabolic trough plants possessing approximately 13.5% greater total installed costs and 14% – 15.5% higher LCOEs, and dry-cooled central receivers approximately 5% greater costs and 8% – 9.5% higher LCOEs. This was attributed to the higher capital and O&M costs and efficiency penalties associated with the use of dry cooling. Wet cooling is therefore considered theoretically superior to dry cooling if ample cooling water is available, however, in water-stressed regions such as the Northern Cape of South Africa where large volumes of water may not be available, dry-cooling is considered the optimal choice.

Dry Cooling Dramatically Reduces Water Consumption

The use of dry cooling resulted in an annual reduction in water consumption of more than 90% for all CSP plants, when compared to equivalent wet-cooled plants in the same location. It is thus concluded that the use of dry cooling in regions with limited access to cooling water, or in cases where the cost of water is prohibitively high, will be a necessity and will allow for the realisation of CSP projects in regions that would otherwise not have allowed for them to be economically viable.

Central Receiver Technology Considered Preferable

When compared to the parabolic trough models in this study, the central receiver models were found to produce between 1% and 8% more energy annually across all three locations. This is primarily attributed to their high concentration ratios and optical efficiencies. Central receivers were also found to consume less water annually compared to their equivalent parabolic trough plants – between 6% –11% less for wet-cooled plants and between 7.5% – 13.5% less for dry-cooled plants. In addition, the central receiver plants proved approximately 26% – 35.5% more economical in terms of total installed cost per net capacity and approximately 30% – 33.5% more economical in terms of LCOE than their parabolic trough equivalents. The difference in economy was so great that a dry-cooled central receiver was found to be more economical in terms of LCOE than an equal capacity wet-cooled parabolic trough in same location. The lower costs of central receivers are attributed to their higher annual energy production as well as the difference in fundamental plant design and default component costs in the SAM model. Based on these results, it is concluded that central receiver technology should be given primary consideration when only parabolic trough and central receiver systems are considered.

Upington Identified as Best Location of the Three Considered

Of the three locations considered in this study, namely Upington, Springbok and Bloemfontein, the Upington region was deemed the optimal location for CSP. The reasons for this decision are based on the results that the Upington plants possessed the lowest total installed costs per net capacity, the highest annual energy production, and the lowest LCOE of all the considered locations. Furthermore is was observed that the LCOE for the dry-cooled central receiver plant in Upington (R1.54 /kWh) was lower than that of the wet-cooled central receiver plant in Springbok (R1.56 /kWh), and the same as the wet-cooled central receiver in Bloemfontein (R1.54 /kWh). It is thus concluded that it may be more beneficial to construct a central receiver CSP plant in a region with high

DNI levels but limited access to cooling water, as opposed to an area with lower DNI levels but access to large volumes of water.

11.2.3 Identification of Preferred Technology for Each Site

Based on the results of each of the SAM models, the following technologies were considered the optimal choice for each considered location:

Upington

Due to the scarcity of water in the Upington region of Northern Cape, as well as the negative impacts that could arise for local farms and communities in the region should large quantities of water be drawn from the orange river for plant cooling, it is thought that the optimal CSP plant for the Upington region would be a central receiver plant with dry cooling technology. This is affirmed by the previous conclusion that a dry-cooled CSP plant in a region with high DNI levels may be the optimal plant choice for South Africa considering the water stressed classification of the country.

Springbok

As a consequence of not being able to model the effects of sea water cooling on CSP plant efficiencies and costs, it was only possible to conclude that, based on the results of this study, the optimal CSP plant for the Springbok region would be a central receiver plant. Further research would be required in order to determine whether wet cooling with sea water or dry cooling would be preferable.

Bloemfontein

It is concluded that the optimal CSP technology for the Bloemfontein region – when only parabolic trough and central receiver technologies are considered – would be a central receiver, however, based on the lack of data on permissible volumes of extraction for large water bodies, it is not possible to determine whether wet cooling or dry cooling would be more beneficial. Due to its lower costs and higher efficiency, employing wet cooling would be more economical if cooling water was available in large enough, cost effective quantities, however, more specific site analyses and local water availability studies would be required in order to determine if this was indeed the case, or alternatively if dry cooling would be preferable.

As a final note, it is concluded that the choice of central receiver system as the optimal CSP technology for all three locations is based solely on the comparisons in this study between parabolic troughs and central receivers. Alternative solar technologies such as linear Fresnel, parabolic dish, or even photovoltaics should therefore also be considered and modelled for comparison purposes in future studies and in the context of a large-scale rollout of CSP.

11.2.4 Sensitivity of Results to External Factors

A sensitivity analysis was successfully conducted and used as a means to determine the variation of the LCOE as a function of variation in a few select input variables. The key conclusions drawn from the sensitivity analysis are summarised under their respective headings.

LCOE Most Sensitive to Financing Assumptions

The resulting LCOE from the SAM models was found to be most sensitive to the financing assumptions of the project, such as the inflation rate, debt fraction and minimum required IRR. The loan rate and real discount rate were also found to affect the LCOE, however, to a lesser extent. The solar field cost was also identified as affecting the resulting LCOE, primarily due to it representing the largest factor in the plant capital costs. It is thus concluded that financial constraints, rather than plant capital costs, have the largest influence over the resulting LCOE. This result was echoed in the SAM (2010) documentation.

LCOE Least Sensitive to Cost of Cooling Water

The cost of cooling water (as represented by the variable cost by generation input) was found to have the least effect on the resulting plant LCOE, with maximum increases of approximately only R0.01 per kWh observed. Furthermore, even when increased to its maximum value in the sensitivity analysis, the wet-cooled plants still proved more economical than their dry-cooled equivalents. Based on this result, it is concluded that the availability of raw cooling water, rather than its current cost, will be the limiting factor in the use of wet cooling technology.

11.2.5 Validation of SAM Findings

SAM Model Results Successfully Validated

The results from the SAM models were validated by means of comparison with those found in the literature. The results achieved in this study were found to be in the same order of magnitude as those in the literature, and were often similar within 10% – 20%.

LCOE Data Found to be Similar to South African Models Created by EPRI

Of the literature results used for comparison and validation purposes, only those from EPRI (2010) contained data specific to CSP plants modelled in the South African environment; however, these were limited to dry-cooled plants only. Although the total plant costs were considerably higher than those given by EPRI (2010), the remaining metrics showed good agreement. The LCOE in particular showed strong agreement, with the dry-cooled parabolic trough value of R2.31/kWh agreeing within approximately 10% to the EPRI value of R2.08/kWh, and the dry-cooled central receiver value of R1.54/kWh varying by less than 2% from the EPRI value of R1.57/kWh.

Total Installed Costs Found to be Higher than Literature Values

Of the results validated, the total installed cost per net capacity, however, was found to be considerably higher than the values stated in the literature, occasionally by more than 50%. The higher than average total installed costs are concluded to be a result of both the SAM default costs – and hence the costs by the WorleyParsons Group – on which they are based, and the conservative cost adjustment factors applied to represent the higher overall capital and O&M costs for construction in South Africa. It was also noted, however, that the total installed cost per net capacity metric was variable for all plants in the literature, and therefore, the fact that the costs used in this study were based on SAM inputs, and that they were in the correct order of magnitude, resulted in them being considered acceptable. It is therefore concluded that the SAM analyses conducted in this study were implemented and conducted successfully.

Additional Validation and Sensitivity Analyses Required

A final conclusion regarding the various validation and sensitivity analyses in this study, is that they were limited to only consider the Upington based plants. It is therefore deemed necessary to conduct more extensive validation and sensitivity analyses for additional locations in further studies.

11.3 Analysis of Research Questions

Through the development of the methodology, the use of the various models and simulations in this dissertation, and the analysis of their results, the topics posed in the research questions have largely been discussed and analysed; however, for the sake of completeness, an explicit analysis summary of each of the four research questions will now be presented under their respective headings.

1. Is it more beneficial in terms of the Levelised Cost of Energy (LCOE) to locate a South African CSP plant in a region with high DNI levels but limited access to cooling water, hence adopting dry cooling; or in a region with lower DNI levels but greater access to larger volumes of water, hence adopting wet cooling?

Is was observed and noted both in the analysis of the SAM model in Chapter 9, as well as in the conclusions relating to the SAM analysis, that the LCOE value of R1.54 /kWh for the dry-cooled central receiver plant in Upington was lower than that of the R1.56 /kWh value for the wet-cooled central receiver plant in Springbok, and the same as the R1.54 /kWh value for the wet-cooled central receiver in Bloemfontein. Furthermore, due to the classification of South Africa as a water-stressed country, it was thus concluded that it may be more beneficial to employ dry cooling and construct a central receiver CSP plant in a region with high DNI levels but limited access to cooling water, as opposed to an area with lower DNI levels but access to large volumes of water and employing wet cooling.

The benefit in terms of LCOE was only found to be true for central receiver plants, however, as when considering parabolic trough plants, the dry-cooled trough plant in Upington had a resulting LCOE of R2.31/kWh while the wet-cooled trough plants in Springbok and Bloemfontein had resulting LCOEs of R2.22/kWh and R2.20/kWh respectively. Even so, the difference in LCOE value between the dry-cooled trough in Upington and the wet-cooled trough in Bloemfontein is less than 5%, and thus considering the water stressed nature of South Africa, dry-cooling may still prove preferable depending on the specific site and situation.

2. Of the CSP technologies considered in this analysis, which would be deemed most optimal at each location?

The discussion and identification of the optimal CSP technology for each of the considered sites, comprising only the CSP technologies modelled, was presented in Sections 9.1, 9.2 and 9.3, as well as in the conclusions relating to the SAM analysis. For all the three sites considered, it was concluded that central receiver plants were preferable, based on the model predictions that central receivers produced between 1% and 8% more energy annually, consumed between 6% and 11% less water for wet-cooled plants and between 7.5% and 13.5% less water for dry-cooled plants, and proved approximately 26% – 35.5% more economical in terms of total installed cost per net capacity and approximately 30% – 33.5% more economical in terms of LCOE than their parabolic trough equivalents. Furthermore, a dry-cooled central receiver was found to be more economical in terms of LCOE than an equal capacity wet-cooled parabolic trough in same location.

Due to the scarcity of water in the Upington region of Northern Cape, as well as the negative impacts that could arise for local farms and communities in the region should large quantities of water be drawn from the orange river for plant cooling, it was further concluded that the use of dry-cooling would be preferable for the Upington site. However, due to the inability to model the use of sea water for cooling purposes along the West Coast of South Africa, and the lack of data on volumes of water permissible for extraction from the large water bodies and rivers, it was not possible to determine weather the use of wet-cooling or dry cooling would be preferable for the locations of Springbok and Bloemfontein respectively. Nevertheless, it may still be more beneficial to make use of dry cooling, as a means to reduce the risk of water supply concerns.

3. Which financial and cost-related model input variables have the greatest effect on the resulting LCOE of the plant, and hence which are the key items to consider when implementing a utility-scale parabolic trough or central receiver CSP plant in South Africa?

A sensitivity analysis of a number of financial and cost-based model inputs was conducted in Chapter 10, as well as in the conclusions relating to the SAM analysis, comprising the debt fraction, inflation rate, loan rate (or cost of debt), minimum IRR, discount rate, fixed cost by capacity, the cost of water (represented by the variable cost by generation), and for parabolic trough plants; the solar field cost. The sensitivity analysis, which was conducted for the Upington based plants only, revealed that the resulting LCOE was

most sensitive to the financing assumptions of the project, such as the inflation rate, debt fraction and minimum required IRR. The loan rate and real discount rate were also found to affect the LCOE, however, to a lesser extent. The solar field cost was also identified as affecting the resulting LCOE, primarily due to it representing the largest factor in the plant capital costs. The cost of cooling water (as represented by the variable cost by generation input) was found to have the least effect on the resulting plant LCOE, and even when increased to its maximum value in the sensitivity analysis, the wet-cooled plants still proved more economical than their dry-cooled equivalents. It was thus concluded that financial constraints, rather than plant capital costs, have the largest influence over the resulting LCOE, and that the availability of raw cooling water, rather than its *current* cost, will be the limiting factor in the use of wet cooling technology.

4. Can a high level analysis and methodology be developed to achieve the objectives of this study, by making use of existing software and modelling tools, available data, or data adapted to reflect South African conditions; and if so, how accurately can this be achieved?

The methodology developed to achieve the objectives set and analyse the research questions posed in this dissertation can be classified into two sub-categories, namely that of the GIS methodology, and that of the methodology developed to analyse South African specific CSP plants within the SAM software.

The GIS methodology allowed for the successful identification and quantification of potential CSP sites in South Africa, and made use of data which was available and specific to South Africa. The methodology developed for the SAM analysis allowed for the creation of a cost and performance analysis of CSP plants in the South African environment; however, certain compromises and approximations had to be made due to a lack of availability of South African specific data. As an example, the three locations of Upington, Springbok and Bloemfontein – whose weather data was used to represent conditions at potential CSP sites – were chosen due to a lack of freely available, detailed hourly weather data for specific geographic coordinates, or regions containing potential CSP sites. Furthermore, as revealed through the creation of the database used to review and compare existing CSP plant design and cost data – discussed in Section 8.4 and in the appendices – it was not possible to obtain a complete dataset for South African CSP plants, and thus further methods were developed to either adjust international data to local conditions, approximate or calculate required inputs, or make use of SAM defaults.

Various key model outputs were also compared to those presented in the literature, as described in Section 9.5 as well as in the conclusions relating to the SAM analysis, and reasonable correlation was found, usually within 10% – 20%. Some of the model results, particularity those of the total installed cost per net capacity, were considerably higher than those stated in the literature, however, and reasons for this have been discussed, and recommendations made for further work.

Although the methodology developed and the model results achieved did identify central receiver technology as being preferable to parabolic trough technology for all three locations considered, an optimal solution in terms of both CSP technology and cooling technology choice was only presented for Upington. Similar predictions were not considered possible for Springbok and Bloemfontein due to the lack of capacity for modelling sea water cooling, and a lack of data pertaining to volumes of water available for extraction from large water bodies respectively. The methodology is therefore limited as an optimisation tool; however, its development and the implementation thereof allowed for the achievement of the dissertation's objectives, and provides a means of identifying potential CSP sites and technologies for further consideration, as well as highlighting the important parameters related to their implementation.

12 Recommendations

Throughout the course of this dissertation, several items have emerged as potential candidates for future work. These include, but are not limited to, data that has been used which could be expanded or improved upon, insufficient data in certain fields, and certain approximations which were made due to lack of data or insufficient supporting research. Therefore, based on these items, as well as drawing from the conclusions in this dissertation, the following recommendations are made:

12.1 Recommendations for further GIS Analysis

12.1.1 Suggested GIS Data Improvements

Obtain Solar Data at Higher Resolution

The spacial resolution of the solar data used in this study was fairly coarse when compared to the resolution of other data sets in this analysis – 40 km × 40 km as opposed to 90 m × 90 m. Therefore, in order to determine variations in DNI levels over smaller distances, and hence achieve grater accuracy in the determination and ranking of potential CSP sites according to DNI levels, it is recommended to obtain DNI data with a higher spacial resolution for use in future studies.

Consider Proximity of CSP Sites to Roads and Load Centres

Although the proximity of an identified potential CSP site to specific infrastructure like the existing national gird was analysed, no consideration was given for the proximity to other existing infrastructure such as roads or load centres. As the distance to towns or load centres, as well as access to road infrastructure greatly affects a project's construction costs, it is recommended to include these items as part of the analysis criteria in future analyses.

Source Better National Grid Data and Consider Proximity to Substations

As stated in Section 6.3.6 as well as in the conclusions, the data used to represent the Eskom national grid was digitised and geo-referenced and thus could not be considered as an accurate, primary source of vector-based data. As a result, no data representing the locations of electrical substations were included in the GIS analysis. As a utility-scale power plant would be required to connect to the national grid via a substation, it is recommended to included the proximity to substations, in addition to the national grid, as analysis criteria in future studies.

Incorporate Land Class Data with Land Costs

Utility-scale CSP plants generally require fairly large areas of land for their solar fields, and thus the cost of land will certainly be a factor when considering potential locations for potential CSP plants. It is therefore recommended to incorporate land class data which includes the cost of land in future GIS-based analyses, as this could be used as a factor in the determination of the optimal location for a potential plant.

12.1.2 Suggestions for Further GIS Models

Analyse Water Bodies According to Permissible Volumes Available for Extraction

The proximity of CSP plants to cooling water was considered as on of the key criteria in the GIS analysis, while the comparison between wet and dry cooling technology formed one of the major themes in this study. The data used to represent the large water bodies in the GIS analysis allowed for the differentiation between large rivers and dams and other smaller water bodies, however, no data was included which defined water flow rates, volumes or what volumes were available for extraction. It is therefore recommend for future studies to identify which of the large water bodies could sustain further water extraction, and in what quantities.

Conduct Further Validation of Local Scale Solar Data

Due to limits in both time and computational resources, it was only possible to make use of the *solar area radiation* calculation algorithm to calculate the DNI levels and duration of daily irradiation (and hence validate the adopted DNI data) for a few of the identified potential sites. It is therefore recommended to conduct further and more detailed validation of solar data at a site-specific scales in any further studies.

Consider Future Grid Expansion

As stated in the conclusions, the density of the existing national grid was found to be a limiting factor for potential CSP sites which required a close proximity to it, particularly in the Northern Cape region. When the 20 km proximity requirement was removed, however, (as in Case 4 and Case 5 of the GIS analysis) the CSP potential was found to increase by more than 4 times. It is therefore recommended to determine whether the expansion of the national grid in certain regions – as a means to realise a greater CSP potential – would be beneficial, and to include the modelling and analysis thereof in future studies.

12.2 Recommendations for further SAM Analysis

12.2.1 Suggested SAM Data Improvements

Obtain Location Specific Weather Data

As stated in Section 8.1, due to the lack of freely available hourly weather data for specific geographic locations, weather data for the towns of Upington, Springbok and Bloemfontein was used to approximate the various weather conditions experienced at different potential CSP sites. Therefore, the data used in this study did not reflect the actual weather data for any specific or optimally identified CSP site. Although it was concluded that the approximated weather data used in this report was adequate for an initial high-level study, it is recommended to obtain location, or site-specific weather data for use with the SAM models in any future studies, in order to model the cost and performance of plants at *actual* specific locations.

Further Customise SAM Default Design Data

Due to the lack of complete and comprehensive design and cost data containing all the inputs required by the SAM models – as discussed in Section 8.4 and illustrated by the comparison databases of Appendix B to Appendix E – many of the plant design inputs were left as their SAM default values. In order to model the performance and costs of *actual* potential plants, it is recommended to make use of plant-specific design and cost data, and to rely less on the SAM default values.

12.2.2 Suggestions for Further SAM Models

Consider Additional Solar and CSP Technologies at Potential Sites

The scope of this dissertation, and time constraints, resulted in only two CSP technologies being considered, analysed and compared, namely parabolic trough and central receiver systems. However, as described in Chapter 3, there exist a number of additional CSP technologies, both commercially available and under development, which could also be considered for implementation at potential sites. Furthermore, one could also consider non-thermal solar power systems such as photovoltaic (PV) solar technology in South Africa. However, as PV systems are able to utilise the diffuse irradiation component of solar irradiation in addition to DNI component, and as the GIS analysis of this dissertation was specific to DNI, additional GIS analyses would be required which consider other forms of irradiation such as latitude tilt irradiation (LTI). The SAM 2010.04.12 software possesses the ability to model both parabolic dish CSP systems and PV systems, in addition to the parabolic trough and central receiver systems considered in this study. It is therefore recommended to include the analyses of these additional technologies within the SAM software in any future studies, particularity in the context of a large-scale rollout.

Include Modelling of Fossil Backup Fuel Hybridisation

Although the use of thermal energy storage was considered for all plants at all locations in this study, no consideration was given to the use of a fossil backup fuel, and hence plant hybridisation. Hybridisation is currently utilised at many existing CSP plants – such as the SEGS parabolic trough plants in the Unites States and many of the plants in Spain – as a means to increase plant availability and capacity factors and render plants better suited to base load power generation. The use of fossil backup fuel is also often limited, with maximum limits of 25% imposed on supplementation for the SEGS plants, while only 15% supplementation is allowed for Spanish plants. The SAM software possesses the ability to include and model both the cost and performance effects of fossil backup with CSP plants, but due to time constraints this was not included in this dissertation. The modelling of plant hybridisation is therefore recommended for future studies.

Conduct Further Validation and Sensitivity Analyses for All Locations

Due to time constraints, it was only possible to compare and validate the SAM results for plants situated at Upington with those found in the literature. It is therefore recommended to conduct further and more detailed validation of the SAM model results for all locations considered in any future studies.

12.3 General Recommendations for Future Studies

The following final recommendations are considered to be difficult to implement into the existing GIS based analysis and to accomplish within the current SAM software. They are thus suggested as general recommendations which may require other means or software in order to be implemented.

Perform Solar DNI Measurements at Potential CSP Sites

As stated in section 6.3.1, as well as in the conclusions of this dissertation, the solar data employed in this study was satellite derived, and had a spacial resolution of 40 km × 40 km. In order to ensure that the true potential and conditions at a particular CSP site are known, and before selecting an area for construction, it is thus recommended that actual solar measurements, as well as the measurement of any other weather data required, be conducted at promising identified sites. These measurements should be conducted for a reasonable period of time in order to gauge the true potential of a site, and are typically conducted over a period of months, or even years.

Model Sea Water Cooling on West Coast and Hybrid Wet-Dry Cooling

When considering the optimal CSP technology for the Springbok location, it was determined that central receiver technology was preferable to parabolic trough, however, it was noted in Section 9.2.6 as well as in the conclusions that additional modelling would be required in order to determine whether a central receiver plant using sea water for wet cooling on the West Coats would in fact be more economical than a dry-cooled central receiver plant. The modelling of the use of sea water for wet cooling purposes was considered beyond the scope of this study and SAM analysis, however, it is recommended that further research be conducted in this area, and attempts made to model the effects on both performance and cost as a result of adopting this technology.

Another cooling technology which was identified in Chapter 4 is that of hybrid wet-dry cooling. The option to include hybrid wet-dry cooling was not presented in the SAM software, and was also not considered to be within the scope of this study. The use of hybrid wet-dry cooling, however, in particular that of water conservation hybrid systems, could be considered advantageous in some scenarios where water reduction is a necessity but efficiency higher than dry cooling is required during the hottest periods of the year. It is thus recommended that attempts should be made to include the analysis of hybrid wet-dry cooling in future studies.

Include the Analysis of Volumetric Central Receiver Systems, Linear Fresnel Technology and Concentrating Photovoltaics

It has already been recommended to consider additional solar technologies at potential CSP sites, and mention was made of the SAM software's ability to model both the performance and cost characteristics of solar PV systems and parabolic dish technology. There are still additional technologies which could be considered, however, such as central receiver technology with volumetric cavity receivers, linear Fresnel technology, compact linear Fresnel reflectors (CLFRs), and concentrating photovoltaics (CPV), some of which are still being commercialised and are considered to be viable alternatives to existing commercial solar technologies. It is therefore recommended to to include the analyses of these additional technologies in future studies, however, in order to accomplish this, more advanced models, additional software packages, and new calculations and procedures may be required.

Perform Environmental Impact Assessments at Promising Identified Sites

In order to reduce the potential for negative environmental impacts, as well as avoid the identification of CSP sites in unsuitable areas, restrictions were imposed in the GIS section of this report in order to exclude potential sites which were either located in unsuitable land class areas, or in any areas not classified as possessing 'least threatened' vegetation. However, as stated in Section 6.3.4, in terms of the Environmental Impact Assessment Regulations of South Africa, EIAs must be conducted before any construction project can begin in a particular area. It is therefore recommended to conduct EIAs at identified sites in order to minimize potentially negative environmental impacts, and as a means to aid the process of selecting an optimal CSP plant location.

Bibliography

Bennett, K. (2010). Informal supervisor meetings and discussion, Energy Research Centre, Department of Mechanical Engineering, University of Cape Town.

Bennett, K. (2011). Informal supervisor meetings and discussion, Energy Research Centre, Department of Mechanical Engineering, University of Cape Town.

Bloomberg (2011). Bloomberg Market Data World Currencies. Retrieved online (16 May 2011) from: `http://www.bloomberg.com/markets/currencies/europe-africa-middle-east/`.

Boyle, G., editor (2004). *Renewable Energy Power for a Sustainable Future. Second Edition.* Oxford University Press, United Kingdom.

Bravo, J. D., Casals, X. G., and Pascua, I. P. (2007). GIS approach to the definition of capacity and generation ceilings of renewable energy technologies. *Energy Policy - Elsevier*, 35:4879–4892.

Brodrick, J. J. L. (2010). A GIS - based assessment of potential sites for large concentrated solar power plants in South Africa. Unpublished Energy Project Report, Energy Research Centre, University of Cape Town.

Broesamle, H., Mannstein, H., Schillings, C., and Trieb, F. (2001). Assessment of solar electricity potentials in North Africa based on satellite data and a Geographic Information System. *Solar Energy – Elsevier*, 70(1):1–12.

Brosseau, D. A., Hlava, P. F., and Kelly, M. J. (2004). Testing thermocline filler materials and molten-salt heat transfer fluids for thermal energy storage systems used in parabolic trough solar power plants. Technical Report SAND2004-3207, Sandia National Laboratories, New Mexico.

Cengel, Y. A. and Boles, M. A. (2006). *Thermodynamics: An Engineering Approach. Fifth edition in SI units.* McGraw-Hill, New York.

City of Johannesburg Council (2011). Amendment of tariff charges for water services and sewerage and sanitation services: 2011/12. COJ : Mayoral Committee 2011-03-17. Available online (6 April 2011) at: http://www.joburg-archive.co.za/2011/tariffs/water_and_sanitation.pdf.

Cohen, G. E., Kearney, D. W., and Kolb, G. J. (1999). Final report on the operation and maintenance improvement program for concentrating solar power plants. Technical report, SAND99-1290.

CSIR (2001a). *South African 30m Land Cover Data, FUNDISADISK*. Council for Scientific and Industrial Research, Pretoria.

CSIR (2001b). *South African DWAF 1:10,000 River and Dam Data, FUNDISADISK*. Council for Scientific and Industrial Research, Pretoria.

CSIR (2001c). *South African Provinces Data, Administrative Section, FUNDISADISK*. Council for Scientific and Industrial Research, Pretoria.

Dersch, J., Geyer, M., Hermann, U., Jones, S., Kelly, B., Kistner, R., Ortmanns, W., Pitz-Paal, R., and Price, H. (2002). Solar Trough Integration Into Combined Cycle Systems. Proceedings of Solar 2002: Sunrise on the Reliable Energy Economy. Reno, Nevada.

DLR (2003). Concrete Storage: Update on the European concrete TES program. Presentation by DLR – German Aerospace Center, Institute of Technical Thermodynamics.

DME (2003). White Paper on Renewable Energy. Technical report, South African Department of Minerals and Energy, Pretoria.

DOE, U.S. (2010). Concentrating solar power commercial application study: Reducing water consumption of concentrating solar power electricity generation. Report to Congress. Technical report, U.S. Department of Energy. Retrieved online (17 July 2010) from: http://www.nrel.gov/csp/troughnet/pubs_power_plant.html#cooling.

Duffie, J. A. and Beckman, W. A. (1974). *Solar Energy Thermal Processes*. John Wiley & Sons, Inc., New York.

Edkins, M., Winkler, H., and Marquard, A. (2009). Large-scale rollout of concentrating solar power in South Africa. Technical report, Energy Research Centre, University of Cape Town.

ENPAT (1998). *South African Major Roads, Secondary Roads, and Towns*. Department of Environmental Affairs and Tourism, Pretoria.

ENPAT (2000). *South African River Data*. Department of Environmental Affairs and Tourism, Pretoria.

EPRI (2010). Power Generation Technology Data for Integrated Resource Plan of South Africa. Technical report, Electric Power Research Institute, Palo Alto, CA.

EPRI and California Energy Commission (2002). Comparison of Alternate Cooling Technologies for California Power Plants: Economic, Environmental, and Other Tradeoffs. Technical report, PIER / EPRI, California. Available online (17 February 2011) at: `http://www.nrel.gov/csp/troughnet/publications.html`.

Eskom (2006). *Environmental Impact Assessment Process – Proposed Concentrating Solar Power (CSP) Plant and Associated Infrastructure in the Northern Cape Area*. Eskom. Retrieved online (25 June 2010) from: `http://www.eskom.co.za/content/BID_Final_English230306.pdf`.

Eskom (2010). *Eskom Power Stations Poster*. Eskom General Communications Department, Pretoria. Retrieved via Private Communications with Eskom Visitors Centre (June 2010), Cape Town.

ESRI (2010a). ArcGIS Documentation on the Solar Area Radiation Toolbox. Available online (11 December 2010) at: `http://webhelp.esri.com/arcgisdesktop/9.2/index.cfm?TopicName=Area_Solar_Radiation`.

ESRI (2010b). The Guide to Geographic Information Systems: What is GIS? Retrieved online (19 July 2010) from: `http://www.gis.com/content/what-gis`.

ESRI Online Forums (2010). ArcGIS Desktop Discussion Forums – Solar Radiation. Retrieved online (19 December 2010) from: `http://forums.esri.com/thread.asp?t=228857&f=995&c=93`.

European Commission (2004). European Research on Concentrated Solar Thermal Energy. Technical Report EUR 20898, European Commission, Brussels.

Fahy, G. (2009). The Analysis of South Africa's Potential to Supply Linear Fresnel Thermal Collector Components. Unpublished Energy Project Report, Energy Research Centre, University of Cape Town.

Fluri, T. P. (2009). The potential of concentrating solar power in South Africa. *Energy Policy - Elsevier*, 37:5075–5080.

Forristall, R. (2003). Heat Transfer Analysis and Modeling of a Parabolic Trough Solar Receiver Implemented in Engineering Equation Solver. Technical Report NREL/TP-550-34169, National Renewable Energy Laboratory. Retrieved online (26 May 2011) from: `http://www.nrel.gov/csp/troughnet/pdfs/34169.pdf`.

Gilman, P. (2010). Solar Advisor Model training course at the University of Stellenbosch, Cape Town, South Africa. Attended in June 2010.

Gilman, P. (2011). Private communication with Paul Gilman regarding NREL SAM.

Herrmann, U., Geyer, M., and Kearney, D. (2002). Overview on Thermal Storage Systems. Presentation by FLABEG Solar International GmbH at the Workshop on Thermal Storage for Trough Power Systems.

IEA (2007). SolarPACES Annual Report 2007. Technical report, Solar Power and Chemical Energy Systems – SolarPACES.

IEA (2008). Energy Technology Perspectives 2008: Scenarios & Strategies to 2050. Technical report, International Energy Agency, Paris.

IEA (2010a). Energy Technology Perspectives 2010: Scenarios & Strategies to 2050. Technical report, International Energy Agency, Paris.

IEA (2010b). *Technology Road Map: Concentrating Solar Power*. International Energy Agency and the OECD, Paris.

Kelly, B. (2006). Nexant Parabolic Trough Solar Power Plant Systems Analysis. Tasks 1-3: January 20, 2005 – December 31, 2005. Technical report, Nexant Inc. Prepared under subcontract for the National Renewable Energy Laboratory. Available online (17 February 2011) at: `http://www.nrel.gov/csp/troughnet/publications.html`.

Kelly, B. and Kearney, D. (2006). Parabolic Trough Solar System Piping Model. Technical Report NREL/SR-550-40165, National Renewable Energy Laboratory. Retrieved online (26 May 2011) from: `http://www.nrel.gov/csp/troughnet/pdfs/40165.pdf`.

Kistler, B. (1986). A User's Manual for DELSOL3: A Computer Code for Calculating the Optical Performance and Optimal System Design for Solar Thermal Central Receiver Plants. Technical Report SAND86-8018, Sandia National Laboratories. Retrieved online (7 June 2010) from: `http://prod.sandia.gov/techlib/access-control.cgi/1986/868018.pdf`.

Lindenberg, N. and Slingsby, T. (2010). Private communication with Nicholas Lindenberg and Thomas Slingsby, GIS Research Laboratory, University of Cape Town.

Meteotest (2011). Meteonorm Overview. Available online (29 April 2011) at: `http://www.meteonorm.com/pages/en/meteonorm.php`.

Meyer, R. (2010). Solar Advisor Model training course at the University of Stellenbosch, Cape Town, South Africa. Attended in June 2010.

Mills, D. (2004). Advances in solar thermal electricity technology. *Solar Energy – Elsevier*, 76:19–31.

Montes, M., Abánades, A., Martínez-Val, J., and Valdés, M. (2009). Solar multiple optimization for a solar-only thermal power plant, using oil as heat transfer fluid in the parabolic trough collectors. *Solar Energy – Elsevier*, 83:2165–2176.

Morse, W. (2009). An analysis into the geophysical and industrial requirements, if South Africa were to evolve its electricity supply to a large emphasis on Concentrated Solar Power. Master's thesis, Energy Research Centre, University of Cape Town.

Mucina, L. and Rutherford, M. C., editors (2006). *The Vegetation of South Africa, Lesotho and Swaziland*. Strelitzia 19, South African National Biodiversity Institute, Pretoria. (Data retrieved in the form of Shapefiles from Electronic Resource CD).

Mukheibir, P. (2007). Qualitative assessment of municipal water resource management strategies under climate impacts: the case of the Northern Cape, South Africa. *Water SA*, 33(4).

Müller-Steinhagen, H. (2011). *Solar Thermal Power Plants - On the Way to Commercial Market Introduction*. DLR, Stuttgart.

NERSA (2009). Renewable Energy Feed In Tariff Guidelines. Technical report, National Energy Regulator of South Africa. Reasons for Decision.

NERSA (2010). Renewable Energy Feed In Tariffs Phase II. Technical report, National Energy Regulator of South Africa. Reasons for Decision.

Novatec Solar (2011). Novatec Solar NOVA-1. Retrieved online (2 June 2011) from: `http://www.novatecsolar.com/20-1-Nova-1.html`.

NREL (2011a). Parabolic Trough Thermal Energy Storage Technology. Retrieved online (17 May 2011) from: `http://www.nrel.gov/csp/troughnet/thermal_energy_storage.html`.

NREL (2011b). Solar Advisor Model Home and Overview. National Renewable Energy Laboratory. Retrieved online (20 May 2011) from: `https://www.nrel.gov/analysis/sam/`.

Pegels, A. (2009). Prospects for Renewable Energy in South Africa: Mobilizing the Private Sector. Discussion Paper. German Development Institute - d.i.e, Bonn, Germany.

Pilkington Solar International GmbH (2000). Survey of Thermal Storage for Parabolic Trough Power Plants. Technical Report NREL/SR-550-27925, National Renewable Energy Laboratory. Prepared for NREL by Pilkington Solar International GmbH, Cologne, Germany.

REN21 (2008). Renewables 2007 Global Status Report. Technical report, Renewable Energy Policy Network for the 21st Century, Paris: REN21 Secretariat and Washington, DC: Worldwatch Institute.

Romero, M., Buck, R., and Pacheco, J. E. (2002). An Update on Solar Central Receiver Systems, Projects, and Technologies. *ASME Journal of Solar Energy Engineering*, 124:98–108.

SAM (2010). Solar Advisor Model 2010 User Guide and Help Documentation. National Renewable Energy Laboratory.

SAM (2011). Screen Captures from Solar Advisor Model 2010 Software. National Renewable Energy Laboratory.

Sargent & Lundy (2003). Assessment of Parabolic Trough and Power Tower Solar Technology Cost and Performance Forecasts. Technical Report NREL/SR-550-34440, National Renewable Energy Laboratory. Prepared for NREL by Sargent & Lundy LLC Consulting Group, Chicago, Illinois.

SARS (2011). South African Revenue Service S.A. Tax System: What Kinds of Tax Do We Pay. Available online (18 May 2011) at: `http://www.sars.gov.za/home.asp?pid=289`.

Solar Millennium AG (2008). The parabolic trough power plants Andasol 1 to 3. Technical report, Solar Millenium AG, Germany.

Solar Millennium AG (2011). Parabolic Trough Plants – Operation. Retrieved online (18 July 2011) from: `http://www.solarmillennium.de/english/technology/parabolic-trough-power-plants/operation/index.html`.

SolarPACES (2011). PS10. Retrieved online (18 July 2011) from: `http://www.solarpaces.org/Tasks/Task1/ps10.htm`.

SRTM (2006). *Shuttle Radar Topography Mission 90m DEM, NASA JPL*. United States Geographic Service (USGS). Available online (7 July 2010) at: `http://www2.jpl.nasa.gov/srtm`.

StatsSA (2011). Consumer Price Index: Index numbers and year-on-year rates. Retrieved online (18 May 2011) from: `http://www.statssa.gov.za/keyindicators/CPI/CPIHistory.pdf`.

Stine, W. B. and Geyer, M. (2001). *Power From The Sun*. Adapted from the original *Solar Energy Systems Design* published by John Wiley and Sons, Inc. 1986. Retrieved Online (20 May 2010) from: `http://www.powerfromthesun.net/book.html`.

Stoddard, L., Abiecunas, J., and O'Connell, R. (2006). Economic, Energy, and Environmental Benefits of Concentrating Solar Power in California. Technical Report NREL/SR-550-39291, Prepared for NREL by Black & Veatch.

SWERA (2010). *Solar: monthly and annual average direct normal (DNI), global horizontal (GHI), latitude tilt, and diffuse data and GIS data at 40km resolution for Africa from NREL, 2006*. Solar and Wind Energy Resource Assessment. Retrieved online (28 June 2010) from: `http://swera.unep.net`.

Torcellini, P., Long, N., and Judkoff, R. (2003). Consumptive Water Use for U.S. Power Production. Technical report, NREL, Colorado. Available online (17 July 2010) at: `http://www.nrel.gov/csp/troughnet/publications.html`.

Torresol Energy (2011). Gemasolar Plant. Retrieved online (27 June 2011) from: `http://www.torresolenergy.com/TORRESOL/gemasolar-plant/en`.

TRNSYS (2011). TRNSYS Official Website - Overview of TRYNSYS. University of Wisconsin, Madison. Available Online (20 May 2011) at: `http://sel.me.wisc.edu/trnsys/features/features.html`.

Turchi, C. (2010). Parabolic Trough Reference Plant for Cost Modeling with the Solar Advisor Model (SAM). Technical Report NREL/TP-550-47605, NREL.

Turchi, C., Mehos, M., Ho, C. K., and Kolb, G. J. (2010). Current and Future Costs for Parabolic Trough and Power Tower Systems in the US Market. Presented at SolarPACES 2010. Conference Paper: NREL/CP-5500-49303.

Van der Merwe, P. (2011). Private Communication with Paul van der Merve from the South African Department of Water Affairs, Pretoria.

Wagner, M. J. (2008). Simulation and Predictive Performance Modeling of Utility-Scale Central Receiver System Power Plants. Master's thesis, University of Wisconsin-Madison. Retrieved online (30 November 2010) from: `http://sel.me.wisc.edu/theses/wagner08.zip`.

Winkler, H., editor (2007). Long Term Mitigation Scenarios. Technical report, Energy Research Centre, prepared for the Department of Environment Affairs and Tourism, South Africa.

Appendices

Appendix A: GIS Methodology

The GIS analysis undertaken in this project can be classified according to three sections, namely; the importing and processing of the necessary data files, the analysis of the data by means of the computer software package ArcGIS, and the generation of maps and calculation results in both ArcGIS and spreadsheet software. The procedures adopted and followed for each of the aforementioned sections will now be described in detail under their respective headings.

1. Import and Process Gathered Data

Solar Data

In a Spreadsheet Program:

1. Open the `csr_africa_data.xls` file.
2. Export the DNI tab into a Comma Separated Value (CSV) file.

In ArcGIS:

1. Load the `csr_afr_poly.shp` Shapefile.
2. Open the South Africa country and provincial borders Shapefile with a UTM 34S projection.
3. Select the `csr_afrpoly.shp` Shapefile grid with a 1 degree buffer using SA provinces to reduce the number of data points.
4. Open the CSV DNI file.
5. Merge the attribute tables of the CSV and Shapefile according to column PSECELLID.

6. Open attribute table of new layer, and adopt a graduated custom scale for CANN (annual values of DNI).
7. A map of South Africa with the solar data DNI for an average year was then created.

Land Slope Data

1. Load the 90m DEM from SRTM which contains the land slope for the country.
2. Create an additional analysis layer of the slope classifying it according to percentage slope.
3. Create a further boolean layer (true or false) with a slope of 1%.

Vegetation Data

1. Load vegetation map of SA retrieved from Mucina and Rutherford (2006).
2. Create a layer from this data according to the attribute of 'least threatened'.
3. Create a dissolve layer for 'least threatened' to reduce polygons and file size.

Rivers and Dams Data and Buffer

1. Import large water bodies and rivers data set.
2. Create a new layer with a radial buffer of 20 km around large rivers and dams.

West Coast Data and Buffer

1. Create a new layer from the SA outline polygon and trim the West Coast from SA-Namibia border to Cape Town harbour.
2. Create a new buffer layer with a 20 km radius from this newly created West Coast line.
3. Merge the rivers, dams and West Coast buffers into one layer called *water buffers*.

Eskom National Grid Data and Buffer

For the national grid the following procedure was followed:

1. Import the SA National Grid jpeg picture file from Eskom (2010).
2. Open the jpeg as a new layer.
3. Make use of the georeferencing procedure to accurately project the jpeg image over the existing SA map.
4. Create a new layer with UTM projection and trace the Eskom national grid from the georeferenced jpeg.
5. Remove the original Eskom 2008 jpeg, leaving only the digitised national grid layer behind.
6. Create a new 20 km radial buffer layer from the Eskom national grid.

Land Cover Data

1. A land cover grid was created in order to exclude areas not suitable for construction. The data imported comprised the *South African 30m Land Cover Data* published by the CSIR (2001a).

   Areas excluded comprised:

   - Water-bodies
   - Wetlands
   - Forests
   - Plantations
   - Urban Areas

2. The various attributes were merged into one layer of excluded areas.

2. Data Analysis

Analysis Cases and Site Identification

1. Convert all vector data to boolean rasters, in order to be able to use the *raster calculator* feature in ArcGIS. This is necessary because the raster calculator functions by analysing each cell of the raster in each layer according to given criteria, but vector data by nature does not possess data comprising of gridded cells (Lindenberg and Slingsby, 2010).

2. Apply an analysis mask of the Eskom power lines, in order to reduce the number of calculations and exclude the rest of the country from unnecessary analysis.

3. Initiate the raster calculator with the following chosen analysis criteria that a potential site must possess:

Case 1: DNI > 6.0 kWh/m^2/d, Proximity to Large Water Bodies

- DNI greater than 6.0 kW/m^2 per day
- Less than 20 km from large water bodies
- Less than 20 km from transmission lines
- Less than 1% land slope
- Region classified as 'least threatened' vegetation
- Region not excluded due to land class restrictions of Section 6.3.3
- Site area greater than 2 km^2

Case 2: DNI > 6.5 kWh/m^2/d, Proximity to Large Water Bodies

- DNI greater than 6.5 kW/m^2 per day
- Less than 20 km from large water bodies
- Less than 20 from transmission lines
- Less than 1% land slope
- Region classified as 'least threatened' vegetation
- Region not excluded due to land class restrictions of Section 6.3.3
- Site area greater than 2 km^2

Case 3: DNI > 7.0 kWh/m^2/d, No Proximity to Large Water Bodies

- DNI greater than 7.0 kW/m^2 per day
- Less than 20 km from transmission lines
- Less than 1% land slope
- Region classified as 'least threatened' vegetation
- Region not excluded due to land class restrictions of Section 6.3.3
- Site area greater than 2 km^2

Case 4: DNI > 6.5 kWh/m^2/d, Proximity to Large Water Bodies, No Grid Proximity

- DNI greater than 6.5 kW/m^2 per day
- Less than 20 km from large water bodies
- Less than 1% land slope
- Region classified as 'least threatened' vegetation
- Region not excluded due to land class restrictions of Section 6.3.3
- Site area greater than 2 km^2

Case 5: DNI > 7.0 kWh/m^2/d, No Proximity to Large Water Bodies, No Grid Proximity

- DNI greater than 7.0 kW/m^2 per day
- Less than 1% land slope
- Region classified as 'least threatened' vegetation
- Region not excluded due to land class restrictions of Section 6.3.3
- Site area greater than 2 km^2

4. Convert the identified potential sites for each of the aforementioned cases back into vector Shapefiles.

5. Perform an intersect with the original solar data from the merged `csr_afrpoly.shp` and `DNI.csv` files and the identified sites, in order to re-populate the identified sites attribute tables with the solar DNI values.

6. Add an additional 'Area' field column to the attribute tables and use the *Calculate Geometry* tool to calculate the area of each site. The intersect used in the previous step, however, causes sites that fall across the solar DNI grid boundaries to be split into separate sites. It is therefore necessary to use the *Summarize* tool to create a new database file from the attribute tables to re–merge sites that have been split, and thus calculate the correct total area of each site. This process is mentioned in Section 6.5.3 and illustrated in Figure 6.12.

Solar Shading and DNI Calculation Algorithm

Unsuccessful Method 1

1. Open the *Area Solar Radiation* tool from the *Solar Radiation* toolbox within *Spacial Analyst*.
2. Import the 90m South African DEM and calculate the appropriate latitude.
3. Set the algorithm to run for a period of 365 days for the year 2006.
4. Run the solar area shading algorithm for the entire country with specified output for: *global radiation*, *direct radiation*, and *daily duration of radiation*.

Unsuccessful Method 2

1. Split the South Africa data layer into $1^\circ \times 1^\circ$ geographic grid cells.
2. Manually select only those $1^\circ \times 1^\circ$ geographic grid cells which contain identified potential CSP sites.
3. Buffer each grid cell with 1 km radial buffer as a means to reduce edge effects in the calculation.
4. Convert DEM to geographic co-ordinates and extract the DEM by mask of the selected buffered grid $1^\circ \times 1^\circ$ cells.
5. Re-run the solar area shading model on each of the $1^\circ \times 1^\circ$ buffered cells by making use of the batch scheduling process, with specified output for: *global radiation*, *direct radiation*, and *daily duration of radiation*. Set the algorithm to run for a period of 365 days for the year 2006. The batch process will automatically calculated the latitude of each of the $1^\circ \times 1^\circ$ grid cells. The algorithm took a number of days to complete.

6. Clip the 1 km radial buffer by means of *extract by mask* for both the DNI calculation and duration shading models, in order to remove the edge effects from the results.

7. Use the mosaic tool to attempt to re-merge the selected $1^\circ \times 1^\circ$ grid cells into a single uniform layer.

Final Successful Method

1. Identify and select a few of the larger CSP sites with higher DNI values by ranking of attributes in their relevant databases.

2. Create a 50 km radial euclidean distance buffer around the selected CSP sites.

3. Extract the DEM by mask of the buffered sites and shrink the extent to eliminate the zero-data values.

4. Re-run the solar area shading model on each of radial buffers by making use of the batch scheduling process, with specified output for: *global radiation*, *direct radiation*, and *daily duration of radiation*. Set the algorithm to run for the period of 365 days for the year 2006.

5. Within *ArcCatalogue*, create new *geo-database*.

6. Create a new *raster catalogue*.

7. Import the results dataset from the algorithm into the geo-database within Arc-Catalogue.

8. Change and specify the colour-ramp to obtain a suitable legend.

3. Calculations and Maps

Although the quantification of the potential sites identified for Case 1, Case 2, Case 3, Case 4 and Case 5 is described in detail in Section 6.5, the analysis procedure adopted for the data will be described briefly below.

1. All the associated database files and attribute tables for each of the identified sites for each of the above cases were exported into Excel® spreadsheet files in order to allow for calculations and further analysis to be performed.

2. For each of the aforementioned cases, the following calculations were performed in a spreadsheet program:

    - Calculate total area available for each case
    - Calculate the total energy available for each analysis case by multiplying each site area by its corresponding DNI value and then summing the resulting totals
    - Calculate the power generation potential for each analysis case by dividing the total available area by the land use value of 28 km^2 per GW
    - Calculate the net energy generation potential for parabolic trough plants by multiplying the power generation potential by the 8760 hours in a year and then by the 38.8% capacity factor
    - Calculate the net energy generation potential for central receiver plants by multiplying the power generation potential by the 8760 hours in a year and then by the 60% capacity factor

3. Finally all the maps in this project, from Figure 6.1 onwards, were created in ArcGIS and exported to a jpeg format for inclusion in this report.

Appendix B: Comparison Database of Parabolic Trough Costs

PARABOLIC TROUGH COST DATA

Trough System Cost

	SAM (2010) Default Values		EPRI (2010)				Turchi et al. (2010)	
	6 hrs - wet	6 hrs - dry	0 hrs - wet	3 hrs - wet	6 hrs - wet	9 hrs - wet	0 hrs - wet	6 hrs - wet
Direct Capital Costs								
Site improvements	20 $/m2							
Solar field	350 $/m2						295 $/m2	
HTF system	50 $/m2						90 $/m	
Storage	70 $/kWht							
Fossil backup	0 $/kWe							
Power plant	920 $/kWe	1140 $/kWe					940 $/kWe gross	
Contingency	10%							
TOTAL Direct Cost	$ 640,556,125.20	$ 764,612,940.45						
Indirect Capital Costs								
Engineer, Procure, Construct % of Direct cost	15%							
Project, Land, Management % of Direct cost	3.5%							
Sales tax applies to % of direct cost	80%							
TOTAL Indirect Cost	$ 158,217,362.92	$ 188,859,396.29						
Total Installed Costs								
Total Installed Costs	$ 798,773,488.12	$ 953,472,336.74						
Est. Total installed cost per net capacity	7,987.66 $/kW	9,080.60 $/kW						
Operation and Maintenance Costs								
Fixed annual cost	0 $/yr							
Fixed cost by capacity	80 $/kW. yr		424 R/kW.yr	513 R/kW.yr	562 R/kW.yr	635 R/kW.yr	70 $/kW. Yr	
Variable cost by generation	3 $/MWh							
Fossil fuel cost	0 $/MMBTU							

	Stoddard et al. (2006)		Sargent & Lundy (2003)	Kelly (2006)		
	6 hrs - wet (2005 $)	6 hrs - wet (2010 $)	SEGS VI no TES	Small no TES	Med no TES	Large no TES
Direct Capital Costs						
Site improvements	$ 2,455,000	$ 3,607,200				
Solar field	$ 230,865,000	$ 339,216,427	250 $/m2			
HTF system	$ 10,009,000	$ 14,706,505		23.09 $/m	25.09 $/m	26.42 $/m
Storage	$ 57,957,000	$ 85,157,847				
Fossil backup						
Power plant	$ 38,754,000	$ 56,942,340	527 $/ kWe			
Contingency						
TOTAL Direct Cost	$ 393,280,000	$ 577,857,346				
Indirect Capital Costs						
Engineer, Procure, Construct % of Direct cost						
Project, Land, Management % of Direct cost						
Sales tax applies to % of direct cost						
TOTAL Indirect Cost	$ 101,106,000	$ 148,557,885				
Total Installed Costs						
Total Installed Costs	$ 494,386,000	$ 726,415,231		$ 267,747,000	$ 465,148,000	$ 600,039,000
Est. Total installed cost per net capacity			3,008 $/kW	3,314 $/kW	3,074 $/kW	2,978 $/kW
Operation and Maintenance Costs						
Fixed annual cost						
Fixed cost by capacity						
Variable cost by generation				24 $/MWh	18 $/MWh	16 $/MWh
Fossil fuel cost						

Appendix C: Comparison Database of Central Receiver Costs

CENTRAL RECEIVER COST DATA

Tower System Cost

	SAM (2010) Default Values			EPRI (2010)		
	6 hrs - wet	6 hrs - dry	No Storage - wet	3 hrs - wet	6 hrs - wet	9 hrs - wet
Direct Capital Costs						
Site improvements	20 $/m2					
Heliostat field	201 $/m2					
Balance of plant	345 $/kWe					
Power Block	575 $/kWe	795 $/kWe	575 $/kWe			
Storage	30 $/kWht					
Fixed solar field cost	0 $					
Fixed tower cost	$ 901,500.00					
Tower cost scaling component	0.01298					
Receiver reference cost	$ 59,148,900.00					
Receiver reference area	1110 m2					
Receiver scaling component	0.7					
Contingency	10%					
TOTAL Direct Cost	$ 459,524,490.89	$ 501,901,154.72	$ 318,820,456.84			
Indirect Capital Costs						
Engineer, Procure, Construct % of Direct cost	15%					
Project, Land, Management % of Direct cost	3.5%	3.5%	3.5%			
Sales tax applies to % of direct cost	80%					
TOTAL Indirect Cost	$ 113,502,549.25	$ 123,969,585.22	$ 78,748,652.84			
Total Installed Costs						
Total Installed Costs	$ 573,027,040.13	$ 625,870,739.94	$ 397,569,109.68			
Est. Total installed cost per net capacity	5,730.21 $/kW	6,258.64 $/kW	3,975.65 $/kW			
Operation and Maintenance Costs						
Fixed annual cost	0 $/yr					
Fixed cost by capacity	80 $/kW. yr			489 R/kW.yr	546 R/kW.yr	603 R/kW.yr
Variable cost by generation	3 $/MWh					
Fossil fuel cost	0 $/MMBTU					

	Romero et al. (2002)				Sargent and Lundy (2003)
	Solar Two	Solar Tres	PS10 (2001 $)	PS10 (2010 $)	Solar Two
Direct Capital Costs					
Site improvements					
Heliostat field			$ 11,717,700	$ 23,423,737	
Balance of plant					
Power Block			$ 8,718,700	$ 17,428,722	
Storage					
Fixed solar field cost					
Fixed tower cost			$ 1,707,200	$ 3,412,701	
Tower cost scaling component					
Receiver reference cost					$ 9,100,000
Receiver reference area					100 m2
Receiver scaling component					
Contingency					
TOTAL Direct Cost					
Indirect Capital Costs					
Engineer, Procure, Construct % of Direct cost					
Project, Land, Management % of Direct cost					
Sales tax applies to % of direct cost					
TOTAL Indirect Cost					
Total Installed Costs					
Total Installed Costs			$ 27,984,800	$ 55,941,745	
Est. Total installed cost per net capacity			2,798.48 $/kW (2001)	5,594.17 $/kW	
Operation and Maintenance Costs					
Fixed annual cost					
Fixed cost by capacity					0.165 $/kWh
Variable cost by generation					
Fossil fuel cost					

Appendix D: Comparison Database of Parabolic Trough Design Data

PARABOLIC TROUGH DESIGN DATA

	SAM (2010) Default		EPRI (2010)	Turchi et al. (2010)		Dersch et al. (2002)		Sargent and Lundy (2003)	Kelly (2006)		
	6 hrs - wet	6 hrs - dry	0 hrs to 9hrs - wet	0 hrs - wet	6 hrs - wet	SEGS	SEGS with TES	SEGS VI no TES	Small no TES	Med no TES	Large no TES
Annual Performance											
System Degradation	0%										
Availability	94%		95%	94%				98%			
Solar Field											
Solar Field Parameters											
Solar multiple	2			1.3	2				1.45		
Field aperture	861590 m2							188,000 m2	541,786 m2	1,015,848 m2	1,354,464 m2
Row spacing	15 m										
Stow angle	170 deg										
Deploy angle	10 deg										
Solar field	H Layout										
Header pipe roughness	4.57e-005 m										
HTF pump efficiency	0.85										
Freeze protection temp	150 °C										
Irradiation at design	950 W/m2										
Allow partial defocusing	No										
Heat Transfer Fluid											
Field HTF fluid	VP-1							VP-1			
Design loop inlet temp	293 °C										
Design outlet inlet temp	391 °C							391 °C			
Min single loop flow rate	1 kg/s										
Max single loop flow rate	12 kg/s										
Min field flow velocity	0.356106 m/s										
Max field flow velocity	4.9655 m/s										
Header design min flow velocity	2 m/s										
Header design max flow velocity	3 m/s										
Initial field temp	100 °C										
Design Point											
Single loop aperture	3762.4 m2										
Loop optical efficiency	0.744601							0.533			
Total loop conversion efficiency	0.716894										
Total required aperture, SM=1	427969 m2	500269 m2									
Required number of loops, SM=1	113.749	132.965									
Actual number of loops	227	266							192	360	480
Actual aperture	854065 m2	1000800 m2						188,000 m2			
Actual solar multiple	2										
Field thermal output	582.936 MWt	681.416 MWt							234.7 MWt	440.0 MWt	586.7 MWt
Collector Orientation											
Collector tilt	0 deg										
Collector azimuth	0 deg										
Mirror Washing											
Water usage per mirror wash	0.6 L/m2							22 l/m2			
Washing frequency	4 days										

Collectors (SCAs)

	SAM (2010) Default		EPRI (2010)	Turchi et al. (2010)		Dersch et al. (2002)		Sargent and Lundy (2003)	Kelly (2006)		
	6 hrs - wet	6 hrs - dry	0 hrs to 9hrs - wet	0 hrs - wet	6 hrs - wet	SEGS	SEGS with TES	SEGS VI no TES	Small no TES	Med no TES	Large no TES
Configuration	Solargenix SGX-1										
Collector Geometry											
Reflective aperture area	470.3 m2							235 m2			
Aperture width total structure	5 m										
Length of collector assembly	100 m							50 m			
Number of modules per assembly	12							12			
Ave surface-to-focus path length	1.8 m										
Piping distance between assemblies	1 m										
Optical Parameters											
Incidence angle modifier coeff 1	1										
Incidence angle modifier coeff 2	0.0506										
Incidence angle modifier coeff 3	-0.1763										
Tracking error	0.994							0.994			
Geometry effects	0.98							0.98			
Mirror reflectance	0.935							0.935			
Dirt on mirror	0.95			0.935				0.931			
General optical error	0.99										
Optical Calculations											
Length of single module	8.33333 m										
Incidence angle modifier	1.00228										
End loss at design	0.980058										
Optical efficiency at design	0.856609							0.533			

Receivers (HCEs)

	SAM (2010) Default		EPRI (2010)	Turchi et al. (2010)		Dersch et al. (2002)		Sargent and Lundy (2003)	Kelly (2006)		
	6 hrs - wet	6 hrs - dry	0 hrs to 9hrs - wet	0 hrs - wet	6 hrs - wet	SEGS	SEGS with TES	SEGS VI no TES	Small no TES	Med no TES	Large no TES
Configuration	Schott PTR70 2008							Luz			
Receiver Geometry											
Absorber tube inner diameter	0.066 m										
Absorber tube outer diameter	0.07 m										
Glass envelope inner diameter	0.115 m										
Glass envelope outer diameter	0.12 m										
Absorber flow plug diameter	0 m										
Internal surface roughness	4.5e-005 m										
Absorber flow pattern	Tube flow										
Absorber material type	304L										
Parameters and Variations											
Variation 1											
Variant weighting fraction	0.985							1			
Absorber absorptance	0.96							0.92			
Absorber emittance	Table							0.18 at 400 °C			
Envelope absorbtance	0.02										
Envelope emittance	0.86										
Envelope transmittance	0.963							0.92			
Broken glass	No										
Annulus gas type	Hydrogen										
Annulus pressure	0.0001 tor										
Estimated ave heat loss	150 W/m										
Bellows shadowing	0.96										
Dirt on receiver	0.98										
Variation 2											
Variant weighting fraction	0.01										
Absorber absorptance	0.96										
Absorber emittance	0.65										
Envelope absorbtance	0.02										
Envelope emittance	0.86										
Envelope transmittance	0.963										
Broken glass	No										
Annulus gas type	Air										
Annulus pressure	750 torr										
Estimated ave heat loss	1100 W/m										
Bellows shadowing	0.96										
Dirt on receiver	0.98										
Variation 3											
Variant weighting fraction	0.005										
Absorber absorptance	0.8										
Absorber emittance	0.65										
Envelope absorbtance	0										
Envelope emittance	1										
Envelope transmittance	1										
Broken glass	Yes										
Annulus gas type	Air										
Annulus pressure	750 torr										
Estimated ave heat loss	1500 W/m										
Bellows shadowing	0.96										
Dirt on receiver	1										
Total Weighted Losses											
Heat loss at design	166.25 W/m										
Optical derate	0.869242										

Power Cycle

	SAM (2010) Default		EPRI (2010)	Turchi et al. (2010)		Dersch et al. (2002)		Sargent and Lundy (2003)	Kelly (2006)		
	6 hrs - wet	6 hrs - dry	0 hrs to 9hrs - wet	0 hrs - wet	6 hrs - wet	SEGS	SEGS with TES	SEGS VI no TES	Small no TES	Med no TES	Large no TES
Plant Capacity											
Design gross output	110 MWe	115.5 MWe									
Estimated gross to net conversion factor	0.9091										
Estimated net output at design (nameplate)	100.001 MWe	105.001 MWe	125 MWe	100 MWe		50 MWe	50 MWe	30 MWe	88 MW	165 MW	220 MW
Power Block Design Point											
Rated cycle conversion efficiency	0.3774	0.339		0.377				0.351			
Design inlet temp	391 °C			391							
Design outlet temp	293 °C										
Boiler operating pressure	100 bar										
Fossil backup boiler LHV efficiency	0.9										
Heat capacity of balance plant	5 kWht/K. MWhe										
Steam cycle blowdown fraction	0.013	0.016									
Plant control											
Fraction of thermal power needed for standby	0.2										
Power block startup time	0.5 hr										
Fraction of thermal power needed for startup	0.2										
Minimum required startup temp	300 °C										
Max turbine over design operation	1.15										
Min turbine operation	0.25										
Cooling System											
Condenser type	Evaporative	Air-cooled				Evaporative	Evaporative	Evaporative	Evaporative	Evaporative	Evaporative
Ambient temp at design	20 °C	33 °C									
Ref. condenser water dT	10 °C	10 °C									
Approach temp	5 °C	5 °C									
ITD at design point	16 °C	16 °C									
Condenser pressure ratio	1.0028	1.0028									

Thermal Storage

	SAM (2010) Default		EPRI (2010)	Turchi et al. (2010)		Dersch et al. (2002)		Sargent and Lundy (2003)	Kelly (2006)		
	6 hrs - wet	6 hrs - dry	0 hrs to 9hrs - wet	0 hrs - wet	6 hrs - wet	SEGS	SEGS with TES	SEGS VI no TES	Small no TES	Med no TES	Large no TES
Storage System											
Full load hours of Thermal Energy Storage	6 hr										
Storage volume	26032 m3	30429.8 m3									
TES thermal capacity	1748.81 MWt	2044.25 MWt				0 MWt	839 MWt				
Parallel tank pairs	1										
Tank height	20 m										
Tank fluid min height	1 m										
Tank diameter	40.7093 m	44.0139 m									
Min fluid volume	1301.6 m3	1521.49 m3									
Tank loss coefficient	0.4 W/m2. K										
Estimated heat loss	0.497096 MWt	0.552161 MWt									
Tank heater set point	250 °C										
Aux heater outlet set temp	391										
Tank heater capacity	25 MWt										
Tank heater efficiency	0.98										
Hot side HX approach temp	5 °C										
Hot side HX approach temp	7 °C										
Heat exchanger derate	0.877551										
Initial TES fluid temp	300 °C										
Storage HTF fluid	Solar Salt										
Fluid temp	342 °C										
TES fluid density	1872.49 kg/m3										
TES specific heat	1.50182 kJ/kg. K										

Parasitics

Piping thermal loss coefficient	0.45 W/m2. K										
Tracking power	125 W/sca										
Req pumping power for HTF through power block	0.55 kJ/kg										
Req pumping power for HTF through storage	0.15 kJ/kg										
Fraction of rated gross power consumed at all times	0.0055										
Balance of plant parasitics	0.02467 MWe/MWcap										
Aux heater, boiler parasitics	0.02273 MWe/MWcap										
Design Point Totals											
Tracking TOTAL	227000 W	266000 W									
TOTAL fixed parasitic load	0.605 MWe	0.635 MWe				3.77 MWe	6.54 MWe		0.443 MWe	0.835 MWe	1.115 MWe
BOP	2.7137 MWe	2.8494 MWe							2.183 MWe	4.053 MWe	5.375 MWe
Aux	2.5003 MWe	2.6253 MWe									

Appendix E: Comparison Database of Central Receiver Design Data

CENTRAL RECEIVER DESIGN DATA

	SAM (2010) Default Values			EPRI (2010)				Romero et al. (2002)			Sargent and Lundy (2003)
	6 hrs - wet	6 hrs - dry	No Storage - wet	0 hrs - wet	3 hrs - wet	6 hrs - wet	9 hrs - wet	Solar Two	Solar Tres	PS10	Solar Two
Annual Performance											
System Degradation	0%										
Availability	94%			92%							
Heliostat Field											
Heliostat Field											
Heliostat width	12.2 m									9.67 m	
Heliostat height	12.2 m									9.57 m	
Ratio of reflective area to profile	0.97										
Use round heliostats	No										
Heliostat area	144.375 m2									91 m2	95 m2
Mirror reflectance and soiling	0.9									0.9	0.95
Heliostat availability	0.99										0.98
Image error	0.002 rad										
Heliostat stow deploy angle	8 deg										
Wind stow speed	15 m/s										
Field Parameters											
Total reflective area	964,712.4 m2	1,012,933.6 m2	668,455.3 m2								80,000 m2
No. heliostats	6682	7016	4630							981	1912
Radial step size for layout	115.628 m	115.628 m	87.5025 m								
Solar Field Layout Constraints											
Max heliostat distance to tower height ratio	7.5										
Min heliostat distance to tower height ratio	0.75										
Tower height	205.56 m		155.56 m								
Max distance from tower	1541.7 m		1166.7 m								
Min distance from tower	154.17 m		116.67 m								
Max realised distance from tower	1310.45 m		1079.2 m								
Radial Zones	12										
Azimuthal Zones	12										
Mirror Washing											
Water use per wash	0.6 l/m2										
Washing frequency	4 days										
Land Area											
Non-solar field land area	180000 m2										
Solar field land area multiplier	1.3										
Calculated total land area	4.65693 km2	5.23026 km2	3.77494 km2	0.0814 km2	0.263 km2						0.4 km2

Tower and Receiver

	SAM (2010) Default Values			EPRI (2010)				Romero et al. (2002)			Sargent and Lundy (2003)
	6 hrs - wet	6 hrs - dry	No Storage - wet	0 hrs - wet	3 hrs - wet	6 hrs - wet	9 hrs - wet	Solar Two	Solar Tres	PS10	Solar Two
Dimensions											
Receiver height	18.8 m	19.91 m	15.17 m							10.5 m	
Receiver diameter	12.44 m		10.67 m							10.5 m	
Tower Height	205.56 m		155.56 m							90 m	
Thermodynamic Characteristics											
Number of panels	24										
Tube outer diameter	40 mm										
Tube wall thickness	1.25 mm										
Required HTF outlet temp	574 °C										565 °C
Max temp to receiver	350 °C										
Coating absorptivity	0.94										0.93
Coating emissivity	0.88										
Heat loss factor	1										
Enable night recirculation in receiver	No										
Recirculation heater efficiency	1										
Max HTF velocity in receiver	6 m/s										
Max flow rate to receiver	3,690,306.6 kg/hr		3,165,238.8 kg/hr								
Max receiver flux	1200 kWt/m2										800 kW/m2
Materials and Flow											
HTF Type	Salt (60%, NaNO3 40% KNO3)										Solar Salt
Material type	Stainless AISI316										
Flow pattern	1										

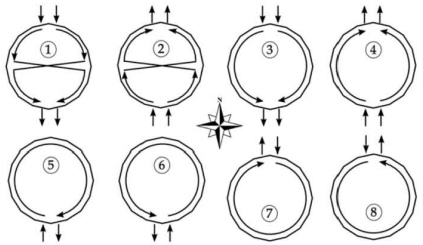

	SAM (2010) Default Values			EPRI (2010)				Romero et al. (2002)			Sargent and Lundy (2003)
	6 hrs - wet	6 hrs - dry	No Storage - wet	0 hrs - wet	3 hrs - wet	6 hrs - wet	9 hrs - wet	Solar Two	Solar Tres	PS10	Solar Two
Power Cycle											
Plant Capacity											
Design turbine gross output	110 MWe										
Estimated gross to net conversion factor	0.9091										
Estimated net output at design (nameplate)	100.001 MWe			125 MWe				10 MW	15 MW	10 MW	10 MW
Power Block Design Point											
Rated cycle conversion efficiency	0.425	0.408	0.425							0.309	0.317
Design thermal power	258.824 MWt	269.608 MWt	258.824 MWt								
Design HTF inlet temp	574 °C										510 °C
Design HTF outlet temp	290 °C										
Boiler steam pressure	100 bar										125 bar
Boiler LHV efficiency	0.9										
Steam cycle blowdown fraction	0.013										
Plant control											
Min temp to load	500 °C										
Low resource standby period	2 hr										
Fraction of thermal power needed for standby	0.2										
Power block startup time	0.5 hr										
Fraction of thermal power needed for startup	0.75										
Min turbine load fraction	0.25										
Max turbine over design operation	1.15										
Cooling System											
Condenser type	Evaporative	Air-cooled	Evaporative								Evaporative
Ambient temp at design	20 °C	33 °C	20 °C								
Ref. condenser water dT	10 °C	10 °C	10 °C								
Approach temp	5 °C	5 °C	5 °C								
ITD at design point	16 °C	16 °C	16 °C								
Condenser pressure ratio	1.0028	1.0028	1.0028								
Thermal Storage											
Storage System											
Storage type	2 tank		None								
Full load hours of Thermal Energy Storage	6 hr		0					110 MWh	610 MWh	18 MWh	3 hr
Storage HTF volume	7224.78 m3	7525.81 m3	-								
Tank diameter	21.4463 m	21.8885 m	-								
Tank height	20 m		-								
Tank fluid min height	1 m		-								
Parallel tank pairs	1		-								
Min fluid volume	361.239 m3	376.291 m3	-								
Max fluid volume	6863.54 m3	7149.52 m3	-								
Tank wetted loss coefficient	0.4 W/m2. K		-								
Tank dry loss coefficient	0.25 W/m2. K		-								
Initial hot HTF temp	574 °C		-								
Initial cold HTF temp	290 °C		-								
Initial hot HTF percent	0.3		-								
Initial hot HTF volume	2167.43 m3	2257.74 m3	-								
Initial cold HTF volume	5057.35 m3	5268.07 m3	-								
Cold tank heater temp set-point	280 °C		-								
Cold tank heater max load	30 MWe		-								
Hot tank heater temp set-point	500 °C		-								
Hot tank heater max load	30 MWe		-								
Tank heater efficiency	0.99		-								
Parasitics											
Startup energy of single heliostat	0.025 kWe										
Tracking power for single heliostat	0.055 kWe										
Receiver HTF pump efficiency	0.85										
Storage pump power	0.01 Mwe/MWt										
Balance of plant power	0.05 Mwe/MWt									1 MW	
Piping loss coefficient	3500 Wt/m										
Total piping length	1500 m										

Appendix F: Final Design Inputs for Parabolic Trough

Overview

The following appendix details the full and final set of inputs used in the SAM parabolic trough models for this study. In order to avoid vast amounts of repetition in the reporting of the input data, many of the following inputs pages have been generalised so as to apply to each of the 6 parabolic trough models (both wet and dry cooling at each of the three locations). In order to accomplish this task of generalisation, many of the values automatically calculated by SAM within each input page (and reported in the blue fields) have been removed as they would only apply to specific cases. In the cases where it was not possible to report one input page for both wet and dry-cooled plants, a separate input page for each of the cooling technologies is listed, however, they are still generalised in the sense that they apply to the wet-cooled and dry-cooled plants at all locations. In some instances, such as the solar field design and annual performance, it was not possible to generalise input pages, and thus all input pages are listed for each location. The input pages for location are not included in the appendix as they are simply specified according to each of the locations in question.

Financing

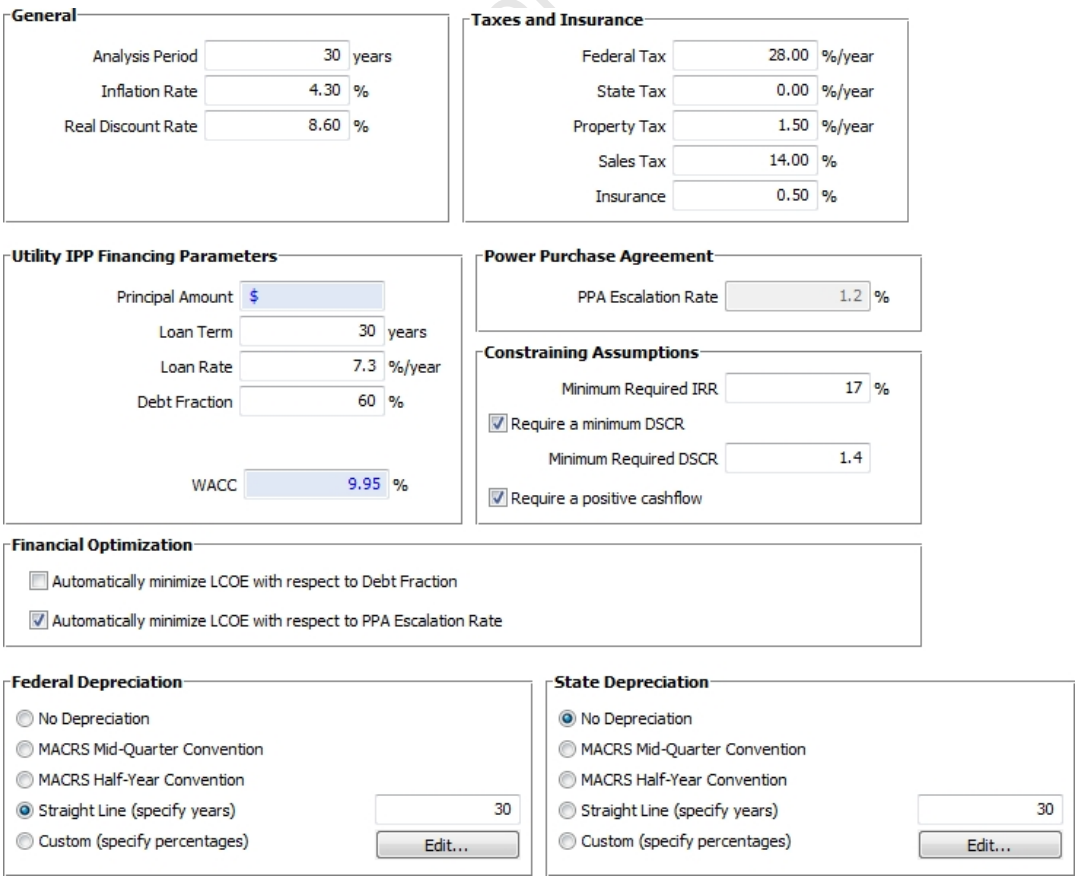

Tax and Payment Incentives

Investment Tax Credit (ITC)

		Amount	Taxable Incentive Federal	Taxable Incentive State	Reduces ITC Basis Federal	Reduces ITC Basis State	Reduces Depreciation Basis Federal	Reduces Depreciation Basis State
Federal	Value	$ 0	N/A	NO	N/A	N/A	☑	☑
State	Value	$ 0	NO	N/A	N/A	N/A	☐	☐
		Percentage	Maximum					
Federal	Value	0 %	$ 1e+099	N/A	NO	N/A	N/A	☑	☑
State	Value	0 %	$ 1e+099	NO	N/A	N/A	N/A	☐	☐

Note:

Depreciation is not used in residential financing, and hence the basis reduction inputs above can be ignored.

Production Tax Credit (PTC)

		Amount	Term	Escalation						
Federal	Value	0 $/kWh	10 years	2 %	N/A	NO	NO	NO	NO	NO
State	Value	0 $/kWh	10 years	2 %	NO	N/A	NO	NO	NO	NO

Investment Based Incentive (IBI)

		Amount									
Federal	Value	$ 0	☑	☑	☐	☐	☐	☐
State	Value	$ 0	☑	☑	☐	☐	☐	☐
Utility	Value	$ 0	☑	☑	☐	☐	☐	☐
Other	Value	$ 0	☑	☑	☐	☐	☐	☐
		Percentage	Maximum								
Federal	Value	0 %	$ 1e+099	☑	☑	☐	☐	☐	☐
State	Value	0 %	$ 1e+099	☑	☑	☐	☐	☐	☐
Utility	Value	0 %	$ 1e+099	☑	☑	☐	☐	☐	☐
Other	Value	0 %	$ 1e+099	☑	☑	☐	☐	☐	☐

Capacity Based Incentive (CBI)

		Amount	Maximum						
Federal	Value	0 $/W	$ 1e+099	☑	☑	☐	☐	☐	☐
State	Value	0 $/W	$ 1e+099	☑	☑	☐	☐	☐	☐
Utility	Value	0 $/W	$ 1e+099	☑	☑	☐	☐	☐	☐
Other	Value	0 $/W	$ 1e+099	☑	☑	☐	☐	☐	☐

Production Based Incentive (PBI)

		Amount	Term	Escalation						
Federal	Value	0 $/kWh	0 years	0 %	☑	☑	NO	NO	NO	NO
State	Value	0 $/kWh	0 years	0 %	☑	☑	NO	NO	NO	NO
Utility	Value	0 $/kWh	0 years	0 %	☑	☑	NO	NO	NO	NO
Other	Value	0 $/kWh	0 years	0 %	☑	☑	NO	NO	NO	NO

Wet-Cooled Parabolic Trough System Costs

Direct Capital Costs

Site Improvements		m2	22.01 $/m2	$
Solar Field		m2	385.13 $/m2	$
HTF System		m2	55.02 $/m2	$
Storage		MWht	77.03 $/kWht	$
Fossil Backup		MWe, Gross	0.00 $/kWe	$ 0.00
Power Plant		MWe, Gross	1,012.35 $/kWe	$
		Contingency	10 %	$
			Total Direct Cost	$

Indirect Capital Costs

	% of Direct Cost	Non-fixed Cost	Fixed Cost	Total
Engineer,Procure,Construct	15 %	$	$ 0.00	$
Project,Land,Management	3.5 %	$	$ 0.00	$

Sales Tax of 14 % applies to 80 % of Direct Cost $

Total Indirect Cost $

Total Installed Costs

Total Installed Cost $

Estimated Total Installed Cost per Net Capacity ($/kW) $

Operation and Maintenance Costs

	First Year Cost		Escalation Rate (above inflation)
Fixed Annual Cost	0.00	$/yr	0 %
Fixed Cost by Capacity	88.03	$/kW-yr	0 %
Variable Cost by Generation	7.04	$/MWh	0 %
Fossil Fuel Cost	0.00	$/MMBTU	0 %

Notes

1) Escalation rates do not apply to O&M annual schedules, only first year values.

2) Fossil fuel cost is not applicable to PV or Dish Stirling systems. Set to zero for these systems.

Dry-Cooled Parabolic Trough System Costs

Direct Capital Costs

Site Improvements		m2	22.01 $/m2	$
Solar Field		m2	385.13 $/m2	$
HTF System		m2	55.02 $/m2	$
Storage		MWht	77.03 $/kWht	$
Fossil Backup		MWe, Gross	0.00 $/kWe	$ 0.00
Power Plant		MWe, Gross	1,254.43 $/kWe	$
		Contingency	10 %	$
			Total Direct Cost	$

Indirect Capital Costs

	% of Direct Cost	Non-fixed Cost	Fixed Cost	Total
Engineer,Procure,Construct	15 %	$	$ 0.00	$
Project,Land,Management	3.5 %	$	$ 0.00	$

Sales Tax of 14 % applies to 80 % of Direct Cost $

Total Indirect Cost $

Total Installed Costs

Total Installed Cost $

Estimated Total Installed Cost per Net Capacity ($/kW) $

Operation and Maintenance Costs

	First Year Cost		Escalation Rate (above inflation)
Fixed Annual Cost	0.00	$/yr	0 %
Fixed Cost by Capacity	88.03	$/kW-yr	0 %
Variable Cost by Generation	3.39	$/MWh	0 %
Fossil Fuel Cost	0.00	$/MMBTU	0 %

Notes

1) Escalation rates do not apply to O&M annual schedules, only first year values.

2) Fossil fuel cost is not applicable to PV or Dish Stirling systems. Set to zero for these systems.

Upington Wet and Dry-Cooled Solar Field Design and Annual Performance

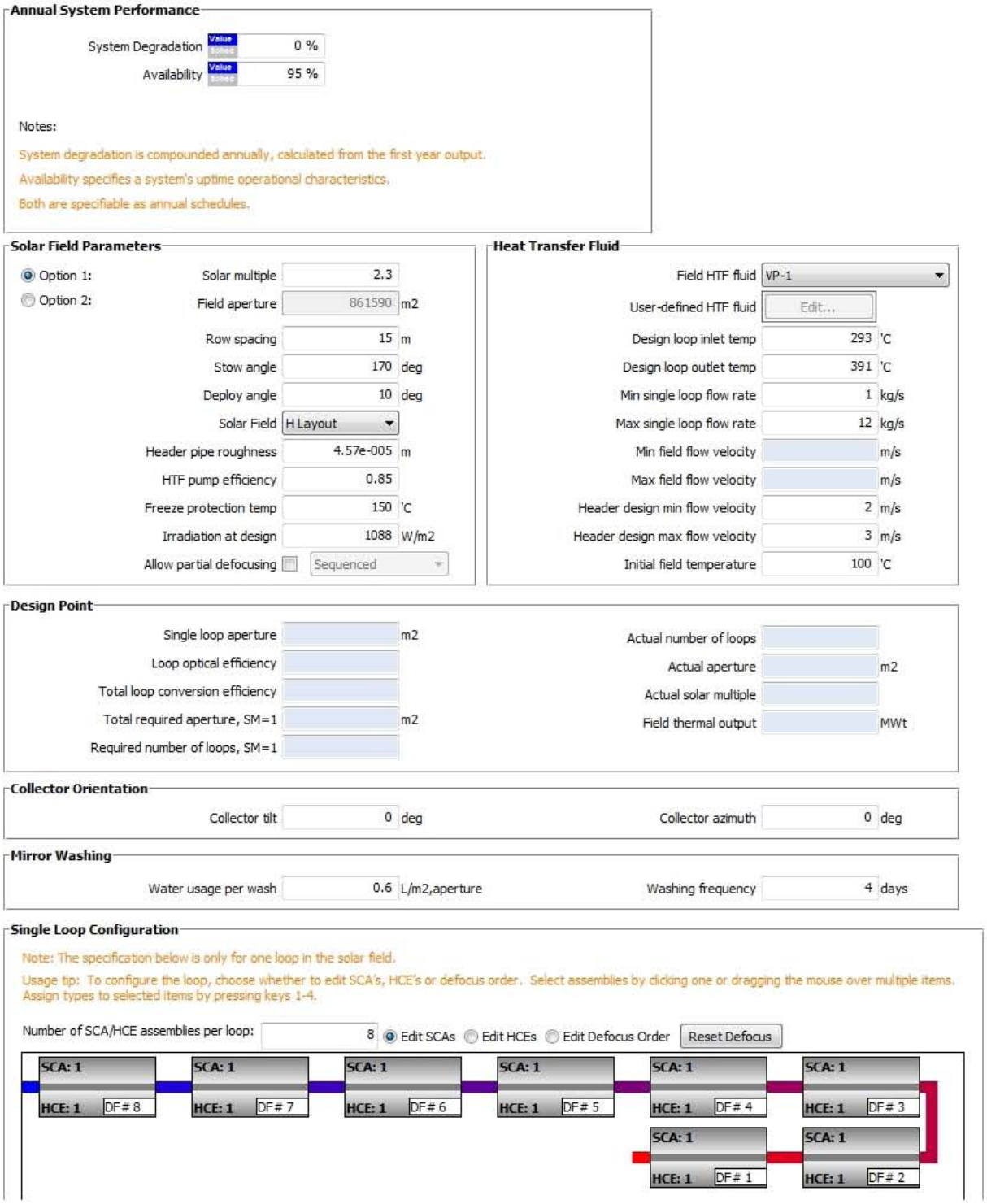

Springbok Wet and Dry-Cooled Solar Field Design and Annual Performance

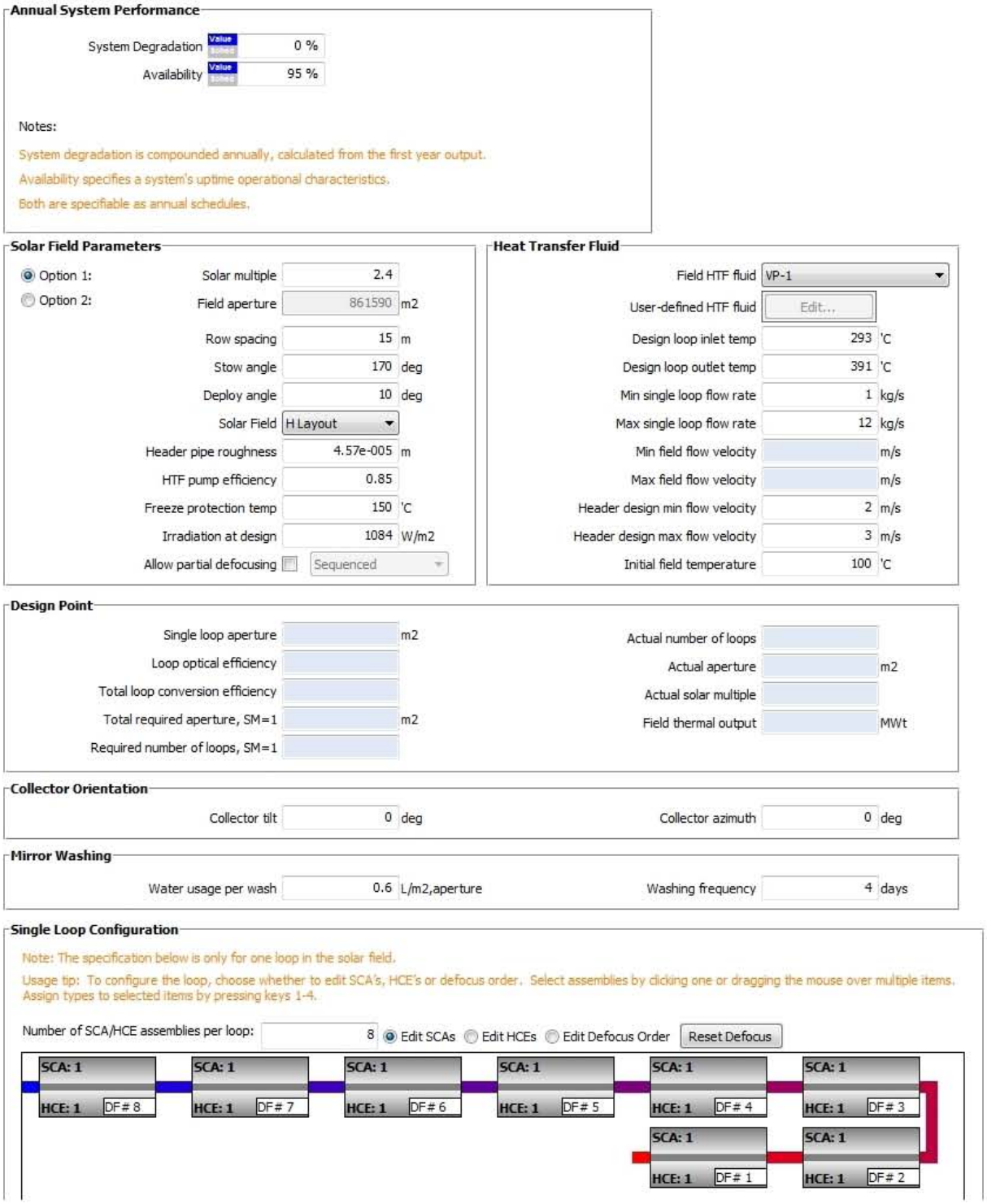

Bloemfontein Wet and Dry-Cooled Solar Field Design and Annual Performance

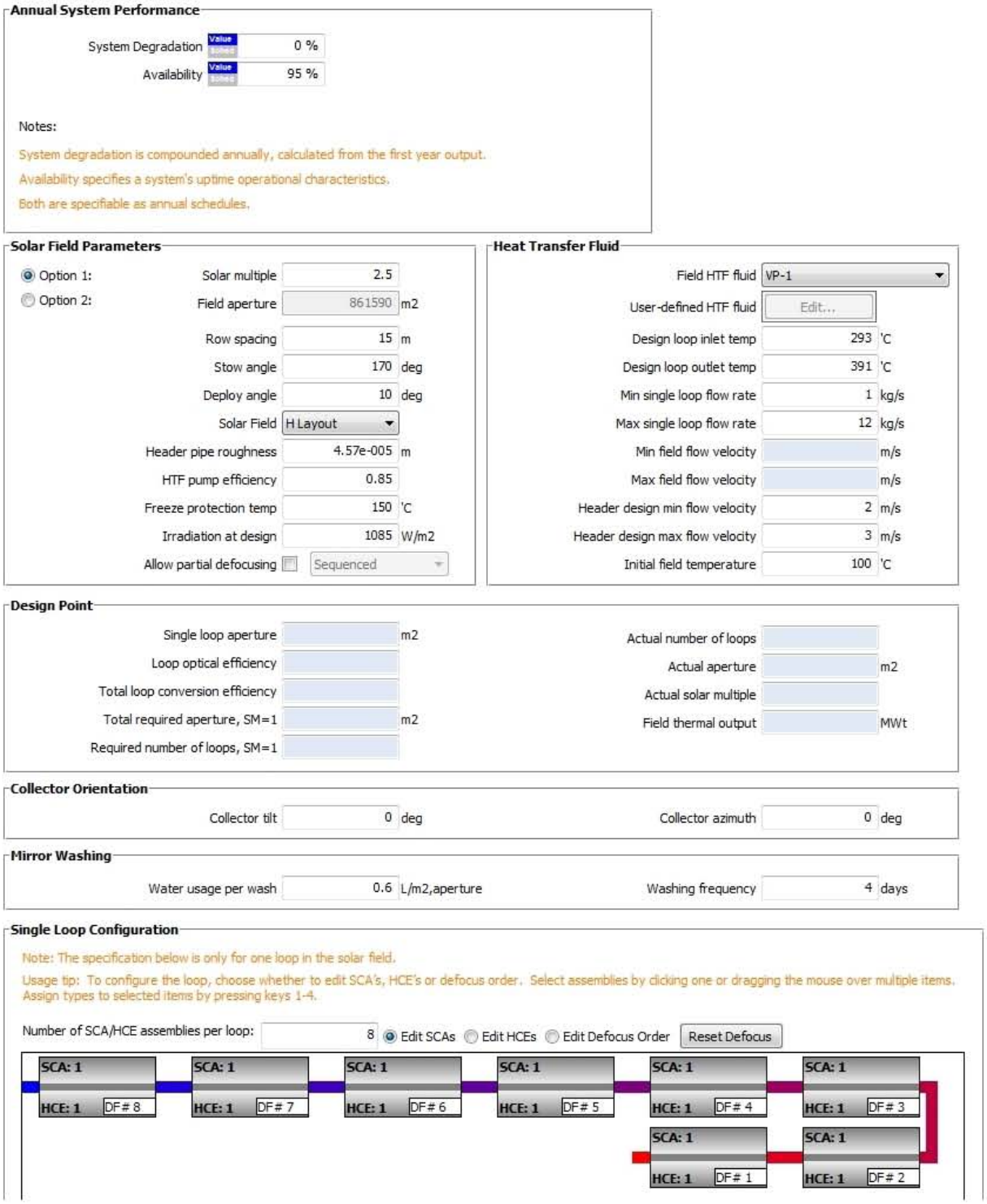

Collectors (SCAs) and Receivers (HCEs)

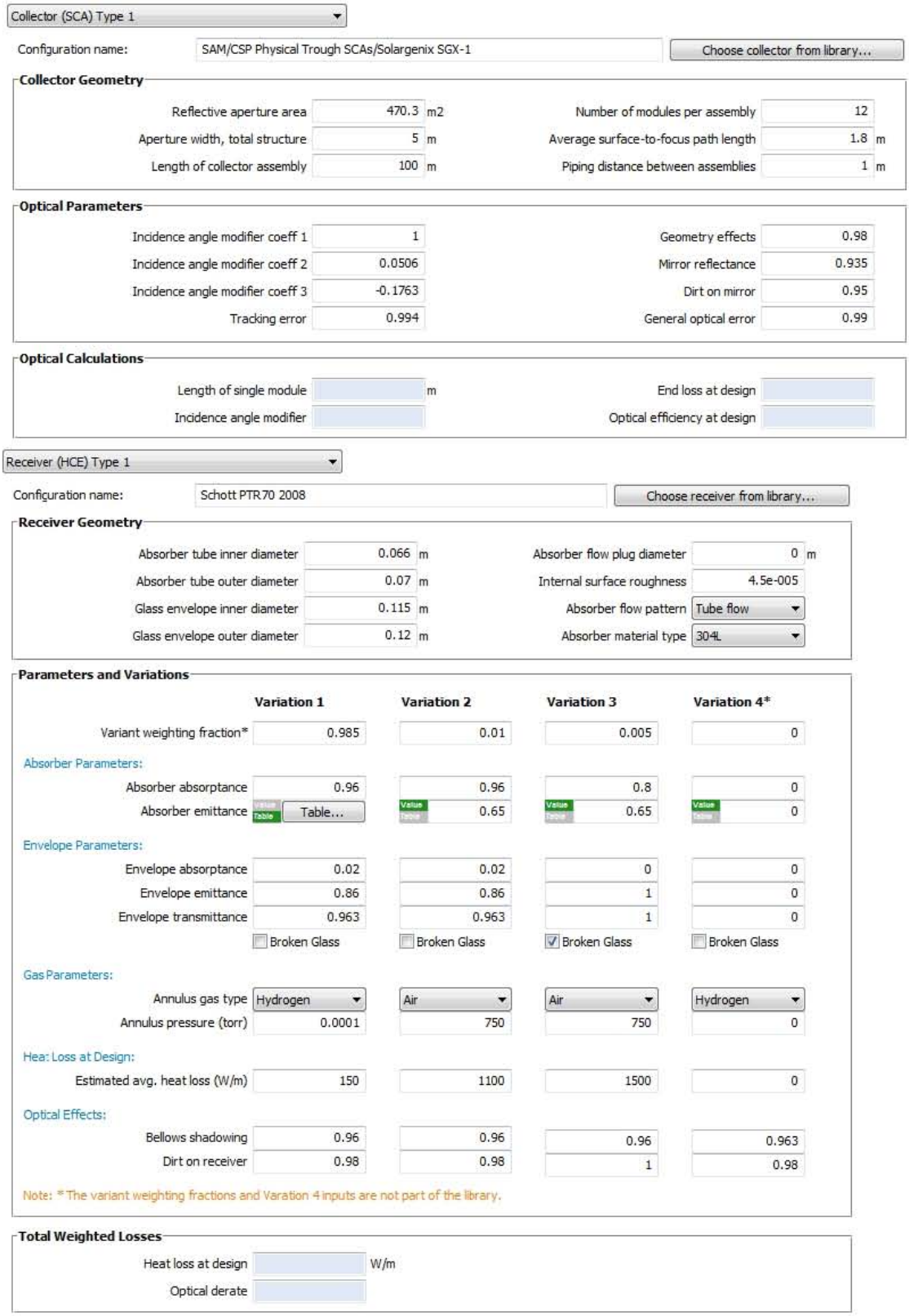

Wet-Cooled Power Cycle

Plant Capacity

Design gross output	110	MWe
Estimated gross to net conversion factor	0.9091	
Estimated net output at design (nameplate)	100.001	MWe

Note: Parasitic losses typically reduce net output to approximately 90 % of design gross power

Power Block Design Point

Rated cycle conversion efficiency	0.3774	
Design inlet temperature	391	'C
Design outlet temperature	293	'C
Boiler operating pressure	100	bar
Fossil backup boiler LHV efficiency	0.9	
Heat capacity of balance of plant	5	kWht/K-MWhe
Steam cycle blowdown fraction	0.013	

Plant Control

Fraction of thermal power needed for standby	0.2	
Power block startup time	0.5	hr
Fraction of thermal power needed for startup	0.2	
Minimum required startup temp	300	'C
Max turbine over design operation	1.15	
Min turbine operation	0.25	

Cooling System

Condenser type	Evaporative	
Ambient temp at design	20	'C
Ref. Condenser Water dT	10	'C
Approach temperature	5	'C
ITD at design point	16	'C
Condenser pressure ratio	1.0028	

Dry-Cooled Power Cycle

Plant Capacity

Design gross output	110	MWe
Estimated gross to net conversion factor	0.9091	
Estimated net output at design (nameplate)	100.001	MWe

Note: Parasitic losses typically reduce net output to approximately 90 % of design gross power

Power Block Design Point

Rated cycle conversion efficiency	0.339	
Design inlet temperature	391	'C
Design outlet temperature	293	'C
Boiler operating pressure	100	bar
Fossil backup boiler LHV efficiency	0.9	
Heat capacity of balance of plant	5	kWht/K-MWhe
Steam cycle blowdown fraction	0.016	

Plant Control

Fraction of thermal power needed for standby	0.2	
Power block startup time	0.5	hr
Fraction of thermal power needed for startup	0.2	
Minimum required startup temp	300	'C
Max turbine over design operation	1.15	
Min turbine operation	0.25	

Cooling System

Condenser type	Air-cooled	
Ambient temp at design	33	'C
Ref. Condenser Water dT	10	'C
Approach temperature	5	'C
ITD at design point	16	'C
Condenser pressure ratio	1.0028	

Wet-Cooled Thermal Storage and Parasitics

Storage System

Full load hours of TES	6	hr	Tank heater capacity	25	MWt
Storage volume	26032	m3	Tank heater efficiency	0.98	
TES Thermal capacity	1748.81	MWt	Hot side HX approach temp	5	'C
Parallel tank pairs	1		Cold side HX approach temp	7	'C
Tank height	20	m	Heat exchanger derate	0.877551	
Tank fluid min height	1	m	Initial TES fluid temp	300	'C
Tank diameter	40.7093	m	Storage HTF fluid	Solar Salt	
Min fluid volume	1301.6	m3	User-defined HTF fluid	Edit...	
Tank loss coeff	0.4	W/m2-K	Fluid Temperature	342	'C
Estimated heat loss	0.497096	MWt	TES fluid density	1872.49	kg/m3
Tank heater set point	250	'C	TES specific heat	1.50182	kJ/kg-K
Aux heater outlet set temp	391				

Thermal Storage Dispatch Control

Current dispatch schedule:

No library match.

Dispatch schedule library...

Note:

Schedule libraries do not affect the Storage Dispatch, Turbine Output and Fossil Fill fractions below.

	Storage Dispatch w/ solar*	Storage Dispatch w/o solar*	Turb. out. fraction*	Fossil fill fraction*
Period 1:	0	0	1.1	0
Period 2:	0	0	1	0
Period 3:	0	0	1	0
Period 4:	0	0	1	0
Period 5:	0	0	1	0
Period 6:	0	0	1	0

Notes:

1. Storage dispatch fractions apply to the maximum energy storage.

2. Turbine output and fossil fill fractions apply to the design turbine thermal input.

Weekday Schedule

	12am	1am	2am	3am	4am	5am	6am	7am	8am	9am	10am	11am	12pm	1pm	2pm	3pm	4pm	5pm	6pm	7pm	8pm	9pm	10pm	11pm
Jan	3	3	3	3	3	3	3	2	2	2	2	1	1	1	1	1	1	2	2	2	2	2	3	3
Feb	3	3	3	3	3	3	3	2	2	2	2	1	1	1	1	1	1	2	2	2	2	2	3	3
Mar	3	3	3	3	3	3	3	2	2	2	2	1	1	1	1	1	1	2	2	2	2	2	3	3
Apr	6	6	6	6	6	6	5	5	4	4	4	4	4	4	4	4	4	4	4	4	4	5	5	5	6
May	6	6	6	6	6	6	6	5	5	4	4	4	4	4	4	4	4	4	4	4	4	4	5	5	5
Jun	6	6	6	6	6	6	6	5	5	4	4	4	4	4	4	4	4	4	4	4	4	4	5	5	5
Jul	6	6	6	6	6	6	6	5	5	4	4	4	4	4	4	4	4	4	4	4	4	4	5	5	5
Aug	6	6	6	6	6	6	6	5	5	4	4	4	4	4	4	4	4	4	4	4	4	4	5	5	5
Sep	6	6	6	6	6	6	6	5	5	4	4	4	4	4	4	4	4	4	4	4	4	4	5	5	5
Oct	6	6	6	6	6	6	5	5	4	4	4	4	4	4	4	4	4	4	4	4	4	5	5	5	6
Nov	6	6	6	6	6	6	5	5	4	4	4	4	4	4	4	4	4	4	4	4	4	5	5	5	6
Dec	3	3	3	3	3	3	3	3	2	2	2	2	1	1	1	1	1	1	2	2	2	2	2	3	3

Weekend Schedule

	12am	1am	2am	3am	4am	5am	6am	7am	8am	9am	10am	11am	12pm	1pm	2pm	3pm	4pm	5pm	6pm	7pm	8pm	9pm	10pm	11pm
Jan	3	3	3	3	3	3	3	3	3	3	3	3	3	3	3	3	3	3	3	3	3	3	3	3
Feb	3	3	3	3	3	3	3	3	3	3	3	3	3	3	3	3	3	3	3	3	3	3	3	3
Mar	3	3	3	3	3	3	3	3	3	3	3	3	3	3	3	3	3	3	3	3	3	3	3	3
Apr	6	6	6	6	6	5	5	5	5	5	5	5	5	5	5	5	5	5	5	5	5	5	5	6
May	6	6	6	6	6	6	5	5	5	5	5	5	5	5	5	5	5	5	5	5	5	5	5	5
Jun	6	6	6	6	6	6	5	5	5	5	5	5	5	5	5	5	5	5	5	5	5	5	5	5
Jul	6	6	6	6	6	6	5	5	5	5	5	5	5	5	5	5	5	5	5	5	5	5	5	5
Aug	6	6	6	6	6	6	5	5	5	5	5	5	5	5	5	5	5	5	5	5	5	5	5	5
Sep	6	6	6	6	6	6	5	5	5	5	5	5	5	5	5	5	5	5	5	5	5	5	5	5
Oct	6	6	6	6	6	5	5	5	5	5	5	5	5	5	5	5	5	5	5	5	5	5	5	6
Nov	6	6	6	6	6	5	5	5	5	5	5	5	5	5	5	5	5	5	5	5	5	5	5	6
Dec	3	3	3	3	3	3	3	3	3	3	3	3	3	3	3	3	3	3	3	3	3	3	3	3

Parasitics

Piping thermal loss coefficient	0.45	W/m2-K
Tracking power	125	W/sca
Required pumping power for HTF through power block	0.55	kJ/kg
Required pumping power for HTF through storage	0.15	kJ/kg
Fraction of rated gross power consumed at all times	0.0055	

Design Point Totals

Tracking W

Fixed MWe

			Factor	Coeff 0	Coeff 1	Coeff 2		
Balance of plant parasitic	0.02467	MWe/MWcap	1	0.483	0.517	0	BOP	MWe
Aux heater,boiler parasitic	0.02273	MWe/MWcap	1	0.483	0.517	0	Aux	MWe

Dry-Cooled Thermal Storage and Parasitics

Storage System

Full load hours of TES	6	hr	Tank heater capacity	25	MWt
Storage volume	28980.8	m3	Tank heater efficiency	0.98	
TES Thermal capacity	1946.9	MWt	Hot side HX approach temp	5	'C
Parallel tank pairs	1		Cold side HX approach temp	7	'C
Tank height	20	m	Heat exchanger derate	0.877551	
Tank fluid min height	1	m	Initial TES fluid temp	300	'C
Tank diameter	42.9532	m	Storage HTF fluid	Solar Salt	
Min fluid volume	1449.04	m3	User-defined HTF fluid	Edit...	
Tank loss coeff	0.4	W/m2-K	Fluid Temperature	342	'C
Estimated heat loss	0.534245	MWt	TES fluid density	1872.49	kg/m3
Tank heater set point	250	'C	TES specific heat	1.50182	kJ/kg-K
Aux heater outlet set temp	391				

Thermal Storage Dispatch Control

Current dispatch schedule:

No library match.

Dispatch schedule library...

Note:

Schedule libraries do not affect the Storage Dispatch, Turbine Output and Fossil Fill fractions below.

	Storage Dispatch w/ solar*	Storage Dispatch w/o solar*	Turb. out. fraction*	Fossil fill fraction*
Period 1:	0	0	1.1	0
Period 2:	0	0	1	0
Period 3:	0	0	1	0
Period 4:	0	0	1	0
Period 5:	0	0	1	0
Period 6:	0	0	1	0

Notes:

1. Storage dispatch fractions apply to the maximum energy storage.

2. Turbine output and fossil fill fractions apply to the design turbine thermal input.

Weekday Schedule

	12am	1am	2am	3am	4am	5am	6am	7am	8am	9am	10am	11am	12pm	1pm	2pm	3pm	4pm	5pm	6pm	7pm	8pm	9pm	10pm	11pm
Jan	3	3	3	3	3	3	3	2	2	2	2	1	1	1	1	1	1	2	2	2	2	2	3	3
Feb	3	3	3	3	3	3	3	2	2	2	2	1	1	1	1	1	1	2	2	2	2	2	3	3
Mar	3	3	3	3	3	3	3	2	2	2	2	1	1	1	1	1	1	2	2	2	2	2	3	3
Apr	6	6	6	6	6	6	5	5	4	4	4	4	4	4	4	4	4	4	4	4	4	5	5	5	6
May	6	6	6	6	6	6	6	5	5	4	4	4	4	4	4	4	4	4	4	4	4	4	5	5	5
Jun	6	6	6	6	6	6	6	5	5	4	4	4	4	4	4	4	4	4	4	4	4	4	5	5	5
Jul	6	6	6	6	6	6	6	5	5	4	4	4	4	4	4	4	4	4	4	4	4	4	5	5	5
Aug	6	6	6	6	6	6	6	5	5	4	4	4	4	4	4	4	4	4	4	4	4	4	5	5	5
Sep	6	6	6	6	6	6	6	5	5	4	4	4	4	4	4	4	4	4	4	4	4	4	5	5	5
Oct	6	6	6	6	6	6	5	5	4	4	4	4	4	4	4	4	4	4	4	4	4	5	5	5	6
Nov	6	6	6	6	6	6	5	5	4	4	4	4	4	4	4	4	4	4	4	4	4	5	5	5	6
Dec	3	3	3	3	3	3	3	3	2	2	2	2	1	1	1	1	1	1	2	2	2	2	2	3	3

Weekend Schedule

	12am	1am	2am	3am	4am	5am	6am	7am	8am	9am	10am	11am	12pm	1pm	2pm	3pm	4pm	5pm	6pm	7pm	8pm	9pm	10pm	11pm
Jan	3	3	3	3	3	3	3	3	3	3	3	3	3	3	3	3	3	3	3	3	3	3	3	3
Feb	3	3	3	3	3	3	3	3	3	3	3	3	3	3	3	3	3	3	3	3	3	3	3	3
Mar	3	3	3	3	3	3	3	3	3	3	3	3	3	3	3	3	3	3	3	3	3	3	3	3
Apr	6	6	6	6	6	5	5	5	5	5	5	5	5	5	5	5	5	5	5	5	5	5	5	6
May	6	6	6	6	6	6	5	5	5	5	5	5	5	5	5	5	5	5	5	5	5	5	5	5
Jun	6	6	6	6	6	6	5	5	5	5	5	5	5	5	5	5	5	5	5	5	5	5	5	5
Jul	6	6	6	6	6	6	5	5	5	5	5	5	5	5	5	5	5	5	5	5	5	5	5	5
Aug	6	6	6	6	6	6	5	5	5	5	5	5	5	5	5	5	5	5	5	5	5	5	5	5
Sep	6	6	6	6	6	6	5	5	5	5	5	5	5	5	5	5	5	5	5	5	5	5	5	5
Oct	6	6	6	6	6	6	5	5	5	5	5	5	5	5	5	5	5	5	5	5	5	5	5	6
Nov	6	6	6	6	6	6	5	5	5	5	5	5	5	5	5	5	5	5	5	5	5	5	5	6
Dec	3	3	3	3	3	3	3	3	3	3	3	3	3	3	3	3	3	3	3	3	3	3	3	3

Parasitics

			Design Point Totals	
Piping thermal loss coefficient	0.45	W/m2-K		
Tracking power	125	W/sca	Tracking	W
Required pumping power for HTF through power block	0.55	kJ/kg		
Required pumping power for HTF through storage	0.15	kJ/kg		
Fraction of rated gross power consumed at all times	0.0055		Fixed	MWe

			Factor	Coeff 0	Coeff 1	Coeff 2		
Balance of plant parasitic	0.02467	MWe/MWcap	1	0.483	0.517	0	BOP	MWe
Aux heater,boiler parasitic	0.02273	MWe/MWcap	1	0.483	0.517	0	Aux	MWe

Appendix G: Final Design Inputs for Central Receiver

Overview

The following appendix details the full and final set of inputs used in the SAM central receiver models for this study. As with Appendix F, in order to avoid vast amounts of repetition in the reporting of the input data, many of the following inputs pages have been generalised so as to apply to each of the 6 central receiver models (both wet and dry cooling at each of the three locations). In order to accomplish this task of generalisation, many of the values automatically calculated by SAM within each input page (and reported in the blue fields) have been removed as they would only apply to specific cases. In the cases where it was not possible to report one input page for both wet and dry-cooled plants, a separate input page for each of the cooling technologies is listed, however, they are still generalised in the sense that they apply to the wet-cooled and dry-cooled plants at all locations. In some instances, such as the heliostat field layout, it was not possible to generalise input pages, and thus all 6 input pages are listed. Once again, the input pages for location are not included in the appendix as they are simply specified according to each of the locations in question.

Financing

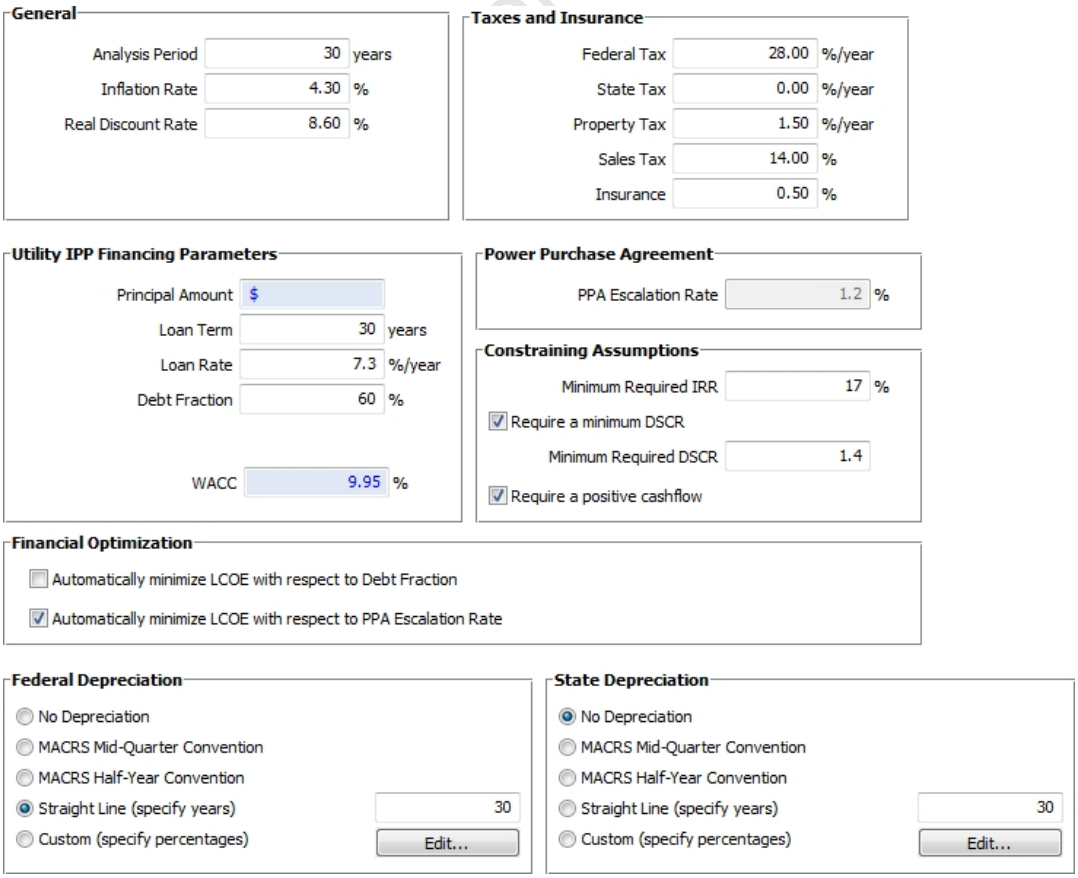

Tax and Payment Incentives

Investment Tax Credit (ITC)

		Amount	Taxable Incentive Federal	Taxable Incentive State	Reduces ITC Basis Federal	Reduces ITC Basis State	Reduces Depreciation Basis Federal	Reduces Depreciation Basis State
Federal	Value	$ 0	N/A	NO	N/A	N/A	☑	☑
State	Value	$ 0	NO	N/A	N/A	N/A	☐	☐
		Percentage	Maximum					
Federal	Value	0 %	$ 1e+099	N/A	NO	N/A	N/A	☑	☑
State	Value	0 %	$ 1e+099	NO	N/A	N/A	N/A	☐	☐

Note:

Depreciation is not used in residential financing, and hence the basis reduction inputs above can be ignored.

Production Tax Credit (PTC)

		Amount	Term	Escalation						
Federal	Value	0 $/kWh	10 years	2 %	N/A	NO	NO	NO	NO	NO
State	Value	0 $/kWh	10 years	2 %	NO	N/A	NO	NO	NO	NO

Investment Based Incentive (IBI)

		Amount									
Federal	Value	$ 0	☑	☑	☐	☐	☐	☐
State	Value	$ 0	☑	☑	☐	☐	☐	☐
Utility	Value	$ 0	☑	☑	☐	☐	☐	☐
Other	Value	$ 0	☑	☑	☐	☐	☐	☐
		Percentage	Maximum								
Federal	Value	0 %	$ 1e+099	☑	☑	☐	☐	☐	☐
State	Value	0 %	$ 1e+099	☑	☑	☐	☐	☐	☐
Utility	Value	0 %	$ 1e+099	☑	☑	☐	☐	☐	☐
Other	Value	0 %	$ 1e+099	☑	☑	☐	☐	☐	☐

Capacity Based Incentive (CBI)

		Amount	Maximum						
Federal	Value	0 $/W	$ 1e+099	☑	☑	☐	☐	☐	☐
State	Value	0 $/W	$ 1e+099	☑	☑	☐	☐	☐	☐
Utility	Value	0 $/W	$ 1e+099	☑	☑	☐	☐	☐	☐
Other	Value	0 $/W	$ 1e+099	☑	☑	☐	☐	☐	☐

Production Based Incentive (PBI)

		Amount	Term	Escalation						
Federal	Value	0 $/kWh	0 years	0 %	☑	☑	NO	NO	NO	NO
State	Value	0 $/kWh	0 years	0 %	☑	☑	NO	NO	NO	NO
Utility	Value	0 $/kWh	0 years	0 %	☑	☑	NO	NO	NO	NO
Other	Value	0 $/kWh	0 years	0 %	☑	☑	NO	NO	NO	NO

Wet-Cooled Central Receiver System Costs

Direct Capital Costs

Site Improvements		m2	22.008 $/m2	$
Heliostat Field		m2	221.175 $/m2	$
Balance of Plant		MWe, Gross	379.63 $/kWe	$
Power Block		MWe, Gross	632.72 $/kWe	$
Storage System		MWht	33.01 $/kWht	$
			Fixed Solar Field Cost	$ 0.00
Fixed Tower Cost	$ 991,988.06			
Tower Cost Scaling Exponent	0.01298		Total Tower Cost	$
Receiver Reference Cost	$ 65,085,970.84			
Receiver Reference Area	1110	m2	Area m2	
Receiver Cost Scaling Exponent	0.7		Total Receiver Cost	$
			Contingency 10 %	$
			Total Direct Cost	$

Indirect Capital Costs

	% of Direct Cost	Non-fixed Cost	Fixed Cost	Total
Engineer,Procure,Construct	15 %	$	$ 0.00	$
Project,Land,Management	3.5 %	$	$ 0.00	$
Sales Tax of 14 % applies to 80 % of Direct Cost				$
			Total Indirect Cost	$

Total Installed Costs

Total Installed Cost	$
Estimated Total Installed Cost per Net Capacity ($/kW)	$

Operation and Maintenance Costs

	First Year Cost		Escalation Rate (above inflation)
Fixed Annual Cost	0.00	$/yr	0 %
Fixed Cost by Capacity	88.03	$/kW-yr	0 %
Variable Cost by Generation	6.16	$/MWh	0 %
Fossil Fuel Cost	0.00	$/MMBTU	0 %

Dry-Cooled Central Receiver System Costs

Direct Capital Costs

Site Improvements		m2	22.008 $/m2	$
Heliostat Field		m2	221.175 $/m2	$
Balance of Plant		MWe, Gross	379.63 $/kWe	$
Power Block		MWe, Gross	874.8 $/kWe	$
Storage System		MWht	33.01 $/kWht	$
			Fixed Solar Field Cost	$ 0.00

Fixed Tower Cost	$ 991,988.06		
Tower Cost Scaling Exponent	0.01298	Total Tower Cost	$
Receiver Reference Cost	$ 65,085,970.84		
Receiver Reference Area	1110 m2	Area m2	
Receiver Cost Scaling Exponent	0.7	Total Receiver Cost	$
		Contingency 10 %	$
		Total Direct Cost	$

Indirect Capital Costs

	% of Direct Cost	Non-fixed Cost	Fixed Cost	Total
Engineer,Procure,Construct	15 %	$	$ 0.00	$
Project,Land,Management	3.5 %	$	$ 0.00	$

Sales Tax of 14 % applies to 80 % of Direct Cost $

Total Indirect Cost $

Total Installed Costs

Total Installed Cost $

Estimated Total Installed Cost per Net Capacity ($/kW) $

Operation and Maintenance Costs

	First Year Cost		Escalation Rate (above inflation)
Fixed Annual Cost	0.00	$/yr	0 %
Fixed Cost by Capacity	88.03	$/kW-yr	0 %
Variable Cost by Generation	3.45	$/MWh	0 %
Fossil Fuel Cost	0.00	$/MMBTU	0 %

Annual Performance and Tower and Receiver Design

Annual System Performance

System Degradation	Value	0 %
Availability	Value	92 %

Notes:

System degradation is compounded annually, calculated from the first year output

Availability specifies a system's uptime operational characteristics.

Both are specifiable as annual schedules.

Dimensions

Receiver Height	15.49	m
Receiver Diameter	12.44	m
Tower Height	216.67	m

Note:

Optimal dimensions are calculated by using the solar field wizard.

Thermodynamic Characteristics

Number of Panels	24	
Tube Outer Diameter	40	mm
Tube Wall Thickness	1.25	mm
Required HTF Outlet Temp.	574	'C
Max. Temp. To Receiver	350	'C
Coating Absorptivity	0.94	
Coating Emissivity	0.88	
Heat Loss Factor	1	
Enable Night Recirculation in Receiver	☐	
Recirculation Heater Efficiency	1	
Max. HTF Velocity in Receiver	6	m/s
Max. Flow Rate to Receiver	3,690,306.6	kg/hr
Max. Receiver Flux	1200	kWt/m2

Materials and Flow

HTF Type	Salt (60% NaNO3 40% KNO3)
Property table for user-defined HTF	Edit...
Material Type	Stainless AISI316
Flow Pattern	2

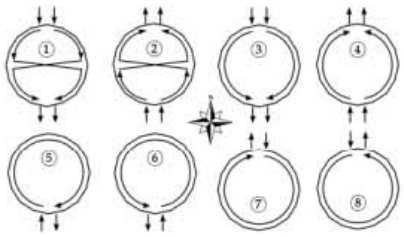

Upington Wet-Cooled Heliostat Field Design

Heliostat Properties

Heliostat Width	12.2	m
Heliostat Height	12.2	m
Ratio of Reflective Area to Profile	0.97	
Use Round Heliostats (D=W)	☐	
Heliostat Area	144.375	m2
Mirror Reflectance and Soiling	0.9	
Heliostat Availability	0.99	
Image Error	0.002	rad
Heliostat Stow Deploy Angle	8	deg
Wind Stow Speed	15	m/s

Circular Field Optimization Wizard

Start Wizard...

The wizard will calculate an optimal distribution of heliostats and populate the zonal grid below. It calculates optimal tower and receiver heights, and receiver diameter. Since some cost and financial parameters help guide the optimization, be sure to set reasonable values before running the wizard. Refer to the documentation for more information.

Field Parameters

Total Reflective Area	1,027,804.2	m2
Number of Heliostats	7119	
Radial Step Size For Layout	121.877	m

Solar Field Layout Constraints

Max Heliostat Distance to Tower Height Ratio	7.5	Max. Distance From Tower	1625.02 m
Min Heliostat Distance to Tower Height Ratio	0.75	Min. Distance From Tower	162.503 m
Tower Height	216.67 m	Max Realized Distance From Tower	1259.39 m

Mirror Washing

Water Usage Per Wash	0.6	L/m2,aperture
Washing Frequency	4	days

Land Area

Non-Solar Field Land Area	180000	m2
Solar Field Land Area Multiplier	1.3	
Calculated Total Land Area	5.14383	km2

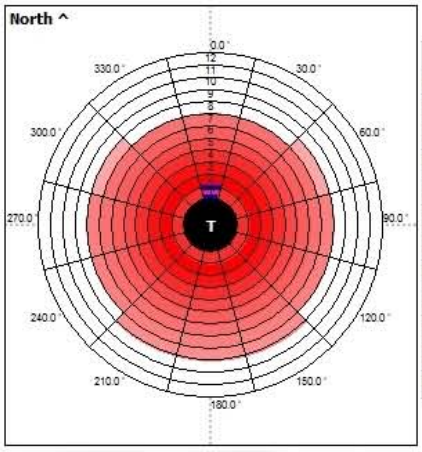

Radial Zones: 12 Azimuthal Zones: 12

	0.0	30.0	60.0	90.0	120.0	150.0	180.0	210.0	240.0	270.0	300.0	330.0
Rad. 1	21	21	21	21	21	21	21	21	21	21	21	21
Rad. 2	60	60	60	60	60	60	60	60	60	60	60	60
Rad. 3	75	75	75	75	75	75	75	75	75	75	75	75
Rad. 4	84	84	84	84	84	84	84	84	84	84	84	84
Rad. 5	88	88	88	88	88	88	88	88	88	88	88	88
Rad. 6	90	90	90	90	90	90	90	90	90	90	90	90
Rad. 7	90	90	90	90	90	90	90	90	90	90	90	90
Rad. 8	0	0	63	90	90	90	90	90	90	90	63	0
Rad. 9	0	0	0	0	0	89	89	89	0	0	0	0
Rad. 10	0	0	0	0	0	0	0	0	0	0	0	0
Rad. 11	0	0	0	0	0	0	0	0	0	0	0	0
Rad. 12	0	0	0	0	0	0	0	0	0	0	0	0

Import Export

Optimization Wizard (Upington Power Tower - 6 hrs TES - Wet)

Solar Field

Solar Multiple	2

Receiver and Tower

Min. Receiver Diameter	8 m
Max. Receiver Diameter	16 m
Optimization Levels for Receiver Diameter	10
Min. Receiver Height/Diameter Ratio	0.8
Max. Receiver Height/Diameter Ratio	1.6
Optimization Levels for Receiver H/D Ratio	10
Min. Tower Height	150 m
Max. Tower Height	250 m
Optimization Levels for Tower Height	10

Upington Dry-Cooled Heliostat Field Design

Heliostat Properties

Heliostat Width	12.2	m
Heliostat Height	12.2	m
Ratio of Reflective Area to Profile	0.97	
Use Round Heliostats (D=W)	☐	
Heliostat Area	144.375	m2
Mirror Reflectance and Soiling	0.9	
Heliostat Availability	0.99	
Image Error	0.002	rad
Heliostat Stow Deploy Angle	8	deg
Wind Stow Speed	15	m/s

Circular Field Optimization Wizard

Start Wizard...

The wizard will calculate an optimal distribution of heliostats and populate the zonal grid below. It calculates optimal tower and receiver heights, and receiver diameter. Since some cost and financial parameters help guide the optimization, be sure to set reasonable values before running the wizard. Refer to the documentation for more information.

Field Parameters

Total Reflective Area	1,010,190.5	m2
Number of Heliostats	6997	
Radial Step Size For Layout	121.877	m

Solar Field Layout Constraints

Max Heliostat Distance to Tower Height Ratio	7.5		Max. Distance From Tower	1625.02 m
Min Heliostat Distance to Tower Height Ratio	0.75		Min. Distance From Tower	162.503 m
Tower Height	216.67	m	Max Realized Distance From Tower	1259.39 m

Mirror Washing

Water Usage Per Wash	0.6	L/m2,aperture
Washing Frequency	4	days

Land Area

Non-Solar Field Land Area	180000	m2
Solar Field Land Area Multiplier	1.3	
Calculated Total Land Area	5.14383	km2

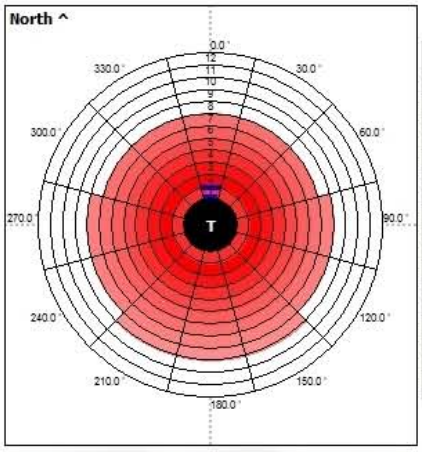

Radial Zones: 12 Azimuthal Zones: 12

	0.0	30.0	60.0	90.0	120.0	150.0	180.0	210.0	240.0	270.0	300.0	330.0
Rad. 1	21	21	21	21	21	21	21	21	21	21	21	21
Rad. 2	60	60	60	60	60	60	60	60	60	60	60	60
Rad. 3	75	75	75	75	75	75	75	75	75	75	75	75
Rad. 4	84	84	84	84	84	84	84	84	84	84	84	84
Rad. 5	88	88	88	88	88	88	88	88	88	88	88	88
Rad. 6	90	90	90	90	90	90	90	90	90	90	90	90
Rad. 7	90	90	90	90	90	90	90	90	90	90	90	90
Rad. 8	0	0	2	90	90	90	90	90	90	90	2	0
Rad. 9	0	0	0	0	0	89	89	89	0	0	0	0
Rad. 10	0	0	0	0	0	0	0	0	0	0	0	0
Rad. 11	0	0	0	0	0	0	0	0	0	0	0	0
Rad. 12	0	0	0	0	0	0	0	0	0	0	0	0

Import Export

Optimization Wizard (Upington Power Tower - 6 hrs TES - Dry)

Solar Field

Solar Multiple	1.9

Receiver and Tower

Min. Receiver Diameter	8 m
Max. Receiver Diameter	16 m
Optimization Levels for Receiver Diameter	10
Min. Receiver Height/Diameter Ratio	0.8
Max. Receiver Height/Diameter Ratio	1.6
Optimization Levels for Receiver H/D Ratio	10
Min. Tower Height	150 m
Max. Tower Height	250 m
Optimization Levels for Tower Height	10

Springbok Wet-Cooled Heliostat Field Design

Heliostat Properties

Heliostat Width	12.2	m
Heliostat Height	12.2	m
Ratio of Reflective Area to Profile	0.97	
Use Round Heliostats (D=W)	☐	
Heliostat Area	144.375	m2
Mirror Reflectance and Soiling	0.9	
Heliostat Availability	0.99	
Image Error	0.002	rad
Heliostat Stow Deploy Angle	8	deg
Wind Stow Speed	15	m/s

Circular Field Optimization Wizard

Start Wizard...

The wizard will calculate an optimal distribution of heliostats and populate the zonal grid below. It calculates optimal tower and receiver heights, and receiver diameter. Since some cost and financial parameters help guide the optimization, be sure to set reasonable values before running the wizard. Refer to the documentation for more information.

Field Parameters

Total Reflective Area	1,028,670.4	m2
Number of Heliostats	7125	
Radial Step Size For Layout	121.877	m

Solar Field Layout Constraints

Max Heliostat Distance to Tower Height Ratio	7.5		Max. Distance From Tower	1625.02 m
Min Heliostat Distance to Tower Height Ratio	0.75		Min. Distance From Tower	162.503 m
Tower Height	216.67	m	Max Realized Distance From Tower	1259.39 m

Mirror Washing

Water Usage Per Wash	0.6	L/m2,aperture
Washing Frequency	4	days

Land Area

Non-Solar Field Land Area	180000	m2
Solar Field Land Area Multiplier	1.3	
Calculated Total Land Area	5.16405	km2

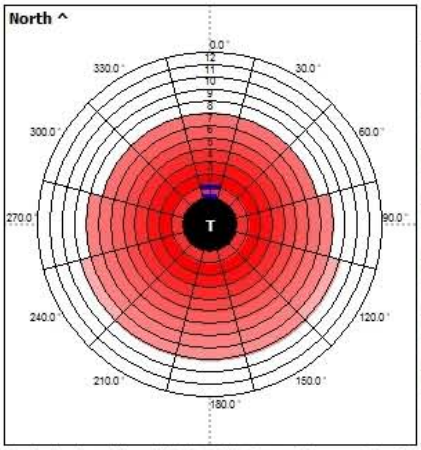

Radial Zones: 12 Azimuthal Zones: 12

	0.0	30.0	60.0	90.0	120.0	150.0	180.0	210.0	240.0	270.0	300.0	330.0
Rad. 1	21	21	21	21	21	21	21	21	21	21	21	21
Rad. 2	60	60	60	60	60	60	60	60	60	60	60	60
Rad. 3	75	75	75	75	75	75	75	75	75	75	75	75
Rad. 4	84	84	84	84	84	84	84	84	84	84	84	84
Rad. 5	88	88	88	88	88	88	88	88	88	88	88	88
Rad. 6	90	90	90	90	90	90	90	90	90	90	90	90
Rad. 7	90	90	90	90	90	90	90	90	90	90	90	90
Rad. 8	0	0	0	90	90	90	90	90	90	90	0	0
Rad. 9	0	0	0	0	66	89	89	89	66	0	0	0
Rad. 10	0	0	0	0	0	0	0	0	0	0	0	0
Rad. 11	0	0	0	0	0	0	0	0	0	0	0	0
Rad. 12	0	0	0	0	0	0	0	0	0	0	0	0

Import Export

Optimization Wizard (Springbok Power Tower - 6 hrs TES - Wet)

Solar Field

Solar Multiple	2

Receiver and Tower

Min. Receiver Diameter	8 m
Max. Receiver Diameter	16 m
Optimization Levels for Receiver Diameter	10
Min. Receiver Height/Diameter Ratio	0.8
Max. Receiver Height/Diameter Ratio	1.6
Optimization Levels for Receiver H/D Ratio	10
Min. Tower Height	150 m
Max. Tower Height	250 m
Optimization Levels for Tower Height	10

Springbok Dry-Cooled Heliostat Field Design

Heliostat Properties

Heliostat Width	12.2	m
Heliostat Height	12.2	m
Ratio of Reflective Area to Profile	0.97	
Use Round Heliostats (D=W)	☐	
Heliostat Area	144.375	m2
Mirror Reflectance and Soiling	0.9	
Heliostat Availability	0.99	
Image Error	0.002	rad
Heliostat Stow Deploy Angle	8	deg
Wind Stow Speed	15	m/s

Circular Field Optimization Wizard

Start Wizard...

The wizard will calculate an optimal distribution of heliostats and populate the zonal grid below. It calculates optimal tower and receiver heights, and receiver diameter. Since some cost and financial parameters help guide the optimization, be sure to set reasonable values before running the wizard. Refer to the documentation for more information.

Field Parameters

Total Reflective Area	1,012,211.7	m2
Number of Heliostats	7011	
Radial Step Size For Layout	121.877	m

Solar Field Layout Constraints

Max Heliostat Distance to Tower Height Ratio	7.5		Max. Distance From Tower	1625.02 m
Min Heliostat Distance to Tower Height Ratio	0.75		Min. Distance From Tower	162.503 m
Tower Height	216.67	m	Max Realized Distance From Tower	1259.39 m

Mirror Washing

Water Usage Per Wash	0.6	L/m2,aperture
Washing Frequency	4	days

Land Area

Non-Solar Field Land Area	180000	m2
Solar Field Land Area Multiplier	1.3	
Calculated Total Land Area	5.16405	km2

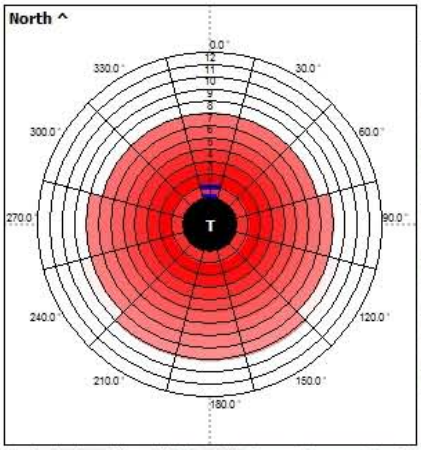

Radial Zones: 12 Azimuthal Zones: 12

	0.0	30.0	60.0	90.0	120.0	150.0	180.0	210.0	240.0	270.0	300.0	330.0
Rad. 1	21	21	21	21	21	21	21	21	21	21	21	21
Rad. 2	60	60	60	60	60	60	60	60	60	60	60	60
Rad. 3	75	75	75	75	75	75	75	75	75	75	75	75
Rad. 4	84	84	84	84	84	84	84	84	84	84	84	84
Rad. 5	88	88	88	88	88	88	88	88	88	88	88	88
Rad. 6	90	90	90	90	90	90	90	90	90	90	90	90
Rad. 7	90	90	90	90	90	90	90	90	90	90	90	90
Rad. 8	0	0	0	90	90	90	90	90	90	90	0	0
Rad. 9	0	0	0	0	9	89	89	89	9	0	0	0
Rad. 10	0	0	0	0	0	0	0	0	0	0	0	0
Rad. 11	0	0	0	0	0	0	0	0	0	0	0	0
Rad. 12	0	0	0	0	0	0	0	0	0	0	0	0

Import Export

Optimization Wizard (Springbok Power Tower - 6 hrs TES - Dry)

Solar Field

Solar Multiple	1.9

Receiver and Tower

Min. Receiver Diameter	8 m
Max. Receiver Diameter	16 m
Optimization Levels for Receiver Diameter	10
Min. Receiver Height/Diameter Ratio	0.8
Max. Receiver Height/Diameter Ratio	1.6
Optimization Levels for Receiver H/D Ratio	10
Min. Tower Height	150 m
Max. Tower Height	250 m
Optimization Levels for Tower Height	10

Bloemfontein Wet-Cooled Heliostat Field Design

Heliostat Properties

Heliostat Width	12.2	m
Heliostat Height	12.2	m
Ratio of Reflective Area to Profile	0.97	
Use Round Heliostats (D=W)	☐	
Heliostat Area	144.375	m2
Mirror Reflectance and Soiling	0.9	
Heliostat Availability	0.99	
Image Error	0.002	rad
Heliostat Stow Deploy Angle	8	deg
Wind Stow Speed	15	m/s

Circular Field Optimization Wizard

Start Wizard...

The wizard will calculate an optimal distribution of heliostats and populate the zonal grid below. It calculates optimal tower and receiver heights, and receiver diameter. Since some cost and financial parameters help guide the optimization, be sure to set reasonable values before running the wizard. Refer to the documentation for more information.

Field Parameters

Total Reflective Area	1,029,247.9	m2
Number of Heliostats	7129	
Radial Step Size For Layout	121.877	m

Solar Field Layout Constraints

Max Heliostat Distance to Tower Height Ratio	7.5		Max. Distance From Tower	1625.02 m
Min Heliostat Distance to Tower Height Ratio	0.75		Min. Distance From Tower	162.503 m
Tower Height	216.67	m	Max Realized Distance From Tower	1259.39 m

Mirror Washing

Water Usage Per Wash	0.6	L/m2,aperture
Washing Frequency	4	days

Land Area

Non-Solar Field Land Area	180000	m2
Solar Field Land Area Multiplier	1.3	
Calculated Total Land Area	5.14383	km2

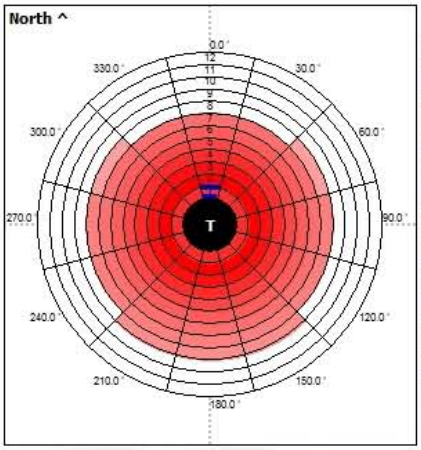

Radial Zones: 12 Azimuthal Zones: 12

	0.0	30.0	60.0	90.0	120.0	150.0	180.0	210.0	240.0	270.0	300.0	330.0
Rad. 1	21	21	21	21	21	21	21	21	21	21	21	21
Rad. 2	60	60	60	60	60	60	60	60	60	60	60	60
Rad. 3	75	75	75	75	75	75	75	75	75	75	75	75
Rad. 4	84	84	84	84	84	84	84	84	84	84	84	84
Rad. 5	88	88	88	88	88	88	88	88	88	88	88	88
Rad. 6	90	90	90	90	90	90	90	90	90	90	90	90
Rad. 7	90	90	90	90	90	90	90	90	90	90	90	90
Rad. 8	0	0	68	90	90	90	90	90	90	90	68	0
Rad. 9	0	0	0	0	0	89	89	89	0	0	0	0
Rad. 10	0	0	0	0	0	0	0	0	0	0	0	0
Rad. 11	0	0	0	0	0	0	0	0	0	0	0	0
Rad. 12	0	0	0	0	0	0	0	0	0	0	0	0

Import Export

Optimization Wizard (Bloem Power Tower - 6 hrs TES - Wet)

Solar Field

Solar Multiple	2

Receiver and Tower

Min. Receiver Diameter	8 m
Max. Receiver Diameter	16 m
Optimization Levels for Receiver Diameter	10
Min. Receiver Height/Diameter Ratio	0.8
Max. Receiver Height/Diameter Ratio	1.6
Optimization Levels for Receiver H/D Ratio	10
Min. Tower Height	150 m
Max. Tower Height	250 m
Optimization Levels for Tower Height	10

Bloemfontein Dry-Cooled Heliostat Field Design

Heliostat Properties

Heliostat Width	12.2	m
Heliostat Height	12.2	m
Ratio of Reflective Area to Profile	0.97	
Use Round Heliostats (D=W)	☐	
Heliostat Area	144.375	m2
Mirror Reflectance and Soiling	0.9	
Heliostat Availability	0.99	
Image Error	0.002	rad
Heliostat Stow Deploy Angle	8	deg
Wind Stow Speed	15	m/s

Circular Field Optimization Wizard

Start Wizard...

The wizard will calculate an optimal distribution of heliostats and populate the zonal grid below. It calculates optimal tower and receiver heights, and receiver diameter. Since some cost and financial parameters help guide the optimization, be sure to set reasonable values before running the wizard. Refer to the documentation for more information.

Field Parameters

Total Reflective Area	1,011,345.5	m2
Number of Heliostats	7005	
Radial Step Size For Layout	121.877	m

Solar Field Layout Constraints

Max Heliostat Distance to Tower Height Ratio	7.5		Max. Distance From Tower	1625.02 m
Min Heliostat Distance to Tower Height Ratio	0.75		Min. Distance From Tower	162.503 m
Tower Height	216.67	m	Max Realized Distance From Tower	1259.39 m

Mirror Washing

Water Usage Per Wash	0.6	L/m2,aperture
Washing Frequency	4	days

Land Area

Non-Solar Field Land Area	180000	m2
Solar Field Land Area Multiplier	1.3	
Calculated Total Land Area	5.14383	km2

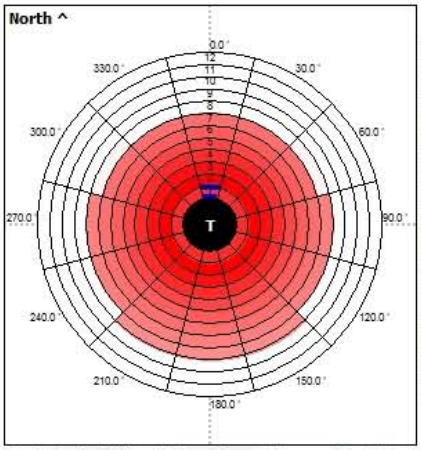

Radial Zones: 12 Azimuthal Zones: 12

	0.0	30.0	60.0	90.0	120.0	150.0	180.0	210.0	240.0	270.0	300.0	330.0
Rad. 1	21	21	21	21	21	21	21	21	21	21	21	21
Rad. 2	60	60	60	60	60	60	60	60	60	60	60	60
Rad. 3	75	75	75	75	75	75	75	75	75	75	75	75
Rad. 4	84	84	84	84	84	84	84	84	84	84	84	84
Rad. 5	88	88	88	88	88	88	88	88	88	88	88	88
Rad. 6	90	90	90	90	90	90	90	90	90	90	90	90
Rad. 7	90	90	90	90	90	90	90	90	90	90	90	90
Rad. 8	0	0	6	90	90	90	90	90	90	90	6	0
Rad. 9	0	0	0	0	0	89	89	89	0	0	0	0
Rad. 10	0	0	0	0	0	0	0	0	0	0	0	0
Rad. 11	0	0	0	0	0	0	0	0	0	0	0	0
Rad. 12	0	0	0	0	0	0	0	0	0	0	0	0

Import Export

Optimization Wizard (Bloem Power Tower - 6 hrs TES - Dry)

Solar Field

Solar Multiple	1.9

Receiver and Tower

Min. Receiver Diameter	8 m
Max. Receiver Diameter	16 m
Optimization Levels for Receiver Diameter	10
Min. Receiver Height/Diameter Ratio	0.8
Max. Receiver Height/Diameter Ratio	1.6
Optimization Levels for Receiver H/D Ratio	10
Min. Tower Height	150 m
Max. Tower Height	250 m
Optimization Levels for Tower Height	10

Wet-Cooled Power Cycle

Plant Capacity

Design Turbine Gross Output	110	MWe
Estimated Gross to Net Conversion Factor	0.9091	
Estimated Net Output at Design (Nameplate)	100.001	MWe

Note: Parasitic losses typically reduce net output to approximately 90 % of design gross power

Power Block Design Point

Rated Cycle Conversion Efficiency	0.425	
Design Thermal Power	258.824	MWt
Design HTF Inlet Temp.	574	'C
Design HTF Outlet Temp.	290	'C
Boiler Steam Pressure	100	Bar
Boiler LHV Efficiency	0.9	
Steam cycle blowdown fraction	0.013	

Plant Control

Min. Temp. To Load	500	'C
Low-resource Standby Period	2	hours
Standby Mode Thermal Fraction	0.2	
Turbine Startup Time	0.5	hours
Turbine Startup Energy Fraction	0.75	
Minimum Load Fraction	0.25	
Max. Over Design Operation	1.15	

Cooling System

Condenser Type	Evaporative	
Design Ambient Temperature	20	'C
Ref. Condenser Water dT	10	'C
Approach Temperature	5	'C
ITD at Design Point	16	'C
Condenser Pressure Ratio	1.0028	

Dry-Cooled Power Cycle

Plant Capacity

Design Turbine Gross Output	110	MWe
Estimated Gross to Net Conversion Factor	0.9091	
Estimated Net Output at Design (Nameplate)	100.001	MWe

Note: Parasitic losses typically reduce net output to approximately 90 % of design gross power

Power Block Design Point

Rated Cycle Conversion Efficiency	0.408	
Design Thermal Power	269.608	MWt
Design HTF Inlet Temp.	574	'C
Design HTF Outlet Temp.	290	'C
Boiler Steam Pressure	100	Bar
Boiler LHV Efficiency	0.9	
Steam cycle blowdown fraction	0.016	

Plant Control

Min. Temp. To Load	500	'C
Low-resource Standby Period	2	hours
Standby Mode Thermal Fraction	0.2	
Turbine Startup Time	0.5	hours
Turbine Startup Energy Fraction	0.75	
Minimum Load Fraction	0.25	
Max. Over Design Operation	1.15	

Cooling System

Condenser Type	Air-cooled	
Design Ambient Temperature	33	'C
Ref. Condenser Water dT	10	'C
Approach Temperature	5	'C
ITD at Design Point	16	'C
Condenser Pressure Ratio	1.0028	

Wet-Cooled Thermal Storage and Parasitics

Storage System

Storage Type	Two Tank		Initial Hot HTF Temp.	574	'C
Full Load Thermal Storage Hours	6	hours	Initial Cold HTF Temp.	290	'C
Storage HTF Volume	7224.78	m3	Initial Hot HTF Percent	30	%
Tank Diameter	21.4463	m	Initial Hot HTF Volume	2167.43	m3
Tank Height	20	m	Initial Cold HTF Volume	5057.35	m3
Min. Tank Fluid Height	1	m	Cold Tank Heater Temp. Set-Point	280	'C
Parallel Tank Pairs	1		Cold Tank Heater Max. Load	30	MWe
Min. Fluid Volume	361.239	m3	Hot Tank Heater Temp. Set-Point	500	'C
Max. Fluid Volume	6863.54	m3	Hot Tank Heater Max. Load	30	MWe
Wetted Loss Coefficient	0.4	Wt/m2-K	Tank Heater Efficiency	0.99	
Dry Loss Coefficient	0.25	Wt/m2-K			

Thermal Storage Dispatch Control

Current dispatch schedule:

No library match.

Dispatch schedule library...

Note:

Schedule libraries do not affect the Storage Dispatch, Turbine Output and Fossil Fill fractions below.

	Storage Dispatch w/ solar*	Storage Dispatch w/o solar*	Turb. out. fraction*	Fossil fill fraction*
Period 1:	0.1	0.1	1.1	0
Period 2:	0.1	0.1	1	0
Period 3:	0.1	0.1	1	0
Period 4:	0.1	0.1	1	0
Period 5:	0.1	0.1	1	0
Period 6:	0.1	0.1	1	0

Notes:

1. Storage dispatch fractions apply to the maximum energy storage.

2. Turbine output and fossil fill fractions apply to the design turbine thermal input.

Weekday Schedule

	12am	1am	2am	3am	4am	5am	6am	7am	8am	9am	10am	11am	12pm	1pm	2pm	3pm	4pm	5pm	6pm	7pm	8pm	9pm	10pm	11pm
Jan	3	3	3	3	3	3	3	2	2	2	2	1	1	1	1	1	1	2	2	2	2	2	3	3
Feb	3	3	3	3	3	3	3	2	2	2	2	1	1	1	1	1	1	2	2	2	2	2	3	3
Mar	3	3	3	3	3	3	3	2	2	2	2	1	1	1	1	1	1	2	2	2	2	2	3	3
Apr	6	6	6	6	6	5	5	4	4	4	4	4	4	4	4	4	4	4	4	4	5	5	5	6
May	6	6	6	6	6	6	5	5	4	4	4	4	4	4	4	4	4	4	4	4	4	5	5	5
Jun	6	6	6	6	6	6	5	5	4	4	4	4	4	4	4	4	4	4	4	4	4	5	5	5
Jul	6	6	6	6	6	6	5	5	4	4	4	4	4	4	4	4	4	4	4	4	4	5	5	5
Aug	6	6	6	6	6	6	5	5	4	4	4	4	4	4	4	4	4	4	4	4	4	5	5	5
Sep	6	6	6	6	6	6	5	5	4	4	4	4	4	4	4	4	4	4	4	4	4	5	5	5
Oct	6	6	6	6	6	5	5	4	4	4	4	4	4	4	4	4	4	4	4	4	5	5	5	6
Nov	6	6	6	6	6	5	5	4	4	4	4	4	4	4	4	4	4	4	4	4	5	5	5	6
Dec	3	3	3	3	3	3	3	2	2	2	2	1	1	1	1	1	1	2	2	2	2	2	3	3

Weekend Schedule

	12am	1am	2am	3am	4am	5am	6am	7am	8am	9am	10am	11am	12pm	1pm	2pm	3pm	4pm	5pm	6pm	7pm	8pm	9pm	10pm	11pm
Jan	3	3	3	3	3	3	3	3	3	3	3	3	3	3	3	3	3	3	3	3	3	3	3	3
Feb	3	3	3	3	3	3	3	3	3	3	3	3	3	3	3	3	3	3	3	3	3	3	3	3
Mar	3	3	3	3	3	3	3	3	3	3	3	3	3	3	3	3	3	3	3	3	3	3	3	3
Apr	6	6	6	6	6	5	5	5	5	5	5	5	5	5	5	5	5	5	5	5	5	5	5	6
May	6	6	6	6	6	6	5	5	5	5	5	5	5	5	5	5	5	5	5	5	5	5	5	5
Jun	6	6	6	6	6	6	5	5	5	5	5	5	5	5	5	5	5	5	5	5	5	5	5	5
Jul	6	6	6	6	6	6	5	5	5	5	5	5	5	5	5	5	5	5	5	5	5	5	5	5
Aug	6	6	6	6	6	6	5	5	5	5	5	5	5	5	5	5	5	5	5	5	5	5	5	5
Sep	6	6	6	6	6	6	5	5	5	5	5	5	5	5	5	5	5	5	5	5	5	5	5	5
Oct	6	6	6	6	6	5	5	5	5	5	5	5	5	5	5	5	5	5	5	5	5	5	5	6
Nov	6	6	6	6	6	5	5	5	5	5	5	5	5	5	5	5	5	5	5	5	5	5	5	6
Dec	3	3	3	3	3	3	3	3	3	3	3	3	3	3	3	3	3	3	3	3	3	3	3	3

Parasitic Energy Consumption

Startup Energy of a Single Heliostat	0.025	kWe-hr
Tracking Power for a Single Heliostat	0.055	kWe
Receiver HTF Pump Efficiency	0.85	
Storage Pump Power	0.01	MWe/MWt
Balance of Plant Power	0.05	MWe/MWt
Piping Loss Coefficient	3500	Wt/m
Total Piping Length	1500	m

Dry-Cooled Thermal Storage and Parasitics

Storage System

Storage Type	Two Tank		Initial Hot HTF Temp.	574	'C
Full Load Thermal Storage Hours	6	hours	Initial Cold HTF Temp.	290	'C
Storage HTF Volume	7525.81	m3	Initial Hot HTF Percent	30	%
Tank Diameter	21.8885	m	Initial Hot HTF Volume	2257.74	m3
Tank Height	20	m	Initial Cold HTF Volume	5268.07	m3
Min. Tank Fluid Height	1	m	Cold Tank Heater Temp. Set-Point	280	'C
Parallel Tank Pairs	1		Cold Tank Heater Max. Load	30	MWe
Min. Fluid Volume	376.291	m3	Hot Tank Heater Temp. Set-Point	500	'C
Max. Fluid Volume	7149.52	m3	Hot Tank Heater Max. Load	30	MWe
Wetted Loss Coefficient	0.4	Wt/m2-K	Tank Heater Efficiency	0.99	
Dry Loss Coefficient	0.25	Wt/m2-K			

Thermal Storage Dispatch Control

Current dispatch schedule:

No library match.

Dispatch schedule library...

Note:

Schedule libraries do not affect the Storage Dispatch, Turbine Output and Fossil Fill fractions below.

	Storage Dispatch w/ solar*	Storage Dispatch w/o solar*	Turb. out. fraction*	Fossil fill fraction*
Period 1:	0.1	0.1	1.1	0
Period 2:	0.1	0.1	1	0
Period 3:	0.1	0.1	1	0
Period 4:	0.1	0.1	1	0
Period 5:	0.1	0.1	1	0
Period 6:	0.1	0.1	1	0

Notes:

1. Storage dispatch fractions apply to the maximum energy storage.

2. Turbine output and fossil fill fractions apply to the design turbine thermal input.

Weekday Schedule

	12am	1am	2am	3am	4am	5am	6am	7am	8am	9am	10am	11am	12pm	1pm	2pm	3pm	4pm	5pm	6pm	7pm	8pm	9pm	10pm	11pm
Jan	3	3	3	3	3	3	3	2	2	2	2	1	1	1	1	1	1	2	2	2	2	2	3	3
Feb	3	3	3	3	3	3	3	2	2	2	2	1	1	1	1	1	1	2	2	2	2	2	3	3
Mar	3	3	3	3	3	3	3	2	2	2	2	1	1	1	1	1	1	2	2	2	2	2	3	3
Apr	6	6	6	6	6	5	5	4	4	4	4	4	4	4	4	4	4	4	4	4	5	5	5	6
May	6	6	6	6	6	6	5	5	4	4	4	4	4	4	4	4	4	4	4	4	4	5	5	5
Jun	6	6	6	6	6	6	5	5	4	4	4	4	4	4	4	4	4	4	4	4	4	5	5	5
Jul	6	6	6	6	6	6	5	5	4	4	4	4	4	4	4	4	4	4	4	4	4	5	5	5
Aug	6	6	6	6	6	6	5	5	4	4	4	4	4	4	4	4	4	4	4	4	4	5	5	5
Sep	6	6	6	6	6	6	5	5	4	4	4	4	4	4	4	4	4	4	4	4	4	5	5	5
Oct	6	6	6	6	6	5	5	4	4	4	4	4	4	4	4	4	4	4	4	4	5	5	5	6
Nov	6	6	6	6	6	5	5	4	4	4	4	4	4	4	4	4	4	4	4	4	5	5	5	6
Dec	3	3	3	3	3	3	3	2	2	2	2	1	1	1	1	1	1	2	2	2	2	2	3	3

Weekend Schedule

	12am	1am	2am	3am	4am	5am	6am	7am	8am	9am	10am	11am	12pm	1pm	2pm	3pm	4pm	5pm	6pm	7pm	8pm	9pm	10pm	11pm
Jan	3	3	3	3	3	3	3	3	3	3	3	3	3	3	3	3	3	3	3	3	3	3	3	3
Feb	3	3	3	3	3	3	3	3	3	3	3	3	3	3	3	3	3	3	3	3	3	3	3	3
Mar	3	3	3	3	3	3	3	3	3	3	3	3	3	3	3	3	3	3	3	3	3	3	3	3
Apr	6	6	6	6	6	5	5	5	5	5	5	5	5	5	5	5	5	5	5	5	5	5	5	6
May	6	6	6	6	6	6	5	5	5	5	5	5	5	5	5	5	5	5	5	5	5	5	5	5
Jun	6	6	6	6	6	6	5	5	5	5	5	5	5	5	5	5	5	5	5	5	5	5	5	5
Jul	6	6	6	6	6	6	5	5	5	5	5	5	5	5	5	5	5	5	5	5	5	5	5	5
Aug	6	6	6	6	6	6	5	5	5	5	5	5	5	5	5	5	5	5	5	5	5	5	5	5
Sep	6	6	6	6	6	6	5	5	5	5	5	5	5	5	5	5	5	5	5	5	5	5	5	5
Oct	6	6	6	6	6	5	5	5	5	5	5	5	5	5	5	5	5	5	5	5	5	5	5	6
Nov	6	6	6	6	6	5	5	5	5	5	5	5	5	5	5	5	5	5	5	5	5	5	5	6
Dec	3	3	3	3	3	3	3	3	3	3	3	3	3	3	3	3	3	3	3	3	3	3	3	3

Parasitic Energy Consumption

Startup Energy of a Single Heliostat	0.025	kWe-hr
Tracking Power for a Single Heliostat	0.055	kWe
Receiver HTF Pump Efficiency	0.85	
Storage Pump Power	0.01	MWe/MWt
Balance of Plant Power	0.05	MWe/MWt
Piping Loss Coefficient	3500	Wt/m
Total Piping Length	1500	m

UNIVERSITY OF CAPE TOWN

DEPARTMENT OF MECHANICAL ENGINEERING

RONDEBOSCH, CAPE TOWN, SOUTH AFRICA

SITE LOCATION AND TECHNO-ECONOMIC ANALYSIS OF UTILITY-SCALE CONCENTRATING SOLAR POWER PLANTS IN SOUTH AFRICA

A dissertation submitted in partial fulfilment of the requirements for the degree of Master of Philosophy in Sustainable Energy Engineering

Author:

Joshua J.L. Brodrick

17th November 2011

Abstract

This dissertation comprises a two-part study concerned with the identification and quantification of potential Concentrating Solar Power (CSP) sites in South Africa; and the performance and cost modelling, optimisation and analysis of two CSP technologies in three locations. A further theme of the study is the consideration of the availability of water for plant cooling purposes, and hence the comparison between, and analysis of optimal CSP technologies and cooling methods for each location.

A Geographic Information System (GIS) based analysis was created and presented in order to identify potential CSP sites, with an emphasis placed on levels of incoming direct normal solar irradiation, as well as proximity to the national electricity grid, and large water sources for cooling purposes. Additional analysis criteria include a suitably flat land slope, and the exclusion of areas deemed unsuitable for construction, or not classed as possessing 'least threatened' vegetation. Five separate analysis cases were considered resulting in a total identified potential land area of between 2,180.5 km^2 and 18,785.6 km^2, total available solar energy levels of between 16.5 TWh/day and 144.3 TWh/day, a power generation potential of between 77.9 GW and 670.9 GW at a land use value of 28 km^2 per GW, and a net energy generation potential of between 264.7 and 3,526.3 TWh/annum, depending on the analysis cases and CSP technologies considered.

A number of computer-based performance and cost models were then created within the Solar Advisor Model (SAM) software for both parabolic trough and central receiver technologies, incorporating both wet and dry cooling at three locations. Of the two CSP technologies considered, central receiver technology was found to be preferable, while wet-cooling was found to be more economical than dry cooling. Dry cooling, however was shown to reduce water consumption by more than 90%. The resulting LCOE from the SAM models was found to be most sensitive to the financing assumptions of the project, rather than the project capital costs, while the cost of cooling water was found to have the least effect on the resulting plant LCOE. Based on these results, in conjunction with the classification of South Africa as a water stressed country, it was thus deduced that the availability of raw cooling water, rather than its current cost, would likely be the limiting factor in the use of wet cooling technology. According to the comparisons between the final model results, it was found that it may be more beneficial to construct a central receiver CSP plant in a region with high DNI levels but limited access to cooling water, as opposed to an area with lower DNI levels but access to large volumes of water.

Declaration

I know the meaning of plagiarism, and declare that all the work in the document, save for that which is properly acknowledged, is my own.

Joshua J.L. Brodrick
17th November 2011
University of Cape Town

Acknowledgements

First and foremost I would like to acknowledge and thank my supervisor, Professor Kevin Bennett, whose leadership was invaluable. His guidance made this research possible and it was a privilege to have worked with him.

My sincerest thanks also go to Nicholas Lindenberg and Thomas Slingsby, both of whom have been an unfathomable source of knowledge, and assistance. Their never ending attitude to help – complimented by their skill with GIS software – allowed for the realization of this project, that otherwise may not have been attempted.

I would also like to acknowledge and thank Paul Gilman, previously from NREL, whose advise and experience regarding the SAM software was invaluable. In particular, his advice relating to the adaptation of SAM to local conditions proved extremely beneficial, and his help was highly valued.

My acknowledgements and thanks also go to South Africa's National Energy Research Institute (SANERI) and the University of Cape Town, for funds allocated towards the fulfilment of my degree. Their financial support allowed for the realisation of this research, and is greatly appreciated.

To Oisin 'Ush' Tummon, whose most cherished friendship, competitive spirit, and constant support have made my engineering years some of the best of my life, thank you for all the encouragement and inspiration.

To my parents, who have given me never ending support, and sacrificed to give me the best education possible. I would not have accomplished what I have today without you. Thank you.

And finally to Or, whose undying support and constant encouragement kept inspiring me through it all.

Table of Contents

List of Tables

List of Figures

Nomenclature

Acronyms and Abbreviations

CLFR	Compact Linear Fresnel Reflector
CPV	Concentrating Photovoltaic
CSIR	Council for Scientific and Industrial Research
CSP	Concentrating Solar Power
DEAT	Department of Environmental Affairs and Tourism
DEM	Digital Elevation Model
DME	Department of Minerals and Energy
DNI	Direct Normal Irradiation
DOE	Department of Energy
DSCR	Debt Service Coverage Ratio
DWA	Department of Water Affairs (formerly the DWAF)
DWAF	Department of Water Affairs and Forestry (now the DWA)
EIA	Environmental Impact Assessment
EPRI	Electric Power Research Institute
EPW	EnergyPlus Weather Data
GHG	Greenhouse Gas
GHI	Global Horizontal Irradiation
HCE	Heat Collection Element
HTF	Heat Transfer Fluid

HVAC	Heating, Ventilation, and Air Conditioning
IEA	International Energy Agency
IPCC	Intergovernmental Panel on Climate Change
IPP	Independent Power Producer
IRR	Internal Rate of Return
LCOE	Levelised Cost of Energy
LTMS	Long Term Mitigation Scenarios
NASA	National Aeronautics and Space Administration
NERSA	National Energy Regulator of South Africa
NREL	National Renewable Energy Laboratory
O&M	Operation and Maintenance
PCM	Phase Change Material
PPA	Power Purchase Agreement
PV	Photovoltaic
REFIT	Renewable Energy Feed-In Tariff
SAM	Solar Advisor Model
SARS	South African Revenue Service
SCAs	Solar Collector Assemblies
SEGS	Solar Energy Generating Systems
SETP	Solar Energy Technologies Program
SRTM	Shuttle Radar Topography Mission
SWERA	Solar and Wind Energy Resource Assessment
TES	Thermal Energy Storage
TMY	Typical Meteorological Year
USGS	United States Geographic Service

UTM	Universal Transverse Mercator
WMAs	Water Management Areas

Units of Measure

$/kl	U.S. Dollars per Kilolitre
$/MWh	U.S. Dollars per Megawatt Hour
¢/kWh	U.S. cents per Kilowatt Hour
GW	Gigawatt
GWh/d	Gigawatt Hours per Day
kl	Kilolitre
kW	Kilowatt
kW_e	Kilowatt Electric
kW.yr	Kilowatt Year
kWh_{th}	Kilowatt Hour Thermal
kWh/m^2	Kilowatt Hours per Square Meter
$kWh/m^2/d$	Kilowatt Hours per Square Meter per Day
MW	Megawatt
MW_e	Megawatt Electric
MW_{th}	Megawatt Thermal
MWh	Megawatt Hour
R	South African Rand
R/kl	South African Rand per Kilolitre
R/MWh	South African Rand per Megawatt Hour
TWh/a	Terrawatt Hours per Annum
TWh/d	Terrawatt Hours per Day
Wh/m^2	Watt Hour per Square Meter

1 Introduction

1.1 Subject and Reason for Investigation

Climate change, unsustainable development, and the depletion of finite fossil resources are some of the prominent issues facing the world in the 21st century. With the increase in extreme weather phenomena, alterations in global climate patterns, and the rise in average global temperatures, the effect that human kind is having on the biosphere is becoming more evident. The Intergovernmental Panel on Climate Change (IPCC), cited by Pegels (2009), confirms this fact, and points to human activity as one of the major causes of global warming, as a direct result of greenhouse gas (GHG) emissions.

In addition, the diminishing supply of crude oil, as well as other fossil fuels, poses a threat to the energy security of all countries worldwide. According to the DME (2003), the South African economy in particular is strained by the import of dollar based fuels, whose burden could be greatly diminished by reducing the need to import them. Furthermore, should global measures such as carbon taxing be introduced that limit the use of fossil fuels, the South African economy would be negatively impacted, as it currently generates revenue from the processing and export of coal.

The increasing global realisation of the need to reduce GHG emissions and progress towards sustainable power production has resulted in renewable energy sources receiving a great deal of attention, and becoming an increasingly important factor in the world energy balance (European Commission, 2004). According to the International Energy Agency (IEA, 2008), solar energy is the most abundant of all renewable energy sources, leading to solar power being considered as a primary contender for renewable power generation. In regions with high levels of direct solar radiation, Concentrating Solar Power (CSP) systems in particular are considered to have the potential to replace conventional fossil fuel technologies (European Commission, 2004; IEA, 2008).

In South Africa, however, even though there are vast renewable resources present – in particular some of the best solar resources in the world – investment in renewable energy technology has been relatively low and these resources have remained largely untapped (DME, 2003). Although financial incentives, such as the Renewable Energy Feed-In Tariff (REFIT), have been proposed by the National Energy Regulator of South Africa (NERSA, 2009), they have yet to realise the development of a large renewable energy sector, and as a result renewable energy targets defined in policy papers still have to be met (Pegels, 2009).

South Africa is also classified as a water-stressed country, with an average annual rainfall less than 60% of the world average (Mukheibir, 2007). The effects of climate change, coupled with a growing population and future development, are expected to add additional pressure to the limited availability of future water resources. As thermal power stations can use in the region of 1.89 - 2.84 litres of water per kilowatt hour (500 - 750 gallons/MWh) of energy produced when employing conventional wet cooling technology (DOE, U.S., 2010), it is thus imperative to consider all future energy generation technologies in the context of their water consumption. Alternative cooling technologies such as dry cooling – which is already adopted in some of the country's newer coal-fired plants – should also be considered as an alternative to more conventional wet cooling methods.

In light of these facts, the subject of this dissertation comprises a multi-part study concerned with the determination of locations for potential CSP plants in South Africa, and subsequently, the conduction of a computer-based performance and cost simulation of parabolic trough and central receiver CSP technologies at a number of locations representing the identified potential sites. Particular attention is paid to the availability of water for plant cooling purposes, and hence the use of both wet cooling and dry cooling technologies is considered. For each location, an attempt is made to identify the optimal CSP technology type, as well as to ascertain whether it would be preferable to adopt wet or dry cooling.

It is hoped that through the conduction of this research, a better understanding of the local technical and economic aspects and key variables associated with the implementation of CSP systems in South Africa will be gained. It is also hoped that by studying multiple CSP technologies at different locations, the relative metrics arising from their comparisons will prove more valuable than if only an absolute value prediction of a single technology or location was made. As stated by the European Commission (2004), a better understanding of the key issues will be beneficial for financiers, researchers and developers, if a successful CSP sector is to be realised globally, as well as here in South Africa.

1.2 Background to Investigation

In the past, the energy sector in both the developed and developing world has been the primary source of GHG emissions, as a direct result of a heavy reliance on fossil fuels as a source for energy production. South Africa in particular relies heavily on fossil fuels for its energy supply, with fossil fuels accounting for 90% of primary energy, and coal representing 75% of the fossil-based supply (DME, 2003). According to the DME, the abundant naturally occurring coal resources have resulted in extensive capital investments in a large-scale, coal-based energy supply system. This in turn saw low electricity prices and relatively little new capacity development taking place in the last decade (Pegels, 2009). However, according to Edkins, cited by Morse (2009), the lack of new capacity investment resulted in South Africa facing an electricity supply crisis and diminishing reserve margin towards the end of 2007. Morse (2009) continues to state that the national electricity supplier, Eskom, proposed two mitigation scenarios to increase capacity while reducing the effects of climate change, both of which include increasing the share of renewables. The first scenario envisages 8.5 GW of solar energy by 2050, while the second sees 30 GW of solar installed.

One of the key reason for the inclusion of solar power is that the majority of South Africa receives more than 2500 hours of sunshine per annum, with an average solar-radiation level ranging between 4.5 and 6.5 kWh/m^2 in one day. This is one of the highest local solar resources in the world, and according to the DME (2003), makes South Africa a prime candidate for solar power generation. In particular, the extremely high levels of annual direct solar irradiation makes the country a prime candidate for CSP systems. Certain CSP technologies are also considered to be relatively mature, with the first commercial parabolic trough plants being commissioned in 1984 as a result of the 1970s oil price shock (Wagner, 2008). Furthermore, as CSP systems typically make use of thermal energy as an intermediate energy phase, they possess the added benefit of being able to store thermal energy for later use, thereby reducing their variability and rendering them more applicable for base-load power generation. In areas with high levels of direct solar radiation, CSP plants prove to be far cheaper then photovoltaic (PV) solar systems, however, they are currently still not yet competitive with fossil fuels or wind power (IEA, 2008). The long-term viability of renewable energy technologies such as CSP therefore depends on the availability of financial subsidies, carbon emission disincentives, and their reliability when competing with more conventional fossil-based power generation systems (Morse, 2009).

Although no major utility-scale CSP plants are currently under construction in South Africa, initial research has been conducted to determine and quantify the potential for CSP plants in South Africa. A geographic information systems (GIS) study conducted by Fluri (2009) identified potential CSP locations throughout the country, however, no consideration was made for plant proximity to sources of cooling water. According to the Renewable Energy Policy Network (REN21, 2008), it is certain that renewable energy technologies will need to be implemented, and that they offer a viable solution to satisfying the growing energy demand, while simultaneously reducing GHG emissions and mitigating climate change. Before the successful and commercially-competitive implementation of these technologies is realised in South Africa, however, favourable policy and financial backing will also be required, and hence additional research will be beneficial in providing a deeper insight into the available technologies and their relationship with the economic environment.

1.3 Objectives

Thus, in light of the identification of South Africa's vast solar resource potential yet water stressed nature, coupled with the fact that Eskom has proposed renewable energy targets which have yet to be fully realised, and the fact that no utility-scale commercial CSP plants have yet been commissioned in South Africa, the objectives of this dissertation, considered in the context of current conditions and boundaries, and with the aim to aid the commencement of CSP in South Africa, are as follows:

1. To develop a methodology for the identification and quantification of potential CSP sites in South Africa, and subsequently, present an approach for creating South African specific, high-level techno-economic models of current commercial CSP technologies at select identified locations.

2. A further aim is to use this approach to attempt to ascertain which of the current commercial CSP technologies modelled would be considered optimal for a considered location, and to determine whether the use of wet cooling or dry cooling technology would be more beneficial.

3. Finally, as at the time of writing, no utility-scale commercial CSP plants have yet been realised in South Africa, a further objective of this study is to derive useful insight into and understanding of the techno-economic criteria and their effect on CSP developments, through the comparison of different model results and hence the arising relative metrics; as opposed to absolute value predictions which are not

the focus of this high level study. This objective is based on advise given by Gilman (2011) – previously of the United States National Renewable Energy Laboratory (NREL) Solar Advisor Model (SAM) division – which was that through consistency in the modelling, and only varying metrics of key interest, the relative metrics will provide more useful information as opposed to the less important and potentially less accurate absolute value predictions.

1.4 Research Questions

Based on the three key objectives of this dissertation, four research questions were posed, which encompassed specific aspects of the objectives, and whose analysis was deemed beneficial in aiding the understanding and accomplishment of the objectives. The research questions posed were:

1. Is it more beneficial in terms of the Levelised Cost of Energy (LCOE) to locate a South African CSP plant in a region with high DNI levels but limited access to cooling water, hence adopting dry cooling; or in a region with lower DNI levels but greater access to larger volumes of water, hence adopting wet cooling?

2. Of the CSP technologies considered in this analysis, which would be deemed most optimal at each location?

3. Which financial and cost-related model input variables have the greatest effect on the resulting LCOE of the plant, and hence which are the key items to consider when implementing a utility-scale parabolic trough or central receiver CSP plant in South Africa?

4. Can a high level analysis and methodology be developed to achieve the objectives of this study, by making use of existing software and modelling tools, available data, or data adapted to reflect South African conditions; and if so, how accurately can this be achieved?

1.5 Methodology

In order to achieve the objectives of this study, as well as to assess the research questions posed, the following methodology was developed and employed:

1. Conduct an in-depth literature review regarding the current environment for Concentrating Solar Power (CSP) stations in South Africa, in particular, considering previous studies on solar resource potential, and the availability of water for power-plant consumption.

2. In addition, assess the current status of CSP plants worldwide, paying particular attention to the latest technological developments, including cooling technology and thermal energy storage.

3. Identify and source the relevant data required to construct a Geographic Information Systems (GIS) model of potential CSP stations in South Africa.

4. Conduct a high-level GIS analysis, in order to identify potential CSP sites in South Africa, based on defined criteria.

5. Acquire detailed hourly weather data for the locations of a select few of the potential CSP sites identified in the GIS analysis.

6. Conduct an in-depth literature review of existing CSP plant designs and costs, in order to determine the necessary technical and financial data required to model various CSP technologies in South Africa.

7. Create performance and cost models for various CSP plants and locations in South Africa with the Solar Advisor Model (SAM) software, and subsequently simulate and optimise the various CSP plant configurations within the SAM models.

8. Analyse the various model results, and attempt to identify the optimal CSP technology for each of the considered locations. Thereafter, compare the results to, and validate them against, results contained in the literature.

9. Perform a sensitivity analysis of various model inputs in order to ascertain their effect on the model results.

10. Draw conclusions from the findings of the study, and make recommendations for further research and potential improvements.

1.6 Scope and Limitations

In light of the aforementioned objectives, this dissertation will include the identification and analysis of potential CSP sites in South Africa by means of a high-level GIS analysis. A performance and cost model will then be constructed within the Solar Advisor Model (SAM) computer software for two utility-scale CSP technology types, namely parabolic trough and central receiver, employing both wet and dry cooling at three identified potential locations. Attempts will be made to identify optimal choices for both CSP technology type and cooling technology within the context of current conditions and boundaries, and the sensitivity of the models to input variables will be assessed.

Due to limitations in the SAM software, and that fact that at the time of writing no utility-scale commercial CSP plants have yet been realised in South Africa, the more established parabolic trough and central receiver systems will thus receive key focus as CSP commencement technologies, and be will be considered and modelled at each location. Emerging technologies will therefore not be considered in this study. Furthermore, due to time constraints, no photovoltaic (PV) or concentrating photovoltaic (CPV) systems will be considered in this study. Due to the lack of freely available, detailed weather data, potential CSP site locations will be approximated with hourly weather data from the closest major town or city. Although the use and modelling of thermal energy storage will be included for CSP plants, time constraints lead to the exclusion of considering and modelling a fossil backup fuel system. Additionally, due to time constraints, and based on the guidelines in the REFIT documentation (NERSA, 2009, 2010), only 6 hours of thermal energy storage will be considered and this capacity will not be varied. Finally, as at the time of writing no utility-scale CSP plants were in existence in South Africa, detailed plant technical, design and cost data had to be sourced from the literature for plants outside of South Africa, before attempts were made to adjust these data to local conditions.

1.7 Plan of Development

The dissertation begins with a review of the literature, pertaining to the current state of CSP research in South Africa, as well as an overview of the SAM software, its method of operation, and its application.

Chapter 3 presents an overview of solar thermal technology, incorporating a review of current CSP technologies as well as their history and current applications worldwide. Chapter 4 then describes thermal power cycles, and the application of various wet and dry cooling technologies, before discussion their respective costs, and effect on plant water consumption. Chapter 5 concludes the initial theory and review chapters, with an overview of thermal energy storage, motivation for its use with CSP plants, and finally a description of various thermal storage technologies and their application.

The GIS analysis is conducted in Chapter 6, which concludes with the identification and quantification of potential CSP sites in South Africa. Chapter 7 then presents a detailed description of the SAM software user interface and its various input pages as a means to better identify required model input data, as well as to determine the applications and limitations of the software. In Chapter 8, a full and detailed description of all the methods and sources used in the determination of the SAM model inputs is given. The optimisation of various plant design criteria is also presented.

The final results from the various models, and the analysis thereof, are presented in Chapter 9, where they are subsequently compared to and validated against similar results contained in the literature. A sensitivity analysis of various key input variables is then conducted in Chapter 10, whereby the effect of varying input conditions on final model outputs is gauged.

In the final two chapters, conclusions are drawn from the findings, before recommendations are made based on the conclusions. The full documentation of the developed GIS methodology, as well as all CSP plant comparison databases and final model inputs are presented in the appendices.

2 Literature Review

Before commencing this research, it was first necessary to review the literature pertaining to the analysis of CSP systems in South Africa. This was done not only in order to gain the theoretical knowledge and data required to completed this analysis, but also to achieve a better understanding and refined scope through the review of the findings and limitations of similar studies that have previously been conducted.

In light of this, the following chapter will present a review of South Africa's solar and CSP potential, and the issues regarding water scarcity and security. A review of the relevant computer software used for the analysis of CSP technologies in this study will also be presented. The review of literature will not be confined to this chapter alone, however, but instead the relevant theory and literature specific to each section will be discussed and developed throughout the course of this dissertation. Furthermore, the data required for the various models and analyses in this study will be sourced from the literature and presented both in the subsequent sections of the report and in the appendices.

2.1 Analysis of South Africa's CSP Potential

The use of geographic information systems (GIS) software to conduct initial high-level evaluations and identify potential CSP sites is becoming more common. In their paper on the *GIS approach to the definition of capacity and generation ceilings of renewable energy technologies*, Bravo et al. (2007) made use of GIS software and modelling to identify and quantify the energy generation potential of CSP sites in Spain. More recently, Fluri (2009) conducted a study on the potential of CSP in South Africa, making use of similar GIS analysis criteria and methodologies to those of Bravo et al. (2007), as well as GIS studies conducted by Pletka et al. and Dahle et al. (as cited by Fluri, 2009).

Fluri (2009) concluded that when considering the potential CSP sites identified in his study with a land use profile of 28 km^2 per gigawatt (GW), South Africa possesses 510.3 GW of nominal generation capacity in the Northern Cape, 25.3 GW in the Free State, 10.5 GW in the Western Cape and 1.6 GW in the Eastern Cape. This results in a total nominal power generation capacity of 547.6 GW for the whole of South Africa. Furthermore, if parabolic trough CSP technology is considered at all locations, with an assumed annual capacity factor of 38.8%, a net energy generation potential of 1861.4 terrawatt hours per annum (TWh/a) could be realised.

Although Fluri (2009) states that a CSP sector of this magnitude would require 6086.7 million m^3 of water per annum, the requirement for potential sites to be within a certain proximity of cooling water was not included in the study. What is noted, however, is that according to the water management areas (WMAs) defined by the South African Department of Water Affairs (DWA) – then the Department of Water Affairs and Tourism (DWAF), and cited by Fluri, 2009) – most potential CSP sites are situated in areas where there is little or no potential for any future development requiring water for consumption purposes. Fluri (2009) therefore concludes that a large roll-out of CSP in South Africa will only be possible if dry-cooling is considered.

2.2 Water Scarcity

As stated in the introduction of this report, South Africa is classified as a water-stressed country, receiving an annual average rainfall of 500mm – less than 60% of the world average (Mukheibir, 2007). Of the 19 water management areas (WMAs) defined by the DWA – then the DWAF – 11 of these faced water deficits in 2004. The Northern Cape province is particularly affected by supply concerns, and had a water supply deficit of 8 million m^3 in 2000 (Mukheibir, 2007). This is of especial concern, as the Northern Cape is one of primary areas considered for potential CSP development.

As CSP plants consume large quantities of water per year – in the region of 500 - 750 gallons per megawatt hour (1.89 - 2.84 litres/kWh) (DOE, U.S., 2010) – it is thus imperative to consider water availability when analysing any potential CSP development site. Should there be insufficient water to supply the plant, or should the price of water become a limiting factor, it may be necessary to consider other areas or provinces with lower solar resources but access to water, or conversely, make use of alternative plant cooling technologies such as dry-cooling – at the expense of plant efficiency and cost.

2.3 The Solar Advisor Model Software

2.3.1 Overview

The Solar Advisor Model (SAM) is a performance and economic software model which was developed by the National Renewable Energy Laboratory (NREL), in collaboration with Sandia National Laboratories and in partnership with the U.S. Department of Energy (DOE) Solar Energy Technologies Program (SETP). Development on SAM was begun in 2004 by SETP to aid and support their analyses. It has since evolved the capacity to model a range of renewable technologies, and is currently used worldwide for planning and evaluating research and development programs, developing project cost and performance estimates, and for academic research (NREL, 2011b). SAM is now designed to aid in the decision making process for many involved in the solar industry, ranging from project managers, engineers, technology developers, incentive designers and researchers (SAM, 2010).

In general, SAM calculates both the performance characteristics for the renewable technology in question, and economic estimates for grid-connected solar power projects in the distributed and central generation markets (SAM, 2010). These attributes, as well as the fact that it has been used and validated in the fields of industry and research for a number of years, make it an ideal choice for use in this study to model, analyse and compare grid-connected, utility-scale parabolic trough and central receiver CSP technologies, incorporating the effects of both wet and dry cooling technologies, at various locations around South Africa.

In order to aid understanding of how SAM accomplishes its task of calculating the performance and economic characteristics of a plant, a brief overview of the workings of the SAM performance and economic components will now be briefly discussed. For the sake of brevity, detailed technical descriptions and actual thermodynamic and economic formulae will not be presented, however, these are available in the SAM (2010) documentation should the need or interest arise to consult them.

2.3.2 Performance Model Component

The SAM plant performance component is based on an hourly simulation engine that runs on the TRNSYS software, developed at the University of Wisconsin Madison, but combined with additional customised components. TRNSYS is a time-series based transient systems simulation program which can simulate the performance of solar thermal and photovoltaic systems, low energy buildings and HVAC systems, renewable energy systems, co-generation, and fuel cells. The TRNSYS software has been commercially available since 1975, and through years of validation has become reference software for engineers and researchers, across multiple fields worldwide (SAM, 2010; TRNSYS, 2011).

TRNSYS makes use of hourly resource data combined with user specified components that represent the power system and the manner in which they are connected. TRNSYS includes a detailed library of multiple components found in thermal and electrical energy systems, but also allows for the creation of additional, user-defined components through a system description language. Once a system is defined by means of components, connections and their interactions, the model then solves the representing mathematical equations in order to describe and predict the system performance (TRNSYS, 2011).

There is no need to purchase or make use of TRNSYS in conjunction with SAM, however, as it is integrated directly into the SAM software. Hence, there is also no requirement of familiarity with the use of TRNSYS in order to run SAM (SAM, 2010). The user need only define the inputs and specifications for the components of a plant in SAM, and when a simulation or model is run, SAM passes these defined inputs, as well as the relevant connection and interaction data, directly into its TRNSYS simulation engine for processing. The results can then used with the economic model components in SAM.

2.3.3 Economic Model Component

The economic model in SAM calculates the cost of generating electricity and the project's cash flow over a specified analysis period, based on provided location, direct and operating cost, financial, and design specification data. In order to accomplish this, the system's hourly output for a single year, as generated by the aforementioned performance model component, is used to calculate a series of annual cash flows for revenues generated from electricity sales and incentive payments, tax liabilities (including any tax credits for which the project is eligible), and loan principal and interest payments.

SAM then produces economic output metrics such as the levelised cost of energy (LCOE), internal rate of return (IRR), minimum debt service coverage ratio (DSCR), and yearly cash flows. The economic model also possesses the ability to represent projects in the residential, commercial, and utility markets, while incorporating a variety of incentive payments and tax credits – which can be based on investment amounts, capacity ratings, and annual electricity production (SAM, 2010).

2.3.4 Model Output and Simulations

Thus in summary, SAM functions by the means of interaction with performance, cost, and finance models to calculate energy output, energy costs, and cash flows. A final means of functionality provided in SAM is the option to run various simulations of the same case study, comprising parametric analyses, sensitivity analyses, optimisation, and statistical analyses. These additional simulations allow for the investigation of the effect that any variation or uncertainty in any of the input data will have on final model results (SAM, 2010).

An overview of the various input pages and layout of the SAM user interface will be covered in greater detail in Chapter 7, while detailed descriptions, methods and motivations for the definition and derivation of inputs used in the SAM model for this study will be given in Chapter 8.

3 Concentrating Solar Technologies

3.1 Solar Thermal Overview

In a concentrating solar power (CSP) system, the sun's rays are focussed by means of optical devises in order to generate large quantities of heat. The heat generated can then be used to power a Stirling engine, generate steam to drive a turbine for electricity production, or alternatively, to drive chemical reactions (European Commission, 2004; IEA, 2010a).

CSP systems make use of mirrors or reflective surfaces which continuously track the sun in order to concentrate and focus the incoming incident radiation onto one or multiple receivers. However, as predicted by classical optical theory, only direct, parallel light rays are capable of being reflected and concentrated. CSP systems are therefore only capable of using the Direct Normal Irradiation (DNI) component of irradiation from the sun, and hence are only suitable in areas that receive high annual averages of DNI (European Commission, 2004; IEA, 2010a). According to the International Energy Agency (IEA), the minimum yearly DNI considered acceptable for the consideration of CSP plants is 2000 kWh/m^2/year (5.48 kWh/m^2/day) (IEA, 2008). This limits the placement of CSP plants to regions such as North Africa, Southern Africa, Western India, the South Western United States, Mexico, some parts of South America, part of Central Asia, and Australia. These promising areas for CSP are presented in Figure 3.1.

The main components of a CSP plant comprise the aforementioned *solar collector field* – constituting the tracking mirrors and reflectors – the *solar receiver*, and an *energy conversion system*. The high temperature heat that is produced when the mirrors or reflectors focus and concentrate the irradiation onto the receiver is then captured and transported to the energy conversion system by a working fluid circulating through the receiver. This process can be accomplished in two ways; either *directly* by using water as the working fluid and generating steam directly in the receiver, or alternatively in an *indirect* process, where a heat transfer fluid (HTF) is circulated through the receiver

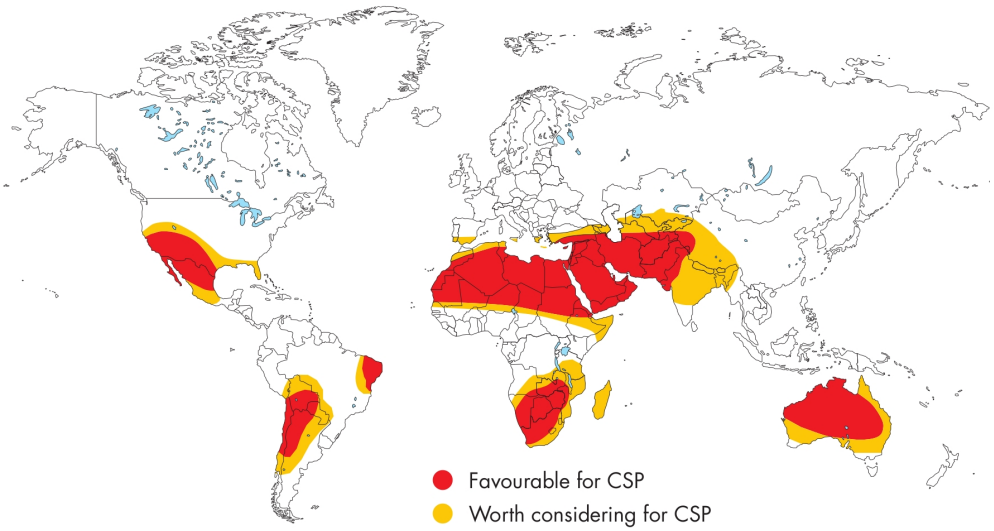

Figure 3.1: Most Promising Areas for CSP Sites (IEA, 2008).

before being used to produce steam in the energy conversion system via a heat exchanger mechanism (EPRI, 2010). The final step of the energy conversion process occurs at the power block or energy conversion system. In an electricity producing CSP plant, the heat can either be used to power a Stirling engine, or alternatively, to generate steam for driving a Rankine cycle turbine. CSP plants also possess the potential to be used in solar desalination projects, or to produce chemical fuels like hydrogen (IEA, 2008).

There are currently four major types of CSP technology, namely *Parabolic Trough*, *Central Receiver* (also know as a Power Tower), *Linear Fresnel*, and *Parabolic Dish* (or Dish Stirling). A schematic representation of each technology is presented in Figure 3.2 below.

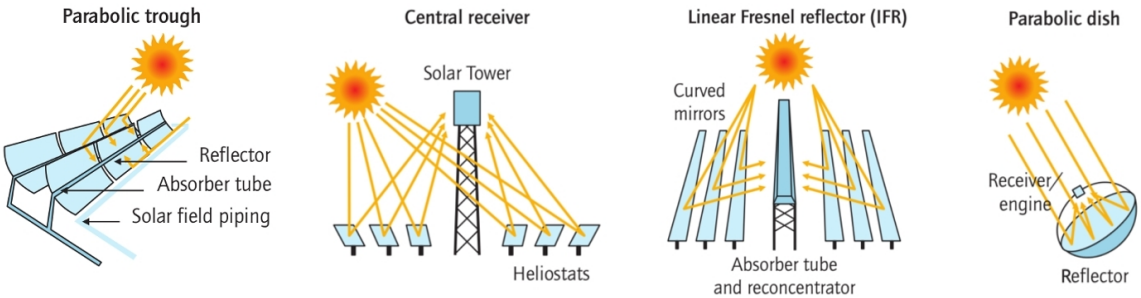

Figure 3.2: Various CSP Technologies. *Source of Images*: (IEA, 2010b).

From the figure, it can be seen that parabolic trough and linear Fresnel systems are line focus technologies, which track the sun along a single axis. Central receiver and parabolic trough technologies, however, are point focus technologies which track the sun across two axes (IEA, 2010a). A brief description of each of the technologies will now be presented under their respective headings.

3.2 Parabolic Trough

Figure 3.3: Parabolic Trough CSP Technology. *Source of Images:* Meyer (2010), Meyer (2010) and Müller-Steinhagen (2011).

Parabolic trough technology, as depicted in Figure 3.3, is the most mature of the CSP technologies, and consists primarily of a large field of single-axis tracking, parabolically-shaped troughs. The troughs are lined with parabolically shaped mirrors, or reflectors, which focus and concentrate the sun's beam radiation onto an integral linear receiver tube running along the length of each trough's focus. The troughs, which can span up to 150m in length, are usually installed in multiple parallel rows, known as solar collector assemblies (SCAs), which can cover areas of multiple square kilometers. The SCAs are typically aligned along a North-South horizontal axis, with each trough – driven by motors and control systems – tracking the sun from East to West throughout the day to ensure that the maximum incoming radiation is captured (EPRI, 2010).

The solar receiver tube, termed a heat collection element (HCE), is usually black-coated and housed in a glass vacuum tube to reduce thermal losses. Currently, all commercial plants make use of an indirect system with a high temperature thermal oil HTF which is circulated through the receiver tube, absorbing heat and reaching temperatures up to 400℃. The HTF is then piped to the power block and fed through heat exchangers in order to produce high temperature steam for the power cycle. Finally, the HTF is piped back to the HCEs for reheating. As a means to reduce costs, and limit the requirement for additional heat exchangers and maintenance, research is also being conducted in the field of direct steam generation (DSG) parabolic trough systems. In these DSG systems, water

is circulated through the receiver tubes to produce superheated steam. The superheated steam is then transported to the power block, where it drives a steam turbine to produce electricity. The water is then condensed and cycled back through the HCEs (EPRI, 2010; European Commission, 2004; Sargent & Lundy, 2003).

3.3 Central Receivers

Figure 3.4: Central Receiver CSP Technology. *Source of Images:* EPRI (2010), Müller-Steinhagen (2011) and Meyer (2010).

A central receiver system, also known as a 'power tower' and depicted in Figure 3.4, makes use of hundreds or thousands of individual two-axis sun-tracking mirrors, known as heliostats, to focus the sun's direct radiation onto a relatively small receiver situated on top of a tower. The receiver usually comprises an area of only a few square meters, while the tower ranges in height from 50m to over 100m depending on the capacity of the plant. Due to the large number of heliostats in the solar field, and the relatively small receiver size, central receiver plants produce extremely high concentration ratios in the order of 1000 suns, which in turn results in higher working temperatures and higher overall efficiencies when compared to parabolic trough plants (EPRI, 2010; European Commission, 2004; Sargent & Lundy, 2003).

The *receiver* is generally classed according to two categories, namely an *indirect irradiation* receiver, or a *direct irradiation* receiver. In an indirect configuration, the receiver consists of a number of metal or ceramic tubes through which the HTF flows. The outer surface of the receiver is heated by the concentrated solar irradiation, and this heat is then transferred to the working fluid. The heat can then be used to generate steam to drive a Rankine cycle turbine for electricity production, or alternatively to provide process heat for chemical processes. In such systems, the HTF typically comprises either water which generates steam within the receiver (as used in the Solar One, PS10 and PS20 plants), or a molten salt (as used in the Solar Two and Gemasolar plants) which is circulated throughout the system and heated to temperatures around 565 ℃ (Wagner, 2008).

In a direct irradiation receiver, also referred to as a volumetric receiver, the atmospheric air absorbs the solar radiation directly, or by intimate contact with a solid surface. The heated air can then be used to drive an open Brayton cycle or to heat nitrogen or helium for closed Brayton cycle operation (Wagner, 2008). At the time of writing, however, this technology is still undergoing research and development.

The use of a molten nitrate salt in a central receiver system has many distinct advantages over the thermal oil typically used in parabolic trough plants. Molten salt has a superior heat transfer capability compared to thermal oil, and is also significantly cheaper. The elimination of the thermal oil also greatly reduces the environmental risks associated with leaks. Molten salt can also be used directly as an energy storage mechanism, thereby reducing system component costs by eliminating the need for additional oil-to-salt heat exchangers – should storage be incorporated in a CSP system. The main disadvantage of a molten salt HTF, however, is that is solidifies at a relatively low temperature of 221 ℃, and therefore requires the use of additional electrical freeze protection mechanisms (EPRI, 2010; Wagner, 2008). The topic of thermal storage, however, will be discussed in more detail in Chapter 5.

Central receiver systems do, however, have larger associated parasitic loads when compared to parabolic trough plants. These arise due to the the fact that each heliostat requires an individual electric drive motor for tracking, and in the case of molten salt systems, the aforementioned electrical freeze protection system. Therefore, due to their size and economies of scale, central receiver systems are best suited for utility-scale application in the 30 MW to 400 MW range (European Commission, 2004). As a final note, due to the modelling limitation in SAM, only indirect irradiation central receiver systems will be considered, with the analysis of volumetric receivers considered beyond the scope of this report and recommended for future studies.

3.4 Linear Fresnel

Linear Fresnel technology, as depicted in Figure 3.5, is similar to the parabolic trough in the sense that it is a line focus technology. A linear Fresnel system differs from the parabolic trough, however, in that it approximates the parabolic shape by using long ground-level rows of flat or slightly curved mirrors. These mirrors are all individually controlled, single axis-tracking reflectors, which focus and concentrate the sun's incoming radiation onto a *fixed* downward-facing linear receiver which is suspended above the collectors (IEA, 2010a; Mills, 2004).

Figure 3.5: Linear Fresnel CSP Technology. *Source of Images:* Müller-Steinhagen (2011), Fahy (2009) and Meyer (2010).

A linear Fresnel system makes use of water as the working fluid and is thus a direct steam generation technology. According to Mills (2004), linear Fresnel systems can be classified into two different design categories, namely; the *Solarmundo* linear Fresnel system and the *Compact Linear Fresnel Reflector* (CLFR) system. The Solarmundo system is a classical linear Fresnel system, with one receiver per field and a relatively high receiver-to-field width ratio. The Solarmundo system makes use of a cavity receiver with a single receiver tube and secondary internal reflector. Mills (2004) continues to state that a Solarmundo system can be expected to deliver an annual average solar to electricity efficiency of between 10% and 12%. An example of a linear Fresnel cavity receiver with an internal secondary reflector, as produced by Novatec Solar (2011), is shown in Figure 3.6.

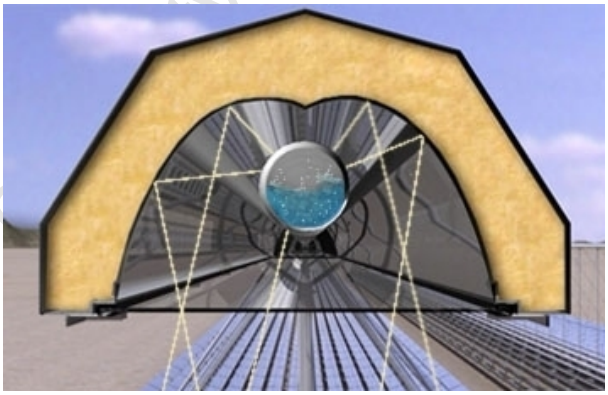

Figure 3.6: Linear Fresnel Cavity Receiver with Internal Secondary Reflector (Novatec Solar, 2011).

The CLFR system differers from a classical linear Fresnel system in that is employs the partial inter-meshing of adjacent fields with multiple receiver towers. This allows for a more efficient use of land space, as well as a significant increase in the optical efficiency of the system. The CLFR system makes use of a flat cavity receiver attached to boiling tubes, but unlike the Solarmundo system, does not make use of a secondary reflector. The CLFR system is reported to possess a peak solar to electricity conversion efficiency

of 19% (Mills, 2004). Both types of linear Fresnel system generate steam directly, which can then be used for electricity production through a Rankine cycle power block, or alternatively generate process heat. A linear Fresnel system is currently in use in Liddell, Australia, where it preheats boiler water for use in a conventional fossil fuel power station (Meyer, 2010).

Linear Fresnel technology is one of the newer developing CSP technologies, but possesses great potential as a low cost and effective system. Due to limitations in the SAM software, and the non-commercial nature of linear Fresnel technology, its use will not be considered or modelled in this analysis, but is recommended for further study.

3.5 Parabolic Dish

Figure 3.7: Parabolic Dish CSP Technology. *Source of Images:* Müller-Steinhagen (2011), Morse (2009) and Meyer (2010).

A parabolic dish system, as show in in Figure 3.7, makes use of a parabolically shaped dish, supported by a single structure and covered in mirrors or reflectors used to focus the sun's incoming radiation onto a receiver. The receiver unit is fixed at the dish's focus, with the whole dish and receiver unit tracking the sun along two axes. Parabolic dishes usually have an independent engine or generator coupled to the receiver, which is typically an external combustion Stirling engine. It is for this reason that a parabolic dish system may also referred to as a Dish Stirling system. Stirling engines are not the only engine used, however, with the possibility existing to make use of Brayton micro-turbines, or alternatively generating steam directly at the receiver. In the case of a Stirling or Brayton cycle, electricity would be generated directly at each receiver unit, while the use of direct steam generation would conversely require a separate power block and Rankine cycle turbine. (European Commission, 2004; IEA, 2010a).

Due to their extremely high concentration ratios, parabolic dish systems offer the greatest conversion efficiencies out of all the current CSP technologies, however, their commercial use is generally limited by their prohibitively high cost (Meyer, 2010). The dishes are generally small in size with diameters ranging between 8 and 10 meters (larger examples do exist, however, such as the *Big Dish* in Canberra, Australia). Due to their size, parabolic dish systems are considered modular by nature, but large installations are generally required to benefit from economies of scale. Their low compatibility with thermal storage, as well as the fact that they do not required cooling water, also puts them in direct competition with photovoltaic systems (European Commission, 2004; IEA, 2010a).

Due to the non-commercial nature of parabolic dish technology, parabolic dish systems will will not be considered in this analysis, however, their analysis is recommended for future studies.

3.6 Efficiency and Availability

The efficiency with which the incoming solar radiation can be converted into thermal energy, and electricity is dependent on a combination of the optical efficiency of the mirrors or reflectors, the heat absorption efficiency of the receiver, and the thermal to electric efficiency of the power block. According to the European Commission (2004), optical efficiencies in the region of 98% are achievable, while heat conversion efficiencies are in the range of 70% to 95%. Experimental parabolic dish systems have shown a peak solar to electric efficiency of 29%, but this is dependent on the technology type. Technologies with the highest concentration ratios, such as parabolic dishes and central receivers, generally achieve higher over all efficiencies when compared to more mature technologies such as parabolic troughs, which only achieve efficiencies around 20% (European Commission, 2004). The choice of cooling system for the power block – either wet or dry cooled – also affects the overall plant efficiency, as well as the system cost. A detailed discussion of thermal power plant cooling technologies will therefore be presented in Chapter 4.

CSP systems are also variable power producers by nature, due to their reliance on the sun and sensitivity to weather conditions. As a means to improve their availability and capacity factors, and hence render them better suited to base-load power generation, some CSP plants incorporate thermal energy storage devices, or are supplemented with a fossil fuel backup boiler (EPRI, 2010; IEA, 2010a). A detailed discussion of thermal storage for CSP systems will therefore be presented in Chapter 5.

3.7 History and Current State of Development of CSP Plants

Initial interest in CSP technology began in the late 1970s, with development beginning in early 1980s, and was primarily a result of the late 1970s world oil crisis. Experimental plants were set up in many countries, including Spain, the United States (U.S.), Japan and Australia, all of which were parabolic trough systems (Meyer, 2010).

CSP technology is still under active development today, however, having received a renewed revival as a result of the growing awareness of climate change and the need to reduce greenhouse gas (GHG) emissions (European Commission, 2004). Research is currently being conducted to improve the efficiency and reduce the cost of all aspects of CSP systems including, mirrors, receivers, HTFs, power blocks and cooling systems. Special attention is also being given to thermal energy storage systems, which would allow CSP plants to meet evening peaks loads, as well as become a firm option for base-load power generation, and hence economically viable competition to fossil fuel plants (IEA, 2010a).

A brief time-line of the development and operational lifetimes of some of the key CSP plants worldwide will now be presented under their respective headings. For the sake of brevity, not every single plant will be mentioned, but an effort made to include some of the major plants representing each technology. A summary of all the technologies covered is also presented in Table 3.1.

Parabolic Trough Plants

The first commercially operating CSP plant was the Solar Energy Generating Systems (SEGS) I parabolic trough plant, commissioned in the Mojave Desert of California in 1984. The plant was expanded in capacity every year from 1984 till 1991 and incorporates SEGS I through to SEGS IX. The total combined capacity of the plant is 354 MW, and the it has been operational ever since it was commissioned. Over the years, its output has increased by 35% while operation and maintenance (O&M) costs decreased by 40%. The plant is supplemented by a natural gas backup, with an upper limit of 25% imposed on supplementation. In the best years, however, only 5% gas backup was required (European Commission, 2004; Meyer, 2010).

Another key CSP plant is that of Nevada Solar One, which is a 64MW parabolic trough plant first commissioned in 2007 in the Nevada Desert. As of writing, this is the largest parabolic trough plant in the U.S. since the the original SEGS plants in 1980s (Meyer, 2010).

A final notable parabolic trough development is that of the Andasol I, II and III plants in Southern Spain. Andasol I and II are currently in operation, with the first plant commissioned in 2009. At the time of writing, Andasol III is still under development. Each plant outputs 50 MW to the electricity grid, which is the upper limit as currently regulated in Spain (Solar Millennium AG, 2008).

Central Receiver Plants

Some of the earliest central receiver CSP plants were the 10 MW Solar One and then later upgraded Solar Two plants in the Mojave Desert, California. Solar One was commissioned in 1982, and subsequently upgraded in 1988 to Solar Two, which incorporated 3 hours of full load thermal energy storage. Both plants operated reliably as development and test plants, and formed the design basis for the Gemasolar (Solar Tres) plant (Sargent & Lundy, 2003; Meyer, 2010).

Gemasolar, which was commissioned in 2011, is a 19.9 MW central receiver in southern Spain, and represents the worlds first central receiver system with 15 hours of molten salt storage. It also makes use of 15% limited natural gas backup (Torresol Energy, 2011).

Two other notable central receiver plants are PS10 and PS20 situated near Seville in southern Spain. Commissioned in 2007, PS10 was Europe's first commercial central receiver system and comprises an 11 MW direct steam system, as well as a steam energy storage system. PS20 was based on PS10 and was commissioned in 2009. At 20 MW rated capacity, it is currently the world's largest central receiver system, and makes use of direct steam generation (Meyer, 2010; Wagner, 2008).

A slightly different and new concept for central receiver systems is that of the 5 MW eSolar plant which was commissioned in 2009 in the U.S. The plant's focus is on modularity and ease of construction, and comprises approximately 12,000 small heliostats in a rectangular field, as opposed to the fewer, larger heliostats is elliptical arrangements, as adopted by many other systems (Meyer, 2010).

Linear Fresnel Plants

Linear Fresnel technology is still relatively undeveloped when compared to parabolic troughs and central receiver systems, however, a few commercial installations have been realised. The first implementation was a 1 MW thermal plant used to preheat boiler water for a coal-fired power station in Liddell, Australia. The plant was commissioned in 2004, and later upgraded to 10 $MW_{thermal}$. Other installations include the 5 MW Kimberlina CLFR plant installed in California in 2008, and the more recent 1.4 MW PE 1 plant installed by Novatec Solar in 2009 in Murcia, Spain (Meyer, 2010; Novatec Solar, 2011).

Parabolic Dish Plants

Parabolic dish technology, like linear Fresnel, is still relatively underdeveloped. Although a number of experimental systems do exist, as of the time of writing there are currently no commercially operating parabolic dish CSP plants (Meyer, 2010).

Table 3.1: Summary of Select Commercial CSP Plant Developments. *Source of Data:* European Commission (2004), Sargent & Lundy (2003), Meyer (2010), Novatec Solar (2011), Torresol Energy (2011) Solar Millennium AG (2008) and Wagner (2008).

Project	CSP Technology	Capacity	Country	Year Commissioned
SEGS I - IX	Parabolic Trough	354 MW	U.S.	1984
Nevada Solar One	Parabolic Trough	64 MW	U.S.	2007
Andasol I	Parabolic Trough	50 MW	Spain	2009
Andasol II	Parabolic Trough	50 MW	Spain	2009
Solar One	Central Receiver	10 MW	U.S.	1982
Solar Two	Central Receiver	10 MW	U.S.	1988
Gemasolar	Central Receiver	19.9 MW	Spain	2011
PS10	Central Receiver	11 MW	Spain	2007
PS20	Central Receiver	20 MW	Spain	2009
eSolar	Central Receiver	5 MW	U.S.	2009
Liddell	Linear Fresnel	10 MW_{th}	Australia	2004
Kimberlina	Linear Fresnel	5 MW	U.S.	2008
Novatec PE 1	CLFR	1.4 MW	Spain	2009

4 Power Plant Cooling Technologies

The Rankine steam power cycle forms the basis for the majority of all thermal power stations, as a means to generate electricity from heat (Cengel and Boles, 2006). The majority of all CSP technologies used for electricity generation are also based on the steam power cycle, the exception being the Stirling dish system which operates on the Stirling cycle (DOE, U.S., 2010). Furthermore, according to the DOE, U.S. (2010), all of the existing commercial parabolic trough CSP plants in the United States use a Rankine steam cycle to convert their thermal energy to electricity, in a similar manner to that used by coal-fired, natural gas and nuclear power stations.

The Rankine steam cycle functions according to the principle that heat enters the system from an external high temperature source, and is rejected to the sink at a low temperature. In an ideal cycle and ignoring any losses, the work done by the steam turbine – and thus the work extracted from the system – is equivalent to the difference in temperatures of the heat source and the heat rejected at the sink (DOE, U.S., 2010). This can be seen in Figure 4.1.

The efficiency of the Rankine cycle is largely affected by the temperatures and pressures at the source and sink of the system, and hence in the case of electricity generation from a steam turbine, the difference in the temperatures and pressures of the steam at the turbine inlet and outlet. The efficiency of the system – and thus power generation potential – can therefore be improved by either increasing the temperature and pressure of the inlet steam, or decreasing the temperature and pressure of the outlet steam (Kelly, 2006). The exit steam in the condenser is a saturated mixture, existing at the saturation temperature relating to the pressure in the boiler. Thus the lower the temperature of the condenser, the lower the exit steam pressure of the turbine, and the greater the efficiency and hence the amount of work that can be extracted from the system (Cengel and Boles, 2006). The process of decreasing the temperature and pressure of the exit steam is illustrated in Figure 4.2.

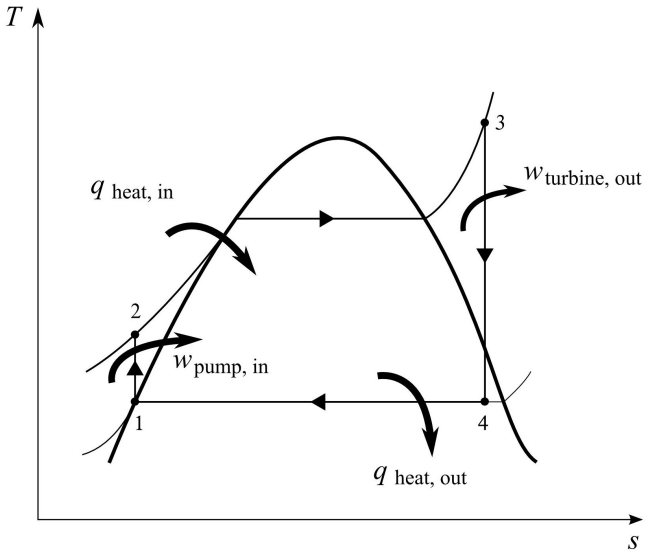

1 - 2 Isentropic compression in pump
2 - 3 Constant pressure addition of heat inside a boiler
3 - 4 Isentropic expansion through a turbine
4 - 1 Constant pressure rejection of heat in a condenser

Figure 4.1: Temperature - Enthalpy Diagram of the Simple Ideal Rankine Cycle.

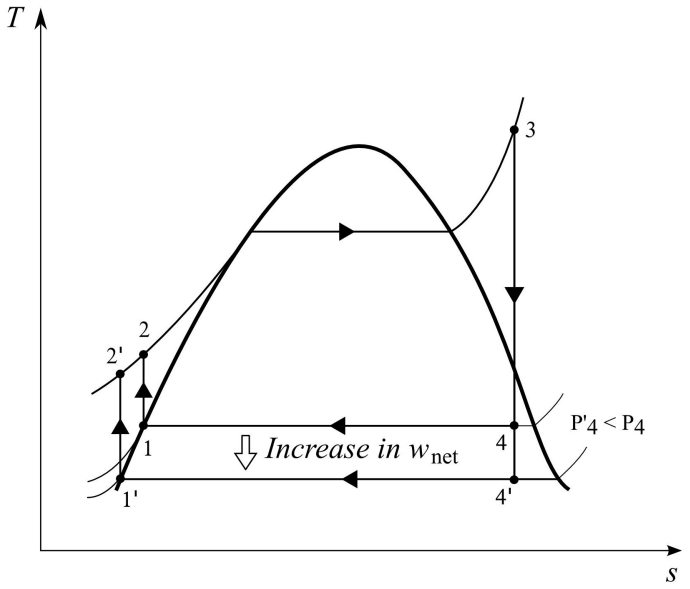

Figure 4.2: Effect of Decreasing Condenser Temperature and Pressure on the Efficiency of the Simple Ideal Rankine Cycle.

The condenser in most systems is therefore maintained at a low pressure, but in order to maintain it, a form of cooling is required in order to decrease its temperature. According to Kelly (2006), the lowest ambient temperature available is the wet bulb temperature, and thus most conventional power plants make use of an evaporation process and cooling towers to provide cooling water to the condenser, thereby achieving a high efficiency. Kelly (2006) continues to state that as the principal of heat transfer for wet cooling requires evaporation, large quantities of water are consumed – as much as 725 000 tons of water for an 80 MW_e parabolic trough CSP plant. In a report to congress concerning the reduction of water consumption in CSP electricity generation plants, the U.S. Department of Energy (DOE, U.S., 2010) state that all the operational CSP plants in the U.S. make use of water cooling, but due to the fact that water use for power plants is becoming more constrained, incentives exist to investigate alternative cooling technologies such as dry cooling, or hybrid wet-dry cooling. The following sections will thus briefly outline the methods and functionality of wet cooling, dry cooling and hybrid wet-dry cooling.

4.1 Wet Cooling

A 2003 study concerning the *Consumptive Water Use for U.S. Power Production* conducted by Torcellini et al. (2003) for NREL, showed that in the year 2000, 89% of electricity in the United States was produced by thermal driven, water-cooled energy conversion cycles. These water-cooled cycles used in thermoelectric plants were shown to evaporate an average of 1.8 litres of water for every kWh of electricity consumed at the point of end use (Torcellini et al., 2003).

In general, water-cooled cycles can be divided into two main categories or methods of accomplishment, namely, *once-through cooling*, and *recirculating evaporative cooling* (DOE, U.S., 2010). These two categories of wet cooling will now be briefly described.

4.1.1 Once-Through Cooling

In a once-through wet cooling cycle, large quantities of water are withdrawn from a waterbody, passed through a heat exchanger in the power cycle's steam condenser, and then returned back to the water source at elevated temperatures. The elevated temperature of the water returned to the source results in increased evaporation of the source itself. This process is represented graphically in Figure 4.3.

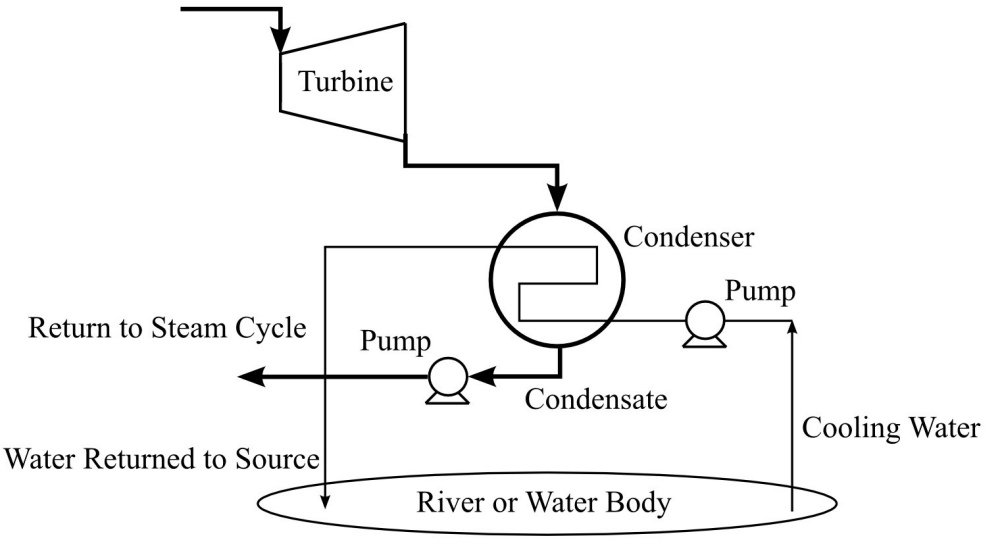

Figure 4.3: Schematic Representation of a Once-Through Wet Cooling System.

The method of once-through wet cooling typically requires volumes of between 87 and 102 litres of water per kWh being extracted from the source, the majority of which is returned and rapidly increases the evaporation rates of the source (DOE, U.S., 2010; Torcellini et al., 2003). The DOE, U.S. (2010) continues to note that the future use of once-through wet cooling in thermoelectric power plants may be restricted, due to environmental concerns regarding the impact of the elevated source temperatures on aquatic life and ecosystems. As a means to reduce these negative environmental impacts associated with this practice, evaporative cooling towers are thus preferred and hence more actively pursued.

4.1.2 Evaporative Cooling

In an evaporative cooling cycle, heat is removed from the system and transferred to the surrounding air by means of the evaporation of water. Unlike the once-through wet cooling cycle, the cooling water in the evaporative cycle is recirculated through the system, with a portion of it being continually evaporated in a draft cooling tower (Torcellini et al., 2003). Make-up water is thus required, and is drawn from the source to replenish the water evaporated in the draft cooling tower. This process is represented graphically in Figure 4.4.

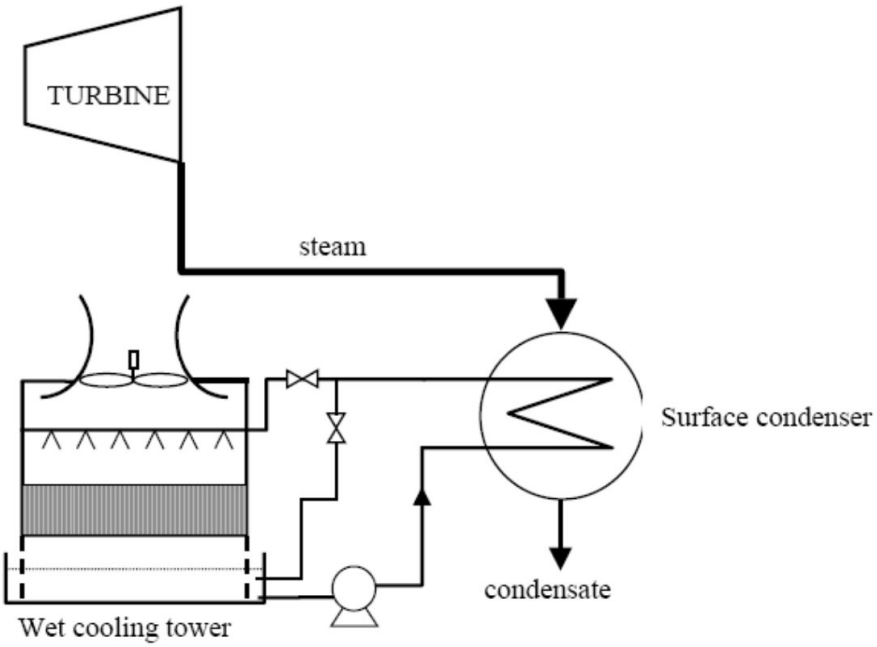

Figure 4.4: Schematic Representation of an Evaporative Wet Cooling System (DOE, U.S., 2010).

The recirculating evaporative cooling process results in far lower quantities of water being withdrawn from the source – between 1.89 and 2.46 litres per kWh – but the majority of the water which is withdrawn is consumed through evaporation (DOE, U.S., 2010). These figures are thus in agreement with the consumption figure of 1.8 litres per kWh stated by Torcellini et al. (2003) in section 4.1.

A further item for consideration with evaporative cooling is that any minerals, salts or water treatment chemicals present in the cooling water will become more concentrated over time as they are left behind in the evaporation process. This creates the need to drain a portion of the cooling water in order to remove these particulates. The waste drainage water is known as *blowdown*, and is a potential environmental hazard. Furthermore, any chemicals which are evaporated along with the cooling water can be a source a particulate pollution (DOE, U.S., 2010).

Therefore in summary of wet cooling, if a recirculating evaporative system is used, the volume of water withdrawn from the source is low, but the consumption of that water is relatively high. Conversely, if a once-through cooling system is used, larger quantities of water are drawn from the source, with evaporation rates at the power plant being low, but the elevated water source temperatures resulting in greater evaporation at the source, and increased total evaporation overall (Torcellini et al., 2003).

4.2 Dry Cooling

A dry cooling cycle operates without the need for cooling water, instead rejecting the heat from the steam cycle to the surrounding air. This process can be achieved through a number of methods, which will be described in the following sections.

A typical thermoelectric plant operating with dry cooling is thus a highly attractive alternative when considering water withdrawals and consumption. The only water withdrawal required for a conventional plant operating with dry cooling is for the steam cycle blowdown and make-up water, as well as domestic uses on site. A CSP plant using this technology, however, would require additional water withdrawals for mirror cleaning. The DOE, U.S. (2010) suggest that a conventional thermoelectric plant making use of dry cooling consumes less than 10% of the water of an equivalent plant employing evaporative wet cooling.

Although dry cooling was seen primarily as a means to address water limitations in areas where there was abundant fuel but little water, there are a number of additional or alternate reasons for its consideration. The majority of these considerations either stem from environmental or aesthetic concerns and comprise items such as reduction of waste-water discharge, and the abatement of the evaporation vapour plume visibility. According to EPRI and California Energy Commission (2002), in many cases the use of dry cooling also reduces licensing approval times by removing the need for a review of water related issues and rights, thus shortening the "time to market".

The use of dry cooling is becoming increasingly common with thermoelectric plants, but there are, however, disadvantages associated with the technology. Dry cooling represents a higher initial capital investment cost, and requires more auxiliary power to run when compared to wet cooling cycles. As the lowest temperature available to dry cooling is the dry bulb temperature – which is higher than the wet bulb temperature, especially on hotter days – the Rankine cycle efficiency is also reduced. This is a result of the increased temperature causing an increase in the condenser pressure and decreasing the turbine efficiency. The IEA (2010b) state that the use of dry cooling with a parabolic trough CSP plant can reduce its efficiency and annual electricity production by 7%, increasing the cost of the electricity it produces by 10%, when compared to the same plant using wet cooling technology. These figures are comparable to the 5% electricity production reduction and 7-9% increase in electricity price, as found by the DOE, U.S. (2010) in their analysis.

As with wet cooling, dry cooling cycles can also be differentiated according to two main categories or methods of accomplishment, namely, *direct* dry cooling, and *indirect* dry cooling. These two categories will now be briefly described.

4.2.1 Direct Systems

Direct dry cooling systems are the most common, and function by means of routing the turbine exhaust steam directly to an air-cooled condenser. The air cooled condenser is essentially a liquid-to-air surface heat exchanger with multiple finned tubes, usually arranged in an A-frame configuration. The multiple fins serve to increase the surface area for heat exchange and thus the heat transfer efficiency. The heat exchanger is typically fitted with fans in order to aid the heat transfer process via forced convection (DOE, U.S., 2010; Torcellini et al., 2003). The process is represented in Figure 4.5.

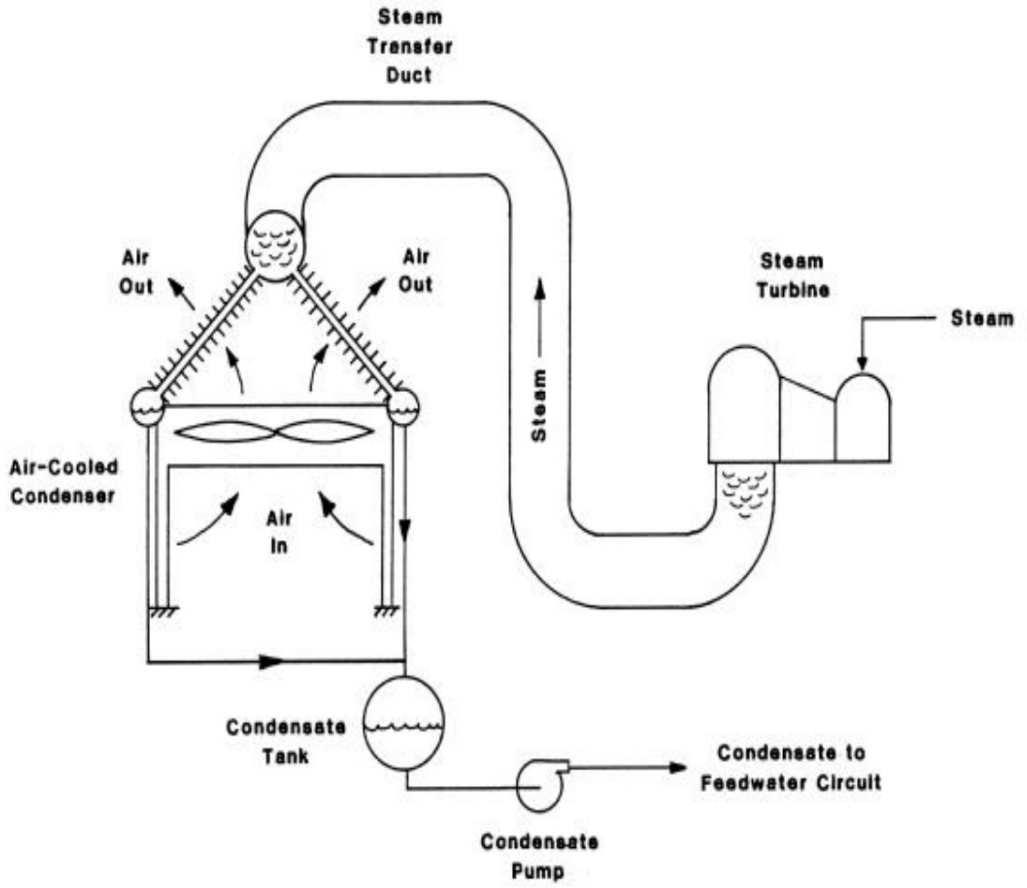

Figure 4.5: Schematic Representation of a Direct Dry Cooling System (EPRI and California Energy Commission, 2002).

4.2.2 Indirect Systems

In an indirect dry cooling system, a separate condenser is used in which the steam is condensed. This can be either a conventional shell-and-tube surface condenser, or a barometric condenser which condenses the steam directly on a spray of cooling water. In both types, the cooling water used to condense the steam is then circulated in a separate cycle through an air-cooled heat exchanger which ultimately rejects the heat to the atmosphere (EPRI and California Energy Commission, 2002). The former system is illustrated in Figure 4.6 and the latter in Figure 4.7.

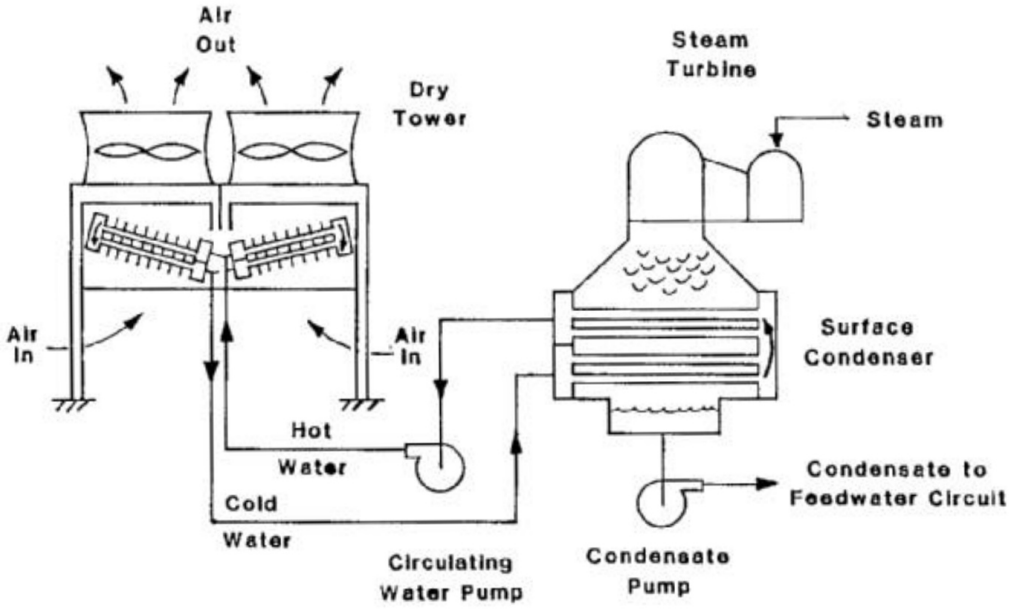

Figure 4.6: Schematic Representation of an Indirect Dry Cooling System with Surface Condenser and Mechanical Draft Tower (EPRI and California Energy Commission, 2002).

The latter system depicted in Figure 4.7 – which makes use of the barometric condenser – is usually coupled to a natural draft cooling tower, and known as a *Heller* system. As with all dry cooling technologies, they are characterised by a high initial capital cost, and generally a high operational and maintenance cost as well. They are used in several installations around the world, and represent the most likely retrofit solution for the rare occasion that an existing wet cooled plant would want to convert to dry cooling (EPRI and California Energy Commission, 2002).

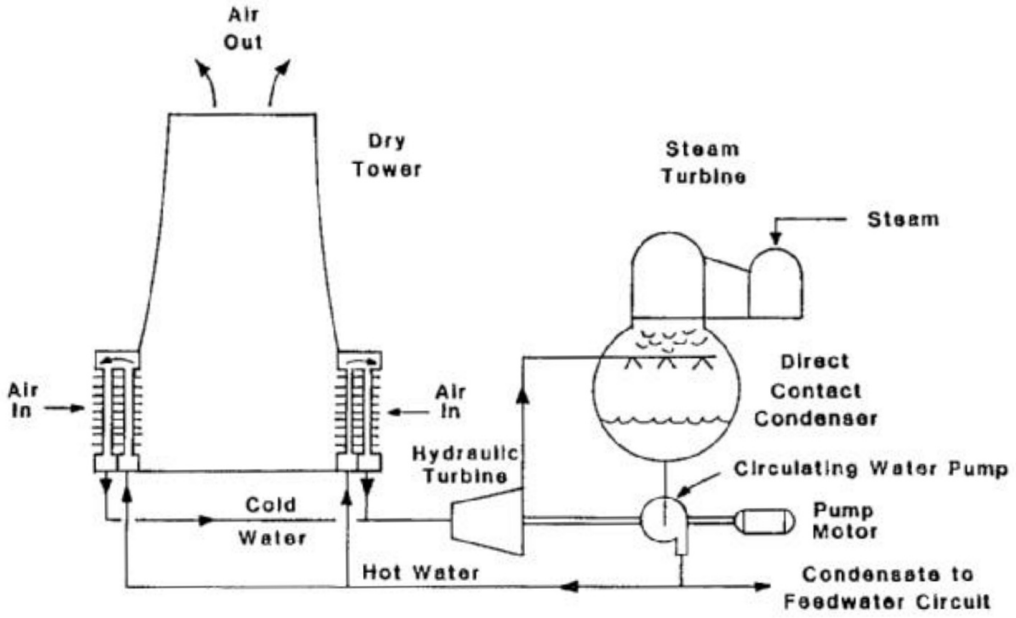

Figure 4.7: Schematic Representation of a Indirect Dry Cooling System with Direct Contact Condenser and Natural Draft Tower (EPRI and California Energy Commission, 2002).

4.3 Hybrid Wet-Dry Cooling

A hybrid wet-dry cooling system functions by means of employing a combination of both wet and dry cooling technologies. The use of hybrid cooling can generally be classified according to its purpose, namely a water conservation system or a plume abatement system. Initial interest in the technology occurred primarily in the 1970s – at the same time interest and research in dry cooling was taking place – and the primary focus was on plume abatement design. According to EPRI and California Energy Commission (2002), this trend in prioritising hybrid systems for plume abatement design as opposed to water conservation is still largely the case today.

4.3.1 Plume Abatement Systems

A plume abatement system is essentially a wet cooling system with a small dry-cooled component. The dry component's sole purpose is to dry out the exhaust plume during particularly cold and highly humid periods, when it would be most visible. Although this is primarily as aesthetic purpose, other benefits include reducing winter icing (caused by the exhaust plume) on nearby roads. The cold and highly humid conditions mentioned

are generally not present in areas deemed most suitable for CSP generation, however, and thus plume abatement is not considered a pressing issue for CSP sites (DOE, U.S., 2010; EPRI and California Energy Commission, 2002).

4.3.2 Water Conservation Systems

The purpose of a water conservation system is to reduce, but not completely eliminate the use of cooling water for power cycle heat rejection. The idea is that the plant will operate on a dry cooling cycle for the majority of the year – as a means to drastically reduce water consumption – but during the hottest periods of the year, a small amount of cooling water is used as a means to mitigate the largest losses in system efficiency that would be experienced in an all-dry system. According to EPRI and California Energy Commission (2002), water conservation hybrid schemes can limit annual water usage to between 2% and 5% (but generally between 20% to 80%) of that consumed by an all-wet cooling system, while simultaneously achieving greater efficiency and capacity advantages over an all-dry system during the hottest periods of the year. The DOE, U.S. (2010) echo this view, and estimate that water conservation hybrid systems save about 80% of water when compared to all-wet systems, while reducing the energy cost penalty below that of dry-cooled systems. Water conservation systems also possess the added advantage of plume abatement due to the wet part of the system not operating during the colder periods of the year when a plume is most likely to be visible.

4.3.3 Design Arrangements

A multitude of different designs exist for hybrid cooling systems, and can be summarised according to the following tower and condenser designs (EPRI and California Energy Commission, 2002):

Tower Designs

- Single structure with combined tower
- Separate wet and dry towers
- Parallel or series airflow paths through the wet and dry systems
- Parallel or series connected cooling water circuits

Condenser Designs

- Common condenser
- Separate condenser
- Divided water box separating the cooling water flows from the wet and dry towers

A generic hybrid parallel cooling system is shown in Figure 4.8. The system functions by making use of a dry cooling system as the primary heat rejection system for the majority of the year. During hot periods, the system efficiency is enhanced by routing some of the turbine exit steam to a separate wet cooling system which only rejects a portion of the total waste heat.

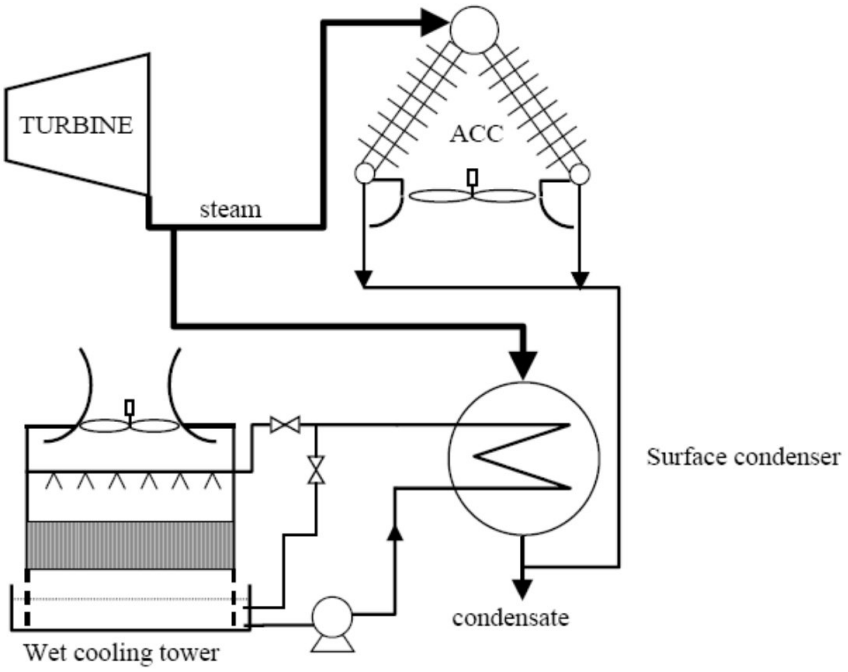

Figure 4.8: Schematic Representation of a Generic Parallel Hybrid Wet-Dry Cooling System (DOE, U.S., 2010).

4.4 Technology Comparisons and Costs

The majority of all new fossil fuel based plants make us of an evaporative wet cooling cycle to reject the steam power cycle heat to the atmosphere. A typical coal or nuclear power station will consume in the region of 500 gallons of water per MWh (1.89 litres per kWh) of electricity produced. In comparison, a typical parabolic trough or central receiver CSP plant making use of an evaporative wet cooling will consume similar amounts of water, with the parabolic trough plant consuming slightly more on average – in the region of 800 gallons per MWh (3.03 litres per kWh). Of this water consumed, approximately 2% is used for mirror washing and cleaning (DOE, U.S., 2010).

As discussed in Section 4.2, dry cooling is typically far less economical than wet cooling due to its poorer thermal efficiency characteristics (especially during hotter periods of the year) as well as its higher initial capital investment costs. This is also true for CSP plants. However, as the most suitable CSP sites are generally located in regions with high levels of solar irradiation resulting from many hours of direct sunlight, these sites also tend to have minimal access to water sources (DOE, U.S., 2010). With the ever increasing pressure for power plants to reduce their water consumption, coupled with the great difficulty and expense of having to secure water in these arid regions, new CSP sites need to consider dry cooling technologies more than ever before.

According to the DOE, U.S. (2010) studies have shown that plant location as well as power plant type affect the efficiency and cost associated with dry cooling. As an example a parabolic trough plant located in the Mojave Desert operating on dry cooling would produce 5% less electricity and the cost of electricity would increase by 7% - 9%. A similar dry cooled plant located in New Mexico would only see an electricity price increase of 2%, however, as the maximum daytime temperatures are lower.

Furthermore, additional studies predicted that central receiver plants would only see a reduction in efficiency of 1.3% compared to a 4.6% reduction for parabolic trough plants. This is though to be due to the higher concentration ratios and associated high operating temperatures of the central receiver plants compared to parabolic trough plants, which diminishes the effect of the increased dry cooled condenser temperature. It has also been suggested that the net present value of a dry cooled CSP plant could be improved by using a larger collector field in order to offset the lower Rankine cycle efficiencies associated with dry cooling (DOE, U.S., 2010).

It is thus concluded that although dry cooling may increase plant initial capital investment costs, as well as running costs and ultimately the final electricity price in the short term, it will most likely become a necessity for all new CSP plants in the future. Finally, the costs associated with dry cooling are both location and technology dependent, with the local micro-climate, local water availability and extraction costs, as well as demand for electricity, all playing a significant role.

For ease of comparison purposes, the above section data is summarised and presented in Table 4.1 with water consumption, relative efficiency, and electricity cost data.

Table 4.1: Comparison of Water Consumption and Relative Electricity Costs for Different Power Plants using Different Cooling Technologies. *Source of Data:* DOE, U.S. (2010)

Power Plant Type	Cooling Technology	Gallons/MWh	Litres/kWh	Efficiency Reduction*	Elec. Cost Increase
Coal / Nuclear	Once Through Wet	23 000 - 27 000**	87.06 - 102.21		
	Recirculating Wet	400 - 750	1.51 - 2.84		
	Dry Cooled	50 - 60	0.19 - 0.23		
Natural Gas	Recirculating Wet	200	0.76		
Central Receiver	Recirculating Wet	500 - 750***	1.89 - 2.84		
	Hybrid Parallel	90 - 250	0.34 - 0.95	1 - 3%	5%
	Dry Cooled	90	0.34	1.3%	
Parabolic Trough	Recirculating Wet	800	3.03		
	Hybrid Parallel	100 - 450	0.38 - 1.70	1 - 4%	8%
	Dry Cooled	78	0.30	4.5 - 5%	2 - 9%
Linear Fresnel	Recirculating Wet	1000***	3.79		
Dish Stirling	Mirror Washing	20	0.08		

* Annual energy output loss compared to most efficient cooling technology

** Majority returned to source, but at elevated temperature

*** Estimate

5 Thermal Energy Storage

5.1 Need and Motivation for Energy Storage

The solar energy received on earth's surface is not a constant, but is instead a time-dependant energy resource, affected by both the time of day and variable weather conditions. The energy demands that are met by thermal power station are also time-dependant, and vary throughout the day, but usually in a different manner to the solar energy supply. Consequently, if a solar energy generation system or CSP plant is required to meet the majority of this demand, or operate as a base-load plant, energy storage in some form will be required (Duffie and Beckman, 1974). By extending the operational hours of a CSP plant, the incorporation of energy storage can increase plant capacity factors from below 25% to above 50% and hence greatly increase a plant's dispatchability (Morse, 2009).

5.1.1 Advantages of Energy Storage in CSP Plants

The incorporation of a low capacity energy storage system in a CSP plant allows for the storage of energy as a 'buffer', which can be used to smooth electricity production considerably, as well as be dispatched during periods of intermittent cloud cover. This eliminates the short-term variations in CSP plant output, thereby increasing turbine efficiency (IEA, 2010b; Pilkington Solar International GmbH, 2000; Wagner, 2008).

A moderate size energy storage system is also beneficial in areas where peak energy demand occurs after sunset, or at a different time to the daily solar irradiation peak. In these situations, a plant can store energy during periods of high solar radiation and dispatch it later, allowing for a separation between the collection of energy and the operation of the power block. This in turn extends the operational hours of the plant without the need to burn an axillary fossil back-up fuel, and hence reduces the unpredictability in-

herent in the use of solar energy, rendering CSP technology closer to the dispatchability of a base-load plant (Pilkington Solar International GmbH, 2000; SAM, 2010; Wagner, 2008).

In some CSP plants the size of the solar field is increased relative to the rated turbine output capacity – thereby increasing the plant solar multiple – to allow the power block to operate at its rated capacity for more hours of the day. In these plants, with an absence of an energy storage system, some of the solar collectors would need to be 'defocussed' during the periods of maximum solar irradiation, as the solar field would produce more heat then the system could utilise. The incorporation of an energy storage system, however, would allow for this excess energy to be diverted to storage, thereby reducing unnecessary energy loss whilst simultaneously extending the operating hours of the plant after sunset (SAM, 2010). The discussion of the trade-off's associated with the increase in solar multiple, as well the the optimisation of CSP plant solar multiples will be presented in Section 8.8.5.

5.1.2 Method of Operation

The method of operation for energy storage in a CSP plant is fairly simple to define. Throughout the day, during periods of high solar irradiation, excess energy generated by the solar field is diverted to a storage system. During any periods of intermittent solar irradiation, and primarily after the sun sets or solar irradiation levels drop below those required to run the power block at rated capacity, the stored energy is released into the steam power generation cycle to either supplement the solar energy, or solely run the power block (IEA, 2010b).

In some instances, a backup or supplementary fossil fuel boiler is incorporated into the power cycle, to provide further energy to run the power block. This system, defined as hybridisation, is beyond the scope of this study, however, and will not be considered in any of the forthcoming analyses. The modelling of its inclusion is recommended for further studies. A graphic representation of the effect of energy storage (as well as hybridisation) on a CSP plant is shown in Figure 5.1.

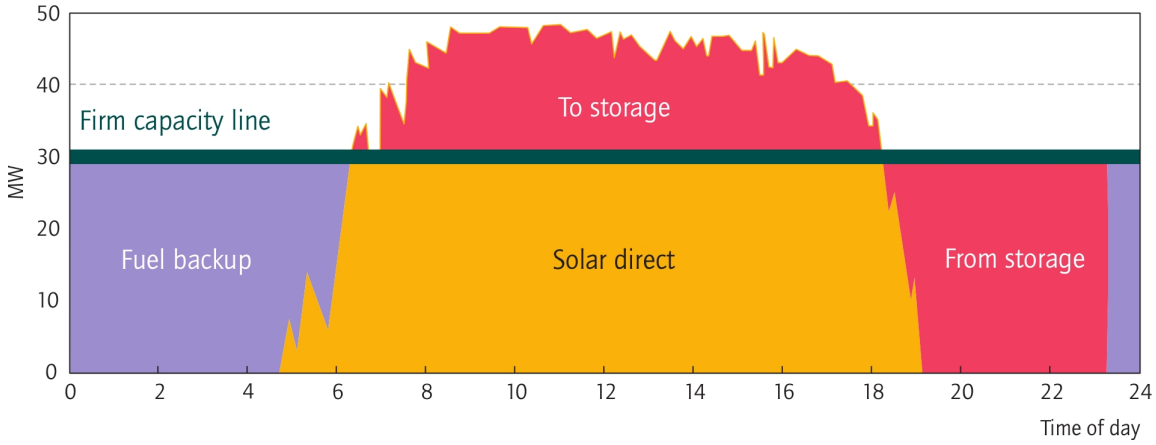

Figure 5.1: Effect of Energy Storage and Hybridisation on a CSP Plant (IEA, 2010b).

5.2 Classification of Energy Storage Technologies

5.2.1 Primary Forms of Energy Storage

Energy storage can exist in many forms, but can generally be classified according to four primary forms; namely *electrical* energy storage, *mechanical* energy storage, *thermal* energy storage (TES) and *chemical* energy storage. Of these primary forms, thermal energy storage is considered by many to be the most viable energy storage mechanism for use with CSP plants (EPRI, 2010; Morse, 2009; Wagner, 2008; Pilkington Solar International GmbH, 2000), with many of the existing commercial and pilot CSP plants already incorporating a form of TES. The characteristics, as well as advantages and disadvantages, of the remaining primary energy storage forms will thus not be discussed in this report, and instead, readers are referred to the dissertation by Morse (2009) for an in-depth review.

CSP plants therefore possess a distinct advantage when compared to other renewable energy technologies such as wind or photovoltaics, in that they produce thermal energy directly, which can easily be stored without the need to first convert energy from another form. The direct storage of electricity generated by these other technologies is considered to be far more complex and costly when compared to thermal energy storage (Pilkington Solar International GmbH, 2000; Wagner, 2008).

5.2.2 Thermal Energy Storage Mechanisms

Thermal energy storage can be classified according to three main storage mechanisms, namely; *sensible-heat*, *latent heat* – or phase change materials (PCMs), and *thermo-chemical*. Each one of these mechanisms can be further classified as *active* or *passive* depending on the storage design (Pilkington Solar International GmbH, 2000; Stine and Geyer, 2001).

Sensible-Heat Storage

Sensible-heat storage refers to the process of storing energy by increasing the the temperature, and thus internal energy, of the storage medium. The magnitude of energy stored by the medium can be calculated by the product of the mass, average specific heat and temperature change of the medium. Sensible-heat storage systems usually employ solids or liquids as the heat storage medium, however combinations resulting in mixed-media storage are also used (Pilkington Solar International GmbH, 2000; Stine and Geyer, 2001).

Typical examples of sensible-heat storage technologies include solid media such as concrete, packed-bed media such as rock and sand, as well as mixed-media systems comprising a packed bed with a liquid such as thermal oil. Mixed-media systems generally make use of thermal stratification; however, parasitic losses and high pressure drops are some of the disadvantages associated with this system (Pilkington Solar International GmbH, 2000).

Other examples include the use of liquids for sensible-heat storage. Water can be used to generate high pressures steam for storage purposes, however, thermal oils and molten salts are often used due to their higher temperature limits. Liquids used for TES can either be stored in single tanks, making use of thermal stratification, or alternatively in a two-tank system. Due to concerns over the negative environmental impacts of synthetic thermal oils, molten salts are often preferred; however, due to their higher melting points, auxiliary heaters are required to prevent freezing (Pilkington Solar International GmbH, 2000). More detailed descriptions of some of the sensible-heat storage technologies, however, will be give in Section 5.3.

Latent Heat Storage

Latent heat storage is based on the principle that energy can be released or absorbed nearly isothermally during the phase change of a material. This phase change can be from solid-to-liquid, liquid-to-vapour, or solid-to-solid crystalline, however, in terms of CSP thermal storage, solid-to-liquid phase change materials (PCMs) are most common. One of the major advantages of using PCMs for energy storage is that the latent heat of fusion is typically much higher than the sensible-heat, which allows for a greater energy density of the storage media. This in turn allows for a reduction in volume and size of latent heat storage systems when compared to single-phase sensible-heat systems, thereby reducing material costs (Duffie and Beckman, 1974; Pilkington Solar International GmbH, 2000; Stine and Geyer, 2001).

The selection of a suitable PCM is a difficult task, however, as the material must be able to sustain a large number of phase change cycles without degrading. Furthermore, as a PCM can exist in solid phase, it is not possible to circulate the storage media directly as the HTF. Instead, a separate cycle is required, with additional heat exchangers carefully designed to accommodate the typically low thermal diffusivity of the solid material. This ultimately results in an increased system cost (Stine and Geyer, 2001).

As latent heat energy storage is nearly an isothermal process, the storage media remains at a fairly constant temperature whether charging or discharging. Conversely, sensible-heat storage systems typically undergo a large temperature change during charging or discharging, rendering them more suited to conditions in a high temperature CSP plant. The lower temperature latent heat storage systems are thus deemed more suited to applications which required constant temperatures and compact designs. According to Stine and Geyer (2001), due to the high cost of latent heat storage systems, as well as the availability of sensible-heat storage systems, latent heat storage systems have yet to be widely adopted in high-temperature CSP systems.

Thermochemical Storage

A thermochemical energy storage system is based on the principle of using heat to drive completely reversible, endothermic chemical reactions, thereby storing energy. As the rupture of chemical bonds is highly energy intensive, this mechanisms results in a storage media with a high energy density. The products of the thermochemical reaction are also typically non-reactive at ambient temperatures, and can be stored separately, rendering them suitable for long term energy storage. When energy is required from storage, the reaction can be reversed at elevated temperatures, releasing the stored energy in the

process. Catalysts are also sometimes required to release the stored energy, adding to the level of system control (Duffie and Beckman, 1974; Pilkington Solar International GmbH, 2000; Stine and Geyer, 2001).

Some of the key advantages of thermochemical energy storage comprise its associated high energy density, nearly infinite storage potential as a result of the chemical product stability at ambient temperatures, and the potential to create 'solar-fuels' such as hydrogen, which can be easily transported. However, although thermochemical energy storage systems are theoretically promising, uncertainties regarding the thermodynamic properties of the reaction components and long term reversibility of the reactions, have resulted in it being far from the point of adoption in CSP plants. As of writing, there are currently no utility-scale commercial CSP plants employing thermochemical energy storage (Pilkington Solar International GmbH, 2000; Stine and Geyer, 2001).

5.2.3 Thermal Energy Storage Design Concepts

Direct and Indirect Active Systems

In an active TES system, the storage medium itself circulates, and is generally characterised by forced convection heat transfer. Active systems also usually make use of tank storage to contain the storage medium.

An active system can be further subdivided into *direct* and *indirect* systems. In a direct system, the heat transfer fluid (HTF) itself – which receives energy from the solar field – serves as the storage medium, eliminating the need for an additional storage medium and heat exchangers. Conversely, an indirect active system makes use of a separate secondary loop containing a storage medium, which is charged and discharged by the HTF via means of heat exchangers (Pilkington Solar International GmbH, 2000; SAM, 2010).

Passive Systems

A passive TES system – also referred to as a regenerator – differs from an active systems in that the storage medium itself does not circulate. Instead, the HTF passes through the storage medium only when charging or discharging. Passive systems usually make use of dual-medium storage, which can comprise liquids, solids or PCMs. A disadvantage with passive systems, however, is that the heat transfer rates are low, especially when using solid media, and there is usually no direct contact between the HTF and storage media as a result of heat exchangers (Pilkington Solar International GmbH, 2000).

5.3 Thermal Energy Storage Technologies

As a means of concluding the review of thermal energy storage, this final section will present and briefly outline the method of operation for some of the more prominent TES technologies.

5.3.1 Molten Salt Energy Storage

Indirect Two-Tank Molten Salt System

In an indirect two-tank molten salt system, thermal energy from the solar field is circulated by means of an HTF – typically a synthetic thermal oil – in a separate cycle to the storage system. During periods of peak solar irradiation, excess heat collected by the synthetic oil HTF is directed via heat exchangers to molten salt in the storage system cycle. During the charging process, the molten salt flows from the cold tank into the hot tank, where it is stored for later use. When additional energy is required to drive the power block, the hot salt flows back from the hot tank, through the storage system heat exchangers, to the cold tank, adding additional energy to the HTF. The energy from the synthetic oil HTF passes through an additional heat exchanger used to heat water and generate steam for the Rankine power cycle (Sargent & Lundy, 2003). This process, usually adopted in parabolic trough plants, is illustrated graphically in Figure 5.2.

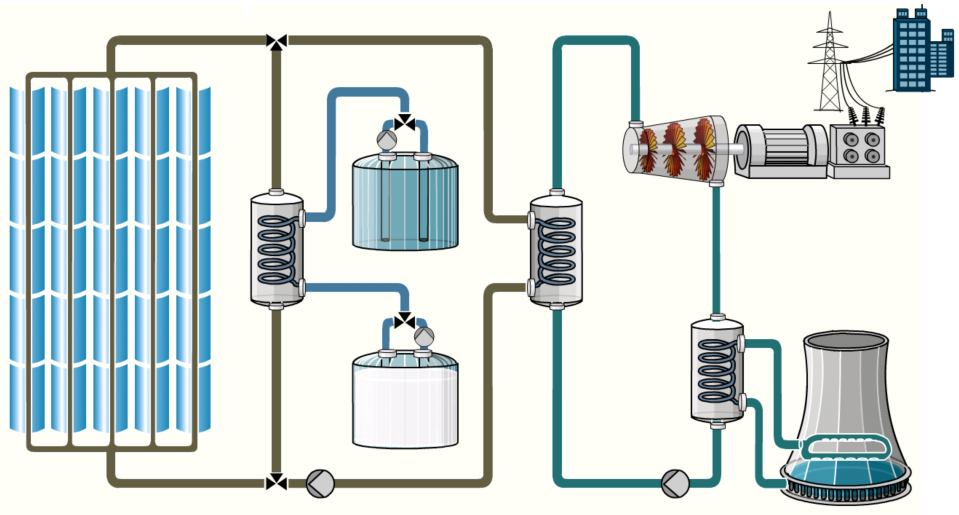

Figure 5.2: Schematic of Parabolic Trough Plant with Two-Tank Indirect Molten Salt Storage (Solar Millennium AG, 2011).

Direct Two-Tank Molten Salt System

Unlike the indirect molten salt storage system with synthetic oil HTF adopted by parabolic trough systems, some central receiver CSP plants adopt a direct molten salt system, where the HTF is the same fluid as the storage media. This allows for the direct thermal energy storage of the HTF itself, resulting in a substantial cost reduction through the elimination of the oil-to-salt heat exchangers (with their associated parasitic losses) as well as the need for thermal oil (EPRI, 2010).

In such a system, liquid salt at 290 ℃ is pumped from the cold storage tank through the receiver, where it is heated to 565 ℃. The heated molten salt then flows to the hot tank where it is stored for later use. When additional energy is required to drive the power block, the hot salt is pumped from the hot tank through the steam generating heat exchangers, used to heat water and generate steam for the Rankine power cycle. Once through the heat exchanger, the salt is then pumped back to the cold tank where it is stored until pumped back through the receiver for reheating (Sargent & Lundy, 2003). This process is illustrated graphically in Figure 5.3.

Images of a two-tank molten salt storage system under construction at the Andasol I parabolic trough plant in Spain, and a direct two-tank system at the Solar Two central receiver plant in the U.S. are shown in Figure 5.4

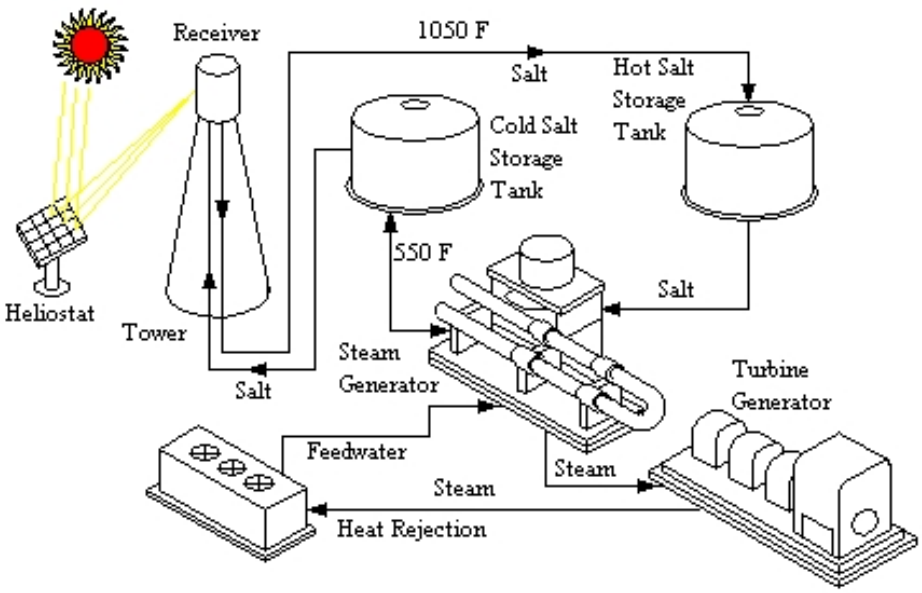

Figure 5.3: Schematic of Central Receiver Plant with Two-Tank Direct Molten Salt Storage (Sargent & Lundy, 2003).

Figure 5.4: Two-Tank Molten Salt Storage at Andasol I in Spain and Solar Two in the United States. *Source of Images:* Müller-Steinhagen (2011) and Meyer (2010).

5.3.2 Thermal Oil, Rock and Sand Thermocline Systems

As a means to reduce thermal energy storage costs associated with two-tank systems, thermocline system make use of a single tank to store both the hot and cold storage medium. This system relies on thermal buoyancy to maintain thermal stratification, with the hot fluid remaining at the top of the tank and the cold fluid sinking to the bottom. The boundary area within the tank where the hot and cold fluids meet is defined as a thermocline (Brosseau et al., 2004; NREL, 2011a; SAM, 2010).

As a means to reduce the thermal storage fluid volume – and thus further reduce costs – the single tank can be filled with a low-cost packed-bed filler material, comprising rock and sand, or potentially, other materials. This low-cost filler material then becomes the primary energy storage media in the mixed-media system, with a liquid such as thermal oil circulating through it (Brosseau et al., 2004; NREL, 2011a).

A thermocline system can either act as a direct system, with the HTF fluid itself flowing through the storage media when charging, or alternatively it can be adopted as an indirect system, utilising a separate thermal storage fluid such as thermal oil. The Solar One central receiver CSP plant in the U.S. utilises thermal oil combined with rock and sand in a single tank thermocline TES system (Brosseau et al., 2004; Meyer, 2010). A schematic of an indirect thermocline system is presented in Figure 5.5 while an image of the Solar One single tank storage system is shown in Figure 5.6.

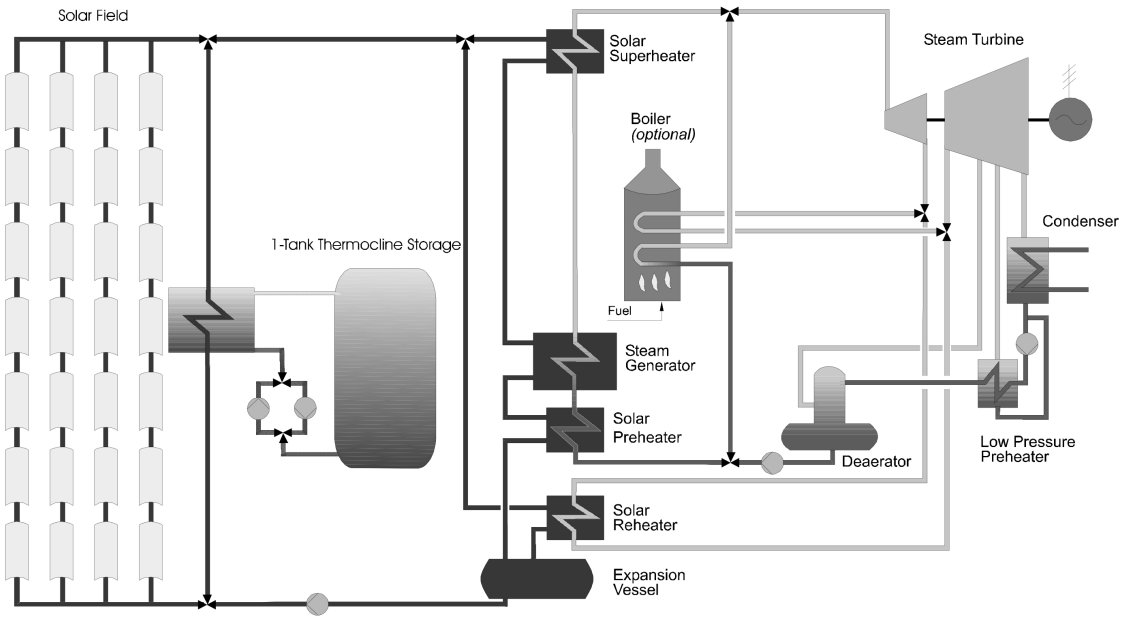

Figure 5.5: Schematic Diagram of Indirect Thermocline Energy Storage (Herrmann et al., 2002).

Figure 5.6: Solar One's Single-Tank Thermocline Energy Storage Comprising Thermal Oil, Rock and Sand (Meyer, 2010).

5.3.3 High Pressure Steam Storage

In plants which make use of water as the HTF – hence operating as direct steam generation systems – it is possible store the high pressure steam itself in a direct steam thermal energy storage system. The high pressure saturated steam is stored in a number of tanks, depending on their level of charge. During periods of intermittent solar irradiation, the stored energy in the steam storage tanks is release to power the Rankine cycle turbine (SolarPACES, 2011).

This method of direct steam storage was adopted in the PS10 central receiver plan in Spain, and allowed for a storage capacity of 20 $MWh_{thermal}$ – which equates to 50 minutes of turbine operation at 50% load (Meyer, 2010; SolarPACES, 2011). Direct steam storage systems – also referred to as a steam accumulators – are only economically suitable as buffer storage devices, however, and are not economically applicable for long term energy storage (Morse, 2009). A schematic of a central receiver with direct steam storage is presented in Figure 5.7, while an image of the four steam storage tanks at PS10 plant in Spain is shown in Figure 5.8.

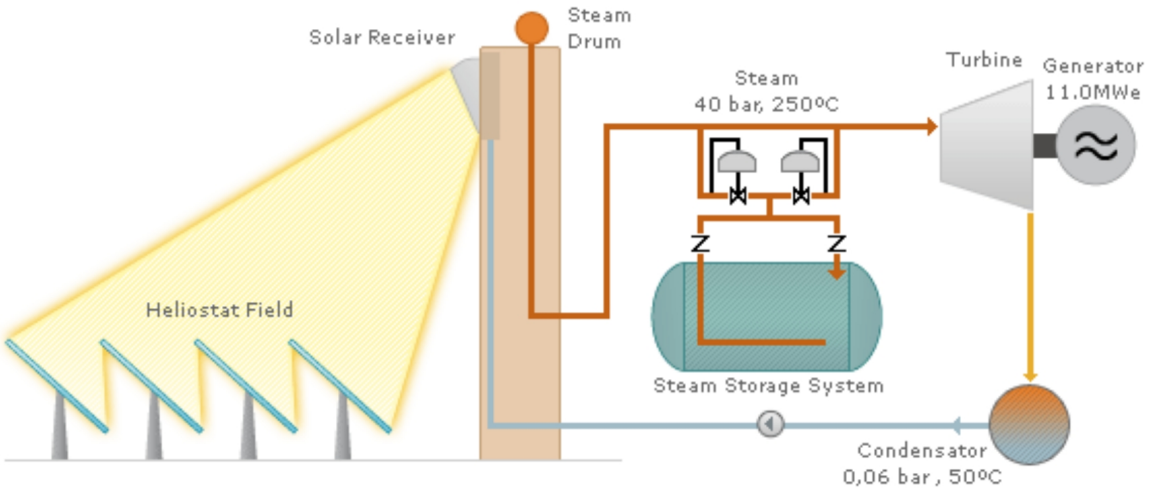

Figure 5.7: Schematic Diagram of Central Receiver Plant with Steam TES (IEA, 2007).

Figure 5.8: The Four Steam Storage Tanks at the Base of the PS10 Central Receiver Plant (SolarPACES, 2011).

5.3.4 Concrete and Solid Media Storage

As a means to reduce the cost of thermal energy storage system, as well as increase their modularity, the German Aerospace Center (DLR) has been conducting research into the use of solid media storage devices comprising concrete, or cast ceramics. In such a system, the standard HTF fluid from the solar field is circulated through an array of pipes embedded in the solid storage medium, thereby transferring the thermal energy to and from storage during the charging and discharging processes (DLR, 2003; NREL, 2011a).

As previously stated, the main advantage of such a system over other TES systems is the low cost of the storage media, however, primary issues such as large pressures drops, low thermal transfer rates, and maintaining good contact between the concrete and piping do exist (NREL, 2011a; Pilkington Solar International GmbH, 2000). A schematic of a concrete energy storage system is depicted in Figure 5.9, while images of concrete storage test blocks from the DLR are shown in Figure 5.10.

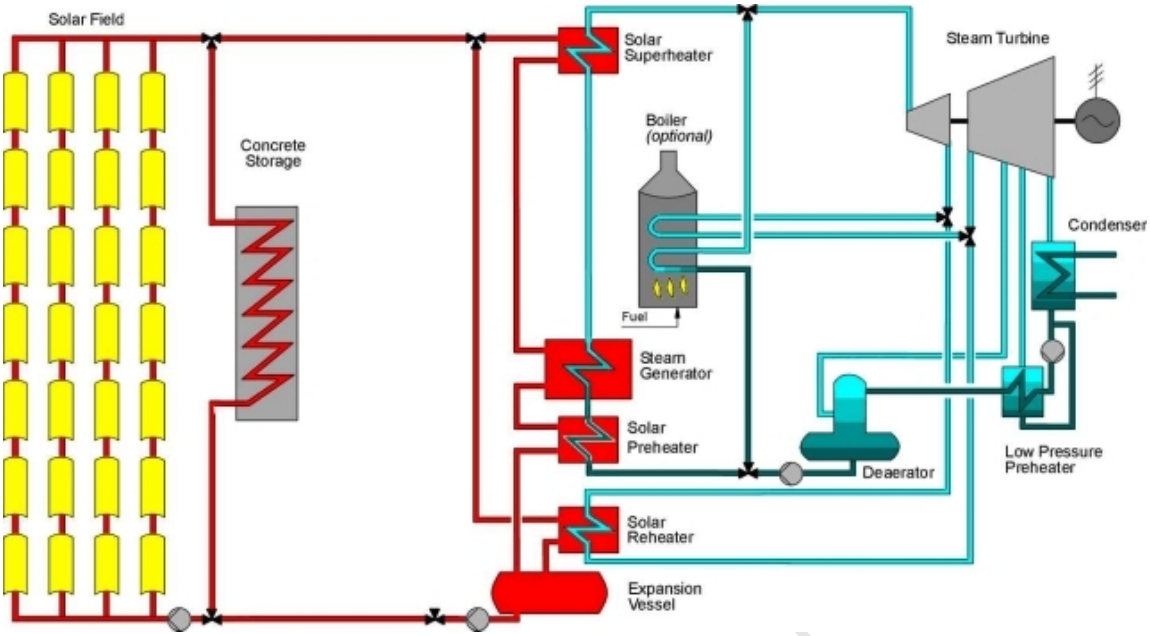

Figure 5.9: Schematic of a CSP Plant with Concrete TES (Herrmann et al., 2002).

Figure 5.10: Concrete Storage Test Blocks (DLR, 2003).

5.3.5 Phase Change Materials

The use of phase change materials (PCMs) in a storage system allows for large amounts of energy to be stored in relatively small volumes, resulting in low energy storage costs. Although PCMs were initially considered for use with thermal oil parabolic trough plants, research conducted by the DLR has shown them to be more suitable for use with direct steam generation parabolic trough plants (NREL, 2011a).

In such a system, a single PCM material – chosen such that its phase change occurs in the temperature region of the HTF thermal source – is either encapsulated within a highly conducive thermal solid, or within a matrix of expanded graphite (Morse, 2009). The HTF fluid from the receiver then flows through a heat exchanger embedded in the PCM storage, allowing for charging and discharging of the storage media. Due to the complexity of these systems, however, further research on the use of PCMs is still being conducted (NREL, 2011a). A graphic representation and an image of a salt PCM latent heat storage module is presented in Figure 5.11.

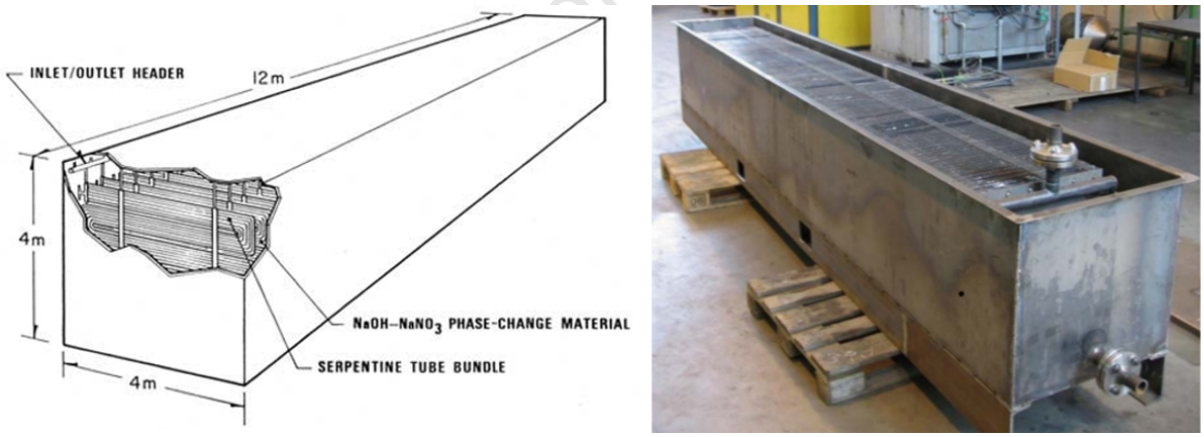

Figure 5.11: Latent-Heat Thermal Energy Storage Module with Salt PCM. *Source of Images*: Stine and Geyer (2001) and Müller-Steinhagen (2011).

6 Site Location and Geographic Information Systems Analysis

6.1 Overview of GIS Software and Analysis

A Geographic Information System (GIS) is defined by ESRI (2010b) as the integration of hardware, software and data, which is used for the capture, management, analysis and display of all forms of geographically referenced information.

As previously stated, the use of GIS software to identify and quantify potential CSP sites is becoming more common, as it allows for one to visualise, analyse and interpret data in a unique and efficient manner. This in turn not only renders trends and relationships in data more evident, but also allows for identification of locations based on specified criteria, the mapping of these locations, and the extraction and calculation of new data that would otherwise not be readily visible (ESRI, 2010b).

In this study, GIS software was used extensively to identify and quantify potential sites for CSP plants in South Africa. The GIS analysis and methodology was based on the use of a number of predefined analysis criteria, which were created and represented in the software in the form of data layers. These data layers were then used as screens, whereby the software was set to search for instances, or locations, where all of the analysis criteria were satisfied simultaneously. The search was performed at a predefined spacial resolution of 90m by 90m cells – as governed by the spacial resolution of the majority of the analysis layers. Once potential CSP sites were identified, it was then possibly to analyse and calculate various attributes, as well as depict the findings visually in topographical format. Key characteristics and attributes of the identified potential sites are also presented numerically in tabular format. The full GIS analysis and methodology will now be presented in the following sections of this chapter, while a more detailed description of the exact GIS procedure developed for this study is given in Appendix A.

6.2 Previously Conducted Studies

When considering a potential CSP site, a number of physical and topographical criteria – such as minimum solar irradiation levels and close proximity to suitable infrastructure – need to be satisfied to ensure that construction is not only possible, but also economically viable. In addition, it is imperative to consider the environmental connotations of such a project, and take precautions to avoid causing any negative impacts.

As discussed briefly in the literature review of Chapter 2, previous studies making use of GIS software to analyse CSP potential in various counties and regions have been conducted, with a more recent study by Fluri (2009) focussing specifically on South Africa. When reviewing previous GIS studies conducted by Bravo et al. (2007), Pletka et al., Dahle et al. (cited by Fluri, 2009) and Fluri (2009), it can be seen that they all make use of similar analysis criteria to a varying degree.

In their assessment of capacity and generation ceilings of renewable energy technologies for Spain, Bravo et al. (2007) required that all potential sites have a land slope of between 2% and 7% for slopes facing SE to SW and a slope below 2% for all other orientations. In addition, potential sites were considered and grouped according to average daily solar direct normal irradiation (DNI) values of 1500, 1750 and 2000 kWh/m^2/annum, which equates to approximately 4.1, 4.8 and 5.5 kWh/m^2/day respectively.

In their studies on potential CSP sites in the United States, Pletka et al. and Dahle et al. (as cited by Fluri, 2009) both required a land slope of less than 1%, and DNI values greater than 6.5 and 6.75 kWh/m^2/day respectively.

In his study on *the potential of concentrating solar power in South Africa*, Fluri (2009) stipulated a land slope of less than 1% and a daily DNI value of 7.0 kWh/m^2/day. Furthermore, Fluri also included the additional analysis criteria comprising the exclusion of: sensitive or 'threatened' vegetation areas, built-up areas, water surfaces and other unsuitable areas. Potential sites were also required to be of an area larger than 2 km^2 in order to be considered.

A final consideration for potential CSP site locations is the proximity to high voltage transmission lines and/or substations. Distances considered acceptable in the aforementioned studies range from 1 km to 25 miles (40.2 km) (Fluri, 2009). The analysis criteria of the previous studies are summarised in Table 6.1.

Table 6.1: GIS Analysis Considerations from Select Previous Studies. *Source of Data:* Bravo et al. (2007), Fluri (2009).

Reviewed Study:	Bravo et al. (2007)	Pletka et al. (2007)	Dahle et al. (2008)	Fluri (2009)
Slope (%)	$< 7\%$ (SE to SW) $< 2\%$ (other)	$< 1\%$	$< 1\%$	$< 1\%$
DNI (kWh/m^2/day)	> 4.1, > 4.8, > 5.5	> 6.5	> 6.75	> 7.0
Proximity to Transmission Lines	Not Considered	< 1.0km	< 40.2km	< 20.0km

In order to quantify the energy generation potential from the identified potential sites in South Africa, Fluri assumed a land use profile of 28 km^2/GW, with a 38.8% capacity factor for parabolic trough plants. Furthermore he assumed a specific water requirement of 3.27 m^3/MWh for the CSP plants. His study identified a vast number of suitable locations for potential CSP plants in South Africa, and a summary of the key results is given in Table 6.2.

Table 6.2: Results and Findings of Fluri's Study on the Potential for CSP in South Africa. *Source of Data:* Fluri (2009).

	Total for South Africa
Suitable Land Area (km^2)	15334.0
Power Generation Potential (GW)	547.6
Net Energy Generation (TWh/a)	1861.4
Water Requirement Wet-Cooled (million m^3/a)	6086.7

What is noted, however, is that although Fluri (2009) states that a CSP sector of this magnitude would require 6086.7 million m^3 of water per annum, the close proximity to large water bodies was not considered as a requirement for a potential CSP site in Fluri's study. Considering the previously discussed water-stressed classification of South Africa, as well as the large water requirements of wet-cooled CSP plants for cooling and mirror cleaning purposes (Cohen et al., 1999; Edkins et al., 2009), it was decided to include the proximity to large water bodies as a key requirement in this study. An initial GIS assessment was conducted by the author in a preliminary unpublished GIS study (Brodrick, 2010), however, the GIS analysis conducted and presented in this dissertation serves to improve upon and greatly extend the scope and validation of the initial investigation.

6.3 Analysis Criteria

Based on the various data layers and analysis criteria stated in the aforementioned literature, it was decided to adopt a similar GIS methodology, and make use of a similar number of data layer analysis criteria in the GIS section of this study. The multiple analysis criteria used to analyse potential CSP sites in this study will now be identified and discussed under their respective headings.

6.3.1 Solar Irradiation

When incoming solar radiation enters the Earth's atmosphere, a portion of it is scattered, resulting in ambient white light classified as *diffuse irradiation*. The remaining light, which is seen to come directly from the sun – or solar disk – consist of parallel rays capable of casting a shadow, and is classified as *direct irradiation* or *beam irradiation*. The light that is 'seen' on the Earth's surface is thus a combination of diffuse and direct irradiation, the ratio of which depends on the amount of cloud cover and other light refracting particles in the atmosphere (Boyle, 2004).

Although the diffuse irradiation portion may contain high amounts of energy, in general, CSP technologies are only capable of focussing the direct irradiation portion onto the receiver (Duffie and Beckman, 1974). Thus for the remainder of this analysis, only the level of solar *direct normal irradiation* (DNI) will be considered for the identification of potential CSP site locations.

DNI can be described as a measure of the sun's energy falling on the Earth's surface, and is quantified in the units of watt hours per square meter (Wh/m^2). As defined in Table 6.1, previous studies required a potential CSP site to have total daily DNI values in a range above 4 kWh/m^2/day (Fluri, 2009). In this analysis, three initial cases will be considered with required daily DNI values ranging from > 6.0 kWh/m^2/day, > 6.5 kWh/m^2/day and > 7.0 kWh/m^2/day, depending on the availability of water. The exact requirements, however, will be described in detail in Section 6.4.

The solar irradiation data used in this analysis was derived from satellite imagery and was processed by the United States National Renewable Energy Laboratory (NREL). The data has a spacial resolution of 40 km $\times$ 40 km with an accuracy of 10% (Fluri, 2009; SWERA, 2010). The data was made publicly available by means of the Solar and Wind Energy Resource Assessment website (SWERA, 2010).

The solar data was included in the GIS software as the first data analysis layer. Based on this data, a map depicting the average daily DNI values over South Africa for different months of the year was created, and is presented in Figure 6.1. A second map depicting the data analysis layer for the annual average daily DNI values for South Africa can be seen in Figure 6.2. From the figures it is evident that the DNI values for the summer months are considerably higher than those of the winter months, with areas in the Northern Cape receiving the highest DNI values throughout the year. It can also be seen that the Northern Cape receives average annual daily DNI values in excess of 7.0 kWh/m^2/day, which are though to be some of the highest worldwide, and in excess of areas such as California, Nevada, Morocco and Spain (Edkins et al., 2009).

6.3.2 Land Slope

Large utility-scale CSP sites generally require relatively large, flat areas of land, usually comprising areas greater than 2 km^2 in size (Broesamle et al., 2001; Morse, 2009). Of all the commercially implemented CSP plant technologies, parabolic trough plants are the most sensitive to land slope, and require flatter areas of land when compared to technologies such as central receiver systems. This is a result of parabolic troughs making use of single-axis tracking, where as the two-axis tracking heliostats used in central receiver systems provide more flexibility with regard to land slope (EPRI, 2010). In previous studies, the land slope requirement for parabolic trough plants was usually a slope of less than 1% (Fluri, 2009) – as can be seen in Table 6.1 – however, some studies such as that done by Broesamle et al. (2001) only required a land slope of 2% or less. In their study on South Africa EPRI (2010), suggest a land slope criteria of between 1% and 3%.

In this study, a land slope requirement of less than 1% was enforced, in order to allow for the consideration of both parabolic trough and central receiver CSP systems. The land slope data used in this study to create the land slope GIS analysis layer was derived from a 90 m Digital Elevation Model (DEM), courtesy of NASA's Shuttle Radar Topography Mission (SRTM), and published by the United States Geographic Service (USGS). The DEM has a spacial resolution of 90 m $\times$ 90 m.

Using this DEM data, a map depicting the percentage land slope analysis layer was created, and is shown in Figure 6.3. It is noted that a large majority of areas with between 0% and 1% slope also coincide with the regions with high DNI values in the Northern Cape, North West Province and Free State, as evident when compared to Figure 6.2.

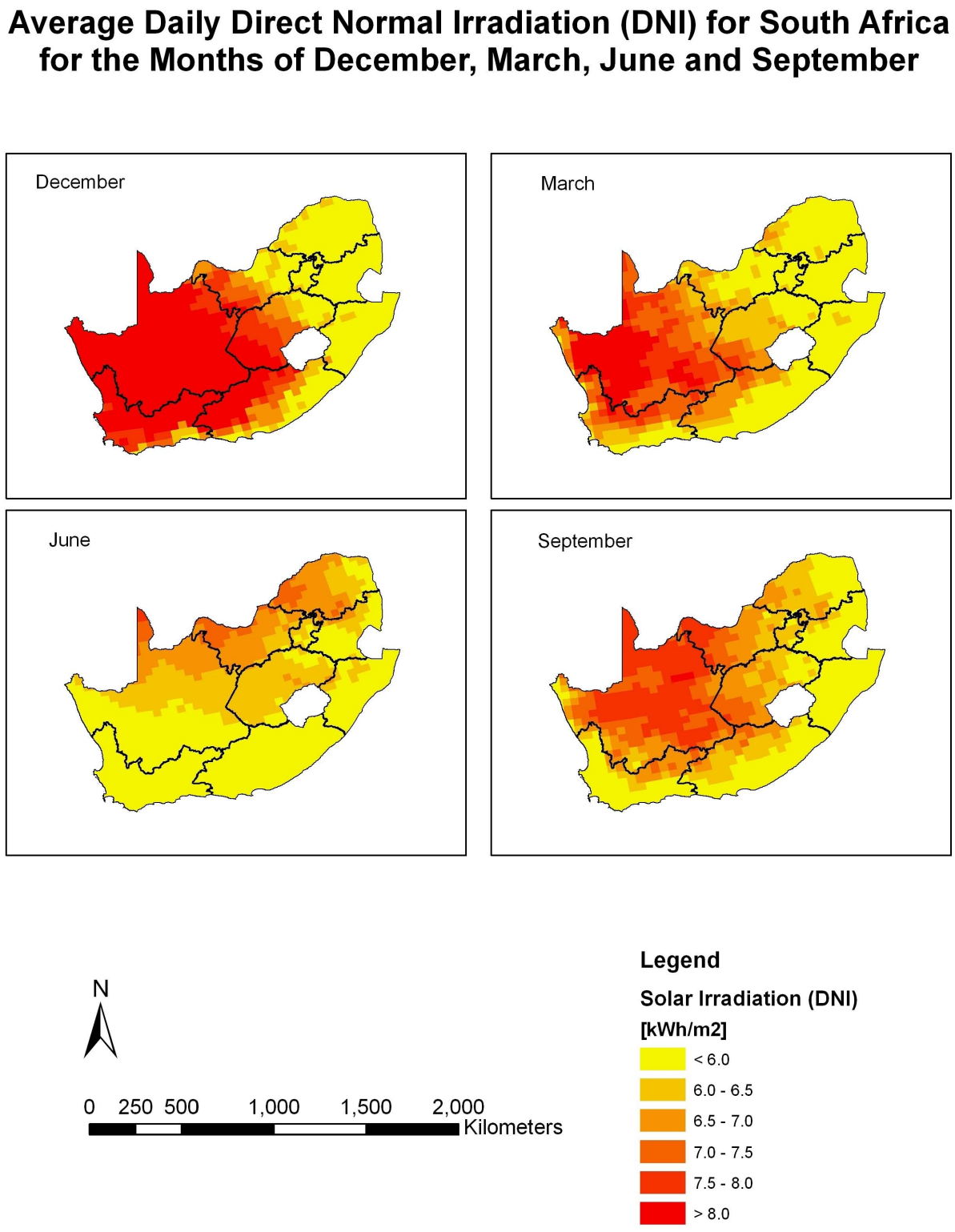

Figure 6.1: Map of Monthly Average Daily Direct Normal Irradiation (DNI) for South Africa for the Months of December, March, June and September (Brodrick, 2010). *Source of Data:* SWERA (2010) and CSIR (2001c).

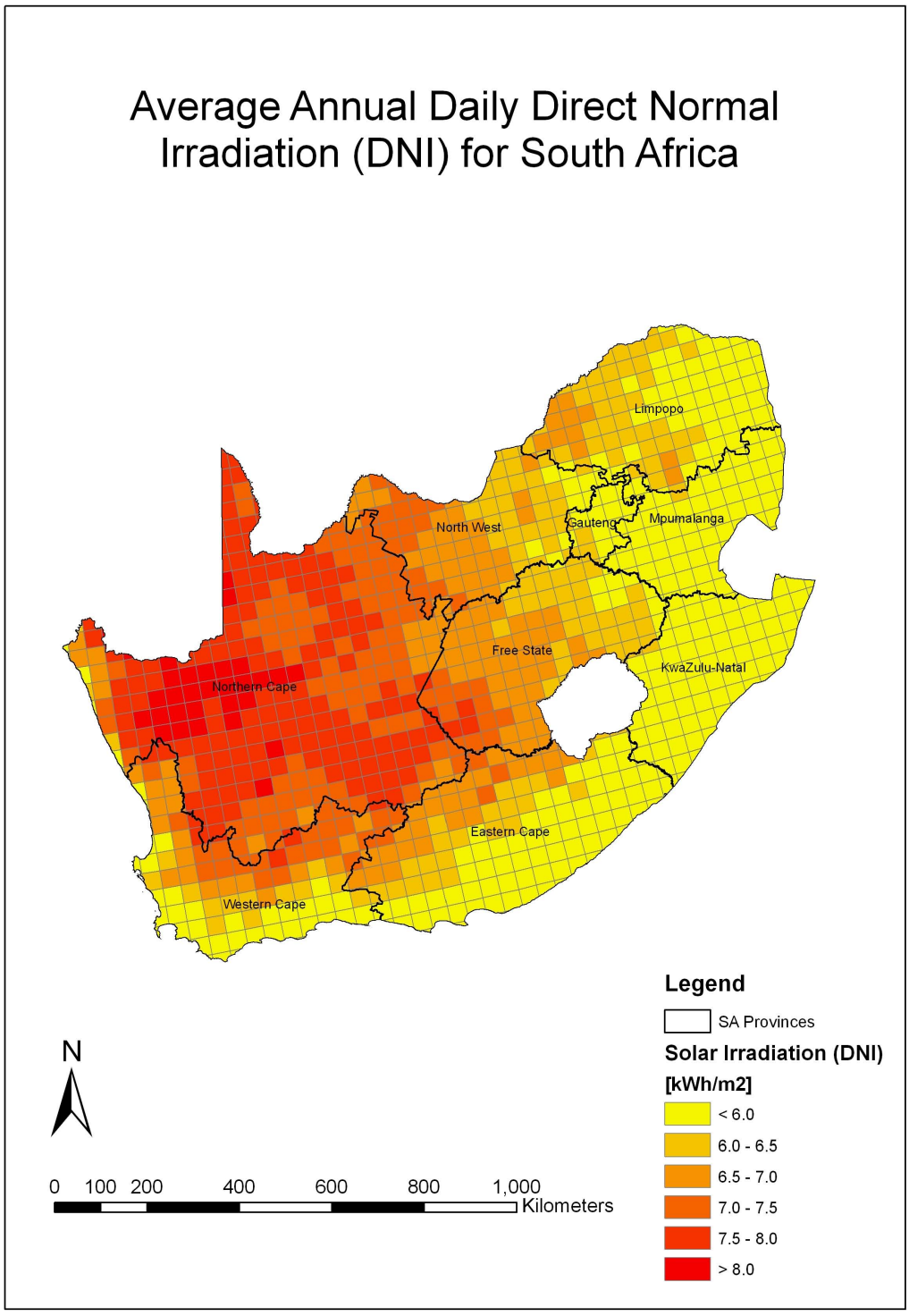

Figure 6.2: Map of Annual Average Daily Direct Normal Irradiation (DNI) for South Africa (Brodrick, 2010). *Source of Data:* SWERA (2010) and CSIR (2001c).

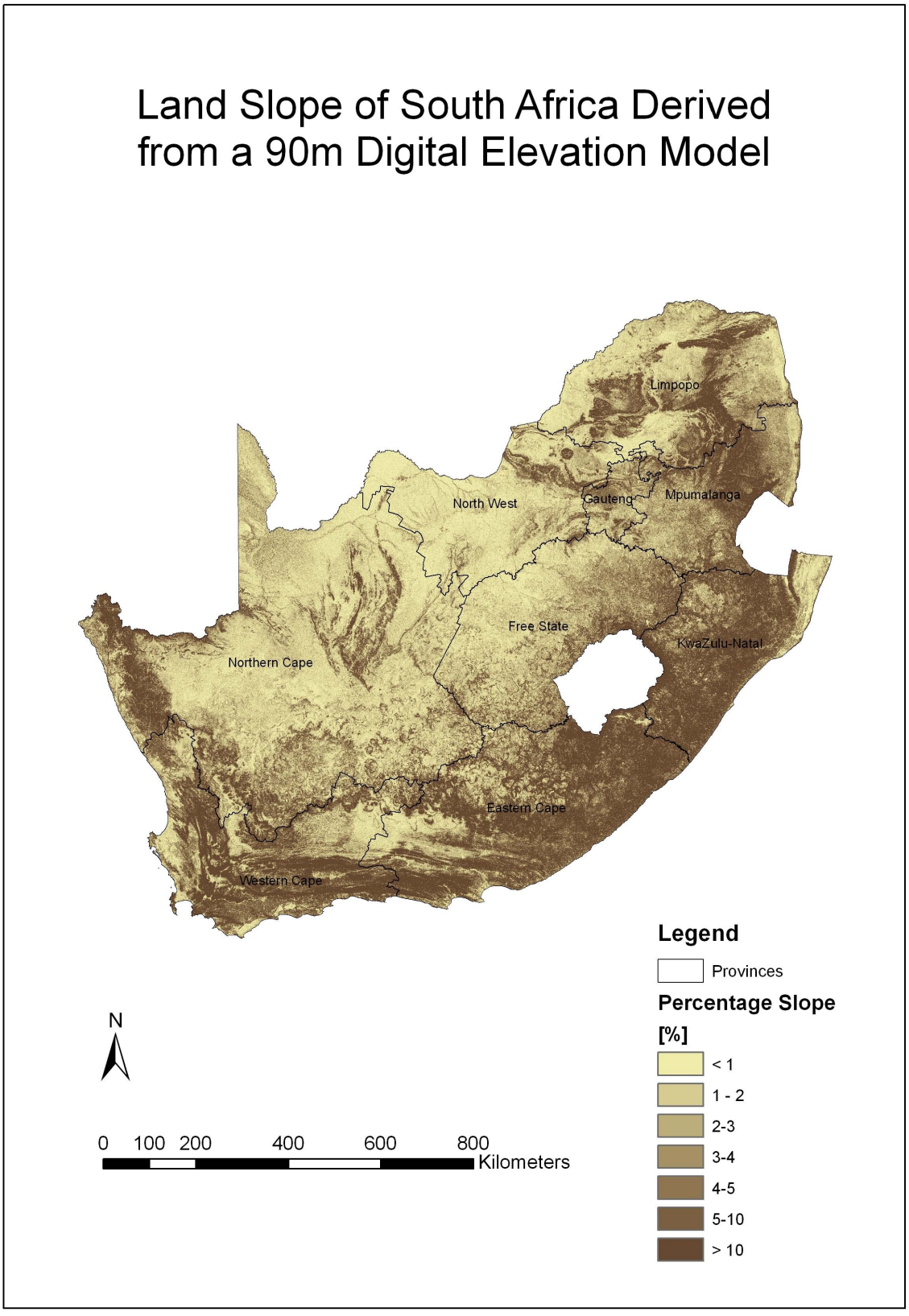

Figure 6.3: Map of the Land Slope of South Africa Derived from a 90m Digital Elevation Model (DEM) (Brodrick, 2010). *Source of Data:* SRTM (2006) and CSIR (2001c).

6.3.3 Excluded Areas

When choosing a potential suitable location for any power station, certain areas must be excluded from the analysis due to the unsuitable nature of their land class. In his study of the potential of CSP in South Africa, Fluri (2009) excluded areas such as water surfaces, built–up areas, military bases and airports.

In this analysis, land use was classified according to the *South African 30m Land Cover Data* published by the CSIR (2001a), and the following land class areas were excluded from consideration:

- Water-bodies
- Wetlands
- Forests
- Plantations
- Urban Areas

By making use of the land class data, and merging the various excluded land classes into one body of excluded areas, the excluded areas data analysis layer was created in the GIS software. A map created depicting the data analysis layer of the excluded land class areas is presented in Figure 6.4. From the figure, it can be seen that the majority of the Northern Cape – except for cultivated areas near the Orange river – is not excluded from the analysis, as it is one of the least urbanised provinces in South Africa. It is also noted, when compared to the map of Solar Irradiation in Figure 6.2, that the majority of areas with the highest DNI values coincide with the non-excluded areas.

6.3.4 Vegetation

In terms of the Environmental Impact Assessment (EIA) Regulations of South Africa, before any construction project can begin in a particular area, it must be authorised by the National Department of Environmental Affairs and Tourism (DEAT). In order to obtain this authorisation, multiple independent EIAs must be conducted, in order to minimize potentially negative environmental impacts (Eskom, 2006).

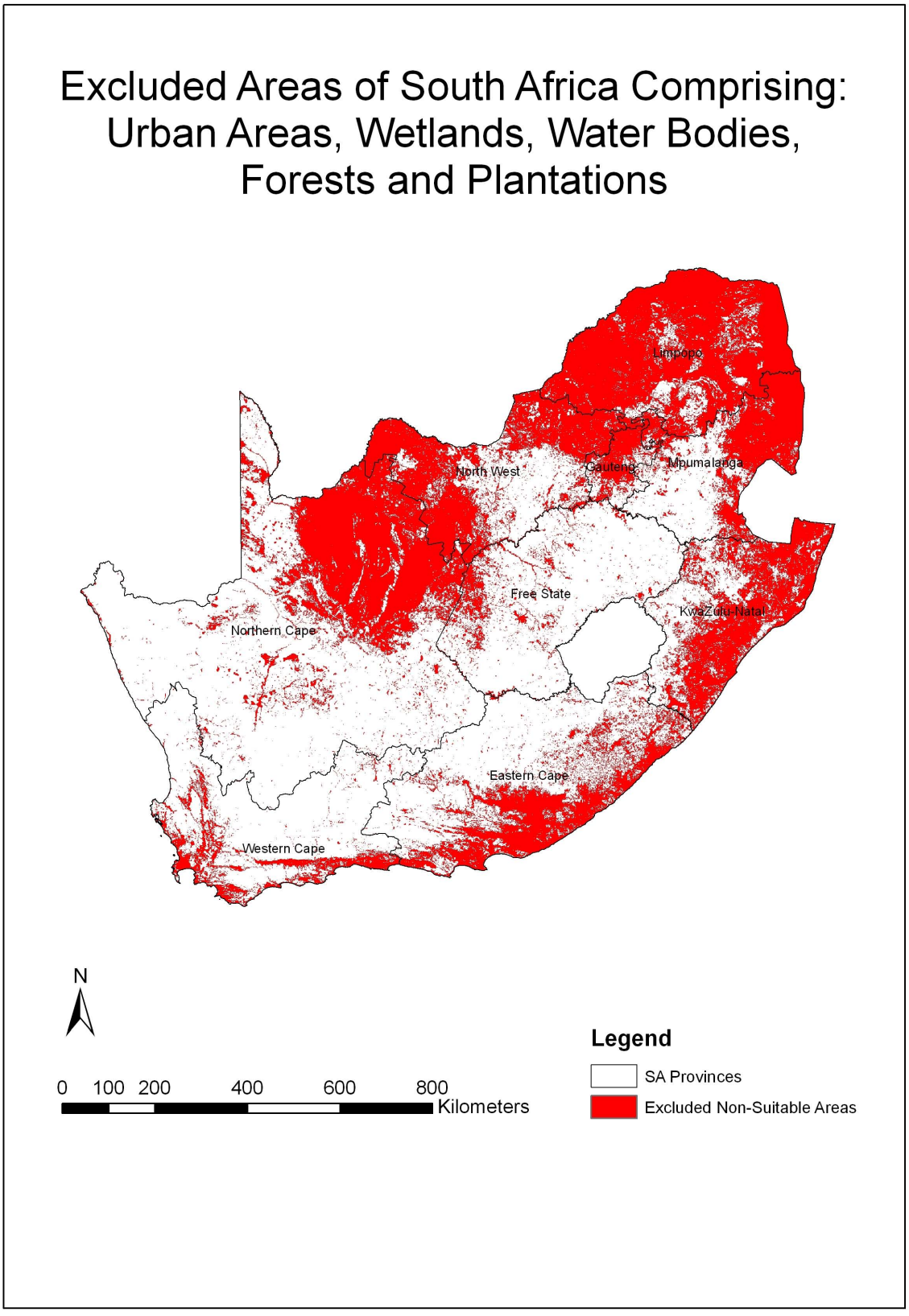

Figure 6.4: Map of Areas in South Africa Excluded from the GIS Analysis (Brodrick, 2010). *Source of Data:* CSIR (2001a) and CSIR (2001c).

Obtaining EIAs for potential sites was beyond the scope of this analysis; however, in order to reduce the likelihood of possible negative environmental impacts, potential CSP sites were only considered if they fell inside areas classed by Mucina and Rutherford (2006) as *'least threatened'* vegetation.

Using the data presented by Mucina and Rutherford (2006) in their publication, *The Vegetation of South Africa, Lesotho and Swaziland*, a data analysis layer comprising areas classified as 'least threatened' was created in the GIS software. A map was then created depicting this data analysis layer, which can be seen in Figure 6.5. It is noted, when compared to the map of solar DNI in Figure 6.2, that the majority of areas with high DNI values also coincide with the areas classed as 'least threatened' vegetation.

6.3.5 Water Availability

As previously discussed, the availability of water for plant cooling purposes is deemed an important factor for consideration in the implementation of any large CSP plant, and the analysis thereof is one of the key themes of this study. According to Edkins et al. (2009), the 100 Megawatt (MW) Central Receiver plant planned by Eskom for Upington is expected to consume in the region of 300,000 m^3 of water per annum. Furthermore, Cohen et al. (1999) state that for the Solar Energy Generating Systems (SEGS) CSP parabolic trough plants in the United States, more than 90% of water usage is a result of the Rankine power cycle cooling, while only 1.4% is used for mirror cleaning. Hence, the proximity to large water sources, water bodies and rivers was included as a data analysis layer and was considered as a requirement for some of potential CSP site locations.

In some of the GIS analysis cases, potential CSP sites were required to be situated within 20 km of a large perennial river, dam, or the Atlantic Ocean on the West Coast of South Africa. In order to represent this requirement, data comprising the *1:10,000 River and Dam Data* from the South African Department of Water Affairs and Forestry (DWAF) – supplied by the CSIR (2001b) – and the *South African River Data* from the South African Department of Environmental Affairs and Tourism – supplied by ENPAT (2000) – was used in the creation of the water proximity analysis layer. A map created depicting the data analysis layer of the 20 km buffer from large perennial rivers, dams, and the South African West Coast can be seen in Figure 6.6.

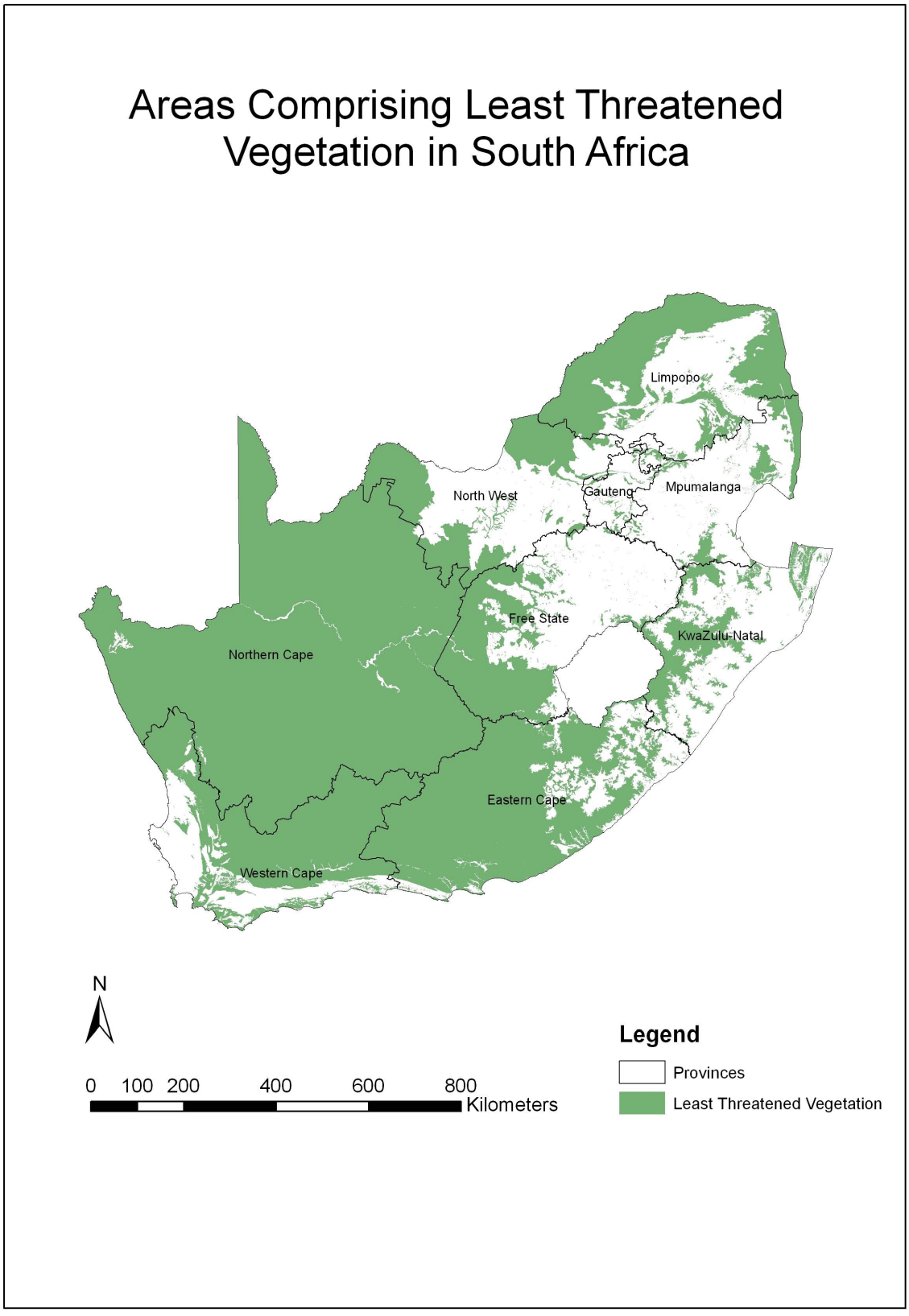

Figure 6.5: Map showing Areas of Least Threatened Vegetation in South Africa (Brodrick, 2010). *Source of Data:* Mucina and Rutherford (2006) and CSIR (2001c).

6.3.6 Proximity to Power Grid

A close proximity to high voltage transmission lines in a necessity for any large power station, in order to allow for the electricity produced to be distributed efficiently and economically to the rest of the country (Morse, 2009). Morse (2009) continues to state that for a 100 MW CSP plant, a minimum transmission line power rating of 132 kV with a line length not exceeding 100 km is required in order to reduce electrical losses. Thus for the final analysis layer criterion, and in keeping with the analysis figures used by Fluri (2009) and stated by Edkins et al. (2009), potential sites were only considered if they fell within a 20 km radial buffer from transmission lines. In addition, only transmission lines with a power rating greater than or equal to 132 kV were considered.

The data used in the creation of this analysis layer comprised the major Eskom national grid, whose spacial data in turn was implemented through the digital geo-referencing of a poster issued by Eskom (2010). A map created using this data, and depicting the analysis layer of the 20 km buffer from the Eskom national gird can be seen in Figure 6.6. It is noted that there is not a large portion or capacity of the national grid in the Northern Cape; however, according to Morse (2009) there are plans for further development of grid capacity in this region.

As a means to investigate potential areas and corridors for future grid expansion, further GIS analyses were conducted by removing the criteria for potential CSP sites to be in close proximity to the existing national grid. This method therefore allowed for the identification of potential sites that would otherwise have been excluded. Furthermore, the identification of large concentrations of sites could be used as a means to guide future grid expansion. This topic, however, will be discussed further in Section 6.5.2.

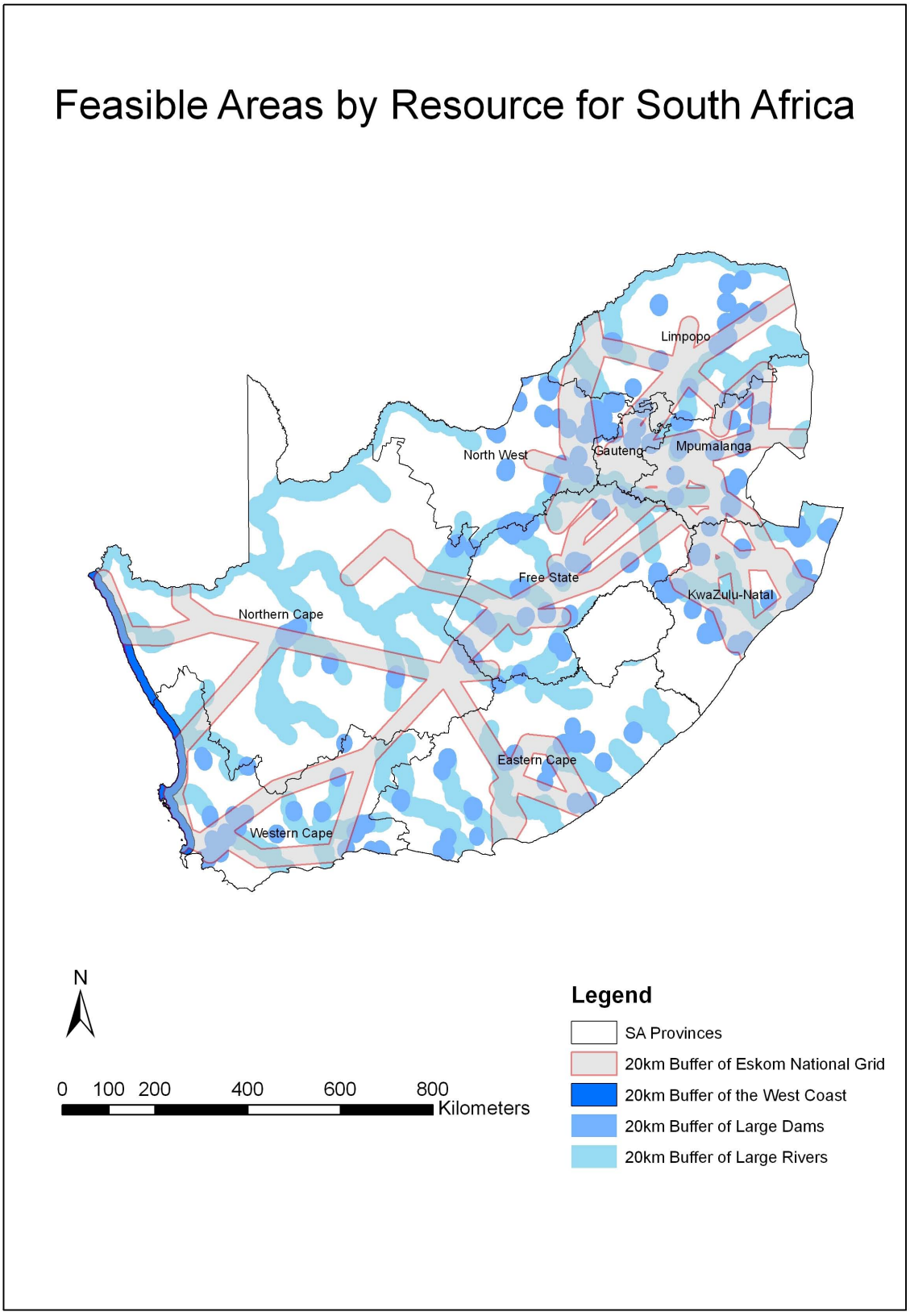

Figure 6.6: Map showing Areas in South Africa within a 20 km Radius of Large Water Bodies and of the National Grid (Brodrick, 2010). *Source of Data:* Eskom (2010), ENPAT (2000), CSIR (2001b) and CSIR (2001c).

6.4 Analysis Cases

The analysis criteria discussed in Section 6.3 were then grouped to create a number of unique analysis cases. The various analysis cases were created in order to allow for the identification of potential CSP sites with differing characteristics, depending on the criteria that needed to be satisfied. Five different analysis cases, or scenarios, were created in total, all of which will now be described and discussed in the following sections.

6.4.1 Cases Concerned with and without Proximity to Water

The initial three analysis cases were created in order to considered and identify various potential CSP sites based on the availability of water in the surrounding regions. Case 1 and Case 2 both require a potential CSP site to be within a certain distance from large water bodies, but have less stringent DNI requirements – of which Case 1 possesses the lowest DNI requirement. Conversely, Case 3 has no requirement for close proximity to cooling water – hence assuming the probable adoption of dry cooling – but requires the highest DNI levels of all the cases in order to offset the efficiency reductions if dry cooling were adopted at the site. The three cases are defined technically as follows:

Case 1: DNI > 6 kWh/m^2/d, Proximity to Large Water Bodies

- DNI greater than 6.0 kW/m^2 per day
- Less than 20 km from large water bodies
- Less than 20 km from transmission lines
- Less than 1% land slope
- Region classified as 'least threatened' vegetation
- Region not excluded due to land class restrictions of Section 6.3.3
- Site area greater than 2 km^2

Case 2: DNI > 6.5 kWh/m^2/d, Proximity to Large Water Bodies

- DNI greater than 6.5 kW/m^2 per day
- Less than 20 km from large water bodies
- Less than 20 from transmission lines
- Less than 1% land slope
- Region classified as 'least threatened' vegetation
- Region not excluded due to land class restrictions of Section 6.3.3
- Site area greater than 2 km^2

Case 3: DNI > 7 kWh/m^2/d, No Proximity to Large Water Bodies

- DNI greater than 7.0 kW/m^2 per day
- Less than 20 km from transmission lines
- Less than 1% land slope
- Region classified as 'least threatened' vegetation
- Region not excluded due to land class restrictions of Section 6.3.3
- Site area greater than 2 km^2

6.4.2 Cases Considering Future Grid Expansion

The final two cases that were considered were derived from Case 2 and Case 3 respectively, but were modified by removing the single condition for a 20 km proximity to transmission lines. This was done in order to assess the country's CSP potential if it were not limited by the location and density of the existing grid. Furthermore, the identification of large concentrations of potential CSP sites in areas without grid access could be used as a guide for possible future grid expansions, as mentioned at the end of Section 6.3.6 and described in Section 6.5.2.

Case 4: DNI > 6.5 kWh/m^2/d, Proximity to Large Water Bodies, No Grid Proximity

- DNI greater than 6.5 kW/m^2 per day
- Less than 20 km from large water bodies
- Less than 1% land slope
- Region classified as 'least threatened' vegetation
- Region not excluded due to land class restrictions of Section 6.3.3
- Site area greater than 2 km^2

Case 5: DNI > 7 kWh/m^2/d, No Proximity to Large Water Bodies, No Grid Proximity

- DNI greater than 7.0 kW/m^2 per day
- Less than 1% land slope
- Region classified as 'least threatened' vegetation
- Region not excluded due to land class restrictions of Section 6.3.3
- Site area greater than 2 km^2

6.4.3 GIS Methodology

A completed and detailed description of the GIS methodology and procedures that were developed and followed in order to successfully complete the GIS analysis – comprising the import and processing of data as well as the quantification of results – is given in Appendix A. Due to its length, and hence for the sake of brevity, the full methodology will not be presented in the body of the report.

6.5 Model Results and Identified Sites

A separate GIS analysis was conducted for each of the five analysis cases outlined in Section 6.4. The results obtained regarding the identified potential sites for each of the five cases will now be presented and discussed.

6.5.1 Identified Potential Sites with Close Gird Proximity

Case 1: DNI > 6 kWh/m^2/d, Proximity to Large Water Bodies

The identified potential CSP sites for Case 1, superimposed on the Digital Elevation Model (DEM), were recorded in topographical format and are presented in Figure 6.7. From the figure it can be initially observed that the large majority of the identified potential sites – depicted in black – fall within the boundaries of the Northern Cape, which is to be expected due to the Northern Cape receiving the highest average daily DNI levels throughout the year. Potential sites in the Free State and the Western Cape provinces are also identified; however, these to a much lesser extent.

Although not clearly visible from the country-sized scale of the map, the potential sites are constituted of a multitude of small square cells, which is a direct result of the 90m × 90m spacial resolution adopted in the analysis. Furthermore, the potential sites are not always completely uniform in shape, which is caused by the strict land slope requirement resulting in the elimination of some of the smaller 90m × 90m grid cells. These features are more evident in subsequent maps, however, which depict areas in greater detail.

When reviewing the results in conjunction with national grid data, it can be seen that the potential sites are limited by the lack of national grid capacity in the Northern Cape, made evident by the fact that all the sites are clustered around the few large transmission lines. Lack of water also plays a limiting role, however, as the only potential sites are situated close to the very few large water bodies. Although these results are expected due to the analysis criteria that were stipulated in Section 6.3, the resulting map greatly aids in coherent display of this information, that would otherwise be hard to visualise.

A final observation from this particular analysis is that only a very small portion of the West Coast appears suitable for CSP plants. This is mainly due to the combination of a lack of large grid capacity in the region, the decrease of DNI levels towards the coast, and the 'threatened vegetation' on the West Coast of the Western Cape.

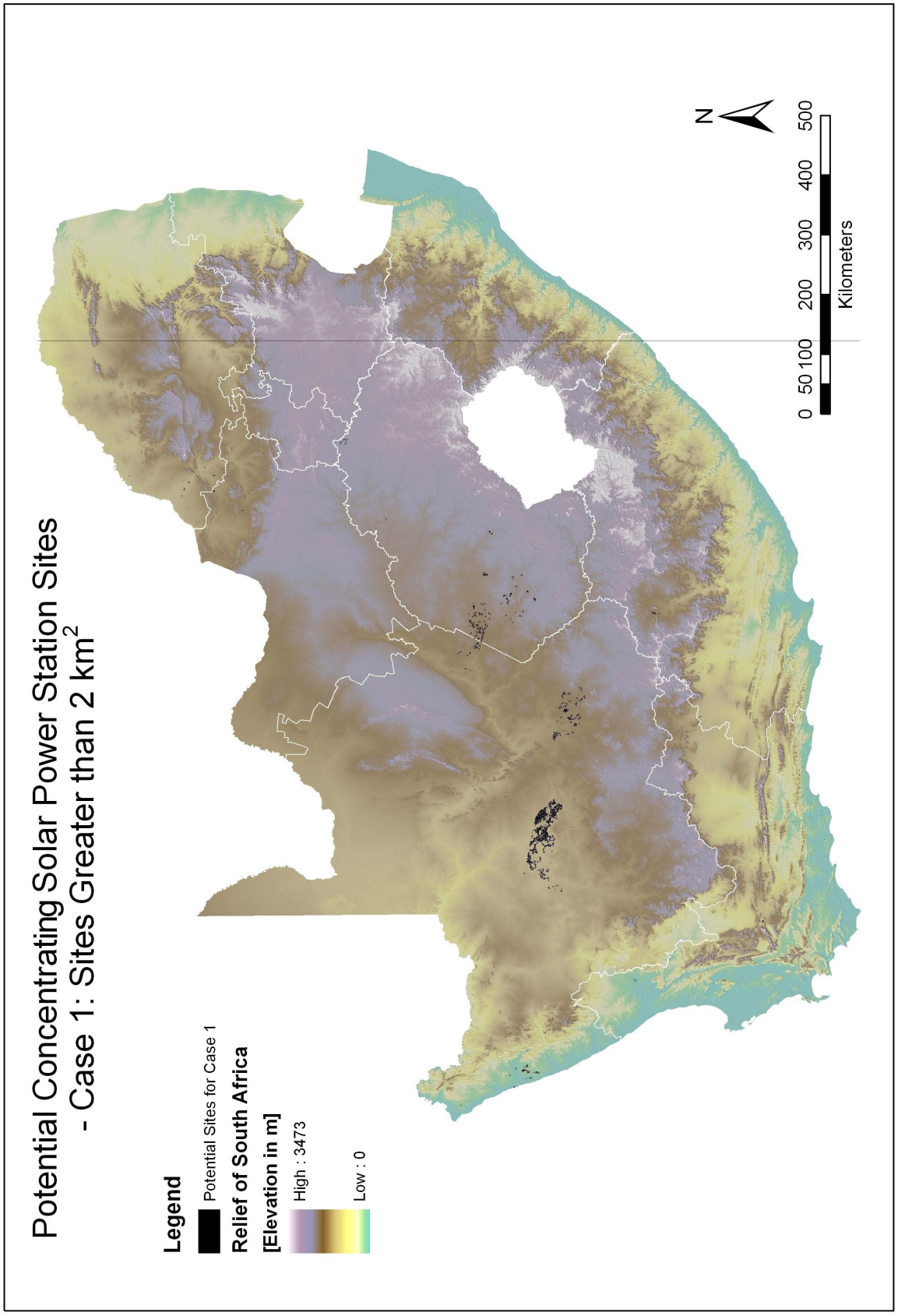

Figure 6.7: Map Identifying Potential Locations for CSP Plants in South Africa, as Governed by the Criteria in Case 1. *Source of Data:* Same as included layers.

Case 2: DNI > 6.5 kWh/m^2/d, Proximity to Large Water Bodies

The identified potential CSP sites for Case 2, superimposed on the DEM, were recorded in topographical format and are presented in Figure 6.8. From the map it is evident that the results are very similar to those of Case 1, only with a slight decrease in the total number – and area – of potential CSP sites. This is to be expected, however, as the only difference between the requirements for Case 1 and Case 2 is the higher DNI requirement of 6.5 kWh/m^2/day for Case 2, which in turn results in additional sites being excluded due to their slightly lower DNI values. For the remainder of the potential sites, the explanation is unchanged from that given in Case 1.

Case 3: DNI > 7 kWh/m^2/d, No Proximity to Large Water Bodies

The identified potential CSP sites for Case 3, superimposed on the DEM, were recorded in topographical format and are presented in Figure 6.9. It is immediately clear that, when compared to the previous two analysis cases, Case 3 produces the largest number and area of potential CSP sites. This is primarily due to the removal of the requirement for a close proximity to large water bodies, the reason being that even though the DNI requirement is increased to above 7.0 kWh/m^2/day, the Northern Cape does not possess many large water resources, but the majority of it does, however, possess solar resources in excess of 7.0 kWh/m^2/day.

The implications of this are that by reducing the need for cooling water and using alternative cooling technologies such as dry cooling, a far greater CSP potential could be realised in terms of mere number of sites and potential area. Finally, as in the previous cases, the potential CSP sites are clustered around the national grid transmission network, and the lack of extensive grid capacity in the region is again one of the limiting factors.

6.5.2 Identified Potential Sites with No Grid Proximity Requirement

As previously stated, the final two cases, Case 4 and Case 5, are derivatives of Case 2 and Case 3 respectively, but with the removal of the condition for a 20 km proximity to the national grid.

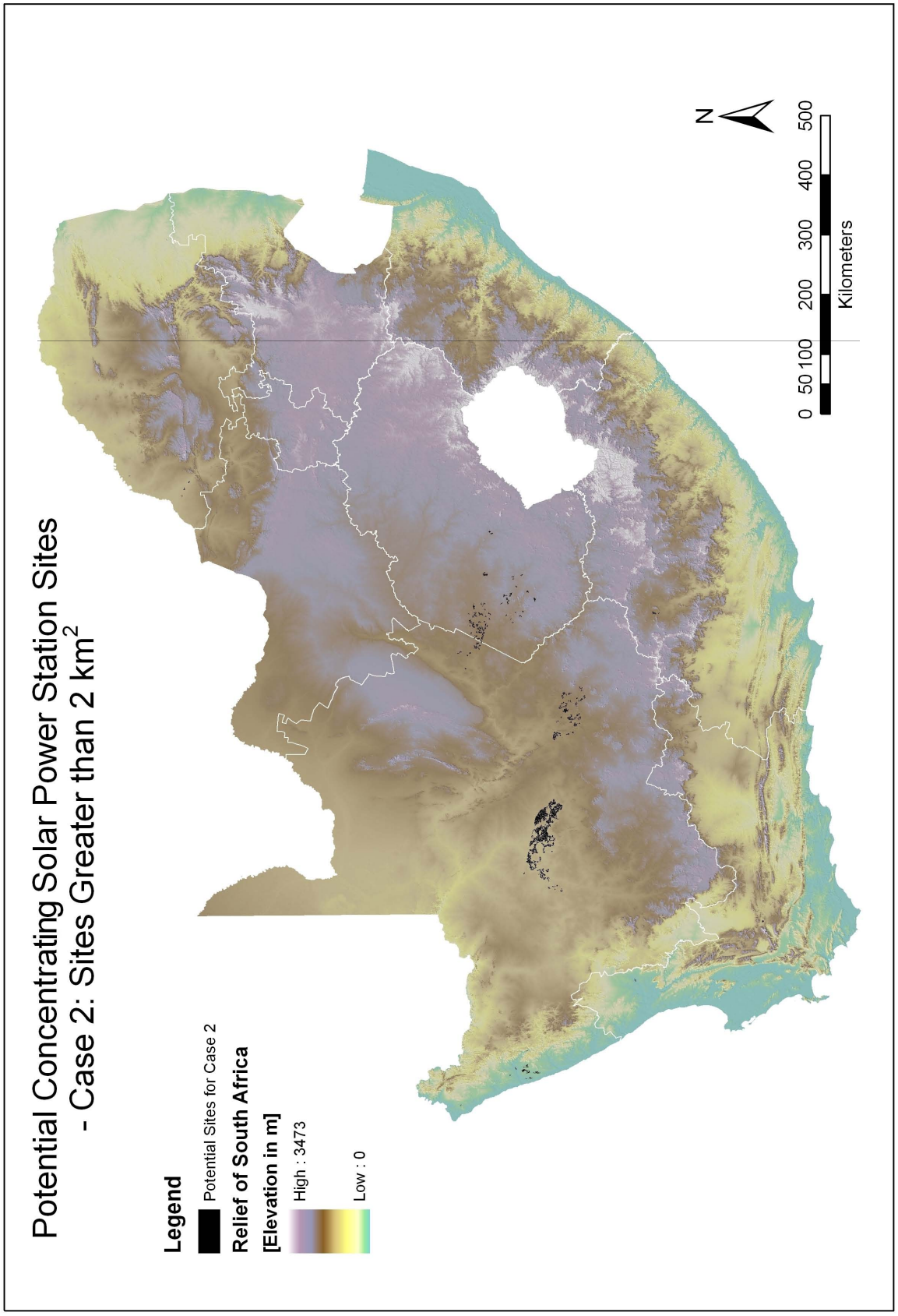

Figure 6.8: Map Identifying Potential Locations for CSP Plants in South Africa, as Governed by the Criteria in Case 2. *Source of Data:* Same as included layers.

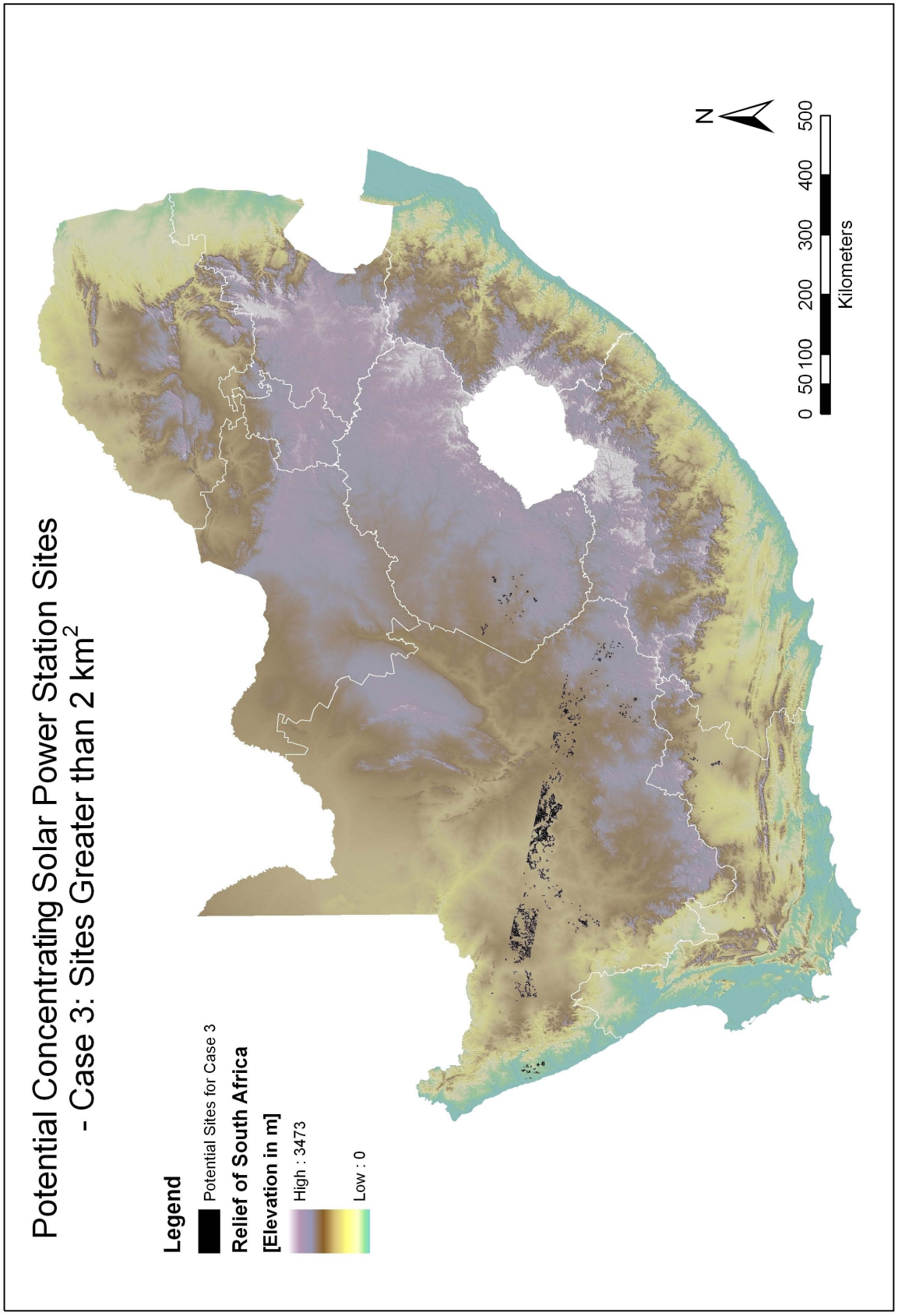

Figure 6.9: Map Identifying Potential Locations for CSP Plants in South Africa, as Governed by the Criteria in Case 3. *Source of Data:* Same as included layers.

Case 4: DNI > 6.5 kWh/m^2/d, Proximity to Large Water Bodies, No Grid Proximity

The identified potential CSP sites for Case 4, superimposed on the DEM, were recorded in topographical format and are presented in Figure 6.8. The existing Eskom national grid was also included in the map – represented by the grey dashed lines – in order to better illustrate how close the identified sites are to the existing infrastructure, as well as to highlight potential areas that may not be close to the existing grid at all.

When reviewing the map of the Case 4 potential sites, it can be seen that although there is no requirement for the potential sites to be near the existing grid, a large number of the sites are still situated fairly close, particularity in the Northern Cape. The limited distribution of sites is thought to be primarily a result of the requirement for close proximity to cooling water, as well as the strict land slope requirement. When compared to Case 2 – from which Case 4 is derived – it is clear that there is certainly a large increase in the number of identified potential sites, particularity in the Western Cape, Eastern Cape, Free State and North West Provinces, This is to be expected, however, due to the relaxation of the 20 km grid proximity requirement.

Case 5: DNI > 7 kWh/m^2/d, No Proximity to Large Water Bodies, No Grid Proximity

The identified potential CSP sites for Case 5, superimposed on the Digital Elevation Model (DEM), were recorded in topographical format and are presented in Figure 6.8. As in Case 4, the existing Eskom national grid was also included in the map – represented by the grey dashed lines.

From the map of Case 5 potential sites, it is immediately clear that the removal of both the requirements for close proximity to the national grid and large water bodies greatly increases the number of identified potential sites, with Case 5 identifying by far the largest number compared to any other analysis case. As was the situation in Case 4, a large number of the identified sites are still located fairly close to the national grid in the Northern Cape, primarily due to its high DNI values and level ground. An additional number of sites are also identified further North of the Orange River, as well as on the border between the Northern Cape and North West Province. Due to the increase in the DNI requirement to 7.0 kWh/m^2/day, however, a number of potential sites identified by Case 4 in the Free States Province have now been eliminated.

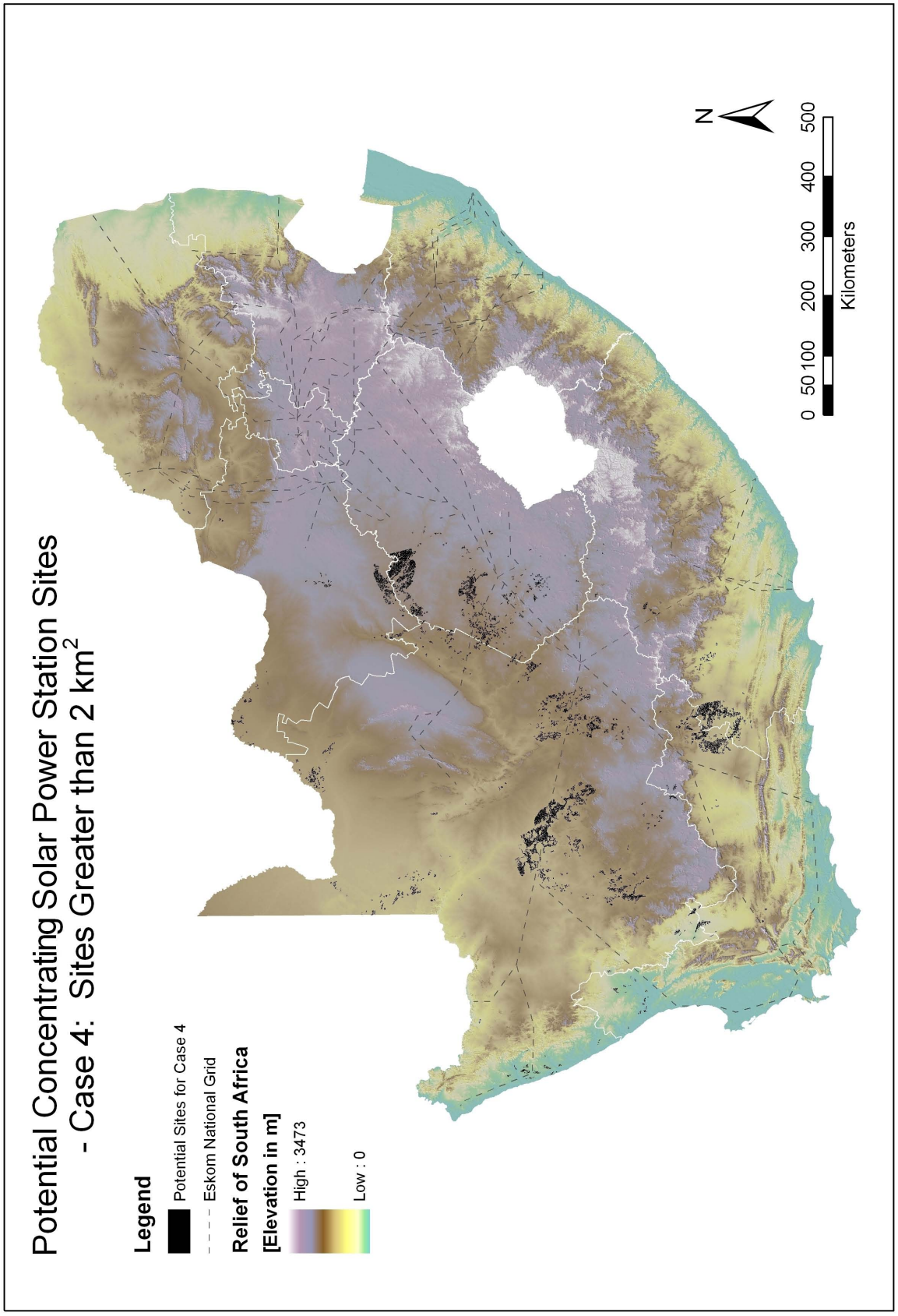

Figure 6.10: Map Identifying Potential Locations for CSP Plants in South Africa, as Governed by the Criteria in Case 4. *Source of Data:* Same as included layers.

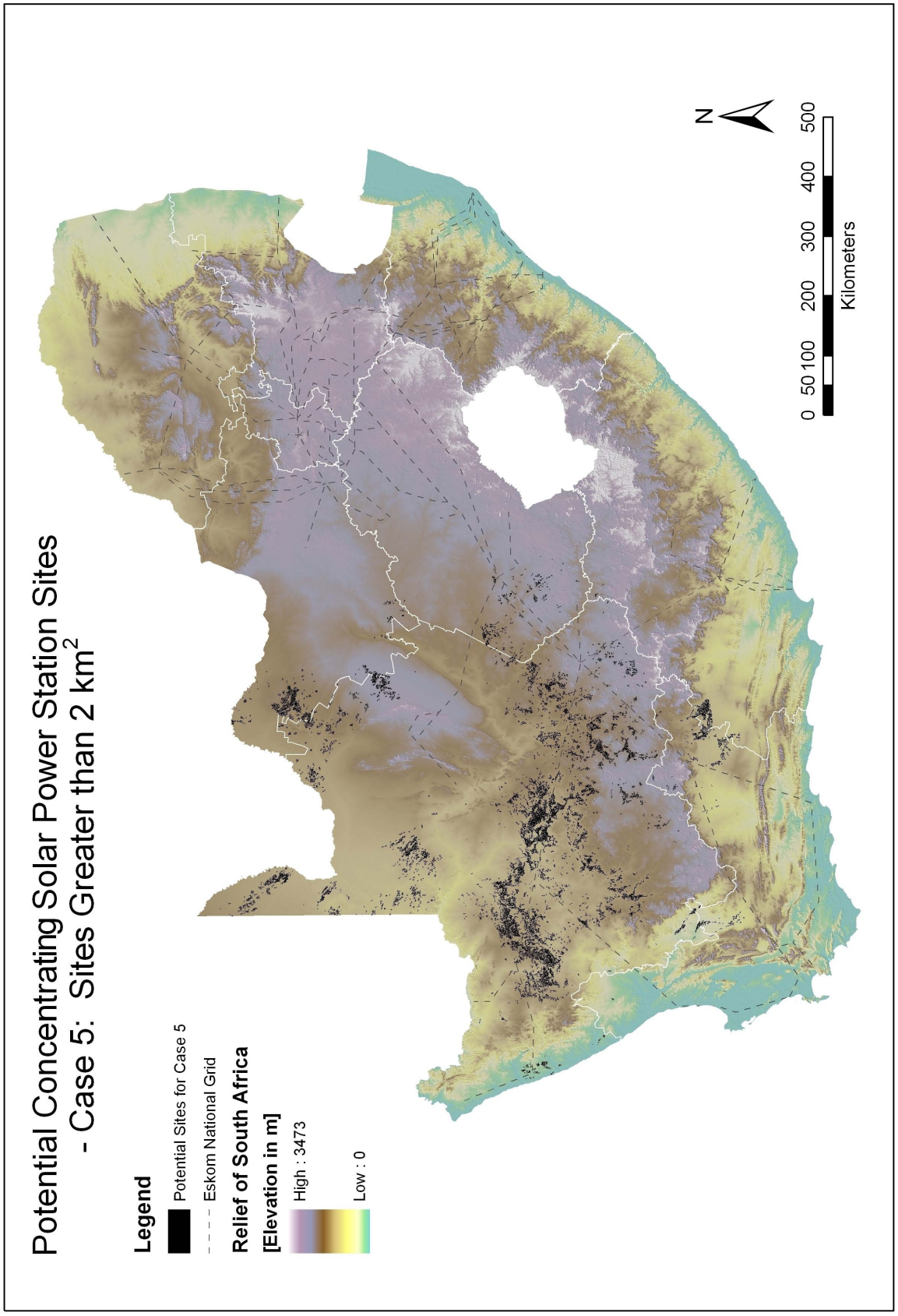

Figure 6.11: Map Identifying Potential Locations for CSP Plants in South Africa, as Governed by the Criteria in Case 5. *Source of Data:* Same as included layers.

6.5.3 Quantification and Characteristics of Potential Sites

In order to allow for the quantification of the results for the potential CSP sites, database files containing the total area, perimeter, location, and DNI values for each of the sites were created within the GIS software. The total available solar energy in terrawatt hours per day (TWh/d) was then calculated for each site by multiplying the site area by its particular DNI value. As the cell size for each analysis block is 90 m × 90 m – as dictated by the special resolution of the Digital Elevation Model (DEM) – each cell in a potential site was also assigned the identification number of the site containing it. This was done in order to overcome the possible scenario that a potential site fell across the boundary of differing DNI values on the larger 40 km × 40 km DNI grid, which would then cause the GIS software to consider it as two separate sites. The sites were then redefined according to their original site numbers, as described in Item 6 of Appendix A on page 214. This method allowed for the correct calculation of the total area and hence solar energy available for each potential site. The method is illustrated graphically in Figure 6.12.

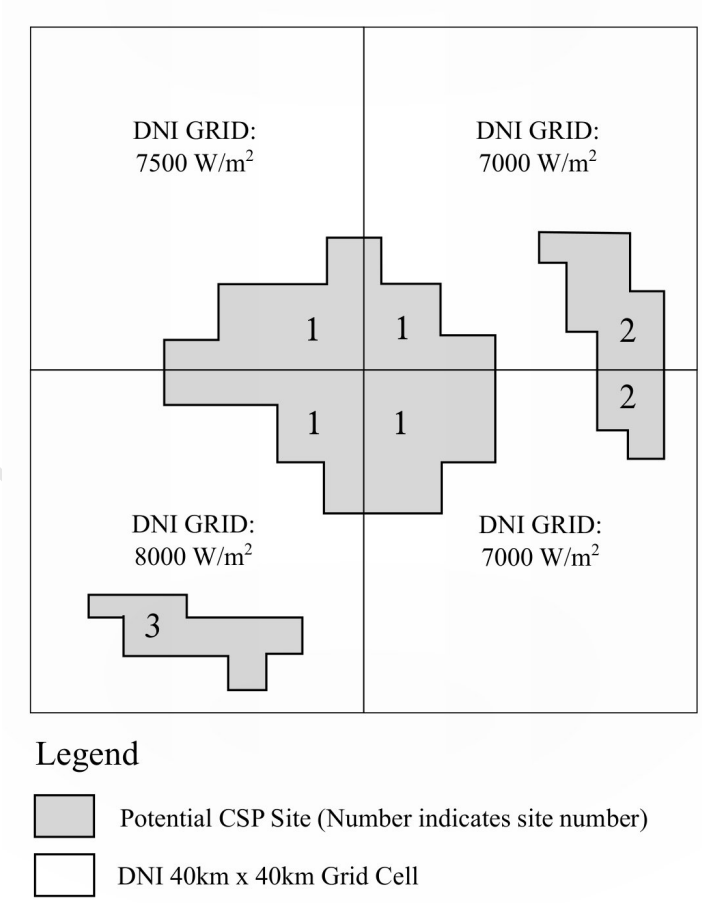

Figure 6.12: Method of Summarising Sites to Overcome Splitting by DNI Grid.

Once the total available solar energy had been calculated for each site, the total power generation potential in gigawatts (GW) was then calculated. This was accomplished by adopting a land use value of 28 km^2 per GW, in accordance with Pletka et al. (as cited by Fluri, 2009). Finally, an average plant capacity factor of 38.8% was assumed for parabolic trough plants (Fluri, 2009), while a capacity factor of 60.0% was assumed for central receivers (Winkler, H., editor, 2007), which allowed for the prediction of the net energy generation potential in Terrawatt hours per annum (TWh/a).

For the first set of calculations, all potential site areas were included in the quantification, even those with areas less than 2 km^2. Theses results are presented in Table 6.3. However, due to the extremely large amount of data produced from the Case 5 analysis when sites smaller than 2 km^2 weren't excluded, the resulting database file was too large to be completely imported and analysed in Microsoft Excel®. The Case 5 values could therefore not be included in the table. All these values were only calculated for interest sake, however, and were not deemed critical for the completion of this investigation.

For the second set of calculations, only sites with areas greater than 2 km^2 were considered and quantified, as stipulated in the actual analysis cases. These results are presented in Table 6.4. In this instance, the data for Case 5 was now small enough to be analysed completely, and its results are therefore included in the table along with those of the first four analysis cases.

Table 6.3: Total Potential Area, Average Daily DNI, Total Available Solar Energy, Power Generation Potential and Net Energy Generation (Including potential sites with areas less than 2 km^2).

	Case 1	Case 2	Case 3	Case 4	Case 5
Total Potential Area (km^2)	7,158.0	6,848.4	15,337.3	32,917.8	–
Average Daily DNI (kWh/m^2/day)	7.2	7.3	7.7	7.4	–
Total Available Solar Energy (TWh/d)	52.4	50.5	118.7	241.0	–
Power Generation Potential at 28 km^2/GW (GW)	255.6	244.6	547.8	1,175.6	–
Net Energy Generation - Parabolic Trough with 38.8% Capacity Factor (TWh/a)	868.9	831.3	1,861.8	3,995.8	–
Net Energy Generation - Central Receiver with 60.0% Capacity Factor (TWh/a)	1,343.7	1,285.5	2,879.0	6,179.1	–

Table 6.4: Total Potential Area, Average Daily DNI, Total Available Solar Energy, Power Generation Potential and Net Energy Generation (Excluding potential sites with areas less than 2 km^2).

	Case 1	Case 2	Case 3	Case 4	Case 5
Total Potential Area (km^2)	2,219.3	2,180.5	4,294.0	9,994.3	18,785.6
Average Daily DNI (kWh/m^2/day)	7.3	7.4	7.8	7.3	7.6
Total Available Solar Energy (TWh/d)	16.8	16.5	33.5	72.5	144.3
Power Generation Potential at 28 km^2/GW (GW)	79.3	77.9	153.4	356.9	670.9
Net Energy Generation - Parabolic Trough with 38.8% Capacity Factor (TWh/a)	269.4	264.7	521.2	1,213.2	2,280.4
Net Energy Generation - Central Receiver with 60.0% Capacity Factor (TWh/a)	416.6	409.3	806.0	1,876.1	3,526.3

When reviewing the results presented in the two tables, it is observed that they affirm the trends identified from the maps of the analysis cases. Case 2 results in the lowest identified site area and hence energy generation potential, caused by its stricter DNI requirement of 6.5 kWh/m^2/day (compared to 6.0 kWh/m^2/day of Case 1). Case 3 results in the greatest site area and energy generation potential of the first three cases that consider grid proximity. Furthermore, the increase in site area and energy generation potential in Case 4 and Case 5 is dramatic – more than four times that of the equivalent Case 2 and Case 3 scenarios – and is attributed to the removal of the grid proximity requirement. Finally, although the exclusion of sites with areas less than 2 km^2 greatly reduces the total overall area and energy generation potential, vast areas still remain for consideration.

As a means of validating these results, a comparison was made to the those achieved by Fluri (2009) in his GIS study of CSP potential in South Africa. Fluri (2009) calculated a total suitable land area of 15,334.0 km^2, a power generation potential of 547.6 GW and a net energy generation potential of 1861.4 TWh/annum. Comparing this to the suitable land area of 15,337.3 km^2, a power generation potential of 547.8 GW and a net energy generation potential of 1,861.8 Wh/annum calculated in Case 3 in this study – which made use of virtually identical analysis criteria to those used by Fluri – and *including* sites smaller than 2 km^2, a strong resemblance is visible. However, when compared to the results from Case 1 and Case 2, which required a close proximity to water bodies, the values calculated in this study are considerably lower – 2180.5 km^2, 77.9 GW and 264.7 TWh/annum for Case 2 *excluding* sites smaller than 2 km^2.

The reasons for these discrepancies are twofold: Firstly, the obvious factor that the requirement for a close proximity to water greatly reduces the number of potential sites in this study, compared to Fluri's, which didn't require a water proximity characteristic. And secondly, even though the analysis criteria in this study for Case 3 were virtually identical to Fluri's, different data was used for some analysis layers, and different land class exclusions were applied in this study, as can be see in Figure 6.4.

It is therefore concluded that although the requirement for a close proximity to large water bodies greatly reduces the area and energy generation potential of CSP sites in South Africa, a large number of sites do still exist. In order to truly realise the solar resource potential in South Africa, however, it may be more beneficial to make use of dry cooling technologies to reduce the need for plant cooling water, and hence greatly expand the total potential area and number of potential sites for future CSP installations. The investigation of this possibility will thus be conducted in Chapter 8 through to Chapter 10. Finally, if the the national grid were to be further extended into areas with high CSP potential, the total available area and energy generation potential could be greatly increased. The cost benefit analysis of the extension of the national grid is beyond the scope of this study however, and will not be considered.

6.6 Solar Shading and DNI Calculation Model

6.6.1 Background and Motivation

The DNI data used in this analysis, as stated in Section 6.3.1, was processed by NREL and has a spacial resolution of 40 km × 40 km with an accuracy of 10%. At the time of writing, this data was the best freely available data for South Africa with the highest spacial resolution, and was used by Fluri (2009), as well as recommended by Meyer (2010).

All the remaining raster-based analysis criteria, however, have a spacial resolution of 90 m × 90 m, as derived from the spacial resolution of the DEM. Potential CSP sites thus comprise a collection of 90 m × 90 m cells, and can total an area of a number of kilometers. This in turn results in the DNI data having a far coarser resolution than than other analysis layer or identified potential CSP sites. The sun's irradiation, however, is thought to be far more constant over a larger area, than that of land slope for instance, and thus for the sake of this study, the resolution is considered acceptable.

The 40 km × 40 km spacial resolution of the DNI grid, however, is not able to capture variations in DNI caused by local terrain and surroundings. These potential variations could arise from hills or mountains casting shadows on nearby flatter areas at certain times of the day. Although the analysis cases used should generally exclude areas that would be shaded by hills – as a result of the strict land slope criteria (less than 1%) – there may be the odd case where a potential CSP site could fall in a valley that is flat but surrounded by high hills or mountains. Thus, as a means to verify the eligibility of potential CSP sites, it was decided to make use of the shading and DNI calculation algorithm from the *Area Solar Radiation* toolbox within the ArcGIS software package.

The Area Solar Radiation calculation algorithm is fairly complex in nature, with a large number of user defined variables, and is able calculate and output the incoming direct radiation, diffuse radiation, and duration of direct radiation for any area defined by a DEM raster (ESRI, 2010a). This makes it an ideal tool not only for calculating the average hours of daylight that a particular sight may experience over a year – taking into account shading from surrounding elevations – but also as a means to verify the actual DNI values of the NREL data through comparison with its algorithmically calculated values.

6.6.2 Theory and User Defined Inputs

The Solar Radiation Algorithm calculates solar irradiation and duration of direct radiation based on a number of input parameters, and the surrounding topography contained within the DEM. It is thus purely a calculated indication, and is not based on any actual measurements at the potential sites. The accuracy of the calculations can be increased by controlling a number of the algorithm's input parameters, however, as stated by ESRI (2010a) in the documentation, it is imperative to obtain the correct balance between processing time and accuracy. This is due to the fact the radiation calculations can be time consuming, with calculations for large DEMs running for hours and sometimes days.

The algorithm functions by dividing the sky into a hemispherical dome comprising a number of defined cells. Then, by making use of the latitude of the area in question as well as times and dates, the position and track of the sun is calculated as it moves across the sky for each defined day interval. The direct radiation received on a surface is then calculated by the positions and tracks of the sun – as stored in the *sunmap* – for a specified period of time. In this case the simulation was run for an entire year to obtain an annual daily average. A specified number of *viewsheds* are created and horizon

angles are traced for all areas within the DEM, in order to take into account shading and blocking by topographical features, and thereby yield a quantified duration of received daily direct radiation (ESRI, 2010a).

As the latest NREL DNI data used in this study was for the year 2006, the Solar Radiation algorithm was run for the same time period – from 1st January 2006 to 31st December 2006. This was done in order to allow for an equal comparison between the measured and calculated results. The majority of the remaining solar area model inputs were left at the suggested default values, in order to obtain adequate accuracy without significantly increasing processing time. Location specific inputs such as the site latitude were automatically calculated by the software based on the input data of the areas in question.

6.6.3 Unsuccessful Methods

It was initially thought that the most efficient method for calculating the direct irradiation and duration of radiation from the solar area radiation algorithm would be to import the 90 m DEM for South Africa, and run the calculation algorithm for the entire country. This method would therefore cover all previously identified potential sites, and allow for the direct comparison and verification between them. It soon became apparent, however, that the algorithm was extremely computationally intensive, and crashed before any results could be obtained. After reading user's reviews and comments regarding the algorithm on ESRI's online forums (ESRI Online Forums, 2010) it was revealed that this was a common issue encountered when processing large DEMs for long time periods, especially when running the algorithm on 32 bit operating systems with their associated memory limit – as opposed to a 64 bit operating system.

In order to reduce the computational size of the data extent that needed to be processed by the solar radiation algorithm, it was subsequently decided to divide the South African 90m DEM into multiple geographic $1° \times 1°$ grid cells, and then only run the solar radiation algorithm on those $1° \times 1°$ grid cells that contained identified potential sites. In theory, once the algorithm had run for each of the $1° \times 1°$ grid cells, the separate results could then be merged back together to form one single data layer.

It was also decided to add a small euclidean distance buffer around each of the $1° \times 1°$ grid cells, as recommended by Lindenberg and Slingsby (2010). This was done in an attempt to reduce edge effects on the resulting calculated data, that would not have arisen had the algorithm been run once over the entire country as a whole. These edge effects could appear along the boundaries of each of the $1° \times 1°$ grid cells as a result of there not being any data on the external surrounding, which, in reality, would have affected the calculations for the included data. By increasing the extent of each of the $1° \times 1°$ grid cells by a certain distance, the edge effects would then also be moved outwards. Then, in theory, when merging all the calculation results from the $1° \times 1°$ grid cells together after the algorithm had been run, the excess overlapping euclidean buffers could be clipped away, thereby reducing the model's edge effects. Full details and description of this method are given in Appendix A.

The solar radiation calculation was subsequently run on the chosen $1° \times 1°$ grid cells and their buffers. The algorithm and calculation process was still highly computationally intensive, and took multiple days to run. It did, however, ultimately produce results without crashing. Attempts where made to merge, or *mosaic*, the processed individual $1° \times 1°$ grid cells back together, however, due to unknown and unexplained reasons, the results produced from the merge were erroneous and unreliable.

The graphic results of the DNI, and duration of average daily DNI for the $1° \times 1°$ grid cells calculated by the algorithm, as well as the failed attempt at their re-merging are presented in topographical format in Figure 6.13 and Figure 6.14 respectively. In the figures, boundary lines can clearly be seen that appear to suggest that the calculations for each $1° \times 1°$ grid cell were not consistent between cells, with the resulting merge not appearing continuous. Furthermore, two of the $1° \times 1°$ grid cells contained erroneous DNI values of 0 kWh/m^2/d for the entire cell, depicted by the two yellow cells in Figure 6.13.

6.6.4 Modified Successful Method

Due to the lack of success in calculating the DNI and duration of daily DNI for large areas of South Africa, it was decided to adopt a more focussed approach. As the calculation of DNI and duration of daily DNI is primarily for the purpose of validating the NREL DNI data – and hence the results achieved in the analysis cases – it was deemed acceptable to only run the calculation algorithm for a few small areas containing a few potential CSP sites, thereby reducing the size of calculation for the algorithm, and hence computational time.

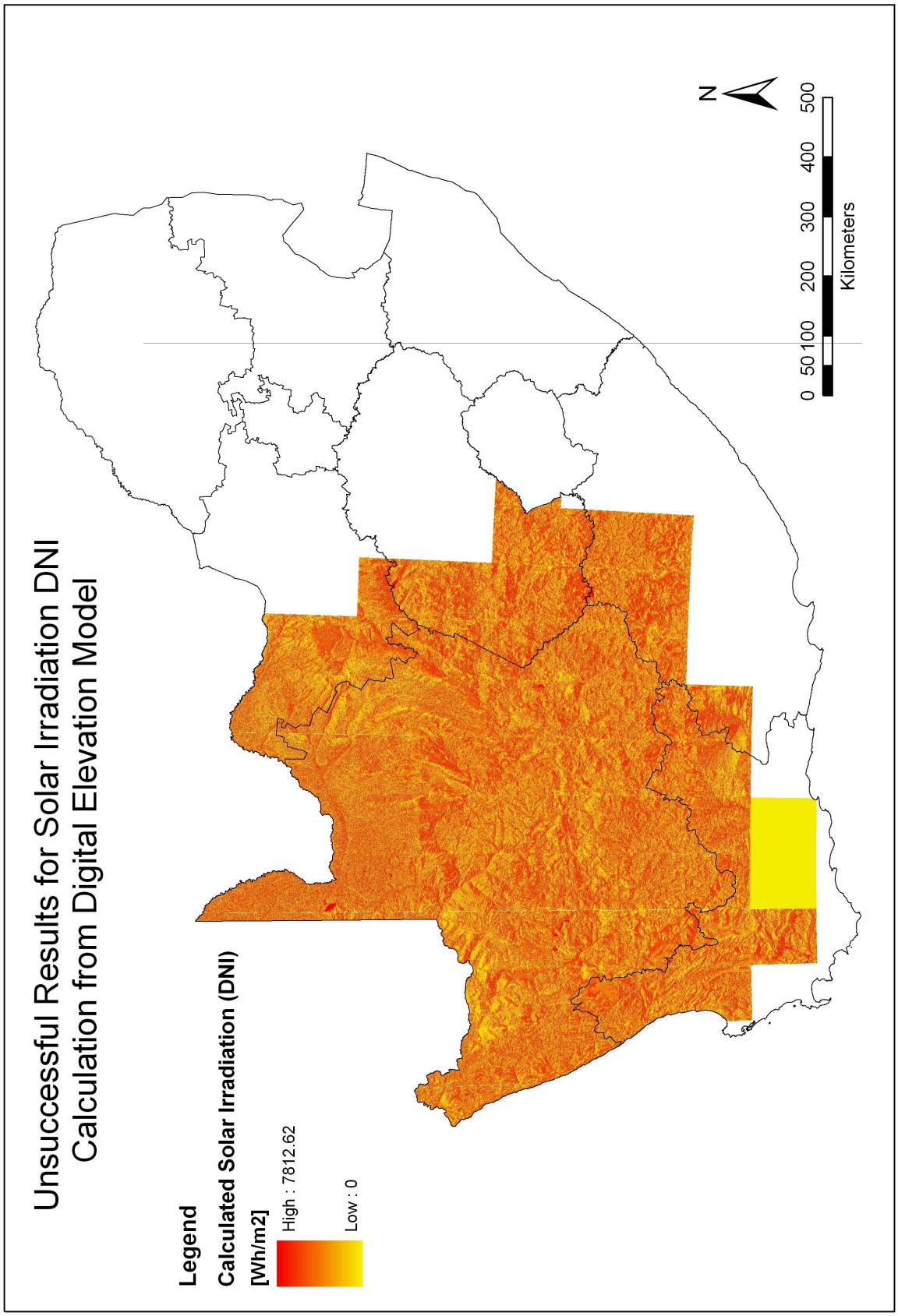

Figure 6.13: Map Illustrating the Failed Merge and Edge Effects for the Daily Solar DNI Calculation Algorithm. *Source of Data:* CSIR (2001c) and DNI Calculation Algorithm.

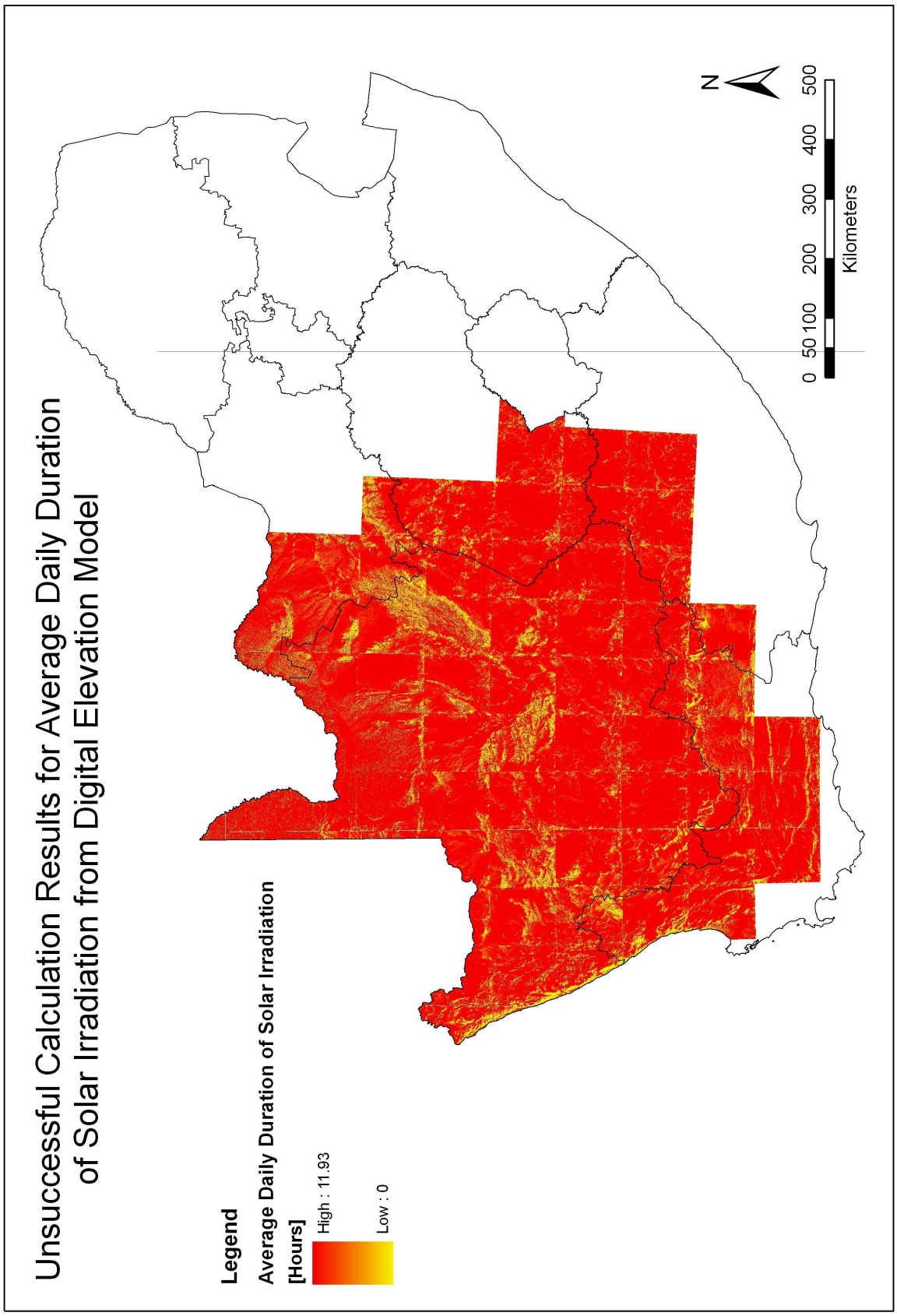

Figure 6.14: Map Illustrating the Failed Merge and Edge Effects for the Solar Shading and Duration Calculation Algorithm. *Source of Data:* CSIR (2001c) and DNI Calculation Algorithm.

In order to accomplish this task, two potential sites identified from Case 4 with fairly high DNI values and large total areas were chosen, while one site closer to the West Coast was chosen from Case 5. A 50 km radial buffer was then created around each of the sights to account for edge effects. The calculation algorithm was run on each one these three buffered site areas. As the areas for each calculation were smaller than a $1° \times 1°$ geographic grid cell, no re-merging or 'mosaicing' was required. The results of the solar irradiation DNI calculation for Case 4 and Case 5 are presented in Figure 6.15 and Figure 6.17 respectively, while the results from the duration of solar irradiation calculations are presented in Figure 6.16 and Figure 6.18.

When reviewing the DNI calculation results shown in Figure 6.15 and Figure 6.17, a few trends were observed. Firstly the algorithm calculates DNI levels lower than those measured by the NREL satellite derived data. Secondly the identified potential CSP sites do indeed fall in areas with calculated high DNI levels, although the algorithm does predict some higher DNI levels on the more steeply sloped terrain (evident when reviewed in conjunction with the DEM over which the results are superimposed).

When reviewing the duration of daily solar irradiation maps shown in Figure 6.16 and Figure 6.18, however, it can be seen the the potential CSP sites identified in this study fall in areas which receive high average daily durations of solar irradiation – in the region of 11.8 hours. The areas on the steeper slopes that appeared to have higher calculated DNI levels in the first calculation can be seen to receive lower durations of average daily solar irradiation.

Therefore, based on this rather limited method of validation, it is concluded that the results for the potential CSP sites identified in the analysis cases do indeed coincide with areas receiving high amounts of annual DNI. It is also concluded that the analysis cases were completed successfully in the GIS software, with all the specified analysis criteria being satisfied simultaneously. However, as will be discussed in Chapter 12, further validation and more extensive analyses considering local-scale DNI levels are recommend for future studies.

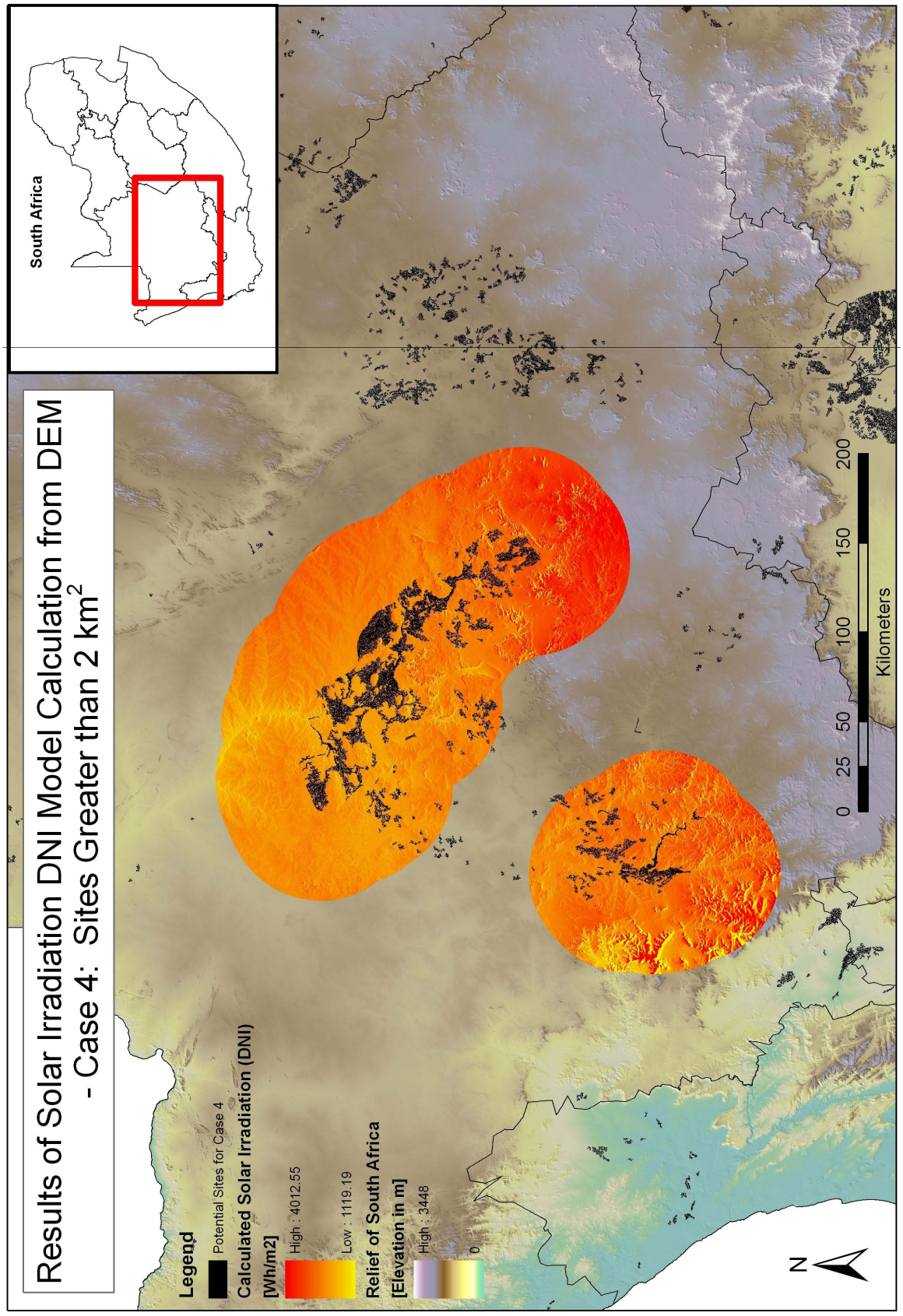

Figure 6.15: Map Illustrating the Successful Model Area Surrounding Potential Sites for the Daily Solar DNI Calculation Algorithm for Case 4. *Source of Data:* Same as included layers.

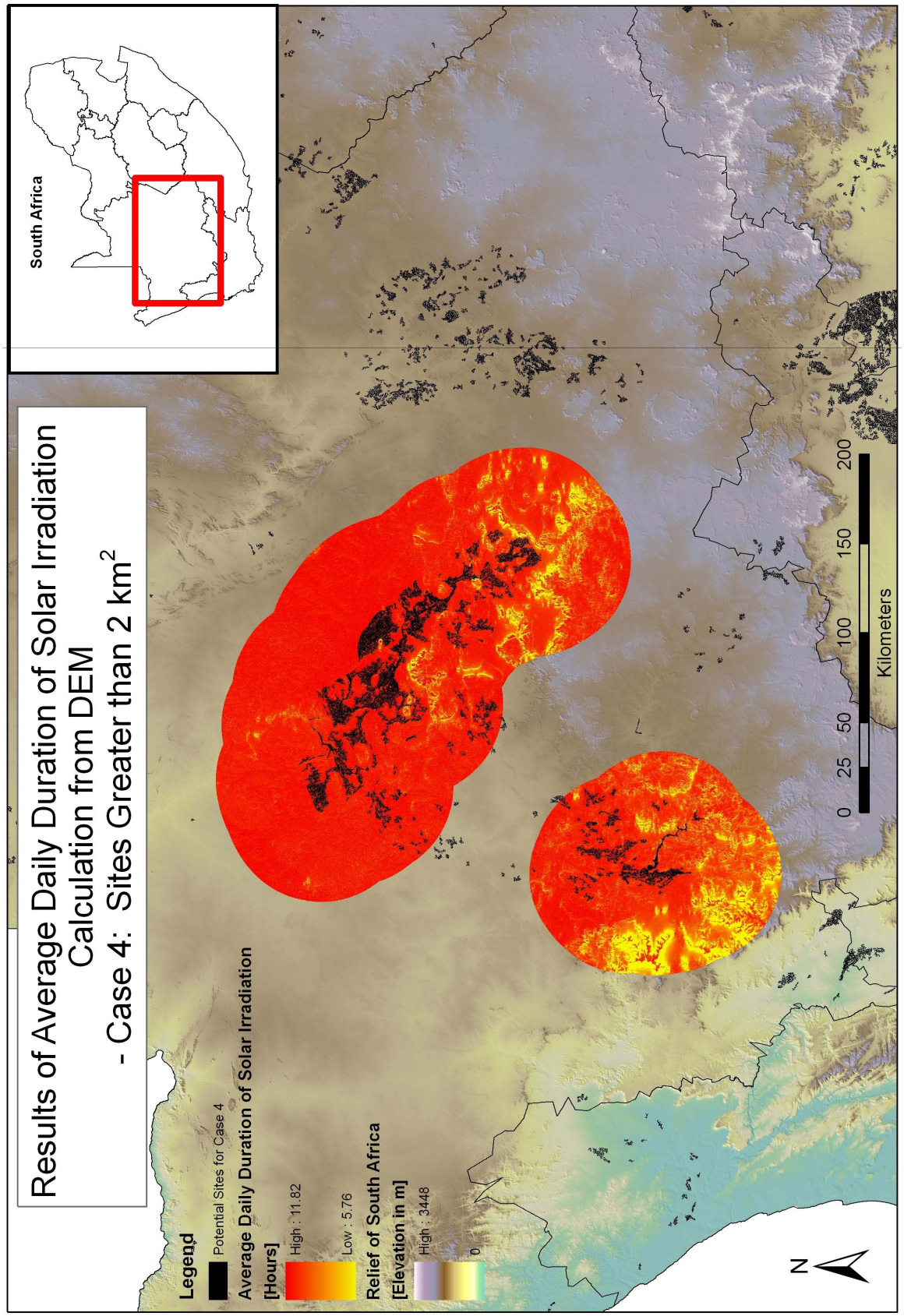

Figure 6.16: Map Illustrating the Successful Model Area Surrounding Potential Sites for the Solar Shading and Duration Calculation Algorithm for Case 4. *Source of Data:* Same as included layers.

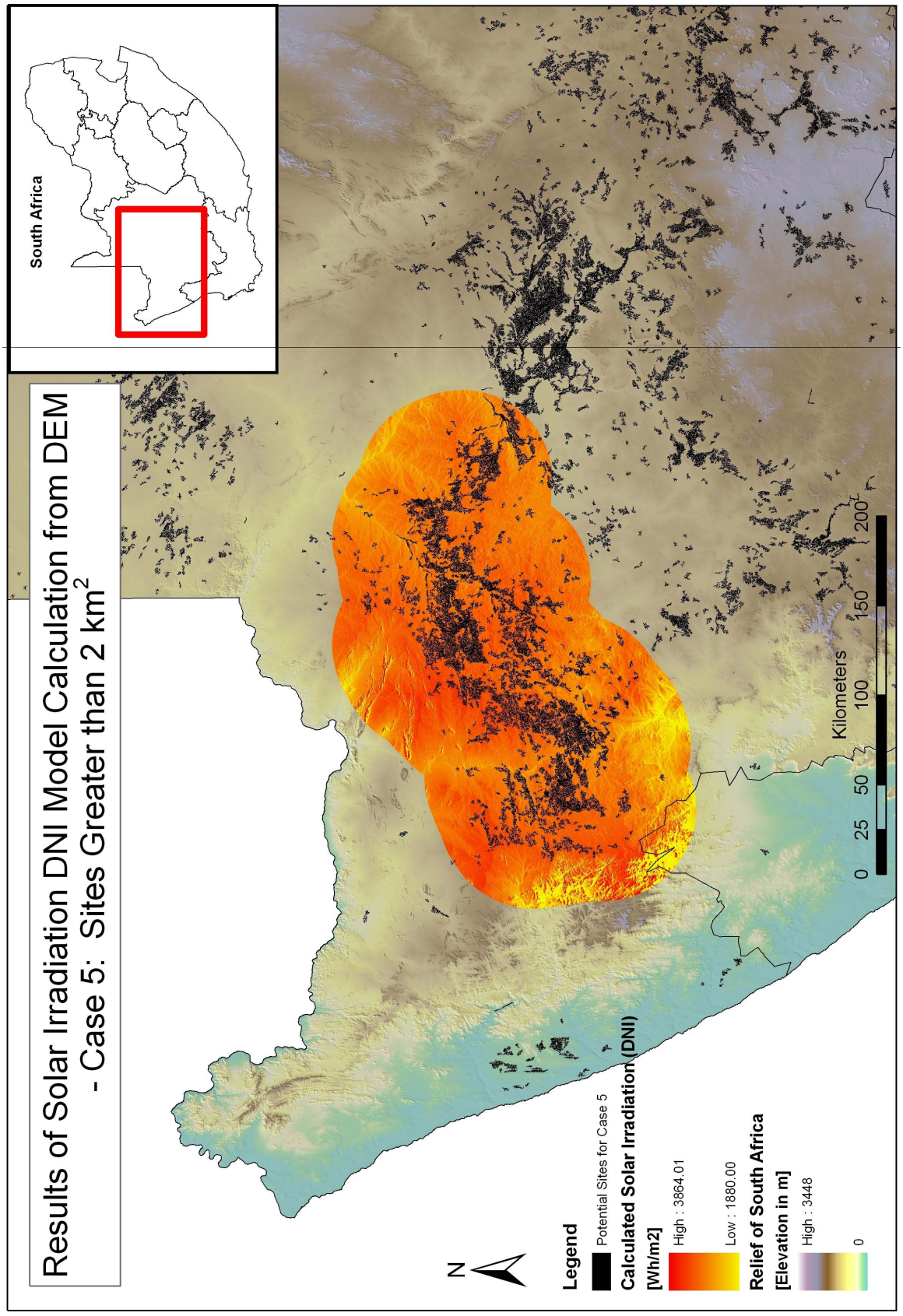

Figure 6.17: Map Illustrating the Successful Model Area Surrounding Potential Sites for the Daily Solar DNI Calculation Algorithm for Case 5. *Source of Data:* Same as included layers.

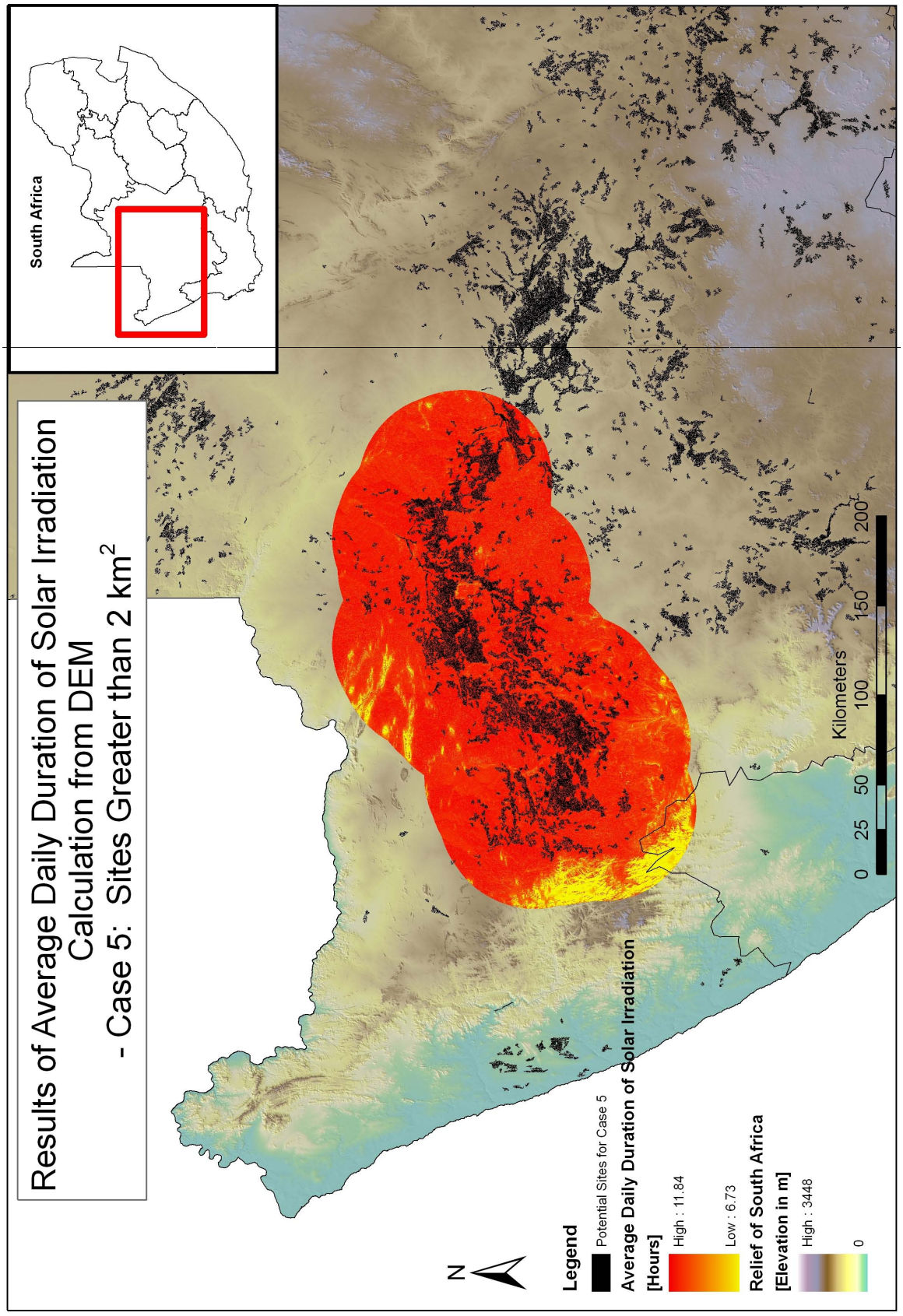

Figure 6.18: Map Illustrating the Successful Model Area Surrounding Potential Sites for the Solar Shading and Duration Calculation Algorithm for Case 5. *Source of Data:* Same as included layers.

7 System Modelling using SAM

The following chapter will present a brief overview of the SAM software user interface and input pages, reported in a similar order in which they would be found in the program. This not only allows for a better understanding of what input data is required in order to accurately model a CSP plant with SAM, but also further aids in the understanding of the applications and limitations of the software.

7.1 Program Version and User Interface

The latest version of the SAM software at the time of commencing this analysis was SAM version number 2010.04.12. This is the version that was used for the entirety of the study, and all further inputs and descriptions are made with reference to this version.

As mentioned in Section 2.3, the SAM software presents the user with a graphical user interface comprising a number of input pages, each of which requires a number of data inputs to be entered. Once all the data inputs on the relevant pages have been satisfied, the user is presented with options to configure and run various simulations, before viewing the results within the software or alternatively exporting them to a spreadsheet program. It is also possible to run a number of cases or scenarios for a project, changing only a few key variables in one in order to ascertain and compare their effects. Brief overviews of each of the input pages within SAM will now be outlined under their respective headings.

7.2 Technology and Market

The initial step in defining a project in SAM is to define which technology it comprises. Choices include *Concentrating Solar Power* (CSP), *Photovoltaic*, or a *Generic Fossil-fuel System*. Since this study is concerned with the modelling and analysis of CSP plants only, no further discussion will be presented on the other technology types. Further description of the different CSP technology types included in SAM is given in Section 7.5.

The second input of the technology and market pages requires the definition of the energy market which best describes the project in question. Depending on which technology choice was made initially, different financing option become available. Choices include *Residential*, *Commercial*, or *Utility IPP* projects. Once again, SAM will display different input variable pages depending on which market choice was made (SAM, 2010).

7.3 Weather Data

7.3.1 Overview of Accepted Data

The SAM software makes use of detailed weather data specific to each project location in order to run simulations and calculate the system performance outputs. SAM only accepts weather data in a text file format which contains hourly weather data describing solar resource, as well as a number of other environmental variables, for a specific location. The text data can be in either Typical Meteorological Year 3 (TMY3), Typical Meteorological Year 2 (TMY2) or EnergyPlus Weather Data (EPW) file format. The weather data encapsulated in these files may contain data for a single complete year, or for a typical year made up of assimilated data from a number of years. By definition, a TMY2 file normally represents data from a number of years ranging from 1961 - 1990, while a TMY3 represents more recent data from 1991 - 2005. These data types are generally suited for economic analysis and performance predictions of a project over a long analysis period. Single year data on the other hand is better suited for analysis of a project's economics and performance in a particular year, and for analyses involving rate structure or load data for a given year. All data sets, however, possess the standard assumption of 8760 hours per year, and do not account for leap years (SAM, 2010).

7.3.2 Weather Data Elements and Uses

The data encapsulated in the weather files contains information for a number of variables, including latitude and longitude, elevation, global horizontal irradiation (GHI), direct normal irradiation (DNI), diffuse irradiation, wind velocity, wet and dry bulb temperatures, pressure and albedo (SAM, 2010). Although not all these variables may be used in the simulation of each and every technology type, the SAM software only accepts a complete dataset with all variables as standard. For the CSP plants being analysed in this study, the key values of importance are the solar DNI levels, the location, and variables such as wind speed and temperature which would be needed for thermodynamic calculations and determining heat transfer losses to the environment.

7.4 Financing and Incentives

7.4.1 Economics and Financing

As discussed in Section 2.3.3, SAM possesses a detailed financial and economic model component. The financing inputs page displays the variables and inputs that are used by this model component to calculate the project cash flow, as well as other related financial metrics. As previously stated, the input variables available for each simulation depend on the technology choice and financing option as specified in the 'Technology and Market' section of the SAM software. As this study is concerned with utility scale CSP plants in South Africa, the *Utility IPP* market was deemed the obvious choice for the SAM model and simulations, and thus only Utility IPP model options will be discussed further.

According to the SAM (2010) definition, a utility project earns revenue by the selling of electricity at a rate determined through a power purchase agreement (PPA). The PPA rate is fixed for a year, and then either remains fixed, or escalates at a defined annual escalation rate. When a utility IPP market is chosen for a project, it is assumed that the utility owner pays cash for the equity portion of the total installed project cost in year zero, and makes interest and principal loan payments in the following years. SAM then calculates the electricity PPA price required to meet the internal rate of return (IRR), minimum debt service coverage ratio (DSCR) and positive cash flow requirements as defined by the user in the financial inputs page. Utility projects (and commercial projects for that matter) also have the added ability to be modelled with or without depreciation – using MACRS depreciation schedules or various other user-defined depreciation methods (SAM, 2010).

7.4.2 Tax Credit Incentives

SAM also allows for the optional inclusion of tax credit incentives in its economic model, with the option to include both investment based credits or production based credits. An investment tax credit will reduce the project's annual tax liability in the first year of the project cash flow, whereas a production tax credit will reduce the project's annual tax liability in the first year of the cash flow as well as subsequent years up to and including a specified final year. It is also possible to define whether tax credit amounts themselves are taxable, and whether or not they affect the depreciation of the project. Once calculated, SAM then displays the tax credits and income tax payments in the project cash flow results (SAM, 2010).

7.4.3 Payment Incentives

As with tax credit incentives, SAM can also optionally include payment incentives within the economic model. These can be defined either as investment based incentives, capacity based incentives or production based incentives. All types represent an amount paid towards the project that contributes to the project's annual income in the first or subsequent years of the project's life. Once again, as with tax credit incentives, it is possible to define whether the incentives themselves are taxable, and whether or not they affect the depreciation of the project. Once calculated, SAM then displays the payment incentives in the project cash flow results (SAM, 2010).

7.5 System Design and Costing

Depending on which technology choice was made initially, as described in Section 7.2, a number of technology specific design and cost input pages are shown, each of which require further data inputs to be defined. However, as previously mentioned, this study will only focus on those inputs relevant to CSP parabolic trough and central receiver technologies.

7.5.1 System Costs

The economic modelling component in SAM makes use of the system costs to calculate the project investment costs and annual operating costs as reported in the project cash flow output. SAM requires cost input data which describes the entire spectrum of the project, including detailed direct and indirect capital costs as well as operation and maintenance (O&M) costs.

A full description of all the costs data used in this project in given in Sections 8.5 to 8.7 of Chapter 8, with full tabulated data presented in Appendix B, Appendix C, Appendix F and Appendix G. Thus for the sake of brevity, and due to the sheer number of cost input categories available for both parabolic trough and central receiver plants, the various cost inputs will not be listed again in this section.

7.5.2 Parabolic Trough Model

When modelling a parabolic trough CSP plant, SAM offers the user a choice between two plant models. The first model developed is that of the *empirical parabolic trough model*, which makes use of a set of equations, based on empirical analysis of data collected from existing parabolic trough installations, in order to predict the performance of trough components. However, as the empirical model makes use of a set of curve-fit equations derived from the regression analysis of data measured from existing systems, one is limited to only being able to include system components for which measured data exists. The empirical model is based on the *Excelergy* model which was initially developed for internal use at the National Renewable Energy Laboratory (NREL) (SAM, 2010).

The second and most recent parabolic trough model available is that of the *physical trough system model*, which was first introduced in March 2010. This model differs from the empirical model in the fact that it characterises the performance of system components based on the first principals of thermodynamics and heat transfer. These mathematical models allow for far greater flexibility when defining system components and removes the limitation of only being able to model existing components with measured data. The disadvantage of the physical model, however, is that it does add more uncertainty to performance predictions when compared to the empirical model. The empirical model is technically reliable when modelling plants very similar in design to an existing plant from which it was derived, however, for new plant designs not based on existing plants, the physical trough model may be more applicable. A further key advantages of the physical model, apart from its added flexibility, is that its relatively short simulation run-time allows for additional simulations and parametric analyses to be run (SAM, 2010). The physical trough model is based on NREL's collector Excelergy model, and comprises a receiver heat loss model by Forristall (2003), a field piping pressure drop model developed by Kelly and Kearney (2006) and the power cycle performance model used in the SAM central receiver model, developed by Wagner (2008).

As with the system costs input page, the parabolic trough model contains multiple data input pages relating to the physical plant design. Once again, a full review of the design input data is given Section 8.8 of this report, with full tabulated data presented in Appendix D and Appendix F. These inputs will therefore not be presented again in this section.

7.5.3 Central Receiver Model

Unlike the parabolic trough technology model in the SAM software, there is only one choice of model for central receiver systems. The central receiver performance model makes use of TRNSYS components developed at the University of Wisconsin, and is described in the research conducted by Wagner (2008). The central receiver model was first included in the more recent versions of SAM.

Like the parabolic trough models, the central receiver model also presents the user with a number of data input pages relating to the physical design and layout of the plant. The number of inputs are greatly increased, however, by the fact that a central receiver system contains thousands of heliostats, all of which require positioning and layout data. Various mathematical algorithms do exist which aid in the generation of the heliostat field layout based on ray tracing or other methods, but in order to simply the process, SAM includes its own optimisation and layout wizard.

According to the SAM (2010) documentation, "the power tower optimization wizard simplifies the task of choosing values for the relatively large number of input parameters required to specify the power tower solar field and receiver." The optimisation of the heliostat field size is considered a crucial step in the design process, as the heliostat field alone accounts for more than 40% of the total installation cost (Sargent & Lundy, 2003). The SAM optimisation wizard functions by searching for a set of optimal design parameters that result in the lowest levelised cost of energy (LCOE). This optimisation process is separate and run prior to the full simulation process, and produces input variables which are then used to populate the data input fields used in the final performance simulation. Unlike other optimisation techniques such as genetic algorithms, the technique adopted in SAM is more of a 'brute-force' method, where a range and increment size is given for each input variable and then discrete combinations are run individually to see which produces the lowest LCOE while satisfying performance requirements (SAM, 2010). The wizard may not always produce an optimal field layout, however, and may require adjustment to value ranges through an iterative process. If the wizard is unable to locate a reasonable field layout, it will always display a message with suggestions for adjustments of limits or step sizes.

The optimisation wizard makes use of, and holds constant, the capital costs defined in the system costs input page, as well as the solar multiple, nameplate capacity, heliostat width and height, and the receiver maximum flux rating. The various heliostat optical and dimension inputs are also used.

The optimiser then finds and populates the following optimal design values:

- Receiver Diameter
- Receiver Height
- Tower Height
- Radial Step Size for Layout
- Total Reflective Area
- Number of Heliostats
- Number of Heliostats per Radial Zone

The optimisation wizard's underlying algorithm is based on the DELSOL3 code from Sandia National Laboratory (Kistler, 1986), and was implemented in SAM through the PTGen program described by Wagner (2008). A full review of the design input data is given in Section 8.9 of this report, with tabulated data presented in Appendix E and final input data (including inputs to the optimisation wizard) given in Appendix G.

7.6 Thermal Storage and Fossil Fuel Backup

The theory and motivation for thermal energy storage in CSP plants has already been covered in Chapter 5, and hence only its implementation and configuration within SAM will be covered in this section. The user inputs for thermal storage in SAM are divided into two categories, namely thermal energy storage (TES) design parameters, and thermal storage dispatch controls. Should it be required, SAM also possesses the ability to model and include a fossil fuel backup system, whose use is also defined and controlled within the dispatch schedule.

7.6.1 Thermal Storage Systems and Dispatch

The inputs in the TES category are used to define the TES storage capacity and its type – direct, indirect, single tank, two tank – as well as its efficiency parameters. The central receiver TES model differs slightly from the parabolic model, however, in the sense that it calculates the storage tank geometry, but requires that the heat transfer fluid volume, tank loss coefficients, and tank temperatures be specified in order to do so. SAM calculates the storage tank geometry by ensuring that the storage system can supply enough

energy to the power block at its rated design thermal input capacity, for the total number of hours specified (SAM, 2010). As with previous sections, the full list of all the inputs for each technology is presented in tabulated form along with the other plant design data in Appendix D, Appendix E, Appendix F and Appendix G.

The inputs in the thermal storage dispatch determine when energy from the TES system – and fossil backup system if included – is released to the power block. This process can be defined by up to six different dispatch schedule periods. The SAM software analyses the thermal dispatch process according to the following algorithm (SAM, 2010):

- For each hour in the simulation process, SAM makes a decision whether or not to operate the power cycle based on how much energy is available in the TES, how much energy is being delivered by the solar field, and the input values of the thermal storage dispatch control parameters. It is also possible to define when the power cycle operates according to the aforementioned six dispatch schedule periods for both weekdays and weekends.
- For each hour of the simulation, SAM analyses the amount of energy available in the TES at the beginning of the hour, and decides whether or not it should operate the power cycle, if it is not already running. This decision is based on two targets, namely one for periods of sunshine and one for periods without.
- During periods of sunshine when there is insufficient energy from the solar field to drive the power cycle at its specified load requirement, the system dispatches energy from storage, but only when energy in storage is greater than or equal to the dispatch target. A dispatch target exists for each dispatch period and is defined as the product of the storage dispatch fraction for that period, and the thermal storage capacity defined by the TES thermal capacity input variable.
- Similarly during periods of no sunshine, when no thermal power is being produced by the solar field, the power block will not run, except for when the energy available in TES is greater or equal to the dispatch target as defined above.

Thus in order to define and control the dispatch schedule, one simply defines a turbine output fraction and a storage dispatch fraction for each dispatch period. A turbine output fraction of 1.0 is equivalent to requiring an energy output defined by the systems nameplate gross output capacity. For hours when the system is not able to produce the required amount of energy from the solar field, the power cycle will then run on energy from both the solar field and TES. For hours when the energy from the solar field exceeds that of the output requirement defined, the power block will run at said capacity while excess energy is diverted to TES – provided it is not full.

7.6.2 Fossil Fuel Backup and Dispatch

If one decides to include a fossil fuel backup system with the CSP plant, its specification and schedule are defined within SAM by means of a dispatch schedule similar to that of the thermal storage system. The fossil fuel dispatch schedule is defined by means of a fossil fill fraction for each dispatch period. The fossil fill fraction defines the solar output level of the system for each hour at which the backup fossil fuel system runs. A fossil fill fraction of 1.0 requires the fossil backup to run and supplement the system to 100% design output power for every hour that the solar energy alone would not be enough to accomplish this. A fossil fill fraction of 0.5 would only allow the fossil backup to engage and supplement the system when the solar output of the plant drops below 50% (SAM, 2010).

SAM also incorporates and calculates the cost of fossil fuel for the backup system – as defined in the system costs page – and reports the results in the levelised cost of energy as well as other result metrics. The energy equivalent of the fuel consumption is also calculated and reported in the results.

A full description and graphic representation of the dispatch schedules used to define the thermal energy storage systems in this analysis is presented in Section 8.10 of this report, and hence no examples will be given here. The use of a fossil backup fuel is not considered in this study, however, and hence no modelling or data inputs relating to its use will be discussed or included.

7.7 Parasitics and Losses

The final input page in the SAM software is that of *Parasitics*, which allows for the inclusion of parameters that define the parasitic electrical loads and losses in the system. The parasitic losses are calculated according to two sections, namely the total parasitic losses used to calculate the power block design thermal input, and the hourly values calculated during the simulation of the system's performance. SAM includes a default set of parasitic parameters for a range of systems, which are then automatically scaled to match the size of the actual plant being modelled. The actual calculated parasitic losses are then reported in the results of the analysis (SAM, 2010). The parasitic loss inputs for the parabolic trough and central receiver systems are discussed in Section 8.8 and Section 8.9 respectively, and presented in tabular format along with the other design inputs for each technology in Appendix D, Appendix E, Appendix F and Appendix G.

8 System Inputs for SAM Model

The derivation and correct identification of inputs for the SAM model is extremely important, as with any model, the results achieved are only as good as the input data used to ascertain them. The following sections will thus describe in detail the methods and sources used in the determination of the inputs to the SAM software models in this study. The sections are described in an order relating to their structure in the SAM software.

8.1 Site Selection and Weather Data

8.1.1 Background and Method

After the successful conduction of the GIS potential site analysis, the next step was to select a number of potential sites for further analysis, and subsequently to obtain detailed weather data for these sites. The means of determining or selecting the *most* optimal sites is not a simple task, however, and would require a closer level of inspection and lower level analysis than the high level GIS analysis presented in this study. Furthermore, the selection of potential sites for a CSP project would depend on project-specific requirements, and would potentially require a method which ranked and weighted sites according to criteria considered most important for that particular project.

The difficulty of site selection for analysis in this study is compounded by the fact that the SAM software requires very detailed weather data for a potential site, as discussed in Section 7.3. Acquiring this weather data for a specific location given by geographic co-ordinates is either achieved by direct measurements from a weather station set up at the site in question, or otherwise from satellite derived or interpolated data (Meyer, 2010). The first method would require site measurements to be taken for a period of at least a year, which would be extremely costly and is thus judged beyond the scope of this study. The latter method, although technically easier and cheaper, still requires the use of proprietary software or data for any location not centred near a city, large town, or

weather station with publicly available data (Meyer, 2010). Software such as Meteonorm is capable of providing the required hourly data for any geographic location, accomplished by means of combining satellite derived data with interpolated weather data from known weather stations; however, at the time of writing this software was not freely available (Meteotest, 2011; Meyer, 2010).

Detailed hourly weather data for a meteorological year (in EPW format) was, however, available for a number of major cities and towns around South Africa, included with the SAM training course as presented by Gilman (2010) and Meyer (2010). The sites in South Africa for which data was supplied and possessed are listed in Table 8.1.

Table 8.1: South African Locations for which Detailed Hourly Data Weather Data was Already Obtained.

Location Name	Province
Bethlehem	Free State
Bloemfontein	Free State
Lephalale	Limpopo
Saldanha	Western Cape
Springbok	Northern Cape
Sutherland	Northern Cape
Upington	Northern Cape

After discussion with Bennett (2010), it was decided to make use of this weather data already in possession, and subsequently, select three potential CSP sites for consideration by means of comparison and superposition of the weather data locations and the potential sites identified in the GIS analysis. This would eliminate the need to invest in expensive weather data, as well as remove the need for a lower level analysis required for identifying the *absolute optimal* sites. This decision was made based on the scope and detail required for this high-level study; however, for future research, it is recommended to make use of more accurate site specific weather data as well as lower-level site evaluation and selection methods. The method adopted in this study for choosing the three locations will now be presented.

8.1.2 Chosen Sites

Of the locations for which weather data was available, only three were deemed close enough to the identified potential sites to be of value to the analysis. These sites comprise the town of *Upington* in the Northern Cape, the town of *Springbok* in the Northern Cape, and the city of *Bloemfontein* in the Free State. A map of these three chosen locations superimposed on the identified potential CSP sites from Case 5 (DNI > 7 kWh/m^2/day, No Proximity to Large Water Bodies, No Grid Proximity) is shown in Figure 8.1.

From the map it can be seen that the three chosen towns are not only located close to identified potential CSP sites, but are also evenly distributed across the region. Furthermore, each of the three locations possesses slightly different characteristics, either in a region with high DNI values and reasonably close to water sources (Bloemfontein), in an area of high DNI but further from water sources (Upington), or in a region of lower DNI but closer to the West Coast (Springbok).

8.1.3 Visualisation and Validation of Site Weather Data

As a means of validating that the assumption to make use of existing town weather data to approximate the weather data at optimal locations is acceptable, the weather data for each of the three town locations was processed and quantified, before being compared to that of the satellite derived NREL DNI data used in the GIS analysis in Section 6.3.1.

The first step in the validation process was to create daily solar profiles of the variation in DNI for an average day for a number of different months. This was done for each of the three locations, before an average annual daily profile was created for visualisation. The results of these daily profiles and average annual daily profiles for Upington, Springbok and Bloemfontein can be seen in Figure 8.2, Figure 8.3 and Figure 8.4 respectively.

From the graphs of the DNI profiles, it is immediately apparent that the daily profiles fit the correct and expected shape for DNI variation, with zero DNI during night hours and an increase to peak DNI around midday. A variation of the average daily profile is also visible from month to month, with the summer months of December and March experiencing a larger and longer plateau – and thus exposure to DNI – when compared to the winter months of June and September. Finally, variation is also observed between locations, with the Upington area receiving higher DNI values when compared to Springbok and Bloemfontein. This is agreement with the satellite derived DNI maps presented in Figure 6.1 and Figure 6.2 of this report.

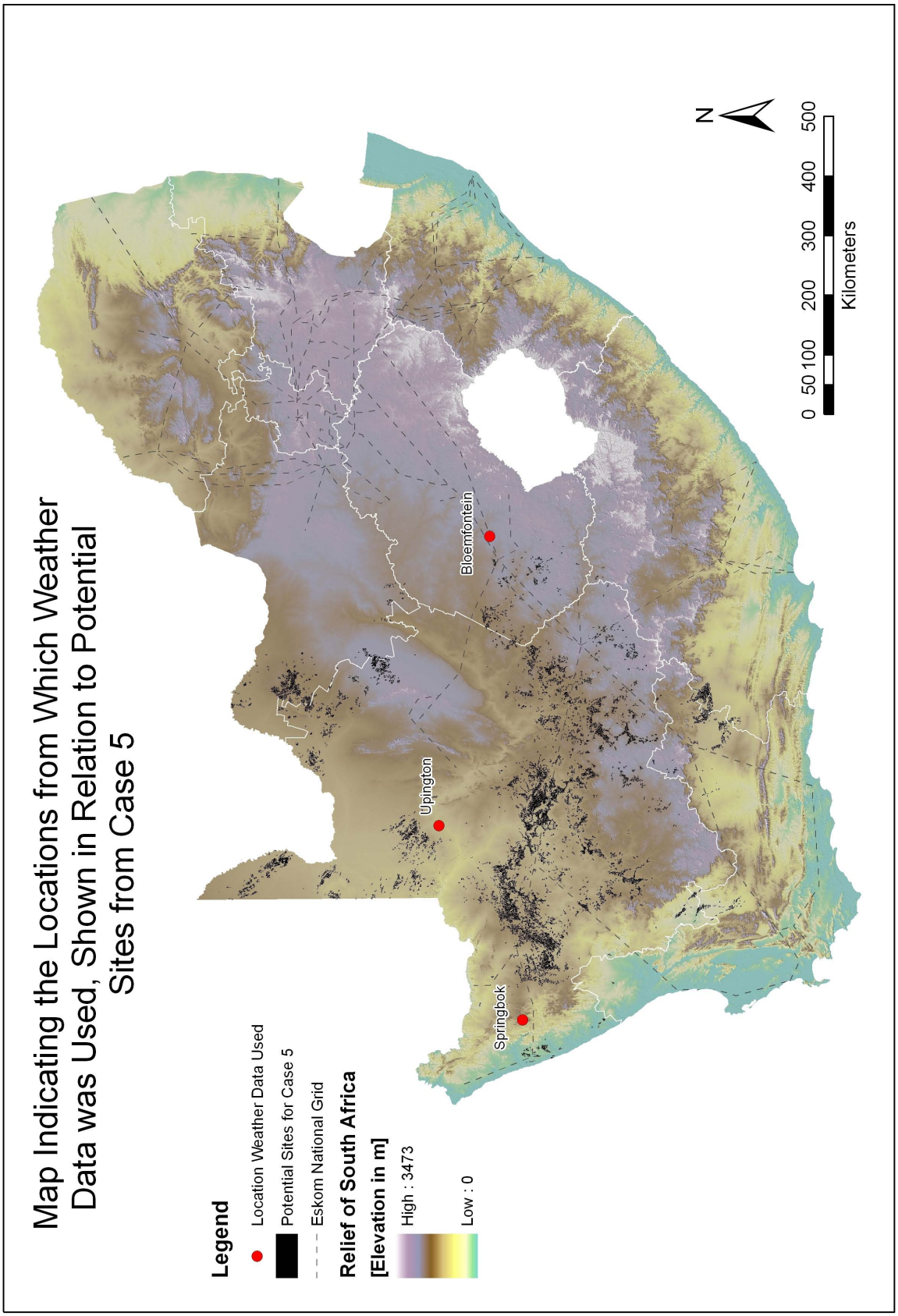

Figure 8.1: Map Indicating the Locations from which Weather Data was Used, Shown in Relation to Potential Sites from Case 5. *Source of Data:* Same as included layers and ENPAT (1998).

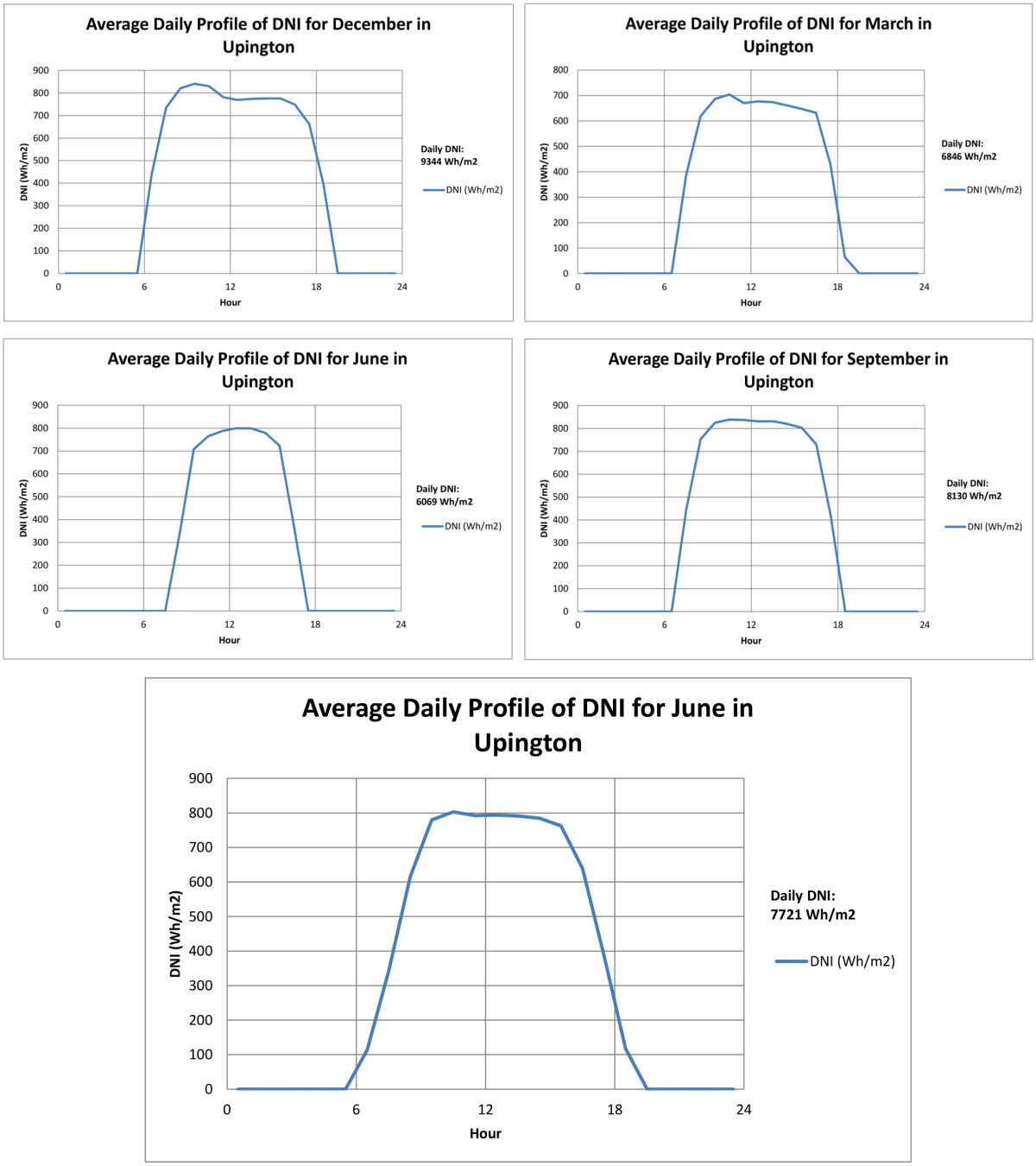

Figure 8.2: Average Daily DNI Profiles for Select Months and Annual Average Daily DNI Profile for Upington.

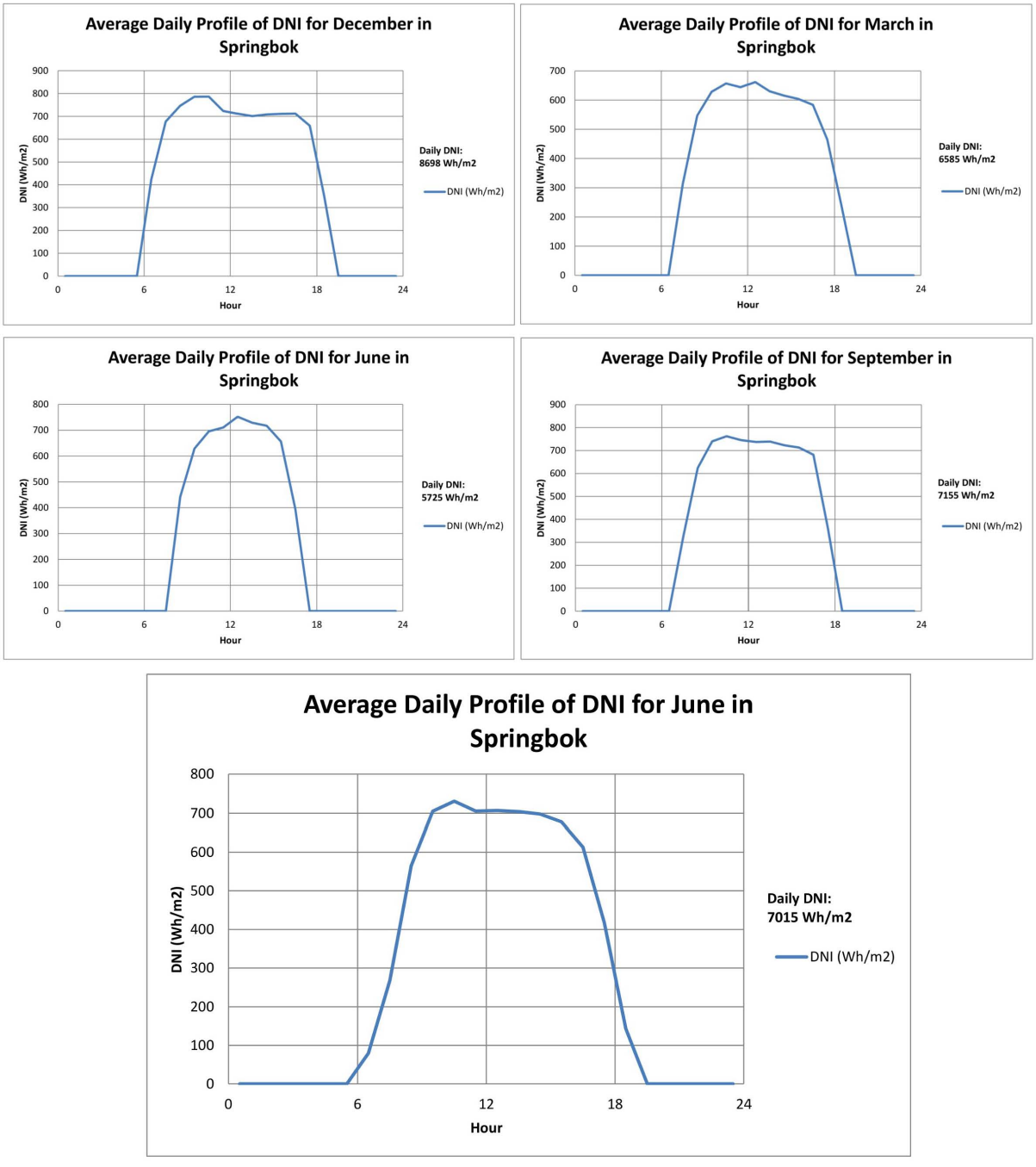

Figure 8.3: Average Daily DNI Profiles for Select Months and Annual Average Daily DNI Profile for Springbok.

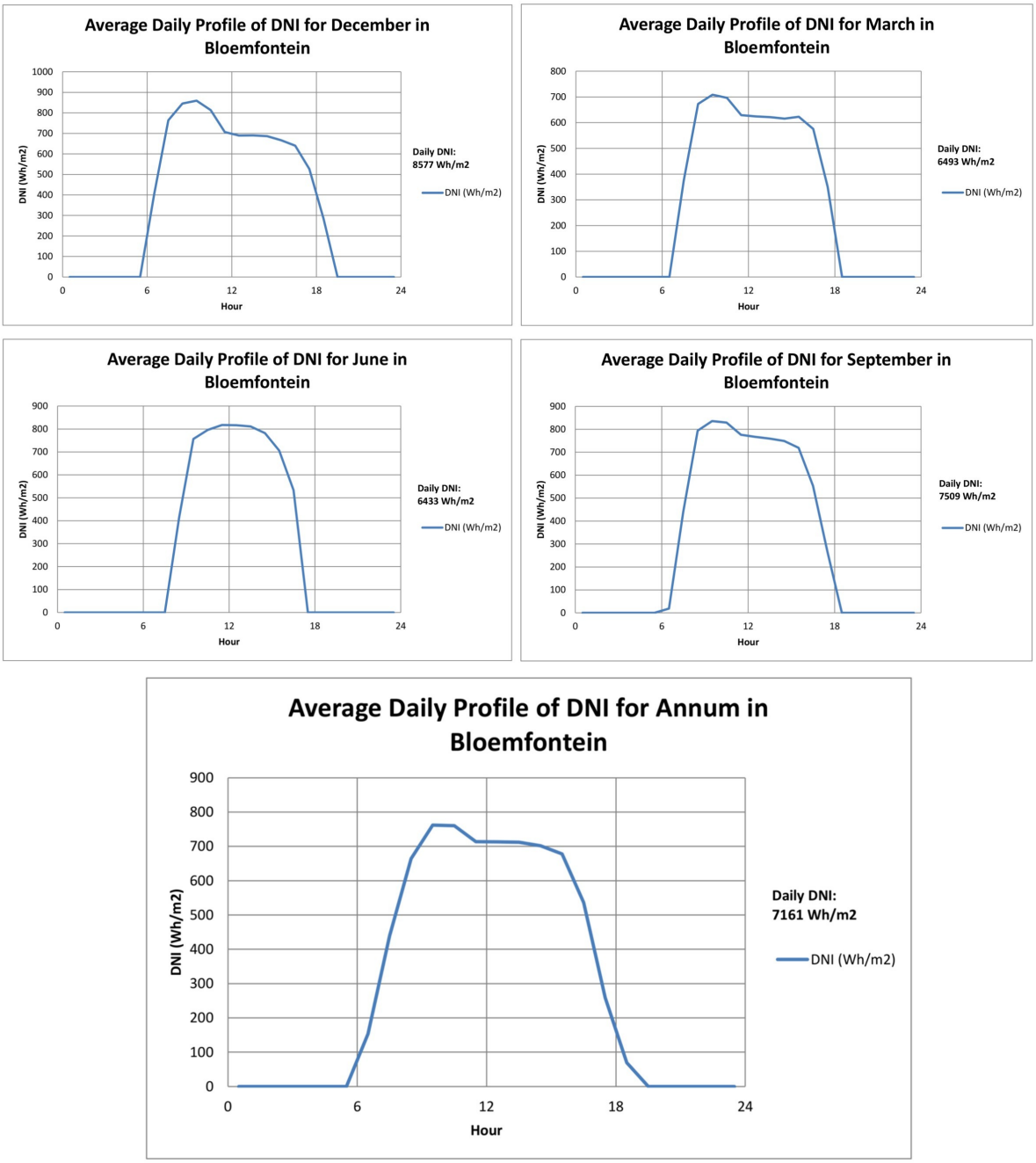

Figure 8.4: Average Daily DNI Profiles for Select Months and Annual Average Daily DNI Profile for Bloemfontein.

The second means of validating the weather data chosen for use in SAM, was to calculate the total daily DNI for an average day of each selected month, and an annual average daily total for the three locations, as a means to quantify and compare it to the satellite derived DNI values given by NREL (SWERA, 2010) and used in the GIS analysis of this report. The results of these calculations are presented in Table 8.2.

Table 8.2: Total Daily DNI for Select Months and Annual Average Total Daily DNI for Upington, Springbok and Bloemfontein.

	Upington	Springbok	Bloemfontein
Total Daily DNI for Average Day in December ($Wh/m^2/day$)	9344	8698	8577
Total Daily DNI for Average Day in March ($Wh/m^2/day$)	6846	6585	6493
Total Daily DNI for Average Day in June ($Wh/m^2/day$)	6069	5725	6433
Total Daily DNI for Average Day in September ($Wh/m^2/day$)	8130	7155	7509
Annual Average Total Daily DNI ($Wh/m^2/day$)	**7721**	**7015**	**7161**

From the above tabulated data, it is clear that the total daily DNI values for each of the locations shows strong agreement with the satellite derived DNI values given by NREL (SWERA, 2010) – and used to identify the potential sites in the GIS section of this report – with the annual daily average for each location being higher than the 7.0 $kWh/m^2/day$ required by the GIS analysis. Once again, the monthly variations are also in accordance with the values predicted by the satellite data in the GIS study, and can be compared to those given in Figure 6.2.

Thus although the towns used to approximate the CSP locations are not situated at any specific or optimal identified sites themselves, the weather data was deemed suitable from a DNI perspective to be used for the SAM model. It is noted that is was not possible to compare other weather data characteristics such as temperature, wind speed, wind direction, and albedo, as these variables were not considered in the GIS study and hence there was no means to quantify how they would differ when compared to the local town weather data. It was therefore assumed that the data used in this report was adequate for an initial high-level study, based on the assumption that the DNI data is considered the primary weather factor for CSP plants, however, it is once again recommended to obtain location specific weather data in future studies.

8.2 Financial Inputs and REFIT

8.2.1 Background and Overview

The SAM model contains a detailed financial analysis component, as discussed in Section 7.4, but the majority of the default values included, however, are specific to the United States (U.S.). It was therefore necessary to review the inputs and adjust them to reflect the local costs and environment in South Africa. In order to determine the financial assumptions required for a South African specific model, the draft reports for the South African Renewable Feed-In Tariff (REFIT) were reviewed. The REFIT is a revolutionary set of proposed tariffs, or rates, at which an appointed buyer is obliged to pay any independent power producer (IPP) for energy supplied to the South African national electricity grid. The feed-in tariffs were calculated for a number of various renewable energy technologies, and the assumptions made for their calculation in a South African environment are listed in the draft reports for REFIT Phase I (NERSA, 2009) and Phase II (NERSA, 2010). Of these assumptions, those of key interest comprised; a debt to equity ratio of 70% debt to 30% equity, a real discount rate of 8% for conventional plants and 12% for renewable plants, a tax rate of 28% and a real cost of debt 6.39%.

As a means to validate these values, as well as determine a number of remaining inputs, a study presented by the Electric Power Research Institute (EPRI) on *Power Generation Technology Data for the Integrated Resource Plan of South Africa* (EPRI, 2010) was reviewed. Their study was not only restricted to CSP plants, but covered most forms of modern electricity generation, and provided detailed descriptions of financial, cost and design inputs for each technology type considered. In their analyses, they adopted a debt to equity ratio of 60% debt to 40% equity, a real discount rate of 8.6%, a tax rate of 28% and a real cost of debt of 7.3%. Furthermore they made use of a combined property tax and insurance value of 2% of project value, and assumed a straight line depreciation model over the entire loan term of 30 years.

As can be seen when comparing the two data sets from NERSA and EPRI, the majority of the values are similar, with EPRI seeming to adopt slightly more conservative values in some cases. It was therefore decided to make use of the EPRI values in the cases where they were more conservative, or when NERSA values were not stated, and adopt the NERSA data for all other inputs. An insurance rate of 0.5% was adopted as suggested by Turchi (2010) and the SAM software, and thus a property tax of 1.5% was adopted in order to sum to the combined 2% value given by EPRI.

In order to assure that the inflation rate and tax rate data was as accurate and up to date as possible, the latest data from the South African Revenue Service (SARS) and Statistics South Africa was consulted. SARS (2011) confirmed the 28% federal tax level – with state tax being equal to zero with no differentiation between Federal and State in South Africa – and a sales tax of 14%. Statistics South Africa gave an average inflation rate for the year 2010 of 4.3% which was adopted in the study (StatsSA, 2011).

8.2.2 Definition of Inputs

The finally adopted values used in this analysis, as discussed above, are presented below in Table 8.3. The default SAM values are also included for reference and comparison purposes.

Table 8.3: Financial Inputs for SAM Model. *Source of Data:* EPRI (2010), NERSA (2010), SARS (2011), StatsSA (2011), Turchi (2010).

	Default SAM Value	Value Used in Analysis	Reference
Analysis Period	30 yr	30 yr	Turchi (2010), EPRI (2010)
Inflation Rate	2.5%	4.3%	StatsSA (2011)
Real Discount Rate	8%	8.6%	EPRI (2010)
Federal Tax	35%	28%	NERSA (2010), SARS (2011)
State Tax	8%	0%	
Property Tax	0%	1.5%	Derived from EPRI (2010)
Sales Tax	7.75%	14%	SARS (2011)
Insurance	0.5%	0.5%	Turchi (2010), EPRI (2010)
Loan Term	20 yr	30 yr	EPRI (2010)
Loan Rate	8%	7.3%	EPRI (2010)
Debt Fraction	40%	60%	EPRI (2010)
Depreciation	MARCS Mid-Quarter	Straight Line 30 Years	EPRI (2010)

8.3 Market Choice and Incentives

8.3.1 Electricity Market Choice

As discussed in Section 7.4, the choice of market type for this study is that of a *Utility IPP*. The choice of this market requires a definition of a PPA escalation rate, as well as a minimum required IRR and a minimum DSCR. In the REFIT Phase II document, NERSA (2010) makes use of an IRR value of 17%, which is 2% higher than the 15% default value given in SAM. No mention of any other values was found in the documents by NERSA (2010) or EPRI (2010), and thus it was decided to adopt the value of 17% for the IRR, and the SAM default value for minimum DSCR. Instead of specifying a PPA escalation rate, it was decided to let SAM automatically calculate the value that resulted in the lowest LCOE. The final adopted market inputs are given in Table 8.4 below.

Table 8.4: Market Constraint Inputs for SAM Model. *Source of Data:* SAM (2010).

	Default SAM Value	Value Used in Analysis
PPA Escalation Rate	1.2%	Automatically Minimize
Minimum IRR	15%	17%
Minimum DSCR	1.4	1.4

8.3.2 Tax Credits and Payment Incentives

At the time of writing, the author was not aware of any tax credit incentives nor any payment incentives for utility-scale CSP projects in South Africa. Therefore although SAM does possess the ability to incorporate the effects of tax credit and payment incentives into a project's financial model – as discussed in Section 7.4 – no allowance or inclusion of any incentives was made in this study.

8.4 Review and Compilation of Existing CSP Plant Designs and Costs

In order to accurately model and simulate a CSP plant within the SAM software, it is necessary to posses and input fairly detailed design and cost related data. However, the determination and acquisition of this plant design and costs data presented a fairly difficult task. This was found to be due to a combination of there being relatively few commercially operating CSP plants worldwide when compared to conventional power stations, and the fact that the level of detail of the data required for existing CSP plants is either not freely available, or otherwise not complete in terms of both cost and design specifications.

As a means to obtain the required data, an extensive literature review was conducted to locate detailed plant cost and design data for existing CSP plants worldwide. A spreadsheet database was then constructed in order to record and compare the reviewed data. Of the documents reviewed, all provided differing levels of detail for various aspects of different plants. The focus of some documents leaned more towards system costs, while others toward the design criteria. The sheer quantity and variety of the design and cost specifications represented in a typical CSP plant (and thus in the documents reviewed) also soon proved to be an issue, resulting in the scope and focus of the database becoming extensive and unclear. It was therefore decided to adopt a slightly different and more focused approach, first compiling all the required inputs from the existing SAM model into the database, and then only seeking those equivalent items out of the literature, as a means for comparison. This new approach allowed for a far more concise and focused database to be construed, without sacrificing any of the detail or accuracy required to construct a new SAM model.

The complete comparison database, adapted to fit on multiple A4 pages is presented in the appendices. The database contains comparison data for both parabolic trough and central receiver CSP plants, and comprises system costs and design data for various existing plants as well as the SAM default plants. Data was sourced from – but not limited to – reports and papers from EPRI (2010), Sargent & Lundy (2003), Turchi et al. (2010), Stoddard et al. (2006), Kelly (2006), Romero et al. (2002) and Dersch et al. (2002). Parabolic trough system costs are presented in Appendix B while Appendix C gives central receiver system costs. Parabolic trough design data is presented in Appendix D, while central receiver design data is presented in Appendix E.

After reviewing the constructed comparison database, it was apparent that no one report or paper presented a complete set of the required data, even after the scope had been narrowed as previously described. Furthermore, while some papers were more complete in terms of cost data, and others in design data, further discrepancies arose due to the fact that the existing CSP plants reviewed were of different sizes and ages. In order to accurately construct the complete set of data required, one would then need to obtain scaling factors as a means to compare all plants on an equal power-output size rating, as well as apply financial discounting to account for the different ages of the plants and associated years of their cost data.

The SAM software itself, however, includes a complete set of default data inputs for a number of different CSP plant types and configurations. The data was commissioned by NREL as part of a study conducted to update the ageing default inputs used in the 2009 version of SAM. The study's findings, as well as the plant designs and costs are given in the report by Turchi (2010). According to Turchi (2010), NREL contracted the WorleyParsons Group, Inc to conduct a design and cost analysis of a generic representative parabolic trough plant, with both wet and dry cooling. The 100 MW plant was given nominal design specifications by NREL, before the complete conceptual design and cost assessment was conducted by the WorleyParsons Group. Turchi (2010), continues to state that "the the primary purpose of the WorleyParsons contract was to develop a line-item cost model that SAM users could manipulate to represent cases of interest".

After reviewing the report and study conducted by NREL and the WorleyParsons Group, it was thought best to make use of the default design parameters and baseline costs for all the CSP plants in this study, but only in the instances that more appropriate and location specific South African values could not be identified or calculated. As a means to validate this reasoning, the method was discussed with Bennett (2011), and contact was made with Gilman (2011) who was previously involved with SAM at NREL. Both Bennett and Gilman affirmed the approach, with Gilman continuing to state that the absolute values are less important in the study then the relative metrics, and thus provided that the default assumptions remain constant across locations, and only the variables of interest are varied, the truly valuable information will arise in the comparison of results and effects measured. The various plant data presented in the comparison database already constructed is still included in the report, however, as a means for comparison and validation.

8.5 System Costs

As discussed in Section 8.4, it was decided to make use of the default cost inputs provided in the SAM software – as derived from the study conducted by NREL and the Worley-Parsons Group (Turchi, 2010) – but to then adapt them to equivalent costs that would have occurred had the same plant been constructed in South Africa. It was also decided to conduct the entire analysis with a base year of 2010 in currency terms, primarily due to the fact that this study was begun in 2010. Fortunately, the default SAM inputs were also defined in 2010 by the WorleyParsons Group, and hence listed in 2010 U.S. Dollars. This ensured that they were realistic and current, and also removed the need to make conversions to other years by means of discounting or appreciation.

The costs used in the SAM model could not simply be converted to local South African values by means of the current currency exchange rate, however, as the costs themselves are dependent on local factors such as local expertise and material availability, imports and shipping distances, labour wage rates and labour productivity. It was therefore decided to make use of a method presented and employed by EPRI (2010) in their aforementioned study and report on *Power Generation Technology Data for the Integrated Resource Plan of South Africa*. As previously stated, their study was not restricted to CSP plants only, but covered most forms of modern electricity generation. For all technologies their method remained the same, however, in the fact that the power plant costs were initially established for U.S. based plants with the same design basis and specifications as the South African plant in question. The costs were then adjusted based on adjustment factors developed by EPRI's subcontractor as well as in-house EPRI assumptions. Finally, once the adjustment was completed, the costs were converted to South African Rand by means of the current currency exchange rate.

This method was deemed ideally suited for use in this study owing to the fact that, like the EPRI study, the CSP plant cost data in this study are also given for U.S. based plants and require conversion in order to accurately represent an equivalent South African based plant. The method as well as the adjustment factors will now be discussed in detail for both the *direct* and *indirect* capital costs, as well as the *operation and maintenance* (O&M) costs.

8.5.1 Method for Direct and Indirect Capital Costs

It was first assumed that a portion of the equipment and materials required for the construction of a South African CSP plant would be imported from outside South Africa, while the remainder of the materials and construction labour would be supplied locally. It is also noted that for all CSP technologies included in this study, no provision was made for new infrastructure nor improvements to existing infrastructure, including transmission lines and roads, because as noted by EPRI (2010), these are "generally quite specific and design requirements can vary from one location to another". Based on cost data from the Medupi Coal Power Station Project, as well as in-house data, EPRI estimated the percentage breakdown of both imported and locally available plant components, labour and material costs for each technology. These percentages are given in Table 8.5.

Table 8.5: Assumptions for Percentage Breakdown of Imported and Locally Available CSP Plant Components, Labour and Material Costs. *Source of Data:* EPRI (2010).

Technology	Imported	Locally Available
CSP Parabolic Trough	50%	50%
CSP Central Receiver	50%	50%

It was then assumed that of the estimated breakdown of *local costs*, a certain percentage comprised material and equipment costs while the remainder comprised local labour costs. This was based on EPRI in-house labour to material ratio data, as well as the assumption that 95% of the imported costs were material or equipment costs (EPRI, 2010). These percentages are given Table 8.6.

Table 8.6: Assumptions for Percentage Breakdown of Materials and Labour for Locally Available CSP Costs. *Source of Data:* EPRI (2010).

Technology	Materials (Local)	Labour (Local)
CSP Parabolic Trough	45%	55%
CSP Central Receiver	45%	55%

A set of conversion factors for adjusting the construction costs in the U.S. gulf coast to the cost of construction in South Africa were developed by EPRI's subcontractor, and are given in Table 8.7 below. These conversion factors were then applied to the breakdown of local materials and local labour presented in Table 8.6 above.

Table 8.7: Conversion Factors for U.S. to South African Local Materials, Local Labour Productivity and Local Labour Wage Rate. *Source of Data:* EPRI (2010).

Category	Materials Factor (Local)	Labour Productivity Factor (Local)	Labour Wage Rate (Local)
Civil	1.00	1.75	0.72
Concrete	1.00	1.75	0.72
Structural Steel	1.00	2.10	0.57
Mechanical	1.00	2.10	0.67
Piping	1.10	2.25	0.68
Valves	1.10	2.25	0.68
Insulation	1.00	2.00	0.62
Electrical Bulks	1.00	1.95	0.52
Instrumentation	1.15	1.95	0.52
Painting	1.00	1.80	0.76
Electrical Equipment	1.00	1.90	0.62
Value Used	**1.00**	**2.10**	**0.65**

From the above data it can be seen that the majority of the materials used in the construction of power plants in South Africa are expected to cost approximately the same as in the U.S. This is due to the fact that the majority of the raw materials required are mined and refined locally (leading to less expensive pricing compared to the U.S.) but that less advanced production techniques and lower labour productivity in South Africa subsequently offset this.

The predicted lower labour productivity in South Africa also causes an increase in the hours required to complete the construction, with an increase ranging from 75% to 125% more labour hours. At the same time, however, the labour wage rates are lower in South Africa compared to the U.S., ranging from 24% to 48% lower. Thus in accordance with the recommendations made by EPRI's subcontractor, an average adjustment factor of 1.00 for materials, 2.10 for labour productivity, and 0.65 for labour wage rates was applied across all their respective cost divisions (EPRI, 2010).

Of the percentage of costs given in Table 8.5 that represent imports, no division was made between labour and materials, and only an shipping factor was applied. It was assumed, however, that the shipping factor would remain 1.00 based on the further assumption that the same transportation costs applied for shipping to the U.S. and South Africa (EPRI, 2010). This in turn resulted in the imported cost remaining the same as the U.S.

Therefore based on the aforementioned breakdowns and factors, the U.S. based direct and indirect capital costs were adjusted to South African costs in the following manner:

1. Each direct and indirect capital cost item was broken down into an imported portion and a locally available portion as per the percentages given in Table 8.5.
2. The imported portion of the cost was assumed to remain the same as the U.S. imported cost.
3. The locally available portion of the cost was then broken down into a materials portion and a labour portion as per the percentages given in Table 8.6.
4. These local material and labour portions were then converted to South African equivalent costs by means of the adjustment values given in Table 8.7.
5. The converted imported and local costs were then all combined to give the final equivalent South Africa cost (still in 2010 U.S. Dollars) for the particular direct or indirect capital cost in question.

It was decided not to complete the final conversion to South African Rand by means of the currency exchange rate at this point, however, due to the fact that the SAM software is based in U.S. dollars. It was instead decided to run the SAM software models using the above calculated South African equivalent U.S. Dollar values, and subsequently convert the final outputs of the model to South Africa Rand by means of the exchange rate. This method has the added benefit of allowing for easier comparisons and validation of the SAM output data to other existing CSP plant data (which is already given in U.S Dollars) at different steps of the analysis process.

A visual representation of the entire conversion process for direct and indirect capital costs is presented in Figure 8.5 in the form of a flow diagram.

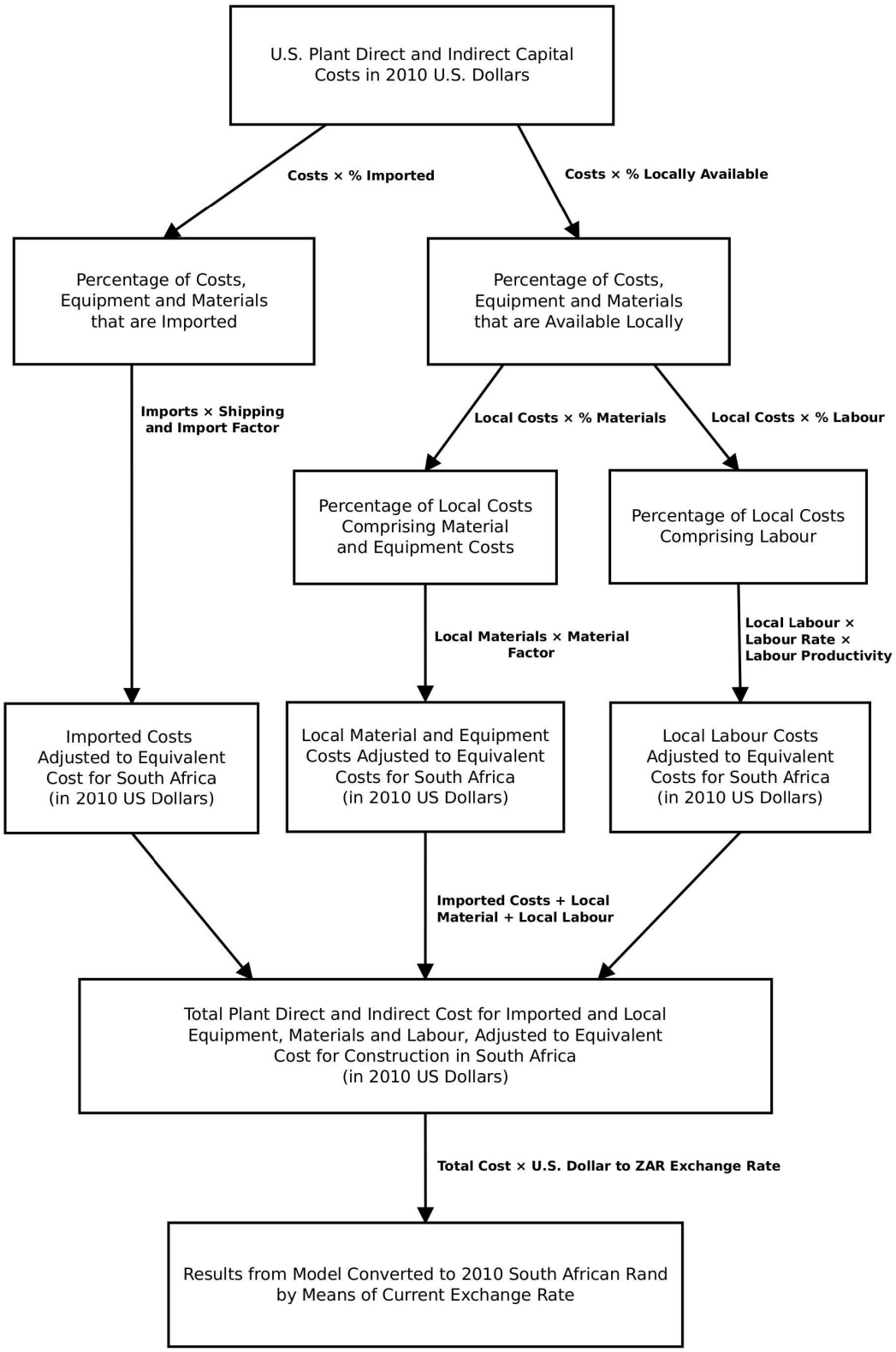

Figure 8.5: Visualisation of Method for Estimating and Converting Foreign CSP Plant Direct and Indirect Capital Costs to South African Based Equivalents.

8.5.2 Method for Operation and Maintenance Costs

The CSP plant operation and maintenance (O&M) costs also required adjusting to to South African conditions and currency. The method adopted for converting the O&M costs was similar to that of the direct and indirect capital costs described in Section 8.5.1. Based on the assumption that *fixed* O&M costs are often scaled with the capital costs of a plant, the same adjustment factors and conversion method used for the direct and indirect capital costs was adopted (EPRI, 2010), namely:

1. Each fixed O&M cost item was broken down into an imported portion and a locally available portion as per the percentages given in Table 8.5.
2. The imported portion of the cost was assumed to remain the same as the U.S. imported cost.
3. The locally available portion of the cost was then broken down into a materials portion and a labour portion as per the percentages given in Table 8.6.
4. These local material and labour portions were then converted to South African equivalent costs by means of the adjustment values given in Table 8.7.
5. The converted imported and local costs were then all combined to give the final equivalent South Africa cost (still in 2010 U.S. Dollars) for the particular O&M cost in question.

Variable O&M costs, however, prove more difficult to analyse with this method, and thus could not be broken down with material and labour factors (EPRI, 2010). Thus for *variable* O&M costs, only a currency exchange rate was applied after the completion of the SAM analysis. A visual representation of the entire conversion process for fixed and variable O&M costs is presented in Figure 8.6 in the form of a flow diagram.

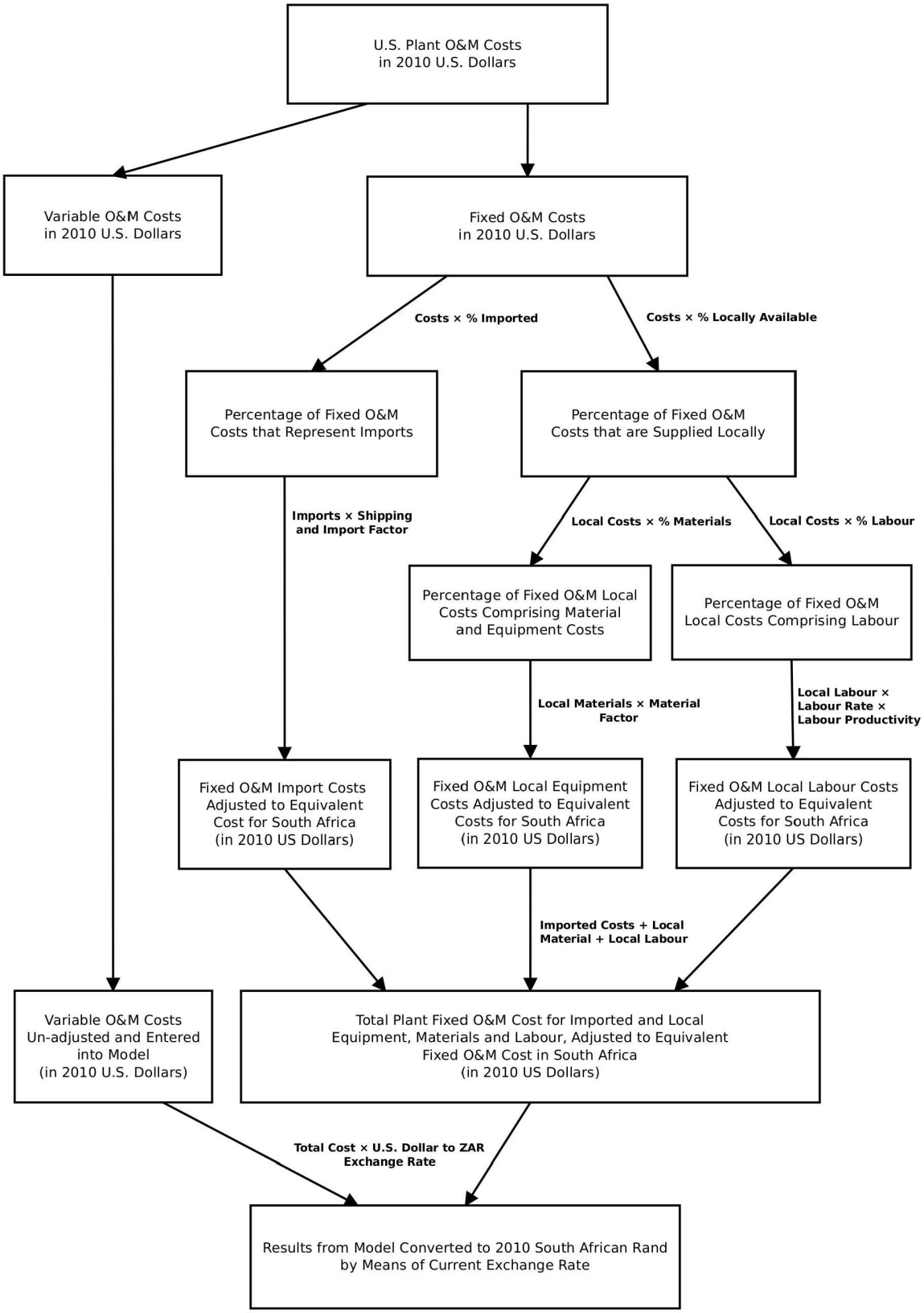

Figure 8.6: Visualisation of Method for Estimating and Converting Foreign CSP Plant O&M Costs to South African Based Equivalents.

8.6 Cost of Water

8.6.1 Background and Incorporation

The availability of cooling water, or lack thereof, is a key area of focus in this study, and its representation in the SAM model was therefore given specific consideration. The SAM software does not allow for, nor present a specific input dedicated to the cost or consumption of cooling water, and it was thus necessary to devise another means to represent it in the model. After discussion with Gilman (2010), it was recommended to incorporate the cost and use of cooling water by means of an additional user-defined O&M cost.

SAM offers the user the ability to add an O&M cost either as a fixed cost by capacity (in $/kW.yr), or as a variable cost by generation (in $/MWh). As the consumption of cooling water is directly dependent on the amount of power produced and not linked directly to the name plate capacity of the plant, it was decided to incorporate it as a variable O&M cost by generation (in $/MWh).

8.6.2 Method of Calculation

As no South African cooling water consumption data was found for parabolic trough or central receiver CSP plants in the required units of $/MWh (or R/MWh), a method was devised in order to calculate the required inputs. The review of cooling technologies in Chapter 4 provided data for water consumption of parabolic trough and central receiver plants. This data was extracted from Table 4.1 and the values used presented in Table 8.8. For the case of wet cooling for central receiver plants where a range of values was given, the average value of 625 Gallons per MWh (2.37 litres/kWh) was used. These values were then converted to metric units of kilolitres/MWh.

The next step in the calculation process required the determination of cost data for large quantities of cooling water from the local South African municipalities in the areas surrounding the potential sites. Initial searches only revealed the commercial and industrial treated water tariffs for City of Johannesburg Council, at a stated value of R14.82 per kl for consumption exceeding 200 kl (City of Johannesburg Council, 2011). It was therefore decided to contact the South African Department of Water Affairs (DWA) to obtain local tariffs for both treated and untreated water. Van der Merwe (2011) from the DWA stated that the unit charges for bulk raw water supplied from departmental water resource infrastructure to large Eskom coal-fired power stations in the Mpumalanga highveld region

– which supply base-load electricity to the national electricity grid – currently vary from around R2.30 to R8.25 per kl, depending on the physical attributes of the water supply infrastructure. These costs exclude any treatment cost of the raw water for cooling purposes, which would occur at the plant in addition to the aforementioned departmental unit charges. As these costs represent a fairly large range, further inquiry was made, and it was determined that one supplier, Namakwa Water in the Lower Orange River area, contended that it was able to supply its customers with bulk treated water at a cost of R5.50 per kl, although the sustainability of this supply at this price is not known (Van der Merwe, 2011).

As a final means to obtain a reasonable value for the cost of cooling water, the Sargent & Lundy (2003) report for NREL on the *Assessment of Parabolic Trough and Power Tower Solar Technology Cost and Performance Forecasts* was consulted. In their report, a review is given of the SunLab cost model, where SunLab estimates (based on the SEGSVI/VII CSP plants) give a raw water cost of $0.32 per kl, and treatment costs of $0.043 and $0.540 per kl for cooling water chemical treatment and demineralizer chemical treatment respectively. Thus at a rand-dollar exchange rate of R7.02 to the U.S Dollar as of the 16th May 2011 (Bloomberg, 2011) the SunLab raw water cost of $0.32 equates to a cost of approximately R2.25, which is very similar to the lower limit of R2.30 as stated by Van der Merwe (2011).

It was finally decided, however, to employ a conservative approach and adopt an average value from Van der Merwe (2011) of approximately R5.28 for raw water costs, but then to vary the range during the sensitivity analysis as described in Chapter 10. When converted using the aforementioned exchange rate, this resulted in a raw water cost of $0.75 per kl. The chemical treatment and demineralization costs from SunLab were then added to the raw water cost to yield the total cooling water cost in $/kl, as given in Table 8.8.

The final step in the calculation process was then to multiply the total cooling water cost in $/kl by the water usage in kl/MWh to obtain the final cooling water O&M cost in $/MWh. The results of the final calculation for each technology are give in Table 8.8. It is also noted that for the remainder of this report, the term 'wet cooling' will refer to the technology of recirculating wet cooling, as once through wet cooling is not a considered technology in this analysis.

Table 8.8: Values Used in Calculation of O&M Cost of Cooling Water for Various Power Plants using Different Cooling Technologies. *Source of Data:* DOE, U.S. (2010), Van der Merwe (2011), Sargent & Lundy (2003).

	Parabolic Trough		Central Receiver	
	Wet Cooling	Dry Cooled	Wet Cooling	Dry Cooled
Water Usage (Gallons/MWh)	800	78	625*	90
Water Usage (kl/MWh)	3.028	0.295	2.366	0.341
Raw Water Cost (R/kl)	5.275*	5.275*	5.275*	5.275*
Raw Water Cost ($/kl)	0.751	0.751	0.751	0.751
Cooling Water Chemical Cost ($/kl)	0.043	0.043	0.043	0.043
Demineraliser Chemical Cost ($/kl)	0.540	0.540	0.540	0.540
Total Water Cost ($/kl)	1.334	1.334	1.334	1.334
Calculated Cooling Water O&M Cost ($/MWh)	**4.04**	**0.39**	**3.16**	**0.45**

* Average Value

8.7 Final Locally Adjusted Cost Inputs for SAM

The conversion method as described in Section 8.5 was applied to the default cost data supplied with the SAM software, which is recorded in Appendix B and Appendix C. The additional cost for cooling water as calculated in Section 8.6 was then added to the existing O&M variable cost by generation section. The results from the conversion process and the final cost inputs as used in the SAM software model are recorded below in tabular format. Table 8.9 lists the final calculated inputs for the parabolic trough plant, while Table 8.10 lists the final calculated inputs for the central receiver plant. The final cost inputs for the various parabolic trough and central receiver models are also listed in their entirety in Appendix F and Appendix G respectively.

Table 8.9: Locally Adjusted Final Cost Inputs as Used in SAM Models for Parabolic Troughs.

Parabolic Trough	**Wet Cooled**	**Dry Cooled**
Direct Capital Costs		
Site Improvement	22.008 $/m^2	
Solar Field	385.131 $/m^2	
HTF System	55.019 $/m^2	
Storage	77.026 $/kWh$_{th}$	
Fossil Backup	0.000 $/kW$_e$	
Power Plant	1012.345 $/kW$_e$	1254.428 $/kW$_e$
Contingency	10%	
Indirect Capital Costs		
Engineer, Procure, Construct	15% of Direct Cost	
Project, Land, Management	3.5% of Direct Cost	
Sales tax Applies to:	80% of Direct Cost	
O&M Costs		
Fixed Annual Cost	0.000 $/yr	
Fixed Cost by Capacity	88.030 $/kW.yr	
Variable Cost by Generation	7.040 $/MWh	3.390 $/MWh
Fossil Fuel Cost	0.000 $/MMBTU	

* Unadjusted value left as SAM default

Table 8.10: Locally Adjusted Final Cost Inputs as Used in SAM Models for Central Receivers.

Central Receiver	Wet Cooled	Dry Cooled
Direct Capital Costs		
Site Improvement	22.008 $/m^2	
Heliostat Field	221.175 $/m^2	
Balance of Plant	379.629 $/kW$_e$	
Power Block	632.716 $/kW$_e$	874.798 $/kW$_e$
Storage	33.011 $/kWh$_{th}$	
Fixed Solar Field Cost	$ 0.000	
Fixed Tower Cost	$ 991,988.06	
Tower Cost Scaling Component	0.01298	
Fossil Backup	0.000 $/kW$_e$	
Receiver Reference Cost	$ 65,085,970.84	
Receiver Reference Area	1110 m^2	
Receiver Scaling Component	0.7	
Contingency	10%	
Indirect Capital Costs		
Engineer, Procure, Construct	15% of Direct Cost	
Project, Land, Management	3.5% of Direct Cost	
Sales tax Applies to:	80% of Direct Cost	
O&M Costs		
Fixed Annual Cost	0.000 $/yr	
Fixed Cost by Capacity	88.030 $/kW.yr	
Variable Cost by Generation	6.160 $/MWh	3.450 $/MWh
Fossil Fuel Cost	0.000 $/MMBTU	

* Unadjusted value left as SAM default

8.8 Parabolic Trough Design Specifications

The following sections will cover some of the key plant design and performance related inputs for the parabolic trough models in SAM. For the sake of brevity, only the inputs which have been specifically adapted for South African conditions, or otherwise modified from the SAM default inputs, will be covered in the following sections. A full list of the SAM default design inputs for the parabolic trough model is presented in Appendix D, while the final design and performance inputs used in this study for the parabolic trough models are presented in Appendix F.

8.8.1 Design Gross Output and Nameplate Capacity

As stated in Section 8.4 it was decided to adopt the WorleyParsons Group, and SAM default parabolic trough plant size of 100 MW nameplate capacity. This approach was adopted as all technical and design related data included in SAM is specific to a plant of this size. Furthermore, 100 MW is also the plant capacity adopted by Eskom (2006) for their prosed central receiver plant in the Northern Cape. In order to produce a nameplate capacity of 100 MW, a gross design output of 110 MW was required to account for the parasitic and other losses in the system (SAM, 2010). Although this value has not been changed from the SAM default, it is included in this section as a reference and reminder of the parabolic trough plant size in this study.

8.8.2 Availability and Performance

According to EPRI (2010), parabolic troughs are expected to have an annual availability of up to 95%. This is due to the existing commercial nature of parabolic trough plants, as well as the fact that the solar fields do not operate at night, thereby allowing for much of the maintenance to take place during this down time. Furthermore, the modular nature of the SCAs and HCEs means that repairs can be carried out on a single unit, while the remainder of the plant remains in operation.

As no mention of any degradation assumptions are made in the EPRI (2010) study, it was decided to adopt the SAM default value of 0% degradation, which assumes adequate maintenance is conducted on the plant throughout its lifetime.

8.8.3 Solar Irradiation Design Point Calculation

The solar irradiation design point value is generally defined as the maximum annual incident DNI value (in W/m^2) experienced at a location in a typical meteorological year. SAM makes use of this value to calculate the required solar field aperture from the user-specified solar multiple value. According to the SAM (2010) documentation, the choice of this value is of great importance, as the value has a significant impact on the calculated field aperture size. An example is given where a 110 MW plant with a solar multiple of 2 and an irradiation design point value of 950 W/m^2 requires a field aperture of 862,000 m^2, but the same system with an irradiation design point value of 800 W/m^2 requires a field aperture of 1,030,000 m^2. It is thus imperative to make use of an accurate value, as choosing too low a value will result in an oversized solar field which would then lead to excessive collector defocusing. Conversely, too high a value would result in an undersized solar field which can rarely drive the power block at its rated capacity.

The SAM documentation continues to state that an irradiation design point value of 950 W/m^2 would be suitable for a plant in the Mojave Desert in the U.S. while a value of 800 W/m^2 is typical for Southern Spain. It is suggested, however, to calculate the correct maximum irradiation design point value for each location being modelled, by making use of the location weather data and the field collector tilt and azimuth. This value can be calculated in SAM by the following method:

1. Initialise a parabolic trough simulation in SAM.
2. Choose and input the weather data for the site in question.
3. Adjust the solar field collector tilt and azimuth values from their default values of 0° tilt and 0° North-South orientations.
4. Run the simulation and view the hourly result database.
5. The maximum annual incident DNI value for each hour of the simulation is given by the the $Collector\_DNI\text{-}x\text{-}CosTh$ variable.
6. This data can then be exported and examined in a spreadsheet program in order to determine the absolute maximum value and hence the irradiation at design value.

The maximum annual incident DNI value, and hence the irradiation design point value, was calculated for the Upington, Springbok and Bloemfontein locations by following the above procedure. The resulting values are presented in Table 8.11.

Table 8.11: Calculated Solar Irradiation Design Point Values for Upington, Springbok and Bloemfontein.

	Calculated Solar Irradiation Design Point (W/m^2)	Value Used in Analysis (W/m^2)
Upington	1088.1	1088
Springbok	1084.1	1084
Bloemfontein	1085.4	1085

Although the calculated values above are slightly higher than the 950 W/m^2 values assumed for the Mojave Desert in the U.S., this is to be expected, as according to the Edkins et al. (2009) as stated in Section 6.3.1, the Northern Cape receives average annual daily DNI values which are though to be some of the highest worldwide, and in excess of areas such as California. This is further confirmed by the solar resource maps created for South Africa in the GIS section of this report.

8.8.4 Cooling Technology Choice

It has already been noted that the use of cooling water – and hence cooling technology choice – is one of the key points of interest in this study. It was therefore necessary to consider and model both a parabolic trough plant with wet cooling and one with dry cooling for each location, in order to ascertain the effects the cooling technology choice would have on water use, efficiency and ultimately cost.

The SAM software presents the user with a choice of two standard library models for cooling systems, namely an evaporative wet cooled system and an air-cooled condenser (dry cooled) system. For each location, one parabolic trough model was set up with wet cooling, and a second model with dry cooling. The resulting design-related input data for each technology is presented in Table 8.12. It is noted that for the case of wet cooling, the ambient temperature at design is the wet bulb temperature, while for the dry cooled system, the ambient temperature at design is the dry bulb temperature. The reference condenser water temperature change value and approach temperature are specific to evaporative cooling only, and are used by SAM in the calculation of the cooling water mass flow rate and turbine back pressure. Similarly, the initial temperature difference at design point value and condenser pressure ratio are specific to dry cooling only, and are used by SAM in the calculation of the pressure drop across the condenser and the corresponding parasitic power required to maintain the air flow rate (SAM, 2010).

Table 8.12: Parabolic Trough Cooling Technology Design Input Variables. *Source of Data:* SAM (2010).

Parabolic Trough	Wet Cooling	Dry Cooling
Condenser Type	Evaporative	Air-cooled
Ambient Temperature at Design	20 ℃	33 ℃
Reference Condenser Water dT	10 ℃	–
Approach Temperature	5 ℃	–
Initial Temperature Difference at Design Point	–	16 ℃
Condenser Pressure Ratio	–	1.0028
Power Block Rated Cycle Conversion Efficiency	0.3774	0.3390
Steam Cycle Blowdown Fraction	0.013	0.016

It is noted that the overall efficiency of the power block when running on a wet cooling cycle is higher than that of dry cooling, which is to be expected. In addition, the steam cycle blowdown fraction – which accounts for water used in steam cycle make-up and replenishment – is higher for dry cooling in order to account for wet-surface air cooling for critical Rankine cycle components (SAM, 2010).

8.8.5 Solar Multiple Optimisation

The solar multiple of a CSP system is defined as the ratio between the thermal power produced by the solar field at its design point, and the thermal power required by the power block under normal operational conditions (Montes et al., 2009). A solar multiple of 1.0 would imply that the solar field of a plant is just sufficient to drive the power block at full rated capacity when experiencing its maximum DNI design point value. A typical parabolic trough plant with a solar multiple of 1.0 would therefore only operate at its design point for only a few hours of every year. In an attempt to overcome this limitation, the majority of CSP plants possess oversized solar fields – and hence solar multiples greater than 1.0 – thereby allowing the plant to operate closer to its design point for more hours of the year. However, over-sizing the soar field does mean that excess thermal energy will be generated during times of high solar irradiation. In a system without storage, this excess energy is lost, while in a system with thermal energy storage, this excess energy will be diverted to the storage system for later use (Montes et al., 2009; SAM, 2010). This process is illustrated graphically in Figure 8.7.

A system with a solar multiple greater than 1.0 therefore produces more electricity, consequently reducing the system's LCOE. The increase in solar field size also increases the capital and O&M costs of the plant, however, and hence a balance needs to be found

between the increased electricity production and increased system cost. In most systems, a turning point will be reached, after which the higher system cost associated with increasing the solar multiple outweighs the benefit of the added electricity production. The complexity of the relationship is also increased when one considers a system with thermal storage, as TES can increase electricity output by storing energy from an even larger solar field, but has associated higher system costs and thermal losses. According to the SAM documentation, the optimal solar multiple for a parabolic trough system with no storage is between 1.4 and 1.5, while that for a system with storage is generally higher.

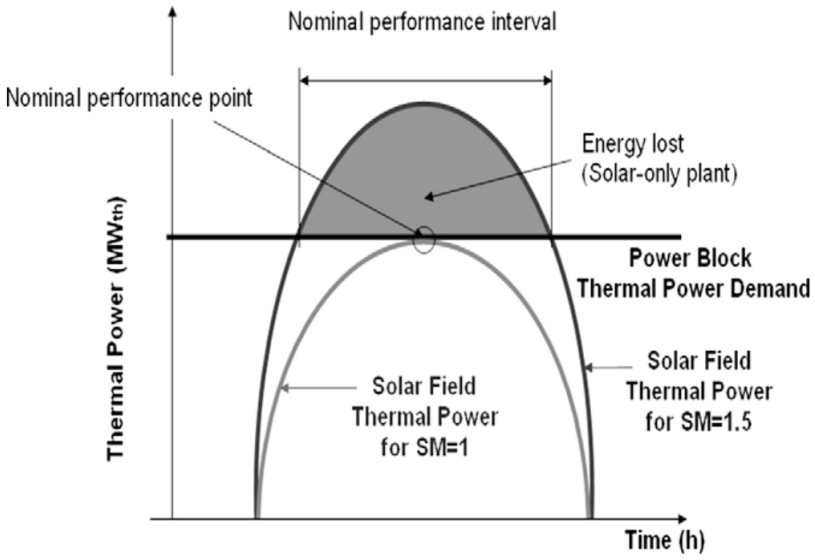

Figure 8.7: Daily Thermal Power Production from a Plant with No Thermal Storage for Different Solar Field Multiples (Montes et al., 2009).

In order to determine the optimal solar multiple value for each plant in this study, for all locations and cooling technologies, a parametric analysis within the SAM software was chosen. This method is recommended by the SAM documentation, due to the complex relationship between the solar multiple and LCOE for a plant with storage. For each of the parabolic trough models, both wet and dry cooled, and at each location, a simulation was run to calculate the LCOE of the plant with solar multiples ranging from 1.0 to 3.0 in increments of 0.1. Thus for each model with 6 hours of thermal storage, 21 simulations were run. The results were then exported to a spreadsheet program for analysis and graphing purposes. The simulations took a fair amount of time to run, and thus the incremental resolution was not increased to below 0.1. This value was considered acceptable, however, as the SAM software defaults to an increment of only 0.25. The graphic results of the optimisation process for each plant type situated at Upington, Springbok and Bloemfontein are presented in Figure 8.8, Figure 8.9 and Figure 8.10 respectively.

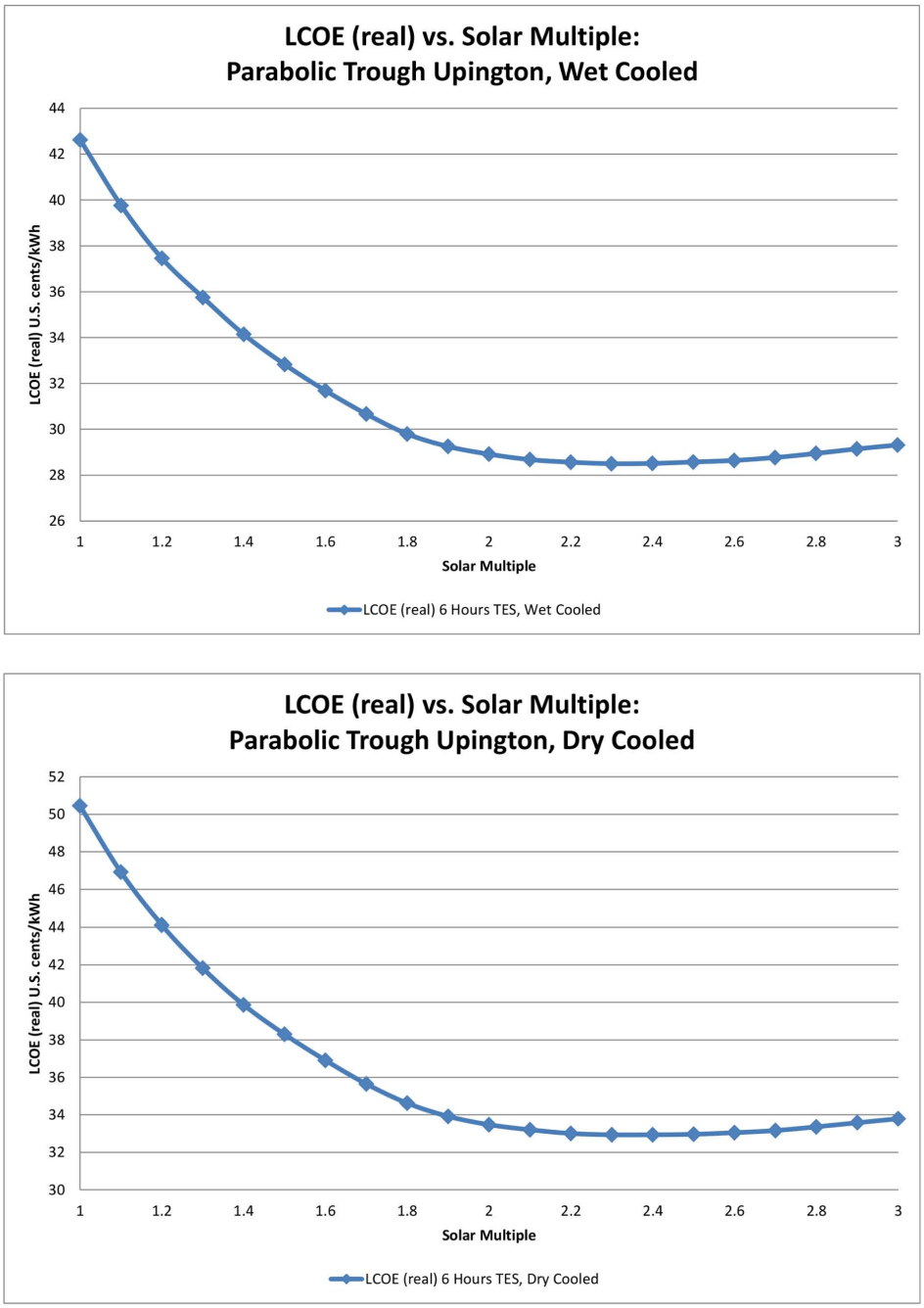

Figure 8.8: LCOE as a Function of Solar Multiple for Wet and Dry Cooling, Used to Determine Optimal Solar Multiple Value for Upington.

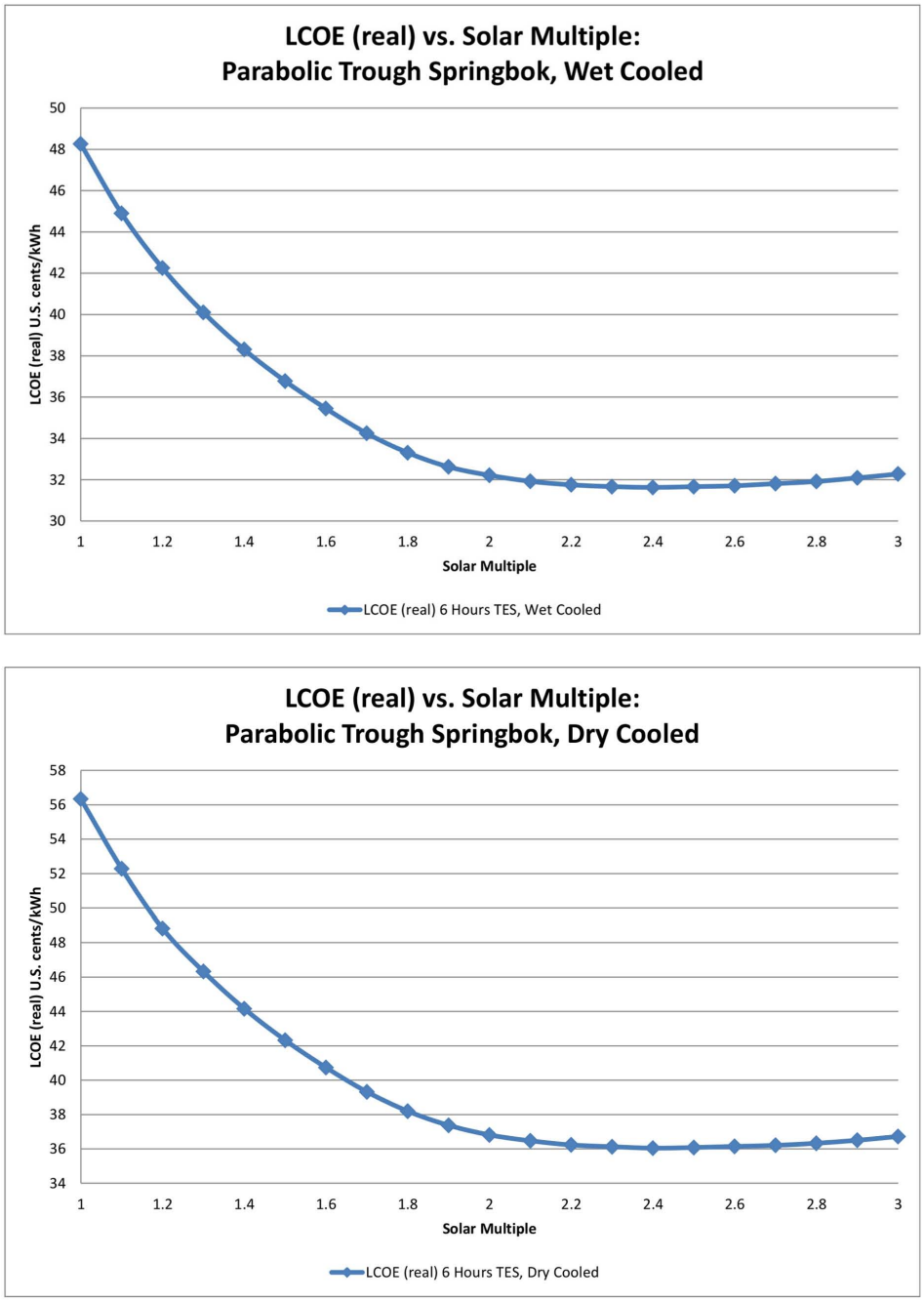

Figure 8.9: LCOE as a Function of Solar Multiple for Wet and Dry Cooling, Used to Determine Optimal Solar Multiple Value for Springbok.

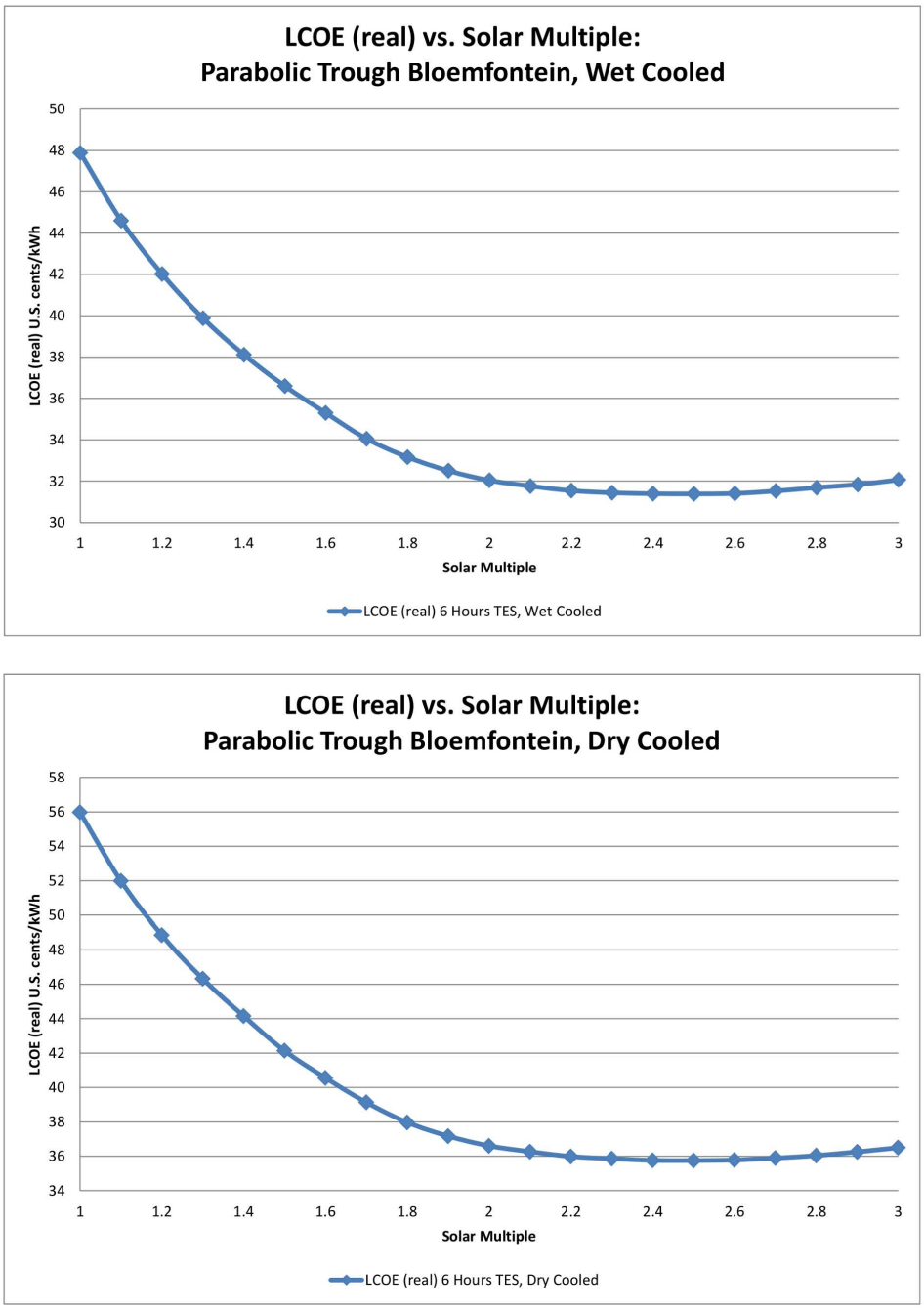

Figure 8.10: LCOE as a Function of Solar Multiple for Wet and Dry Cooling, Used to Determine Optimal Solar Multiple Value for Bloemfontein.

From the graphs, it is evident that the LCOE initially decreases rapidly with an increase in solar multiple, until it is eventually overwhelmed by the increasing system costs. For all three locations, the optimal solar multiple value occurs in the region of 2.3 to 2.5, with a slight variation in each location. Although there is an obvious difference in LCOE price between wet cooled and dry cooled systems, both system types possessed the same optimal solar multiple in each location. The optimal solar multiple values determined and used in the remainder of this study for each cooling technology and each location are presented in Table 8.13.

Table 8.13: Calculated Optimal Solar Multiples for Parabolic Trough Models with Wet and Dry Cooling in Upington, Springbok and Bloemfontein.

Location	Optimal Solar Multiple for Parabolic Trough Model	
	Wet Cooling	Dry Cooling
Upington	2.3	2.3
Springbok	2.4	2.4
Bloemfontein	2.5	2.5

As a means of validating the above results, the graphs from the solar multiple optimisation in this study were compared to those found by Montes et al. (2009) and depicted in Figure 8.11. The same shape and trend is found in both, while the difference in position of the optimal solar multiple observed is primarily due to the exclusion of thermal storage in the Montes et al. study. The optimal solar multiple values of 2.3 to 2.5 found in this study are also strongly comparable to the values of between 2.0 and 2.25 found in the SAM documentation optimisation example of a plant with 6 hours TES (SAM, 2010).

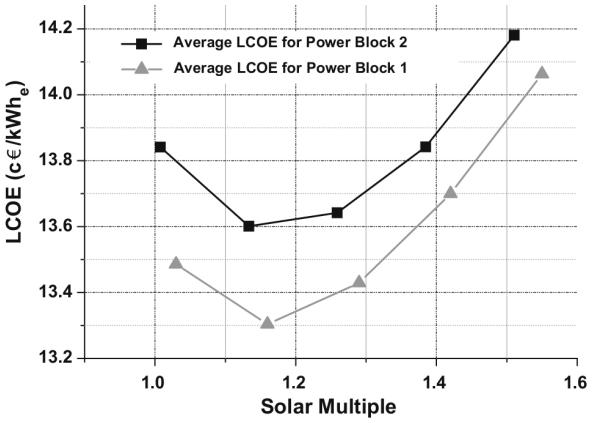

Figure 8.11: Average Electricity Cost for Every Solar Multiple Considered and Two Configurations of the Power Block with No Storage (Montes et al., 2009).

8.9 Central Receiver Design Specifications

As with the parabolic trough model, the following sections will cover some of the key plant design and performance related inputs for the central receiver models in SAM. Once again, for the sake of brevity, only the inputs which have been specifically adapted for South African conditions, or otherwise modified from the SAM default inputs, will be covered in the following sections. A full list of the SAM default design inputs for the central receiver model is presented in Appendix E, while the final design and performance inputs used in this study for the central receiver models are presented in Appendix G.

8.9.1 Design Gross Output and Nameplate Capacity

As for the case of the parabolic trough models, a plant size of 100 MW nameplate capacity was adopted for all central receiver models. Once again, a gross design output of 110 MW was needed in order to produce a nameplate capacity of 100 MW due to parasitics and losses. Although this value has not been changed from the SAM default, it is included in this section as a reference.

8.9.2 Availability and Performance

EPRI (2010) state that central receivers are expected to have an availability of 92%, which is less than the 95% for parabolic troughs. This is primarily due to the early commercial status of central receivers, however, this value is expected to increase in the future as more systems are deployed. For this analysis, the stated value of 92% was adopted.

As with the parabolic trough model, it was also decided to adopt the SAM default value of 0% degradation, which assumes that adequate maintenance is conducted on the plant throughout its lifetime.

8.9.3 Tower, Heliostat Field and Solar Multiple Optimisation

The central receiver optimisation wizard attempts to locate the best design parameters for the heliostat field, tower and receiver by searching through a discrete number of inputs defined by the search range. However, all calculations are based on a specified solar multiple value for the model in question, whose value is *not* varied or optimised by the wizard. As in the case of the parabolic trough model, the optimal solar multiple value for the central receiver plants at each location was also unknown prior to the analysis. It

was therefore decided to first run the optimisation wizard with a number of different solar multiples covering a similar range of values to those for the parabolic trough models, for each cooling technology type and at each location, but to retain the default search ranges and increments. The wizard would then define the optimal heliostat field layout, tower height and receiver dimensions for *that particular* solar multiple. Subsequently, using the resulting heliostat field layout, tower and receiver dimensions for that particular solar multiple, a full simulation was then run for each possible configuration in order to determine which solar multiple produced the heliostat field layout, tower height and receiver design which resulted in the lowest LCOE.

The results for each optimisation wizard run with each solar multiple, and full simulation calculated LCOE are presented in the following sections. For the sake of brevity, the full heliostat field layout, tower, and receiver dimensions will not be presented for each and every optimisation wizard run, but only for the run with the *optimal* solar multiple which resulted in the lowest LCOE in the full simulation.

Solar Multiple Optimisation

From the results of the previous solar multiple optimisation performed in the parabolic trough model, it was expected that the optimal solar multiple would occur in the region of 2.0; however, in order to determine the optimal solar multiple values for each plant, the solar multiple values were iterated from 1.0 to 2.6, by which stage it could be observed that the turning point had been passed. As was the case for the parabolic trough models, the calculated LCOE values from the simulation runs for each solar multiple were then exported to a spreadsheet program for analysis and graphing purposes. Due to the added step of having to run the tower and heliostat optimisation wizard first for each solar multiple value (and hence not being able to make use of a parametric analysis) the simulation and optimisation process took a fair amount of time to complete. The same parabolic trough incremental resolution of 0.1 was therefore adopted. The graphic results for the variation of LCOE with solar multiple for central receiver plants at all locations utilising wet cooling technology are presented in the first graph of Figure 8.12, while those for dry cooling at all locations are presented in the second graph of Figure 8.12.

The graphic results suggest that the optimal solar multiple for all the central receiver plants with *wet* cooling at all three locations in this study is 2.0. Similarly, the predicted optimal solar multiple for all the central receiver plants with *dry* cooling at all three locations in this study is 1.9. These values are strongly comparable to the solar multiple value of 1.9 as used by the SAM example central receiver model with 6 hours TES in California, and were therefore adopted for the remainder of this study.

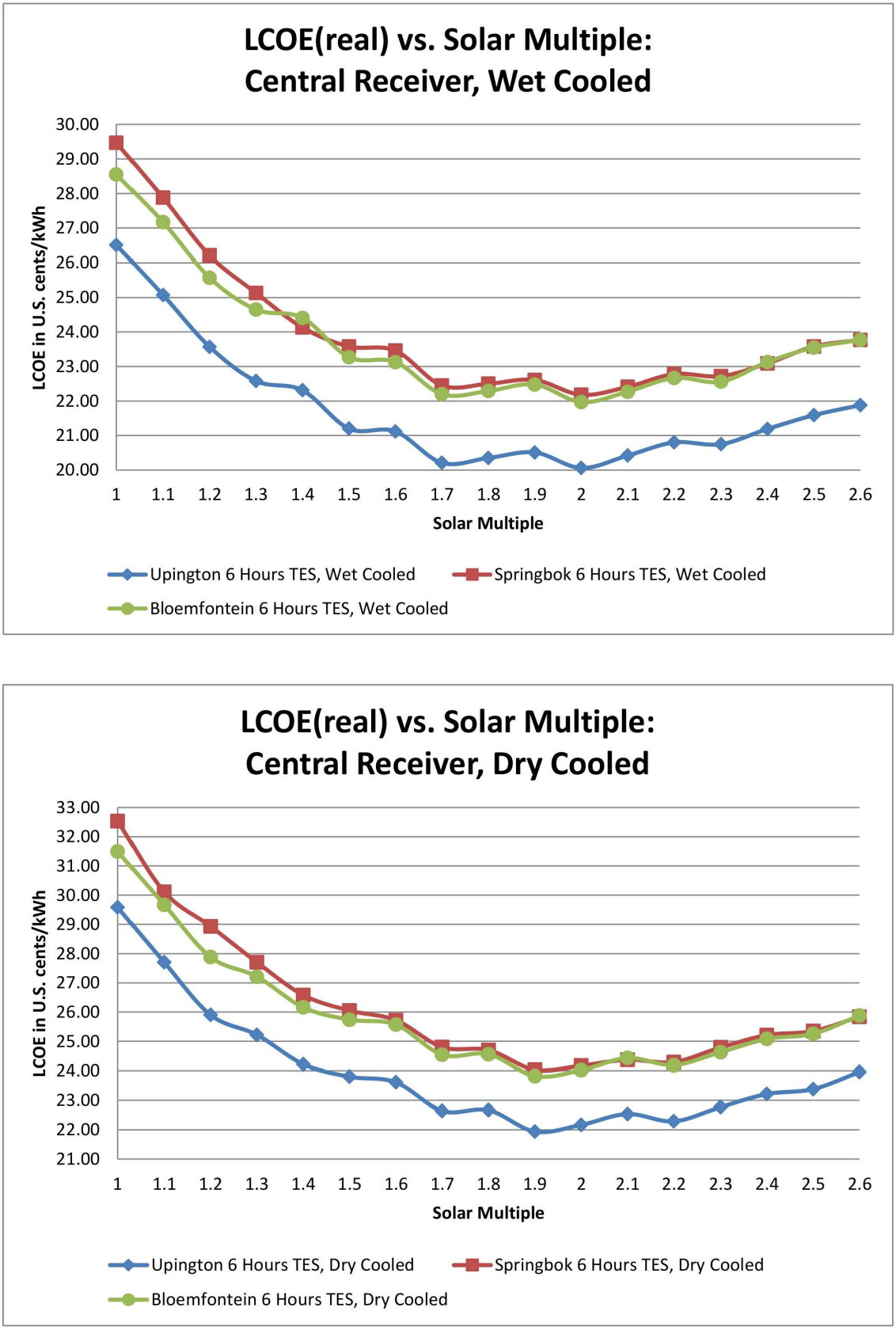

Figure 8.12: LCOE as a Function of Solar Multiple for Wet and Dry Cooling, Used to Determine Optimal Solar Multiple for Central Receiver Plants.

Heliostat Field Layout and Characteristics

The optimal heliostat field layouts generated by the optimisation wizard for each location and each cooling technology type – utilising a solar multiple of 2.0 for wet systems and 1.9 for dry systems – are depicted visually in Figure 8.13 and Figure 8.14. Each image represents an aerial view of the circular fields, which are divided into 12 radial segments with 12 rows each. The darker red areas indicate a higher density of heliostats.

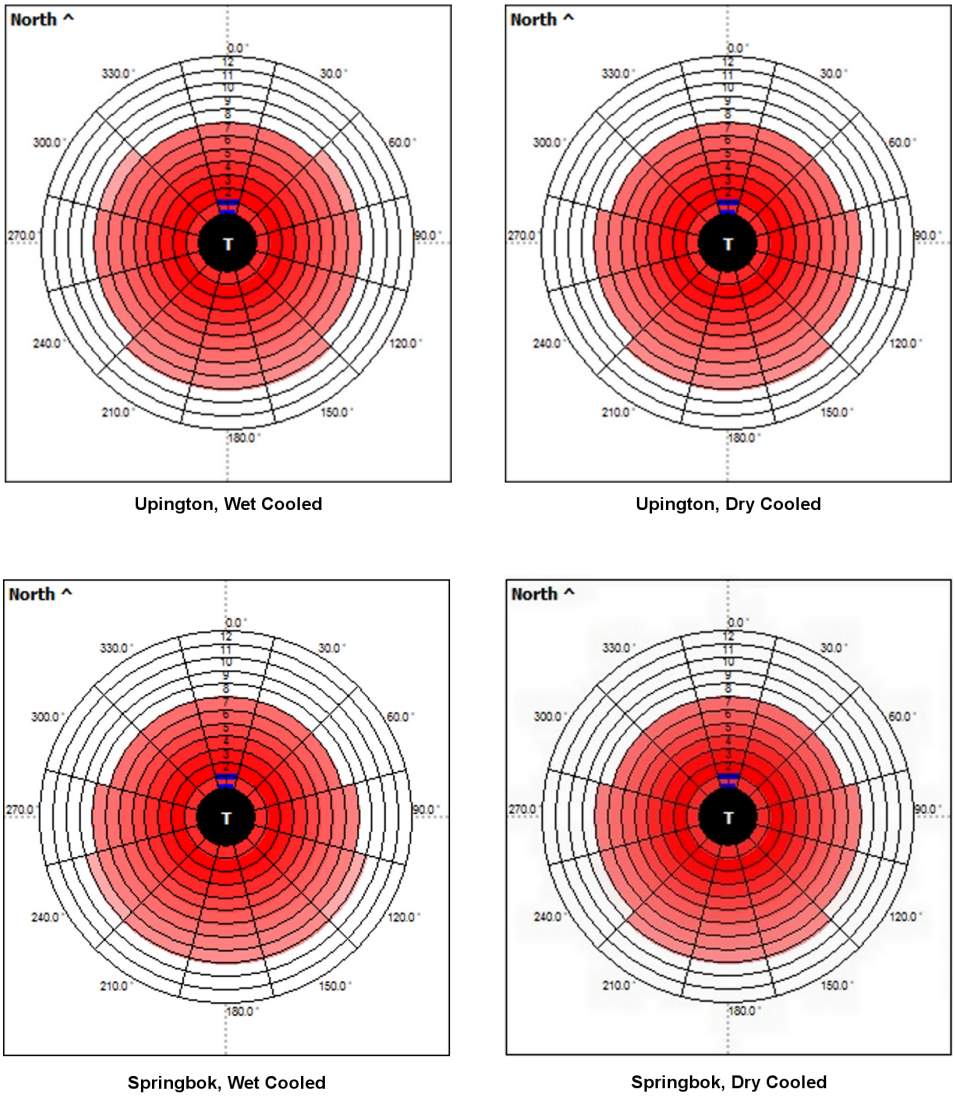

Figure 8.13: Optimal Heliostat Field Layout Diagram for a Central Receiver Plant with Wet and Dry Cooling at Upington and Springbok.

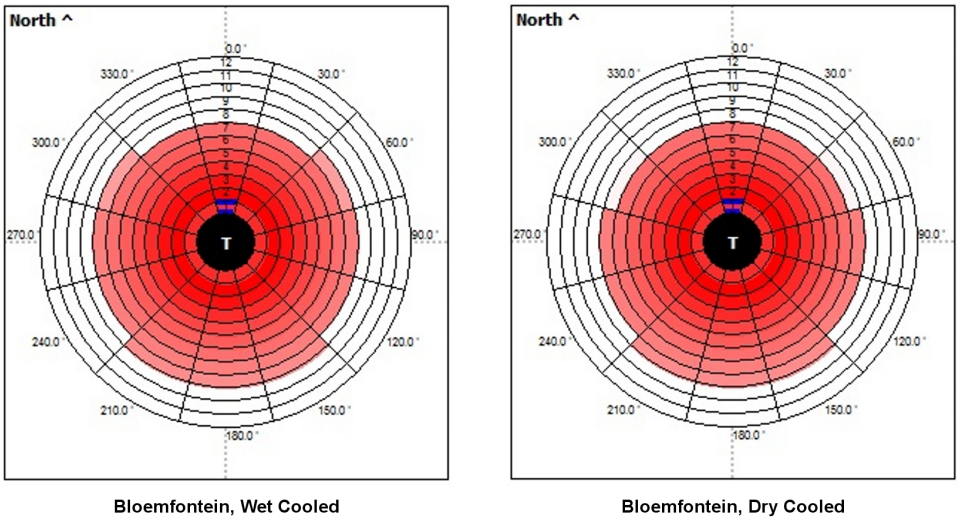

Figure 8.14: Optimal Heliostat Field Layout Diagram for a Central Receiver Plant with Wet and Dry Cooling at Bloemfontein.

As one would expect, the large majority of the heliostats in the field are located on the Southern side of the tower, thereby reducing cosine effect losses and increasing optical efficiency for locations in the Southern Hemisphere. This process is best visualised by means of the diagram shown in Figure 8.15. In order to focus the sun's rays onto the receiver, a heliostat must position itself so that its surface normal bisects the angle between the sun's rays and the line from the heliostat to the tower. The effective reflection area of the heliostat is then reduced by the cosine of one-half of the angle subtended. In the Southern Hemisphere, heliostats in the South field generally have their surface normal pointing Northwards towards the tower, thereby suffering less cosine reduction when compared to heliostats in the North field (Stine and Geyer, 2001).

The total number of heliostats in the field, as well as the total reflective area, and minimum and maximum distances from the tower calculated for each location and cooling technology are presented in Table 8.14. From the results it is evident that all of the plants have approximately 7000 heliostats, which is strongly comparable to the estimate of 6000 heliostats suggested by Eskom (2006) for their proposed 100 MW central receiver plant in the Northern Cape. The maximum distance from the tower of approximately 1260 m is also within the 2.0 km range for a large CSP plant, as suggested by the SAM (2010) documentation.

Table 8.14: Calculated Optimal Heliostat Field Layout Parameters for Central Receiver Models with Wet and Dry Cooling in Upington, Springbok and Bloemfontein.

		Number of Heliostats	Total Reflective Area (m^2)	Min. Distance from Tower (m)	Max. Distance from Tower (m)
Upington	Wet:	7119	1,027,804.2	162.5	1259.4
	Dry:	6997	1,010,190.5	162.5	1259.4
Springbok	Wet:	7125	1,028,670.4	162.5	1259.4
	Dry:	7011	1,012,211.7	162.5	1259.4
Bloemfontein	Wet:	7129	1,029,247.9	162.5	1259.4
	Dry:	7005	1,011,345.5	162.5	1259.4

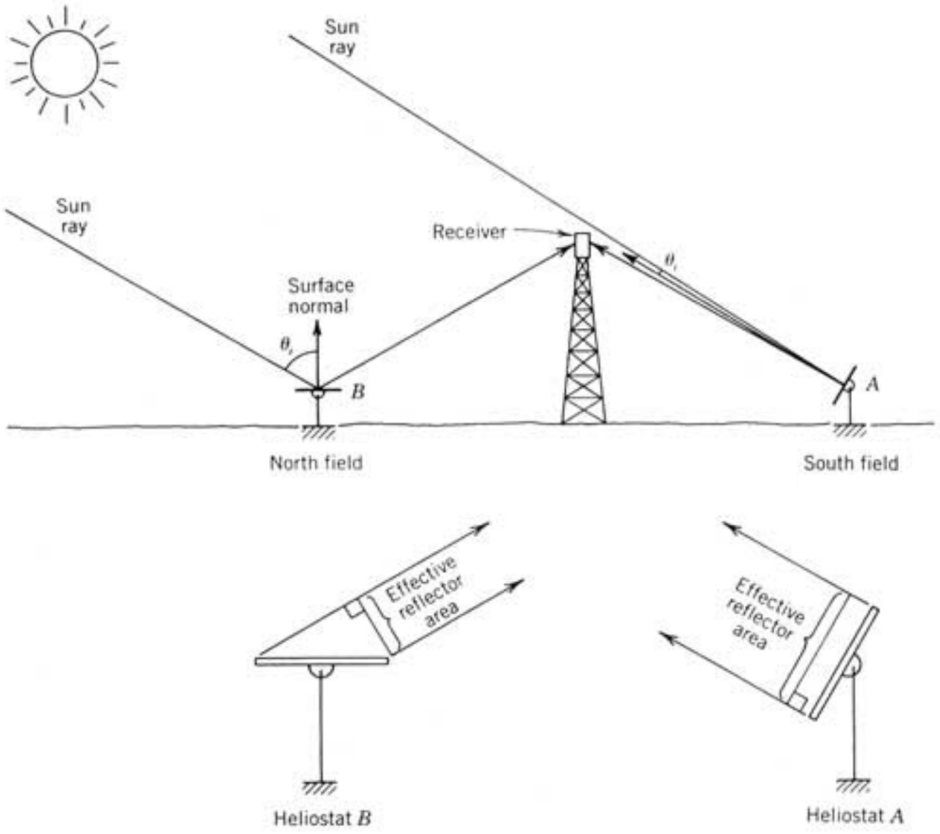

Figure 8.15: Cosine Effect of Two Heliostats in the Southern Hemisphere. *Adapted from Image:* Stine and Geyer (2001).

Tower and Receiver Dimensions

The optimal tower heigh as defined by the optimisation wizard occurred at a height of 216.67 m. This height was deemed the optimum value for all locations with both wet and dry cooling – with associated solar multiples of 2.0 and 1.9 respectively. This value is also strongly comparable to the estimated tower heigh of 210 m suggested by Eskom (2006) for their 100 MW proposed plant in the Northern Cape.

The optimal receiver heigh and diameter predicted by the optimisation wizard were 15.49 m and 12.44 m respectively. Once again this was standard when considering all locations, cooling types and solar multiples. Eskom (2006) estimated a receiver height in the region of 20 m for their 100 MW plant, thus once again affirming the credibility of the optimisation wizard results. The results for both tower height and receiver dimensions are presented in Table 8.15.

Table 8.15: Calculated Optimal Tower and Receiver Dimensions for Central Receiver Models with Wet and Dry Cooling in Upington, Springbok and Bloemfontein.

		Tower Height (m)	Receiver Height (m)	Receiver Diameter (m)
Upington	Wet Cooling:	216.67	15.49	12.44
	Dry Cooling:	216.67	15.49	12.44
Springbok	Wet Cooling:	216.67	15.49	12.44
	Dry Cooling:	216.67	15.49	12.44
Bloemfontein	Wet Cooling:	216.67	15.49	12.44
	Dry Cooling:	216.67	15.49	12.44

8.9.4 Receiver HTF Flow Configuration

In his study and creation of the central receiver model for SAM, Wagner (2008) identified 8 possible flow configurations for the HTF through the receiver. These flow configurations are presented in Figure 8.16. The cross-over flow pattern labelled as *Configuration 1* in the image is the one adopted at Solar II and is also the SAM default for its example plant in the Northern Hemisphere. In this configuration, the HTF enters through the Northern-most panels and then proceeds in series through half of the panels, before finally exiting from the two Southern-most panels of the receiver.

In this study, however, it was decided to adopt the same cross-over flow configuration, but to instead use the configuration identified by *Configuration 2* in the figure. This is due to the CSP plants in this study being located in the Southern Hemisphere, thereby requiring the HTF to enter from the Southern-most panels of the receiver.

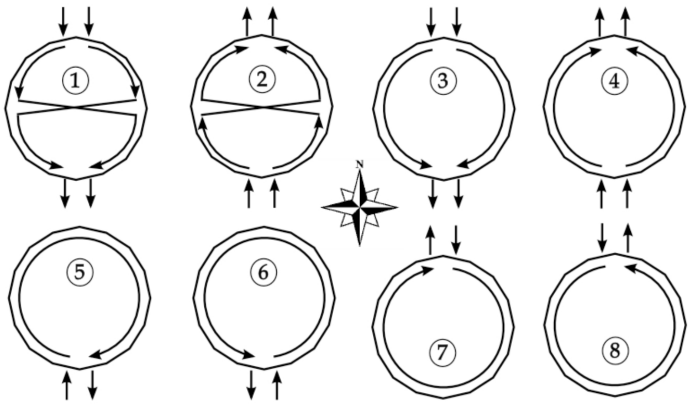

Figure 8.16: Possible Flow Configurations for External Receiver (Wagner, 2008).

8.9.5 Cooling Technology Choice

As for the case of the parabolic trough model, for each location, one central receiver model was set up with wet cooling, and a second model with dry cooling. The resulting design-related input data for each cooling technology is presented in Table 8.16. Once again it is noted that the overall efficiency of the power block when running on a wet cooling cycle is higher than that of dry cooling, while the steam cycle blowdown fraction is higher for dry cooling in order to account for wet-surface air cooling for critical Rankine cycle components (SAM, 2010).

Table 8.16: Central Receiver Cooling Technology Design Input Variables. *Source of Data:* SAM (2010).

Central Receiver	Wet Cooling	Dry Cooling
Condenser Type	Evaporative	Air-cooled
Ambient Temperature at Design	20 ℃	33 ℃
Reference Condenser Water dT	10 ℃	–
Approach Temperature	5 ℃	–
Initial Temperature Difference at Design Point	–	16 ℃
Condenser Pressure Ratio	–	1.0028
Power Block Rated Cycle Conversion Efficiency	0.425	0.408
Steam Cycle Blowdown Fraction	0.013	0.016

8.10 Thermal Storage

A thermal energy storage system comprising two-tank molten salt storage was chosen for both the parabolic trough and central receiver CSP models in this study, as per the SAM software defaults. The two-tank molten salt storage system was considered an appropriate choice, based on the review of thermal storage technologies in Chapter 5, which identified sensible-heat storage as the current most commercially viable TES technology. Furthermore, molten salt storage is also the adopted storage technology in the more recent CSP plants such as Andasol I - III, Solar Two and Gemasolar (Solar Tres) (Meyer, 2010; Torresol Energy, 2011).

In keeping with the plant design data assumptions from the previous sections, the default thermal storage design inputs were adopted for both the parabolic trough and central receiver models. An indirect two-tank molten salt system was specified for the parabolic trough plant, while a direct two-tank molten salt system was specified for the central receiver plants. Once again, the complete set of input variables for the parabolic trough and central receiver plants is presented in Appendix F and Appendix G respectively.

8.10.1 Full Load Hours of Thermal Storage

Although it is possible to simulate both parabolic trough and central receiver models with varying hours of thermal storage, it was decided to only study systems with 6 hours of full load TES in this analysis. This decision was made primarily due to time constraints, as the inclusion of a variation in hours of storage would more than double the number of models being run in this study. Furthermore, the value of 6 hours was chosen not only because is it the default SAM value for both parabolic trough and central receiver systems – hence full data for its inclusion is available – but it also represents the required number of storage hours specified by NERSA for both parabolic trough and central receiver plants in the South African REFIT (NERSA, 2010).

8.10.2 Storage Dispatch Schedule

As discussed in Section 7.6.1, the thermal storage dispatch schedule determines how and when the energy flows between the solar field, the thermal energy storage system and the power block, for up to six different dispatch periods. SAM presents a library of default dispatch schedules, with the SCE dispatch schedule representing the software default. The SCE default dispatch schedule is presented in Figure 8.17, with its legend shown in Table 8.17. A storage dispatch value of 0 indicates that the system will always

dispatch stored energy in any hour assigned to the given dispatch period, if required. A turbine output fraction of 1.0 requires the turbine gross output to be met in full, with supplementation from storage if it is available. A value of 0 for fossil fill fraction ensures that no fossil backup is utilised under any circumstance.

It was decided to employ the SAM default SCE dispatch schedule for thermal storage in this study, however, it was first necessary to modify it for conditions relevant to the Southern Hemisphere. This is evident, as it can be seen in Figure 8.17 that the default peak turbine output occurs over the months of June to September, instead of the Southern Hemisphere summer months of December to March. The entire dispatch schedule was thus shifted forward by six months, thereby retaining its form but adapting it to the local Souther Hemisphere climate. The resulting adapted dispatch schedule used in this study is presented in Figure 8.18.

Weekday Schedule

	12am	1am	2am	3am	4am	5am	6am	7am	8am	9am	10am	11am	12pm	1pm	2pm	3pm	4pm	5pm	6pm	7pm	8pm	9pm	10pm	11pm
Jan	6	6	6	6	6	6	5	5	4	4	4	4	4	4	4	4	4	4	4	4	4	5	5	5
Feb	6	6	6	6	6	6	5	5	4	4	4	4	4	4	4	4	4	4	4	4	4	5	5	5
Mar	6	6	6	6	6	6	5	5	4	4	4	4	4	4	4	4	4	4	4	4	4	5	5	5
Apr	6	6	6	6	6	5	5	4	4	4	4	4	4	4	4	4	4	4	4	4	5	5	5	6
May	6	6	6	6	6	5	5	4	4	4	4	4	4	4	4	4	4	4	4	4	5	5	5	6
Jun	3	3	3	3	3	3	3	2	2	2	2	1	1	1	1	1	1	2	2	2	2	2	3	3
Jul	3	3	3	3	3	3	3	2	2	2	2	1	1	1	1	1	1	2	2	2	2	2	3	3
Aug	3	3	3	3	3	3	3	2	2	2	2	1	1	1	1	1	1	2	2	2	2	2	3	3
Sep	3	3	3	3	3	3	3	2	2	2	2	1	1	1	1	1	1	2	2	2	2	2	3	3
Oct	6	6	6	6	6	5	5	4	4	4	4	4	4	4	4	4	4	4	4	4	5	5	5	6
Nov	6	6	6	6	6	6	5	5	4	4	4	4	4	4	4	4	4	4	4	4	4	5	5	5
Dec	6	6	6	6	6	6	5	5	4	4	4	4	4	4	4	4	4	4	4	4	4	5	5	5

Weekend Schedule

	12am	1am	2am	3am	4am	5am	6am	7am	8am	9am	10am	11am	12pm	1pm	2pm	3pm	4pm	5pm	6pm	7pm	8pm	9pm	10pm	11pm
Jan	6	6	6	6	6	6	5	5	5	5	5	5	5	5	5	5	5	5	5	5	5	5	5	5
Feb	6	6	6	6	6	6	5	5	5	5	5	5	5	5	5	5	5	5	5	5	5	5	5	5
Mar	6	6	6	6	6	6	5	5	5	5	5	5	5	5	5	5	5	5	5	5	5	5	5	5
Apr	6	6	6	6	6	5	5	5	5	5	5	5	5	5	5	5	5	5	5	5	5	5	5	6
May	6	6	6	6	6	5	5	5	5	5	5	5	5	5	5	5	5	5	5	5	5	5	5	6
Jun	3	3	3	3	3	3	3	3	3	3	3	3	3	3	3	3	3	3	3	3	3	3	3	3
Jul	3	3	3	3	3	3	3	3	3	3	3	3	3	3	3	3	3	3	3	3	3	3	3	3
Aug	3	3	3	3	3	3	3	3	3	3	3	3	3	3	3	3	3	3	3	3	3	3	3	3
Sep	3	3	3	3	3	3	3	3	3	3	3	3	3	3	3	3	3	3	3	3	3	3	3	3
Oct	6	6	6	6	6	5	5	5	5	5	5	5	5	5	5	5	5	5	5	5	5	5	5	6
Nov	6	6	6	6	6	6	5	5	5	5	5	5	5	5	5	5	5	5	5	5	5	5	5	5
Dec	6	6	6	6	6	6	5	5	5	5	5	5	5	5	5	5	5	5	5	5	5	5	5	5

Figure 8.17: Default SAM SCE Dispatch Schedule (SAM, 2011).

Table 8.17: Thermal Dispatch Schedule Legend. *Source of Data:* SAM (2010).

	Storage Dispatch: With Solar	Storage Dispatch: Without Solar	Turbine Output Fraction	Fossil Fill Fraction
Period 1	0	0	1.1	0
Period 2	0	0	1	0
Period 3	0	0	1	0
Period 4	0	0	1	0
Period 5	0	0	1	0
Period 6	0	0	1	0

Weekday Schedule

	12am	1am	2am	3am	4am	5am	6am	7am	8am	9am	10am	11am	12pm	1pm	2pm	3pm	4pm	5pm	6pm	7pm	8pm	9pm	10pm	11pm
Jan	3	3	3	3	3	3	3	2	2	2	2	1	1	1	1	1	1	2	2	2	2	2	3	3
Feb	3	3	3	3	3	3	3	2	2	2	2	1	1	1	1	1	1	2	2	2	2	2	3	3
Mar	3	3	3	3	3	3	3	2	2	2	2	1	1	1	1	1	1	2	2	2	2	2	3	3
Apr	6	6	6	6	6	5	5	4	4	4	4	4	4	4	4	4	4	4	4	4	5	5	5	6
May	6	6	6	6	6	6	5	5	4	4	4	4	4	4	4	4	4	4	4	4	4	5	5	5
Jun	6	6	6	6	6	6	5	5	4	4	4	4	4	4	4	4	4	4	4	4	4	5	5	5
Jul	6	6	6	6	6	6	5	5	4	4	4	4	4	4	4	4	4	4	4	4	4	5	5	5
Aug	6	6	6	6	6	6	5	5	4	4	4	4	4	4	4	4	4	4	4	4	4	5	5	5
Sep	6	6	6	6	6	6	5	5	4	4	4	4	4	4	4	4	4	4	4	4	4	5	5	5
Oct	6	6	6	6	6	5	5	4	4	4	4	4	4	4	4	4	4	4	4	4	5	5	5	6
Nov	6	6	6	6	6	5	5	4	4	4	4	4	4	4	4	4	4	4	4	4	5	5	5	6
Dec	3	3	3	3	3	3	3	2	2	2	2	1	1	1	1	1	1	2	2	2	2	2	3	3

Weekend Schedule

	12am	1am	2am	3am	4am	5am	6am	7am	8am	9am	10am	11am	12pm	1pm	2pm	3pm	4pm	5pm	6pm	7pm	8pm	9pm	10pm	11pm
Jan	3	3	3	3	3	3	3	3	3	3	3	3	3	3	3	3	3	3	3	3	3	3	3	3
Feb	3	3	3	3	3	3	3	3	3	3	3	3	3	3	3	3	3	3	3	3	3	3	3	3
Mar	3	3	3	3	3	3	3	3	3	3	3	3	3	3	3	3	3	3	3	3	3	3	3	3
Apr	6	6	6	6	6	5	5	5	5	5	5	5	5	5	5	5	5	5	5	5	5	5	5	6
May	6	6	6	6	6	6	5	5	5	5	5	5	5	5	5	5	5	5	5	5	5	5	5	5
Jun	6	6	6	6	6	6	5	5	5	5	5	5	5	5	5	5	5	5	5	5	5	5	5	5
Jul	6	6	6	6	6	6	5	5	5	5	5	5	5	5	5	5	5	5	5	5	5	5	5	5
Aug	6	6	6	6	6	6	5	5	5	5	5	5	5	5	5	5	5	5	5	5	5	5	5	5
Sep	6	6	6	6	6	6	5	5	5	5	5	5	5	5	5	5	5	5	5	5	5	5	5	5
Oct	6	6	6	6	6	5	5	5	5	5	5	5	5	5	5	5	5	5	5	5	5	5	5	6
Nov	6	6	6	6	6	5	5	5	5	5	5	5	5	5	5	5	5	5	5	5	5	5	5	6
Dec	3	3	3	3	3	3	3	3	3	3	3	3	3	3	3	3	3	3	3	3	3	3	3	3

Figure 8.18: Dispatch Schedule Used in Analysis and Adapted for Southern Hemisphere.

9 Model Results and Analysis

The final inputs for the various CSP technologies and models, as identified, determined and discussed in Chapter 8 were used to create twelve separate, final SAM simulations. These twelve simulations comprise parabolic trough models with wet cooling and with dry cooling, and central receiver models with wet and dry cooling for each of the three stipulated locations. The following chapter will now present and discuss the results obtained from the running of the twelve individual simulations, as well as identify any trends and discuss the optimal CSP configuration for each of the three locations in South Africa. Before the results are presented, however, a brief definition and description of the key considered output metrics will be given.

Annual Energy Production

The annual energy production metric is a measure of the total electric generation, in kWh, for the first year that a plant operates. This first year is equivalent to year one in the project's cash flow. The annual energy output may decrease over the plant's lifetime should a degradation rate value be included. The annual energy production value is a direct result of the plant performance calculations in the SAM model and is thus affected by the plant design and weather conditions (SAM, 2010).

Total Installed Cost per Net Capacity

The total installed cost per net capacity for a plant is simply a measure of the sum of all the capital costs, both direct and indirect, divided by the plant's nameplate rated net capacity (SAM, 2010). In this analysis, the total installed cost per net capacity is calculated by summing all the cost inputs stated in the final costs of Section 8.7 and in Table 8.9 and Table 8.10, and then dividing the total value by the nameplate capacity of 100,001.00 kW (100 MW).

Levelised Cost of Energy

The levelised cost of energy is a value in cents (or Rand) per kilowatt hour, whose value is the amount that a utility-scale project must receive for each unit of electricity it sells, in order to meet the financial requirements defined by a positive cash-flow, the minimum IRR and the minimum DSCR. The LCOE takes into account the project capital costs, financing, tax and operating costs over its lifetime, as well its electricity production (SAM, 2010). The LCOE is defined mathematically by the following formula:

$$\text{LCOE}_{\text{real}} = \frac{\sum_{n=0}^{N} \frac{R_n}{(1+d_{\text{nominal}})^n}}{\sum_{n=1}^{N} \frac{Q_n}{(1+d_{\text{real}})^n}} \tag{9.1}$$

Where,

N = Total project lifetime in years.
Q_n = Total annual energy production in year n.
R_n = The revenue generated from electricity sales in year n, calculated by the product of the annual energy production and electricity PPA price.
d_{real} = The real discount rate.
d_{nominal} = The nominal discount rate, calculated by the following formula:

$$d_{\text{nominal}} = (1+d_{\text{real}})(1+I) - 1$$

I = Inflation rate.

One of the key advantages of using an LCOE, is that it allows for the comparison of alternative technology choices, with different project lifetimes and performance characteristics. The LCOE provides a means to compare all technologies on an equal basis, while capturing the trade-off's between projects with different capital costs and O&M costs (SAM, 2010).

The SAM software calculates the LCOE in both real and nominal terms. According to the SAM (2010) documentation, it is generally advisable to make use of the nominal LCOE for projects with short lifetimes, while projects with longer lifetimes are generally analysed and compared with the real LCOE, thereby accounting for inflation over the project's life. Therefore, due to the 30 analysis periods used in this study, the *real* LCOE was adopted as the comparison metric of choice.

Capacity Factor

The capacity factor of a plant is defined as the ratio of the plant's actual energy output in the first year of operation, to the potential energy output that would have resulted had the plant operated at its nameplate capacity for the entire year. Capacity factors are an important consideration for the analysis of the merits of any plant, and also aid in the determination of whether a plant is better suited for base load generation, mid-merit, or for peaking loads (SAM, 2010).

The capacity factor is defined mathematically as:

$$\text{CF} = \frac{E_{\text{Actual Output Year 1}}}{P_{\text{Nameplate Capacity}} \cdot 8760} \tag{9.2}$$

Where,

CF = Capacity factor.
$E_{\text{Actual Output Year 1}}$ = Total annual energy generation in kWh in year 1 of the project cash-flow.
$P_{\text{Nameplate Capacity}}$ = The rated system nameplate capacity in kW.

9.1 Upington

Of the twelve final simulations, the first four were run for the Upington location. The key results and output metrics for these simulations are presented in Table 9.1. Each of the key areas for the different technologies in Upington will now be briefly discussed and compared under their relevant headings.

9.1.1 Annual Energy Production

The total annual energy produced by each plant type in Upington ranges from 370,088,244 kWh_e for the dry-cooled parabolic trough plant, to 417,100,874 kWh_e for the wet-cooled central receiver plant. As would be expected, the central receiver plants produce greater annual energy output, when compared to the parabolic trough plants, as a result of their higher concentration ratios and greater overall efficiency. The wet-cooled plants for both parabolic trough and central receiver plants also produce more energy than their dry-cooled equivalents as a result of the lower power cycle efficiencies associated with dry cooling.

Table 9.1: Cost and Performance Results for Parabolic Trough and Central Receiver Models with Wet and Dry Cooling in Upington.

Upington	Parabolic Trough		Central Receiver	
	Wet Cooling	Dry Cooling	Wet Cooling	Dry Cooling
Rated Net Capacity	100 MW	100 MW	100 MW	100 MW
Availability	95 %	95 %	92 %	92 %
Economic Life	30 yrs	30 yrs	30 yrs	30 yrs
Annual Energy Produced (kWh_e)	385,626,991.3	370,088,244.3	417,100,874.0	393,061,979.1
Total Direct Cost	$ 704,851,935.08	$ 800,658,637.32	$ 518,441,957.40	$ 545,371,791.37
Total Indirect Cost	$ 209,341,024.72	$ 237,795,615.28	$ 153,977,261.35	$ 161,975,422.04
Total Installed Cost	$ 914,192,959.80	$ 1,038,454,252.60	$ 672,419,218.75	$ 707,347,213.41
Total Installed Cost per Net Capacity	$ 9,141.84 /kW R 64,175.72 /kW	$ 10,384.44 /kW R 72,898.77 /kW	$ 6,724.12 /kW R 47,203.32 /kW	$ 7,073.40 /kW R 49,655.27 /kW
LCOE – real *	28.50 ¢/kWh R 2.00 /kWh	32.93 ¢/kWh R 2.31 /kWh	20.06 ¢/kWh R 1.41 /kWh	21.94 ¢/kWh R 1.54 /kWh
1st Year PPA Price	40.81 ¢/kWh R 2.86 /kWh	47.63 ¢/kWh R 3.34 /kWh	28.33 ¢/kWh R 1.99 /kWh	31.24 ¢/kWh R 2.19 /kWh
Capacity Factor	44.02 %	42.25 %	47.61 %	44.87 %
Annual Water Usage	1,507,891.7 m^3 3.91 l/kWh 1032.97 gal/MWh	89,460.5 m^3 0.24 l/kWh 63.86 gal/MWh	1,410,134.3 m^3 3.38 l/kWh 893.11 gal/MWh	82,446.8 m^3 0.21 l/kWh 55.41 gal/MWh

* ¢/kWh refers to U.S. cents per kilowatt hour.

9.1.2 Installed Cost per Net Capacity

The total installed cost per net capacity for the CSP models in Upington ranges from R47,203.32 /kW ($6,724.12 /kW) for the wet-cooled central receiver model, to R72,898.77 /kW ($10,384.44 /kW) for the dry-cooled parabolic trough plant. Both the central receiver plants are more economical when compared to the parabolic trough plants, which is a result of the difference in system component costs and plant designs between the two CSP technology types. Making use of dry cooling also increases plant costs, which is consistent with the higher capital and maintenance costs associated with the use of dry cooling technology. Furthermore, it is noted that the model predicts a central receiver plant with dry cooling in Upington is more economical in terms of cost per net capacity than the wet-cooled parabolic trough plant with equivalent 100 MW rating in the same location.

9.1.3 Levelised Cost of Energy

The LCOE for the different models in Upington ranges from R1.41 /kWh (20.06 U.S. ¢/kWh) to R2.31 /kWh (32.93 U.S. ¢/kWh) for the wet-cooled central receiver and dry-cooled parabolic trough respectively. The resulting LCOE for the central receiver plants is lower than that of the parabolic trough plants, while wet cooling is more economical than dry cooling for both technologies.

It is also noted that the calculated first year PPA prices of R1.99 /kWh and R2.19 /kWh for the central receiver models with wet and dry cooling respectively, are relatively close to the R2.31 /kWh 2009 value as stated in the REFIT Phase II document released by NERSA (2010) for central receiver plants with 6 hours TES. The PPA prices of R2.86 /kWh and R3.34 /kWh for the parabolic trough models with wet and dry cooling respectively, however, are higher than the 2009 value of R2.10 /kWh suggested by NERSA (2010) in the REFIT Phase II document for parabolic trough plants with 6 hours TES.

9.1.4 Capacity Factor

The capacity factors for the different plants in Upington range from 42.25% for the dry-cooled parabolic trough plant, to 47.61% for the wet cooled central receiver plant. The central receiver plants generally have higher capacity factors when compared to the parabolic trough plants, which is thought to be due the the previously mentioned higher concentration ratios and hence efficiency. Dry cooling also decreases capacity factors due to its negative effect on plant efficiency.

9.1.5 Annual Water Consumption

The difference in the annual water consumption between wet and dry cooling is vast, with the dry cooled central receiver consuming only 82,446.8 m^3 (0.21 litres/kWh) compared to the 1,507,891.7 m^3 (3.91 litres/kWh) of the wet-cooled parabolic trough. The central receiver plants also consume less water annually when compared to parabolic troughs, which is expected, and discussed in Section 4.4 of Chapter 4. Furthermore, the values of 3.91 litres/kWh and 3.38 litres/kWh for the wet-cooled parabolic trough and central receiver plants respectively, are similar to the values of 3.03 litres/kWh and 2.84 litres/kWh stated in Table 4.1, albeit approximately 0.54 - 0.88 litres/kWh higher.

9.1.6 Preferred Technology for Upington

Based on the above results, as well as the output data listed in Table 9.1, it is concluded that the central receiver plants in Upington are superior and more economical than their equivalent parabolic trough plants. It is also noted that of the two central receiver plants, the wet-cooled plant proves more economical in terms of LCOE and PPA price, which is to be expected. However, the scarcity of water in the Upington region of Northern Cape, as well as the negative impact on local farming and communities in the region should large quantities of water be drawn from the orange river for plant cooling (Morse, 2009), raise concerns over the security of supply of the cooling water and hence its cost. According to Morse (2009), the city of Upington consumes approximately 12.3 million m^3 of water per annum. A potential CSP plant with wet cooling would therefore consume more than a 10^{th} of the volume of water as the entire city of Upington.

In addition, according to the model results a central receiver plant with dry cooling is even more cost effective in terms of the LCOE and PPA price, than the same capacity parabolic trough making use of wet cooling. Therefore, due to these concerns over the security of supply of water in the region, it is thought that the optimal CSP plant for the Upington region would be a central receiver plant with dry cooling.

9.2 Springbok

The subsequent four simulations were run for the Springbok location. The key results and output metrics for these simulations are presented in Table 9.2. Each of the key areas for the different technologies in Springbok will now be briefly discussed and compared under their relevant headings.

Table 9.2: Cost and Performance Results for Parabolic Trough and Central Receiver Models with Wet and Dry Cooling in Springbok.

Springbok	Parabolic Trough		Central Receiver	
	Wet Cooling	Dry Cooling	Wet Cooling	Dry Cooling
Rated Net Capacity	100 MW	100 MW	100 MW	100 MW
Availability	95 %	95 %	92 %	92 %
Economic Life	30 yrs	30 yrs	30 yrs	30 yrs
Annual Energy Produced (kWh_e)	356,160,487.5	346,887,632.4	376,179,962.7	358,737,976.1
Total Direct Cost	$ 725,891,696.52	$ 823,611,104.34	$ 518,673,680.08	$ 545,912,477.63
Total Indirect Cost	$ 215,589,833.87	$ 244,612,497.99	$ 154,046,082.98	$ 162,136,005.86
Total Installed Cost	$ 941,481,530.38	$ 1,068,223,602.33	$ 672,719,763.06	$ 708,048,483.48
Total Installed Cost per Net Capacity	$ 9,414.72 /kW R 66,091.33 /kW	$ 10,682.13 /kW R 74,988.55 /kW	$ 6,727.13 /kW R 47,224.45 /kW	$ 7,080.41 /kW R 49,704.48 /kW
LCOE – real *	31.63 ¢/kWh R 2.22 /kWh	36.04 ¢/kWh R 2.53 /kWh	22.18 ¢/kWh R 1.56 /kWh	24.03 ¢/kWh R 1.69 /kWh
1st Year PPA Price	45.38 ¢/kWh R 3.19 /kWh	52.18 ¢/kWh R 3.66 /kWh	31.37 ¢/kWh R 2.20 /kWh	34.23 ¢/kWh R 2.40 /kWh
Capacity Factor	40.66 %	39.60 %	42.94 %	40.95 %
Annual Water Usage	1,388,420.6 m^3 3.90 l/kWh 1029.82 gal/MWh	88,879.7 m^3 0.26 l/kWh 67.69 gal/MWh	1,271,440.6 m^3 3.38 l/kWh 892.87 gal/MWh	79,800.6 m^3 0.22 l/kWh 58.76 gal/MWh

* ¢/kWh refers to U.S. cents per kilowatt hour.

9.2.1 Annual Energy Production

The total annual energy produced by each plant in Springbok ranges from 346,887,632.4 kWh_e for the dry-cooled parabolic trough plant, to 376,179,962.7 kWh_e for the wet-cooled central receiver. As was the case for Upington, the central receiver plants produce greater annual energy yields, when compared to the parabolic trough plants, as a result of their higher concentration ratios and greater cycle efficiency. Both the wet-cooled parabolic trough and central receiver plants once again produce more energy than their dry-cooled equivalents, as a result of the lower power cycle efficiencies associated with dry cooling.

9.2.2 Installed Cost per Net Capacity

The total installed cost per net capacity for the CSP models in Springbok ranges from R47,224.45 /kW ($6,727.13 /kW) for the wet-cooled central receiver model, to R74,988.55 /kW ($10,682.13 /kW) for the dry-cooled parabolic trough plant. As in Upington, both the central receiver plants are more economical when compared to the parabolic trough plants, while the use of dry cooling also increases plant costs. It is again noted that the model predicts a central receiver plant with dry cooling is more economical in terms of cost per net capacity than the equivalent 100 MW capacity wet-cooled parabolic trough plant in the same location.

9.2.3 Levelised Cost of Energy

The LCOE for the different models in Springbok ranges from R1.56 /kWh (22.18 U.S. ¢/kWh) to R2.53 /kWh (36.04 U.S. ¢/kWh) for the wet-cooled central receiver and dry-cooled parabolic trough respectively. Once again, the LCOE for the central receiver plants is lower than that of the parabolic trough plants, while wet cooling is more economical than dry cooling for both technologies.

The resulting required first year PPA prices of R2.20 /kWh and R2.40 /kWh for the central receiver models with wet and dry cooling respectively, are relatively close to R2.31 /kWh 2009 value as stated in the REFIT Phase II document (NERSA, 2010) for central receiver plants with 6 hours TES, albeit approximately R0.20 /kWh higher than the PPA prices for Upington. The PPA prices of R3.19 /kWh and R3.66 /kWh for the parabolic trough models with wet and dry cooling respectively, however, are considerably higher than the 2009 value of R2.10 /kWh suggested by NERSA (2010) in the REFIT Phase II document for parabolic trough plants with 6 hours TES, and are approximately R0.32 higher than the Upington trough prices. The higher energy prices experienced in

Springbok are related to the lower annual energy yields on account of the lower annual DNI levels at Springbok when compared to Upington.

9.2.4 Capacity Factor

The capacity factors for the different plants in Springbok range from 39.60% for the dry-cooled parabolic trough plant, to 42.94% for the wet cooled central receiver. Once again, the central receiver plants generally have higher capacity factors when compared to the parabolic trough plants, thought to be due the the aforementioned higher concentration ratios and efficiency. Dry cooling also decreases capacity factors due to its negative effect on plant efficiency. The capacity factors for Springbok are approximately 3% lower than those in Upington, which is likely due to the lower total annual DNI in Springbok resulting in the plants operating at their rated capacity for less time throughout the year.

9.2.5 Annual Water Consumption

The difference in the annual water consumption between wet and dry cooling in Springbok is also vast, with the dry-cooled central receiver consuming only 79,800.6 m^3 (0.22 litres/kWh) compared to the 1,388,420.6 m^3 (3.90 litres/kWh) of the wet-cooled parabolic trough. The central receiver plants in Springbok also also consume less water annually when compared to parabolic troughs. Furthermore, the values of 3.90 litres/kWh and 3.38 litres/kWh for the wet-cooled parabolic trough and central receiver plants respectively, are similar to the values of 3.03 litres/kWh and 2.84 litres/kWh stated in Table 4.1 and virtually identical (but slightly lower) to those in Upington.

9.2.6 Preferred Technology for Springbok

Based on the above results, as well as the output data listed in Table 9.2, it is concluded that the central receiver plants in Springbok are superior and more economical than their equivalent parabolic trough plants. It is also noted that of the two central receiver plants, the wet-cooled plant proves more economical in terms of LCOE and PPA price, which is to be expected. The decision for the optimal CSP technology near Springbok is complicated, however, as although plants in this region, like Upington, are situated in the dry Northern Cape, with its associated water scarcity – and hence security of water supply concerns – the possibility also exists for plants to be located along the west coast, as can be seen in Figure 8.1. A CSP plant situated at the coast could then potentially make use of wet cooling, drawing its cooling water from the Atlantic Ocean.

The use of sea water for wet cooling is not considered or incorporated into the SAM software in this study, however, and is considered beyond the scope of this report. A dry-cooled central receiver plant is also a potential candidate for the optimal CSP technology near Springbok, with it being more cost effective in terms of the LCOE and PPA price, than the same capacity parabolic trough making use of wet cooling. Additional modelling would therefore be required in order to determine whether a central receiver plant using sea water for wet cooling – with its associated complexities – would in fact be more economical than a dry-cooled central receiver plant. Hence, it can only be concluded, based on the results from this analysis, that the optimal CSP plant for the Springbok region would be a central receiver plant, but more research is required to determine whether wet cooling with sea water or dry cooling is preferable.

9.3 Bloemfontein

The final four simulations were run for the Bloemfontein location. The key results and output metrics for the these simulations are presented in Table 9.3. Each of the key areas for the different technologies in Bloemfontein will now be briefly discussed and compared under their relevant headings.

9.3.1 Annual Energy Production

The total annual energy produced by each plant in Bloemfontein ranges from 358,081,166.8 kWh_e for the dry-cooled parabolic trough plant, to 380,078,179.4 kWh_e for the wet-cooled central receiver plant. As was the case for both Upington and Springbok, the central receiver plants produce greater annual energy yields, when compared to the parabolic trough plants, as a result of their higher concentration ratios and greater overall efficiencies. The wet-cooled plants for both parabolic trough and central receiver plants once again also produced more energy than their dry-cooled equivalents, as a result of the lower power cycle efficiencies associated with dry cooling.

9.3.2 Installed Cost per Net Capacity

The total installed cost per net capacity for the CSP models in Bloemfontein ranges from R47,238.49 /kW ($6,729.13 /kW) for the wet-cooled central receiver model, to R76,904.17 /kW ($10,955.01 /kW) for the dry-cooled parabolic trough plant. As in the both the Upington and Springbok cases, both the central receiver plants are more economical when compared to the parabolic trough plants. Making use of dry cooling also

Table 9.3: Cost and Performance Results for Parabolic Trough and Central Receiver Models with Wet and Dry Cooling in Bloemfontein.

Bloemfontein	Parabolic Trough		Central Receiver	
	Wet Cooling	Dry Cooling	Wet Cooling	Dry Cooling
Rated Net Capacity	100 MW	100 MW	100 MW	100 MW
Availability	95 %	95 %	92 %	92 %
Economic Life	30 yrs	30 yrs	30 yrs	30 yrs
Annual Energy Produced (kWh_e)	367,781,069.3	358,081,166.8	380,078,179.4	361,868,799.9
Total Direct Cost	$ 745,018,752.37	$ 844,650,865.78	$518,828,161.87	$ 545,680,754.95
Total Indirect Cost	$ 221,270,569.45	$ 250,861,307.14	$ 154,091,964.07	$ 162,067,184.22
Total Installed Cost	$ 966,289,321.82	$ 1,095,512,172.91	$ 672,920,125.94	$ 707,747,939.17
Total Installed Cost per Net Capacity	$ 9,662.80 /kW R 67,832.86 /kW	$ 10,955.01 /kW R 76,904.17 /kW	$ 6,729.13 R 47,238.49 /kW	$ 7,077.41 R 49,683.42 /kW
LCOE – real *	31.38 ¢/kWh R 2.20 /kWh	35.75 ¢/kWh R 2.51 /kWh	21.97 ¢/kWh R 1.54 /kWh	23.82 ¢/kWh R 1.67 /kWh
1st Year PPA Price	45.05 ¢/kWh R 3.16 /kWh	51.76 ¢/kWh R 3.63 /kWh	31.06 ¢/kWh R 2.18 /kWh	33.93 ¢/kWh R 2.38 /kWh
Capacity Factor	41.98 %	40.88 %	43.39 %	41.31 %
Annual Water Usage	1,434,814.3 m^3 3.90 l/kWh 1030.61 gal/MWh	92,379.5 m^3 0.26 l/kWh 68.15 gal/MWh	1,283,893.8 m^3 3.38 l/kWh 892.37 gal/MWh	79,981.9 m^3 0.22 l/kWh 58.39 gal/MWh

* ¢/kWh refers to U.S. cents per kilowatt hour.

increased plant costs. It is again noted that the model predicts a central receiver plant with dry cooling in Bloemfontein is more economical in terms of cost per net capacity than the wet-cooled parabolic trough plant with an equivalent 100 MW rating in the same location.

9.3.3 Levelised Cost of Energy

The LCOE for the different models in Bloemfontein ranges from R1.54 /kWh (21.97 U.S. ¢/kWh) to R2.51 /kWh (35.75 U.S. ¢/kWh) for the wet-cooled central receiver and dry-cooled parabolic trough respectively. Once again, the LCOE for the central receiver plants is lower than that of the parabolic trough plants, while wet cooling is more economical than dry cooling for both technologies.

The resulting required first year PPA prices of R2.18 /kWh and R2.38 /kWh for the central receiver models with wet and dry cooling respectively, are relatively close to R2.31 /kWh 2009 value as stated in the REFIT Phase II document (NERSA, 2010) for central receiver plants with 6 hours TES, albeit R0.19 /kWh higher than the PPA prices for Upington. The PPA prices of R3.16 /kWh and R3.63 /kWh for the parabolic trough models with wet and dry cooling respectively, however, are considerably higher than the 2009 value of R2.10 /kWh suggested by NERSA (2010) in the REFIT Phase II document for parabolic trough plants with 6 hours TES, and are approximately R0.30 higher than the Upington trough prices. The higher energy prices experienced in Bloemfontein, as in Springbok, are thought to be primarily related to the lower annual energy yields on account of the lower annual DNI levels at Bloemfontein when compared to Upington.

9.3.4 Capacity Factor

The capacity factors for the different plants in Upington range from 40.88% for the dry-cooled parabolic trough plant, to 43.39% for the wet cooled central receiver plant. Once again, the central receiver plants generally have higher capacity factors when compared to the parabolic trough plants, which is thought to be due the the previously mentioned higher concentration ratios and efficiency. Dry cooling also decreases capacity factors due to its negative effect on plant efficiency. The capacity factors for Bloemfontein are also generally in the region of 2% lower than those in Upington, but approximately 1% higher than Springbok. This is again likely due to the differences in total annual DNI received at each location.

9.3.5 Annual Water Consumption

The difference in the annual water consumption between wet and dry cooling in Bloemfontein is again vast, with the dry cooled central receiver consuming only 79,981.9 m^3 (0.22 litres/kWh) compared to the 1,434,814.3 m^3 (3.90 litres/kWh) of the wet-cooled parabolic trough. The central receiver plants in Bloemfontein also also consume less water annually when compared to parabolic troughs. Furthermore, the values of 3.90 litres/kWh and 3.38 litres/kWh for the wet-cooled parabolic trough and central receiver plants respectively, are similar to the values of 3.03 litres/kWh and 2.84 litres/kWh stated in Table 4.1 and virtually identical (but slightly lower) to those in Upington.

9.3.6 Preferred Technology for Bloemfontein

Based on the above results, as well as all the output data listed in Table 9.3, it is concluded that the central receiver plants in Bloemfontein, as in the previous two location, are superior and more economical than their equivalent parabolic trough plants. It is also noted that of the two central receiver plants, the wet-cooled plant proves more economical in terms of LCOE and PPA price, which once again is to be expected. The decision for the optimal CSP technology near Bloemfontein is complex, however, as depending on the plant location, water for wet cooling may be accessible from large dams, rivers or other water sources in the region. This can be seen in Figure 6.6, which depicts rivers and large water bodies throughout the country in the GIS analysis section of this report. Nevertheless, it may still be more beneficial to make use of dry cooling, as a means to reduce the risk of water supply concerns. A dry-cooled central receiver plant near Bloemfontein, is still more cost effective in terms of the LCOE and PPA price, than the same capacity parabolic trough making use of wet cooling.

It is therefore concluded that more specific site analyses and local water availability studies would be required in order to determine whether a central receiver plant using wet cooling, or a dry-cooled central receiver plant would be more optimal. It can, however, be concluded that the optimal CSP technology – when only parabolic trough and central receiver technologies are considered – for the Bloemfontein region would be a central receiver.

9.4 Comparison of All Technologies and Locations

Although all the CSP technologies and cooling type configurations have been analysed at their various locations, it was deemed necessary to compare all the technologies at all locations based on four key metrics. This was done in order to address the third objective defined in this study through the comparison of the relative metrics; and to determine any trends in the results. The *LCOE*, *total installed cost per net capacity*, *annual water consumption*, and *annual energy production* data from Table 9.1, Table 9.2 and Table 9.3 was used to create the four graphs in Figure 9.1, to Figure 9.4 respectively. Any trends identified will be now discussed under their subsequent headings.

9.4.1 Comparison of Total Installed Cost per Net Capacity

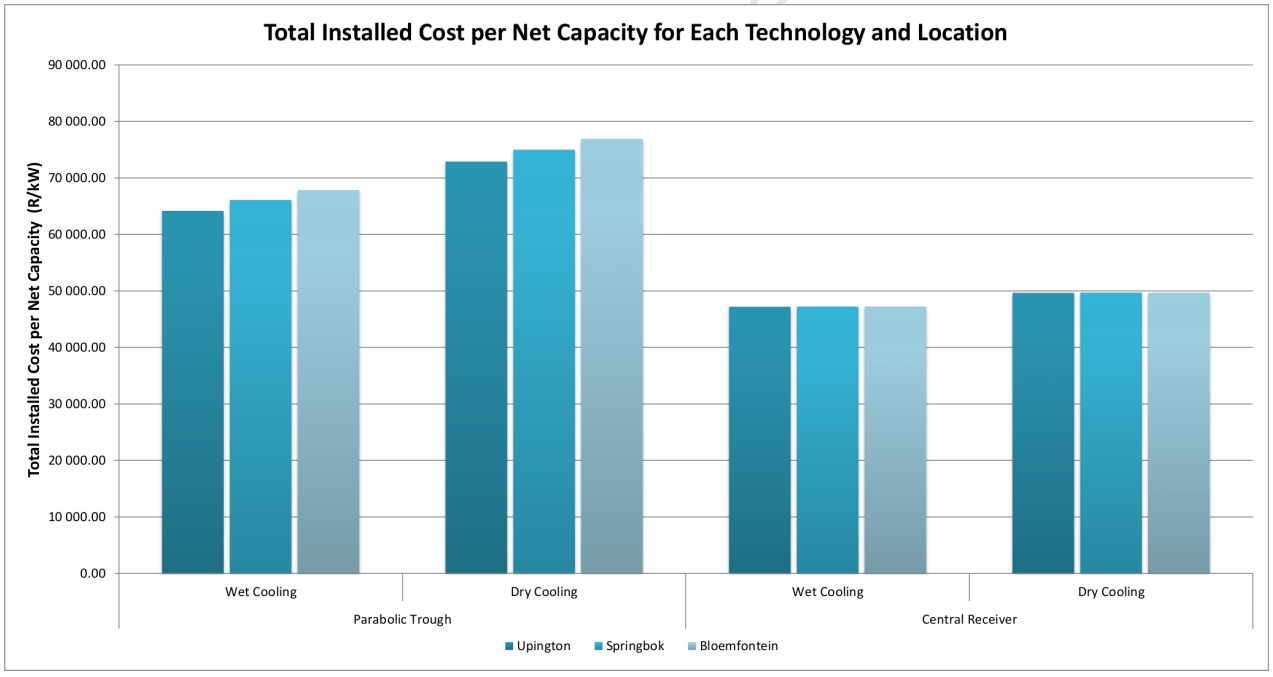

Figure 9.1: Comparison of Plant Total Installed Cost per Net Capacity for Each Technology and Location.

From Figure 9.1 three broad trends are initially evident. Firstly, for both wet and dry-cooled parabolic trough plants, the total installed cost per net capacity increases between Upington, Springbok and Bloemfontein, by approximately 3% between Upington and Springbok and a further 3% between Springbok and Bloemfontein; whereas for central receiver plants, the total installed cost per net capacity appears less influenced by location

with less than 0.1% variation. This is most likely related to the solar multiple of the plants, as the solar multiple influences the solar field size, and hence cost of the plant. As was discussed and shown in Table 8.13 and Figure 8.12, the parabolic trough plants have different solar multiples for each location (with Upington possessing the lowest and Bloemfontein the highest), while the central receiver plants have the same solar multiple for each location (but different solar multiples for wet and dry cooling).

Secondly, the dry-cooled plants for both parabolic trough and central receivers result in higher total installed costs, which is explained by their higher associated capital costs. The dry-cooled parabolic trough plants were shown to have approximately 13.5% greater total installed costs then their wet-cooled equivalents, while the dry-cooled central receivers were shown to have approximately 5% greater total installed costs then their wet-cooled equivalents. For the central receiver plants, the fact that the dry-cooled plants for all locations have a lower solar multiple than the wet-cooled plants (1.9 as opposed to 2.0) does help to reduce the difference in capital cost, however the dry-cooled systems are still more costly.

Finally, it is clear that central receiver plants have lower installed costs per net capacity than their equivalent capacity parabolic trough plants – approximately 26% – 30% less for wet cooling and approximately 31.5% – 35.5% less for dry cooling. As previously stated, this is due to different fundamental plant designs, components used, and component costs.

9.4.2 Comparison of Annual Energy Production

From Figure 9.2 the main trends identified are as follows; firstly, that location clearly has an effect on the annual energy production, with plants in Upington producing the most energy annually, followed by Bloemfontein and the least at Springbok. This trend closely follows the difference in annual DNI levels for each of the locations. Springbok was shown to produce approximately 6% – 10% less energy annually than Upington, while Bloemfontein was shown to produce approximately 3% – 9% less energy annually than Upington.

Secondly, all plant types making use of dry-cooling produce lower annual energy yields of approximately 2.5% – 6% less then their wet-cooled equivalents, which is attributed to the lower cycle efficiency of dry cooling.

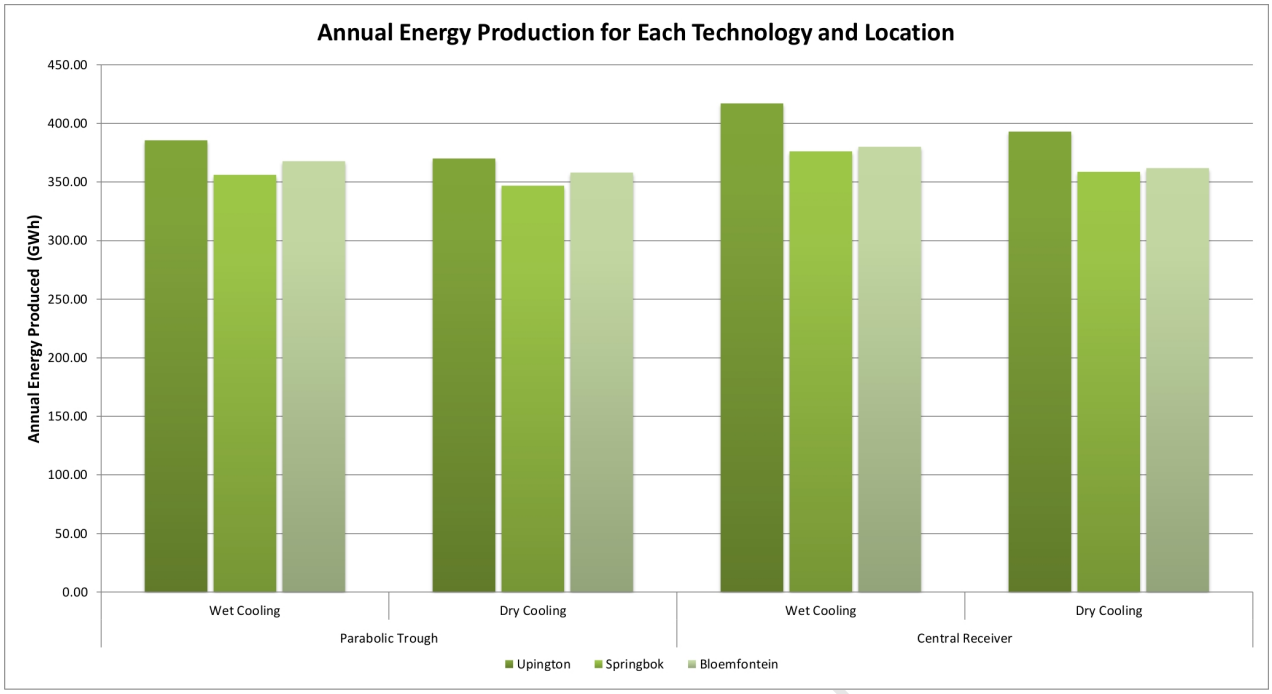

Figure 9.2: Comparison of Annual Energy Production for Each Technology and Location.

Finally, the results show that central receiver systems produce higher annual energy yields of between 1% – 8% more than their equivalent parabolic trough plants for all locations, which has previously been attributed to their higher concentration ratios and grater optical and overall efficiency. The magnitude of increase is also linked to location, however, with the Upington plants showing the greatest increase and the Bloemfontein plants the least.

9.4.3 Comparison of LCOE

The comparison of the LCOE for all technologies and locations, as presented in Figure 9.3 presents slightly different trends than those presented in the previous two graphs. Thus in order to attempt to understand these trends better, the results need to be considered in the context of the governing LCOE equation defined in Equation 9.1.

From the equation, it can be seen that the numerator contains a reference to the revenue generated from electricity sales, which in turn is related to the plant costs which need to be covered (PPA price). The denominator, however, contains a reference to the annual energy production of the plant. It is therefore evident that both the plant costs and energy production will have an effect on the LCOE of the plant in question.

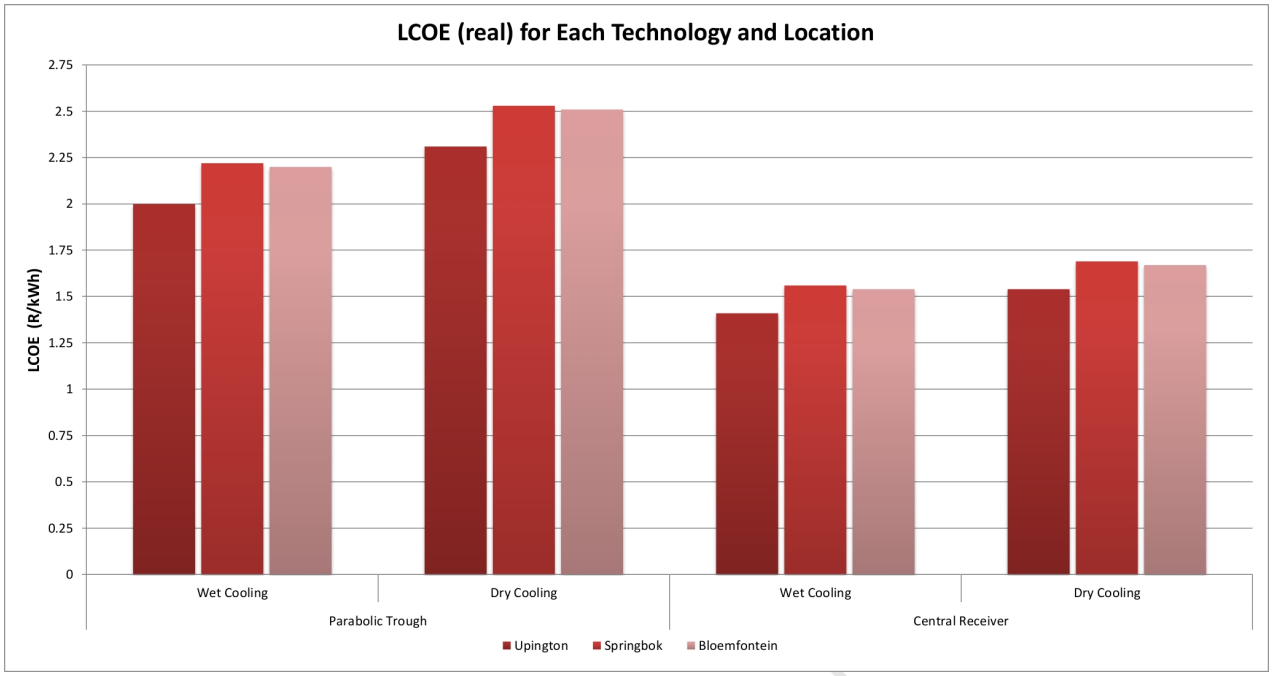

Figure 9.3: Comparison of LCOE (real) for Each Technology and Location.

The graph depicts that for both the parabolic trough and central receiver plants, the lowest LCOE occurs at Upington, whose location also represents the highest annual energy production with the lowest total system cost per net capacity. Bloemfontein, however, has the highest system cost on average, but also has a higher annual energy yield compared to Springbok, which in turn results in it having approximately an 8% – 10% higher LCOE than Upington (although lower than Springbok). Conversely, Springbok has a lower total installed cost per capacity than Bloemfontein, but also has a lower annual energy production value, which ultimately results in Springbok possessing the highest LCOE of all three locations – approximately 9% – 11% higher than Upington. This complex relationships between the LCOE, annual energy production and plant cost is a prime example of why it was necessary to perform the solar multiple optimisations in Chapter 8, in order to obtain the optimum balance between solar multiple (and hence plant size and cost) and energy production.

A second observation for the LCOE is that dry-cooled plants at all locations comprise higher LCOE values then their wet-cooled equivalents – between 14% and 15.5% higher for parabolic troughs and between 8% and 9.5% higher for central receivers. This is due to the higher system cost associated with dry cooling, as well as the reduction in efficiency and annual energy production.

Thirdly, the LCOE values for central receiver plants at all locations are lower than those of the parabolic trough plants – approximately 30% lower for wet-cooled plants and 33.5% lower for dry-cooled plants. This can be explained by both the lower system costs and higher energy output from the central receiver systems.

A final observation is that the LCOE for the dry-cooled central receiver plant in Upington (R1.54/kWh) is lower than that of the wet-cooled central receiver plant in Springbok (R1.56/kWh), and the same as the wet-cooled central receiver in Bloemfontein (R.154/kWh). The implications of this are that it may therefore be more beneficial to construct a central receiver CSP plant in a region with higher DNI levels but limited access to large volumes of cooling water, as opposed to an area with lower DNI levels but access to large volumes of water.

9.4.4 Comparison of Annual Water Consumption

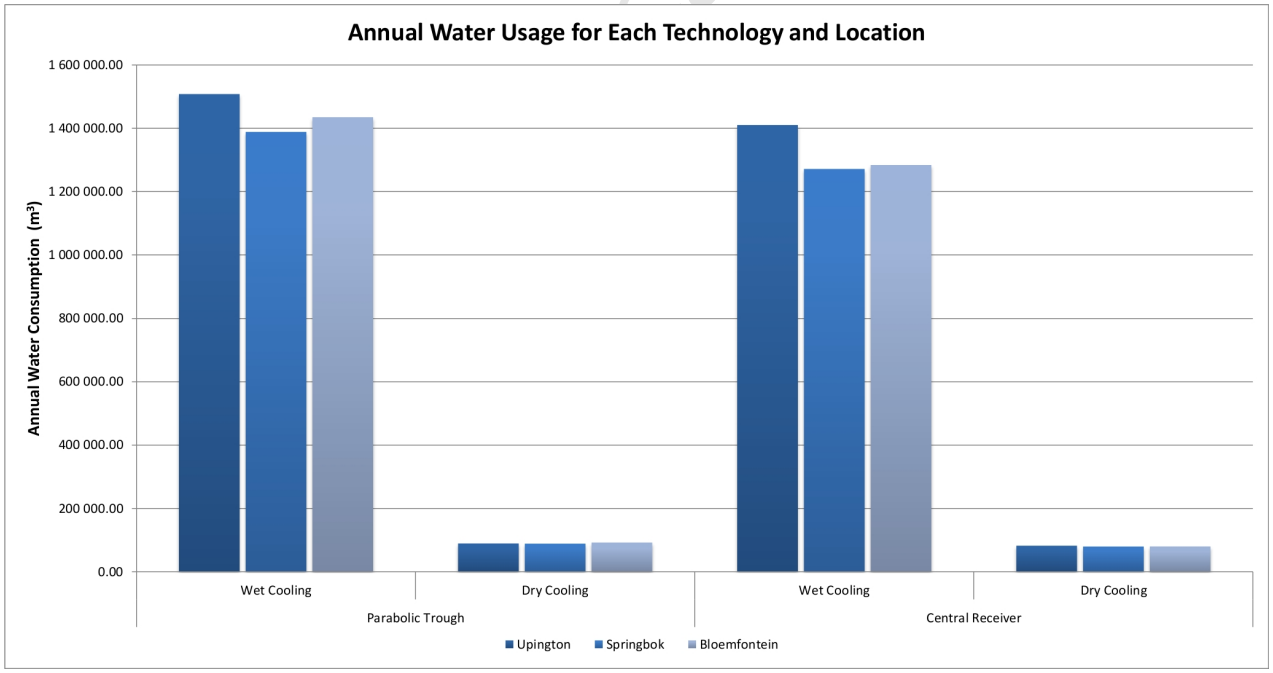

Figure 9.4: Comparison of Annual Water Usage for Each Technology and Location.

Figure 9.4 depicts three major trends for the water consumption of the CSP plants at all three locations. The first and most obvious is that wet-cooling consumes far more water annually than dry cooling. This is true for all locations for both parabolic trough and central receiver technologies, with the results showing dry cooling to eliminate more than 90% of annual plant water usage.

Secondly, as water consumption is directly linked to energy generation, the more energy a plant produces each year, the longer it runs closer to maximum capacity and the more water the power cycle consumes. This is can be seen for the plants located at Upington – as it receives the highest annual DNI values and produces the most energy annually, it also consumes the most water. Similar trends are visible when comparing the annual energy production depicted in Figure 9.2 to the water consumption shown in Figure 9.4.

Finally, it can be seen that all the central receiver plants consume less water by volume than their equivalent parabolic trough plants at all three locations – between 6% – 11% less for wet-cooled plants and between 7.5% – 13.5% less for dry-cooled plants. This has been previously discussed in Section 9.1.5 as well as in Section 4.4 of Chapter 4.

9.5 Validation and Comparison to Literature

In order to ensure that the results obtained in this analysis from the various model runs and simulations are reasonable and accurate, a comparison to similar results presented in the literature was conducted for validation purposes. Although the SAM software itself has been validated and used in industry and academia over the last few years, the comparison of the results in this study to those in the literature not only reaffirms SAM's credibility, but also helps to ensure that the assumptions and calculations made in this particular study in the adaptation of the simulations to South African conditions were reasonable and implemented accurately. In addition, the validation process also seeks to eliminate the possibility of user error when configuring and entering the data within the SAM software.

For the sake of brevity and due to time constraints, apart from in Table 9.8, only the results from the parabolic trough and central receiver models conducted for Upington were used in the validation and comparison process. It was assumed that as one of the primary differences between the Upington models and the others is in location, if the Upington models prove to be accurate, the models at the other locations would hopefully be as well.

The model results for the wet-cooled and dry-cooled parabolic troughs in Upington were compared to result data from the Sargent & Lundy (2003) report (containing both Sargent and Lundy, and SunLab data), as well as data from the International Energy Agency (IEA, 2010b) and the SAM (2010) default data. It is noted that for the wet-cooled parabolic trough models, no literature data was found pertaining to trough models in South Africa, and thus the comparison data presented is left in U.S. dollars for ease of comparison. For the dry-cooled trough, comparisons were made to data from the EPRI (2010) report, which was conducted for South Africa, and hence the results were reported in South African Rand. The results from the parabolic trough comparisons are tabulated and presented in Table 9.4 and Table 9.5.

The model results for both the wet-cooled and dry-cooled central receiver models were compared to the result data from the Sargent & Lundy (2003) report (which contained data for both the then Solar Tres and the proposed Solar100) and EPRI's own local South African modelling. The default SAM data was also used for validation purposes, with its results converted to South Africa Rand by means of the exchange rate stated in Chapter 8. The results from the central receiver comparisons are tabulated and presented in Table 9.6 and Table 9.7.

In addition, the model results for the percentage reduction in annual energy production and percentage increase in LCOE as a result of employing dry cooling instead of wet cooling, for both the parabolic trough and central receiver plants at all three locations, were compared to the percentage values stated in the literature by the IEA (2010b) and the DOE, U.S. (2010). The results of this comparison are present in Table 9.8. A brief discussion regarding the accuracy of each of the metrics will now follow under their respective headings.

Table 9.4: Validation of Upington Wet-Cooled Parabolic Trough Results. *Source of Data:* Sargent & Lundy (2003), IEA (2010b), SAM (2010).

Parabolic Trough	Wet-Cooled	SunLab	S&L	IEA	SAM	This Study
Total Plant Cost or Overnight Cost	($/kW)	4,859.00	4,816.00	–	7,987.66	9,141.84
LCOE	(¢/kWh)	±9.9	±10.2	20.0-29.5	15.34	28.50
Capacity Factor	(%)	53.5	–	–	41.25	44.02
Water Usage	(l/kWh)	–	–	–	3.97	3.91

Table 9.5: Validation of Upington Dry-Cooled Parabolic Trough Results. *Source of Data:* EPRI (2010), SAM (2010).

Parabolic Trough	Dry-Cooled	EPRI	SAM	This Study
Total Plant Cost or Overnight Cost	(R/kW)	43,385.00	63,745.81	72,898.77
LCOE	(R/kWh)	2.08	1.25	2.31
Capacity Factor	(%)	36.30	39.63	42.25
Water Usage	(l/kWh)	0.245	0.252	0.242

Table 9.6: Validation of Upington Wet-Cooled Central Receiver Results. *Source of Data:* Sargent & Lundy (2003), IEA (2010b), SAM (2010).

Central Receiver	Wet-Cooled	Solar Tres		Solar100		SAM	This Study
		SunLab	S&L	SunLab	S&L		
Total Plant Cost or Overnight Cost	($/kW)	7,135	9,090	3,103	4,608	5,730	6,724
LCOE	(¢/kWh)	11.5	14.3	4.8	6.8	10.46	20.06
Capacity Factor	(%)	–	–	–	–	46.21	47.61
Water Usage	(l/kWh)	–	–	–	–	3.30	3.38

Table 9.7: Validation of Upington Dry-Cooled Central Receiver Results. *Source of Data:* EPRI (2010), SAM (2010).

Parabolic Trough	Dry-Cooled	EPRI	SAM Default	This Study
Total Plant Cost or Overnight Cost	(R/kW)	32,190.00	43,935.65	49,655.27
LCOE	(R/kWh)	1.57	0.82	1.54
Capacity Factor	(%)	36.70	44.54	44.87
Water Usage	(l/kWh)	0.295	0.197	0.210

Table 9.8: Validation of Cooling Technology Effect on Plant Efficiency and Water Consumption. *Source of Data:* DOE, U.S. (2010), IEA (2010b).

Plant Type	Source	Reduction of Annual Energy Production*	Increase in LCOE*
Dry-Cooled Parabolic Trough	IEA (2010b)	7%	10%
Dry-Cooled Parabolic Trough	DOE, U.S. (2010)	4.5 - 5%	2 - 9%
Dry-Cooled Central Receiver	DOE, U.S. (2010)	1.3%	–
Upington, Dry-Cooled Trough	This Study	4.0%	15.5%
Upington, Dry-Cooled Tower	This Study	5.8%	9.2%
Springbok, Dry-Cooled Trough	This Study	2.6%	14.0%
Springbok, Dry-Cooled Tower	This Study	4.6%	8.3%
Bloemfontein, Dry-Cooled Trough	This Study	2.6%	14.1%
Bloemfontein, Dry-Cooled Tower	This Study	4.8%	8.4%

* When compared to equivalent plant with wet cooling technology

9.5.1 Validation of Total Installed Cost per Net Capacity

The total installed cost per net capacity for both the parabolic trough and central receiver models are in the same order of magnitude as those from the literature, albeit occasionally more than 50% higher. The only case where the costs in this study are less than those in the literature is for the then Solar Tres central receiver plant. The higher than average total installed costs for the plants in this study are attributed to both the SAM default costs (and hence the costs by the WorleyParsons Group) on which they are based, and to the conservative cost adjustment factors applied in Section 8.5.1 to represent the higher overall capital and O&M costs in South Africa. It is also noted, however, that the total installed cost per net capacity metric is variable for all plants in the literature, and therefore, the fact that the costs used in this study were based on SAM inputs, and that they were in the correct order of magnitude, renders them deemed acceptable.

9.5.2 Validation of LCOE

In contrast to the total installed cost per net capacity data, the LCOE values calculated in this study are not only in the same order of magnitude to those in the literature, but are approximately within 10% of those EPRI (2010) achieved for South Africa. The wet-cooled trough and central receiver models achieved slightly higher LCOE values than those in the literature, but the trough values were still within the range suggested by the IEA (2010b). The LCOE values were higher than the default SAM values, however, but this is primarily due to the SAM values representing plants in the U.S as opposed to South Africa.

9.5.3 Validation of Capacity Factor

The capacity factors achieved in this study were on average higher than those in the literature, but usually not by more than 20%. The higher capacity factors in this study can be attributed to the higher DNI levels in Upington compared to the plant locations in the literature, as well as the 6 hour storage capacity used in this analysis.

9.5.4 Validation of Annual Water Usage

The annual water consumption results from this study were extremely similar to those in the literature, usually with less than a 10% difference. As the water consumption is related to the annual energy output of the plant, some variability was experienced.

9.5.5 Cooling Technology Effect on Plant Efficiency and Water Consumption

The percentage reductions in annual energy production as a result of employing dry cooling for all the plants are in the same order of magnitude to those stated in the literature, and similar in *value* to within approximately 4.5%. The results for the parabolic trough models are slightly lower than those predicted in the literature, while the results for the central receivers are slightly higher than the literature values. The percentage increases in LCOE as a result of employing dry cooling are also in the same order of magnitude to those stated in the literature, with the parabolic trough values slightly higher by a *value* of approximately 4 - 5.5% and the central receiver values within the expected range stated for parabolic troughs. No value was found in the literature for the increase in LCOE as a result of dry cooling adoption in central receiver plants.

9.5.6 Major Cost Categories Breakdown

As a further means of verifying that the total installed costs are indeed primarily a result of the conservatively high SAM default values and South African conversion factors, and are not disproportionate to each other nor contain any other errors, a major cost category breakdown was created for comparison with the literature. Once again, for the sake of brevity, this major cost category breakdown was only created for the Upington plants, in particular only the wet-cooled parabolic trough and central receiver models. Both model cost breakdowns were compared to similar graphs presented in the Sargent & Lundy (2003) report. The graphic comparisons for the wet-cooled parabolic trough are presented in Figure 9.5 and Figure 9.6, while the wet-cooled central receiver comparisons are presented in Figure 9.7 and Figure 9.8.

From Figure 9.5 and Figure 9.6, it is evident that proportion and distribution of the major costs for the wet-cooled parabolic trough plants in this study are very similar to those of the 2004, 100 MW trough plant described in the Sargent & Lundy (2003) study, albeit that the Sargent and Lundy plant possesses 12 hours of TES compared to the 6 hours used in this study. The percentage cost distribution across all categories, except the solar field, are within 4% of each other, while the solar field values are within 7%.

From Figure Figure 9.7 and Figure 9.8, it is evident that proportion and distribution of the major costs for the wet-cooled central receiver plants in this study are very similar to those of the proposed Solar 220 plant outlined in the Sargent & Lundy (2003) study. The percentage cost distribution across all categories, except for the power block and balance of plant, are within 3% of each other. The power block and balance of plant values are within 7% of each other.

The strong agreement between the cost category results for both the wet-cooled parabolic trough and central receiver models in this study and those in the literature therefore suggests that although the final magnitude of the cost are slightly higher in this study, the distribution and proportion of the major cost categories are still strongly comparable to the literature.

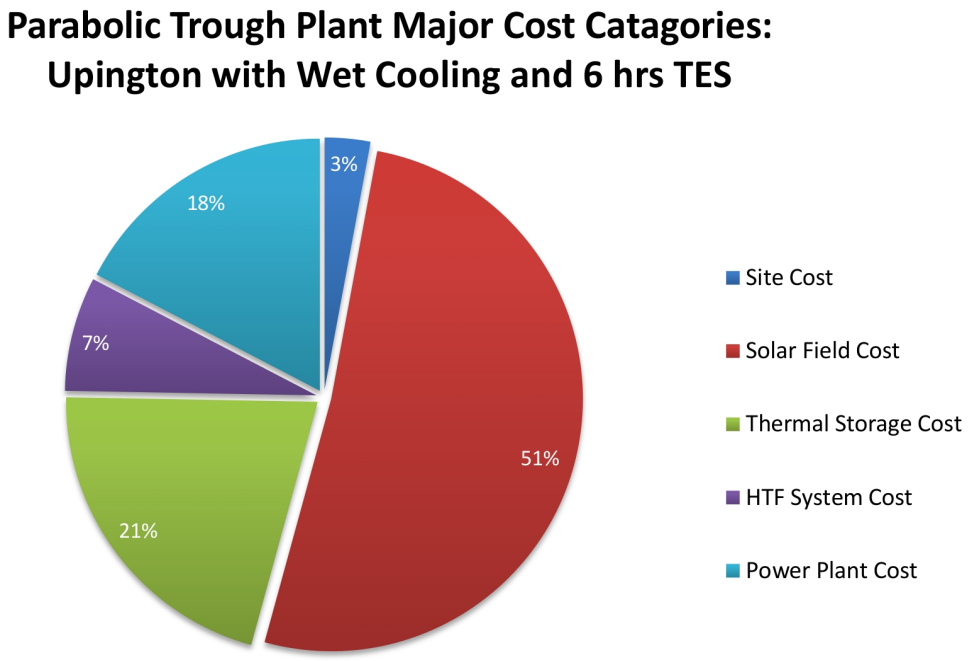

Figure 9.5: Parabolic Trough Major Cost Components for Upington with Wet Cooling.

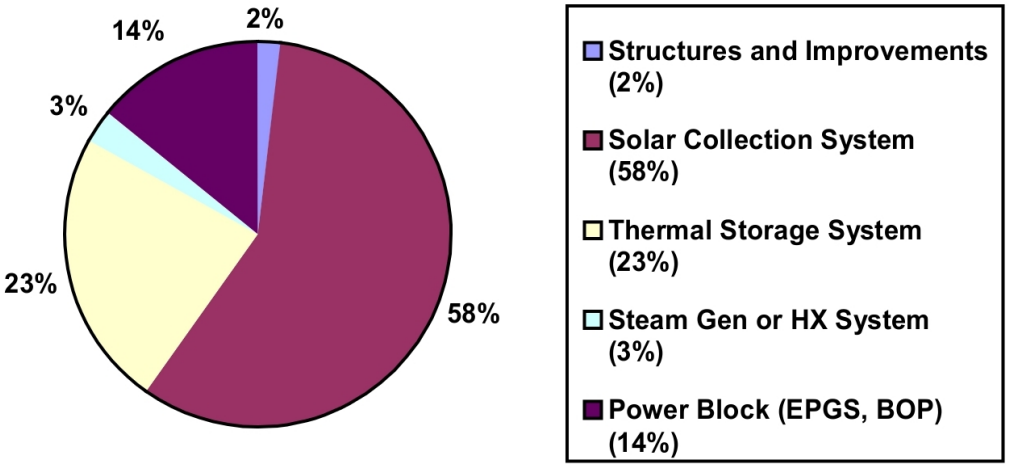

Figure 9.6: Major Cost Categories for Parabolic Trough Plant 2004 Near-Term Case: 100 MW_e, 12 hours TES, 2.5 Solar Multiple (Sargent & Lundy, 2003).

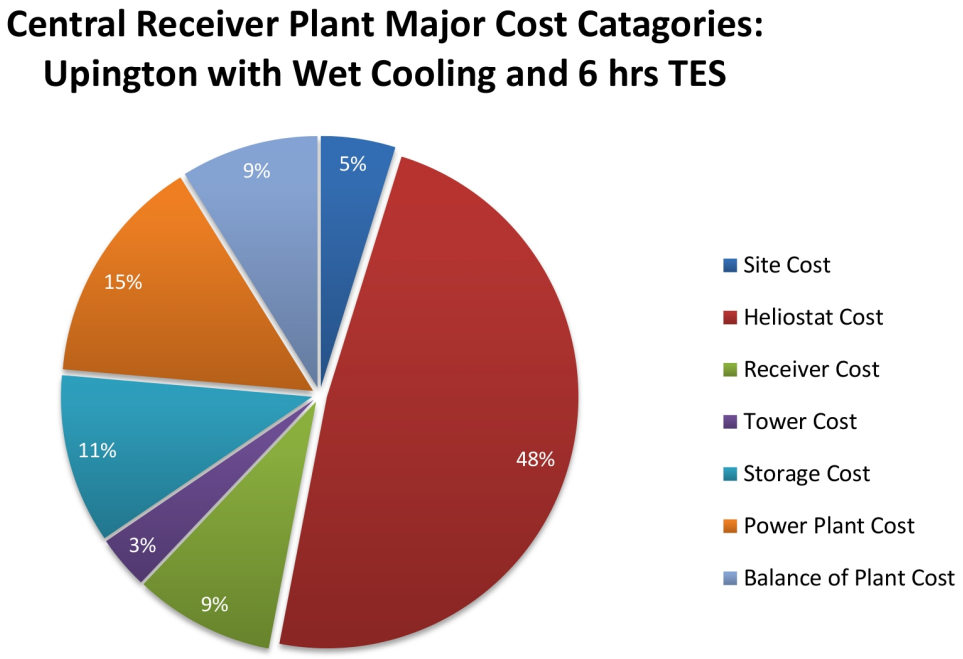

Figure 9.7: Central Receiver Major Cost Components for Upington with Wet Cooling.

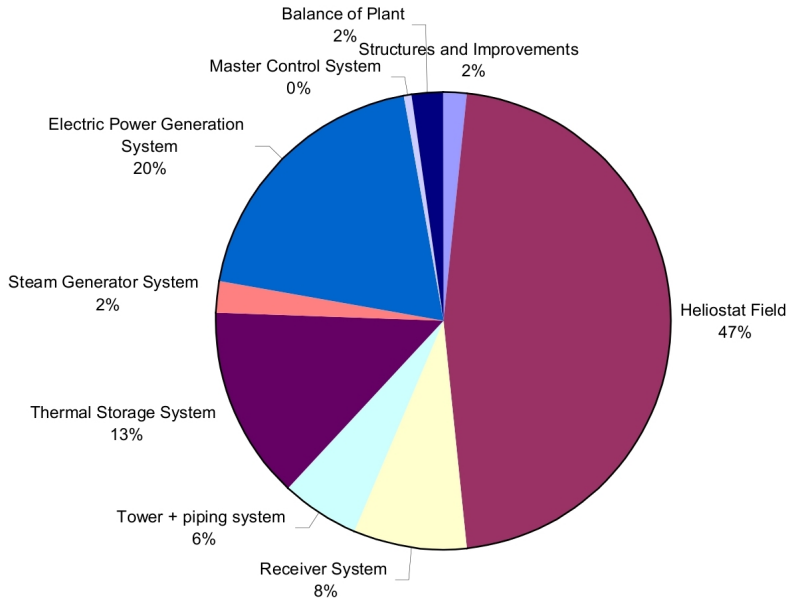

Figure 9.8: Capital Cost Categories for Solar 220 (Sargent & Lundy, 2003).

9.5.7 Daily Generation Profiles

As a final means of validation, solar generation profiles were created from the performance component of the SAM models, and compared to similar generation profiles presented in the EPRI (2010) report. The solar generation profiles display the total incident power from the solar field (Q_SF: in red), the thermal energy directed to the thermal energy storage (Q_to_TES: in blue), the thermal energy directed from the TES to the power block (Q_from_TES: in green), the total thermal energy entering the power block (Q_to_PB: in purple), the gross energy output from the power block (E_gross or Cycle_power: in orange), and finally the net output from the power plant (E_net: in yellow). The generation profiles depict these metrics at hourly intervals over a 24 hour period of a chosen day, and allow for the visual determination of magnitude, timing and distribution of energy flows within the plant. The review of this data can then be used as a means to visually determine whether the energy flows within the plant are reasonable, and hence that the performance model component is functioning accurately.

The solar generation profile for the dry-cooled central receiver plant in Upington for the 16th of January is shown in Figure 9.9 while the generation profile for the EPRI (2010) dry-cooled parabolic trough plant on the 15th of January is shown in Figure 9.10. It was not possible to include solar generation profiles for this study's parabolic trough models, however, as the variables used to depict the energy flow to and from storage (Q_to_TES and Q_from_TES) were not available as outputs in the SAM parabolic trough model.

By comparing the two figures, it is clear that both the model in this study and that used by EPRI follow the same overall trends. The incident solar power varies throughout the day, increasing to its maximum around midday, before decreasing towards the evening. Whenever there is excess energy from the solar field, usually during the hottest period of the day, some of the thermal energy is diverted to storage, as expected. During periods of intermittent solar irradiation, and towards the evening, the excess energy from the TES is then diverted back to the power block, supplementing the energy from the solar field (and replacing it after sunset), in order to allow for continued operation of the plant at its rated capacity. Finally, the energy output from the plant is observed to be less than the energy diverted to the power block, which is a result of losses in the cycle.

The plant generation profile clearly illustrates that the plant operates exactly as expected and designed, and in addition, follows the same pattern of the generation profile depicted in the literature. It is therefore confirmed that the SAM performance model used in this study was executed accurately, and that the results predicted by it are fair.

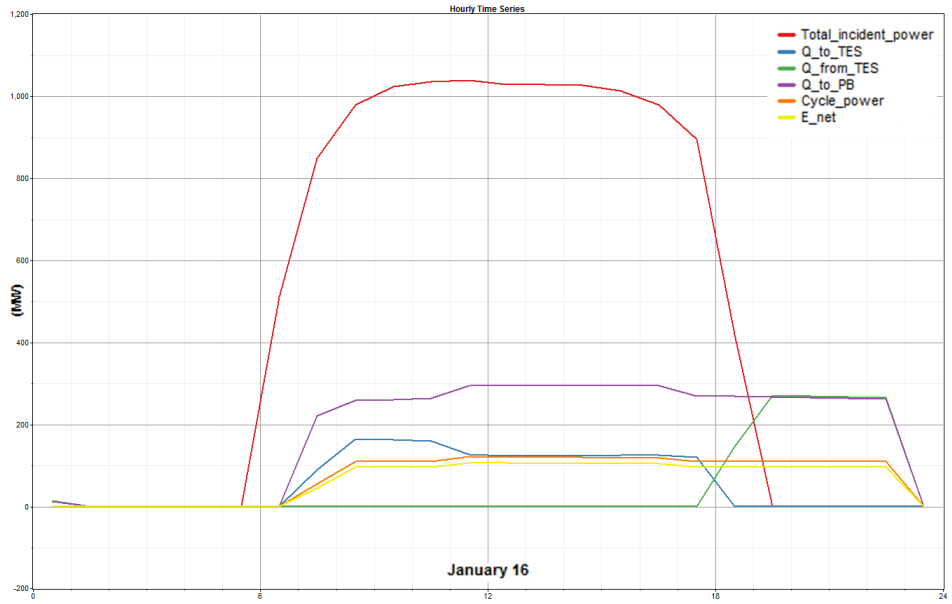

Figure 9.9: Solar Profile for Central Receiver with Dry Cooling and 6 Hours TES in Upington in Summer.

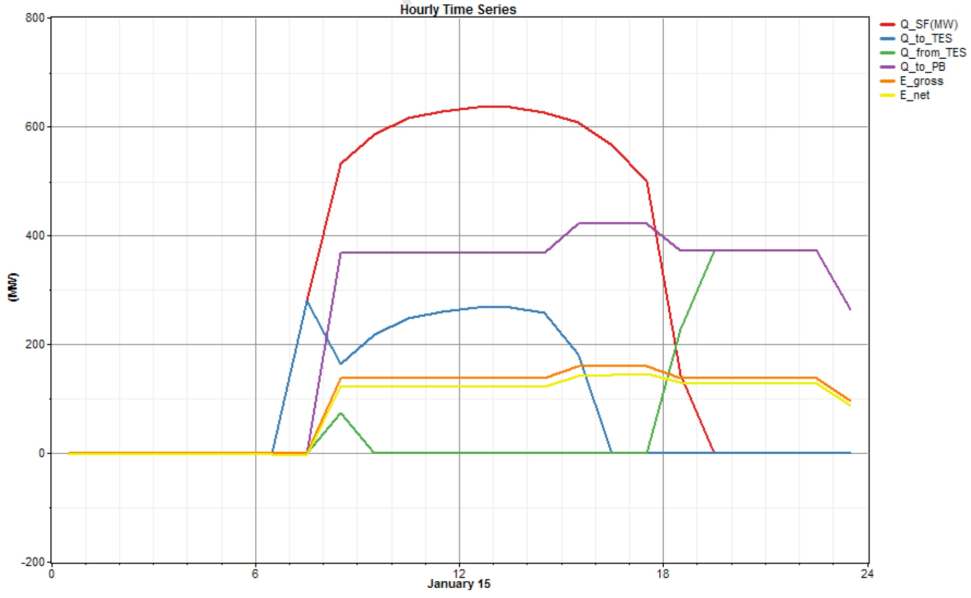

Figure 9.10: Solar Profile for Parabolic Trough with Dry Cooling and 6 Hours TES in Summer (EPRI, 2010).

10 Sensitivity Analysis of Model Inputs

Although the results from this study have been presented and validated, it is important to consider that for any technology, both new and mature, some degree of uncertainty is generally expected in the cost and performance input data used in its modelling. As eluded to in Chapter 8, fairly new or non-commercialised technologies such as the central receiver do not have extensive histories or track records from which to draw complete data, and thus estimates are often used. Even more mature or commercialised technologies such as the parabolic trough are prone to uncertainties stemming from the uniqueness of local conditions (EPRI, 2010). It is therefore necessary to no only be aware of the uncertainties in the input data, but also to attempt to predict and understand how these uncertainties will influence the model results, while determining which inputs have the greatest effect on the final model output.

In order to accomplish this, a sensitivity analysis was conducted for a various number of the input variables used in this study. The input variables considered comprise the following financial inputs: the debt fraction, inflation rate, loan rate (or cost of debt), minimum IRR and real discount rate. The following cost inputs were also analysed: the fixed cost by capacity, the cost of water (represented by the variable cost by generation), and for parabolic trough plants; the solar field cost. Due to the nature of the heliostat optimisation wizard for the central receiver model in SAM, it was not possible to directly integrate the solar field cost into the sensitivity analysis for central receiver plants. Once again, for the sake of brevity, the sensitivity analysis was only conducted for the models of plants in Upington, as it was assumed similar trends would occur for the plants in Springbok and Bloemfontein.

For each one of the input variables, a range of possible values were assigned, based on values suggested in the literature. These limits will now be discussed briefly, while a final summary is presented in Table 10.1.

10.1 Limits and Ranges for Input Variables

An upper limit of 70% was adopted for the debt fraction, based on the value stated in the REFIT Phase II document (NERSA, 2010). A lower limit of 50% was adopted in order to assess the effects of a lower debt fraction.

For the variation in inflation rate, it was decided to adopt a 1% variation in the lower limit and 2% in the upper limit, in order to account for the fluctuation in inflation rate. This resulted in a lower limit inflation rate value of 3.3% and an upper value of 6.3%.

The base case value of 7.3% for the cost of debt was adopted from EPRI (2010) as stated in Chapter 8, however, NERSA (2010) made use of a value of 6.39% while Sargent & Lundy (2003) adopted a value of 8.5%. Using these values as a reference, a lower cost of debt limit of 6.3% and an upper limit of 8.3% was adopted in this study.

Although NERSA (2010) make use of a minimum IRR value of 17% in the REFIT II document (which is the base case value adopted in this study) the SAM default value was 15%, while Sargent & Lundy (2003) made use of a value of 14%. As the adopted base case value of 17% is rather conservative, it was decided to use a lower limit of 15% while increasing the upper limit by only 1% to yield 18%.

NERSA (2010) make use of a real discount rate of 12% in the REFIT Phase II, which is considerably higher than the 8.6% adopted in this study. It was therefore decided to vary the discount rate between 8% and 12% to cover the majority of commonly accepted values.

For variations in both capital and O&M costs, Sargent & Lundy (2003) suggest making use of a ±10% variation around the base case value. This method was therefore chosen for the sensitivity analysis in this study.

As was discussed in Section 8.6 of Chapter 8, a wide range of water costs were listed, with ultimately the mean raw cost from Van der Merwe (2011) being adopted before being combined with treatment costs listed in the Sargent & Lundy (2003) report. For the sensitivity analysis, the full range of the costs given by Van der Merwe (2011) were considered, before being combined once again with the treatment costs from Sargent and Lundy. The final calculated values are listed in Table 10.1.

Table 10.1: Variation Limits of Input Variables for Sensitivity Analysis.

	Base Case	Lower Limit	Upper Limit	Reference
Financing Assumptions				
Debt Fraction	60%	50%	70%	NERSA (2010)
Inflation	4.3%	3.3%	6.3%	
Cost of Debt	7.3%	6.3%	8.3%	NERSA (2010); Sargent & Lundy(2003)
Minimum Required IRR	17%	15%	18%	SAM (2010)
Real Discount Rate	8.6%	8.0%	12.0%	NERSA (2010)
O&M Costs				
Fixed Cost by Capacity	$ 88.03	-10%	+10%	Sargent & Lundy (2003)
Variable Cost by Generation (Incorporating Cost of Water)				
Parabolic Trough Wet Cooling	$ 7.04	$ 5.76	$ 8.32	Calculated from: van der Merwe (2011); Sargent & Lundy (2003)
Parabolic Trough Dry Cooling	$ 3.39	$ 3.26	$ 3.52	
Central Receiver Wet Cooling	$ 6.16	$ 5.16	$ 7.16	
Central Receiver Dry Cooling	$ 3.45	$ 3.31	$ 3.59	
Capital Costs				
Solar Field Cost (Parabolic Trough Only)	$ 385.13	-10%	+10%	Sargent & Lundy (2003)

10.2 Sensitivity Analysis Results

The chosen output metric used to determine the sensitivity of the model to the aforementioned sensitivity input metrics, was that of the LCOE. The LCOE was chosen for the same reasons as stated in the beginning of Chapter 9, in that it provides a means to compare all technologies on an equal basis, while capturing the trade-offs between projects with different designs, capital and O&M costs, and financing parameters (SAM, 2010). The results from the sensitivity analysis are presented in graphical format for both the Upington wet-cooled and dry-cooled parabolic trough and central receiver plants in Figure 10.1 to Figure 10.4 respectively.

As can be seen from the figures, the LCOE is most sensitive to the values stipulated for the inflation rate, closely followed in second by the debt fraction. For both these inputs, an increase in their value results in a decrease in the LCOE, due to the reduction in comparable magnitude of the initial capital outlay. Variations in these inputs can see the LCOE ranging from approximately R1.81 to R2.16 per kWh for the wet-cooled parabolic trough, R2.10 to R2.51 per kWh for the dry-cooled parabolic trough, R1.28 to R1.52 per kWh for the wet-cooled central receiver, and R1.40 to R1.66 per kWh for the dry-cooled central receiver.

The third most influential input of those considered is that of the minimum required IRR, which sees an increase in LCOE with an increase in its value. This is in-line with it being one of the constraining inputs in the financial model. The solar field cost (only applied to the parabolic trough models) closely follows as the next most influential input, and represents a large portion of the project capital cost – as can be seen by its share in Figure 9.5. Intuitively, an increase in the capital cost sees an increase in the LCOE. Variations in these two inputs result in the LCOE ranging from approximately R1.90 to R2.09 per kWh for the wet-cooled parabolic trough, and R2.20 to R2.42 per kWh for the dry-cooled parabolic trough.

The subsequent three inputs, comprising the loan rate, real discount rate, and fixed cost by capacity all have a relatively small effect on the LCOE, with the *overall influence* ranging from approximately R0.10 per kWh down to R0.02 per kWh on either side of the base case value. For all three inputs, an increase in their value also results in an increase in the LCOE.

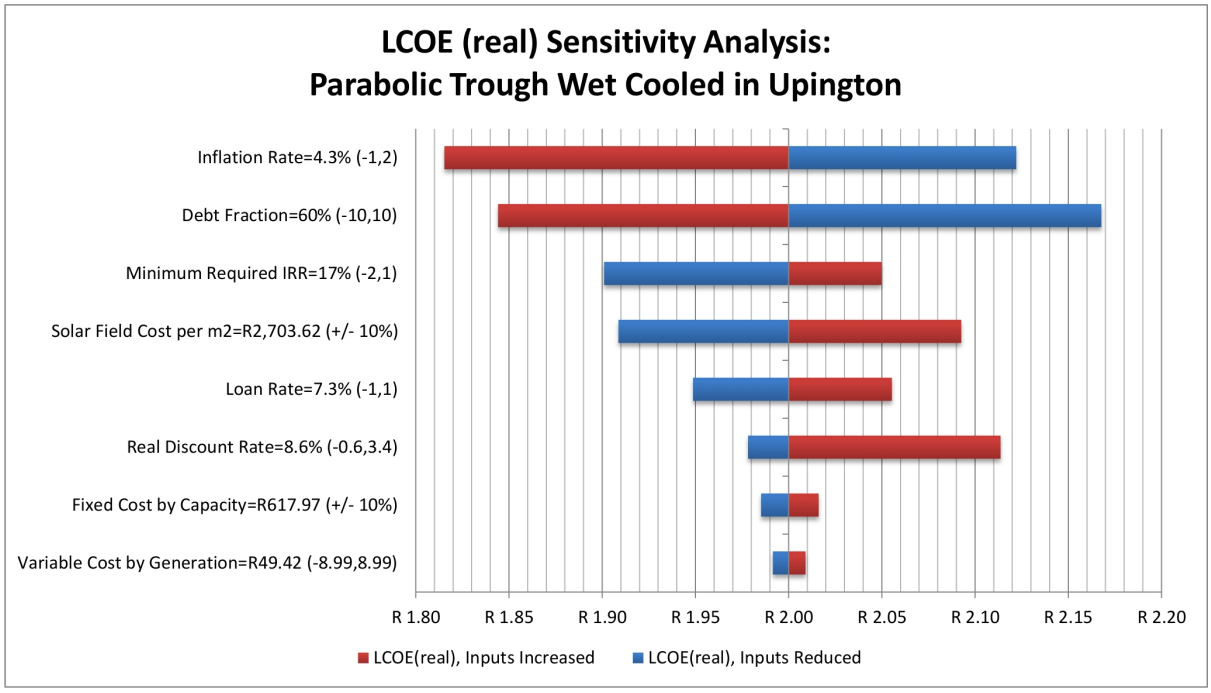

Figure 10.1: Sensitivity Analysis of LCOE (real) for Parabolic Trough with Wet Cooling in Upington.

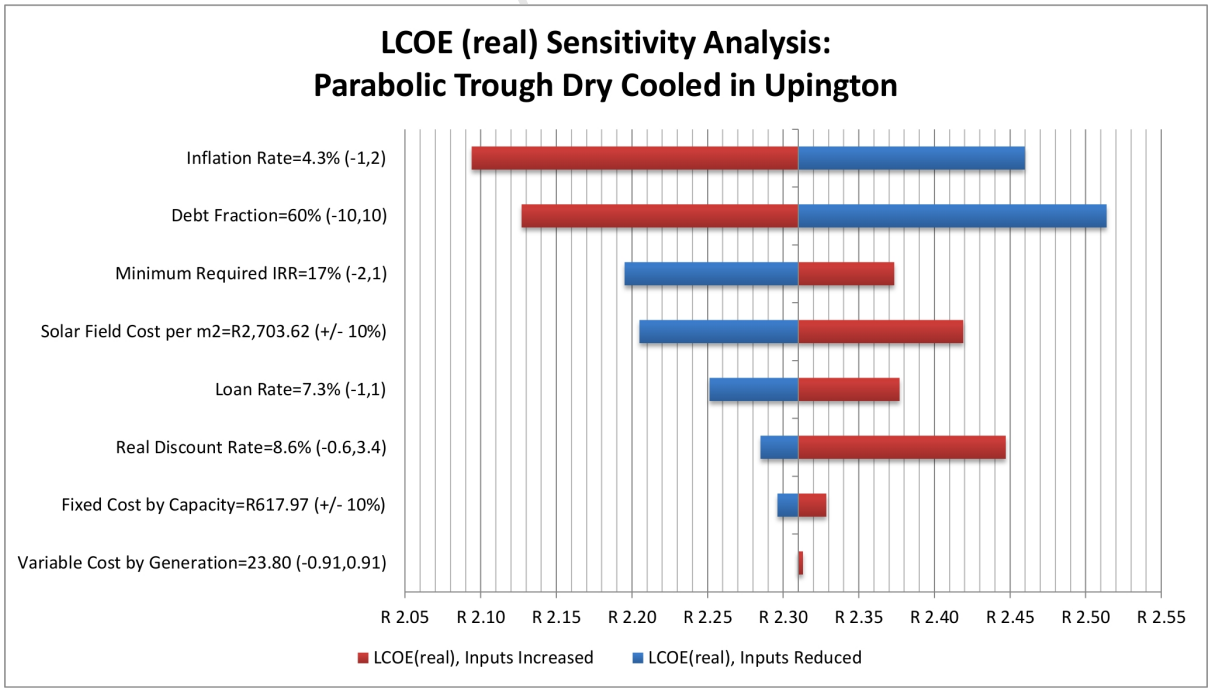

Figure 10.2: Sensitivity Analysis of LCOE (real) for Parabolic Trough with Dry Cooling in Upington.

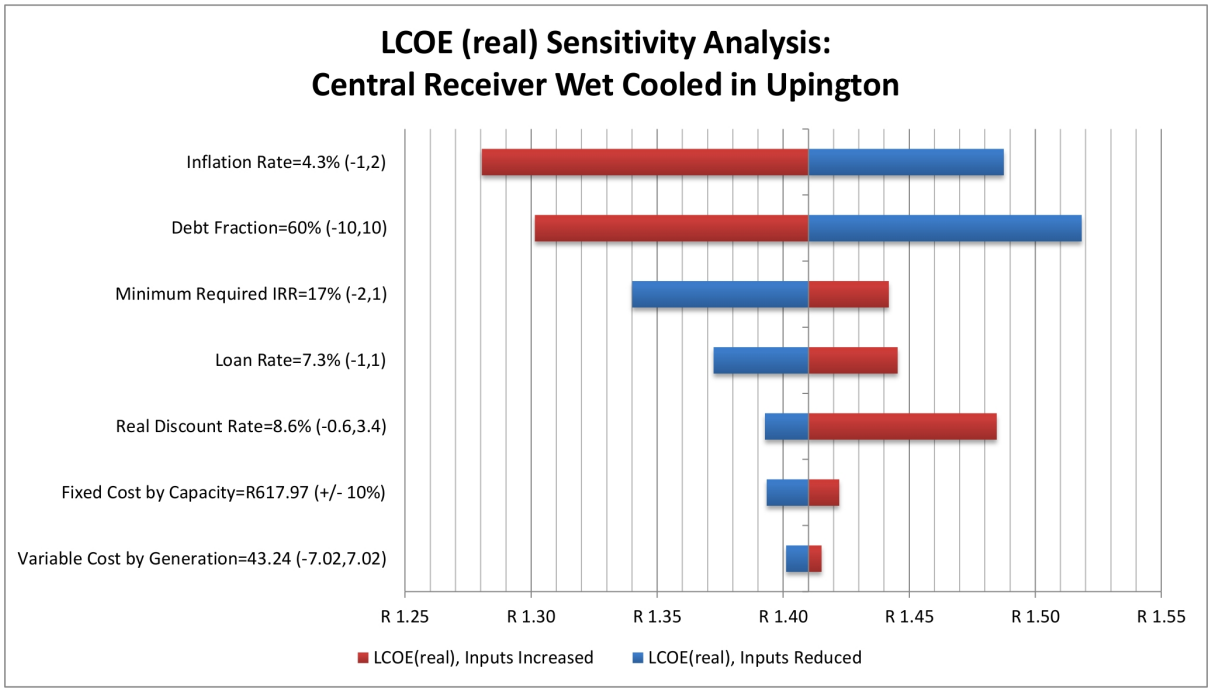

Figure 10.3: Sensitivity Analysis of LCOE (real) for Central Receiver with Wet Cooling in Upington.

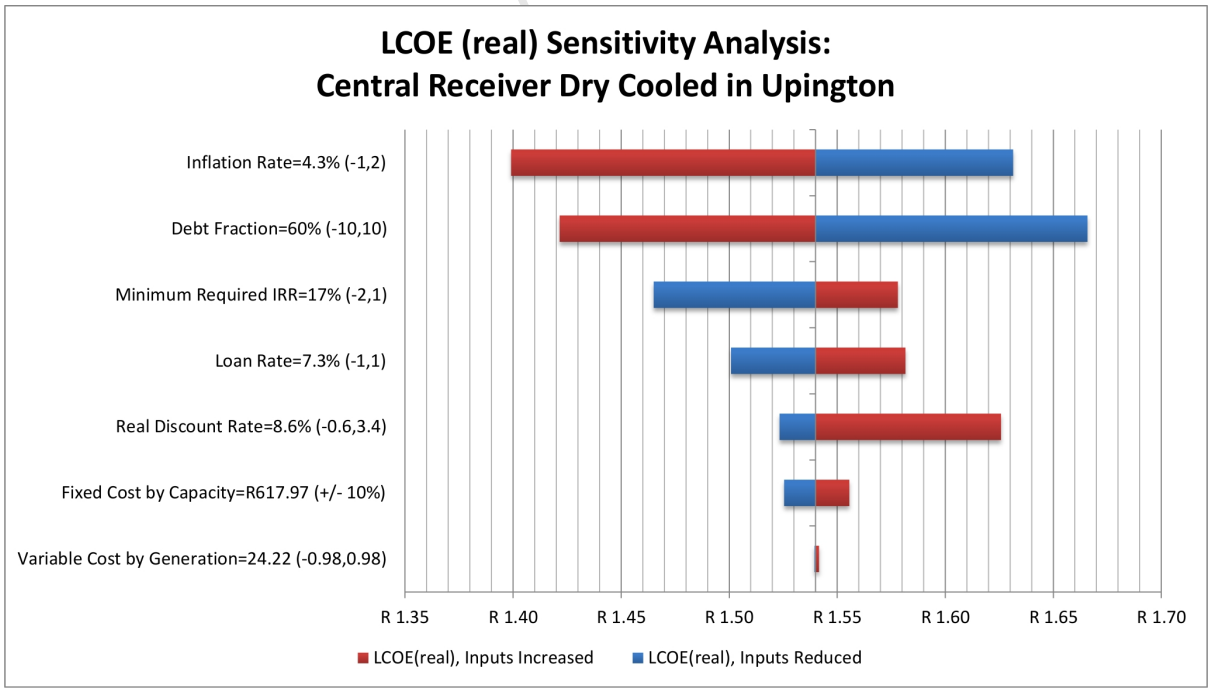

Figure 10.4: Sensitivity Analysis of LCOE (real) for Central Receiver with Dry Cooling in Upington.

Of all the input variables considered in the sensitivity analysis, that which has the least effect on the LCOE is the cost of water (represented by the variable cost by generation). Although an increase in the cost of cooling water does lead to an increase in the LCOE, the increase is approximately R0.01 per kWh for both the wet-cooled parabolic trough and central receiver plants, and less than R0.01 per kWh for the dry-cooled plants. Therefore, according to the model, it is implied that even if the cost of raw water increases to the upper limit of R8.25 per kilolitre, the wet-cooled plants will still be more cost affective – in terms of LCOE – than their dry-cooled equivalents. This in turn implies that the availability of raw cooling water, rather than its current cost, will limit the use of wet cooling technology.

10.3 Validation of Sensitivity Analysis Results

One of the major outcomes of the sensitivity analysis is the prediction that the financial constraints, rather than the plant capital costs, have the largest influence over the resulting LCOE. This result is consistent with statements made in the SAM (2010) documentation, which state that long term projects are very sensitive to values specified for the minimum IRR, minimum DSCR and the requirement of a positive cash flow. The documentation continues to state that in some instances it is possible that these financial constraints can render the project capital investment cost a relatively insignificant factor in the LCOE calculation (SAM, 2010).

11 Conclusions

The aims of this dissertation comprised thee key objectives, the first of which was to develop a methodology for the identification and quantification of potential CSP sites in South Africa, and subsequently, present an approach for creating South African specific, high-level techno-economic models of current commercial CSP technologies at select identified locations within the context of current conditions and boundaries. Secondly, to use this approach to attempt to ascertain which of the CSP technologies modelled would be considered optimal for each location, and to determine whether the use of wet cooling or dry cooling technology would be more beneficial. And thirdly, as at the time of writing, no utility-scale commercial CSP plants had yet been realised in South Africa, the final objective of this study was to derive useful insight into and understanding of the techno-economic criteria and their effect on CSP developments, through the comparison of different model results and hence the arising relative metrics, as opposed to absolute value predictions.

The work presented in this dissertation represents the fulfilment of these objectives, in that a methodology was developed whereby potential sites were successfully identified and quantified within the ArcGIS software package, and South African specific performance and cost-based models were created for both parabolic trough and central receiver technologies at each location by means of the SAM software package and the adaptation of model data to South African conditions. Attempts were made to identify the optimal CSP technology and cooling technology for each site considered, and key techno-economic criteria were identified through the comparison of model data and sensitivity analyses.

Thus, based upon the analyses, results and findings of this study, the following conclusions have been drawn and are presented in three categories relating to the GIS analysis, SAM analysis, and analysis of research questions:

11.1 Conclusions Drawn from GIS Analysis

11.1.1 Data, Analysis Criteria and GIS Methodology

Successful Sourcing of Data and Creation of GIS Methodology

Through the conduction of a literature review of previous studies concerned with GIS-based CSP-potential analysis, the characteristics required for potential CSP sites in this study were successfully identified, and relevant analysis criteria developed. The analysis criteria included the level of direct normal solar irradiation, a land slope of less than 1%, areas excluded due to land class, areas classed as 'least threatened' vegetation, and less than 20 km proximity to large water bodies and 132 kV transmission lines. The required data for the study was determined and sourced, thereby allowing for a comprehensive, high-level GIS analysis to be conducted.

An efficient GIS analysis methodology was also successfully researched and developed, and presented in its entirety in Appendix A. The implementation of the methodology in the GIS software allowed for the visualisation, analysis and interpretation of the imported data, which in turn made the creation of maps and the extraction and quantification of information possible.

Potential for Data Improvements

The solar data from NREL (SWERA, 2010) only had a spacial resolution of 40 km $\times$ 40 km, and hence could not depict small-scale variations in DNI caused by changes in local terrain or surroundings. Although this data was the best freely available data for South Africa with the highest spacial resolution, it was decided to make use of the shading and DNI calculation algorithm within the ArcGIS software package, as a means to verify the NREL data (and hence the results achieved), and attempt to predict location specific DNI levels. The DNI calculation algorithm was run with mixed success, and ultimately only used to calculate location specific variations in DNI for a few potential sites. It is concluded, however, that the results for the identified potential CSP sites arising from the analysis cases do indeed coincide with areas receiving high amounts of annual DNI, and hence that the NREL DNI data is acceptable for a high-level study. Further validation and more extensive analyses including the sourcing of higher resolution DNI data is recommended, however.

A further conclusion drawn regarding the data used in the GIS analysis, is that the large water bodies and rivers analysis layer, although suitable for this high-level study, did not contain information regarding the magnitude of water flow-rates, nor the volumes that are permissible for extraction. It was therefore not possible to determine whether a potential site situated near one of these water bodes would in fact be permitted to extract water from it, and if were, what quantities would be available. Furthermore, the transmission and national grid data employed was digitised and geo-referenced from an image, and it is hence concluded that the sourcing of a primary source of grid data would be beneficial for future studies.

A final conclusion regarding data for the GIS analysis surrounds the adopted land class data. The land class data employed in the study did not contain any information regarding the land value associated with a particular area. Data regarding various land area costs could be greatly beneficial to developers in further determining optimal CSP sites, based on the ranking of sites according to the cost associated with either the purchase or rental of the land in question.

11.1.2 Potential CSP Site Identification

Potential CSP Sites Successfully Identified and Quantified

The GIS analysis allowed for the successful identification of a large number of potential CSP sites for each of the five analysis cases. Of the identified potential CSP sites, the vast majority were situated in the Northern Cape, but were limited by the lack of national grid capacity and availability of large water sources in the cases where they formed part of the analysis criteria. Other provinces which contained identified potential sites included the Western and Eastern Cape, the Free State and North West Province.

A number of potential sites were also identified along the West Coast of South Africa, however, the identified potential areas only comprised a small portion of the total West Coast coastline. This is mainly attributed to the combination of a lack of extensive grid capacity in the region, the decrease of DNI levels towards the coast, and the 'threatened vegetation' on the West Coast of the Western Cape. The few potential sites identified could prove to be viable locations if sea water is to be adopted for plant cooling purposes, however as stated in Section 9.2.6, the modelling of sea water cooling was beyond the scope of this report, and thus further analysis is required – including the local measurement of coastal DNI levels and other weather data – in order to determine whether it would be more economical than adopting dry cooling.

The quantification of the five analysis cases – when only considering sites with individual areas grater than 2 km^2 – predicted a total potential land area for CSP in South Africa of anywhere between 2,180.5 km^2 and 18,785.6 km^2, with total available solar energy levels between 16.5 TWh/day and 144.3 TWh/day, depending on which analysis criteria were adopted. These values were more than tripled if the requirement for a site to have an area greater than 2 km^2 was removed and hence all potential areas were included. Of the five analysis cases, Case 2 resulted in the lowest identified site area and hence energy generation potential, caused by its stricter DNI requirement of 6.5 $kWh/m^2/day$ (compared to 6.0 $kWh/m^2/day$ of Case 1) as well a requirements for a 20 km proximity to both large water bodies and the national grid. Of the first three analysis cases (concerned with existing grid proximity) Case 3 resulted in the greatest site area and energy generation potential. When the requirement for close proximity to the national grid was excluded, as in Case 4 and Case 5, the increase in site area and energy generation potential was dramatic, with increases of more than fourfold being realised over their equivalent Case 2 and Case 3 scenarios. From these analysis case results the following additional conclusions are drawn:

Vast Potential for CSP in South Africa

Even when constrained by the requirement for CSP sites to be larger than 2 km^2 in order to be considered, vast potential still exists for a utility-scale CSP sector in South Africa. Furthermore, if one considers the higher capacity factors of central receiver plants compared to parabolic troughs, as well as the central receiver's better tolerance for land slope, central receiver technology is deemed a superior choice for adoption.

Requirement for Site Proximity to Large Water Bodies a Limiting Factor

The requirement for a close site proximity to large water bodies greatly reduces the area and hence energy generation potential of CSP sites in South Africa. The implications of this are that by reducing reliance on cooling water or adopting alternative cooling technologies such as dry cooling, a far greater CSP potential could be realised in terms of number of sites and total potential area. It is thus concluded that in order to fully realise the solar resource potential in South Africa, it may be necessary to make use of dry cooling technologies for the majority of all new CSP plants.

Limitations Arising from Existing National Gird

The number of potential CSP sites are also limited by the lack of national grid capacity in regions with high DNI levels, especially in the Northern Cape. This is evident by the

fact that all the identified sites are clustered around the few large transmission lines in the region. If the the national grid were to be further extended into areas with high CSP potential, the total available area and energy generation potential for CSP could be greatly increased. The site areas identified in Case 4 and Case 5, or similar areas identified by future analyses, could also be used to determine the optimal areas in which future national grid expansion would be beneficial. The cost benefit analysis of the extension of the national grid was considered beyond the scope of this study, but it is deemed a key requirement for future studies.

11.1.3 Validation of CSP Site Identification

Successful Validation of CSP Site Identification

The results achieved in the various GIS analyses were validated by means of comparison with those achieved in a study on South Africa's CSP potential by Fluri (2009). The results achieved in Case 3 of this study – which made use of virtually identical analysis criteria to those used by Fluri – and including sites smaller than 2 km^2, showed a strong resemblance to those achieved by Fluri. The other cases showed less of a resemblance due to the use of different analysis criteria to those used by Fluri. It is therefore concluded that the GIS methodology and analysis conducted in this study was implemented and conducted successfully.

11.2 Conclusions Drawn from SAM Analyses

11.2.1 SAM Model Input Data

Inputs for SAM Models Successfully Sourced and Calculated

The conduction of an extensive literature review of both CSP plant technical design and cost data allowed for the creation of a detailed comparison database, and ultimately lead to the decision to adopt the default SAM input values in the instances where relevant, South African specific data could not be sourced or calculated. A complete set of data inputs for each of the twelve SAM models, adapted to reflect local South African conditions, was successfully created within the SAM software, thereby allowing for a comprehensive performance and cost based analysis to be conducted for each technology at each considered location.

Weather Data from Towns Used to Approximate Potential Sites

The three locations of Upington, Springbok and Bloemfontein – whose weather data was used to represent conditions at potential CSP sites – were chosen due to the lack of freely available detailed weather data for specific geographic coordinates or regions containing potential CSP sites. It is therefore concluded that although this weather data was considered acceptable for this initial study, it will be necessary to obtain detailed, location-specific weather data for future analysis of potential sites. This location-specific data could be obtained commercially, however, the conduction of actual weather and DNI measurements at potential sites will likely be necessary.

11.2.2 Key Findings of SAM Analyses

Each of the twelve SAM models were successfully simulated within the SAM software. Through the analysis and review of the results obtained, the following key conclusions are drawn:

Wet Cooling Most Efficient when Available

The use of wet cooling technology with both parabolic trough and central receiver systems resulted in higher annual energy yields of between 2.5% and 6%, and greater capacity factors than equivalent plants at the same locations making use of dry cooling. This was attributed to the greater efficiencies achievable through the use of wet cooling, as a result of relying on lower wet-bulb temperatures as opposed to the higher dry-bulb temperatures of dry cooling.

The use of wet cooling was also found to result in lower total installed costs per net capacity and lower LCOEs than equivalent dry-cooled plants at the same location, with dry-cooled parabolic trough plants possessing approximately 13.5% greater total installed costs and 14% – 15.5% higher LCOEs, and dry-cooled central receivers approximately 5% greater costs and 8% – 9.5% higher LCOEs. This was attributed to the higher capital and O&M costs and efficiency penalties associated with the use of dry cooling. Wet cooling is therefore considered theoretically superior to dry cooling if ample cooling water is available, however, in water-stressed regions such as the Northern Cape of South Africa where large volumes of water may not be available, dry-cooling is considered the optimal choice.

Dry Cooling Dramatically Reduces Water Consumption

The use of dry cooling resulted in an annual reduction in water consumption of more than 90% for all CSP plants, when compared to equivalent wet-cooled plants in the same location. It is thus concluded that the use of dry cooling in regions with limited access to cooling water, or in cases where the cost of water is prohibitively high, will be a necessity and will allow for the realisation of CSP projects in regions that would otherwise not have allowed for them to be economically viable.

Central Receiver Technology Considered Preferable

When compared to the parabolic trough models in this study, the central receiver models were found to produce between 1% and 8% more energy annually across all three locations. This is primarily attributed to their high concentration ratios and optical efficiencies. Central receivers were also found to consume less water annually compared to their equivalent parabolic trough plants – between 6% –11% less for wet-cooled plants and between 7.5% – 13.5% less for dry-cooled plants. In addition, the central receiver plants proved approximately 26% – 35.5% more economical in terms of total installed cost per net capacity and approximately 30% – 33.5% more economical in terms of LCOE than their parabolic trough equivalents. The difference in economy was so great that a dry-cooled central receiver was found to be more economical in terms of LCOE than an equal capacity wet-cooled parabolic trough in same location. The lower costs of central receivers are attributed to their higher annual energy production as well as the difference in fundamental plant design and default component costs in the SAM model. Based on these results, it is concluded that central receiver technology should be given primary consideration when only parabolic trough and central receiver systems are considered.

Upington Identified as Best Location of the Three Considered

Of the three locations considered in this study, namely Upington, Springbok and Bloemfontein, the Upington region was deemed the optimal location for CSP. The reasons for this decision are based on the results that the Upington plants possessed the lowest total installed costs per net capacity, the highest annual energy production, and the lowest LCOE of all the considered locations. Furthermore is was observed that the LCOE for the dry-cooled central receiver plant in Upington (R1.54 /kWh) was lower than that of the wet-cooled central receiver plant in Springbok (R1.56 /kWh), and the same as the wet-cooled central receiver in Bloemfontein (R1.54 /kWh). It is thus concluded that it may be more beneficial to construct a central receiver CSP plant in a region with high

DNI levels but limited access to cooling water, as opposed to an area with lower DNI levels but access to large volumes of water.

11.2.3 Identification of Preferred Technology for Each Site

Based on the results of each of the SAM models, the following technologies were considered the optimal choice for each considered location:

Upington

Due to the scarcity of water in the Upington region of Northern Cape, as well as the negative impacts that could arise for local farms and communities in the region should large quantities of water be drawn from the orange river for plant cooling, it is thought that the optimal CSP plant for the Upington region would be a central receiver plant with dry cooling technology. This is affirmed by the previous conclusion that a dry-cooled CSP plant in a region with high DNI levels may be the optimal plant choice for South Africa considering the water stressed classification of the country.

Springbok

As a consequence of not being able to model the effects of sea water cooling on CSP plant efficiencies and costs, it was only possible to conclude that, based on the results of this study, the optimal CSP plant for the Springbok region would be a central receiver plant. Further research would be required in order to determine whether wet cooling with sea water or dry cooling would be preferable.

Bloemfontein

It is concluded that the optimal CSP technology for the Bloemfontein region – when only parabolic trough and central receiver technologies are considered – would be a central receiver, however, based on the lack of data on permissible volumes of extraction for large water bodies, it is not possible to determine whether wet cooling or dry cooling would be more beneficial. Due to its lower costs and higher efficiency, employing wet cooling would be more economical if cooling water was available in large enough, cost effective quantities, however, more specific site analyses and local water availability studies would be required in order to determine if this was indeed the case, or alternatively if dry cooling would be preferable.

As a final note, it is concluded that the choice of central receiver system as the optimal CSP technology for all three locations is based solely on the comparisons in this study between parabolic troughs and central receivers. Alternative solar technologies such as linear Fresnel, parabolic dish, or even photovoltaics should therefore also be considered and modelled for comparison purposes in future studies and in the context of a large-scale rollout of CSP.

11.2.4 Sensitivity of Results to External Factors

A sensitivity analysis was successfully conducted and used as a means to determine the variation of the LCOE as a function of variation in a few select input variables. The key conclusions drawn from the sensitivity analysis are summarised under their respective headings.

LCOE Most Sensitive to Financing Assumptions

The resulting LCOE from the SAM models was found to be most sensitive to the financing assumptions of the project, such as the inflation rate, debt fraction and minimum required IRR. The loan rate and real discount rate were also found to affect the LCOE, however, to a lesser extent. The solar field cost was also identified as affecting the resulting LCOE, primarily due to it representing the largest factor in the plant capital costs. It is thus concluded that financial constraints, rather than plant capital costs, have the largest influence over the resulting LCOE. This result was echoed in the SAM (2010) documentation.

LCOE Least Sensitive to Cost of Cooling Water

The cost of cooling water (as represented by the variable cost by generation input) was found to have the least effect on the resulting plant LCOE, with maximum increases of approximately only R0.01 per kWh observed. Furthermore, even when increased to its maximum value in the sensitivity analysis, the wet-cooled plants still proved more economical than their dry-cooled equivalents. Based on this result, it is concluded that the availability of raw cooling water, rather than its current cost, will be the limiting factor in the use of wet cooling technology.

11.2.5 Validation of SAM Findings

SAM Model Results Successfully Validated

The results from the SAM models were validated by means of comparison with those found in the literature. The results achieved in this study were found to be in the same order of magnitude as those in the literature, and were often similar within 10% – 20%.

LCOE Data Found to be Similar to South African Models Created by EPRI

Of the literature results used for comparison and validation purposes, only those from EPRI (2010) contained data specific to CSP plants modelled in the South African environment; however, these were limited to dry-cooled plants only. Although the total plant costs were considerably higher than those given by EPRI (2010), the remaining metrics showed good agreement. The LCOE in particular showed strong agreement, with the dry-cooled parabolic trough value of R2.31/kWh agreeing within approximately 10% to the EPRI value of R2.08/kWh, and the dry-cooled central receiver value of R1.54/kWh varying by less than 2% from the EPRI value of R1.57/kWh.

Total Installed Costs Found to be Higher than Literature Values

Of the results validated, the total installed cost per net capacity, however, was found to be considerably higher than the values stated in the literature, occasionally by more than 50%. The higher than average total installed costs are concluded to be a result of both the SAM default costs – and hence the costs by the WorleyParsons Group – on which they are based, and the conservative cost adjustment factors applied to represent the higher overall capital and O&M costs for construction in South Africa. It was also noted, however, that the total installed cost per net capacity metric was variable for all plants in the literature, and therefore, the fact that the costs used in this study were based on SAM inputs, and that they were in the correct order of magnitude, resulted in them being considered acceptable. It is therefore concluded that the SAM analyses conducted in this study were implemented and conducted successfully.

Additional Validation and Sensitivity Analyses Required

A final conclusion regarding the various validation and sensitivity analyses in this study, is that they were limited to only consider the Upington based plants. It is therefore deemed necessary to conduct more extensive validation and sensitivity analyses for additional locations in further studies.

11.3 Analysis of Research Questions

Through the development of the methodology, the use of the various models and simulations in this dissertation, and the analysis of their results, the topics posed in the research questions have largely been discussed and analysed; however, for the sake of completeness, an explicit analysis summary of each of the four research questions will now be presented under their respective headings.

1. Is it more beneficial in terms of the Levelised Cost of Energy (LCOE) to locate a South African CSP plant in a region with high DNI levels but limited access to cooling water, hence adopting dry cooling; or in a region with lower DNI levels but greater access to larger volumes of water, hence adopting wet cooling?

Is was observed and noted both in the analysis of the SAM model in Chapter 9, as well as in the conclusions relating to the SAM analysis, that the LCOE value of R1.54 /kWh for the dry-cooled central receiver plant in Upington was lower than that of the R1.56 /kWh value for the wet-cooled central receiver plant in Springbok, and the same as the R1.54 /kWh value for the wet-cooled central receiver in Bloemfontein. Furthermore, due to the classification of South Africa as a water-stressed country, it was thus concluded that it may be more beneficial to employ dry cooling and construct a central receiver CSP plant in a region with high DNI levels but limited access to cooling water, as opposed to an area with lower DNI levels but access to large volumes of water and employing wet cooling.

The benefit in terms of LCOE was only found to be true for central receiver plants, however, as when considering parabolic trough plants, the dry-cooled trough plant in Upington had a resulting LCOE of R2.31/kWh while the wet-cooled trough plants in Springbok and Bloemfontein had resulting LCOEs of R2.22/kWh and R2.20/kWh respectively. Even so, the difference in LCOE value between the dry-cooled trough in Upington and the wet-cooled trough in Bloemfontein is less than 5%, and thus considering the water stressed nature of South Africa, dry-cooling may still prove preferable depending on the specific site and situation.

2. Of the CSP technologies considered in this analysis, which would be deemed most optimal at each location?

The discussion and identification of the optimal CSP technology for each of the considered sites, comprising only the CSP technologies modelled, was presented in Sections 9.1, 9.2 and 9.3, as well as in the conclusions relating to the SAM analysis. For all the three sites considered, it was concluded that central receiver plants were preferable, based on the model predictions that central receivers produced between 1% and 8% more energy annually, consumed between 6% and 11% less water for wet-cooled plants and between 7.5% and 13.5% less water for dry-cooled plants, and proved approximately 26% – 35.5% more economical in terms of total installed cost per net capacity and approximately 30% – 33.5% more economical in terms of LCOE than their parabolic trough equivalents. Furthermore, a dry-cooled central receiver was found to be more economical in terms of LCOE than an equal capacity wet-cooled parabolic trough in same location.

Due to the scarcity of water in the Upington region of Northern Cape, as well as the negative impacts that could arise for local farms and communities in the region should large quantities of water be drawn from the orange river for plant cooling, it was further concluded that the use of dry-cooling would be preferable for the Upington site. However, due to the inability to model the use of sea water for cooling purposes along the West Coast of South Africa, and the lack of data on volumes of water permissible for extraction from the large water bodies and rivers, it was not possible to determine weather the use of wet-cooling or dry cooling would be preferable for the locations of Springbok and Bloemfontein respectively. Nevertheless, it may still be more beneficial to make use of dry cooling, as a means to reduce the risk of water supply concerns.

3. Which financial and cost-related model input variables have the greatest effect on the resulting LCOE of the plant, and hence which are the key items to consider when implementing a utility-scale parabolic trough or central receiver CSP plant in South Africa?

A sensitivity analysis of a number of financial and cost-based model inputs was conducted in Chapter 10, as well as in the conclusions relating to the SAM analysis, comprising the debt fraction, inflation rate, loan rate (or cost of debt), minimum IRR, discount rate, fixed cost by capacity, the cost of water (represented by the variable cost by generation), and for parabolic trough plants; the solar field cost. The sensitivity analysis, which was conducted for the Upington based plants only, revealed that the resulting LCOE was

most sensitive to the financing assumptions of the project, such as the inflation rate, debt fraction and minimum required IRR. The loan rate and real discount rate were also found to affect the LCOE, however, to a lesser extent. The solar field cost was also identified as affecting the resulting LCOE, primarily due to it representing the largest factor in the plant capital costs. The cost of cooling water (as represented by the variable cost by generation input) was found to have the least effect on the resulting plant LCOE, and even when increased to its maximum value in the sensitivity analysis, the wet-cooled plants still proved more economical than their dry-cooled equivalents. It was thus concluded that financial constraints, rather than plant capital costs, have the largest influence over the resulting LCOE, and that the availability of raw cooling water, rather than its *current* cost, will be the limiting factor in the use of wet cooling technology.

4. Can a high level analysis and methodology be developed to achieve the objectives of this study, by making use of existing software and modelling tools, available data, or data adapted to reflect South African conditions; and if so, how accurately can this be achieved?

The methodology developed to achieve the objectives set and analyse the research questions posed in this dissertation can be classified into two sub-categories, namely that of the GIS methodology, and that of the methodology developed to analyse South African specific CSP plants within the SAM software.

The GIS methodology allowed for the successful identification and quantification of potential CSP sites in South Africa, and made use of data which was available and specific to South Africa. The methodology developed for the SAM analysis allowed for the creation of a cost and performance analysis of CSP plants in the South African environment; however, certain compromises and approximations had to be made due to a lack of availability of South African specific data. As an example, the three locations of Upington, Springbok and Bloemfontein – whose weather data was used to represent conditions at potential CSP sites – were chosen due to a lack of freely available, detailed hourly weather data for specific geographic coordinates, or regions containing potential CSP sites. Furthermore, as revealed through the creation of the database used to review and compare existing CSP plant design and cost data – discussed in Section 8.4 and in the appendices – it was not possible to obtain a complete dataset for South African CSP plants, and thus further methods were developed to either adjust international data to local conditions, approximate or calculate required inputs, or make use of SAM defaults.

Various key model outputs were also compared to those presented in the literature, as described in Section 9.5 as well as in the conclusions relating to the SAM analysis, and reasonable correlation was found, usually within 10% – 20%. Some of the model results, particularity those of the total installed cost per net capacity, were considerably higher than those stated in the literature, however, and reasons for this have been discussed, and recommendations made for further work.

Although the methodology developed and the model results achieved did identify central receiver technology as being preferable to parabolic trough technology for all three locations considered, an optimal solution in terms of both CSP technology and cooling technology choice was only presented for Upington. Similar predictions were not considered possible for Springbok and Bloemfontein due to the lack of capacity for modelling sea water cooling, and a lack of data pertaining to volumes of water available for extraction from large water bodies respectively. The methodology is therefore limited as an optimisation tool; however, its development and the implementation thereof allowed for the achievement of the dissertation's objectives, and provides a means of identifying potential CSP sites and technologies for further consideration, as well as highlighting the important parameters related to their implementation.

12 Recommendations

Throughout the course of this dissertation, several items have emerged as potential candidates for future work. These include, but are not limited to, data that has been used which could be expanded or improved upon, insufficient data in certain fields, and certain approximations which were made due to lack of data or insufficient supporting research. Therefore, based on these items, as well as drawing from the conclusions in this dissertation, the following recommendations are made:

12.1 Recommendations for further GIS Analysis

12.1.1 Suggested GIS Data Improvements

Obtain Solar Data at Higher Resolution

The spacial resolution of the solar data used in this study was fairly coarse when compared to the resolution of other data sets in this analysis – 40 km × 40 km as opposed to 90 m × 90 m. Therefore, in order to determine variations in DNI levels over smaller distances, and hence achieve grater accuracy in the determination and ranking of potential CSP sites according to DNI levels, it is recommended to obtain DNI data with a higher spacial resolution for use in future studies.

Consider Proximity of CSP Sites to Roads and Load Centres

Although the proximity of an identified potential CSP site to specific infrastructure like the existing national gird was analysed, no consideration was given for the proximity to other existing infrastructure such as roads or load centres. As the distance to towns or load centres, as well as access to road infrastructure greatly affects a project's construction costs, it is recommended to include these items as part of the analysis criteria in future analyses.

Source Better National Grid Data and Consider Proximity to Substations

As stated in Section 6.3.6 as well as in the conclusions, the data used to represent the Eskom national grid was digitised and geo-referenced and thus could not be considered as an accurate, primary source of vector-based data. As a result, no data representing the locations of electrical substations were included in the GIS analysis. As a utility-scale power plant would be required to connect to the national grid via a substation, it is recommended to included the proximity to substations, in addition to the national grid, as analysis criteria in future studies.

Incorporate Land Class Data with Land Costs

Utility-scale CSP plants generally require fairly large areas of land for their solar fields, and thus the cost of land will certainly be a factor when considering potential locations for potential CSP plants. It is therefore recommended to incorporate land class data which includes the cost of land in future GIS-based analyses, as this could be used as a factor in the determination of the optimal location for a potential plant.

12.1.2 Suggestions for Further GIS Models

Analyse Water Bodies According to Permissible Volumes Available for Extraction

The proximity of CSP plants to cooling water was considered as on of the key criteria in the GIS analysis, while the comparison between wet and dry cooling technology formed one of the major themes in this study. The data used to represent the large water bodies in the GIS analysis allowed for the differentiation between large rivers and dams and other smaller water bodies, however, no data was included which defined water flow rates, volumes or what volumes were available for extraction. It is therefore recommend for future studies to identify which of the large water bodies could sustain further water extraction, and in what quantities.

Conduct Further Validation of Local Scale Solar Data

Due to limits in both time and computational resources, it was only possible to make use of the *solar area radiation* calculation algorithm to calculate the DNI levels and duration of daily irradiation (and hence validate the adopted DNI data) for a few of the identified potential sites. It is therefore recommended to conduct further and more detailed validation of solar data at a site-specific scales in any further studies.

Consider Future Grid Expansion

As stated in the conclusions, the density of the existing national grid was found to be a limiting factor for potential CSP sites which required a close proximity to it, particularly in the Northern Cape region. When the 20 km proximity requirement was removed, however, (as in Case 4 and Case 5 of the GIS analysis) the CSP potential was found to increase by more than 4 times. It is therefore recommended to determine whether the expansion of the national grid in certain regions – as a means to realise a greater CSP potential – would be beneficial, and to include the modelling and analysis thereof in future studies.

12.2 Recommendations for further SAM Analysis

12.2.1 Suggested SAM Data Improvements

Obtain Location Specific Weather Data

As stated in Section 8.1, due to the lack of freely available hourly weather data for specific geographic locations, weather data for the towns of Upington, Springbok and Bloemfontein was used to approximate the various weather conditions experienced at different potential CSP sites. Therefore, the data used in this study did not reflect the actual weather data for any specific or optimally identified CSP site. Although it was concluded that the approximated weather data used in this report was adequate for an initial high-level study, it is recommended to obtain location, or site-specific weather data for use with the SAM models in any future studies, in order to model the cost and performance of plants at *actual* specific locations.

Further Customise SAM Default Design Data

Due to the lack of complete and comprehensive design and cost data containing all the inputs required by the SAM models – as discussed in Section 8.4 and illustrated by the comparison databases of Appendix B to Appendix E – many of the plant design inputs were left as their SAM default values. In order to model the performance and costs of *actual* potential plants, it is recommended to make use of plant-specific design and cost data, and to rely less on the SAM default values.

12.2.2 Suggestions for Further SAM Models

Consider Additional Solar and CSP Technologies at Potential Sites

The scope of this dissertation, and time constraints, resulted in only two CSP technologies being considered, analysed and compared, namely parabolic trough and central receiver systems. However, as described in Chapter 3, there exist a number of additional CSP technologies, both commercially available and under development, which could also be considered for implementation at potential sites. Furthermore, one could also consider non-thermal solar power systems such as photovoltaic (PV) solar technology in South Africa. However, as PV systems are able to utilise the diffuse irradiation component of solar irradiation in addition to DNI component, and as the GIS analysis of this dissertation was specific to DNI, additional GIS analyses would be required which consider other forms of irradiation such as latitude tilt irradiation (LTI). The SAM 2010.04.12 software possesses the ability to model both parabolic dish CSP systems and PV systems, in addition to the parabolic trough and central receiver systems considered in this study. It is therefore recommended to include the analyses of these additional technologies within the SAM software in any future studies, particularity in the context of a large-scale rollout.

Include Modelling of Fossil Backup Fuel Hybridisation

Although the use of thermal energy storage was considered for all plants at all locations in this study, no consideration was given to the use of a fossil backup fuel, and hence plant hybridisation. Hybridisation is currently utilised at many existing CSP plants – such as the SEGS parabolic trough plants in the Unites States and many of the plants in Spain – as a means to increase plant availability and capacity factors and render plants better suited to base load power generation. The use of fossil backup fuel is also often limited, with maximum limits of 25% imposed on supplementation for the SEGS plants, while only 15% supplementation is allowed for Spanish plants. The SAM software possesses the ability to include and model both the cost and performance effects of fossil backup with CSP plants, but due to time constraints this was not included in this dissertation. The modelling of plant hybridisation is therefore recommended for future studies.

Conduct Further Validation and Sensitivity Analyses for All Locations

Due to time constraints, it was only possible to compare and validate the SAM results for plants situated at Upington with those found in the literature. It is therefore recommended to conduct further and more detailed validation of the SAM model results for all locations considered in any future studies.

12.3 General Recommendations for Future Studies

The following final recommendations are considered to be difficult to implement into the existing GIS based analysis and to accomplish within the current SAM software. They are thus suggested as general recommendations which may require other means or software in order to be implemented.

Perform Solar DNI Measurements at Potential CSP Sites

As stated in section 6.3.1, as well as in the conclusions of this dissertation, the solar data employed in this study was satellite derived, and had a spacial resolution of 40 km × 40 km. In order to ensure that the true potential and conditions at a particular CSP site are known, and before selecting an area for construction, it is thus recommended that actual solar measurements, as well as the measurement of any other weather data required, be conducted at promising identified sites. These measurements should be conducted for a reasonable period of time in order to gauge the true potential of a site, and are typically conducted over a period of months, or even years.

Model Sea Water Cooling on West Coast and Hybrid Wet-Dry Cooling

When considering the optimal CSP technology for the Springbok location, it was determined that central receiver technology was preferable to parabolic trough, however, it was noted in Section 9.2.6 as well as in the conclusions that additional modelling would be required in order to determine whether a central receiver plant using sea water for wet cooling on the West Coats would in fact be more economical than a dry-cooled central receiver plant. The modelling of the use of sea water for wet cooling purposes was considered beyond the scope of this study and SAM analysis, however, it is recommended that further research be conducted in this area, and attempts made to model the effects on both performance and cost as a result of adopting this technology.

Another cooling technology which was identified in Chapter 4 is that of hybrid wet-dry cooling. The option to include hybrid wet-dry cooling was not presented in the SAM software, and was also not considered to be within the scope of this study. The use of hybrid wet-dry cooling, however, in particular that of water conservation hybrid systems, could be considered advantageous in some scenarios where water reduction is a necessity but efficiency higher than dry cooling is required during the hottest periods of the year. It is thus recommended that attempts should be made to include the analysis of hybrid wet-dry cooling in future studies.

Include the Analysis of Volumetric Central Receiver Systems, Linear Fresnel Technology and Concentrating Photovoltaics

It has already been recommended to consider additional solar technologies at potential CSP sites, and mention was made of the SAM software's ability to model both the performance and cost characteristics of solar PV systems and parabolic dish technology. There are still additional technologies which could be considered, however, such as central receiver technology with volumetric cavity receivers, linear Fresnel technology, compact linear Fresnel reflectors (CLFRs), and concentrating photovoltaics (CPV), some of which are still being commercialised and are considered to be viable alternatives to existing commercial solar technologies. It is therefore recommended to to include the analyses of these additional technologies in future studies, however, in order to accomplish this, more advanced models, additional software packages, and new calculations and procedures may be required.

Perform Environmental Impact Assessments at Promising Identified Sites

In order to reduce the potential for negative environmental impacts, as well as avoid the identification of CSP sites in unsuitable areas, restrictions were imposed in the GIS section of this report in order to exclude potential sites which were either located in unsuitable land class areas, or in any areas not classified as possessing 'least threatened' vegetation. However, as stated in Section 6.3.4, in terms of the Environmental Impact Assessment Regulations of South Africa, EIAs must be conducted before any construction project can begin in a particular area. It is therefore recommended to conduct EIAs at identified sites in order to minimize potentially negative environmental impacts, and as a means to aid the process of selecting an optimal CSP plant location.

Bibliography

Bennett, K. (2010). Informal supervisor meetings and discussion, Energy Research Centre, Department of Mechanical Engineering, University of Cape Town.

Bennett, K. (2011). Informal supervisor meetings and discussion, Energy Research Centre, Department of Mechanical Engineering, University of Cape Town.

Bloomberg (2011). Bloomberg Market Data World Currencies. Retrieved online (16 May 2011) from: `http://www.bloomberg.com/markets/currencies/europe-africa-middle-east/`.

Boyle, G., editor (2004). *Renewable Energy Power for a Sustainable Future. Second Edition.* Oxford University Press, United Kingdom.

Bravo, J. D., Casals, X. G., and Pascua, I. P. (2007). GIS approach to the definition of capacity and generation ceilings of renewable energy technologies. *Energy Policy - Elsevier*, 35:4879–4892.

Brodrick, J. J. L. (2010). A GIS - based assessment of potential sites for large concentrated solar power plants in South Africa. Unpublished Energy Project Report, Energy Research Centre, University of Cape Town.

Broesamle, H., Mannstein, H., Schillings, C., and Trieb, F. (2001). Assessment of solar electricity potentials in North Africa based on satellite data and a Geographic Information System. *Solar Energy – Elsevier*, 70(1):1–12.

Brosseau, D. A., Hlava, P. F., and Kelly, M. J. (2004). Testing thermocline filler materials and molten-salt heat transfer fluids for thermal energy storage systems used in parabolic trough solar power plants. Technical Report SAND2004-3207, Sandia National Laboratories, New Mexico.

Cengel, Y. A. and Boles, M. A. (2006). *Thermodynamics: An Engineering Approach. Fifth edition in SI units.* McGraw-Hill, New York.

City of Johannesburg Council (2011). Amendment of tariff charges for water services and sewerage and sanitation services: 2011/12. COJ : Mayoral Committee 2011-03-17. Available online (6 April 2011) at: http://www.joburg-archive.co.za/2011/tariffs/water_and_sanitation.pdf.

Cohen, G. E., Kearney, D. W., and Kolb, G. J. (1999). Final report on the operation and maintenance improvement program for concentrating solar power plants. Technical report, SAND99-1290.

CSIR (2001a). *South African 30m Land Cover Data, FUNDISADISK*. Council for Scientific and Industrial Research, Pretoria.

CSIR (2001b). *South African DWAF 1:10,000 River and Dam Data, FUNDISADISK*. Council for Scientific and Industrial Research, Pretoria.

CSIR (2001c). *South African Provinces Data, Administrative Section, FUNDISADISK*. Council for Scientific and Industrial Research, Pretoria.

Dersch, J., Geyer, M., Hermann, U., Jones, S., Kelly, B., Kistner, R., Ortmanns, W., Pitz-Paal, R., and Price, H. (2002). Solar Trough Integration Into Combined Cycle Systems. Proceedings of Solar 2002: Sunrise on the Reliable Energy Economy. Reno, Nevada.

DLR (2003). Concrete Storage: Update on the European concrete TES program. Presentation by DLR – German Aerospace Center, Institute of Technical Thermodynamics.

DME (2003). White Paper on Renewable Energy. Technical report, South African Department of Minerals and Energy, Pretoria.

DOE, U.S. (2010). Concentrating solar power commercial application study: Reducing water consumption of concentrating solar power electricity generation. Report to Congress. Technical report, U.S. Department of Energy. Retrieved online (17 July 2010) from: http://www.nrel.gov/csp/troughnet/pubs_power_plant.html#cooling.

Duffie, J. A. and Beckman, W. A. (1974). *Solar Energy Thermal Processes*. John Wiley & Sons, Inc., New York.

Edkins, M., Winkler, H., and Marquard, A. (2009). Large-scale rollout of concentrating solar power in South Africa. Technical report, Energy Research Centre, University of Cape Town.

ENPAT (1998). *South African Major Roads, Secondary Roads, and Towns*. Department of Environmental Affairs and Tourism, Pretoria.

ENPAT (2000). *South African River Data*. Department of Environmental Affairs and Tourism, Pretoria.

EPRI (2010). Power Generation Technology Data for Integrated Resource Plan of South Africa. Technical report, Electric Power Research Institute, Palo Alto, CA.

EPRI and California Energy Commission (2002). Comparison of Alternate Cooling Technologies for California Power Plants: Economic, Environmental, and Other Tradeoffs. Technical report, PIER / EPRI, California. Available online (17 February 2011) at: `http://www.nrel.gov/csp/troughnet/publications.html`.

Eskom (2006). *Environmental Impact Assessment Process – Proposed Concentrating Solar Power (CSP) Plant and Associated Infrastructure in the Northern Cape Area*. Eskom. Retrieved online (25 June 2010) from: `http://www.eskom.co.za/content/BID_Final_English230306.pdf`.

Eskom (2010). *Eskom Power Stations Poster*. Eskom General Communications Department, Pretoria. Retrieved via Private Communications with Eskom Visitors Centre (June 2010), Cape Town.

ESRI (2010a). ArcGIS Documentation on the Solar Area Radiation Toolbox. Available online (11 December 2010) at: `http://webhelp.esri.com/arcgisdesktop/9.2/index.cfm?TopicName=Area_Solar_Radiation`.

ESRI (2010b). The Guide to Geographic Information Systems: What is GIS? Retrieved online (19 July 2010) from: `http://www.gis.com/content/what-gis`.

ESRI Online Forums (2010). ArcGIS Desktop Discussion Forums – Solar Radiation. Retrieved online (19 December 2010) from: `http://forums.esri.com/thread.asp?t=228857&f=995&c=93`.

European Commission (2004). European Research on Concentrated Solar Thermal Energy. Technical Report EUR 20898, European Commission, Brussels.

Fahy, G. (2009). The Analysis of South Africa's Potential to Supply Linear Fresnel Thermal Collector Components. Unpublished Energy Project Report, Energy Research Centre, University of Cape Town.

Fluri, T. P. (2009). The potential of concentrating solar power in South Africa. *Energy Policy - Elsevier*, 37:5075–5080.

Forristall, R. (2003). Heat Transfer Analysis and Modeling of a Parabolic Trough Solar Receiver Implemented in Engineering Equation Solver. Technical Report NREL/TP-550-34169, National Renewable Energy Laboratory. Retrieved online (26 May 2011) from: `http://www.nrel.gov/csp/troughnet/pdfs/34169.pdf`.

Gilman, P. (2010). Solar Advisor Model training course at the University of Stellenbosch, Cape Town, South Africa. Attended in June 2010.

Gilman, P. (2011). Private communication with Paul Gilman regarding NREL SAM.

Herrmann, U., Geyer, M., and Kearney, D. (2002). Overview on Thermal Storage Systems. Presentation by FLABEG Solar International GmbH at the Workshop on Thermal Storage for Trough Power Systems.

IEA (2007). SolarPACES Annual Report 2007. Technical report, Solar Power and Chemical Energy Systems – SolarPACES.

IEA (2008). Energy Technology Perspectives 2008: Scenarios & Strategies to 2050. Technical report, International Energy Agency, Paris.

IEA (2010a). Energy Technology Perspectives 2010: Scenarios & Strategies to 2050. Technical report, International Energy Agency, Paris.

IEA (2010b). *Technology Road Map: Concentrating Solar Power*. International Energy Agency and the OECD, Paris.

Kelly, B. (2006). Nexant Parabolic Trough Solar Power Plant Systems Analysis. Tasks 1-3: January 20, 2005 – December 31, 2005. Technical report, Nexant Inc. Prepared under subcontract for the National Renewable Energy Laboratory. Available online (17 February 2011) at: `http://www.nrel.gov/csp/troughnet/publications.html`.

Kelly, B. and Kearney, D. (2006). Parabolic Trough Solar System Piping Model. Technical Report NREL/SR-550-40165, National Renewable Energy Laboratory. Retrieved online (26 May 2011) from: `http://www.nrel.gov/csp/troughnet/pdfs/40165.pdf`.

Kistler, B. (1986). A User's Manual for DELSOL3: A Computer Code for Calculating the Optical Performance and Optimal System Design for Solar Thermal Central Receiver Plants. Technical Report SAND86-8018, Sandia National Laboratories. Retrieved online (7 June 2010) from: `http://prod.sandia.gov/techlib/access-control.cgi/1986/868018.pdf`.

Lindenberg, N. and Slingsby, T. (2010). Private communication with Nicholas Lindenberg and Thomas Slingsby, GIS Research Laboratory, University of Cape Town.

Meteotest (2011). Meteonorm Overview. Available online (29 April 2011) at: `http://www.meteonorm.com/pages/en/meteonorm.php`.

Meyer, R. (2010). Solar Advisor Model training course at the University of Stellenbosch, Cape Town, South Africa. Attended in June 2010.

Mills, D. (2004). Advances in solar thermal electricity technology. *Solar Energy – Elsevier*, 76:19–31.

Montes, M., Abánades, A., Martínez-Val, J., and Valdés, M. (2009). Solar multiple optimization for a solar-only thermal power plant, using oil as heat transfer fluid in the parabolic trough collectors. *Solar Energy – Elsevier*, 83:2165–2176.

Morse, W. (2009). An analysis into the geophysical and industrial requirements, if South Africa were to evolve its electricity supply to a large emphasis on Concentrated Solar Power. Master's thesis, Energy Research Centre, University of Cape Town.

Mucina, L. and Rutherford, M. C., editors (2006). *The Vegetation of South Africa, Lesotho and Swaziland*. Strelitzia 19, South African National Biodiversity Institute, Pretoria. (Data retrieved in the form of Shapefiles from Electronic Resource CD).

Mukheibir, P. (2007). Qualitative assessment of municipal water resource management strategies under climate impacts: the case of the Northern Cape, South Africa. *Water SA*, 33(4).

Müller-Steinhagen, H. (2011). *Solar Thermal Power Plants - On the Way to Commercial Market Introduction*. DLR, Stuttgart.

NERSA (2009). Renewable Energy Feed In Tariff Guidelines. Technical report, National Energy Regulator of South Africa. Reasons for Decision.

NERSA (2010). Renewable Energy Feed In Tariffs Phase II. Technical report, National Energy Regulator of South Africa. Reasons for Decision.

Novatec Solar (2011). Novatec Solar NOVA-1. Retrieved online (2 June 2011) from: `http://www.novatecsolar.com/20-1-Nova-1.html`.

NREL (2011a). Parabolic Trough Thermal Energy Storage Technology. Retrieved online (17 May 2011) from: `http://www.nrel.gov/csp/troughnet/thermal_energy_storage.html`.

NREL (2011b). Solar Advisor Model Home and Overview. National Renewable Energy Laboratory. Retrieved online (20 May 2011) from: `https://www.nrel.gov/analysis/sam/`.

Pegels, A. (2009). Prospects for Renewable Energy in South Africa: Mobilizing the Private Sector. Discussion Paper. German Development Institute - d.i.e, Bonn, Germany.

Pilkington Solar International GmbH (2000). Survey of Thermal Storage for Parabolic Trough Power Plants. Technical Report NREL/SR-550-27925, National Renewable Energy Laboratory. Prepared for NREL by Pilkington Solar International GmbH, Cologne, Germany.

REN21 (2008). Renewables 2007 Global Status Report. Technical report, Renewable Energy Policy Network for the 21st Century, Paris: REN21 Secretariat and Washington, DC: Worldwatch Institute.

Romero, M., Buck, R., and Pacheco, J. E. (2002). An Update on Solar Central Receiver Systems, Projects, and Technologies. *ASME Journal of Solar Energy Engineering*, 124:98–108.

SAM (2010). Solar Advisor Model 2010 User Guide and Help Documentation. National Renewable Energy Laboratory.

SAM (2011). Screen Captures from Solar Advisor Model 2010 Software. National Renewable Energy Laboratory.

Sargent & Lundy (2003). Assessment of Parabolic Trough and Power Tower Solar Technology Cost and Performance Forecasts. Technical Report NREL/SR-550-34440, National Renewable Energy Laboratory. Prepared for NREL by Sargent & Lundy LLC Consulting Group, Chicago, Illinois.

SARS (2011). South African Revenue Service S.A. Tax System: What Kinds of Tax Do We Pay. Available online (18 May 2011) at: `http://www.sars.gov.za/home.asp?pid=289`.

Solar Millennium AG (2008). The parabolic trough power plants Andasol 1 to 3. Technical report, Solar Millenium AG, Germany.

Solar Millennium AG (2011). Parabolic Trough Plants – Operation. Retrieved online (18 July 2011) from: `http://www.solarmillennium.de/english/technology/parabolic-trough-power-plants/operation/index.html`.

SolarPACES (2011). PS10. Retrieved online (18 July 2011) from: `http://www.solarpaces.org/Tasks/Task1/ps10.htm`.

SRTM (2006). *Shuttle Radar Topography Mission 90m DEM, NASA JPL*. United States Geographic Service (USGS). Available online (7 July 2010) at: `http://www2.jpl.nasa.gov/srtm`.

StatsSA (2011). Consumer Price Index: Index numbers and year-on-year rates. Retrieved online (18 May 2011) from: `http://www.statssa.gov.za/keyindicators/CPI/CPIHistory.pdf`.

Stine, W. B. and Geyer, M. (2001). *Power From The Sun*. Adapted from the original *Solar Energy Systems Design* published by John Wiley and Sons, Inc. 1986. Retrieved Online (20 May 2010) from: `http://www.powerfromthesun.net/book.html`.

Stoddard, L., Abiecunas, J., and O'Connell, R. (2006). Economic, Energy, and Environmental Benefits of Concentrating Solar Power in California. Technical Report NREL/SR-550-39291, Prepared for NREL by Black & Veatch.

SWERA (2010). *Solar: monthly and annual average direct normal (DNI), global horizontal (GHI), latitude tilt, and diffuse data and GIS data at 40km resolution for Africa from NREL, 2006*. Solar and Wind Energy Resource Assessment. Retrieved online (28 June 2010) from: `http://swera.unep.net`.

Torcellini, P., Long, N., and Judkoff, R. (2003). Consumptive Water Use for U.S. Power Production. Technical report, NREL, Colorado. Available online (17 July 2010) at: `http://www.nrel.gov/csp/troughnet/publications.html`.

Torresol Energy (2011). Gemasolar Plant. Retrieved online (27 June 2011) from: `http://www.torresolenergy.com/TORRESOL/gemasolar-plant/en`.

TRNSYS (2011). TRNSYS Official Website - Overview of TRYNSYS. University of Wisconsin, Madison. Available Online (20 May 2011) at: `http://sel.me.wisc.edu/trnsys/features/features.html`.

Turchi, C. (2010). Parabolic Trough Reference Plant for Cost Modeling with the Solar Advisor Model (SAM). Technical Report NREL/TP-550-47605, NREL.

Turchi, C., Mehos, M., Ho, C. K., and Kolb, G. J. (2010). Current and Future Costs for Parabolic Trough and Power Tower Systems in the US Market. Presented at SolarPACES 2010. Conference Paper: NREL/CP-5500-49303.

Van der Merwe, P. (2011). Private Communication with Paul van der Merve from the South African Department of Water Affairs, Pretoria.

Wagner, M. J. (2008). Simulation and Predictive Performance Modeling of Utility-Scale Central Receiver System Power Plants. Master's thesis, University of Wisconsin-Madison. Retrieved online (30 November 2010) from: `http://sel.me.wisc.edu/theses/wagner08.zip`.

Winkler, H., editor (2007). Long Term Mitigation Scenarios. Technical report, Energy Research Centre, prepared for the Department of Environment Affairs and Tourism, South Africa.

Appendices

Appendix A: GIS Methodology

The GIS analysis undertaken in this project can be classified according to three sections, namely; the importing and processing of the necessary data files, the analysis of the data by means of the computer software package ArcGIS, and the generation of maps and calculation results in both ArcGIS and spreadsheet software. The procedures adopted and followed for each of the aforementioned sections will now be described in detail under their respective headings.

1. Import and Process Gathered Data

Solar Data

In a Spreadsheet Program:

1. Open the `csr_africa_data.xls` file.
2. Export the DNI tab into a Comma Separated Value (CSV) file.

In ArcGIS:

1. Load the `csr_afr_poly.shp` Shapefile.
2. Open the South Africa country and provincial borders Shapefile with a UTM 34S projection.
3. Select the `csr_afrpoly.shp` Shapefile grid with a 1 degree buffer using SA provinces to reduce the number of data points.
4. Open the CSV DNI file.
5. Merge the attribute tables of the CSV and Shapefile according to column PSECELLID.

6. Open attribute table of new layer, and adopt a graduated custom scale for CANN (annual values of DNI).
7. A map of South Africa with the solar data DNI for an average year was then created.

Land Slope Data

1. Load the 90m DEM from SRTM which contains the land slope for the country.
2. Create an additional analysis layer of the slope classifying it according to percentage slope.
3. Create a further boolean layer (true or false) with a slope of 1%.

Vegetation Data

1. Load vegetation map of SA retrieved from Mucina and Rutherford (2006).
2. Create a layer from this data according to the attribute of 'least threatened'.
3. Create a dissolve layer for 'least threatened' to reduce polygons and file size.

Rivers and Dams Data and Buffer

1. Import large water bodies and rivers data set.
2. Create a new layer with a radial buffer of 20 km around large rivers and dams.

West Coast Data and Buffer

1. Create a new layer from the SA outline polygon and trim the West Coast from SA-Namibia border to Cape Town harbour.
2. Create a new buffer layer with a 20 km radius from this newly created West Coast line.
3. Merge the rivers, dams and West Coast buffers into one layer called *water buffers*.

Eskom National Grid Data and Buffer

For the national grid the following procedure was followed:

1. Import the SA National Grid jpeg picture file from Eskom (2010).
2. Open the jpeg as a new layer.
3. Make use of the georeferencing procedure to accurately project the jpeg image over the existing SA map.
4. Create a new layer with UTM projection and trace the Eskom national grid from the georeferenced jpeg.
5. Remove the original Eskom 2008 jpeg, leaving only the digitised national grid layer behind.
6. Create a new 20 km radial buffer layer from the Eskom national grid.

Land Cover Data

1. A land cover grid was created in order to exclude areas not suitable for construction. The data imported comprised the *South African 30m Land Cover Data* published by the CSIR (2001a).

   Areas excluded comprised:

   - Water-bodies
   - Wetlands
   - Forests
   - Plantations
   - Urban Areas

2. The various attributes were merged into one layer of excluded areas.

2. Data Analysis

Analysis Cases and Site Identification

1. Convert all vector data to boolean rasters, in order to be able to use the *raster calculator* feature in ArcGIS. This is necessary because the raster calculator functions by analysing each cell of the raster in each layer according to given criteria, but vector data by nature does not possess data comprising of gridded cells (Lindenberg and Slingsby, 2010).

2. Apply an analysis mask of the Eskom power lines, in order to reduce the number of calculations and exclude the rest of the country from unnecessary analysis.

3. Initiate the raster calculator with the following chosen analysis criteria that a potential site must possess:

Case 1: DNI > 6.0 kWh/m^2/d, Proximity to Large Water Bodies

- DNI greater than 6.0 kW/m^2 per day
- Less than 20 km from large water bodies
- Less than 20 km from transmission lines
- Less than 1% land slope
- Region classified as 'least threatened' vegetation
- Region not excluded due to land class restrictions of Section 6.3.3
- Site area greater than 2 km^2

Case 2: DNI > 6.5 kWh/m^2/d, Proximity to Large Water Bodies

- DNI greater than 6.5 kW/m^2 per day
- Less than 20 km from large water bodies
- Less than 20 from transmission lines
- Less than 1% land slope
- Region classified as 'least threatened' vegetation
- Region not excluded due to land class restrictions of Section 6.3.3
- Site area greater than 2 km^2

Case 3: DNI > 7.0 kWh/m^2/d, No Proximity to Large Water Bodies

- DNI greater than 7.0 kW/m^2 per day
- Less than 20 km from transmission lines
- Less than 1% land slope
- Region classified as 'least threatened' vegetation
- Region not excluded due to land class restrictions of Section 6.3.3
- Site area greater than 2 km^2

Case 4: DNI > 6.5 kWh/m^2/d, Proximity to Large Water Bodies, No Grid Proximity

- DNI greater than 6.5 kW/m^2 per day
- Less than 20 km from large water bodies
- Less than 1% land slope
- Region classified as 'least threatened' vegetation
- Region not excluded due to land class restrictions of Section 6.3.3
- Site area greater than 2 km^2

Case 5: DNI > 7.0 kWh/m^2/d, No Proximity to Large Water Bodies, No Grid Proximity

- DNI greater than 7.0 kW/m^2 per day
- Less than 1% land slope
- Region classified as 'least threatened' vegetation
- Region not excluded due to land class restrictions of Section 6.3.3
- Site area greater than 2 km^2

4. Convert the identified potential sites for each of the aforementioned cases back into vector Shapefiles.

5. Perform an intersect with the original solar data from the merged `csr_afrpoly.shp` and `DNI.csv` files and the identified sites, in order to re-populate the identified sites attribute tables with the solar DNI values.

6. Add an additional 'Area' field column to the attribute tables and use the *Calculate Geometry* tool to calculate the area of each site. The intersect used in the previous step, however, causes sites that fall across the solar DNI grid boundaries to be split into separate sites. It is therefore necessary to use the *Summarize* tool to create a new database file from the attribute tables to re–merge sites that have been split, and thus calculate the correct total area of each site. This process is mentioned in Section 6.5.3 and illustrated in Figure 6.12.

Solar Shading and DNI Calculation Algorithm

Unsuccessful Method 1

1. Open the *Area Solar Radiation* tool from the *Solar Radiation* toolbox within *Spacial Analyst*.
2. Import the 90m South African DEM and calculate the appropriate latitude.
3. Set the algorithm to run for a period of 365 days for the year 2006.
4. Run the solar area shading algorithm for the entire country with specified output for: *global radiation*, *direct radiation*, and *daily duration of radiation*.

Unsuccessful Method 2

1. Split the South Africa data layer into $1^\circ \times 1^\circ$ geographic grid cells.
2. Manually select only those $1^\circ \times 1^\circ$ geographic grid cells which contain identified potential CSP sites.
3. Buffer each grid cell with 1 km radial buffer as a means to reduce edge effects in the calculation.
4. Convert DEM to geographic co-ordinates and extract the DEM by mask of the selected buffered grid $1^\circ \times 1^\circ$ cells.
5. Re-run the solar area shading model on each of the $1^\circ \times 1^\circ$ buffered cells by making use of the batch scheduling process, with specified output for: *global radiation*, *direct radiation*, and *daily duration of radiation*. Set the algorithm to run for a period of 365 days for the year 2006. The batch process will automatically calculated the latitude of each of the $1^\circ \times 1^\circ$ grid cells. The algorithm took a number of days to complete.

6. Clip the 1 km radial buffer by means of *extract by mask* for both the DNI calculation and duration shading models, in order to remove the edge effects from the results.

7. Use the mosaic tool to attempt to re-merge the selected $1^\circ \times 1^\circ$ grid cells into a single uniform layer.

Final Successful Method

1. Identify and select a few of the larger CSP sites with higher DNI values by ranking of attributes in their relevant databases.

2. Create a 50 km radial euclidean distance buffer around the selected CSP sites.

3. Extract the DEM by mask of the buffered sites and shrink the extent to eliminate the zero-data values.

4. Re-run the solar area shading model on each of radial buffers by making use of the batch scheduling process, with specified output for: *global radiation*, *direct radiation*, and *daily duration of radiation*. Set the algorithm to run for the period of 365 days for the year 2006.

5. Within *ArcCatalogue*, create new *geo-database*.

6. Create a new *raster catalogue*.

7. Import the results dataset from the algorithm into the geo-database within Arc-Catalogue.

8. Change and specify the colour-ramp to obtain a suitable legend.

3. Calculations and Maps

Although the quantification of the potential sites identified for Case 1, Case 2, Case 3, Case 4 and Case 5 is described in detail in Section 6.5, the analysis procedure adopted for the data will be described briefly below.

1. All the associated database files and attribute tables for each of the identified sites for each of the above cases were exported into Excel® spreadsheet files in order to allow for calculations and further analysis to be performed.

2. For each of the aforementioned cases, the following calculations were performed in a spreadsheet program:

    - Calculate total area available for each case
    - Calculate the total energy available for each analysis case by multiplying each site area by its corresponding DNI value and then summing the resulting totals
    - Calculate the power generation potential for each analysis case by dividing the total available area by the land use value of 28 km^2 per GW
    - Calculate the net energy generation potential for parabolic trough plants by multiplying the power generation potential by the 8760 hours in a year and then by the 38.8% capacity factor
    - Calculate the net energy generation potential for central receiver plants by multiplying the power generation potential by the 8760 hours in a year and then by the 60% capacity factor

3. Finally all the maps in this project, from Figure 6.1 onwards, were created in ArcGIS and exported to a jpeg format for inclusion in this report.

Appendix B: Comparison Database of Parabolic Trough Costs

PARABOLIC TROUGH COST DATA

Trough System Cost

	SAM (2010) Default Values		EPRI (2010)				Turchi et al. (2010)	
	6 hrs - wet	6 hrs - dry	0 hrs - wet	3 hrs - wet	6 hrs - wet	9 hrs - wet	0 hrs - wet	6 hrs - wet
Direct Capital Costs								
Site improvements	20 $/m2							
Solar field	350 $/m2						295 $/m2	
HTF system	50 $/m2						90 $/m	
Storage	70 $/kWht							
Fossil backup	0 $/kWe							
Power plant	920 $/kWe	1140 $/kWe					940 $/kWe gross	
Contingency	10%							
TOTAL Direct Cost	$ 640,556,125.20	$ 764,612,940.45						
Indirect Capital Costs								
Engineer, Procure, Construct % of Direct cost	15%							
Project, Land, Management % of Direct cost	3.5%							
Sales tax applies to % of direct cost	80%							
TOTAL Indirect Cost	$ 158,217,362.92	$ 188,859,396.29						
Total Installed Costs								
Total Installed Costs	$ 798,773,488.12	$ 953,472,336.74						
Est. Total installed cost per net capacity	7,987.66 $/kW	9,080.60 $/kW						
Operation and Maintenance Costs								
Fixed annual cost	0 $/yr							
Fixed cost by capacity	80 $/kW. yr		424 R/kW.yr	513 R/kW.yr	562 R/kW.yr	635 R/kW.yr	70 $/kW. Yr	
Variable cost by generation	3 $/MWh							
Fossil fuel cost	0 $/MMBTU							

	Stoddard et al. (2006)		Sargent & Lundy (2003)	Kelly (2006)		
	6 hrs - wet (2005 $)	6 hrs - wet (2010 $)	SEGS VI no TES	Small no TES	Med no TES	Large no TES
Direct Capital Costs						
Site improvements	$ 2,455,000	$ 3,607,200				
Solar field	$ 230,865,000	$ 339,216,427	250 $/m2			
HTF system	$ 10,009,000	$ 14,706,505		23.09 $/m	25.09 $/m	26.42 $/m
Storage	$ 57,957,000	$ 85,157,847				
Fossil backup						
Power plant	$ 38,754,000	$ 56,942,340	527 $/ kWe			
Contingency						
TOTAL Direct Cost	$ 393,280,000	$ 577,857,346				
Indirect Capital Costs						
Engineer, Procure, Construct % of Direct cost						
Project, Land, Management % of Direct cost						
Sales tax applies to % of direct cost						
TOTAL Indirect Cost	$ 101,106,000	$ 148,557,885				
Total Installed Costs						
Total Installed Costs	$ 494,386,000	$ 726,415,231		$ 267,747,000	$ 465,148,000	$ 600,039,000
Est. Total installed cost per net capacity			3,008 $/kW	3,314 $/kW	3,074 $/kW	2,978 $/kW
Operation and Maintenance Costs						
Fixed annual cost						
Fixed cost by capacity						
Variable cost by generation				24 $/MWh	18 $/MWh	16 $/MWh
Fossil fuel cost						

Appendix C: Comparison Database of Central Receiver Costs

CENTRAL RECEIVER COST DATA

Tower System Cost

	SAM (2010) Default Values			EPRI (2010)		
	6 hrs - wet	6 hrs - dry	No Storage - wet	3 hrs - wet	6 hrs - wet	9 hrs - wet
Direct Capital Costs						
Site improvements	20 $/m2					
Heliostat field	201 $/m2					
Balance of plant	345 $/kWe					
Power Block	575 $/kWe	795 $/kWe	575 $/kWe			
Storage	30 $/kWht					
Fixed solar field cost	0 $					
Fixed tower cost	$ 901,500.00					
Tower cost scaling component	0.01298					
Receiver reference cost	$ 59,148,900.00					
Receiver reference area	1110 m2					
Receiver scaling component	0.7					
Contingency	10%					
TOTAL Direct Cost	$ 459,524,490.89	$ 501,901,154.72	$ 318,820,456.84			
Indirect Capital Costs						
Engineer, Procure, Construct % of Direct cost	15%					
Project, Land, Management % of Direct cost	3.5%	3.5%	3.5%			
Sales tax applies to % of direct cost	80%					
TOTAL Indirect Cost	$ 113,502,549.25	$ 123,969,585.22	$ 78,748,652.84			
Total Installed Costs						
Total Installed Costs	$ 573,027,040.13	$ 625,870,739.94	$ 397,569,109.68			
Est. Total installed cost per net capacity	5,730.21 $/kW	6,258.64 $/kW	3,975.65 $/kW			
Operation and Maintenance Costs						
Fixed annual cost	0 $/yr					
Fixed cost by capacity	80 $/kW. yr			489 R/kW.yr	546 R/kW.yr	603 R/kW.yr
Variable cost by generation	3 $/MWh					
Fossil fuel cost	0 $/MMBTU					

	Romero et al. (2002)				Sargent and Lundy (2003)
	Solar Two	Solar Tres	PS10 (2001 $)	PS10 (2010 $)	Solar Two
Direct Capital Costs					
Site improvements					
Heliostat field			$ 11,717,700	$ 23,423,737	
Balance of plant					
Power Block			$ 8,718,700	$ 17,428,722	
Storage					
Fixed solar field cost					
Fixed tower cost			$ 1,707,200	$ 3,412,701	
Tower cost scaling component					
Receiver reference cost					$ 9,100,000
Receiver reference area					100 m2
Receiver scaling component					
Contingency					
TOTAL Direct Cost					
Indirect Capital Costs					
Engineer, Procure, Construct % of Direct cost					
Project, Land, Management % of Direct cost					
Sales tax applies to % of direct cost					
TOTAL Indirect Cost					
Total Installed Costs					
Total Installed Costs			$ 27,984,800	$ 55,941,745	
Est. Total installed cost per net capacity			2,798.48 $/kW (2001)	5,594.17 $/kW	
Operation and Maintenance Costs					
Fixed annual cost					
Fixed cost by capacity					0.165 $/kWh
Variable cost by generation					
Fossil fuel cost					

Appendix D: Comparison Database of Parabolic Trough Design Data

PARABOLIC TROUGH DESIGN DATA

	SAM (2010) Default		EPRI (2010)	Turchi et al. (2010)		Dersch et al. (2002)		Sargent and Lundy (2003)	Kelly (2006)		
	6 hrs - wet	6 hrs - dry	0 hrs to 9hrs - wet	0 hrs - wet	6 hrs - wet	SEGS	SEGS with TES	SEGS VI no TES	Small no TES	Med no TES	Large no TES
Annual Performance											
System Degradation	0%										
Availability	94%		95%	94%				98%			
Solar Field											
Solar Field Parameters											
Solar multiple	2			1.3	2				1.45		
Field aperture	861590 m2							188,000 m2	541,786 m2	1,015,848 m2	1,354,464 m2
Row spacing	15 m										
Stow angle	170 deg										
Deploy angle	10 deg										
Solar field	H Layout										
Header pipe roughness	4.57e-005 m										
HTF pump efficiency	0.85										
Freeze protection temp	150 °C										
Irradiation at design	950 W/m2										
Allow partial defocusing	No										
Heat Transfer Fluid											
Field HTF fluid	VP-1							VP-1			
Design loop inlet temp	293 °C										
Design outlet inlet temp	391 °C							391 °C			
Min single loop flow rate	1 kg/s										
Max single loop flow rate	12 kg/s										
Min field flow velocity	0.356106 m/s										
Max field flow velocity	4.9655 m/s										
Header design min flow velocity	2 m/s										
Header design max flow velocity	3 m/s										
Initial field temp	100 °C										
Design Point											
Single loop aperture	3762.4 m2										
Loop optical efficiency	0.744601							0.533			
Total loop conversion efficiency	0.716894										
Total required aperture, SM=1	427969 m2	500269 m2									
Required number of loops, SM=1	113.749	132.965									
Actual number of loops	227	266							192	360	480
Actual aperture	854065 m2	1000800 m2						188,000 m2			
Actual solar multiple	2										
Field thermal output	582.936 MWt	681.416 MWt							234.7 MWt	440.0 MWt	586.7 MWt
Collector Orientation											
Collector tilt	0 deg										
Collector azimuth	0 deg										
Mirror Washing											
Water usage per mirror wash	0.6 L/m2							22 l/m2			
Washing frequency	4 days										

Collectors (SCAs)

	SAM (2010) Default		EPRI (2010)	Turchi et al. (2010)		Dersch et al. (2002)		Sargent and Lundy (2003)	Kelly (2006)		
	6 hrs - wet	6 hrs - dry	0 hrs to 9hrs - wet	0 hrs - wet	6 hrs - wet	SEGS	SEGS with TES	SEGS VI no TES	Small no TES	Med no TES	Large no TES
Configuration	Solargenix SGX-1										
Collector Geometry											
Reflective aperture area	470.3 m2							235 m2			
Aperture width total structure	5 m										
Length of collector assembly	100 m							50 m			
Number of modules per assembly	12							12			
Ave surface-to-focus path length	1.8 m										
Piping distance between assemblies	1 m										
Optical Parameters											
Incidence angle modifier coeff 1	1										
Incidence angle modifier coeff 2	0.0506										
Incidence angle modifier coeff 3	-0.1763										
Tracking error	0.994							0.994			
Geometry effects	0.98							0.98			
Mirror reflectance	0.935							0.935			
Dirt on mirror	0.95			0.935				0.931			
General optical error	0.99										
Optical Calculations											
Length of single module	8.33333 m										
Incidence angle modifier	1.00228										
End loss at design	0.980058										
Optical efficiency at design	0.856609							0.533			

Receivers (HCEs)

	SAM (2010) Default		EPRI (2010)	Turchi et al. (2010)		Dersch et al. (2002)		Sargent and Lundy (2003)	Kelly (2006)		
	6 hrs - wet	6 hrs - dry	0 hrs to 9hrs - wet	0 hrs - wet	6 hrs - wet	SEGS	SEGS with TES	SEGS VI no TES	Small no TES	Med no TES	Large no TES
Configuration	Schott PTR70 2008							Luz			
Receiver Geometry											
Absorber tube inner diameter	0.066 m										
Absorber tube outer diameter	0.07 m										
Glass envelope inner diameter	0.115 m										
Glass envelope outer diameter	0.12 m										
Absorber flow plug diameter	0 m										
Internal surface roughness	4.5e-005 m										
Absorber flow pattern	Tube flow										
Absorber material type	304L										
Parameters and Variations											
Variation 1											
Variant weighting fraction	0.985							1			
Absorber absorptance	0.96							0.92			
Absorber emittance	Table							0.18 at 400 °C			
Envelope absorbtance	0.02										
Envelope emittance	0.86										
Envelope transmittance	0.963							0.92			
Broken glass	No										
Annulus gas type	Hydrogen										
Annulus pressure	0.0001 tor										
Estimated ave heat loss	150 W/m										
Bellows shadowing	0.96										
Dirt on receiver	0.98										
Variation 2											
Variant weighting fraction	0.01										
Absorber absorptance	0.96										
Absorber emittance	0.65										
Envelope absorbtance	0.02										
Envelope emittance	0.86										
Envelope transmittance	0.963										
Broken glass	No										
Annulus gas type	Air										
Annulus pressure	750 torr										
Estimated ave heat loss	1100 W/m										
Bellows shadowing	0.96										
Dirt on receiver	0.98										
Variation 3											
Variant weighting fraction	0.005										
Absorber absorptance	0.8										
Absorber emittance	0.65										
Envelope absorbtance	0										
Envelope emittance	1										
Envelope transmittance	1										
Broken glass	Yes										
Annulus gas type	Air										
Annulus pressure	750 torr										
Estimated ave heat loss	1500 W/m										
Bellows shadowing	0.96										
Dirt on receiver	1										
Total Weighted Losses											
Heat loss at design	166.25 W/m										
Optical derate	0.869242										

Power Cycle

	SAM (2010) Default		EPRI (2010)	Turchi et al. (2010)		Dersch et al. (2002)		Sargent and Lundy (2003)	Kelly (2006)		
	6 hrs - wet	6 hrs - dry	0 hrs to 9hrs - wet	0 hrs - wet	6 hrs - wet	SEGS	SEGS with TES	SEGS VI no TES	Small no TES	Med no TES	Large no TES
Plant Capacity											
Design gross output	110 MWe	115.5 MWe									
Estimated gross to net conversion factor	0.9091										
Estimated net output at design (nameplate)	100.001 MWe	105.001 MWe	125 MWe	100 MWe		50 MWe	50 MWe	30 MWe	88 MW	165 MW	220 MW
Power Block Design Point											
Rated cycle conversion efficiency	0.3774	0.339		0.377				0.351			
Design inlet temp	391 °C			391							
Design outlet temp	293 °C										
Boiler operating pressure	100 bar										
Fossil backup boiler LHV efficiency	0.9										
Heat capacity of balance plant	5 kWht/K. MWhe										
Steam cycle blowdown fraction	0.013	0.016									
Plant control											
Fraction of thermal power needed for standby	0.2										
Power block startup time	0.5 hr										
Fraction of thermal power needed for startup	0.2										
Minimum required startup temp	300 °C										
Max turbine over design operation	1.15										
Min turbine operation	0.25										
Cooling System											
Condenser type	Evaporative	Air-cooled				Evaporative	Evaporative	Evaporative	Evaporative	Evaporative	Evaporative
Ambient temp at design	20 °C	33 °C									
Ref. condenser water dT	10 °C	10 °C									
Approach temp	5 °C	5 °C									
ITD at design point	16 °C	16 °C									
Condenser pressure ratio	1.0028	1.0028									

Thermal Storage

	SAM (2010) Default		EPRI (2010)	Turchi et al. (2010)		Dersch et al. (2002)		Sargent and Lundy (2003)	Kelly (2006)		
	6 hrs - wet	6 hrs - dry	0 hrs to 9hrs - wet	0 hrs - wet	6 hrs - wet	SEGS	SEGS with TES	SEGS VI no TES	Small no TES	Med no TES	Large no TES
Storage System											
Full load hours of Thermal Energy Storage	6 hr										
Storage volume	26032 m3	30429.8 m3									
TES thermal capacity	1748.81 MWt	2044.25 MWt				0 MWt	839 MWt				
Parallel tank pairs	1										
Tank height	20 m										
Tank fluid min height	1 m										
Tank diameter	40.7093 m	44.0139 m									
Min fluid volume	1301.6 m3	1521.49 m3									
Tank loss coefficient	0.4 W/m2. K										
Estimated heat loss	0.497096 MWt	0.552161 MWt									
Tank heater set point	250 °C										
Aux heater outlet set temp	391										
Tank heater capacity	25 MWt										
Tank heater efficiency	0.98										
Hot side HX approach temp	5 °C										
Hot side HX approach temp	7 °C										
Heat exchanger derate	0.877551										
Initial TES fluid temp	300 °C										
Storage HTF fluid	Solar Salt										
Fluid temp	342 °C										
TES fluid density	1872.49 kg/m3										
TES specific heat	1.50182 kJ/kg. K										

Parasitics

Piping thermal loss coefficient	0.45 W/m2. K										
Tracking power	125 W/sca										
Req pumping power for HTF through power block	0.55 kJ/kg										
Req pumping power for HTF through storage	0.15 kJ/kg										
Fraction of rated gross power consumed at all times	0.0055										
Balance of plant parasitics	0.02467 MWe/MWcap										
Aux heater, boiler parasitics	0.02273 MWe/MWcap										
Design Point Totals											
Tracking TOTAL	227000 W	266000 W									
TOTAL fixed parasitic load	0.605 MWe	0.635 MWe				3.77 MWe	6.54 MWe		0.443 MWe	0.835 MWe	1.115 MWe
BOP	2.7137 MWe	2.8494 MWe							2.183 MWe	4.053 MWe	5.375 MWe
Aux	2.5003 MWe	2.6253 MWe									

Appendix E: Comparison Database of Central Receiver Design Data

CENTRAL RECEIVER DESIGN DATA

	SAM (2010) Default Values			EPRI (2010)				Romero et al. (2002)			Sargent and Lundy (2003)
	6 hrs - wet	6 hrs - dry	No Storage - wet	0 hrs - wet	3 hrs - wet	6 hrs - wet	9 hrs - wet	Solar Two	Solar Tres	PS10	Solar Two
Annual Performance											
System Degradation	0%										
Availability	94%			92%							
Heliostat Field											
Heliostat Field											
Heliostat width	12.2 m									9.67 m	
Heliostat height	12.2 m									9.57 m	
Ratio of reflective area to profile	0.97										
Use round heliostats	No										
Heliostat area	144.375 m2									91 m2	95 m2
Mirror reflectance and soiling	0.9									0.9	0.95
Heliostat availability	0.99										0.98
Image error	0.002 rad										
Heliostat stow deploy angle	8 deg										
Wind stow speed	15 m/s										
Field Parameters											
Total reflective area	964,712.4 m2	1,012,933.6 m2	668,455.3 m2								80,000 m2
No. heliostats	6682	7016	4630							981	1912
Radial step size for layout	115.628 m	115.628 m	87.5025 m								
Solar Field Layout Constraints											
Max heliostat distance to tower height ratio	7.5										
Min heliostat distance to tower height ratio	0.75										
Tower height	205.56 m		155.56 m								
Max distance from tower	1541.7 m		1166.7 m								
Min distance from tower	154.17 m		116.67 m								
Max realised distance from tower	1310.45 m		1079.2 m								
Radial Zones	12										
Azimuthal Zones	12										
Mirror Washing											
Water use per wash	0.6 l/m2										
Washing frequency	4 days										
Land Area											
Non-solar field land area	180000 m2										
Solar field land area multiplier	1.3										
Calculated total land area	4.65693 km2	5.23026 km2	3.77494 km2	0.0814 km2	0.263 km2						0.4 km2

Tower and Receiver

	SAM (2010) Default Values			EPRI (2010)				Romero et al. (2002)			Sargent and Lundy (2003)
	6 hrs - wet	6 hrs - dry	No Storage - wet	0 hrs - wet	3 hrs - wet	6 hrs - wet	9 hrs - wet	Solar Two	Solar Tres	PS10	Solar Two
Dimensions											
Receiver height	18.8 m	19.91 m	15.17 m							10.5 m	
Receiver diameter	12.44 m		10.67 m							10.5 m	
Tower Height	205.56 m		155.56 m							90 m	
Thermodynamic Characteristics											
Number of panels	24										
Tube outer diameter	40 mm										
Tube wall thickness	1.25 mm										
Required HTF outlet temp	574 °C										565 °C
Max temp to receiver	350 °C										
Coating absorptivity	0.94										0.93
Coating emissivity	0.88										
Heat loss factor	1										
Enable night recirculation in receiver	No										
Recirculation heater efficiency	1										
Max HTF velocity in receiver	6 m/s										
Max flow rate to receiver	3,690,306.6 kg/hr		3,165,238.8 kg/hr								
Max receiver flux	1200 kWt/m2										800 kW/m2
Materials and Flow											
HTF Type	Salt (60%, NaNO3 40% KNO3)										Solar Salt
Material type	Stainless AISI316										
Flow pattern	1										

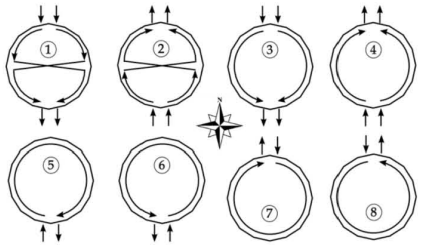

	SAM (2010) Default Values			EPRI (2010)				Romero et al. (2002)			Sargent and Lundy (2003)
	6 hrs - wet	6 hrs - dry	No Storage - wet	0 hrs - wet	3 hrs - wet	6 hrs - wet	9 hrs - wet	Solar Two	Solar Tres	PS10	Solar Two
Power Cycle											
Plant Capacity											
Design turbine gross output	110 MWe										
Estimated gross to net conversion factor	0.9091										
Estimated net output at design (nameplate)	100.001 MWe			125 MWe				10 MW	15 MW	10 MW	10 MW
Power Block Design Point											
Rated cycle conversion efficiency	0.425	0.408	0.425							0.309	0.317
Design thermal power	258.824 MWt	269.608 MWt	258.824 MWt								
Design HTF inlet temp	574 °C										510 °C
Design HTF outlet temp	290 °C										
Boiler steam pressure	100 bar										125 bar
Boiler LHV efficiency	0.9										
Steam cycle blowdown fraction	0.013										
Plant control											
Min temp to load	500 °C										
Low resource standby period	2 hr										
Fraction of thermal power needed for standby	0.2										
Power block startup time	0.5 hr										
Fraction of thermal power needed for startup	0.75										
Min turbine load fraction	0.25										
Max turbine over design operation	1.15										
Cooling System											
Condenser type	Evaporative	Air-cooled	Evaporative								Evaporative
Ambient temp at design	20 °C	33 °C	20 °C								
Ref. condenser water dT	10 °C	10 °C	10 °C								
Approach temp	5 °C	5 °C	5 °C								
ITD at design point	16 °C	16 °C	16 °C								
Condenser pressure ratio	1.0028	1.0028	1.0028								
Thermal Storage											
Storage System											
Storage type	2 tank		None								
Full load hours of Thermal Energy Storage	6 hr		0					110 MWh	610 MWh	18 MWh	3 hr
Storage HTF volume	7224.78 m3	7525.81 m3	-								
Tank diameter	21.4463 m	21.8885 m	-								
Tank height	20 m		-								
Tank fluid min height	1 m		-								
Parallel tank pairs	1		-								
Min fluid volume	361.239 m3	376.291 m3	-								
Max fluid volume	6863.54 m3	7149.52 m3	-								
Tank wetted loss coefficient	0.4 W/m2. K		-								
Tank dry loss coefficient	0.25 W/m2. K		-								
Initial hot HTF temp	574 °C		-								
Initial cold HTF temp	290 °C		-								
Initial hot HTF percent	0.3		-								
Initial hot HTF volume	2167.43 m3	2257.74 m3	-								
Initial cold HTF volume	5057.35 m3	5268.07 m3	-								
Cold tank heater temp set-point	280 °C		-								
Cold tank heater max load	30 MWe		-								
Hot tank heater temp set-point	500 °C		-								
Hot tank heater max load	30 MWe		-								
Tank heater efficiency	0.99		-								
Parasitics											
Startup energy of single heliostat	0.025 kWe										
Tracking power for single heliostat	0.055 kWe										
Receiver HTF pump efficiency	0.85										
Storage pump power	0.01 Mwe/MWt										
Balance of plant power	0.05 Mwe/MWt									1 MW	
Piping loss coefficient	3500 Wt/m										
Total piping length	1500 m										

Appendix F: Final Design Inputs for Parabolic Trough

Overview

The following appendix details the full and final set of inputs used in the SAM parabolic trough models for this study. In order to avoid vast amounts of repetition in the reporting of the input data, many of the following inputs pages have been generalised so as to apply to each of the 6 parabolic trough models (both wet and dry cooling at each of the three locations). In order to accomplish this task of generalisation, many of the values automatically calculated by SAM within each input page (and reported in the blue fields) have been removed as they would only apply to specific cases. In the cases where it was not possible to report one input page for both wet and dry-cooled plants, a separate input page for each of the cooling technologies is listed, however, they are still generalised in the sense that they apply to the wet-cooled and dry-cooled plants at all locations. In some instances, such as the solar field design and annual performance, it was not possible to generalise input pages, and thus all input pages are listed for each location. The input pages for location are not included in the appendix as they are simply specified according to each of the locations in question.

Financing

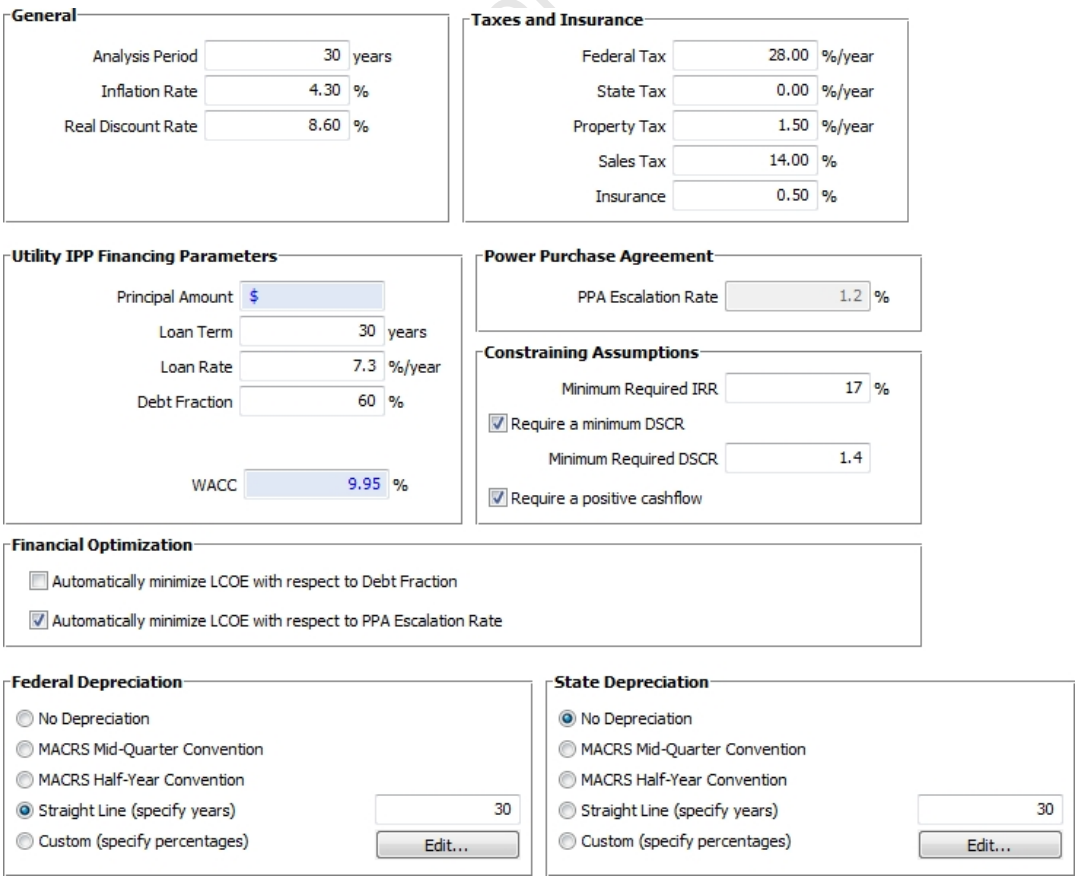

Tax and Payment Incentives

Investment Tax Credit (ITC)

		Amount	Taxable Incentive Federal	Taxable Incentive State	Reduces ITC Basis Federal	Reduces ITC Basis State	Reduces Depreciation Basis Federal	Reduces Depreciation Basis State
Federal	Value	$ 0	N/A	NO	N/A	N/A	☑	☑
State	Value	$ 0	NO	N/A	N/A	N/A	☐	☐
		Percentage	Maximum					
Federal	Value	0 %	$ 1e+099	N/A	NO	N/A	N/A	☑	☑
State	Value	0 %	$ 1e+099	NO	N/A	N/A	N/A	☐	☐

Note:

Depreciation is not used in residential financing, and hence the basis reduction inputs above can be ignored.

Production Tax Credit (PTC)

		Amount	Term	Escalation						
Federal	Value	0 $/kWh	10 years	2 %	N/A	NO	NO	NO	NO	NO
State	Value	0 $/kWh	10 years	2 %	NO	N/A	NO	NO	NO	NO

Investment Based Incentive (IBI)

		Amount									
Federal	Value	$ 0	☑	☑	☐	☐	☐	☐
State	Value	$ 0	☑	☑	☐	☐	☐	☐
Utility	Value	$ 0	☑	☑	☐	☐	☐	☐
Other	Value	$ 0	☑	☑	☐	☐	☐	☐
		Percentage	Maximum								
Federal	Value	0 %	$ 1e+099	☑	☑	☐	☐	☐	☐
State	Value	0 %	$ 1e+099	☑	☑	☐	☐	☐	☐
Utility	Value	0 %	$ 1e+099	☑	☑	☐	☐	☐	☐
Other	Value	0 %	$ 1e+099	☑	☑	☐	☐	☐	☐

Capacity Based Incentive (CBI)

		Amount	Maximum						
Federal	Value	0 $/W	$ 1e+099	☑	☑	☐	☐	☐	☐
State	Value	0 $/W	$ 1e+099	☑	☑	☐	☐	☐	☐
Utility	Value	0 $/W	$ 1e+099	☑	☑	☐	☐	☐	☐
Other	Value	0 $/W	$ 1e+099	☑	☑	☐	☐	☐	☐

Production Based Incentive (PBI)

		Amount	Term	Escalation						
Federal	Value	0 $/kWh	0 years	0 %	☑	☑	NO	NO	NO	NO
State	Value	0 $/kWh	0 years	0 %	☑	☑	NO	NO	NO	NO
Utility	Value	0 $/kWh	0 years	0 %	☑	☑	NO	NO	NO	NO
Other	Value	0 $/kWh	0 years	0 %	☑	☑	NO	NO	NO	NO

Wet-Cooled Parabolic Trough System Costs

Direct Capital Costs

Site Improvements		m2	22.01 $/m2	$
Solar Field		m2	385.13 $/m2	$
HTF System		m2	55.02 $/m2	$
Storage		MWht	77.03 $/kWht	$
Fossil Backup		MWe, Gross	0.00 $/kWe	$ 0.00
Power Plant		MWe, Gross	1,012.35 $/kWe	$
		Contingency	10 %	$
			Total Direct Cost	$

Indirect Capital Costs

	% of Direct Cost	Non-fixed Cost	Fixed Cost	Total
Engineer,Procure,Construct	15 %	$	$ 0.00	$
Project,Land,Management	3.5 %	$	$ 0.00	$

Sales Tax of 14 % applies to 80 % of Direct Cost $

Total Indirect Cost $

Total Installed Costs

Total Installed Cost $

Estimated Total Installed Cost per Net Capacity ($/kW) $

Operation and Maintenance Costs

	First Year Cost		Escalation Rate (above inflation)
Fixed Annual Cost	0.00	$/yr	0 %
Fixed Cost by Capacity	88.03	$/kW-yr	0 %
Variable Cost by Generation	7.04	$/MWh	0 %
Fossil Fuel Cost	0.00	$/MMBTU	0 %

Notes

1) Escalation rates do not apply to O&M annual schedules, only first year values.

2) Fossil fuel cost is not applicable to PV or Dish Stirling systems. Set to zero for these systems.

Dry-Cooled Parabolic Trough System Costs

Direct Capital Costs

Site Improvements		m2	22.01 $/m2	$
Solar Field		m2	385.13 $/m2	$
HTF System		m2	55.02 $/m2	$
Storage		MWht	77.03 $/kWht	$
Fossil Backup		MWe, Gross	0.00 $/kWe	$ 0.00
Power Plant		MWe, Gross	1,254.43 $/kWe	$
		Contingency	10 %	$
			Total Direct Cost	$

Indirect Capital Costs

	% of Direct Cost	Non-fixed Cost	Fixed Cost	Total
Engineer,Procure,Construct	15 %	$	$ 0.00	$
Project,Land,Management	3.5 %	$	$ 0.00	$

Sales Tax of 14 % applies to 80 % of Direct Cost $

Total Indirect Cost $

Total Installed Costs

Total Installed Cost $

Estimated Total Installed Cost per Net Capacity ($/kW) $

Operation and Maintenance Costs

	First Year Cost		Escalation Rate (above inflation)
Fixed Annual Cost	0.00	$/yr	0 %
Fixed Cost by Capacity	88.03	$/kW-yr	0 %
Variable Cost by Generation	3.39	$/MWh	0 %
Fossil Fuel Cost	0.00	$/MMBTU	0 %

Notes

1) Escalation rates do not apply to O&M annual schedules, only first year values.

2) Fossil fuel cost is not applicable to PV or Dish Stirling systems. Set to zero for these systems.

Upington Wet and Dry-Cooled Solar Field Design and Annual Performance

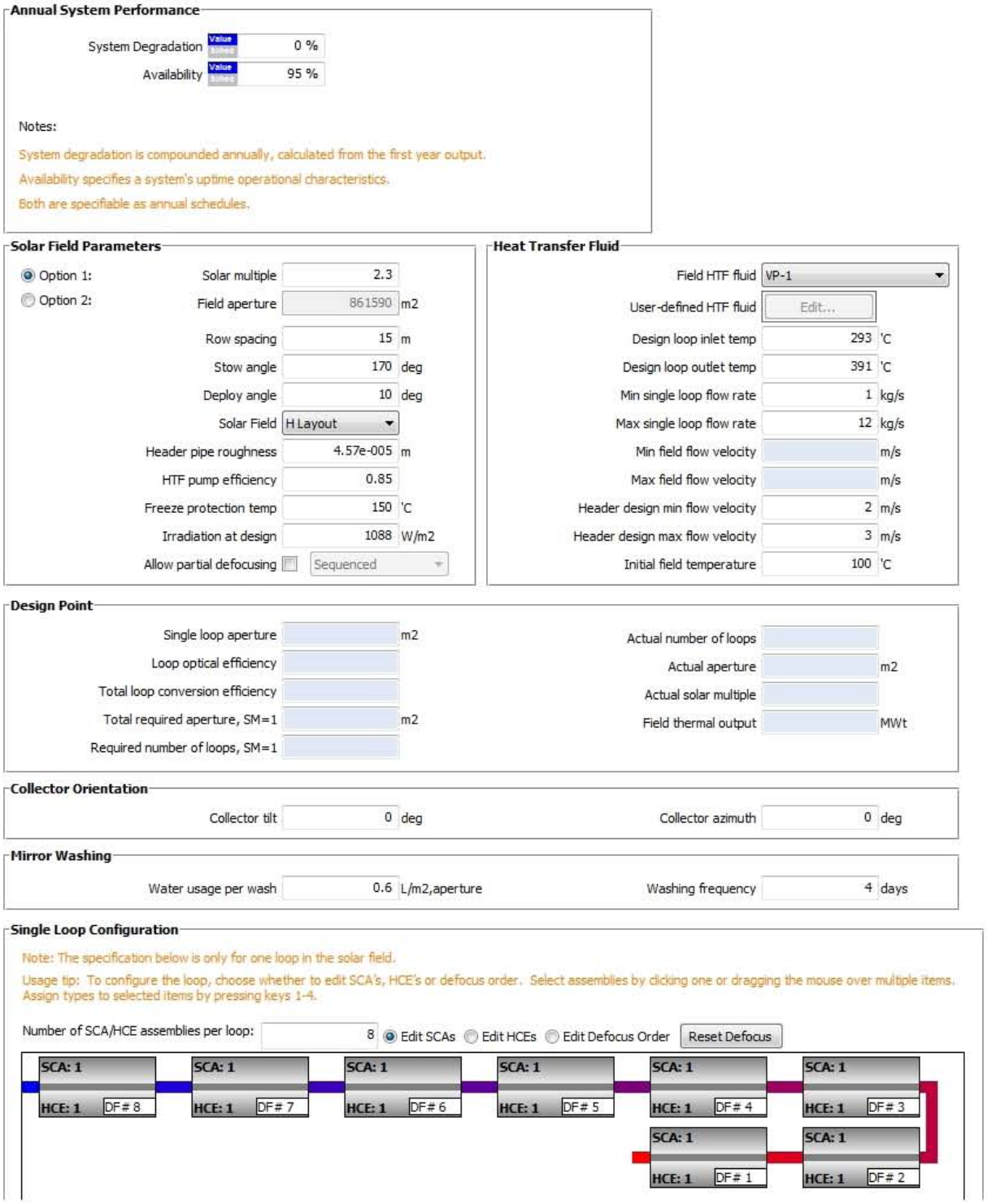

Springbok Wet and Dry-Cooled Solar Field Design and Annual Performance

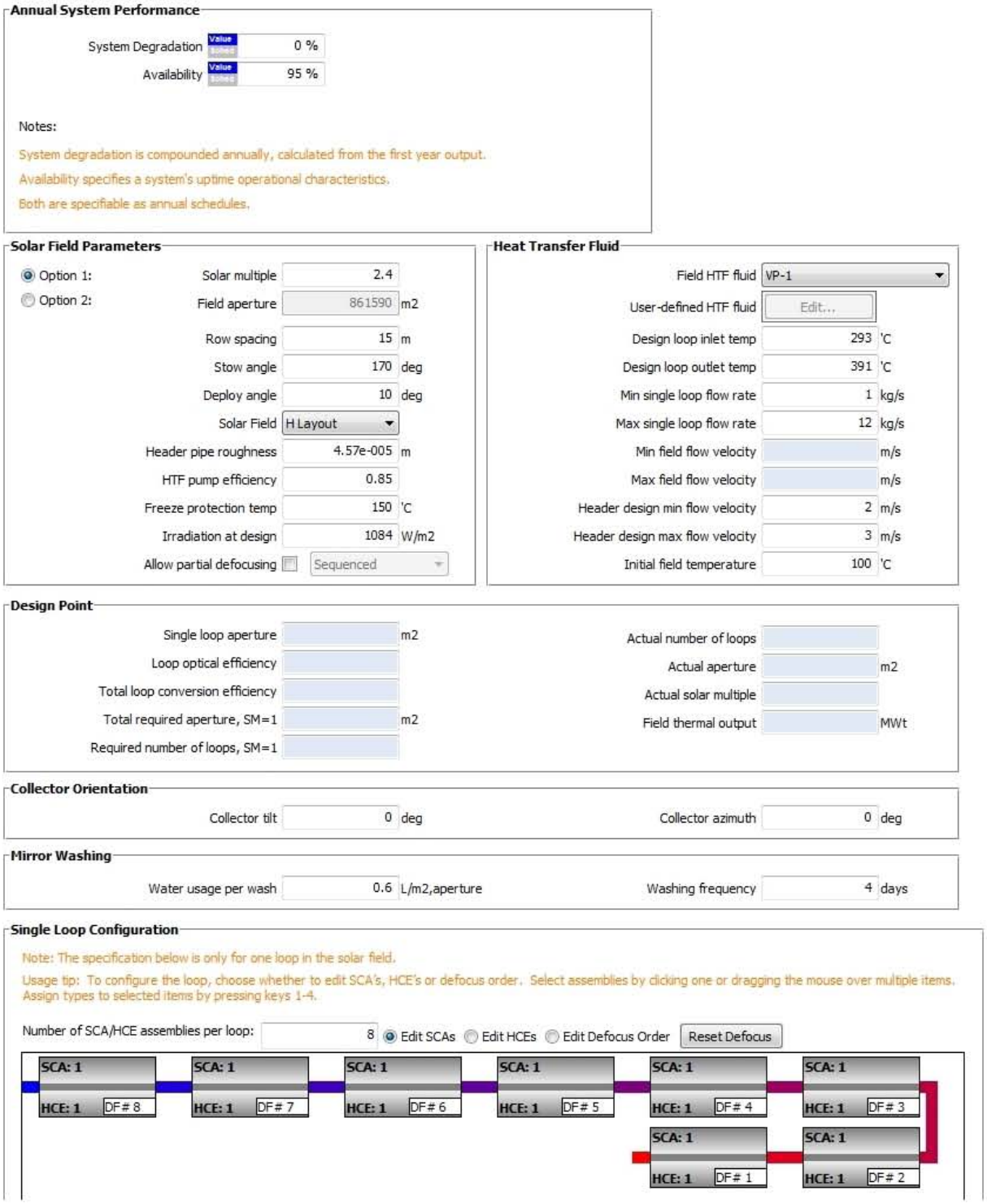

Bloemfontein Wet and Dry-Cooled Solar Field Design and Annual Performance

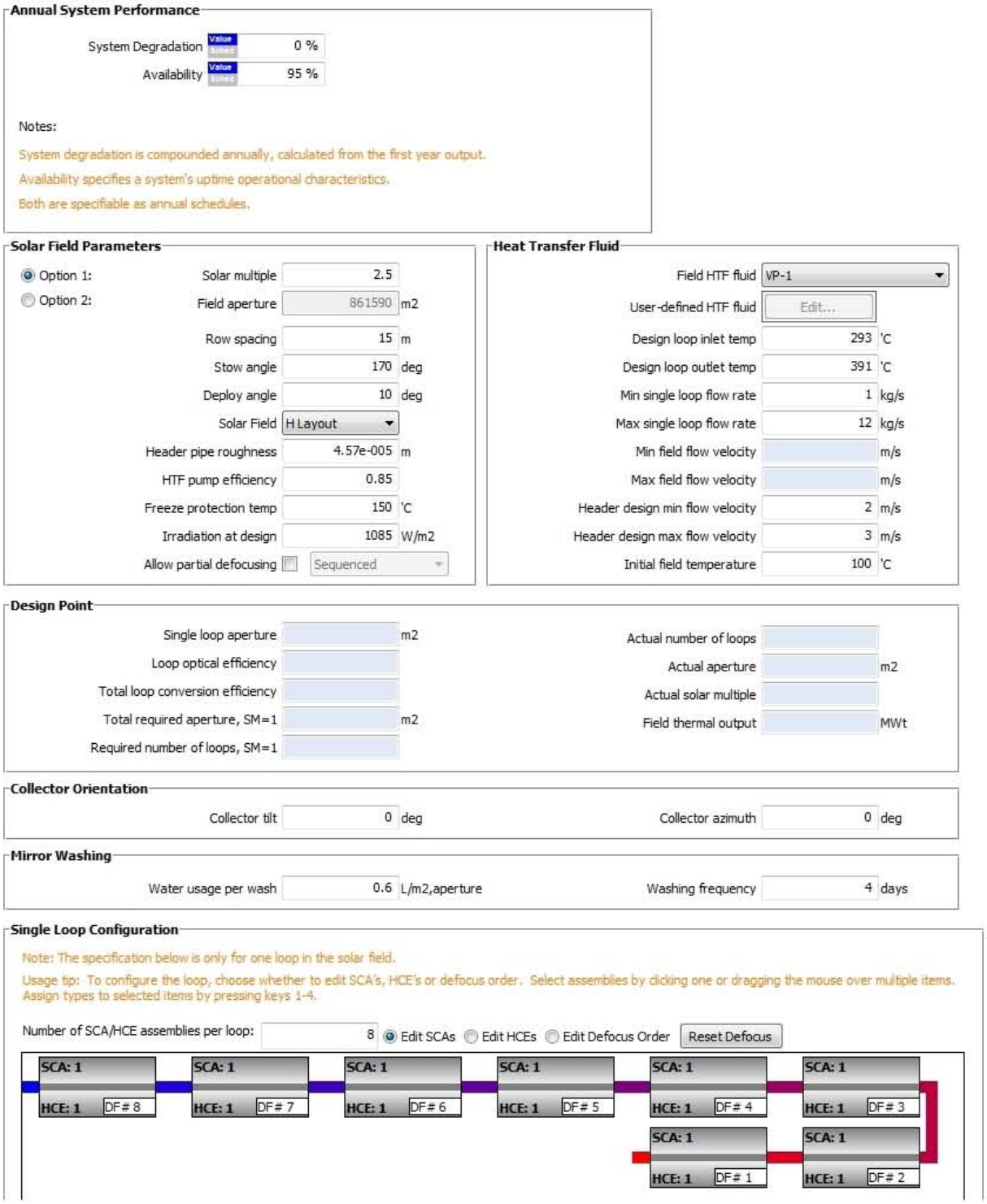

Collectors (SCAs) and Receivers (HCEs)

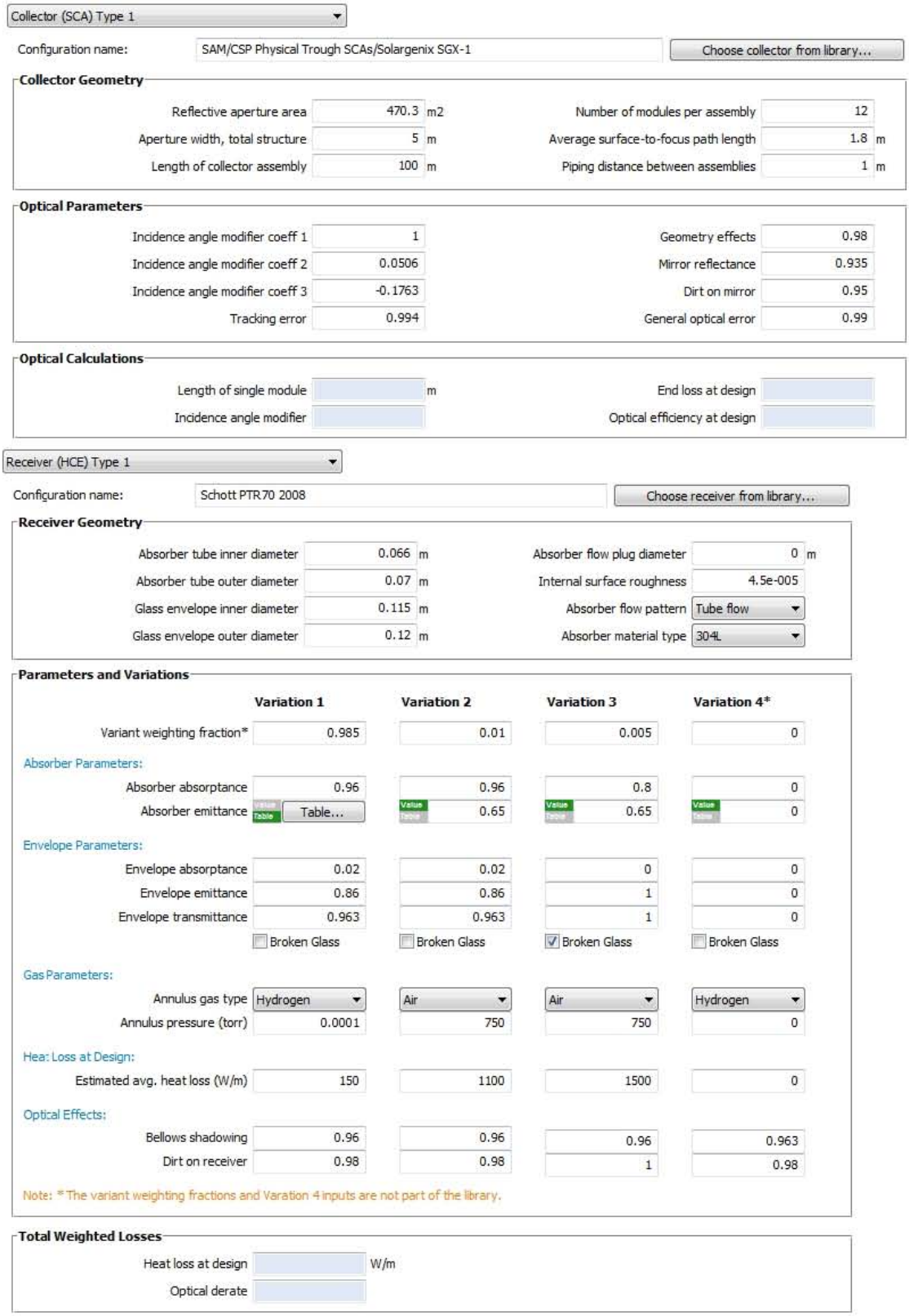

Wet-Cooled Power Cycle

Plant Capacity

Design gross output	110	MWe
Estimated gross to net conversion factor	0.9091	
Estimated net output at design (nameplate)	100.001	MWe

Note: Parasitic losses typically reduce net output to approximately 90 % of design gross power

Power Block Design Point

Rated cycle conversion efficiency	0.3774	
Design inlet temperature	391	'C
Design outlet temperature	293	'C
Boiler operating pressure	100	bar
Fossil backup boiler LHV efficiency	0.9	
Heat capacity of balance of plant	5	kWht/K-MWhe
Steam cycle blowdown fraction	0.013	

Plant Control

Fraction of thermal power needed for standby	0.2	
Power block startup time	0.5	hr
Fraction of thermal power needed for startup	0.2	
Minimum required startup temp	300	'C
Max turbine over design operation	1.15	
Min turbine operation	0.25	

Cooling System

Condenser type	Evaporative	
Ambient temp at design	20	'C
Ref. Condenser Water dT	10	'C
Approach temperature	5	'C
ITD at design point	16	'C
Condenser pressure ratio	1.0028	

Dry-Cooled Power Cycle

Plant Capacity

Design gross output	110	MWe
Estimated gross to net conversion factor	0.9091	
Estimated net output at design (nameplate)	100.001	MWe

Note: Parasitic losses typically reduce net output to approximately 90 % of design gross power

Power Block Design Point

Rated cycle conversion efficiency	0.339	
Design inlet temperature	391	'C
Design outlet temperature	293	'C
Boiler operating pressure	100	bar
Fossil backup boiler LHV efficiency	0.9	
Heat capacity of balance of plant	5	kWht/K-MWhe
Steam cycle blowdown fraction	0.016	

Plant Control

Fraction of thermal power needed for standby	0.2	
Power block startup time	0.5	hr
Fraction of thermal power needed for startup	0.2	
Minimum required startup temp	300	'C
Max turbine over design operation	1.15	
Min turbine operation	0.25	

Cooling System

Condenser type	Air-cooled	
Ambient temp at design	33	'C
Ref. Condenser Water dT	10	'C
Approach temperature	5	'C
ITD at design point	16	'C
Condenser pressure ratio	1.0028	

Wet-Cooled Thermal Storage and Parasitics

Storage System

Full load hours of TES	6	hr	Tank heater capacity	25	MWt
Storage volume	26032	m3	Tank heater efficiency	0.98	
TES Thermal capacity	1748.81	MWt	Hot side HX approach temp	5	'C
Parallel tank pairs	1		Cold side HX approach temp	7	'C
Tank height	20	m	Heat exchanger derate	0.877551	
Tank fluid min height	1	m	Initial TES fluid temp	300	'C
Tank diameter	40.7093	m	Storage HTF fluid	Solar Salt	
Min fluid volume	1301.6	m3	User-defined HTF fluid	Edit...	
Tank loss coeff	0.4	W/m2-K	Fluid Temperature	342	'C
Estimated heat loss	0.497096	MWt	TES fluid density	1872.49	kg/m3
Tank heater set point	250	'C	TES specific heat	1.50182	kJ/kg-K
Aux heater outlet set temp	391				

Thermal Storage Dispatch Control

Current dispatch schedule:

No library match.

Dispatch schedule library...

Note:

Schedule libraries do not affect the Storage Dispatch, Turbine Output and Fossil Fill fractions below.

	Storage Dispatch w/ solar*	Storage Dispatch w/o solar*	Turb. out. fraction*	Fossil fill fraction*
Period 1:	0	0	1.1	0
Period 2:	0	0	1	0
Period 3:	0	0	1	0
Period 4:	0	0	1	0
Period 5:	0	0	1	0
Period 6:	0	0	1	0

Notes:

1. Storage dispatch fractions apply to the maximum energy storage.

2. Turbine output and fossil fill fractions apply to the design turbine thermal input.

Weekday Schedule

	12am	1am	2am	3am	4am	5am	6am	7am	8am	9am	10am	11am	12pm	1pm	2pm	3pm	4pm	5pm	6pm	7pm	8pm	9pm	10pm	11pm
Jan	3	3	3	3	3	3	3	2	2	2	2	1	1	1	1	1	1	2	2	2	2	2	3	3
Feb	3	3	3	3	3	3	3	2	2	2	2	1	1	1	1	1	1	2	2	2	2	2	3	3
Mar	3	3	3	3	3	3	3	2	2	2	2	1	1	1	1	1	1	2	2	2	2	2	3	3
Apr	6	6	6	6	6	6	5	5	4	4	4	4	4	4	4	4	4	4	4	4	4	5	5	5	6
May	6	6	6	6	6	6	6	5	5	4	4	4	4	4	4	4	4	4	4	4	4	4	5	5	5
Jun	6	6	6	6	6	6	6	5	5	4	4	4	4	4	4	4	4	4	4	4	4	4	5	5	5
Jul	6	6	6	6	6	6	6	5	5	4	4	4	4	4	4	4	4	4	4	4	4	4	5	5	5
Aug	6	6	6	6	6	6	6	5	5	4	4	4	4	4	4	4	4	4	4	4	4	4	5	5	5
Sep	6	6	6	6	6	6	6	5	5	4	4	4	4	4	4	4	4	4	4	4	4	4	5	5	5
Oct	6	6	6	6	6	6	5	5	4	4	4	4	4	4	4	4	4	4	4	4	4	5	5	5	6
Nov	6	6	6	6	6	6	5	5	4	4	4	4	4	4	4	4	4	4	4	4	4	5	5	5	6
Dec	3	3	3	3	3	3	3	3	2	2	2	2	1	1	1	1	1	1	2	2	2	2	2	3	3

Weekend Schedule

	12am	1am	2am	3am	4am	5am	6am	7am	8am	9am	10am	11am	12pm	1pm	2pm	3pm	4pm	5pm	6pm	7pm	8pm	9pm	10pm	11pm
Jan	3	3	3	3	3	3	3	3	3	3	3	3	3	3	3	3	3	3	3	3	3	3	3	3
Feb	3	3	3	3	3	3	3	3	3	3	3	3	3	3	3	3	3	3	3	3	3	3	3	3
Mar	3	3	3	3	3	3	3	3	3	3	3	3	3	3	3	3	3	3	3	3	3	3	3	3
Apr	6	6	6	6	6	5	5	5	5	5	5	5	5	5	5	5	5	5	5	5	5	5	5	6
May	6	6	6	6	6	6	5	5	5	5	5	5	5	5	5	5	5	5	5	5	5	5	5	5
Jun	6	6	6	6	6	6	5	5	5	5	5	5	5	5	5	5	5	5	5	5	5	5	5	5
Jul	6	6	6	6	6	6	5	5	5	5	5	5	5	5	5	5	5	5	5	5	5	5	5	5
Aug	6	6	6	6	6	6	5	5	5	5	5	5	5	5	5	5	5	5	5	5	5	5	5	5
Sep	6	6	6	6	6	6	5	5	5	5	5	5	5	5	5	5	5	5	5	5	5	5	5	5
Oct	6	6	6	6	6	5	5	5	5	5	5	5	5	5	5	5	5	5	5	5	5	5	5	6
Nov	6	6	6	6	6	5	5	5	5	5	5	5	5	5	5	5	5	5	5	5	5	5	5	6
Dec	3	3	3	3	3	3	3	3	3	3	3	3	3	3	3	3	3	3	3	3	3	3	3	3

Parasitics

Piping thermal loss coefficient	0.45	W/m2-K
Tracking power	125	W/sca
Required pumping power for HTF through power block	0.55	kJ/kg
Required pumping power for HTF through storage	0.15	kJ/kg
Fraction of rated gross power consumed at all times	0.0055	

Design Point Totals

Tracking W

Fixed MWe

			Factor	Coeff 0	Coeff 1	Coeff 2		
Balance of plant parasitic	0.02467	MWe/MWcap	1	0.483	0.517	0	BOP	MWe
Aux heater,boiler parasitic	0.02273	MWe/MWcap	1	0.483	0.517	0	Aux	MWe

Dry-Cooled Thermal Storage and Parasitics

Storage System

Full load hours of TES	6	hr	Tank heater capacity	25	MWt
Storage volume	28980.8	m3	Tank heater efficiency	0.98	
TES Thermal capacity	1946.9	MWt	Hot side HX approach temp	5	'C
Parallel tank pairs	1		Cold side HX approach temp	7	'C
Tank height	20	m	Heat exchanger derate	0.877551	
Tank fluid min height	1	m	Initial TES fluid temp	300	'C
Tank diameter	42.9532	m	Storage HTF fluid	Solar Salt	
Min fluid volume	1449.04	m3	User-defined HTF fluid	Edit...	
Tank loss coeff	0.4	W/m2-K	Fluid Temperature	342	'C
Estimated heat loss	0.534245	MWt	TES fluid density	1872.49	kg/m3
Tank heater set point	250	'C	TES specific heat	1.50182	kJ/kg-K
Aux heater outlet set temp	391				

Thermal Storage Dispatch Control

Current dispatch schedule:

No library match.

Dispatch schedule library...

Note:

Schedule libraries do not affect the Storage Dispatch, Turbine Output and Fossil Fill fractions below.

	Storage Dispatch w/ solar*	Storage Dispatch w/o solar*	Turb. out. fraction*	Fossil fill fraction*
Period 1:	0	0	1.1	0
Period 2:	0	0	1	0
Period 3:	0	0	1	0
Period 4:	0	0	1	0
Period 5:	0	0	1	0
Period 6:	0	0	1	0

Notes:

1. Storage dispatch fractions apply to the maximum energy storage.

2. Turbine output and fossil fill fractions apply to the design turbine thermal input.

Weekday Schedule

	12am	1am	2am	3am	4am	5am	6am	7am	8am	9am	10am	11am	12pm	1pm	2pm	3pm	4pm	5pm	6pm	7pm	8pm	9pm	10pm	11pm
Jan	3	3	3	3	3	3	3	2	2	2	2	1	1	1	1	1	1	2	2	2	2	2	3	3
Feb	3	3	3	3	3	3	3	2	2	2	2	1	1	1	1	1	1	2	2	2	2	2	3	3
Mar	3	3	3	3	3	3	3	2	2	2	2	1	1	1	1	1	1	2	2	2	2	2	3	3
Apr	6	6	6	6	6	6	5	5	4	4	4	4	4	4	4	4	4	4	4	4	4	5	5	5	6
May	6	6	6	6	6	6	6	5	5	4	4	4	4	4	4	4	4	4	4	4	4	4	5	5	5
Jun	6	6	6	6	6	6	6	5	5	4	4	4	4	4	4	4	4	4	4	4	4	4	5	5	5
Jul	6	6	6	6	6	6	6	5	5	4	4	4	4	4	4	4	4	4	4	4	4	4	5	5	5
Aug	6	6	6	6	6	6	6	5	5	4	4	4	4	4	4	4	4	4	4	4	4	4	5	5	5
Sep	6	6	6	6	6	6	6	5	5	4	4	4	4	4	4	4	4	4	4	4	4	4	5	5	5
Oct	6	6	6	6	6	6	5	5	4	4	4	4	4	4	4	4	4	4	4	4	4	5	5	5	6
Nov	6	6	6	6	6	6	5	5	4	4	4	4	4	4	4	4	4	4	4	4	4	5	5	5	6
Dec	3	3	3	3	3	3	3	3	2	2	2	2	1	1	1	1	1	1	2	2	2	2	2	3	3

Weekend Schedule

	12am	1am	2am	3am	4am	5am	6am	7am	8am	9am	10am	11am	12pm	1pm	2pm	3pm	4pm	5pm	6pm	7pm	8pm	9pm	10pm	11pm
Jan	3	3	3	3	3	3	3	3	3	3	3	3	3	3	3	3	3	3	3	3	3	3	3	3
Feb	3	3	3	3	3	3	3	3	3	3	3	3	3	3	3	3	3	3	3	3	3	3	3	3
Mar	3	3	3	3	3	3	3	3	3	3	3	3	3	3	3	3	3	3	3	3	3	3	3	3
Apr	6	6	6	6	6	5	5	5	5	5	5	5	5	5	5	5	5	5	5	5	5	5	5	6
May	6	6	6	6	6	6	5	5	5	5	5	5	5	5	5	5	5	5	5	5	5	5	5	5
Jun	6	6	6	6	6	6	5	5	5	5	5	5	5	5	5	5	5	5	5	5	5	5	5	5
Jul	6	6	6	6	6	6	5	5	5	5	5	5	5	5	5	5	5	5	5	5	5	5	5	5
Aug	6	6	6	6	6	6	5	5	5	5	5	5	5	5	5	5	5	5	5	5	5	5	5	5
Sep	6	6	6	6	6	6	5	5	5	5	5	5	5	5	5	5	5	5	5	5	5	5	5	5
Oct	6	6	6	6	6	6	5	5	5	5	5	5	5	5	5	5	5	5	5	5	5	5	5	6
Nov	6	6	6	6	6	6	5	5	5	5	5	5	5	5	5	5	5	5	5	5	5	5	5	6
Dec	3	3	3	3	3	3	3	3	3	3	3	3	3	3	3	3	3	3	3	3	3	3	3	3

Parasitics

			Design Point Totals	
Piping thermal loss coefficient	0.45	W/m2-K		
Tracking power	125	W/sca	Tracking	W
Required pumping power for HTF through power block	0.55	kJ/kg		
Required pumping power for HTF through storage	0.15	kJ/kg		
Fraction of rated gross power consumed at all times	0.0055		Fixed	MWe

			Factor	Coeff 0	Coeff 1	Coeff 2		
Balance of plant parasitic	0.02467	MWe/MWcap	1	0.483	0.517	0	BOP	MWe
Aux heater,boiler parasitic	0.02273	MWe/MWcap	1	0.483	0.517	0	Aux	MWe

Appendix G: Final Design Inputs for Central Receiver

Overview

The following appendix details the full and final set of inputs used in the SAM central receiver models for this study. As with Appendix F, in order to avoid vast amounts of repetition in the reporting of the input data, many of the following inputs pages have been generalised so as to apply to each of the 6 central receiver models (both wet and dry cooling at each of the three locations). In order to accomplish this task of generalisation, many of the values automatically calculated by SAM within each input page (and reported in the blue fields) have been removed as they would only apply to specific cases. In the cases where it was not possible to report one input page for both wet and dry-cooled plants, a separate input page for each of the cooling technologies is listed, however, they are still generalised in the sense that they apply to the wet-cooled and dry-cooled plants at all locations. In some instances, such as the heliostat field layout, it was not possible to generalise input pages, and thus all 6 input pages are listed. Once again, the input pages for location are not included in the appendix as they are simply specified according to each of the locations in question.

Financing

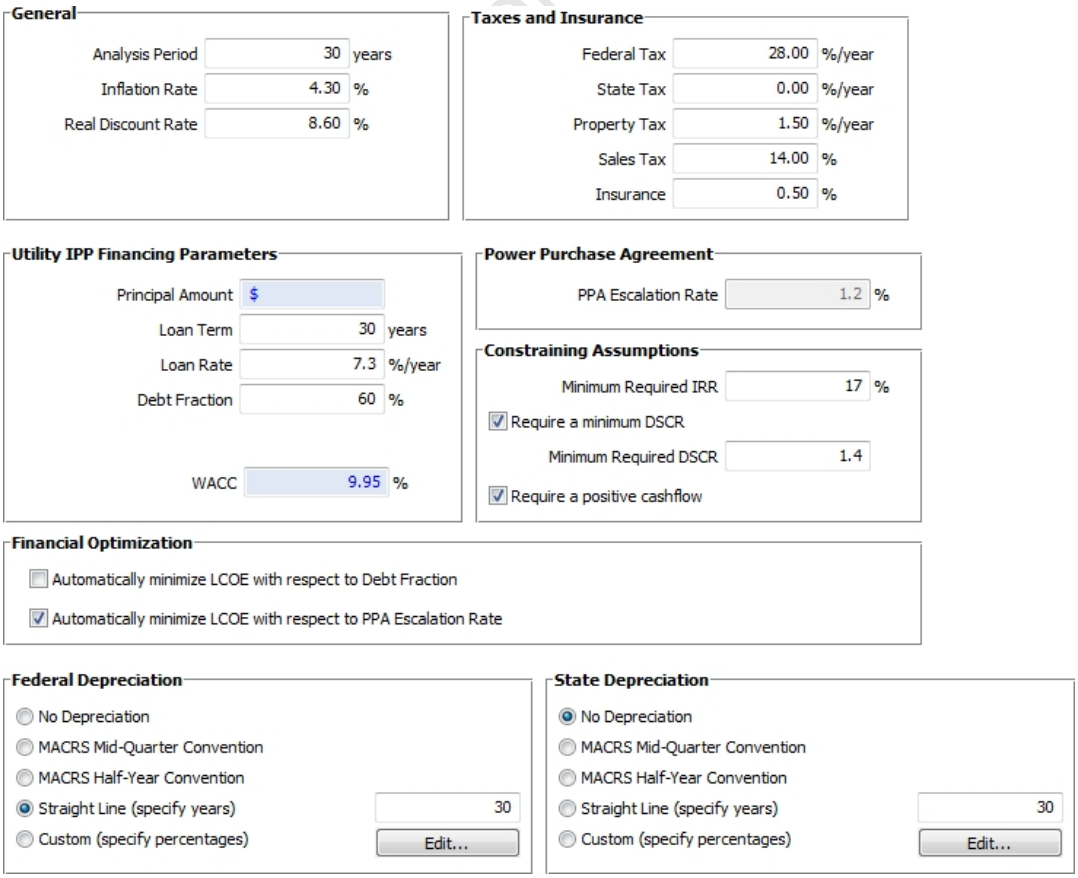

Tax and Payment Incentives

Investment Tax Credit (ITC)

		Amount	Taxable Incentive Federal	Taxable Incentive State	Reduces ITC Basis Federal	Reduces ITC Basis State	Reduces Depreciation Basis Federal	Reduces Depreciation Basis State
Federal	Value	$ 0	N/A	NO	N/A	N/A	☑	☑
State	Value	$ 0	NO	N/A	N/A	N/A	☐	☐
		Percentage	Maximum					
Federal	Value	0 %	$ 1e+099	N/A	NO	N/A	N/A	☑	☑
State	Value	0 %	$ 1e+099	NO	N/A	N/A	N/A	☐	☐

Note:

Depreciation is not used in residential financing, and hence the basis reduction inputs above can be ignored.

Production Tax Credit (PTC)

		Amount	Term	Escalation						
Federal	Value	0 $/kWh	10 years	2 %	N/A	NO	NO	NO	NO	NO
State	Value	0 $/kWh	10 years	2 %	NO	N/A	NO	NO	NO	NO

Investment Based Incentive (IBI)

		Amount									
Federal	Value	$ 0	☑	☑	☐	☐	☐	☐
State	Value	$ 0	☑	☑	☐	☐	☐	☐
Utility	Value	$ 0	☑	☑	☐	☐	☐	☐
Other	Value	$ 0	☑	☑	☐	☐	☐	☐
		Percentage	Maximum								
Federal	Value	0 %	$ 1e+099	☑	☑	☐	☐	☐	☐
State	Value	0 %	$ 1e+099	☑	☑	☐	☐	☐	☐
Utility	Value	0 %	$ 1e+099	☑	☑	☐	☐	☐	☐
Other	Value	0 %	$ 1e+099	☑	☑	☐	☐	☐	☐

Capacity Based Incentive (CBI)

		Amount	Maximum						
Federal	Value	0 $/W	$ 1e+099	☑	☑	☐	☐	☐	☐
State	Value	0 $/W	$ 1e+099	☑	☑	☐	☐	☐	☐
Utility	Value	0 $/W	$ 1e+099	☑	☑	☐	☐	☐	☐
Other	Value	0 $/W	$ 1e+099	☑	☑	☐	☐	☐	☐

Production Based Incentive (PBI)

		Amount	Term	Escalation						
Federal	Value	0 $/kWh	0 years	0 %	☑	☑	NO	NO	NO	NO
State	Value	0 $/kWh	0 years	0 %	☑	☑	NO	NO	NO	NO
Utility	Value	0 $/kWh	0 years	0 %	☑	☑	NO	NO	NO	NO
Other	Value	0 $/kWh	0 years	0 %	☑	☑	NO	NO	NO	NO

Wet-Cooled Central Receiver System Costs

Direct Capital Costs

Site Improvements		m2	22.008 $/m2	$
Heliostat Field		m2	221.175 $/m2	$
Balance of Plant		MWe, Gross	379.63 $/kWe	$
Power Block		MWe, Gross	632.72 $/kWe	$
Storage System		MWht	33.01 $/kWht	$
			Fixed Solar Field Cost	$ 0.00
Fixed Tower Cost	$ 991,988.06			
Tower Cost Scaling Exponent	0.01298		Total Tower Cost	$
Receiver Reference Cost	$ 65,085,970.84			
Receiver Reference Area	1110	m2	Area m2	
Receiver Cost Scaling Exponent	0.7		Total Receiver Cost	$
			Contingency 10 %	$
			Total Direct Cost	$

Indirect Capital Costs

	% of Direct Cost	Non-fixed Cost	Fixed Cost	Total
Engineer,Procure,Construct	15 %	$	$ 0.00	$
Project,Land,Management	3.5 %	$	$ 0.00	$
Sales Tax of 14 % applies to 80 % of Direct Cost				$
			Total Indirect Cost	$

Total Installed Costs

Total Installed Cost	$
Estimated Total Installed Cost per Net Capacity ($/kW)	$

Operation and Maintenance Costs

	First Year Cost		Escalation Rate (above inflation)
Fixed Annual Cost	0.00	$/yr	0 %
Fixed Cost by Capacity	88.03	$/kW-yr	0 %
Variable Cost by Generation	6.16	$/MWh	0 %
Fossil Fuel Cost	0.00	$/MMBTU	0 %

Dry-Cooled Central Receiver System Costs

Direct Capital Costs

Site Improvements		m2	22.008 $/m2	$
Heliostat Field		m2	221.175 $/m2	$
Balance of Plant		MWe, Gross	379.63 $/kWe	$
Power Block		MWe, Gross	874.8 $/kWe	$
Storage System		MWht	33.01 $/kWht	$
			Fixed Solar Field Cost	$ 0.00

Fixed Tower Cost	$ 991,988.06		
Tower Cost Scaling Exponent	0.01298	Total Tower Cost	$
Receiver Reference Cost	$ 65,085,970.84		
Receiver Reference Area	1110 m2	Area m2	
Receiver Cost Scaling Exponent	0.7	Total Receiver Cost	$
		Contingency 10 %	$
		Total Direct Cost	$

Indirect Capital Costs

	% of Direct Cost	Non-fixed Cost	Fixed Cost	Total
Engineer,Procure,Construct	15 %	$	$ 0.00	$
Project,Land,Management	3.5 %	$	$ 0.00	$

Sales Tax of 14 % applies to 80 % of Direct Cost $

Total Indirect Cost $

Total Installed Costs

Total Installed Cost $

Estimated Total Installed Cost per Net Capacity ($/kW) $

Operation and Maintenance Costs

	First Year Cost		Escalation Rate (above inflation)
Fixed Annual Cost	0.00	$/yr	0 %
Fixed Cost by Capacity	88.03	$/kW-yr	0 %
Variable Cost by Generation	3.45	$/MWh	0 %
Fossil Fuel Cost	0.00	$/MMBTU	0 %

Annual Performance and Tower and Receiver Design

Annual System Performance

System Degradation	Value	0 %
Availability	Value	92 %

Notes:

System degradation is compounded annually, calculated from the first year output

Availability specifies a system's uptime operational characteristics.

Both are specifiable as annual schedules.

Dimensions

Receiver Height	15.49	m
Receiver Diameter	12.44	m
Tower Height	216.67	m

Note:

Optimal dimensions are calculated by using the solar field wizard.

Thermodynamic Characteristics

Number of Panels	24	
Tube Outer Diameter	40	mm
Tube Wall Thickness	1.25	mm
Required HTF Outlet Temp.	574	'C
Max. Temp. To Receiver	350	'C
Coating Absorptivity	0.94	
Coating Emissivity	0.88	
Heat Loss Factor	1	
Enable Night Recirculation in Receiver	☐	
Recirculation Heater Efficiency	1	
Max. HTF Velocity in Receiver	6	m/s
Max. Flow Rate to Receiver	3,690,306.6	kg/hr
Max. Receiver Flux	1200	kWt/m2

Materials and Flow

HTF Type	Salt (60% NaNO3 40% KNO3)
Property table for user-defined HTF	Edit...
Material Type	Stainless AISI316
Flow Pattern	2

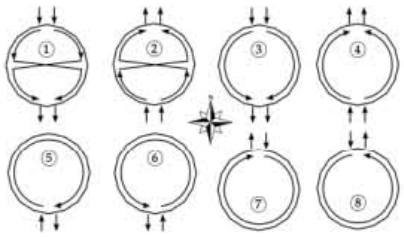

Upington Wet-Cooled Heliostat Field Design

Heliostat Properties

Heliostat Width	12.2	m
Heliostat Height	12.2	m
Ratio of Reflective Area to Profile	0.97	
Use Round Heliostats (D=W)	☐	
Heliostat Area	144.375	m2
Mirror Reflectance and Soiling	0.9	
Heliostat Availability	0.99	
Image Error	0.002	rad
Heliostat Stow Deploy Angle	8	deg
Wind Stow Speed	15	m/s

Circular Field Optimization Wizard

Start Wizard...

The wizard will calculate an optimal distribution of heliostats and populate the zonal grid below. It calculates optimal tower and receiver heights, and receiver diameter. Since some cost and financial parameters help guide the optimization, be sure to set reasonable values before running the wizard. Refer to the documentation for more information.

Field Parameters

Total Reflective Area	1,027,804.2	m2
Number of Heliostats	7119	
Radial Step Size For Layout	121.877	m

Solar Field Layout Constraints

Max Heliostat Distance to Tower Height Ratio	7.5	Max. Distance From Tower	1625.02 m
Min Heliostat Distance to Tower Height Ratio	0.75	Min. Distance From Tower	162.503 m
Tower Height	216.67 m	Max Realized Distance From Tower	1259.39 m

Mirror Washing

Water Usage Per Wash	0.6	L/m2,aperture
Washing Frequency	4	days

Land Area

Non-Solar Field Land Area	180000	m2
Solar Field Land Area Multiplier	1.3	
Calculated Total Land Area	5.14383	km2

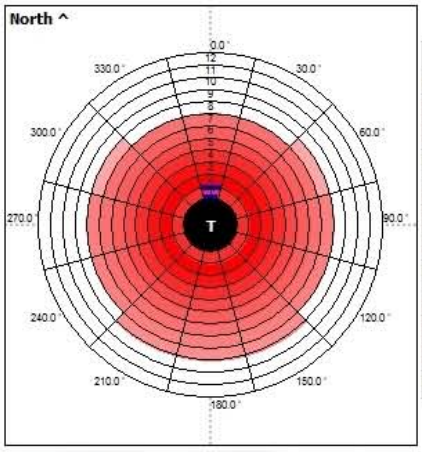

Radial Zones: 12 Azimuthal Zones: 12

	0.0	30.0	60.0	90.0	120.0	150.0	180.0	210.0	240.0	270.0	300.0	330.0
Rad. 1	21	21	21	21	21	21	21	21	21	21	21	21
Rad. 2	60	60	60	60	60	60	60	60	60	60	60	60
Rad. 3	75	75	75	75	75	75	75	75	75	75	75	75
Rad. 4	84	84	84	84	84	84	84	84	84	84	84	84
Rad. 5	88	88	88	88	88	88	88	88	88	88	88	88
Rad. 6	90	90	90	90	90	90	90	90	90	90	90	90
Rad. 7	90	90	90	90	90	90	90	90	90	90	90	90
Rad. 8	0	0	63	90	90	90	90	90	90	90	63	0
Rad. 9	0	0	0	0	0	89	89	89	0	0	0	0
Rad. 10	0	0	0	0	0	0	0	0	0	0	0	0
Rad. 11	0	0	0	0	0	0	0	0	0	0	0	0
Rad. 12	0	0	0	0	0	0	0	0	0	0	0	0

Import Export

Optimization Wizard (Upington Power Tower - 6 hrs TES - Wet)

Solar Field

Solar Multiple	2

Receiver and Tower

Min. Receiver Diameter	8 m
Max. Receiver Diameter	16 m
Optimization Levels for Receiver Diameter	10
Min. Receiver Height/Diameter Ratio	0.8
Max. Receiver Height/Diameter Ratio	1.6
Optimization Levels for Receiver H/D Ratio	10
Min. Tower Height	150 m
Max. Tower Height	250 m
Optimization Levels for Tower Height	10

Upington Dry-Cooled Heliostat Field Design

Heliostat Properties

Heliostat Width	12.2	m
Heliostat Height	12.2	m
Ratio of Reflective Area to Profile	0.97	
Use Round Heliostats (D=W)	☐	
Heliostat Area	144.375	m2
Mirror Reflectance and Soiling	0.9	
Heliostat Availability	0.99	
Image Error	0.002	rad
Heliostat Stow Deploy Angle	8	deg
Wind Stow Speed	15	m/s

Circular Field Optimization Wizard

Start Wizard...

The wizard will calculate an optimal distribution of heliostats and populate the zonal grid below. It calculates optimal tower and receiver heights, and receiver diameter. Since some cost and financial parameters help guide the optimization, be sure to set reasonable values before running the wizard. Refer to the documentation for more information.

Field Parameters

Total Reflective Area	1,010,190.5	m2
Number of Heliostats	6997	
Radial Step Size For Layout	121.877	m

Solar Field Layout Constraints

Max Heliostat Distance to Tower Height Ratio	7.5		Max. Distance From Tower	1625.02 m
Min Heliostat Distance to Tower Height Ratio	0.75		Min. Distance From Tower	162.503 m
Tower Height	216.67	m	Max Realized Distance From Tower	1259.39 m

Mirror Washing

Water Usage Per Wash	0.6	L/m2,aperture
Washing Frequency	4	days

Land Area

Non-Solar Field Land Area	180000	m2
Solar Field Land Area Multiplier	1.3	
Calculated Total Land Area	5.14383	km2

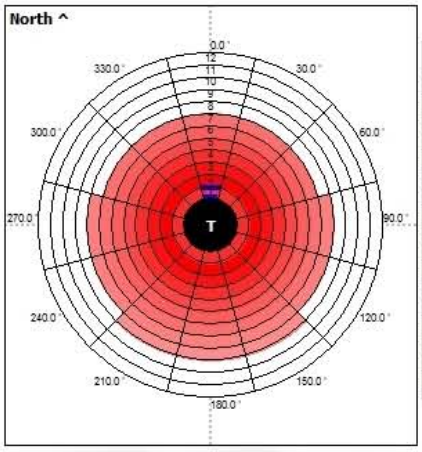

Radial Zones: 12 Azimuthal Zones: 12

	0.0	30.0	60.0	90.0	120.0	150.0	180.0	210.0	240.0	270.0	300.0	330.0
Rad. 1	21	21	21	21	21	21	21	21	21	21	21	21
Rad. 2	60	60	60	60	60	60	60	60	60	60	60	60
Rad. 3	75	75	75	75	75	75	75	75	75	75	75	75
Rad. 4	84	84	84	84	84	84	84	84	84	84	84	84
Rad. 5	88	88	88	88	88	88	88	88	88	88	88	88
Rad. 6	90	90	90	90	90	90	90	90	90	90	90	90
Rad. 7	90	90	90	90	90	90	90	90	90	90	90	90
Rad. 8	0	0	2	90	90	90	90	90	90	90	2	0
Rad. 9	0	0	0	0	0	89	89	89	0	0	0	0
Rad. 10	0	0	0	0	0	0	0	0	0	0	0	0
Rad. 11	0	0	0	0	0	0	0	0	0	0	0	0
Rad. 12	0	0	0	0	0	0	0	0	0	0	0	0

Import Export

Optimization Wizard (Upington Power Tower - 6 hrs TES - Dry)

Solar Field

Solar Multiple	1.9

Receiver and Tower

Min. Receiver Diameter	8 m
Max. Receiver Diameter	16 m
Optimization Levels for Receiver Diameter	10
Min. Receiver Height/Diameter Ratio	0.8
Max. Receiver Height/Diameter Ratio	1.6
Optimization Levels for Receiver H/D Ratio	10
Min. Tower Height	150 m
Max. Tower Height	250 m
Optimization Levels for Tower Height	10

Springbok Wet-Cooled Heliostat Field Design

Heliostat Properties

Heliostat Width	12.2	m
Heliostat Height	12.2	m
Ratio of Reflective Area to Profile	0.97	
Use Round Heliostats (D=W)	☐	
Heliostat Area	144.375	m2
Mirror Reflectance and Soiling	0.9	
Heliostat Availability	0.99	
Image Error	0.002	rad
Heliostat Stow Deploy Angle	8	deg
Wind Stow Speed	15	m/s

Circular Field Optimization Wizard

Start Wizard...

The wizard will calculate an optimal distribution of heliostats and populate the zonal grid below. It calculates optimal tower and receiver heights, and receiver diameter. Since some cost and financial parameters help guide the optimization, be sure to set reasonable values before running the wizard. Refer to the documentation for more information.

Field Parameters

Total Reflective Area	1,028,670.4	m2
Number of Heliostats	7125	
Radial Step Size For Layout	121.877	m

Solar Field Layout Constraints

Max Heliostat Distance to Tower Height Ratio	7.5		Max. Distance From Tower	1625.02 m
Min Heliostat Distance to Tower Height Ratio	0.75		Min. Distance From Tower	162.503 m
Tower Height	216.67	m	Max Realized Distance From Tower	1259.39 m

Mirror Washing

Water Usage Per Wash	0.6	L/m2,aperture
Washing Frequency	4	days

Land Area

Non-Solar Field Land Area	180000	m2
Solar Field Land Area Multiplier	1.3	
Calculated Total Land Area	5.16405	km2

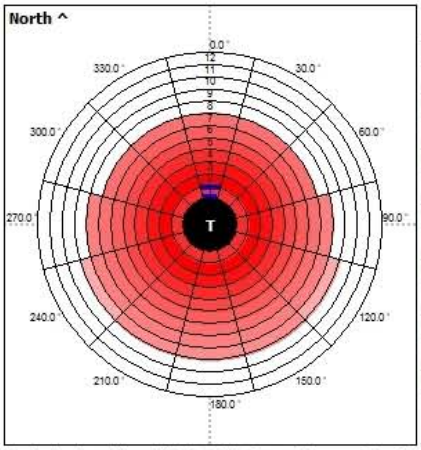

Radial Zones: 12 Azimuthal Zones: 12

	0.0	30.0	60.0	90.0	120.0	150.0	180.0	210.0	240.0	270.0	300.0	330.0
Rad. 1	21	21	21	21	21	21	21	21	21	21	21	21
Rad. 2	60	60	60	60	60	60	60	60	60	60	60	60
Rad. 3	75	75	75	75	75	75	75	75	75	75	75	75
Rad. 4	84	84	84	84	84	84	84	84	84	84	84	84
Rad. 5	88	88	88	88	88	88	88	88	88	88	88	88
Rad. 6	90	90	90	90	90	90	90	90	90	90	90	90
Rad. 7	90	90	90	90	90	90	90	90	90	90	90	90
Rad. 8	0	0	0	90	90	90	90	90	90	90	0	0
Rad. 9	0	0	0	0	66	89	89	89	66	0	0	0
Rad. 10	0	0	0	0	0	0	0	0	0	0	0	0
Rad. 11	0	0	0	0	0	0	0	0	0	0	0	0
Rad. 12	0	0	0	0	0	0	0	0	0	0	0	0

Import Export

Optimization Wizard (Springbok Power Tower - 6 hrs TES - Wet)

Solar Field

Solar Multiple	2

Receiver and Tower

Min. Receiver Diameter	8 m
Max. Receiver Diameter	16 m
Optimization Levels for Receiver Diameter	10
Min. Receiver Height/Diameter Ratio	0.8
Max. Receiver Height/Diameter Ratio	1.6
Optimization Levels for Receiver H/D Ratio	10
Min. Tower Height	150 m
Max. Tower Height	250 m
Optimization Levels for Tower Height	10

Springbok Dry-Cooled Heliostat Field Design

Heliostat Properties

Heliostat Width	12.2	m
Heliostat Height	12.2	m
Ratio of Reflective Area to Profile	0.97	
Use Round Heliostats (D=W)	☐	
Heliostat Area	144.375	m2
Mirror Reflectance and Soiling	0.9	
Heliostat Availability	0.99	
Image Error	0.002	rad
Heliostat Stow Deploy Angle	8	deg
Wind Stow Speed	15	m/s

Circular Field Optimization Wizard

Start Wizard...

The wizard will calculate an optimal distribution of heliostats and populate the zonal grid below. It calculates optimal tower and receiver heights, and receiver diameter. Since some cost and financial parameters help guide the optimization, be sure to set reasonable values before running the wizard. Refer to the documentation for more information.

Field Parameters

Total Reflective Area	1,012,211.7	m2
Number of Heliostats	7011	
Radial Step Size For Layout	121.877	m

Solar Field Layout Constraints

Max Heliostat Distance to Tower Height Ratio	7.5		Max. Distance From Tower	1625.02 m
Min Heliostat Distance to Tower Height Ratio	0.75		Min. Distance From Tower	162.503 m
Tower Height	216.67	m	Max Realized Distance From Tower	1259.39 m

Mirror Washing

Water Usage Per Wash	0.6	L/m2,aperture
Washing Frequency	4	days

Land Area

Non-Solar Field Land Area	180000	m2
Solar Field Land Area Multiplier	1.3	
Calculated Total Land Area	5.16405	km2

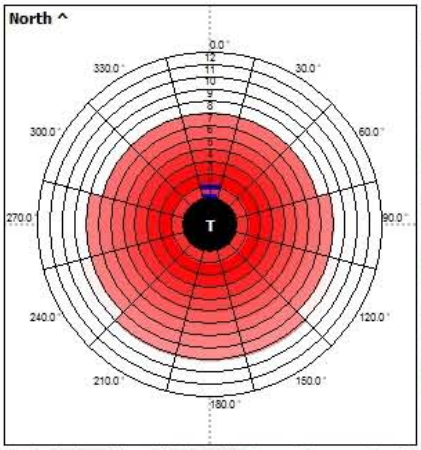

Radial Zones: 12 Azimuthal Zones: 12

	0.0	30.0	60.0	90.0	120.0	150.0	180.0	210.0	240.0	270.0	300.0	330.0
Rad. 1	21	21	21	21	21	21	21	21	21	21	21	21
Rad. 2	60	60	60	60	60	60	60	60	60	60	60	60
Rad. 3	75	75	75	75	75	75	75	75	75	75	75	75
Rad. 4	84	84	84	84	84	84	84	84	84	84	84	84
Rad. 5	88	88	88	88	88	88	88	88	88	88	88	88
Rad. 6	90	90	90	90	90	90	90	90	90	90	90	90
Rad. 7	90	90	90	90	90	90	90	90	90	90	90	90
Rad. 8	0	0	0	90	90	90	90	90	90	90	0	0
Rad. 9	0	0	0	0	9	89	89	89	9	0	0	0
Rad. 10	0	0	0	0	0	0	0	0	0	0	0	0
Rad. 11	0	0	0	0	0	0	0	0	0	0	0	0
Rad. 12	0	0	0	0	0	0	0	0	0	0	0	0

Import Export

Optimization Wizard (Springbok Power Tower - 6 hrs TES - Dry)

Solar Field

Solar Multiple	1.9

Receiver and Tower

Min. Receiver Diameter	8 m
Max. Receiver Diameter	16 m
Optimization Levels for Receiver Diameter	10
Min. Receiver Height/Diameter Ratio	0.8
Max. Receiver Height/Diameter Ratio	1.6
Optimization Levels for Receiver H/D Ratio	10
Min. Tower Height	150 m
Max. Tower Height	250 m
Optimization Levels for Tower Height	10

Bloemfontein Wet-Cooled Heliostat Field Design

Heliostat Properties

Heliostat Width	12.2	m
Heliostat Height	12.2	m
Ratio of Reflective Area to Profile	0.97	
Use Round Heliostats (D=W)	☐	
Heliostat Area	144.375	m2
Mirror Reflectance and Soiling	0.9	
Heliostat Availability	0.99	
Image Error	0.002	rad
Heliostat Stow Deploy Angle	8	deg
Wind Stow Speed	15	m/s

Circular Field Optimization Wizard

Start Wizard...

The wizard will calculate an optimal distribution of heliostats and populate the zonal grid below. It calculates optimal tower and receiver heights, and receiver diameter. Since some cost and financial parameters help guide the optimization, be sure to set reasonable values before running the wizard. Refer to the documentation for more information.

Field Parameters

Total Reflective Area	1,029,247.9	m2
Number of Heliostats	7129	
Radial Step Size For Layout	121.877	m

Solar Field Layout Constraints

Max Heliostat Distance to Tower Height Ratio	7.5		Max. Distance From Tower	1625.02 m
Min Heliostat Distance to Tower Height Ratio	0.75		Min. Distance From Tower	162.503 m
Tower Height	216.67	m	Max Realized Distance From Tower	1259.39 m

Mirror Washing

Water Usage Per Wash	0.6	L/m2,aperture
Washing Frequency	4	days

Land Area

Non-Solar Field Land Area	180000	m2
Solar Field Land Area Multiplier	1.3	
Calculated Total Land Area	5.14383	km2

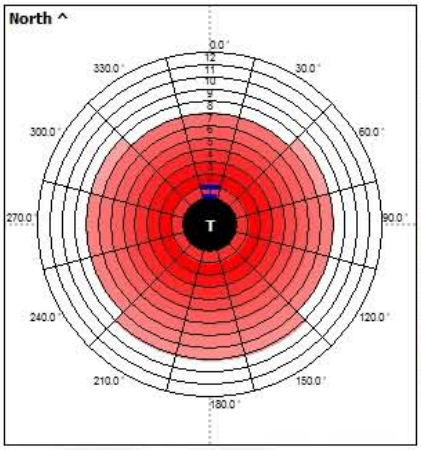

Radial Zones: 12 Azimuthal Zones: 12

	0.0	30.0	60.0	90.0	120.0	150.0	180.0	210.0	240.0	270.0	300.0	330.0
Rad. 1	21	21	21	21	21	21	21	21	21	21	21	21
Rad. 2	60	60	60	60	60	60	60	60	60	60	60	60
Rad. 3	75	75	75	75	75	75	75	75	75	75	75	75
Rad. 4	84	84	84	84	84	84	84	84	84	84	84	84
Rad. 5	88	88	88	88	88	88	88	88	88	88	88	88
Rad. 6	90	90	90	90	90	90	90	90	90	90	90	90
Rad. 7	90	90	90	90	90	90	90	90	90	90	90	90
Rad. 8	0	0	68	90	90	90	90	90	90	90	68	0
Rad. 9	0	0	0	0	0	89	89	89	0	0	0	0
Rad. 10	0	0	0	0	0	0	0	0	0	0	0	0
Rad. 11	0	0	0	0	0	0	0	0	0	0	0	0
Rad. 12	0	0	0	0	0	0	0	0	0	0	0	0

Import Export

Optimization Wizard (Bloem Power Tower - 6 hrs TES - Wet)

Solar Field

Solar Multiple	2

Receiver and Tower

Min. Receiver Diameter	8 m
Max. Receiver Diameter	16 m
Optimization Levels for Receiver Diameter	10
Min. Receiver Height/Diameter Ratio	0.8
Max. Receiver Height/Diameter Ratio	1.6
Optimization Levels for Receiver H/D Ratio	10
Min. Tower Height	150 m
Max. Tower Height	250 m
Optimization Levels for Tower Height	10

Bloemfontein Dry-Cooled Heliostat Field Design

Heliostat Properties

Heliostat Width	12.2	m
Heliostat Height	12.2	m
Ratio of Reflective Area to Profile	0.97	
Use Round Heliostats (D=W)	☐	
Heliostat Area	144.375	m2
Mirror Reflectance and Soiling	0.9	
Heliostat Availability	0.99	
Image Error	0.002	rad
Heliostat Stow Deploy Angle	8	deg
Wind Stow Speed	15	m/s

Circular Field Optimization Wizard

Start Wizard...

The wizard will calculate an optimal distribution of heliostats and populate the zonal grid below. It calculates optimal tower and receiver heights, and receiver diameter. Since some cost and financial parameters help guide the optimization, be sure to set reasonable values before running the wizard. Refer to the documentation for more information.

Field Parameters

Total Reflective Area	1,011,345.5	m2
Number of Heliostats	7005	
Radial Step Size For Layout	121.877	m

Solar Field Layout Constraints

Max Heliostat Distance to Tower Height Ratio	7.5		Max. Distance From Tower	1625.02 m
Min Heliostat Distance to Tower Height Ratio	0.75		Min. Distance From Tower	162.503 m
Tower Height	216.67	m	Max Realized Distance From Tower	1259.39 m

Mirror Washing

Water Usage Per Wash	0.6	L/m2,aperture
Washing Frequency	4	days

Land Area

Non-Solar Field Land Area	180000	m2
Solar Field Land Area Multiplier	1.3	
Calculated Total Land Area	5.14383	km2

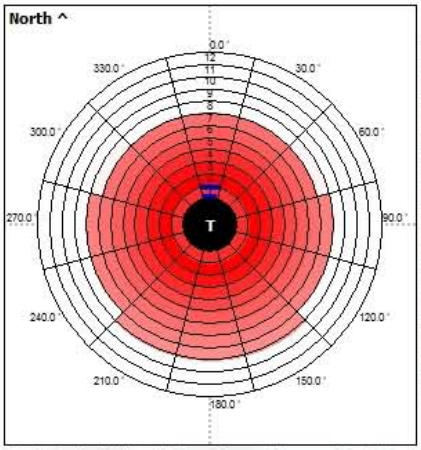

Radial Zones: 12 Azimuthal Zones: 12

	0.0	30.0	60.0	90.0	120.0	150.0	180.0	210.0	240.0	270.0	300.0	330.0
Rad. 1	21	21	21	21	21	21	21	21	21	21	21	21
Rad. 2	60	60	60	60	60	60	60	60	60	60	60	60
Rad. 3	75	75	75	75	75	75	75	75	75	75	75	75
Rad. 4	84	84	84	84	84	84	84	84	84	84	84	84
Rad. 5	88	88	88	88	88	88	88	88	88	88	88	88
Rad. 6	90	90	90	90	90	90	90	90	90	90	90	90
Rad. 7	90	90	90	90	90	90	90	90	90	90	90	90
Rad. 8	0	0	6	90	90	90	90	90	90	90	6	0
Rad. 9	0	0	0	0	0	89	89	89	0	0	0	0
Rad. 10	0	0	0	0	0	0	0	0	0	0	0	0
Rad. 11	0	0	0	0	0	0	0	0	0	0	0	0
Rad. 12	0	0	0	0	0	0	0	0	0	0	0	0

Import Export

Optimization Wizard (Bloem Power Tower - 6 hrs TES - Dry)

Solar Field

Solar Multiple	1.9

Receiver and Tower

Min. Receiver Diameter	8 m
Max. Receiver Diameter	16 m
Optimization Levels for Receiver Diameter	10
Min. Receiver Height/Diameter Ratio	0.8
Max. Receiver Height/Diameter Ratio	1.6
Optimization Levels for Receiver H/D Ratio	10
Min. Tower Height	150 m
Max. Tower Height	250 m
Optimization Levels for Tower Height	10

Wet-Cooled Power Cycle

Plant Capacity

Design Turbine Gross Output	110	MWe
Estimated Gross to Net Conversion Factor	0.9091	
Estimated Net Output at Design (Nameplate)	100.001	MWe

Note: Parasitic losses typically reduce net output to approximately 90 % of design gross power

Power Block Design Point

Rated Cycle Conversion Efficiency	0.425	
Design Thermal Power	258.824	MWt
Design HTF Inlet Temp.	574	'C
Design HTF Outlet Temp.	290	'C
Boiler Steam Pressure	100	Bar
Boiler LHV Efficiency	0.9	
Steam cycle blowdown fraction	0.013	

Plant Control

Min. Temp. To Load	500	'C
Low-resource Standby Period	2	hours
Standby Mode Thermal Fraction	0.2	
Turbine Startup Time	0.5	hours
Turbine Startup Energy Fraction	0.75	
Minimum Load Fraction	0.25	
Max. Over Design Operation	1.15	

Cooling System

Condenser Type	Evaporative	
Design Ambient Temperature	20	'C
Ref. Condenser Water dT	10	'C
Approach Temperature	5	'C
ITD at Design Point	16	'C
Condenser Pressure Ratio	1.0028	

Dry-Cooled Power Cycle

Plant Capacity

Design Turbine Gross Output	110	MWe
Estimated Gross to Net Conversion Factor	0.9091	
Estimated Net Output at Design (Nameplate)	100.001	MWe

Note: Parasitic losses typically reduce net output to approximately 90 % of design gross power

Power Block Design Point

Rated Cycle Conversion Efficiency	0.408	
Design Thermal Power	269.608	MWt
Design HTF Inlet Temp.	574	'C
Design HTF Outlet Temp.	290	'C
Boiler Steam Pressure	100	Bar
Boiler LHV Efficiency	0.9	
Steam cycle blowdown fraction	0.016	

Plant Control

Min. Temp. To Load	500	'C
Low-resource Standby Period	2	hours
Standby Mode Thermal Fraction	0.2	
Turbine Startup Time	0.5	hours
Turbine Startup Energy Fraction	0.75	
Minimum Load Fraction	0.25	
Max. Over Design Operation	1.15	

Cooling System

Condenser Type	Air-cooled	
Design Ambient Temperature	33	'C
Ref. Condenser Water dT	10	'C
Approach Temperature	5	'C
ITD at Design Point	16	'C
Condenser Pressure Ratio	1.0028	

Wet-Cooled Thermal Storage and Parasitics

Storage System

Storage Type	Two Tank		Initial Hot HTF Temp.	574	'C
Full Load Thermal Storage Hours	6	hours	Initial Cold HTF Temp.	290	'C
Storage HTF Volume	7224.78	m3	Initial Hot HTF Percent	30	%
Tank Diameter	21.4463	m	Initial Hot HTF Volume	2167.43	m3
Tank Height	20	m	Initial Cold HTF Volume	5057.35	m3
Min. Tank Fluid Height	1	m	Cold Tank Heater Temp. Set-Point	280	'C
Parallel Tank Pairs	1		Cold Tank Heater Max. Load	30	MWe
Min. Fluid Volume	361.239	m3	Hot Tank Heater Temp. Set-Point	500	'C
Max. Fluid Volume	6863.54	m3	Hot Tank Heater Max. Load	30	MWe
Wetted Loss Coefficient	0.4	Wt/m2-K	Tank Heater Efficiency	0.99	
Dry Loss Coefficient	0.25	Wt/m2-K			

Thermal Storage Dispatch Control

Current dispatch schedule:

No library match.

Dispatch schedule library...

Note:

Schedule libraries do not affect the Storage Dispatch, Turbine Output and Fossil Fill fractions below.

	Storage Dispatch w/ solar*	Storage Dispatch w/o solar*	Turb. out. fraction*	Fossil fill fraction*
Period 1:	0.1	0.1	1.1	0
Period 2:	0.1	0.1	1	0
Period 3:	0.1	0.1	1	0
Period 4:	0.1	0.1	1	0
Period 5:	0.1	0.1	1	0
Period 6:	0.1	0.1	1	0

Notes:

1. Storage dispatch fractions apply to the maximum energy storage.

2. Turbine output and fossil fill fractions apply to the design turbine thermal input.

Weekday Schedule

	12am	1am	2am	3am	4am	5am	6am	7am	8am	9am	10am	11am	12pm	1pm	2pm	3pm	4pm	5pm	6pm	7pm	8pm	9pm	10pm	11pm
Jan	3	3	3	3	3	3	3	2	2	2	2	1	1	1	1	1	1	2	2	2	2	2	3	3
Feb	3	3	3	3	3	3	3	2	2	2	2	1	1	1	1	1	1	2	2	2	2	2	3	3
Mar	3	3	3	3	3	3	3	2	2	2	2	1	1	1	1	1	1	2	2	2	2	2	3	3
Apr	6	6	6	6	6	5	5	4	4	4	4	4	4	4	4	4	4	4	4	4	5	5	5	6
May	6	6	6	6	6	6	5	5	4	4	4	4	4	4	4	4	4	4	4	4	4	5	5	5
Jun	6	6	6	6	6	6	5	5	4	4	4	4	4	4	4	4	4	4	4	4	4	5	5	5
Jul	6	6	6	6	6	6	5	5	4	4	4	4	4	4	4	4	4	4	4	4	4	5	5	5
Aug	6	6	6	6	6	6	5	5	4	4	4	4	4	4	4	4	4	4	4	4	4	5	5	5
Sep	6	6	6	6	6	6	5	5	4	4	4	4	4	4	4	4	4	4	4	4	4	5	5	5
Oct	6	6	6	6	6	5	5	4	4	4	4	4	4	4	4	4	4	4	4	4	5	5	5	6
Nov	6	6	6	6	6	5	5	4	4	4	4	4	4	4	4	4	4	4	4	4	5	5	5	6
Dec	3	3	3	3	3	3	3	2	2	2	2	1	1	1	1	1	1	2	2	2	2	2	3	3

Weekend Schedule

	12am	1am	2am	3am	4am	5am	6am	7am	8am	9am	10am	11am	12pm	1pm	2pm	3pm	4pm	5pm	6pm	7pm	8pm	9pm	10pm	11pm
Jan	3	3	3	3	3	3	3	3	3	3	3	3	3	3	3	3	3	3	3	3	3	3	3	3
Feb	3	3	3	3	3	3	3	3	3	3	3	3	3	3	3	3	3	3	3	3	3	3	3	3
Mar	3	3	3	3	3	3	3	3	3	3	3	3	3	3	3	3	3	3	3	3	3	3	3	3
Apr	6	6	6	6	6	5	5	5	5	5	5	5	5	5	5	5	5	5	5	5	5	5	5	6
May	6	6	6	6	6	6	5	5	5	5	5	5	5	5	5	5	5	5	5	5	5	5	5	5
Jun	6	6	6	6	6	6	5	5	5	5	5	5	5	5	5	5	5	5	5	5	5	5	5	5
Jul	6	6	6	6	6	6	5	5	5	5	5	5	5	5	5	5	5	5	5	5	5	5	5	5
Aug	6	6	6	6	6	6	5	5	5	5	5	5	5	5	5	5	5	5	5	5	5	5	5	5
Sep	6	6	6	6	6	6	5	5	5	5	5	5	5	5	5	5	5	5	5	5	5	5	5	5
Oct	6	6	6	6	6	5	5	5	5	5	5	5	5	5	5	5	5	5	5	5	5	5	5	6
Nov	6	6	6	6	6	5	5	5	5	5	5	5	5	5	5	5	5	5	5	5	5	5	5	6
Dec	3	3	3	3	3	3	3	3	3	3	3	3	3	3	3	3	3	3	3	3	3	3	3	3

Parasitic Energy Consumption

Startup Energy of a Single Heliostat	0.025	kWe-hr
Tracking Power for a Single Heliostat	0.055	kWe
Receiver HTF Pump Efficiency	0.85	
Storage Pump Power	0.01	MWe/MWt
Balance of Plant Power	0.05	MWe/MWt
Piping Loss Coefficient	3500	Wt/m
Total Piping Length	1500	m

Dry-Cooled Thermal Storage and Parasitics

Storage System

Storage Type	Two Tank		Initial Hot HTF Temp.	574	'C
Full Load Thermal Storage Hours	6	hours	Initial Cold HTF Temp.	290	'C
Storage HTF Volume	7525.81	m3	Initial Hot HTF Percent	30	%
Tank Diameter	21.8885	m	Initial Hot HTF Volume	2257.74	m3
Tank Height	20	m	Initial Cold HTF Volume	5268.07	m3
Min. Tank Fluid Height	1	m	Cold Tank Heater Temp. Set-Point	280	'C
Parallel Tank Pairs	1		Cold Tank Heater Max. Load	30	MWe
Min. Fluid Volume	376.291	m3	Hot Tank Heater Temp. Set-Point	500	'C
Max. Fluid Volume	7149.52	m3	Hot Tank Heater Max. Load	30	MWe
Wetted Loss Coefficient	0.4	Wt/m2-K	Tank Heater Efficiency	0.99	
Dry Loss Coefficient	0.25	Wt/m2-K			

Thermal Storage Dispatch Control

Current dispatch schedule:

No library match.

Dispatch schedule library...

Note:

Schedule libraries do not affect the Storage Dispatch, Turbine Output and Fossil Fill fractions below.

	Storage Dispatch w/ solar*	Storage Dispatch w/o solar*	Turb. out. fraction*	Fossil fill fraction*
Period 1:	0.1	0.1	1.1	0
Period 2:	0.1	0.1	1	0
Period 3:	0.1	0.1	1	0
Period 4:	0.1	0.1	1	0
Period 5:	0.1	0.1	1	0
Period 6:	0.1	0.1	1	0

Notes:

1. Storage dispatch fractions apply to the maximum energy storage.

2. Turbine output and fossil fill fractions apply to the design turbine thermal input.

Weekday Schedule

	12am	1am	2am	3am	4am	5am	6am	7am	8am	9am	10am	11am	12pm	1pm	2pm	3pm	4pm	5pm	6pm	7pm	8pm	9pm	10pm	11pm
Jan	3	3	3	3	3	3	3	2	2	2	2	1	1	1	1	1	1	2	2	2	2	2	3	3
Feb	3	3	3	3	3	3	3	2	2	2	2	1	1	1	1	1	1	2	2	2	2	2	3	3
Mar	3	3	3	3	3	3	3	2	2	2	2	1	1	1	1	1	1	2	2	2	2	2	3	3
Apr	6	6	6	6	6	5	5	4	4	4	4	4	4	4	4	4	4	4	4	4	5	5	5	6
May	6	6	6	6	6	6	5	5	4	4	4	4	4	4	4	4	4	4	4	4	4	5	5	5
Jun	6	6	6	6	6	6	5	5	4	4	4	4	4	4	4	4	4	4	4	4	4	5	5	5
Jul	6	6	6	6	6	6	5	5	4	4	4	4	4	4	4	4	4	4	4	4	4	5	5	5
Aug	6	6	6	6	6	6	5	5	4	4	4	4	4	4	4	4	4	4	4	4	4	5	5	5
Sep	6	6	6	6	6	6	5	5	4	4	4	4	4	4	4	4	4	4	4	4	4	5	5	5
Oct	6	6	6	6	6	5	5	4	4	4	4	4	4	4	4	4	4	4	4	4	5	5	5	6
Nov	6	6	6	6	6	5	5	4	4	4	4	4	4	4	4	4	4	4	4	4	5	5	5	6
Dec	3	3	3	3	3	3	3	2	2	2	2	1	1	1	1	1	1	2	2	2	2	2	3	3

Weekend Schedule

	12am	1am	2am	3am	4am	5am	6am	7am	8am	9am	10am	11am	12pm	1pm	2pm	3pm	4pm	5pm	6pm	7pm	8pm	9pm	10pm	11pm
Jan	3	3	3	3	3	3	3	3	3	3	3	3	3	3	3	3	3	3	3	3	3	3	3	3
Feb	3	3	3	3	3	3	3	3	3	3	3	3	3	3	3	3	3	3	3	3	3	3	3	3
Mar	3	3	3	3	3	3	3	3	3	3	3	3	3	3	3	3	3	3	3	3	3	3	3	3
Apr	6	6	6	6	6	5	5	5	5	5	5	5	5	5	5	5	5	5	5	5	5	5	5	6
May	6	6	6	6	6	6	5	5	5	5	5	5	5	5	5	5	5	5	5	5	5	5	5	5
Jun	6	6	6	6	6	6	5	5	5	5	5	5	5	5	5	5	5	5	5	5	5	5	5	5
Jul	6	6	6	6	6	6	5	5	5	5	5	5	5	5	5	5	5	5	5	5	5	5	5	5
Aug	6	6	6	6	6	6	5	5	5	5	5	5	5	5	5	5	5	5	5	5	5	5	5	5
Sep	6	6	6	6	6	6	5	5	5	5	5	5	5	5	5	5	5	5	5	5	5	5	5	5
Oct	6	6	6	6	6	5	5	5	5	5	5	5	5	5	5	5	5	5	5	5	5	5	5	6
Nov	6	6	6	6	6	5	5	5	5	5	5	5	5	5	5	5	5	5	5	5	5	5	5	6
Dec	3	3	3	3	3	3	3	3	3	3	3	3	3	3	3	3	3	3	3	3	3	3	3	3

Parasitic Energy Consumption

Startup Energy of a Single Heliostat	0.025	kWe-hr
Tracking Power for a Single Heliostat	0.055	kWe
Receiver HTF Pump Efficiency	0.85	
Storage Pump Power	0.01	MWe/MWt
Balance of Plant Power	0.05	MWe/MWt
Piping Loss Coefficient	3500	Wt/m
Total Piping Length	1500	m